Jevy a procesy v neživé přírodě v kontextu vývoje současné krajiny a archeologického záznamu

Lenka Lisá

Habilitační práce

Brno 2016

Masarykova univerzita
Přírodovědecká fakulta
Ústav geologických věd

Obsah:

The phenomena and processes in the inanimate nature in context of recent landscape development and archaeological record

Summary

The presented work is generally focused on the study of the phenomena and processes in the inanimate nature during the Quaternary, i.e. the period covering approximately the last 2.5 Ma. However the phenomena and processes important to the understanding of the current landscape on the Earth took place not only during the Quaternary, but in essence continuously flowed logically from the beginning of the Earth's development. Therefore, the main factors of the development of the countryside generally can be summarized under the concept of Geodiversity. This is a complex, constantly changing and evolving system influenced by a multitude of both exogenous as well as endogenous factors. At the same time, it can be understood as the driving engine for the formation of ekofactors, therefore, the landscape as a whole, which inevitably to some extent also affects us and our perception of cultural values.

In the first part the work, a general introduction to the study of formation processes is provided. Here, the basic formation processes of the quaternary sediments corresponding to the type of environment in which they form are summarized, and at the same time the consequences of these processes, both in the natural and archaeological context are described. Discussion of the individual environment is conceived either methodically or in relation to climate change and anthropogenic influences on the evolution of the current landscape. The methodological tools commonly used in the context of these studies are summarized in the second part of the work. These mainly include basic sedimenthological descriptions, micromorphological characteristics in natural or anthropogenic contexts, grain size analysis, environmental magnetism, and chemical composition of studied sediments and soils. For over 10 years I have published 29 papers with impact factor, which have had great impact on these themes and now I am presenting 13 papers, accompanied by one published in the peer-reviewed Journal of the Moravian Museum in Brno. These works I consider to be essential for the chosen topic, and therefore I decided to always present two for each of the described formation process. The study of quaternary sediments in relation to climate trends or anthropogenic context is a multidisciplinary topic, therefore, these works are created mostly in the broader team of co-authors while my specialization was and is mostly of a general concept description of the formation processes, micromorphology and grain size analysis, environmental magnetism and chemistry.

It might be said that this work is more or less the insight into my previous academic experience. It can be noted that the study of cave sediments and the work on the application of provenience methods in my thesis, in essence, predetermined the direction of my scientific career. The provenance studies of aeolian sediment (the main topic of my thesis) deepened my knowledge about provenience methods focused on the association of heavy minerals, geochemistry of garnets or zircon typology. These studies were so far the most comprehensive works on the provenance of the rich geometry of sediments in the territory of our republic. At the same time I managed to incorporate the method of quartz grain micromorphology, into the methodology of provenance studies which I used later several times with success in other directed studies. The benefit of this methodology was for example the recognition of sediment transport by iceberg in the case of the Šumava lakes, or the recognition of aeolian input into the sedimentary archives in the case of Labský důl in Krkonoše Mountains. Although my currently published studies are still concerned with climatic

changes, my other career direction was influenced by the integration into the project of Cambridge University and the beginning of cooperation with archaeologists. Gradually there are several studies within the scope of this project focused on the relationship of changing climate, formation processes in the landscape and human impact, especially during MIS3 (Marine Isotope stage 3). However it was not possible to perform the study of the formation processes in a natural and archaeological context, without deeper knowledge of geoarchaeological methods as for examples micromorfology, environmental magnetism, or geochemical characteristics of the studied sediments. Gradually it was possible to establish a certain methodology of Geoarchaeology, which is now commonly used in the Czech Republic and lectured at several universities. The most important projects in recent years, funded mainly by the Czech Grant Agency, include research of the wooden bailey in Veselí nad Moravou, which in a complex globally unique multidisciplinary study directed on the maintenance of the medieval stables was published. Another study was focused on Neolithic rondels, in which we have conducted the first study to compare the fillings of sharp point ditches of enclosures from the time of the Neolithic and Roman periods. One more example is the research of the early medieval site at Roztoky u Prahy, where it was possible to identify and interpret the emergence, development and disappearance of objects and, above all, their floor scales. The current study of the formation processes is an essential part of environmental studies and there is a visible effort to incorporate this methodological perspective into archaeological research. The methodological approaches used in this direction are constantly developing and it seems, that this field of study has great potential for the future.

Předmluva

Předkládaná práce je zaměřena obecně na studium jevů a procesů v neživé přírodě během kvartéru, tedy období cca posledních 2,5 mil. let (2.588 ± 0.005 Ma; Cohen et al., 2013). Toto období je specifické z mnoha hledisek. Chtělo by se egoisticky říci, že tím hlavním faktorem vyčlenění kvartéru jako posledního období kenozoika je objev a rozšíření hominidů postupně na všech kontinentech. Hlavní důvody, které však vedly stratigrafickou komisi k oddělení tohoto období od toho předcházejícího - neogénu (hranice je stanovena paleomagneticky), jsou závislé především na změnách vývoje klimatu řízeného střídáním Milankovičových cyklů (Hays et al., 1976) podmiňujících opakovaný nárůst a odtávání ledovců na obou polokoulích a s tím související periodické střídání chladných (resp. sušších) a teplejších (resp. vlhčích) výkyvů. Zároveň dochází k vývoji současného utváření říční sítě nebo vzniku eolických sedimentů. Samotná role vlivu člověka na krajinu jako takovou je markantnější až v posledním teplém (resp. humidním) výkyvu, který nazýváme holocén a oddělujeme ho na základě klimatických změn od předcházejícího pleistocénu a pliocénu. Hranice začátku holocénu je kladena do období 11,7 ka (Cohen et al., 2013). Posledních 200 let je potom nazýváno antropocénem (Zalasiewicz, et. al., 2011), protože současně s industriální revolucí začala být role člověka na planetě Zemi mnohem výraznější.

To bylo řečeno obecně k úvodu do stratigrafie, který bylo nutno minimálně takto předestřít k předkládanému tématu. Jevy a procesy důležité k pochopení současné krajiny však na Zemi probíhají nejen během kvartéru, ale v podstatě kontinuálně, logicky od začátku vývoje Země. Proto lze hlavní faktory vývoje krajiny obecně shrnout pod pojem geodiverzita (v naší literatuře např. **Bajer et al., 2015**). Geodiverzita je komplexní, neustále se měnící a vyvíjející se systém ovlivněný množstvím jak exogenních, tak endogenních faktorů. Zároveň ji lze chápat jako hnací motor pro formování ekofaktorů, tedy krajiny jako celku, který zákonitě do jisté míry ovlivňuje i nás samotné a naše vnímání kulturních hodnot. Základem geodiverzity, potažmo diverzity současné krajiny, je v první řadě složení horninového substrátu. Již první pohled na geologickou mapu českých zemí nám odhalí, že na jejich stavbě se podílejí dvě geologické jednotky prvního řádu - Český masiv, který buduje celé Čechy a zhruba dvě třetiny Moravy a Slezska, a Západní Karpaty, jejichž vnější pásmo včetně předhlubně se táhne podél celé jihovýchodní hranice Českého masivu. Nedílnou součástí geologického podloží je i jeho nejsvrchnější „slupka“ na hranici geosféry a atmosféry tvořená kvartérními sedimenty a půdami. Ty jsou v klasickém geologickém pojetí často opomíjeny, jsou však neodmyslitelně důležitou součástí krajinné geodiverzity. Dalším faktorem modifikujícím krajinu je sám člověk. Studium zaměřené na interakci člověka s krajinou v archeologii spadá do oboru geoarcheologie. Základní práce zabývající se geodiverzitou danou formačními procesy a v návaznosti na činnost člověka a geoarcheologické přístupy jsou shrnuty například v pracích Goldberga a MacPhaila (2006), Frenche (2005) nebo Robertse (2014).

Následující práce je v první části koncipována jako obecný úvod do studia formačních procesů. Jsou zde shrnuty základní formační procesy kvartérních sedimentů odpovídající typu prostředí, ve kterém vznikaly, a zároveň jsou zde popsány důsledky těchto procesů jak v přirozeném, tak antropogenním kontextu. Diskuze k jednotlivým prostředím je koncipována buďto metodicky, nebo ve vztahu ke změnám klimatu a antropogenním vlivům na vývoj současné krajiny. Úmyslem této práce nebylo představit vyčerpávající rozbor všech typů sedimentů vznikajících v jednotlivých prostředích, ale zaměřit se především na témata, která jsem publikovala ať již jako hlavní autor, nebo spoluautor přibližně v posledních 10 letech. Obecně jsou v rámci kvartérních sedimentů vyčleňovány sedimenty klastické a chemické (Kukal, 1986, Růžičková et al., 2003). Typ sedimentu odpovídá typu procesu a prostředí, v rámci kterého vznikl. Tak lze následně vyčlenit: 1. svahové procesy; 2. fluviální (říční) procesy; 3. eolické (větrné) procesy; 4. glacigenní (ledovcové) procesy; 5. procesy probíhající v prostředí jezer a mokřadů; 6. procesy probíhající v jeskynním prostředí; 7. procesy vyvolané zemědělstvím; 8. procesy akumulace odpadního a konstrukčního materiálu. Posledním typem je proces při vývoji půd. Ten však není vzhledem k jeho komplexnosti a náročnosti tohoto samostatného tématu zařazen do předkládané práce. Diskuze k recentním půdám a paleopůdám je však zmiňována v kontextu s jinými formačními procesy (**Lisá a Bajer, 2014**). Metodické nástroje běžně používané v rámci těchto studií jsou shrnuty v druhé části práce. Zahrnují především základní sedimentologický popis, mikromorfologickou charakteristiku v přirozeném nebo antropogenním kontextu, zrnitostní analýzu, environmentální magnetismus a chemismus studovaných sedimentů nebo půd. Při studiu formačních procesů platí pravidlo vždy postupovat od tzv. makra k mikru, tzn. přistupovat k detailnějším a zároveň i finančně nákladnějším metodám až po dokonalé znalosti okolní geologie, resp. sedimentologie a geomorfologie. Ač se to zdá logické, v reálu je toto pravidlo bohužel až příliš často opomíjeno.

Z celkového počtu 29 impaktovaných prací, které jsem za posledních cca 10 let publikovala, zde předkládám 13 článků doplněných o jednu publikaci zveřejněnou v recenzovaném časopise Moravského zemského muzea. Tyto práce považuji za zásadní pro zvolené téma, a proto jsem vybrala vždy dvě pro každý popisovaný formační proces. Studium kvartérních sedimentů ve vztahu k vývoji klimatu nebo antropogennímu kontextu je multioborovým tématem, proto jsou tyto práce vytvářeny povětšinou v širším autorském týmu, přičemž mou specializací byl a je převážně obecný koncept popisu formačních procesů, mikromorfologická a zrnitostní analýza, environmentální magnetismus a chemismus. Ostatní práce publikované v „pouze“ recenzovaných časopisech (kterých je do dnešního dne již několik desítek) nebo v monografiích neuváděných na Web of Science nepovažuji za „horší“, tyto jen neodpovídají svým zařazením tomu, jak je dnes scientometrie nastavena. Přesto však na tyto publikace alespoň zčásti odkazuji v diskuzích k jednotlivým tématům a jejich seznam je následně uveden v kapitole 3. Použitá literatura. Pro přehlednost jsou všechny práce, ve kterých jsem hlavním autorem nebo spoluautorem, označeny tučně. Na konci této kapitoly je zároveň uveden seznam zkratek používaných v textu. Výše zmiňovaný koncept procesů hrajících roli při vývoji současné krajiny vychází z mé přednáškové činnosti (předmět Geoarcheologie vyučovaný každoročně a dlouhodobě na FF MU v Brně, FF ZU v Plzni) a byl v poslední době publikován v monografiích **Lisé a Bajera** (**2014**; Manuál geoarcheologa); **Bajera et al.** (**2014**; Micromorphology in natural and antropogenical context) a **Bajera et al.** (**2015;** Krajina a geodiverzita - Neživá příroda jako základ krajinných a kulturních hodnot). Vzhledem k rozsahu předkládané práce jsou její kostrou pouze základní charakteristiky jednotlivých prostředí a základní metodické nástroje geoarcheologie. Tento koncept byl již v minulosti částečně publikován ve výše zmíněných monografiích, zde je však výrazně rozšířen a doplněn odkazy na příkladové studie, které jsem publikovala v posledních zhruba 10 letech.

Na tomto místě bych ráda poděkovala všem, kteří mne provázejí mým profesním životem a pomáhají mi nejen v týmové práci. Jsou to kolegové z mé mateřské instituce Geologického ústavu Akademie Věd České republiky a spoluautoři z nejrůznějších institucí v naší republice i mimo ni. Neocenitelné díky však patří i mé rodině a mým rodičům, největší potom mému muži Pavlovi a dceři Markétce za jejich pochopení při plánování mých víkendových cest a dovolených v terénu. Čtyři kolegové, kteří mne v životě výrazně ovlivnili nejen na mé profesní cestě, ale i ve způsobu, jak chápat dění kolem sebe, a kterým bych tímto chtěla poděkovat, jsou paní Vlasta Jankovská z Botanického ústavu AVČR v Brně, pan Václav Cílek z Geologického ústavu AVČR v Praze, pan Martin Jones z Cambridge University v UK a pan Rudolf Musil z mé alma mater, Masarykovy univerzity v Brně.

Za cenné připomínky k předkládané práci bych tímto ráda poděkovala kolegům Pavlovi Bosákovi z Geologického ústavu AVČR v Praze, Petrovi Nerudovi z Moravského zemského muzea v Brně a Alešovi Bajerovi z Mendelovy univerzity v Brně.

Seznam použitých zkratek

BC (before Christ) – před začátkem našeho letopočtu

BP (before present) – před současností

Cox – oxidovatelný uhlík

CHKO – chráněná krajinná oblast

ka – (for killoannus) - tisíc let

LOI (Loss on Ignition) – ztráta žíháním

LGM (Last Glacial Maximum) – Poslední glaciální maximum

LGT (Last Glacial Terminal)- terminální část posledního glaciálu

Ma (for megaannus) - milion let

MIS3 – Marine Isotope stage 3

MIS4 – Marine Isotope stage 4

PK1 – Pedokomplex 1

TOC (total organic carbon) – celkový obsah uhlíku

W1/2; W2/3 – zkratky pro starší členění würmu

1. Přirozené formační procesy vývoje současné krajiny

1.1. Svahové procesy

Svahové sedimenty vznikají jako postupná akumulace zvětralého materiálu v důsledku gravitačních procesů. Způsob, jakým se materiál pohybuje, závisí na množství faktorů a je silně ovlivněn mírou nasycení vodou. Pro tyto procesy, resp. pro výsledný typ sedimentů, který v jejich rámci vzniká, existuje v literatuře široké spektrum terminologických výrazů. Lze se tedy setkat s pojmy jako např. koluviální, deluviální, geliflukční nebo soliflukční sediment. Všechny tyto výrazy popisují odchylky ve způsobu svahové depozice, resp. faktory, které při ní hrají roli. Hlavním faktorem při svahovém způsobu depozice, která působí na nakloněné ploše, je zemská přitažlivost (gravitace). Proto tyto sedimenty nazýváme obecně jako sedimenty svahové nebo gravitační. Dalším používaným synonymem svahových nebo gravitačních sedimentů/procesů je termín koluviální (výraz coluvial převzatý z anglosaské literatury). Tyto tři pojmy (gravitační/svahový/koluviální) v sobě zahrnují širokou škálu vlivů, které mohou typ výsledných procesů/sedimentů modifikovat. Platí pravidlo, že pokud nejsme schopni identifikovat přesněji vlivy, které při gravitační depozici hrály roli, můžeme sediment obecně nazvat jako gravitační, svahový nebo koluviální. Naproti tomu například termín deluviální už je specifičtější a charakterizuje sediment, na jehož vzniku se podílela jak gravitace, tak nasycení vodou a výsledný proces byl poměrně rychlý. Odpovídá například ronu, plošnému splachu nebo rychlému bahnotoku. V okamžiku, kdy se ke gravitaci přidá saturace sedimentu vodou a pohyb po svahu je pomalý, můžeme vzniklý proces/sediment označit jako soliflukční. Známkou pomalé soliflukce je například tzv. hákování, tj. ohýbání kmenů stromů ve směru depozice. Pokud je voda v sedimentu alespoň částečně zmrzlá, vzniká geliflukční sediment. Ve svahových sedimentech jsou křemenná zrna písčité frakce obvykle ostrohranná, jejich tvar odráží rychlost a sílu krátkodobé depozice.

Svahové sedimenty jsou v podstatě nejrozšířenějším typem kvartérního sedimentu na území naší republiky a vznikaly v různé míře jak během glaciálních, tak interglaciálních období. Typ svahových sedimentů je obvykle závislý silně na podložní geologii a na klimatu, ve kterém vznikaly. Tak například ve vyšších partiích Českomoravské vysočiny (Dráteník, Tři palice) nebo v okrajových pohořích, které lemují naši republiku (Šumava – Čertova stěna, Krkonoše – Labský důl), můžeme identifikovat balvanitá pole jako odraz glaciálních podmínek. Na druhou stranu například i dnes vznikají v oblasti Moravskoslezského flyše rozsáhlá sesuvná území tvořená hlinitopísčitými sedimenty a podmíněná především výskytem smykových zón a přítomností vody v geologickém podloží (Hradecký a Pánek, 2008; Šilhán a Pánek, 2010; Pánek et al., 2011), zatímco na úpatí skal pevných, zejména vulkanických hornin, se vytvářejí volné hrubé sutě – droliny. Svahové procesy mohou být iniciovány jak přirozenými, tak antropogenními faktory. Poměrně často se lze setkat se svahovými jevy a jejich důsledky (hiáty) - například ve sprašových sedimentech posledního glaciálu. Typickým příkladem jsou chybějící A horizonty integlaciálních půd, případně redepozice interstadiálních černozemí (**Hošek et al., 2015**) nebo interstadiálních půd na lokalitě Tvarožná (**Škrdla et al., 2009**) nebo v Dolních Věstonicích (**Lisá et al., 2013a**; **Lisá et al., 2014**). Tato problematika byla autorkou dlouhodobě studována především v jihomoravské sprašové oblasti. Zvýšená intenzita svahových procesů je evidentně vázána především na rozdílné rozložení srážek na přechodu mezi výrazně studenými (suchými) glaciálními podmínkami a relativně teplejšími (vlhčími) interglaciálními nebo interstadiálními podmínkami.

Jedním z příkladů toho, jak svahové formační procesy ovlivnily dlouhodobě uznávanou terminologii, je na našem území období MIS 3 spojené s klasifikací pedokomplexu PK1. Během MIS 3 (období marinního izotopového stadia 3 – pro archeologii klíčového pro řešení problematiky počátku mladého paleolitu) proběhla tři relativně výrazná oteplení (moershooftd, hengelo a denekamp). Mírné oteplení hengelo bylo spojováno s interstadiálem W 1/2 (alpská klasifikace používaná v naší starší literatuře) a denekamp s W 2/3 (Valoch 1971). V dnešním pojetí spadají moershooftd, hengelo i denekamp do interpleniglaciálu v průběhu MIS 3 (Valoch, 2012). Z tohoto období byl do naší stratigrafie zaveden pojem PK1, který souhrnně charakterizuje půdní komplex vznikající v těchto obdobích (Kukla, 1969). Smolíková (1969, 1973) pedokomplex 1 popsala následovně: pseudoglej v autochtonní pozici, arktická hnědozem, arktická hnědozem z čisté spraše na bázi. Problém související přímo s gravitačními formačními procesy, které ovlivňují nejen současnou krajinu, ale i stratigrafický záznam, je však v tom, že pojmem PK1 bývá označován téměř vždy jen jeden půdní horizont přiřazovaný obvykle k poslednímu z těchto interstadiálů denecamp. Charakteristika PK1 se však opírala pouze o radiokarbonově datovanou svrchní půdu s gravettienem v Dolních Věstonicích srovnávanou se stillfriedem B v Dolním Rakousku (dřívějším W 2/3). Jedině v tomto pojetí lze tedy PK1 chápat a používat (Valoch, 2012). V profilech, které byly využity pro model chrono-stratigrafického vývoje pleistocenních sedimentů (Kukla, 1969), nebyly zbývající půdní horizonty vzniklé v předchozích interstadiálech zastiženy, a nebyly proto popsány a očíslovány. Absence zmiňovaných paleopůd je z velké míry způsobena právě erozí v důsledku svahových procesů způsobených již zmiňovanými vyššími srážkovými úhrny, resp. rozdílným rozložením srážkových úhrnů během roku. Typickým příkladem půdy, která nebyla do tohoto schématu zahrnuta z výše zmíněných důvodů, je Bohunická půda (Haesaerts, 1985) odpovídající nejlépe půdě „Willendorf (Bohunice)“ o stáří ±41 ka (Haesaerts a Teyssandier 2003).

Komplex sprašových sedimentů s tenkými vrstvičkami asociovanými Šroubkem et al. (2001) s interstadiálními půdami ve vstupním portálu jeskyně Kůlny byl nesprávně interpretován jako eolická sedimentace přerušovaná pedogenezí. Ve skutečnosti šlo v tomto případě opět o svahový sediment uložený během výrazně vlhčí erozní události, (pravděpodobně během MIS 4), přičemž tenké vrstvičky představují erodované rothlemové půdy z prostoru mimo jeskyni (**Lisá et al., 2013b**). Vstupním částem jeskyní povětšinou dominují nejrůznější typy svahových procesů. Obvykle jsou sedimenty těchto prostředí v naší literatuře interpretovány jako opady z komínů (Musil, 1993), v poslední době však bylo revizí dvou jeskyní – jeskyně Pod hradem a jeskyně Kůlny - zjištěno, že se jedná téměř výhradně o materiál deponovaný svahovými procesy (pomalou geliflukcí nebo deluviálními procesy) z prostoru osypového kužele před jeskyní (případ jeskyně Pod hradem – **Nejman et al., 2013**), které na jedné straně usazují kryoturbačně ovlivněné spraším podobné sedimenty, na druhé straně erodují sedimenty vzniklé ve starších fázích depozice (příklad jeskyně Kůlna – **Lisá et al., 2013b**). Typické texturní prvky indikující geliflukční procesy jsou zachytitelné i v tzv. otevřených stanovištích (open-air sites), a sice například ve sprašové sérii v Dolních Věstonicích. Zde byla v kontextu s lidským osídlením zachycena geliflukcí postižená poloha s gravetienským ohništěm (**Lisá et al., 2014**).

Svahové procesy lze velmi dobře studovat v antropogenním kontextu. Na lokalitě Sovín na západním okraji Prahy byly pomocí sedimentologického, mikrostratigrafického a paleobotanického výzkumu identifikovány mocné horizonty diluviálních sedimentů vzniklé v důsledku pravěkých zemědělských praktik (**Lisá, 2011**). K nastartování svahových procesů v tomto případě přispěla především lidská činnost (rozorání až příliš velkých ploch) v kombinaci s nepříznivými vlastnostmi podložních hornin (cenomanské písky). Svahové procesy lze ovšem také studovat v mnohem menším měřítku. Velmi dobrým příkladem jsou výplně archeologických objektů. Častým dotazem archeologů při studiu těchto výplní je otázka, zda byl materiál do objektu intencionálně přemístěn, nebo zda jde o přirozenou depozici v důsledku například svahových procesů (**Tichý et al, 2010**). Tato problematika byla studována podrobně na příkladu hrotovitých příkopů. Ty se v archeologickém záznamu objevují ve větší míře především v neolitu při výstavbě rondelových struktur a později v době římské při výstavbě krátkodobých postupových táborů. Sedimentologickou analýzou těchto výplní podpořenou mikromorfologickou charakteristikou bylo statisticky dokázáno, že formační procesy v rámci rondelových výplní a v rámci příkopů římských táborů se diametrálně liší. Zatímco u rondelových příkopů docházelo v první fázi k poměrně rychlé sedimentaci gravitací, při které vznikaly poměrně tenké vrstvičky redeponované spraše a redeponované a částečně *in situ* vzniklé půdy, v druhé fázi docházelo k periodickým splachům a průběžnému zarůstání vegetací. Druhá fáze trvala v řádech stovek let. Třetí fáze výplní je charakteristická antropogenním vlivem, tj. rychlým přemístěním materiálu valu, který byl v okolí příkopu deponován při jeho výstavbě (**Lisá et al., 2013c, 2015**; **Válek et al., 2013**). Oproti tomu v případě římských táborů je první fáze depozice charakteristická intencionální depozicí valu směrem do příkopu následovanou dlouhodobou, v rámci stovek let dlouhou gravitační depozicí z okolí spojenou s průběžným zarůstáním. Třetí fází je opět intencionální odstranění zbytku valu a zarovnání povrchu pro účely zemědělského využití (**Lisá et al., 2015**; **Komoroczy et al., 2014**).

1.2. Fluviální (říční) procesy

Fluviální neboli říční sedimenty jsou neodmyslitelnou součástí krajiny. Poslední roky o nich slýcháváme čím dál častěji, a to především v souvislosti s povodněmi. Fluviální procesy však neprobíhají pouze během povodní. Činností řek, přesněji řečeno jejich erozními schopnostmi, se již od miocénu (třetihory) začala formovat současná říční síť. Vzniká tak velmi specifická morfologie krajiny, která po tisíciletí ovlivňuje migrace rostlin, zvířat i lidí, protože vytváří jeden z typů krajinného koridoru. Říční údolí má vždy průřez tvaru V, na rozdíl od údolí modelovaného ledovcem, které má průřez tvaru U. Vývoj říčního koryta a architektury říční nivy se mění v čase a v závislosti na klimatu nebo lidském impaktu. Lze vyčlenit rozdílné základní typy řek: divočící, anastomozující a meandrující.

Když hovoříme o fluviálních procesech/sedimentech, myslíme tím výhradně prostředí spojené s proudící vodou, nemusí se ale vždy jednat o říční koryto. Fluviální sedimenty dělíme obecně na sedimenty korytové a aluviální. Korytové sedimenty se usazují v korytech řek, konkrétně na jejich bázi. V rámci těchto prostředí vznikají facie, které odrážejí rozdílnou energii vodního fluida. Korytové sedimenty jsou většinou ve frakci písku až štěrku, jsou vytříděné a v rámci koryta tvoří rozpoznatelné morfologické tvary, například jesepy. Tím, jak do sebe jednotlivá zrnka písku během transportu narážejí, se část zrn odlamuje, a vznikají tak charakteristické důlky. Následný transport tyto důlky vyhlazuje do tvaru jamek. Celkově jsou zrna, která jsou transportována ve vodním fluidu, na svém povrchu hladká a lesklá, protože vodní film nárazy brzdí. Relikty korytových sedimentů, které zůstaly zachovány na svazích údolí poté, co se řeka zahloubila v důsledku klimatických nebo tektonických procesů níže do geologického podloží, se nazývají terasy. Obecně platí, že terasy výše na svahu jsou starší než terasy položené níže ve svahu.

Naproti tomu aluviální sedimenty, jinak také nazývané povodňové sedimenty nebo sedimenty inundační zóny, jsou ukládány proudící vodou v době povodňové aktivity řeky. Voda se ve formě obohacené suspenze vylije z koryta, a jemnozrnný materiál se tak dostává mimo něj a usazuje se v rozlivové zóně v blízkém okolí řeky. Podle vzdálenosti od říčního koryta vyčleňujeme tzv. proximální (blízkou) nebo distální (vzdálenou) nivu. Morfologicky znatelný přechod mezi korytovými sedimenty a sedimenty aluviální zóny je tzv. levées neboli agradační val. Pod tímto pojmem je možné si představit jakýsi mírně vyvýšený val v těsné blízkosti koryta, který vzniká během povodňové aktivity. Je tvořen prachovitopísčitými sedimenty, které jsou s poměrně velkou energií doslova vyhazovány z koryta řeky. Během vyšších povodňových stavů následně může dojít k protržení valů a k jejich resedimentaci do výsledné formy kuželu situovaného směrem do povodňové zóny. V dnešní krajině je většina velkých řek regulovaná a k agradaci povodňových sedimentů téměř nedochází, přesněji řečeno jejich agradace je prostorově výrazně odlišně rozložena, než tomu bylo v minulosti. Přesto lze nalézt na našem území místa s neregulovanými toky (například Osypané břehy v CHKO Strážnické Pomoraví), kde lze sledovat víceméně přirozenou aktivitu řeky zahrnující agradaci aluviálních sedimentů, erozi a vznik i zánik jednotlivých říčních koryt. Pokud si prohlédneme například satelitní snímky z Google Earth, nalezneme v dnes odvodněných aluviálních zónách větších řek množství pozůstatků po činnosti řek, respektive stavbě říční architektury. Výplně zaniklých koryt se totiž většinou litologicky a zrnitostně liší od okolní aluviální zóny. Jsou většinou bohatší na organiku a saturaci vodou, proto na snímcích vystupují jako tmavší plochy - do sebe propletená ramena již mrtvé řeky.

Dynamika říční sedimentace se liší nejen v průběhu vodního koryta, v závislosti na tom, jaký typ materiálu je do říčního koryta erodován a jakou energií, ale také v závislosti na klimatických podmínkách. Jinou dynamiku mají například řeky v mírném pásu a jinou řeky v subtropických oblastech. Nejvýrazněji se klimatické změny ve formačních procesech fluviálních sedimentů projevují u velkých řek v extrémně klimaticky proměnlivých oblastech. Typickým příkladem toho může být například povodí Nilu. Při studiu nilských sedimentů v rámci šestého Nilského kataraktu byla v rámci úzkého údolí pohoří Sabaloka, kterým Nil protéká těsně před kataraktem, popsána extrémně proměnlivá depozice sedimentů vznikajících v zálivových oblastech (tzv. slack water deposits), v rámci kterých lze velmi dobře rozčlenit jednotlivé fáze povodně (**Lisá et al., 2012**). Počáteční fáze je typická redepozicí lehkého materiálu klastické frakce. Následně vzniká prachovitopísčitý sediment bohatý na organickou hmotu a obsahující množství uhlíků a především mikrouhlíků a propálených fytolitů (částeček opálů) z vypalované vegetace. Následná fáze sedimentace je typická střídáním jemnozrnějších nebo hrubozrnějších facií s minimem organické hmoty, a to převážně prachovitopísčité až písčité frakce. Variabilita je proměnlivá a tento typ facie je často během povodně usazován a znovu erodován. Finální fáze povodně je typická prachovitojílovitým sedimentem bohatým na jemnozrnnou organickou hmotu. Formační procesy této facie probíhají již v pomalu odtékající vodě, tj. v suspenzi s malou energií, kdy z roztoku vypadávají nejmenší částice, které jsou povodní deponovány.

Většina velkých řek na našem území je již regulována a to ztěžuje studium jejich přírodních archivů. Jednou z oblastí, kde je možné studovat environmentální záznam v říční nivě, je neregulovaný úsek řeky Moravy ve strážnickém Pomoraví. Nivní zóna je v této oblasti pokryta několika metry jemnozrnných sedimentů usazovaných od konce posledního glaciálního maxima a během posledního tisíciletí prošla mnoha výraznými změnami (Kadlec et al., 2009; **Grygar et al., 2010**). Poměrně rychlá agradace aluviálních sedimentů v posledním tisíciletí stejně jako nárůst prachovité frakce v nivních sedimentech Moravy byla spojovaná se změnami v zemědělském využití krajiny již v sedmdesátých letech (Prudič, 1978). Podobný trend byl zachycen nedávno například v sedimentech Svratky (**Parma et al., 2015**), přičemž tento scénář je předpokládán pro většinu evropských řek (de Moor et al., 2008; Notebaert et al., 2009; Hoffmann et al., 2009). Současné názory na důvody agradace nivy Moravy však stále nejsou sjednoceny. Kadlec et al. (2009) navrhuje podobný scénář jako Prudič (1978), zatímco **Matys Grygar (2011)** poukazuje na možnou souvislost s klimatickými výkyvy. Jeho závěry jsou založeny na faktu, že zvýšená říční agradace byla zdokumentována pro 13. a konec 16. století a koresponduje s hlavními evropskými klimatickými extrémy. Mimo jiné bylo zjištěno, že v období mezi ~1000 a ~1900 AD se aktuální sedimentační rychlost pohybovala v závislosti na různých depozičních faciích mezi 0,2 – 0,6 mm/rok^{-1} **(Grygar et al., 2010)**.

1.3. Eolické (větrné) procesy

Výsledkem eolických neboli větrných procesů jsou eolické sedimenty. Jejich základní členění se odvíjí především od zrnitosti, tudíž je dělíme na váté prachy, později přeměněné do spraší, a na váté písky (Kukal, 1986, Růžičková et al., 2003). Eolické sedimenty vznikají v důsledku větrné depozice. Kromě fluida – větru - je druhým faktorem přítomnost vhodného materiálu, který je větrem přemísťován, tzn. na jedné straně erodován, na druhé straně usazován v podobě eolických sedimentů. V případě vátých prachů, běžně definovaných pojmem spraš nebo sprašové hlíny, které vznikaly převážně na konci glaciálního období, jsou za zdroj považovány aluviální sedimenty velkých řek (Smalley et al., 2009) a lokálně i mrazově rozvětraná eluvia hornin (**Lisá, 2004**; **Lisá a Uher, 2006**;

Lisá et al., 2009), která nebyla pokryta vegetací (*in situ* zvětralé horniny). Právě menší vegetační pokryv umožnil, že se rozvětraný materiál dostal do vznosu a byl dále transportován ve větrné suspenzi. Poté, co energie depozice poklesla, materiál ze suspenze vypadl (převážně prachová frakce). K poklesu transportační energie dochází za překážkou, jako je například kopcovitý terén nebo hrana říčního údolí, kde vzniká nejčastější geomorfologický tvar – závěj. Postupným zarůstáním vegetací, která svými kořeny prachovitou frakci zpevňovala a zároveň impregnovala roztoky bohatými na karbonáty, vznikl typ sedimentu, který nazýváme spraš. Morfologicky jsou na našem území častější závěje. Je to dáno podložní geologií, resp. od toho se odvíjející starší geomorfologií a s tím souvisejícím vývojem říční sítě. Kombinace směru toku našich řek (převážně S-J) a tedy i převažujících směrů větších údolí spolu s převažujícím prouděním větru v době depozice spraší od Z – V, případně SZ JV, JZ – SV (**Lisá et al., 2005**) způsobila, že vznikaly v době glaciálních maxim převážně závěje na závětrných stranách takto orientovaných údolí. Hlavní složkou spraší je křemen, živec a slída s příměsí uhličitanu vápenatého, vytvářejícího hrudky („cicváry“), a jílu. Barva je obvykle světle okrová a převažující zrnitostní složka je 2 – 63 µm. Pokud váté prachy neobsahují karbonáty, jsou obecně nazývány sprašové hlíny nebo spraším podobné sedimenty.

Návětrné strany jsou u větších řek pokryty vátými písky vynesenými dostatečnou větrnou energií z písčitých korytových sedimentů. Zdrojem vátých písků však mohou být i starší písčité akumulace související například s marinní nebo jezerní sedimentací. Stáří písčitých akumulací je jak glaciální, tak holocenní a akumulace vátých písků jsou v současnosti často reaktivovány. Písčitý materiál je obvykle transportován skákáním (saltací) nebo válením po povrchu, protože jednotlivá zrna jsou zároveň váhově mnohem těžší, než je tomu u prachové frakce. Váté písky mohou být vápnité nebo nevápnité v závislosti na obsahu karbonátů ve zdrojových sedimentech. Protože jednotlivá zrna jsou různě veliká, dochází při transportu k jejich vzájemnému oděru, jehož důsledkem je výrazné zakulacení povrchu a jeho zmatnění. Tím, jak do sebe jednotlivá zrnka písku narážejí, vznikají na jejich povrchu malé důlky.

Váté neboli eolické sedimenty jsou na našem území druhým nejrozšířenějším typem sedimentů. Typické spraše bychom nalezli hlavně v teplejších a sušších oblastech, jako je Polabí nebo jižní Morava (Dyjskosvratecký a Dolnomoravský úval). Jejich výskyt je také většinou limitován nadmořskou výškou cca 300 m n. m. Spraším podobné sedimenty, často označované jako sprašové hlíny, tj. sedimenty, které nemají všechny parametry spraší, lze potom nalézt i ve vyšších nadmořských výškách nebo v oblastech s vyššími srážkami (severní Morava, okraje Českomoravské vysočiny). Mocné sprašové profily tak, jak je známe například z Kalendáře věků v Dolních Věstonicích, však nejsou tvořeny čistě spraší. Jde o komplexní záznam posledního klimatického cyklu, kdy se eolická sedimentace probíhající v chladnějších fázích glaciálů střídala s klidovými teplejšími a na srážky bohatšími obdobími (interglaciály, interstadiály), během kterých se již na vytvořených spraších začaly vytvářet půdy. Přechod mezi chladnými a teplými fázemi vývoje klimatu je typický erozními procesy, v důsledku kterých vznikají redeponované spraše, hlínopísky nebo jiné typy svahových sedimentů. Při bližším pohledu na sprašové profily lehce zjistíme, že se díváme na sled jednotlivých událostí charakterizovaný různými typy sedimentů.

Jednou z dlouhodobě řešených otázek týkajících se eolických sedimentů je provenience jejich zdrojového materiálu. Jde totiž o velmi specifický typ sedimentu, který známe převážně z období kvartéru, a to pouze ze specifických oblastí, které nebyly překryty ledovcem. Naše republika je jednou z takových oblastí, protože je součástí jakéhosi koridoru ze severu ohraničeného severoevropským a z jihu alpským zaledněním. Znalost provenience eolického materiálu a způsob jeho depozice proto vypovídá mnohé o obecných formačních procesech spojených s dynamikou danou geomorfologií a klimatem. Metodicky jsou zde aplikovány tzv. provenienční studie, tj. převážně mineralogické metody detekce zdrojů minerálů. Nejvhodnějšími minerály pro provenienční metody jsou těžké minerály. Jsou to akcesorické minerály o specifické hustotě vyšší než křemen. Výhoda těchto minerálů pro provenienční studie spočívá v tom, že se vyskytují povětšinou samotné nebo pouze jejich určitá asociace, typická pro tu kterou horninu. Klasickou prací na toto téma pro naše území, zaměřenou ovšem na provenienční studie v rámci detekce zdroje u fluviálních sedimentů v rámci Moravského krasu, je práce Burkhartla, Šeberla (1965) a Krystka (1981). Provenience eolických sedimentů v rámci Moravy a Slezska byla studována v rámci mé dizertační práce množstvím provenienčních metod zaměřených jak na detekci asociací těžkých minerálů (**Lisá et al., 2002**; **Kvítková a Buriánek, 2005**), tak například na specifické vlastnosti jednotlivých minerálů, např. granátů (**Lisá et al., 2009**) nebo zirkonů (**Lisá a Uher, 2006**). Provenience spraší interpretovaná na základě mikrostruktur na povrchu křemenných zrn je zhodnocena v práci **Lisá (2004)**. Kombinace studia provenience zirkonů spolu s měřením radioaktivity přinesla zajímavé výsledky. Zirkony typu P23 a P24 typické pro durbachity Třebíčského masivu byly v eolických sedimentech detekovány na vzdálenost cca 50 km od zdrojové horniny (**Kvítková, 2002**). A tímto se dostáváme k samotné problematice aplikace provenienčních metod na eolické sedimenty. Těžké minerály jsou, jak již bylo zmíněno, zastoupeny v horninách akcesoricky. To znamená, že je nutno je před samotnou analýzou zkoncentrovat. K tomu se používá jejich specifická hustota, separace má však svá omezení a je v podstatě ideální separovat frakci cca 63 – 2 500 µm. Vzhledem k tomu, že spraše jsou však primárně prachový sediment, tj. obsahují maximum frakce pod 63 µm, lze tudíž provenienčními metodami studovat provenienci pouze části materiálu a otázkou je, zda je tato část zdrojově typická či spíše atypická. Nabízí se i studium například chemického signálu nebo studium jílových minerálů (Adamová a Havlíček, 1996), zde však narážíme na absenci srovnávacích dat mnohdy i jejich nízkou informační hodnotu. Další možnou metodou je již zmiňované studium mikrostruktur na povrchu křemenných zrn (viz kapitola 2.3). Pokus o tyto studie (**Lisá, 2004**) však nepřinesl očekávané výsledky. Bylo možné identifikovat zrna pocházející například ze zvětralého eluvia, fluviálních sedimentů nebo glacigenních sedimentů, ne však v dostatečně statisticky průkazném souboru. Problém je opět v prachové frakci. Křemenná zrna, která tvoří převážnou část spraší, jsou nejideálnějším materiálem pro exoskopickou analýzu, protože křemenná zrna jsou dostatečně měkká na to, aby se na nich zachytily textury vznikající během transportu, a zároveň dostatečně tvrdá na to, aby textury zůstaly zachovány (**Křížová et al., 2011**). Problém je však v jejich velikosti. Pro vznik identifikovatelných mikrostruktur je zapotřebí dostatečná energie, při které o sebe jednotlivá zrna vzájemně narážejí. K tomu však v prachovité suspenzi dochází jen v malé míře.

Fenomén spraše je zajímavý nejen z obecného hlediska poznání provenience a dynamiky eolického transportu, ale je také klíčový pro klimatické studie související s poznáním prostředí, které zde panovalo v minulosti a do jisté míry ovlivňovalo možnosti pohybu lidí i zvířat v krajině, což výrazně ovlivňovalo chování našich předků (**Lisá et al. 2013a**; **Hošek et al., 2015**; **Wisniewski et al, 2015**). V letech 2006 – 2009 probíhal pod záštitou University v Cambridge projekt s názvem „Moravian Gate project“. V rámci něho byly studovány nejvýznačnější paleolitické lokality v transektu od Dunaje směrem k Odře (Dolní Věstonice, Předmostí a Hošťálkovice). Sedimentologický záznam podpořený dalšími environmentálními metodami se v rámci tohoto transektu výrazně liší (**Lisá et al., 2013a, 2014**). Markantní je zvyšující se množství srážek směrem k severu, což byl pravděpodobně i důvod přesouvajícího se gravetienského osídlení směrem k polským pláním (**Lisá et al., 2014**). Dalším dokladem rozdílného klimatu během posledního glaciálu na území naší republiky je evidentně sušší prostředí na jižní Moravě v kontrastu s vlhčími oceánským klimatem ovlivněnými oblastmi středních Čech (**Hošek et al., 2015**). Zvyšující se zrnitost spraší ve svrchním pleniglaciálu kontrastuje s progresivním zjemňováním zrnitostní frakce v oblastech blíže k severoevropskému zalednění. Lovci mamutů ve svrchním pleniglaciálu se evidentně dovedli velmi dobře orientovat v krajině a přizpůsobit se postupné změně klimatu. Přítomnost vody v krajině byla v pravěku stejně jako dnes jedním z klíčových aspektů přežití. Voda byla vázaná v glaciálech především na údolí velkých řek a na prameny s hlubokým oběhem, tj. na místa na tektonických zlomech. Pro orientaci v krajině využívali gravetienští lovci pravděpodobně i přítomnost výraznějších morfologických vyvýšenin bílé barvy v kombinaci s vodními zdroji, ať již to byly mramory (údolí Dunaje – Krems), nebo vápencová skaliska (Dolní Věstonice, Předmostí), případně antropogenní akumulace vybělených mamutích kostí (souhrnně v **Lisá et al., 2013a**).

1.4. Glacigenní (ledovcové) procesy

Za ledovcové sedimenty jsou obecně považovány takové sedimenty, které vznikly v souvislosti s činností ledovce. Tato definice zahrnuje sedimenty vzniklé nejen v přímé interakci se samotným ledem, ale například i ty, které vznikly odtokem tavných vod. Podle energie formačních procesů probíhajících v přímém kontaktu s tělesem ledovce se rozlišují typy sedimentů popsaných jako glacigenní sediment nebo till s mnoha přívlastky označujícími další varianty prostředí. Ledovcové sedimenty jsou nadřazeným termínem, který zahrnuje glacigenní (tilly), glacifluviální a glacilakustrinní sedimenty. Vzhledem k tomu je jasné, že i variabilita facií bude enormní, protože odrážejí především typ a energii transportu. Energie a typ transportu jsou z hlediska ledovcových procesů dosti rozdílné. Shodná transportní energie může být pod ledovcem i na jeho povrchu, a přesto je typ transportu naprosto odlišný, což se projeví v určitém typu vznikajících sedimentů. Samotný led má obrovskou erozní schopnost a doslova odírá podložní horniny, na kterých se pohybuje. Erodovaný materiál poté transportuje nejen ve svém vlastním tělese, ale i pod ním, na bocích a na svém čele. Vznikají tak nevytříděné sedimenty morén. Poté, co ledovec začne tát, jeho tavné vody erodují a transportují již jemnější materiál a usazuji ho ve formě sedimentů ne nepodobných těm fluviálním nebo jezerním. Výsledné geomorfologické tvary ledovcových sedimentů jsou například moréna, esker, kam, kamová terasa, v širším kontextu potom výplavová plošina nebo výplně jezer (varvy). Křemenná zrna pocházející z glacigenního typu transportu jsou typická výskytem tzv. konchoidálních textur nebo odlomením velkého bloku z plochy zrnka. Tyto textury vznikají třecími silami způsobenými tlakem a střihem obvykle na bázi nebo uvnitř ledovce.

Typickým příkladem jezerních sedimentů ledovcových jezer (glacilakustrinní sedimenty) využívaných pro datování (analogickou metodou je například dendrochronologie) jsou laminované varvy (vrstvičky) odrážející fáze sedimentace s organickou hmotou v zimním období nebo bez organické hmoty v letním období. Hrubší a světlejší letní vrstvička vzniká v důsledku zvýšeného průtoku a dostupnosti kapalné vody. V období, kdy varvy vznikaly, byla léta poměrně krátká (2 – 4 měsíce) a po zámrzu jezera docházelo postupně k vypadávání jemnozrnného materiálu ze suspenze, a to včetně planktonu, proto jsou „zimní“ vrstvičky tenčí, jemnozrnné a obsahují více organiky. Z hlediska času se však nejedná o zimu, kdy došlo k jejich sedimentaci, ale spíše o podzim až začátek zimy. Během zimy a jara, než došlo k roztátí jezera, prakticky žádná sedimentace neprobíhala. Stratigrafie na základě varv je srovnatelná například s dendrochronologií.

Výskyt ledovcových sedimentů na našem území je omezen na relikty severoevropského zalednění, které naši republiku postihlo ze severu. Mohli bychom dnes najít již jen opravdu sedimentární zbytky bez výrazných původních morfologických prvků. Na naše území zasáhl ledovec pravděpodobně celkem třikrát (Nývlt et al., 2011) a své sedimenty zanechal pouze v nejsevernějších výběžcích naší republiky - ve Frýdlantském a Šluknovském výběžku, na Liberecku, v Hradecké pánvi a na severní Moravě na Ostravsku, Opavsku a v Moravské bráně. Dalšími typy ledovcových sedimentů, které bychom mohli na našem území nalézt, jsou malé horské ledovce, které nezávisle na severoevropském nebo alpském zalednění fungovaly v Krkonoších a na Šumavě. Jejich relikty, poskytující velmi dobré environmentální archivy, můžeme dnes najít v podobě výplní karů (Labský důl, Obří důl, NP Krkonoše). Výzkum sedimentů, resp. klimatického záznamu spojeného s formačními procesy ledovcových sedimentů (resp. malých horských zalednění) byl úspěšně aplikován v Krkonoších (**Engel et al, 2010**) nebo na Šumavě (**Mentlík et al., 2010**). V oblasti Labského dolu v Krkonoších byl nalezen cca 15 metrů mocný sedimentární záznam pokrývající cca posledních 30 ka. Jedná se tak o první kontinuální záznam vegetační historie od pozdního glaciálu a holocénu až po současnost v oblasti Sudet. Sedimentární záznam spodní části profilu ukazuje, že v době počátku sedimentace, tj. před cca 30 ka lety (cca začátek MIS 2), byl již kar bez ledu. Klimatická křivka reprezentující následující období je velmi variabilní, přičemž nejstudenější období připadá cca na 18 ka BP, tedy dle obecných modelů konec LGM (Last Glacial Maximum) a nástup LGT (Last Glacial

Terminal). Další výrazné ochlazení zjistitelné v tomto profilu je srovnatelné s mladším dryasem, tj. cca 12 ka BP. Během tohoto období byl v karu Labského dolu stálý malý ledovec, což dokládají mikrovrstvičky ledovcových sedimentů, a zdrojová oblast pro sedimenty byla bez stromové vegetace. Poměrně stabilní klimatické podmínky se objevují až od cca 5 ka BP. Dvě fáze zvýšené sedimentace byly zaznamenány v období 9,2 – 7,5 ka BP a 5,8 – 5,5 ka BP. Tyto fáze odpovídají environmentálním změnám během přechodu mezi subboreálem a atlantikem (**Engel et al., 2010**). Druhou podobně studovanou oblastí byla Stará jímka na Šumavě. Sedimentární záznam v této oblasti není tak komplexní, přesto je však zřejmé, že v porovnání se záznamem v Krkonoších je zalednění na Šumavě mnohem více ovlivněno relativní blízkostí Alp a trvalo v této oblasti až do mladého dryasu (**Mentlík et al., 2010**)

1.5. Procesy probíhající v prostředí jezer a mokřadů

Pro vznik jezerních a mokřadních sedimentů je klíčová přítomnost vody a morfologické sníženiny. Jejich bližší charakteristika se odvíjí od rozsahu a hloubky deprese, od množství a složení vody, která hraje zásadní roli v utváření sedimentárního záznamu. Podle toho rozlišujeme typy prostředí: jezera, slatiny, rašeliniště, vrchoviště a tzv. backswamps, tj. prostředí opuštěných říčních koryt v distální nivě. Jezerní neboli lakustrinní sedimenty mohou mít opět větší množství variant podle toho, na jaké prostředí jsou navázány. Například v souvislosti s činností ledovce vznikají glacilakustrinní sedimenty, v prostředí plošně rozsáhlých jezer s dotací vodními toky – hydrologicky otevřených jezer vznikají odlišné sedimenty než v uzavřených bezodtokových jezerech nebo v nádržích vázaných na prameny, dočasně hrazených jezerech a karových jezerech. Zvláštní kapitolou je jezerní prostředí vznikající v krasových oblastech v důsledku zahlcení odvodňovacích jeskynních systémů v krasových oblastech (polje).

Na prostředí s velkou dotací podzemní nebo srážkové vody jsou vázány organogenní sedimenty (organozemě). Postupnou akumulací organické hmoty vznikají vrchoviště, slatiniště nebo rašeliniště přechodového typu. Obecně tato tři prostředí můžeme charakterizovat jako mokřad nebo bažinu se specifickým typem sedimentu. Vznikají tak organogenní a chemogenní sedimenty pouze s malým podílem klastických sedimentů. Popisovaná prostředí se liší podle typu dotace vodou, jejího složení a typu vegetace, která zvodnělé plochy zarůstá. Slatiniště jsou minerálně bohatá, vznikají z trav a ostřic, nicméně na vzniku výplní se často podílí i dřevo, kůra a kořeny s malou příměsí mechorostů. Slatiniště jsou většinou neutrální nebo jen slabě kyselá (v Polabí přecházejí na bázi až do jezerní křídy, která zde tvoří celá ložiska vzniklá ve staroholocenních kalcitrofních jezerech). Rozšířená jsou u nás převážně v nížinách a v nivách řek (v našem prostředí jsou nížiny obecně minerálně bohaté, což neplatí v sousedním Polsku a Německu); reliktní zbytky nacházíme zejména ve středním Polabí na místech, která byla ušetřena meliorace, a rozsáhlejší výskyty jsou zaznamenány v CHKO Litovelské Pomoraví. Vrchoviště naopak nejsou minerálně bohatá, vznikají převážně z mechorostu rašeliníku a jsou vázána na kyselé až velmi kyselé prostředí. U nás je najdeme převážně na plochých horských pramenných pláních na minerálně chudých podkladech (např. Božídarské rašeliniště v Krušných horách, Úpské rašeliniště v Krkonoších a tzv. slatě na Šumavě). Rašeliniště přechodového typu se vyskytují v rozsáhlých pánevních oblastech s nepropustným podložím - u nás zejména v CHKO Třeboňsko, ale také třeba Velké Dářko v CHKO Žďárské vrchy nebo rašeliniště Rejvíz a Skřítek v CHKO Jeseníky – a na jejich tvorbě se podílí především rašeliník a jsou většinou kyselé.

Jedním z enigmatických jezer České republiky je Komořanské jezero, a to hned z několika důvodů. Jednak se jedná o naše nejrozsáhlejší jezero, jednak bylo v minulém století totálně vytěženo z důvodu těžby uhelných slojí na Mostecku. Třetí důležitý fakt je spojitost jezera s lidským osídlením, což dokumentoval Neústupný (1985) a Neústupný et al. (2008). Komořanské jezero lze zařadit mezi jezera říční (Hurník, 1969) a ve svém vývoji zaznamenalo všechna tři stádia vývoje typická pro jezera říčního typu. První fáze, která proběhla v době ukládání anorganických sedimentů na hranici pleistocénu a holocénu, byla oligotrofního charakteru. Druhá fáze, která probíhala během preboreálu a zaznamenávala eutrofní období, se vyznačovala akumulací rozsivkové zeminy až gyttjy. Od období atlantiku nastala třetí fáze vývoje jezera, které se stává distrofním a postupně přechází v močály a rašeliniště (Hurník, 1969, **Bešta, 2015**). Na konci pleistocénu byla oblast jezerní pánve denudována řekou Bílinou a jejími přítoky na úroveň sp. miocénních sedimentů mostecké pánve (Řeháková, 1986). Řeháková (1986) polemizuje s názorem, že Komořanské jezero vzniklo v důsledku sesuvů fonolitových hornin mezi Hněvínem (408 m. n. m) a Špičákem (399 m. n. m.), které přehradily tok řeky Bíliny v jižní části města Starý Most. Přestože okolí jezera bylo od pravěku osídleno (Neústupný et al., 2008), jezerní sedimenty zkoumané multidisciplinárně **Běštou et al. (2015)** nepotvrdily výrazný lidský impakt. Jeden z mála dokladů působení člověka na okolní prostředí je v jezerních sedimentech Komořanského jezera zaznamenán zvýšeným množstvím pylů rodů *Corylus* a *Populus* během neolitu. Zajímavá je například absence mikrouhlíků pro stejné období. Ta je obyčejně uváděna jako intenzivní doklad žháření předestírající počátky zemědělství na začátku neolitu, což se v tomto případě nepotvrdilo a ukazuje to nejspíše na již existující bezlesí na dostatečně velké ploše, která mohla být zemědělsky obdělávána.

Dalším příkladem studia jezerních sedimentů v kontextu s lidským osídlením může být jezero Švancemberk v Třeboňské pánvi (**Hošek et al., 2014**). V jezerních sedimentech zde byl detekován záznam paleoenvironmentálních změn během pozdního pleistocénu a holocénu. Důležitost této lokality spočívá především v tom, že jde prozatím o jedinou lokalitu v tranzitní zóně mezi oceánským a kontinentálním klimatem. Získaná data, která lze korelovat lépe s oceánským typem klimatického režimu, dokládají, že první polovina mladšího dryasu byla spíše humidnější oproti té druhé, relativně sušší části. Tyto změny se výrazně projevily v okolní vegetaci, dynamice sedimentace a úrovni vodní hladiny během přechodu mezi mladším dryasem a preboreálem. Zvýšená intenzita eroze v povodí však mohla být také ovlivněna mezolitickým osídlením (Šída et al., 2007; Pokorný et al., 2010).

Velmi dobrý příklad využívání sezónního kolísání hladiny vodní plochy bychom našli v povodí Nilu. Geomorfologická sníženina na okraji egyptských hrobek na okraji Saqqary a Abusíru v Káhiře se nazývá Abusírský rybník. Je to výrazný topografický prvek spojený s „krajinou pyramid“ (Jeffreys a Tavares, 1994; Bárta, 2005). Jezero samotné bylo využíváno v době stavitelů pyramid (cca 3 ka BC) jako hlavní přístupová cesta k hrobkám severní a centrální Saqqary a Abusíru (Bárta, 1999). Díky vysokému výskytu žabí populace bylo také asociováno s bohyní Hequet, staroegyptské bohyně zrození a vzkříšení (Bárta, 1999). Voda se v této depresi objevuje často při záplavách, jde však především o vzdutí podzemní vody, ne tak povodňové vody Nilu. Při výzkumech v roce 2007 bylo několik desítek centimetrů pod povrchem objeveno podloží tvořené terasovými sedimenty Nilu, které slouží jako zvodeň a na kterých bylo vytvořeno dláždění sloužící jako přístupová cesta k hrobkám. Toto dláždění bylo evidentně v pozdějších fázích částečně zničeno při erozních fázích typických splachy z wadi Fetekti a následně překryto vrstvami čistého písku deponovaného větrem. Fáze eolické depozice je spojována se zvyšující se aridizací této oblasti. Přestože je tato sníženina nazývána jezerem či rybníkem, nebyla v pravém slova smyslu pravděpodobně nikdy trvalou vodní plochou (**Cílek et al., 2010, 2012**).

Záznam o minulém klimatu případně v souvislosti s antropogenním impaktem lze velmi dobře studovat i na takových sedimentárních archivech, jakými jsou například zaniklá říční koryta. V anglické literatuře jsou taková prostředí nazývána backswamps, tedy sníženiny často lokalizované v distální nivě. Jedním z příkladů je studium zaniklého meandru Labe na lokalitě Chrást (**Petr et al., 2013**). Sedimentární profil zachycuje časový úsek od 11 500 BP, tj. téměř od počátku holocénu. Na bázi profilu je zachycena změna říčního koryta při přechodu konce pozdního glaciálu a holocénu. Hlavní část sedimentárního profilu tvoří sedimenty pozdního glaciálu a středního holocénu. Jsou to období poměrně dynamická, charakteristická extenzivní vegetací a sedimentárními změnami od štěrků po prachovitou frakci nebo vrstvy karbonátů s množstvím schránek plžů. Nejsvrchnější část profilu je tvořena sedimenty slatiny těženými a spalovanými ve středověku. Zajímavý byl nález vrstvy dopleritu, tj. druhotně vzniklého minerálu v důsledku protékajících huminových kyselin, který byl zpočátku makroskopicky asociován s vrstvami bohatými na železo. Jedná se však o postsedimentární textury.

1.6. Procesy probíhající v jeskynním prostředí

Jeskyně představují zvláštní typ prostředí, ve kterém lze studovat nejrůznější typy sedimentů. Jde však povětšinou pouze o výsledky posledního sedimentačního cyklu, pozůstatky starších sedimentárních fází jsou relativně řídké (Bosák 2008). V podstatě se zde dají najít všechny typy a facie terestrických sedimentačních prostředí (Bosch a White, 2004) od eolického po fluviální, lakustrinní, gravitační a ve vstupních faciích dokonce prostředí spojené s ledovcovou činností. Typ sedimentace odráží klimatické změny probíhající mimo jeskynní systém, měnící se provenienci sedimentů nebo změny v hydrologickém systému. Obecně se jeskynní sedimenty dělí na dvě hlavní skupiny (Kukla a Ložek 1958). Jednak jsou to sedimenty vnitrojeskynní facie, tj. sedimenty vznikající v důsledku sedimentárních procesů uvnitř jeskyně, v systému, který je poměrně uzavřený od prostředí mimo jeskyni. Kromě klastických sedimentů sem řadíme i chemogenní sedimenty – hlavně všechny typy speleotém vznikající druhotnou krystalizací karbonátů uvnitř jeskyně. Tyto sedimenty se používají pro izotopové paleoklimatické studie a radiometrické datování (pro shrnutí viz Ford a Williams, 2013; Fairchild et al., 2012) a pro svůj obsah pylových zrn i pro statigrafii (např. Bastin, 1979). Druhým typem jeskynních sedimentů jsou uloženiny vchodové facie. Ta je intenzívně studována pro statigrafickou významnost vrstevního sledu, často v kontextu s archeologickými a paleontologickými nálezy. Tato facie geneticky pokrývá sedimenty vznikající přímo ve vchodové části jeskyně ovlivňované sedimentací z prostředí před jeskyní a zahrnuje i tzv. kužel vchodové facie. Kužel vchodové facie vzniká erozí sedimentů nad vchodem jeskyně a postupným opadem do prostoru před jeskyní. Sedimenty, které nejsou z tohoto prostoru dále erodovány do jeskyně, zůstávají mimo ni a tvoří nejcennější stratigrafický a klimatický záznam. Rozsah sedimentace vchodové facie se odvíjí zejména od množství faktorů, mezi základní patří morfologie jeskyně a okolního terénu.

Jeskyně jsou vázány na krasový fenomén (**Bajer et al., 2015**). U nás jsou povětšinou nejznámější jeskyně, které byly v minulosti obývány člověkem. Nejstarší osídlení je dokumentováno např. pro jeskyni Šipka u Štramberka, Javoříčské jeskyně, jeskyni Kůlna v severní části Moravského krasu, jeskyně s tábořišti lovců sobů a dále jeskyni Pekárna nebo Švédův stůl v jižní části Moravského krasu. Jednou z nejslavnějších jeskyní s halštatským pohřbem je jeskyně Býčí skála ve střední části Moravského krasu.

Geoarcheologicky byla v poslední době poměrně detailně revidována výše zmiňovaná jeskyně Kůlna (**Lisá et al., 2013b**). Jeskyně Kůlna je jednou z nejdůležitějších středo- a mladopaleolitických lokalit střední Evropy, a proto jsou poznatky z této jeskyně popsány v následujícím textu detailněji. Jeskyně Kůlna se nachází cca 45 km severně od Brna na severním okraji Moravského krasu. Je to v podstatě 87 m dlouhý tunel s maximální výškou 25 m a šířkou 8 m (Valoch et al. 2011). Jeskyně má dva vchody, menší orientovaný směrem na sever a větší orientovaný směrem na JJZ do Sloupského údolí. Geomorfologie celé oblasti je zvýrazněna Sloupským údolím široce rozevřeným na sever, které směrem k jihu přechází do úzkého Pustého žlebu. Detailní archeologický výzkum vedený K. Valochem probíhal v jeskyni v letech 1961 – 1976 (Valoch, 1988, 2002). Nejúplnější stratigrafii popsal K. Valoch ve vstupní části jeskyně (Valoch et al., 1969), kde postupně rozlišil celkem 14 hlavních geologických vrstev složených především z klastických sedimentů lišících se homogenitou a zrnitostí od prachu po brekcie tvořené devonskými vápenci či písky a štěrky. Nikdy zde však nebyl proveden detailní sedimentologický výzkum. Revizní geoarcheologické studium sedimentů jeskyně Kůlny, které proběhlo v letech 2010 – 2013 (**Lisá et al., 2013b**), přineslo následující poznatky:

Na základě provedených analýz bylo možné definovat možné odpovědi související s dlouho diskutovanou chronostratigrafickou situací jeskyně Kůlny. Rozdíl mezi vrstvami 5 a 6 lze identifikovat na základě zrnitostního složení, resp. míry zvětrávání. Tyto vrstvy vznikaly pravděpodobně během LGM pomalou soliflukcí a byly ovlivněny kontinuálním promrzáním; na základě měření hodnot frekvenčně závislé magnetické susceptibility lze odlišit vrstvu 6a od vrstev 6 a 5. Sedimentace, která probíhala v rámci starší fáze mladého paleolitu (EUP) byla buď značně omezená, nebo byla poškozena pravděpodobně v důsledku kryogenních pochodů. V každém případě se v sedimentární výplni objevuje nejméně jeden hiát, který by se měl nacházet mezi vrstvami 6a a 6. Mikrostruktury jednotlivých vzorků v kombinaci s dalšími proxy-daty zároveň ukazují, že výrazně chladnější období panovalo během ukládání vrstev 5–6a, 7c a 8. Naopak vrstvy 11 a 9b vykazují známky relativně teplejšího a humidnějšího klimatu, což rámcově koresponduje s dosud uznávanou stratigrafickou koncepcí (souhrnná chronostratigrafická tabule v práci **Lisá et al., 2013b**). Podobné podmínky, i když pouze mírně teplejšího charakteru, pravděpodobně převládaly i v době ukládání vrstvy 7a. Následně však tato vrstva byla postdepozičně mrazově postižena, což zřejmě způsobilo vertikální redepozici archeologických nálezů (Neruda in press). Archeologicky sterilní vrstva 7b vznikla v důsledku rychlých svahových procesů a jsou v ní zakomponovány starší sedimenty (rip-up klasty) v předchozích výzkumech mylně Šroubkem et al. (2001) interpretované jako paleopůdy. Tato vrstva mohla vznikat během chladnější fáze MIS 4, kdy docházelo k výrazné změně vegetace a s tím související možné erozi. Pokud byl však důvodem eroze humidnější event, lze tuto vrstvu interpretovat spíše jako důsledek zvýšeného srážkového úhrnu na počátku MIS 3. MIS 4 by potom mohlo být na základě mikromorfologických pozorování kladeno spíše do vrstvy 8. Teplejší a humidnější klima, které je dle chronostratrigrafického kontextu předpokládáno pro vrstvu 11–13, lze doložit pouze na základě výrazně zvýšených hodnot frekvenčně závislé magnetické susceptibility a indexu zvětrávání charakterizovaného poměrem jíl/prach.

Multidisciplinární studium vnitrojeskynních sedimentů, které odráží neuvěřitelnou variabilitu procesů ovlivňujících jeskynní sedimenty, bylo velmi dobře v poslední době aplikováno například v jeskyních slovinského krasu (Hajan et al., 2008). Dalším podobným příkladem je i výzkum v jeskyni Botovskaja (**Kadlec, 2009**). Ta je typickým příkladem dvourozměrného labyrintu o celkové délce dosud prozkoumaných chodeb cca 60 km. Představuje tak nejdelší jeskynní systém v Ruské federaci. Klastické jeskynní sedimenty tvořící výplně chodeb se liší jak po stránce mineralogické, tak po stránce magnetických vlastností a byly ukládány v různých hydrologických podmínkách. Nejstarší část jeskynních sedimentů byla derivována z pískovců, které překrývají zkrasovělý masiv, zatímco nejmladší výplně jsou tvořeny především redeponovanými půdami a produkty zvětrávání vznikajícími na plató nad jeskyní. Jeskynní sedimenty prošly opakovanými depozičními událostmi a erozí během terciéru a pleistocénu. Poslední katastrofická erozní událost je v jeskynních sedimentech zaznamenána z doby cca před 350 ka. Voda prosakující skrz nadložní pískovce způsobuje kolapsy pískovcových tabulí ze stropů jeskynních chodeb, a vytváří tak nejmladší jeskynní výplně.

1.7. Formační procesy v archeologickém kontextu

Do výčtu kvartérních sedimentů, respektive procesů a prostředí, ve kterých sedimenty vznikají, by měly patřit i procesy vyvolané antropogenní činností. Můžeme je rozdělit na procesy vyvolané zemědělstvím nebo běžnou každodenní činností člověka, která ve svém důsledku představuje akumulaci konstrukčního a odpadního materiálu. Procesy vyvolané kultivací půdního A horizontu nejsou na rozdíl od konkrétních archeologických struktur příliš viditelné, přestože jejich důsledky jsou v krajině běžně přítomné. Výraznější zásahy do půdního fondu jsou známy již od neolitu. Odlesňování a s tím spojená eroze půd byly popsány v mnoha studiích, které dokumentují fáze uhlíkatých vrstev překrytých splachy. Splachy iniciované kultivací nejsou mnohdy na povrchu zřetelné, protože tyto sedimenty rychle zarůstají vegetací a splývají s okolní krajinou. Pokud nejde o splach nahromaděný před nějakou zábranou, není geomorfologicky příliš výrazný. Menší dočasné potůčky (vznikají při nárazových deštích nebo při odtávajícím sněhu), které erodují ornici, mohou vytvářet morfologicky zřetelné výplavové vějíře. Kultivace může zanechávat povrchové morfologické změny, například při hluboké orbě zůstávají menší příkopy a akumulace. Orba prohlubuje A horizont, zanechává „plough marks“ a hranice mezi A horizontem a B nebo C horizontem zůstává ostrá. Kultivace může způsobovat tvorbu iluviálních horizontů nebo jinak zvýrazněných kompaktních vrstev (impregnace FeOH). Zemědělství má na svědomí změnu chemizmu půd, což je mnohdy v přímé relaci k zachování archeologických situací. Hnojení půd organickými a minerálními hnojivy (např. vápnem, vápencem nebo popelem) totiž významně ovlivňuje půdní reakci. V závislosti na antropogenním ovlivnění sedimentů a půd, a to i samotnými pohřby, se mění obsahy fosfátů, síry nebo hodnoty magnetické susceptibility.

Lidské aktivity vždy produkují odpad. Většina preindustriálního odpadu byla organického původu a zetlela, přesto lze odpad identifikovat, a to díky mineralizaci nebo humifikaci probíhající v redukčních podmínkách. Mineralizace organických zbytků je celkem častá v důsledku vysoké biologické aktivity. Může se projevovat buď jako impregnace organické hmoty oxidy železa z půdní matrix, nebo jako pseudomorfózy $CaCO_3$ a fosfátů po původních buněčných strukturách. Na základě specifických znaků lze v určitých podmínkách rozpoznat v sedimentu například popel, výkaly nebo konstrukční materiál prehistorických staveb. Industriální společnosti produkují širokou škálu odpadu, který je však na rozdíl od těch prehistorických velmi dobře zachován díky svému složení. Jedním z takových odpadů je struska, která má velkou výpovědní hodnotu o používaných technologiích. Identifikace prehistorického odpadního materiálu je možná většinou za pomoci laboratorních metod zahrnujících chemickou analýzu nebo mikromorfologii.

Další důležitá otázka při studiu formačních procesů se týká přímo stavby, využívání a zániku archeologických objektů a s tím souvisejícího vzniku podlahových horizontů *s. s.* Makroskopický popis výplní objektů často přináší jen částečnou a především pouze popisnou informaci. Detailnější studium zahrnující mikrostratigrafickou a pedogeochemickou charakteristiku je zásadní pro identifikaci provenience materiálu, který výplně tvoří (Milek, 2012), pro zjištění přítomnosti, typu a stavu organické hmoty (Stoops et al., 2010), uhlíků nebo popele (Canti, 2003) a pro objevení množství a typu pórů v jednotlivých vrstvách či texturních prvcích dokumentujících postsedimentární změny ve studované výplni (Stoops et al., 2010). Všechny tyto informace mohou nepřímo ukazovat například na rychlost a způsob zaplňování objektu, přítomnosti nášlapových horizontů, způsobu jejich úpravy nebo přítomnosti přípravných či sanačních horizontů (Milek, 2012; Goldberg a MacPhail, 2006). Tato metodika byla již v minulosti na území naší republiky úspěšně využita při zpracování několika málo výzkumů. Jedná se například o níže detailněji popsaný výzkum dřevohliněného předhradí ve Veselí na Moravě (**Dejmal et al., 2014**), výzkum raně středověkého sídliště v Roztokách u Prahy (**Novák et al., 2012**; **Kuna et al., 2013**) nebo novověkého zahloubeného objektu v Tišnově u Brna (**Lisá et al., 2010**).

Jedním z mála příkladů využití multidisciplinárního výzkumu formačních procesů sedimentů v antropogenním kontextu je, jak již bylo zmíněno výše, dlouhodobé studium dřevěného předhradí hradu Veselí na Moravě (**Plaček et. al., 2015**), resp. výzkum výplně středověké stáje (**Dejmal et al., 2014**). Výsledky multidisciplinárního studia sedimentární výplně středověké stáje ve Veselí nad Moravou lze shrnout do několika základních bodů. Podlaha stáje byla průběžně ošetřována, a to podobně, jak je tomu dnes, tj. samotná podestýlka byla po čase odstraněna a nahrazena novou. Prostor byl po odstranění podestýlky ošetřen tzv. sanační vrstvou, která měla zároveň i akumulační důsledek. Tato vrstva byla složena z běžného odpadu, jenž však vždy obsahoval zbytky popela z otopných zařízení. Tímto způsobem vznikla vrstevnatá výplň stáje, která je ukončena v sedimentárním sledu nevykydanou podestýlkou. Díky studiu této poslední vrstvy bylo zjištěno, že podestýlka se skládala především z trávy a letorostů dřevin. Tato vegetace byla pravděpodobně i zkrmována, zjištěny však byly i obilniny (proso a oves) a k přikrmování sloužilo i semeno konopí. Ostatní zjištěné obilniny (pšenice, žito) se vyskytovaly pouze v nepatrném množství, snad jako zbytky po zkrmování zadiny. Ze získaných výsledků izotopové analýzy je zřejmé, že v době, kdy vznikala zachovaná podestýlka – tedy v pozdním létě, bylo složení skupiny zde ustájených koní z hlediska úrovně výživy poměrně variabilní. To nepřímo indikuje zbývající využití stáje, tj. buď stáje sloužily k ustájení koní námezdní síly, nebo poselských či vojenských koní. V neposlední řadě byla díky studiu výplně objektu rekonstruována i středověká nelesní vegetace zázemí lokality, která odpovídá všem dosud v okolí lokality se vyskytujícím travnatým společenstvům – společenstvu vlhčích až mokrých luk/pastvin (niva Moravy), mezofilním loukám a místy i suchým a velmi suchým pastvinám. Nepřímým výsledkem analýzy je i poměrně dobrá představa o druhovém složení lesů v zázemí lokality. Také obraz lesní vegetace se na kvalitativní úrovni příliš nelišil od recentního stavu (převládají druhy doubrav, případně dubohabřin na různě vlhkých stanovištích). Kvantitativní stránka rekonstrukce lesní vegetace, tedy zejména úroveň odlesnění, ale mohla být výrazně odlišná.

Samotné studium podlahových horizontů je jednou velkou kapitolou geoarcheologického výzkumu. Množství zajímavých situací nalezených na našem území je však prozatím mnohdy rozpracováno pouze do formy posudků a je nutné jejich studiu věnovat více času. Je to otevřené téma s širokými možnostmi budoucího výzkumu. Tzv. podlahové horizonty jsou totiž velmi zajímavým fenoménem. Jedná se o obecný a v praxi často zaměňovaný či naopak nerozpoznaný pojem. Termínem „podlaha“ by měl být navázán vlastně pouze povrch, který přímo sloužil při funkci objektu. Situace je však mnohem složitější. Často narážíme na přípravné vrstvy pro „finální podlahu“ jako například drenáže, (**Lisá et al., 2008**), podlahovou omítku (**Tichý et al., 2012**) nebo na vrstvy související se sanací původního povrchu (**Beran et al., 2014**; **Dejmal et al., 1013**; **Jarošová et al., 2010**). Vrstvy související přímo s užíváním povrchu nejsou naopak tak často zachovány a najdeme je především ve středověkých situacích (např. **Plaček et al., 2015**; **Novák et al., 2012**; **Kuna et al., 2013**). Při archeologických výzkumech bývá někdy za podlahovou vrstvu nesprávně zaměňována vrstva odlišující se konzistencí (často tvrdostí) od okolního prostředí. Může však jít pouze o horizont vzniklý v důsledku postdepozičních procesů při prosakování mobilních prvků směrem do podloží (**Novák et al., 2012**).

Příkladem studia podlahových horizontů v rámci středověkého sídliště v kontextu s celkovým studiem vytváření, užívání a destrukcí objektů je lokalita Roztoky u Prahy. Sídliště kultury pražského typu (6. – 7. stol. n. l.) v Roztokách u Prahy představuje dosud nevyřešenou archeologickou záhadu. Obtížně interpretovatelné je zejména mimořádné množství sídlištních objektů - zahloubených domů. Během záchranných výzkumů v letech 1980–1989, 2001 a 2006–2010, které poskytly reprezentativní vzorek celé lokality, bylo zachyceno kolem 300 zahloubených domů; jejich celkový počet na lokalitě lze odhadnout na 600–700. Pro srovnání uveďme, že na žádné z ostatních 160 známých lokalit daného období v Čechách nebylo dosud nalezeno více než deset domů. Záhadnost situace umocňuje i zvláštní poloha areálu. Lokalita o ploše kolem 20 ha leží vtěsnána na úzké dno hlubokého údolí na levém břehu Vltavy v pásu o šířce cca 100 m a délce 1,6 km. Pouze malá část lokality byla osídlena v pravěku a/nebo v následujících obdobích, její podstatná část naopak obsahuje archeologické doklady pouze z počátků raného středověku. Zcela evidentně tedy právě v tomto období musel existovat zvláštní důvod k pobytu velkého počtu lidí na daném místě, poměrně nevýhodném z hlediska zemědělství a komunikace. Geoarcheologický výzkum přinesl následující výsledky: v domech se uklízelo; vrstva na podlaze nepředstavuje jen doklady užívání, ale i počátek přirozeného zániku objektu v dosud stojícím domě; po opuštění mohly domy zůstat určitou dobu prázdné; během této doby se mohla akumulovat tmavá vrstva nad podlahou; dřevěné konstrukce domu byly po opuštění rozebrány; spodní vrstvu výplně lze interpretovat jako přemístěnou vrstvu podloží vykopaného při stavbě následujícího sousedního domu; přeházeným materiálem ze základů sousedního domu byla zřejmě zaplněna celá zahloubená část opuštěného domu. Během určité doby vrstva sesedla, čímž většinou vzniklo mísovité prohloubení ve středu; do tohoto prohloubení byl dále deponován odpad z následující fáze vývoje sídliště; tento odpadový areál mohl být v určitém okamžiku pokryt kamenným dlážděním. Dláždění mohlo zarovnávat propadající se terén, ale mohlo tvořit „chodníček“ (někdy navazující na destrukci pece) usnadňující přístup k odpadovému areálu. Odpadový areál mohl být užíván jako latrína; nálezy v odpadové vrstvě v horní části výplně nejsou současné s nálezy na podlaze domu, nýbrž nejméně o jednu stavební fázi mladší (**Novák et al., 2012**; **Kuna et al., 2013**).

2. Vybrané metodické nástroje současné geoarcheologie

2.1. Koncept základního popisu

Základním principem kvalitního geoarcheologického výzkumu je nejen postupovat od makra k mikru, ale také umět se zorientovat v již publikované literatuře. Znalost geologických a topografických map je prvním předpokladem pro správnou interpretaci terénních situací. Druhým předpokladem je dobrý makroskopický popis, znalost archeologického kontextu a stanovení základních výzkumných otázek. V návaznosti na tyto kroky jsou následně odebírány vzorky zpracované jednou z následujících metodik nebo lépe jejich kombinací. Při makroskopickém popisu je třeba zohlednit strukturní a texturní prvky, a sice primární a sekundární. Těmi primárními prvky (zvrstvení) se rozumí uspořádání sedimentárního materiálu uvnitř vrstvy odrážející energii a fluidum, díky kterému sedimentace probíhala. Nejčastějším příkladem je zvrstvení horizontální, čočkovité, šikmé nebo gradační. Sekundární prvky odrážejí postdepoziční modifikace. Nejčastějším příkladem mohou být desikační (výsušné) pukliny, textury zvodnění, mikrotektonika, konvolutní struktury nebo mrazové pukliny (klíny). Dalším popisným znakem je přechod do nadloží. Přechod může být jasný, náhlý, pozvolný, difuzní, ostrý, hladký, zvlněný, nerovnoměrný nebo polámaný a odráží formační procesy během sedimentace, pedogenních pochodů nebo druhotných porušení. Půdní typ matrix zase odráží pedogenní vývoj vrstev a druhotně i zrnitostní složení. Vyhodnocení zrnitostní distribuce je zásadní pro pochopení geneze sedimentu. V terénu se provádí zhodnocení promnutím mezi prsty, případně porovnáním se zrnitostní tabulkou, okoskopicky lze určit i poměry jednotlivých frakcí. Existuje množství klasifikací, liší se podle států nebo účelu, ke kterému byly vytvořeny (viz geologická versus pedologická klasifikace, americká versus evropská). Pro účely hodnocení geoarcheologických situací doporučuji používat Wentworthovu klasifikaci. Grafické vyjádření zrnitosti lze následně provést formou kumulační nebo frekvenční křivky. Důležité je také zhodnocení vytřídění sedimentu, obsahu a zaoblení hrubozrnných částí, přičemž limit hrubozrnnosti nebo litologický typ záleží na autorovi popisu. Lze tak velmi dobře odhadnout například procentuální zastoupení uhlíků nebo mazanice o dané velikosti. Míra zaoblení poukazuje na typ zvětrání nebo délku transportu. Dalším důležitým znakem při popisu sedimentárního profilu je určení barvy. Barva sedimentu odráží půdní procesy a obsah inkluzí; indikuje obsah organické hmoty apřítomnost oxidů železa; a určuje se pomocí srovnávací Munsellovy škály, a to na čerstvém profilu při slunečním světle, dodatečné určení probíhá na suchém vzorku v laboratoři. V neposlední řadě je výhodné v terénu zjistit i obsah karbonátů. Ten lze lehce určit reakcí s 10% HCl. Zjištění pH, které obsah karbonátů nepřímo odráží, následně pomáhá při rozhodování o odběru dalších vzorků například pro paleoekologii (zachování pylů, makrozbytků, schránek měkkýšů; **Lisá a Bajer, 2014**).

2.2. Mikromorfologie v archeologickém kontextu

Metoda mikromorfologie představuje v podstatě popis vnitřní stavby sedimentu nebo půdy podrobným studiem půdních výbrusů, tj. materiálu odebraného *in situ* z vysušeného, pryskyřicí naimpregnovaného profilu, vybroušeného do tloušťky cca 30 µm. Mikromorfologie používaná v archeologickém kontextu, která se dnes již běžně objevuje v anglosaské literatuře, je odvozena od půdní mikromorfologie, jejímž zakladatelem byl W. L. Kubiena (1938). Prakticky se jedná o mikroskopické studium půdních výbrusů. Lze tak získat informace o složení hrubé frakce, matrix, množství a velikosti pórů, texturních prvcích a vzájemných vztazích. Na tomto základě lze interpretovat například provenienci materiálu, způsob zaplňování objektu, míru pedologické aktivity, vyluhování, humifikaci, vysychání a mrazové ovlivnění. Je schopná zachytit přítomnost mikroartefaktů, exkrementů i mikrouhlíků či rozeznat spálené úlomky kostí od těch, které prošly trávicím traktem, spálenou organickou hmotu od dlouhodobě oxidované. Mikromorfologická analýza se odlišuje od ostatních geoarcheologických metod ve čtyřech základních aspektech. Zaprvé produkuje set jak kvalitativních (deskriptivních), tak kvantitativních (numerických) dat a interpretace kvalitativních dat se opírá o standardní terminologii, barevnou fotodokumentaci a vizuální srovnání s ostatními vzorky a s referenční sbírkou. Zadruhé, protože není reálné odebírat mikromorfologické vzorky v systematické síti, tj. každých 0,5 – 1 m^2, není možné na výsledky z mikromorfologie aplikovat kvantitativní analýzu, jako například prostorovou analýzu nebo obecný interpolační prostorový model. Jakkoli se toto může zdát limitující, zdá se, že mikromorfologie má mnohem větší interpretační potenciál, protože vzorky jsou odebírány z originálního stratigrafického kontextu v neporušeném stavu a různé prvky, které sediment tvoří (minerály, matrix, organická hmota, postdepoziční akumulace atd.), lze pozorovat simultánně a interpretovat v mnohem specifičtějším kontextu (exkrementy, podestýlka atd.). Ačkoli techniky, jako je například multi-elementární analýza a ztráta žíháním, poskytují kvantitativní informaci o jednotlivých prvcích a organické hmotě, tyto mohou mít mnoho různých zdrojů, které lze snáze identifikovat právě mikromorfologickou analýzou. V neposlední řadě je velkou výhodou mikromorfologie před ostatními geoarcheologickými metodami fakt, že poskytuje informace o procesech, kterými archeologický sediment vzniká a je případně následně modifikován.

Příkladů aplikace mikromorfologické analýzy na interpretaci archeologické situace bylo již v předchozím textu uvedeno několik. Za všechny je v následujícím textu popsána příkladová studie ze zkoumání podlahového komplexu odkrytého v objektu v Modřicích u Brna, který byl následně interpretován jako středověká kovárna (**Beran et al., 2014**). Svou datací (11. stol. n. l.) se tento nález řadí k jeděním z nejstarších zachovaných výrobních objektů tohoto typu na našem území. Kovářské zpracování železa představovalo v raném středověku zdroj základního sortimentu nástrojů pro zemědělskou výrobu, a tedy důležitý prvek nutný pro přežití vesnických komunit. Přesto jsou dosud poznatky o podobě a organizaci výroby značně útržkovité, často se zaměřením především na centrální aglomerace kolem hradišť. Objekt z Modřic představuje zajímavý příklad vesnické kovárny. Přestože výplň objektu nezahrnovala kovářské výrobky, odpad, který se zde nalezl, dokládá kovářskou výrobu a díky výskytu globulárních okují spolehlivě i kovářské svařování. Konkrétní podoba kovárny je vzhledem ke způsobu zániku jen obtížně rekonstruovatelná, přesto lze na základě informací získaných metodou mikromorfologie ze setu podlahových horizontů spolehlivě doložit způsoby úpravy interiéru. Většinu těchto horizontů lze interpretovat jako specifické podlahové úpravy střídající se s typickými nášlapovými horizonty (Goldberg a Macphail, 2006), které jsou v tomto případě silně prosycené uhlíky, což je logické vzhledem k přítomnosti výhně a nutnosti využívat dřevěné uhlí. Časté obnovování úprav podlahy sanačními vrstvami by mohlo souviset i se sezónním využíváním dílny, neboť je poměrně pravděpodobné, že kovář nepředstavoval plně specializovaného výrobce. Pokud nebyl objekt využíván stále, mohlo být nutné před jeho znovuzprovozněním zamezit vzlínání vody a nově upravit podlahu. Pozoruhodná je ovšem tenká průběžná vrstva tvořená organickým odpadem, nejspíše zvířecími exkrementy. Vzhledem k jejímu charakteru nejde o doklad příležitostného ustájení zvířat, ale spíše o další, velmi specifickou úpravu podlahy. Vyšší obsah fosfátů se znovu objevuje, i když pouze jako prosycení písčité složky, v několika opakujících se nadložních vrstvách. Celkově by bylo možné interpretovat takové obohacení fosfáty v důsledku cílené depozice moči, v případě prvně zmiňované vrstvičky dokonce kejdy. Ta byla považována za prostředek s desinfekčním účinkem. Vedle sporné speciální funkce takovéhoto výmazu lze hypoteticky uvažovat i o jeho neprofánním významu, neboť kováři vždy představovali osoby spojované s magickými praktikami širokého rozsahu (Frolec, 2003). Po zániku funkce byl objekt spíše záměrně zaplněn, o čemž svědčí absence dokladů zarůstání vegetací ve finálním zásypu.

2.3. Povrchová morfologie křemenných zrn

Metodu exoskopické analýzy uvedl v roce 1935 A. Cailleux pod názvem Morfoskopie písku. Princip metody spočívá ve studiu křemenných zrn, která během transportu prodělala signifikantní změny na svém povrchu (**Křížová et al., 2011**). Typ fluida, rychlost a délka transportu určují množství vzniklých texturních prvků a zároveň možnosti interpretace procesů, jimiž křemenná zrna během transportu prošla (Le Ribault, 2003a). Povrch křemenných zrn je pozorován pod binokulárním a následně elektronovým mikroskopem při vícenásobném zvětšení. Ideální velikostní frakce zrn pro tuto analýzu je 300 až 500 µm, protože na zrnech této velikosti se nejlépe projevují mechanické i chemické vlivy (Le Ribault, 1975; Censier a Tourenq, 1986; Cremer a Legigan, 1989), jejichž procentuální zastoupení u jemnozrnných sedimentů není zcela jasné (**Lisá, 2004**). Na povrchu zrn se setkáváme se znaky mechanického nebo chemického původu. Lze rozlišit stupeň lesklosti (lesklý až matný) a skulpturní znaky (rýhování, poškrábání, nárazová deprese, vtisky aj.). Matný povrch křemenných zrn písčité frakce bývá většinou spojován s eolickými pochody, lesklý vzniká nejčastěji dlouhým transportem ve vodním prostředí řek nebo vývojem v mořském prostředí. V pouštních podmínkách je lesklý povrch vysvětlován tenkým povlakem pouštního laku chemogenního původu (Petránek, 1963; Le Ribault, 2003b). Geneze sedimentů určovaná metodou exoskopie odvisí od výskytu charakteristických mikrotextur či jejich souborů na povrchu zrn (*sensu* Le Ribault, 1975). Jedná se o takové mikrotextury, které vznikly při zvětrávání, transportu a sedimentaci materiálu a jejichž procentuální zastoupení většinou nepřevyšuje 60 % (Mahaney et al., 2001). V rámci jednoho prostředí mohou být křemenná zrna ovlivněna několika geneticky odlišnými procesy (Alkaseeva, 2005), avšak nejzřetelnější tvary na křemenných zrnech jsou většinou takové, které vznikly během posledního transportu. Kromě procesu, který se podílel na posledním typu transportu, dokáže exoskopie odhalit na jediném zrnu až 8 epizod vývoje (Le Ribault, 1975). Vztahy mezi eluviálními, fluviálními a eolickými prvky se mění se změnami klimatických podmínek. Vliv procesů na mikroreliéf zrna závisí také na trvání transportu a energii transportního média. Intenzita chemické transformace povrchů křemenných zrn je závislá na době působení chemických procesů, klimatu, textuře sedimentů, velikosti zrn minerálů a na pozici v půdním profilu a v reliéfu (Alkaseeva, 2005). Při zkoumání vzorků je třeba mít na zřeteli, že zrna různých genetických typů mohla být během svého transportu smíchána (Mahaney a Kalm, 2000).

Aplikovatelnost této metody byla testována na našem území v Krkonoších (**Křížová et al, 2011**). Kopanými sondami byly získány sedimenty z vybraných geneticky různorodých skupin tvarů, tj. z glacigenních, fluviálních, svahových a eolických. Odběr byl proveden na relativně malé ploše s obdobnými geologickými a fyzickogeografickými podmínkami i s podobnou historií vývoje reliéfu. Výjimku tvoří jen eolické sedimenty, které se v Krkonoších nenacházejí a pro jejichž odběr byla vybrána poloha eolických sedimentů na pražském Klárově. Uvedená metoda exoskopie povrchu křemenných zrn umožňuje stanovit způsob transportu, a tedy i genezi sedimentu, respektive daného tvaru, který je jím budován. U vzorků pocházejících z velmi podobného prostředí však nemusejí být výsledky zcela jasné a je zapotřebí použít více vzorků. Také je nutné znát samotné prostředí, kde byl vzorek odebrán, včetně jeho okolí, aby byly procesy formující povrch zrn správně přiřazeny k jednotlivým genetickým skupinám. Pro rozlišení genetických typů sedimentů nelze vždy přesně určit sadu vyskytujících se mikrotextur, spíše lze hovořit o určitých frekvencích výskytu, při kterých by se znak stal charakteristickým. Tyto frekvence výskytu však nejsou pro všechny znaky stejné. Důležitou roli pro frekvenci výskytu představuje rychlost transportu v prostředí. Lasturnatý lom vzniká zejména po prudkých nárazech a odlomení částice od částice větší, což může nastat v kterémkoli prostředí, zároveň může ale také vzniknout mrazovým zvětráváním. Tyto nárazy jsou ale ve fluviálním prostředí tlumeny, charakteristická je tedy spíše nepřítomnost lasturnatého lomu pro fluviální sedimenty. Tilly jsou charakteristické naopak velmi vysokou četností lasturnatého lomu, což znamená, že tento znak se u nich vyskytuje alespoň ze zhruba 70 %. U jiných znaků však stačí menší procentuální podíl výskytu k tomu, aby byly označeny za charakteristické. Zdaleka ne vždy lze ale vysledovat toto přibližné hraniční procento a je potřeba počítat s polohou, s probíhajícími procesy v prostředí, ze kterého vzorky pochází, a s nalezenými mikrotexturami. Musíme např. uvažovat nad tím, zda byl sediment donesen z vyšších poloh a jaké procesy v těchto vyšších polohách probíhaly, protože zrno nese na svém povrchu v různé míře zachování i starší struktury. Podobně i Mahaney (2002) a Le Ribault (1975) upozorňují na to, že zrna si nesou mikrotextury z dřívějších prostředí. Ze znalosti geomorfologie (např. sklonitosti terénu) jsme schopni odhadnout, v jakých rychlostech zdejší procesy probíhají – v exoskopii např. V-jamky, srpkovité textury a mísovité jamky (Le Ribault, 1975) vypovídají o rychlostech média, kterým je sediment unášen – a tím lépe pochopit výsledky exoskopie a určit, kde je přibližná hranice vysokého a nízkého výskytu jednotlivých mikrotextur. Křemenná zrna glacigenních sedimentů jsou charakteristická výskytem lasturnatých lomů (či štěpných plátků, které jsou typicky vyvinuté na menších zrnech), stupňovitých tvarů, puklinovými plochami a přilnavými částicemi. Eolické sedimenty jsou charakteristické výskytem V-jamek, mísovitých jamek a vyšším zaoblením zrn. Pro deluvium jsou typické lasturnaté lomy, stupňovité tvary, brázdy a zejména abraze hran. Křemenná zrna murových sedimentů byla charakteristická lasturnatými lomy, stupňovitými tvary, brázdami a křemičitými sraženinami. Fluviální sedimenty mají oproti ostatním vzorkům celkově nízkou četnost mikrotextur a typický je pro ně nízký reliéf s vyšší zaobleností zrn a křemičité sraženiny, zvláště křemičité povlaky.

2.4. Zrnitostní analýza

Granulometrie čili zrnitostní analýza je kvantifikační metoda, při které je stanoven procentuální podíl jednotlivých frakcí, obvykle rozčleněných na jíl, prach a písek. Hranice mezi těmito frakcemi se mnohdy liší podle toho, zda se používá geologický, geologicko-inženýrský nebo pedologický systém, obecně je však hranice jíl/prach stanovena na 2 mikrometry (4 µm ve Wenworthově geologické klasifikaci) a hranice prach/písek na 50 nebo 65 µm (rozdíl mezi britským a americkým klasifikačním systémem; Goldberg a Machpail, 2006). Způsoby, jakými lze stanovit zrnitostní distribuci, jsou poměrně široké a závisejí v první řadě na makroskopicky odhadnutelné zrnitosti. Využití stanovení granulometrie je v environmentálních vědách široké, ba dokonce je použití této metody v mnoha případech naprosto nezbytné. Znalost zrnitostní distribuce a vytříděnosti materiálu je důležitá pro identifikaci provenience studovaného materiálu a pro identifikaci formačních procesů, na jejichž základě sediment vznikl.

Velmi jemné frakce je vhodné stanovovat pomocí laserového granulometru; rozsahy těchto přístrojů se většinou pohybují od 0,04 µm do 2 mm. Měření probíhá ve vodní suspenzi, do které je pipetován dispergovaný vzorek. Přes zakalenou suspenzi následně procházejí laserové paprsky, pomocí nichž je možné detekovat hustotu suspenze a velikost jednotlivých zrn. Manipulace s laserovými granulometry je většinou jednoduchá a úspěšnost výsledku závisí na míře ideální dispergace studovaného materiálu. Obvykle je používaná dispergace v KOH podpořená ultrazvukem. Tzv. totální dispergace zahrnuje následné odstranění karbonátové a organické složky sedimentu. Ty by se totiž mohly do sedimentu dostat druhotně, a neodrážet tak primární sedimentační podmínky. Vše je však nutné posuzovat v závislosti na konkrétních kontextech. Pro laserovou granulometrii jsou vhodné jílovité a prachovité sedimenty, protože množství měřeného materiálu se pohybuje v gramech. Standardní je tzv. pipetovací metoda podle Andreasena, při které se využívá Stokesův zákon. Vzorek je dispergován ve válci a začíná se usazovat na jeho dně. Hrubozrnný materiál padá ke dnu rychleji, zatímco jemnozrnný jíl zůstává delší dobu ve vznosu. Rychlost usazování je závislá na teplotě. Ve specifickém intervalu (obvykle 30 sekund až 8 hodin) je sediment odebírán z určité hloubky sloupce, vysušen a zvážen a následně jsou kalkulovány procentuální obsahy jednotlivých frakcí. Princip chování sedimentu v suspenzi podle Stokesova zákona lze také využít pro měření hustoty suspenze v různých časových úsecích. Jde o způsob měření tzv. hustoměrnou (aerometrickou) metodou podle Cassagrandy. V časovém odstupu je hustoměrem měřena suspenze a získané hodnoty jsou poté přepočítávány na procentuální obsahy jednotlivých zrnitostních frakcí. Pokud je třeba stanovit zrnitostní distribuci u materiálu písčité nebo štěrkovité frakce, je vhodné suché nebo mokré síťování. Při této metodě je potřebné větší množství materiálu, obvykle tak 1 kg. Vzorek je po vysušení zvážen a umístěn na systém sít, přičemž síta jsou naskládaná na sobě podle klesající velikosti standardizovaných ok. Materiál je poté buď promýván vodou, nebo vyklepáván, přičemž na povrchu jednotlivých zrn se usadí tzv. nadsítná frakce. Následným opětovným zvážením jednotlivých frakcí lze stanovit váhová procenta.

Znalost zrnitostního rozložení se často používá jako proxy při studiu sprašových environmentálních archivů, často v kontextu s magnetickou susceptibilitou (**Lisá et al., 2013a, 2014**; **Antoine et al., 2013**; **Hošek et al., 2015**). Ze srovnávacího studia environmentální informace ve sprašových sedimentech na Moravě, resp. v transektu napříč Moravou a Slezskem, bylo zřejmé, že všechny lokality vykazovaly podobný trend kolísání zrnitostního rozložení. Směrem k začátku holocénu dochází k pozvolnému hrubnutí. Podobný trend je sledovatelný i směrem od jihu k severu, směrem k severoevropskému zalednění. Lokalita Dolní Věstonice má nejlépe zachovaný sedimentární záznam a současně i výskyt zrnitostně nejjemnějších sedimentů. Zřetelný byl zároveň nárůst jílové frakce v závislosti na přítomnosti tmavších interstadiálních nebo interglaciálních horizontů. Tím pádem byla zřetelná i korelace mezi magnetickou susceptibilitou a nárůstem jílové frakce.

2.5. Environmentální magnetismus

Environmentální magnetismus je klasickým metodickým nástrojem dnes již nezbytným pro paleoenvironmentální studie. Nejčastěji je využívána magnetická susceptibilita a frekvenčně závislá magnetická susceptibilita (Thompson a Oldfield, 1986). Magnetická susceptibilita (MS) je hodnota měřená v indukovaném magnetickém poli se stanovenou frekvencí a je vyjádřena jednotkami Si – jinak řečeno: je to schopnost minerálů namagnetizovat se v určitém indukovaném magnetickém poli. Podle toho, jak se materiál v magnetickém poli chová, tj. podle intenzity signálu, je možné rozdělit materiál do tří skupin: diamagnetický, paramagnetický a feromagnetický. Diamagnetický materiál má zápornou hodnotu susceptibility, paramagnetický reaguje jen po dobu blízkosti silného magnetického pole a feromagnetický má velmi silnou odezvu na vnější magnetické pole. Magnetickou susceptibilitu půd a sedimentů ovlivňují dva hlavní faktory. Prvním je přítomnost oxidů železa, jako je hematit (αFe_2O_3), maghemit (γFe_2O_3) a magnetit (Fe_3O_4), a druhým je stupeň antropogenního ovlivnění. Hodnoty magnetické susceptibility jsou často odezvou signálu odrážejícího více faktorů. Ovlivňuje je jak množství, tak i velikost magnetických minerálů, proto může být interpretace založená pouze na těchto datech mnohdy zavádějící a je účelné používat magnetickou susceptibilitu pouze jako jedno z vodítek pro finální interpretace. Frekvenčně závislá magnetická susceptibilita je veličina závislá na zrnitosti a vzniklá výpočtem z minimálně dvou měření, přičemž pokaždé je vzorek vystavován magnetickému poli s odlišnou frekvencí (Dearing et al, 1996). Výhoda frekvenčně závislé magnetické susceptibility je v tom, že odráží množství superparamagnetických minerálů, které vznikají převážně při pedogenních pochodech (Evans and Heller, 2003).

Jedna z metodických studií zaměřená na vztah mezi magnetickými parametry a ostatními proxy, jako je například zrnitost nebo obsah organické hmoty, byla provedena na aluviálních sedimentech Nilu v prostoru Sabaloky a šestého Nilského kataraktu (**Lisá et al., 2012**), kde bylo na základě těchto proxy vyčleněno celkem 9 různých facií. Nuanci mezi těmito faciemi odpovídají změny v energii depozice a lidský impakt. Tato studie je již částečně zmiňována výše (kap. 1.2.), proto zde uvedu jen přímé vztahy mezi magnetickými a ostatními proxy. Zvýšená magnetická susceptibilita byla detekována především v sedimentech ukládaných s vysokou energií. Tyto sedimenty však obsahují i množství diamagnetického křemene, proto bylo zvýšení susceptibility přímo závislé především na přítomnosti prachové frakce, případně na obsahu makroskopicky rozpoznatelných akumulací těžkých minerálů, které zde vytvářely černé čočky. Zvýšení frekvenčně závislé magnetické susceptibility bylo naopak vázáno především na prostředí nízkoenergetické depozice a přímo korelovalo se zvýšenými hodnotami prachové a jílové frakce. Pokud ovšem sediment obsahoval zároveň zvýšené množství organické hmoty, zůstávaly hodnoty magnetické susceptibility nízké a hodnoty frekvenčně závislé magnetické susceptibility vykazovaly zvýšený trend.

2.6. Geochemie

V rámci předkládané práce není reálné uchopit kapitolu s názvem Geochemie příliš detailně, protože škála geochemických nebo pedogeochemických metod využívaných při studiu environmentálního záznamu a formačních procesů je příliš široká. Množství z těchto metodických přístupů bylo zmíněno již v předcházejícím textu, proto zde uvádím jen velmi stručný přehled možnosti stanovení silikátové analýzy, kationtové výměnné kapacity a obsahu organické hmoty doplněné jednou krátkou případovou studií.

Silikátová analýza je metoda, jejíž pomocí lze zjistit mokrou cestou, tedy rozpuštěním vzorku v daném rozpouštědle (nejčastěji zředěné kyselině chlorovodíkové) a oddělením nerozpustného vzorku, obsah jednotlivých prvků. Typ rozpouštědla, které je použito, zásadně ovlivňuje konkrétní analytická data, na což je třeba brát zřetel při srovnávacích studiích. Nejčastěji jsou tímto způsobem stanovovány obsahy rozpustného oxidu křemičitého (SiO_2), oxidu vápenatého (CaO) a hořečnatého (MgO), seskvioxidů (Al_2O_3, Fe_2O_3) a oxidů dalších kovů. Stanovení obsahu jednotlivých prvků se následně provádí například z ICP spektrometrické analýzy. Poslední dobou je čím dál tím častěji používán přenosný XRF spektrofotometr. Pro stanovení kationtové výměnné kapacity (CEC) se používá celá řada metod. Hlavní rozdíly jsou v používaných rozpouštědlech. Například rozpouštědlem Mehlich III. lze získat informace o živinách přístupných pro rostliny. Každopádně získáváme informace jen o specifické části měřeného materiálu, což nám dává možnost přesnějších interpretací, ale na druhou stranu nám nedovoluje obecnější popis sedimentu. V případě metody měření Melichem III. lze získat data, která mohou být porovnávána s již známými databázemi půdního chemizmu. Tato informace je často klíčová pro posouzení stáří a geneze půd nebo pro schopnost rozlišení půd vzniklých *in situ* nebo svahovými pochody (Bajer, 2003). Pro stanovení obsahu organické hmoty se obvykle používá větší množství metodických přístupů. Relativně nejlevnějším je tzv. LOI (loss on ignition), tedy ztráta žíháním. Tato metoda je však vhodná pouze pro sedimenty, které obsahují velké množství organické hmoty. Z dalších přesnějších metod se používá stanovení C_{ox} (oxidovatelný uhlík). V zahraniční literatuře se často jako ekvivalent C_{ox} objevuje TOC (total organic carbon) stanovený stejnou nebo podobnou metodikou.

Příkladem využití znalosti chemického složení jako jednoho ze střípků mozaiky může být výzkum výplně halštatské zemnice v Modřicích u Brna (Jarošová, 2010). Chemické analýzy sedimentů zahrnovaly však v tomto případě pouze fosfátovou analýzu. Dalšími analýzami, které jsou v předchozím textu popsány pouze částečně, byly stanovení pH, ztráta žíháním, ze které byly následně přepočtem zjištěny obsahy organické hmoty a karbonátů, a měření magnetické susceptibility. Závislosti jednotlivých měřených veličin byly interpretovány v návaznosti na mikromorfologii a makroskopický popis sedimentů. Laminovaná, asi 1 m mocná výplň zemnice byla na základě statigrafie a mikrostratigrafie vysvětlena jako systém podlahových vrstev s přídavnými sanitárními polohami, které zamezují šíření pachu či vlhkosti z rozkladu organické hmoty. Změny ve výplni tvořené vrstvičkami organické hmoty přemístěné spraší, popelovitými vrstvami a uhlíky, se odráží také v hodnotách magnetické susceptibility, obsahu karbonátů, fosforu či organické hmoty. Monotónní hodnoty pH potvrzují stabilitu fosfátů, které jsou vázány především na částečně rozloženou organickou hmotu. Přínos pedogenně ovlivněného materiálu, tzn. pravděpodobná fáze počínajícího zániku zemnice, kdy dojde k destrukci stěn, odkrytí prostoru a do zemnice se začíná přirozenou gravitací zanášet půda z okolí, je zřetelný ve svrchní části výplně. Tato domněnka je podpořena nejen mikrostratigraficky, ale i zvyšujícími se obsahy frekvenčně závislé magnetické susceptibility, které nekorelují se susceptibilitou měřenou při jedné frekvenci. Zároveň s rostoucími hodnotami frekvenčně závislé magnetické susceptibility roste obsah silikátového residua, tj. klesá obsah karbonátů a organické hmoty. Nárůsty obsahů organické hmoty a fosforečnanů korespondují s nárůstem obsahu karbonátů, což je dáno především hustotou vzorkování a následným zkresleným signálem. Sanitární vrstvy tvořené především karbonátovou složkou ze spraše se v tomto případě mísí s vrstvami organické hmoty, která zároveň dotuje hodnoty fosfátů. Mikromorfologie má v tomto případě mnohem větší vypovídací hodnotu.

5. Vlastní práce

5.1. Svahové procesy

Lisa, L., Komoroczy, B., Vlach, M., Válek, D., Bajer, A., Kovárník, J., Rajtár, J., Hüssen, C.M., Šumberová, R. (2015): How were the ditches filled? Sedimentological and micromorphological classification of formation processes within graben-like archaeological objects. Quaternary International, 370, 66-76.

Lisa, L., Hosek, J., Bajer, A., Matys Grygar T., Vandenberghe D. (2014): Geoarchaeology of Upper Palaeolithic loess sites located within a transect through Moravian valleys, Czech Republic.- Quaternary International, 351, 25-37.

Quaternary International 370 (2015) 66–76

Contents lists available at ScienceDirect

Quaternary International

journal homepage: www.elsevier.com/locate/quaint

How were the ditches filled? Sedimentological and micromorphological classification of formation processes within graben-like archaeological objects

L. Lisá [a,*], B. Komoróczy [b], M. Vlach [b], D. Válek [c], A. Bajer [d], J. Kovárník [e], J. Rajtár [f], C.M. Hüssen [g], R. Šumberová [h]

[a] Institute of Geology ASCR, Rozvojova 269, Prague 6 165 00, Czech Republic
[b] Institute of Archaeology ASCR Brno, v. v. i., Královopolská 147, 612 00 Brno, Czech Republic
[c] Institute of Archaeology and Museology, Faculty of Arts, Masaryk University, Arna Nováka 1, 602 00 Brno, Czech Republic
[d] Institute of Geology and Pedology, FFWT MENDELU, Zemědělská 3, 613 00 Brno, Czech Republic
[e] Department of Archaeology, Philosophical Faculty, University of Hradec Králové, Rokitanského 62, 500 03 Hradec Králové, Czech Republic
[f] Institute of Archaeology of Nitra, Akademická 2, 949 21 Nitra, Slovakia
[g] Römisch-Germanische Kommission DAI Frankfurt am Main, Palmengartenstraβe 10-12, 60325 Frakfurt am Main, Germany
[h] Institute of Archaeology ASCR Praha, v. v. i., Letenská 2, Prague, Czech Republic

ARTICLE INFO

Article history:
Available online 31 December 2014

Keywords:
Formation processes
Sedimentology
Micromorphology
V-shaped ditch
Neolithic rondel structures
Roman ditch

ABSTRACT

The ways of infilling archaeological objects are among the most common questions given to geoarchaeologists. Convenient subjects for the study of formation processes of archaeological terrain features (contexts) are V-shaped ditches. Their infilling is usually lithologicaly and texturally considerably variable with regular morphology and special archaeological context. The V-shaped ditches are known only from two chronologically, culturally distinctive periods. In first case there are ditches of "rondels" from the Late Neolithic Period, in the second case we are dealing with the fortification ditches of the Roman temporary camps.

On the basis of sedimentological and consequently micromophological study, processes were differentiated in the formation of studied infillings. In Neolithic rondels, two parts of infillings were noted. The lower one typically has straight thin bedded layers, originating due to processes connected with vegetation ingrowth and erosion of the rampart. The upper part of the infilling is usually homogenous, and originated during the human caused grading of the surrounding area. During this phase, remains of rampart constructions were most probably destroyed. The basic type of deposition – especially visible in case of rondels – is lateral planar wash with phases of bioturbation, running pedogenesis on the edges of ditches, or stagnating water. The second main featuring process is mass movement slumping, particularly of upper faces of sloped sides. This process often happens naturally, mainly due to erosion, presence of water, and vegetation. The most distinctive postsedimentary processes determined within the rondel infilling were bioturbation, accumulation of carbonates and movement of clay minerals caused by soil leaching. In the V-shaped ditches of the Roman temporary camps, it was possible to microscopically trace similar records documenting coarse particle sedimentation at the base of ditches, although this layer is not continuous thought the whole width. It indicates the direction from which it was transported. They are remains of intentionally redeposited ramparts. The upper parts are marked by increasing humification and bioturbation as a result of ditch infilling emergence. However, it is possible to trace similar formation processes in both groups of studied V-shaped ditches and to define a basic classification. Prevailing textural and structural features are distinctively different between the groups, due to geological subsoil conditions, hydrological regime and depth of the ditches.

* Corresponding author.
E-mail address: lisa@gli.cas.cz (L. Lisá).

http://dx.doi.org/10.1016/j.quaint.2014.11.049

1. Introduction

The way that archaeological objects were infilled is a frequent question, but usually also hard to answer if the infilling does not contain typical textural features. One of the useful methodological tools which might explain more about the formation processes is micromorphology (Goldberg et al., 1993; Barham and Macphail, 1995; Matthews et al., 1997; Courty, 2001). This approach can also answer various questions such as connections with the past climate or human impact on the landscape (Goldberg and Macphail, 2006; Macphail and Goldberg, 2010; Leopold et al., 2011; Milek, 2012). The graben-like ditch infillings are usually lithologicaly and texturally considerably variable, and have regular shapes and relatively specific archaeological context, which was the reason why this type of archaeological structure was chosen for this study dealing mainly with formation processes detected by micromorphology.

Graben-like ditches in the context of Central Europe alluvial landscapes represent a type of archaeological structure typical only for two cultural periods. The older one represents the Central European Neolithic period, especially its later phases (4900–4500 BC) represented by STK – Stroked pottery culture. The most typical monumental subsurface feature of this period is called a "rondel" in the Czech environment (Pavlů, 1982; Podborský, 1988, 1999; terms used in the literature include Kreisgrabenanlage, circular ditches, circular enclosures, and woodhenges). Those objects are typically situated on the edges of river valleys. A "classic" Late Neolithic rondel is typically considered as a complex of one or several, more or less round ditches with a characteristic sharp profile, and one or more circular concentric channels inside the space demarcated by the ditch with the smallest diameter (Fig. 1). Maximum diameter of such objects is 30–240 m, the width of ditches varies between 1.5 and 14 m, and their depth is usually between 1 and 4.5 m (Řídký et al., 2012). The sedimentary infillings of rondel ditches usually look similar (Fig. 2). The lower part is in most cases bedded, with the thickness of individual thin layers varying from mm to cm, while the upper part of the infilling is more or less homogenous (Zeman and Havlíček, 1988). Válek et al. (2013) and Lisá et al. (2013) suggested the main formation processes of the rondel infillings were mainly washouts for the lower part of the infillings and collapse induced by humans for the upper part of the infilling. The large volumes of material excavated from the ditch suggests the presence of earthwork near the ditch, which might be a source of the material for the infilling (Kovárník and Mangel, 2013; Lenneis, 1977; Modderman, 1983; Němejcová-Pavúková, 1986; Neugebauer, 1986; Oliva, 2004; Válek et al., 2013; Lisá et al., 2013), but there are also authors suggesting that earthworks were not present (Trnka, 1986; Podborský, 1988). Kovárník and Mangel (2013) and Vokolek (1963) described one of the rondel structures near Trebovětice with preserved earthworks located particularly on the outer side of the ditch. Earthwork ramparts' presence inside the rondel or outside the ditches, as well as processes in the origin of the ditch infillings, are still discussed (Lisá et al., 2013).

Fig. 2. Infilling of the rondel ditch with the micromorphology sampling positions; Těšetice-Kyjovice, Southern Moravia (Photo P. Lisý).

The second group of the archaeological features within the region of interest, where the V-shaped ditches are a typical phenomenon, represent camps of the Roman army. The V-shaped ditches, the so-called "Spitzgraben" (Fig. 3), are a symptomatic

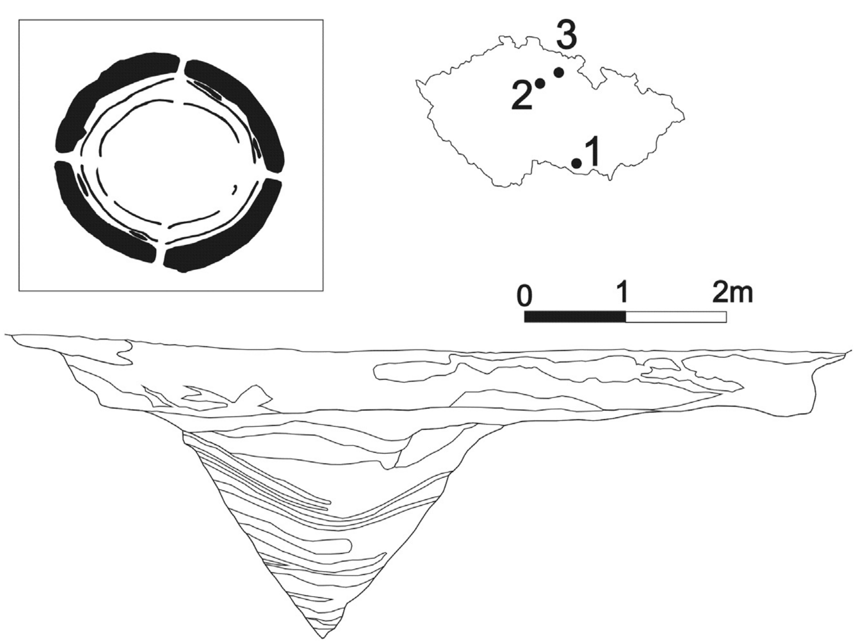

Fig. 1. Typical example of the rondel structure and its ditch infilling; Těšetice-Kyjovice, Southern Moravia.

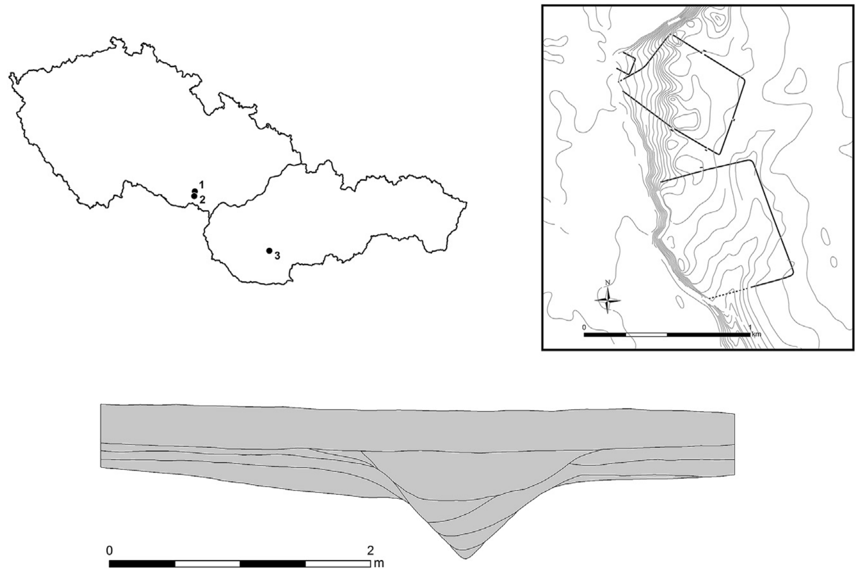

Fig. 3. Typical example of the Roman camp structure and its ditch infillings; Pasohlávky, Southern Moravia.

form of the Roman fortification architecture and are regularly documented in all the types of military installations of the whole Roman Empire (see Fischer, 2012, 253–259). The specificity of the objects in our scope dwells in the fact that they represent temporary military objects in enemy territory. Terminologically, such installations are called "camps", in contrast to the stable long-term types called "forts" and "fortlets", localized in the Roman environment (on terminology see e.g. Webster, 1985; Welfare and Swan, 1995; Jones, 2011, 2012). This fact has significant influence on the infilling development in each case, while it is obvious that the temporary camps, used only for weeks or months, do not contain evidence of further building activities within their stratigraphic units. The Roman temporary camps (incorrectly called "marching camps" in the past) are, beside numerous evidence from Britain (e. g. Welfare/Swan 1995; Jones, 2011, 2012), known also from regions inhabited by the Germanic tribes of Slovakia, Lower Austria, and Moravia. In these regions, they are generally considered to be evidence of the Roman military activities during the period of the Marcomannic wars between 172 and 180 AD and are characterized by the apparent absence of stable build-up areas and limited archaeological finds. On the subject of the Roman temporary camp structure, there also exists evidence in the ancient written sources, whereas the most comprehensively conceived is the work Gromatici Liber de Munitionibus Castrorum by Hyginus (for summary of sources see Jones, 2011, 5–12). This military handbook states clearly that a camp has to be established in vicinity of a river or water source and requires construction of defensive ditches and ramparts. Hyginus mentions two types of defensive ditches, including specified dimensions (Webster, 1985, 172). His basic description of so-called "fossa fastigata" and "fossa Punica" with asymmetrical ditch faces states also mentions small channels in the very bottom of ditches, which might have had served for drying purposes (compared to the mistaken assumption of moat-like use; Fischer, 2012, 255; Jones, 1975, 107; Welfare and Swan, 1995, 17). Material extracted during digging of ditches was used for construction of the core of the rampart (Jones, 1975, 32; Johnson, 1987, 7–10; Fischer, 2012, 253). Concerning the formation processes which probably took a place during the origin of the ditch infilling, Bálek and Šedo (1998) suggested various mechanisms (gradual deposition process or intentional filling; collapse or slip of rampart into ditch; etc.). More detailed observations acquired during the terrain research of the complex fortification system of the central military base located on the hilltop Burgstall at Mušov (Fig. 4), which clearly cannot be considered as a temporary camp (Komoróczy, 2008, 2009a), established that within the ditch infillings sedimentary units containing dried bricks regularly appear, which are reliably associated with the frontal parts of the rampart structure (e.g. Tejral, 2008; Komoróczy, 2008).

The main aim of this paper is to suggest the classification of the formation processes which took place during the formation of the ditch infillings, especially the infillings of graben-like ditches. The classification is based on macroscopic and micromorphologic observations.

2. Methods

The ditch infillings of six localities (three localities with Neolithic rondel ditches and three localities with ditches belonging to the Roman camps) were studied during the last three years on different occasions. The data interpreted in this paper come from different geological and hydrological backgrounds, and the original

Fig. 4. Infilling or the Roman camp ditch with the visible typical internal structure of the coarse grained layer documenting the destroyed body of rampart, Mušov (Photo P. Lisý).

micromorphological descriptions were already published mainly as reports or local papers. Archaeological excavations of the Těšetice-Kyjovice rondel were conducted by Masaryk University; the rondel structure in Kolín was excavated during the rescue excavations of the Institute of Archaeology of Academy of Sciences in Prague. The third Neolithic rondel structure situated in Plotiště n. L was excavated by the Philosophical Faculty of the University in Hradec Králové. Roman ditches situated in Vráble (Slovakia) and Přibice and Mušov-Neurissen (Southern Moravia) were excavated under the Institute of Archaeology of Academy of Sciences, Brno, Institute of Archaeology of Slovak Academy of Sciences Nitra, Austrian Institute of Archaeology Vienna and Römisch-Germanische Kommission DAI Frankfurt am Main.

Cleaned sections were in all cases sedimentologically described and documented. The classification of formation processes suggested in this paper is based on 85 samples which were taken at 6 localities with different geological and cultural backgrounds, from the infillings of graben ditches with different depths. Micromorphological samples usually have dimensions of 120 × 70 or 90 × 50 mm, except at Plotiště n. L. I. Five samples come from the ditch in Těšetice-Kyjovice, 52 samples come from four ditches of Kolín rondel, and 10 samples of the small format 3 × 4 cm come from Plotiště nad Labem I. The Roman ditches in Mušov were studied from two sections, and 5 samples were taken there. The locality of Přibice was studied from 8 samples taken from four ditches. At Vráble, two sections were studied, and 5 samples were taken.

The samples were taken in situ in Kubiena boxes, slowly dried and impregnated in the Laboratory of Geoarchaeology, Institute of Geology, Academy of Sciences in Prague. Thin sections of 120 × 70 mm were completed by Julie Boreham in Reach (www.earthslides.com) and then studied under a binocular and polarising microscope (PPL, XPL and OIL) at magnifications in the range of 1–400*x*. Micromorphological description and interpretations followed mainly Bullock et al. (1985), Stoops (2003), and Stoops et al. (2010).

3. Site description

3.1. Archaeology and general sedimentological context of rondel sites Těšetice, Kolín and Plotiště

All the rondel sites are located in relatively close vicinity of the river network in elevated areas, with good views to the river. The Těšetice-Kyjovice Neolithic rondel (Fig. 2) is located on the south-easterly oriented slope in the area of Sutny I, southwest Moravia (Fig. 1). Sutny I was the most important part of local settlement activities dated to the older stage of Moravian painted ware culture (phase Ia). The rondel itself is composed of one concentric ditch with a diameter of 60 m (Podborský, 1988). The geological background is composed of loess with a Bt interstadial soil horizon at a depth of 3 m. Válek et al. (2013) recently made the revision of the ditch infilling and defined two main horizons developed under different formation processes. The lower part of the infilling shows macroscopic bedding, composed of a set of layers which are more or less continuous. The thickness of those layers varies from mm to tens of centimetres. The upper part of the infilling is composed of a homogenous dark brown matrix with no visible textural features pointing to the possible formation processes. The detailed macroscopical and micromorphological description was published in Lisá et al. (2013).

The largest rondel in the Czech Republic (Šumberová, 2012) was found during construction works in the western part of Kolín city (Fig. 1). The rondel itself is made of four concentric ditches, the outer one with a diameter of 210 m, and the inner one with a diameter of 140 m (Šumberová, 2012). On the basis of the archaeological material from its infilling, the rondel is dated to the Late Neolithic (the later phase of Stroke-Ornamented Pottery culture). The geological background of this area is composed of loess. Macroscopically, the infilling of the ditch is quite similar to the infilling of Těšetice-Kyjovice rondel ditch, i.e. the lower part shows significant lamination with the thickness of the lighter and darker horizons varying form mm to tens of cm, while the upper part of infilling is quite homogenous. The micromorphological observations were done in all studied ditches and a detailed micromorphological description documenting the main features is partly published in Lisá et al. (2013).

Two-thirds of the rondel structure in Plotiště is located within the village urban area near Hradec Králové, on the right terrace of the Elbe River, approximately 5–7 m above the inundation line. The rondel structure is composed of three circular ditches, with the diameter of the outer one of 117 m. The depth of the inner ditch is 240 cm. The rondel structure was dated to the Stroked Pottery Culture (Kovárník, 2012, 2014, in press; Kovárník and Mangel, 2013). The geological background in which the ditches were dug in is composed of alluvial deposits, but the lowermost part of the ditch touched in every case the fluvial deposits located below the alluvium. The sedimentary structure of Plotiště nad Labem I. rondel does not differ significantly from those documented in Těšetice Kyjovice and Kolín. There is a significant presence of bedded more or less continuous horizons of thickness varying in mm and tens of cm in the lower two-thirds of the rondel. The geological background of the locality shows thin lamination due to grain size differentiations resulting from the alluvial process. Two thirds of the infilling contained an erosion layer containing quartz pebbles, with the original provenance in terrace sediments documented below the ditch. These sediments were excavated during the last phase of the ditch construction and deposited on the rampart. The fact that these were observed in the upper part of the recent infilling shows that the rampart was destroyed a long time after the rondel abandonment, probably during the phase of the landscape use for agricultural purposes. The layer of pebble rich aggregate seems to be redeposited from the other side of the ditch (Kovárník, 2013).

3.2. Archaeology and general sedimentological context of Roman fortification ditches Vráble, Přibice and Mušov Burgstahl

All the studied sites are located in vicinity of the river networks in strategic positions in the landscape. Compared with the rondel ditches, those related to the Roman camps are much more shallow and narrower (except the Vráble site), and the internal structure is different. A comprehensive archaeological component complex is situated near Vráble (location Veľké Lehemby) in the northern part of the Danubian Upland (Hrnčiarová et al., 2002) on the left bank terrace of the river Žitava (Fig. 3). The first evidence of the Roman temporary camps was provided by extensive geophysical prospections in 2009 and 2010. Since 2012, the camps have been investigated in terrain within the framework of inter-institutional project cooperation of the Institute of Archaeology of SAS Nitra and Römisch-Germanische Kommission DAI Frankfurt am Main (Hüssen et al. in press). The larger of two camps has known dimensions of 740 by 400 m and the total extent is estimated as roughly 30 ha. In the longer eastern side of the camp fortification, two titulum type gates have been identified. The smaller camp, located on the edge of terrace of the river Žitava, was fortified by a double line of ditches. Its known dimensions are 400 by 255 m, enclosing an estimated area of more than 10 ha. The geological background consists of loess. The micromorphology samples were acquired from small-scale trench excavation in the eastern fortification line, to the north of the northern gate. The terrain situation revealed superposition of two Roman V-shaped ditches with specific soil structures in their infillings. The infilling of the main ditch differs from the infillings of Neolithic rondels, in spite of the fact that the depth and the geological background are comparable. The continuous thin layers we know from Neolithic rondels are missing.

The three temporary camps of the Roman army discovered in Přibice in South Moravia (Fig. 3) count amongst those initially discovered at the beginning of the 1990s, and belong to the best known military installations of this type in Moravia (Bálek et al., 1994; Bálek and Šedo, 1998; Tejral, 1999; Komoróczy, 2009a, 2009b; Komoróczy and Vlach, 2010). The camps are located roughly 8 km to the north of the central fortification of Burgstall at Mušov, on the left bank of the river Jihlava. Two spacious camps designated as Přibice I (~28 ha) and III (~40 ha) are supplemented by the small camp Přibice II (~1 ha), located below the terrace at the edge of alluvial landscape. Camp I also is present within this area. Fortification ditches have been investigated through the limited trench excavations since their discovery (Bálek et al., 1994), although more detailed analyses of fortification ditch infillings have not been conducted. On the basis of the inter-institutional cooperation, selective geophysical prospection of the camps I and II and consequent small-scale trench excavations were accomplished in 2012 and 2013. An excavated area of the eastern gate of the camp I provided suitable conditions for micromorphological sampling. Further excavations aimed to more precisely document the camp II fortification, inaccessible for geophysical prospection. The geological conditions in the excavated gate area consist of fine pebbles of the Jihlava River terrace.

The third ditch is located in the central part of SE slopes of the hilltop Burgstall in South Moravia (Figs. 3 and 4). This ditch was examined within inter-institutional cooperation in 2013. According to its location and archaeological contexts it seems that the structure belongs to an unknown course of the fortification system of the central military base (e.g. Komoróczy, 2006, 2008, 2009a,b). Dating into the frame of the Marcomanniac wars is corroborated also by archaeological finds from particular sections of the infillings. Subsoil of the excavated terrain consisted of fine Cenozoic sandy–clay sediments of the Carpathian Foredeep altering with strata of river

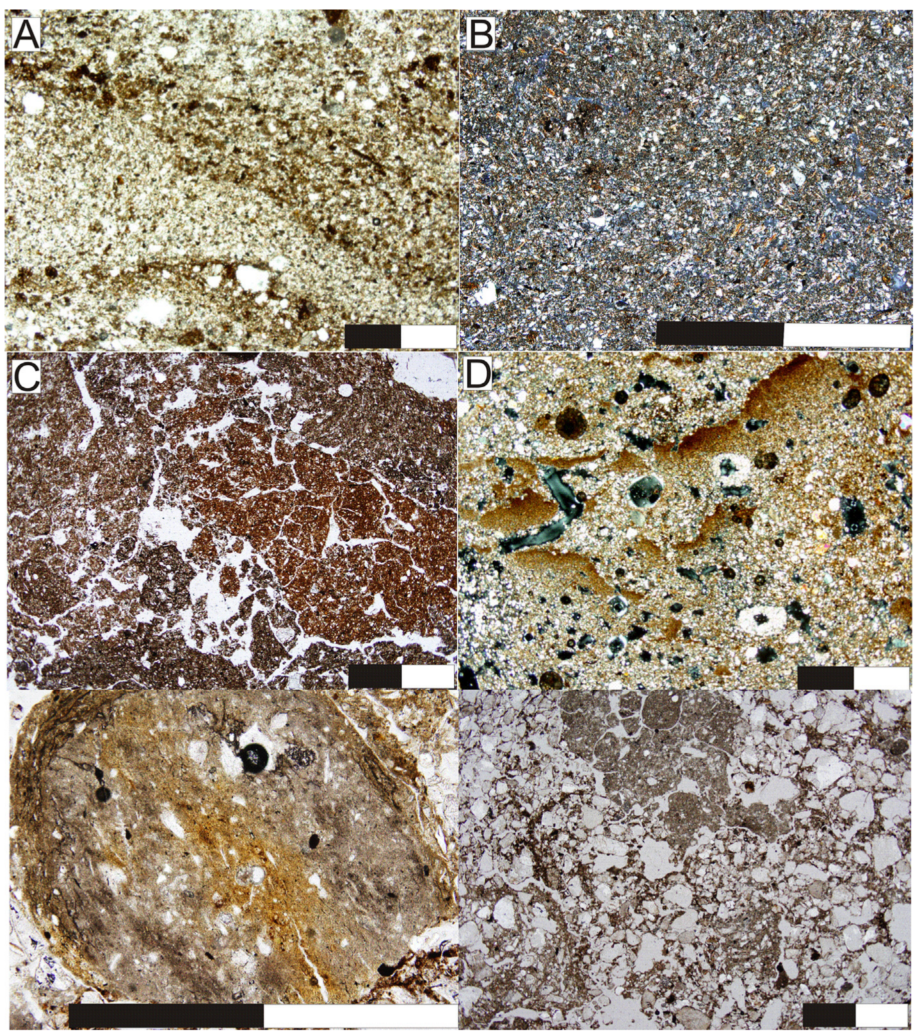

Fig. 5. Micromorphological documentation of natural processes and processes caused by humans observed within infillings of Neolithic ditches and Roman camp ditches; A – layers of material composed of subrounded quartz silt alternating with the layers composed of humus rich aggregates documenting natural colluvial processes, Kolín rondel, ditch 3A, lower part (PPL); B – matrix composed of silty material as well as humic aggregates. The quartz grains show weak orientation along the slope which is result of slow natural colluviation, Těšetice-Kyjovice rondel, central part (XPL); C – rip up clasts composed of clayey aggregates of interglacial soil documenting high energy natural colluviation, Těšetice-Kyjovice rondel, lower part (PPL); D – soil crusts with positive gradation as a result of naturally caused phases of standing water, Kolín rondel, ditch 1, central part (XPL); E – material of human-made mudbrick which were used to consolidate the rampart, Roman camp in Mušov (PPL); F – mechanically deformed material of calcareous claystones, Roman camp in Mušov, (PPL). The length of the scale is 2 mm.

cobblestones and pebbles. Besides numerous archaeological finds, dried bricks (mudbricks) are present in the frontal face of the above-ground part of the fortification. Certain positions of the ditch infillings showed evidence of activity of the local Germanic population after the Roman withdrawal from the region.

4. Macroscopic and micromorphological observations

4.1. Sedimentological and micromorphological features of rondel infillings

Rondel infillings show similar trends in the lithological variability. The uppermost part is usually homogenous and shows signs of pedogenesis. This part of infilling was deposited intentionally (mass movement) and the main reason was probably the levelling of the surface for agriculture. There is a typical lack of primary sedimentary structures occurring during the mass movement and the matrix looks quite homogenous except for bioturbation (Fig. 5A) or postsedimentary textural features, including depletion zones (Fig. 6F), calcium carbonate accumulations (Fig. 6B), or the origin of redoximorphic features (Fig. 6D).

The lower and central parts of the Neolithic rondel infillings are commonly composed not only of thin layers, but also of intercalated massive deposits. These horizons show that the most significant process which took place in formation of the infillings of rondel ditches is the natural deposition under the slope. Features related to the slope processes are visible not only micromorphologically but also macroscopically as thin layers approximately 1–5 cm thick or layers with oriented clasts (Fig. 5A,B). Deposition reflecting high to average energy of sheet wash was documented in the Kolín site by the presence of rip-up clasts (Fig. 5C). The colour and lithological (mainly grain size) difference between single layers detected in lower part of the ditch infilling (Fig. 5A) depends on the type of material deposited into the ditch. Dark layers are composed of redeposited A horizon, partly stabilised by vegetation or bioturbated in situ (Fig. 6A). The stabilisation is documented not only by the presence of bioturbation, but also by the appearance of calcified root cells, carbonate coating, and hypocoating (Fig. 6B). During relatively quick deposition, due to the disruption of the surface of source area, loess material from the walls was partly eroded, and therefore the roundness of soil clasts is due to gravitational movement. On the other hand, the light material detected

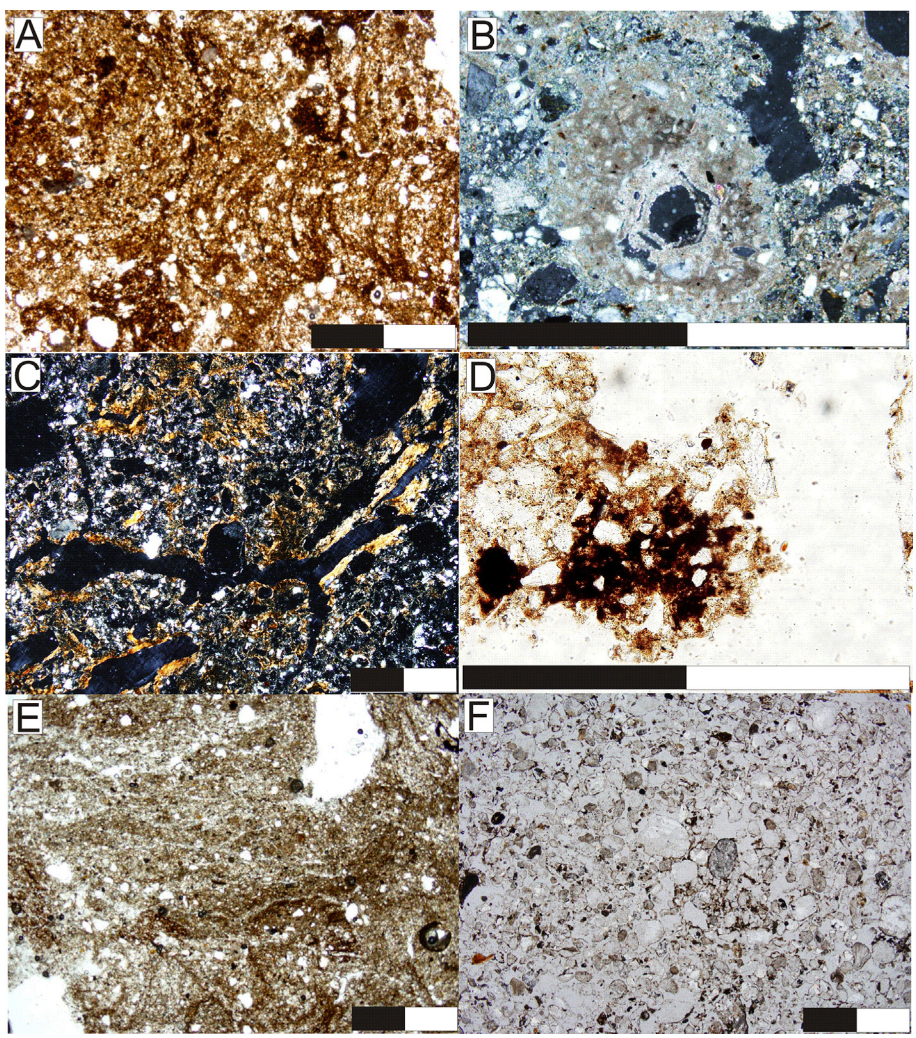

Fig. 6. Micromorphological documentation of postdepositional processes observed within infillings of Neolithic ditches and Roman camp ditches; A – bioturbated matrix by mesofauna, Kolín rondel, ditch 3A, upper part (PPL); B – calcium carbonate coating and hypocoating of void, ditch of Vráble Roman camp, central part (PPL); C – channels with iluviated clay coating, Plotiště rondel, lower part (XPL); D – ferroximorphic nodule documenting redoximorphic conditions of the upper part of Těšetice-Kyjovice rondel infilling (PPL); E – platy microstructure documented within the central part of Kolín rondel, ditch 3A, central part (PPL); F – Depleated part of matrix documented in the infilling of Mušov Roman camp (PPL). The length of the scale is 2 mm.

within this part of the infilling represents the product of degradation of loess or alluvium walls or earthwork near the ditch due to rainsplash, lately influenced by seasonal frost action and producing platy to lenticular microstructure (Fig. 6E). An interesting feature observed in the Kolín site documenting the mechanical destruction of once deposited material under calm humid conditions are soil crusts (Fig. 5D), which are in some cases deposited with negative grading. This feature may suggest previous cleaning of the ditch infilling and the presence of the rampart situated close to the ditch as a source of material. The most significant formation process detected micromorphologically in the Plotiště site and nearly missing in the other studied cases was the postdepositional redeposition of clay material and formation of clay coatings and infillings (Fig. 6C). The source of clay in this case comes from the background alluvial sediments. Moderately sorted silt contains a number of channels and vesicles, and the clay coatings in the inner part composes a porostriated B fabric (Fig. 6C). The intensity of the clay coating does not vary with the depth of the section and was probably formed shortly after the deposition of the infilling.

The very bottom of the rondel ditch infilling is usually composed of bedded colluvium and composed of individual layers predominantly 1–2 mm thick and quite homogenous in composition. Their colour depends on the amount of fine-grained organic matter (humus). In Těšetice, this part of the infilling contained subrounded clasts of the redeposited B horizon of the Eemian luvisol as rip-up clasts (Karkanas and Goldberg, 2013) (Fig. 5C). The B horizon of Eemian Interstadial paleosol is well developed in the background geology of the ditch and was excavated in the final part of the ditch construction. This material was probably translocated to the upper part of the rampart, and therefore was the first to be redeposited to the infilling of the ditch by high energy rainsplash.

4.2. Sedimentological and micromorphological features of Roman fortification ditch infillings

The infillings of Roman fortification ditches do not contain the thin layers and bedding typical for rondel infillings. The layers recognizable macroscopically within the infilling are not usually continuous, and the shape suggests that those layers were deposited in different stages from both sides of the ditch. It is usually possible to recognize 3–4 lithologically different layers which differ by grain size and colour. Usually the bottom of the ditch is more fine grained and homogenous, followed by the unsorted, coarse grained thick layer. This layer has signs of rapid mass movement and may suggest the erosion of a rampart hardened by coarse grained material. The direction of erosion is from the inner to outer part of the camp. The outer part of the ditch is commonly filled by more fine grained material eroded from the walls of the ditch. The uppermost part of the infilling is composed by darker bioturbated arable soil.

No primary structures showing sheet wash deposition were documented, and the macroscopical shape of the layers suggests that the main formation process was rapid mass movement induced by human activity. The typical parts of the observed sediments are aggregates of humus rich particles with subrounded quartz grains. The humification process was minimal before deposition. The most common micromorphological feature is bioturbation. This is probably indicated by the fact that the infillings are quite shallow and the groundwater level is usually quite high. Surprisingly, this feature is usually missing or rare in the lower parts of the infilling, which suggests that the infilling was rapid. Another postsedimentary feature which was observed in all samples of one ditch in Přibice is clay mineral illuviation (Generally Fig. 6C). Clay accumulations are stipple-speckled. The infilling of one ditch located in Mušov – Burgstall in the upper part of the same slope has quite different parameters from the other studied sites, because the geological background is in this case composed of calcareous clays of the Carpathian Foredeep. The lower part of the infilling is composed of rip-up clasts (Fig. 5F) of different shapes and sizes. This material had to be eroded from the excavated original background of the ditch and then was probably deposited into the ditch by mass movement. Some clasts contain partly decomposed organic matter and show signs of mechanical arrangement (Fig. 5E). Such features might be interpreted as a relic of dried mud bricks. In every case, the bioturbation is quite rare, so the formation process of those layers was probably quite quick and might be interpreted as mass movement. The uppermost part of the infilling is rich in bioturbation (Fig. 5A) and also contain signs of human impact in the form of partly burned matrix and charcoal. The lack of primary sedimentary features, relatively good sorting of the sediment, and high degree of bioturbation might suggest slow deposition by sheet wash followed by pedogenetic processes.

The Vráble site differs from the other studied sites because of the different geological background and its depth. Some of the macro and micro parameters of observed layers are at first glance more similar to rondel infillings, but the internal structure of the infilling as a whole is very similar to the other fortification ditches in this study. The most typical feature of the Vráble site is bioturbation, represented by change of fabric or by the presence of channels. The channels were sometime infilled by very porous microaggregates of excrement. Besides bioturbation, the second most significant postsedimentary features are impregnations (Fig. 6B,D) and depletions (Fig. 6F) which originated due to the changes in the water regime, soil humidity, and the presence of plants. Also, temperature which is along with humidity one of the main factor influencing vegetation cover, had to play a role. Water saturated sediment rich in carbonate is quite susceptible to changes of internal structure. The origin of vughy microstructure is probably caused by the escaping air from the pores (Stoops et al., 2010), which was partly replaced by carbonate rich solutions. These solutions are reflected by strong hypocoatings (Fig. 6B). The presence of water in the sediment is also reflected by the origin of different types of Fe rich nodules (Fig. 6D) (Stoops et al., 2010). Micromorphological observation confirmed that the darker layers are composed of subrounded and rounded clasts of humus rich matrix. These clasts were described as rip-up clasts (Fig. 5C) in the sense of Karkanas and Goldberg (2013), the result of high energy deposition. The humus rich aggregates might have come from turf hardening of some kind of rampart, which is generally suggested for the structure of Roman ditches. On the other hand, the humus rich matrix might have originated in humid conditions with rich vegetation quite quickly, so the possibility that these rip-up clasts were derived from newly originated soil cover near the ditch cannot be ruled out. Important information was also derived from the passage features which occurred in some samples. Passage features documented in the infilling originated by macro or mesofauna of the omnivore or carnivore type, because phosphatic nodules were observed within the infilling of passages. Also, fragments of humus rich matrix of the A soil horizon and B horizon of luvisol were detected. These clasts are probably the relicts of former soil cover and may be compared with classical krotovinas.

5. Interpretation and discussion

On one hand, it was possible to identify substantial differences between Neolithic rondel ditch infillings and infillings of ditches surrounding the Roman camps. On the other hand, there are still some similarities in the formation processes of infillings which might be classified visually and in detail by micromorphological observations. Natural or anthropogenic processes which took place during the filling history of archaeological objects, especially rondels, have not been categorised and systematically classified in spite of the fact that there are papers discussing the formation processes in archaeological contexts (Goldberg et al., 1993; Goldberg and Macphail, 2006; Macphail and Goldberg, 2010; Leopold et al., 2011; Milek, 2012). Loishandl-Weisz and Peticzka (2011) noted the processes which might have taken place during the infilling formation of Neolithic rondels in Steinabrunn. Karkanas and Goldberg (2013) have tried to summarize the microscopic features produced by major natural depositional processes acting within a cave environment. These processes are associated mainly with changes in the geomorphic system, climate and the presence of humans, so the classification of both cave and archaeological objects might be very similar. According to Davidson et al. (1992), three main categories of features visible within archaeological objects can be discerned: those related to the source of the sediment, those revealing something about the soil formation processes, and those produced or modified by humans, either deliberately or accidentally. Analyses of soils and sediments can also provide data on long-term processes of deposition and erosion (Renfrew and Bahn, 2000). We propose that the formation processes which took the place in the graben-like ditches might be interpreted as a result of natural deposition, deposition forced by humans, and by the processes which took the place after the primary deposition and might be forced naturally or by humans.

5.1. Natural deposition

The most common type of natural deposits identified macroscopically as well as micromorphologically within the studied infillings are slope deposits. Processes were identified in all studied objects according to the shape and context of sedimentary bodies. Surprisingly, signs of primary sedimentary processes were identified only in the case of Neolithic rondel infillings. Mücher et al. (2010) divided the slope deposits into two main types. The first one cover slope wash, hill wash or rain wash including soil erosion on agricultural land, which seem to be the most typical processes for the lower parts of Neolithic rondels and probably also for the upper parts of Roman ditches. The second type of slope deposition pointed out by Mücher et al. (2010) results in mass deposits. This type includes solifluction, landslides, and debris flow deposits as well as rock fall, dry grain flow, and avalanching. The natural landslides were documented in lower and central parts of Neolithic rondel ditches, while mass movement caused probably by humans was interpreted commonly for the lower part of the Roman ditch infillings. Processes of the slope wash type resulted in Neolithic rondel ditch infillings. Mücher (1974) described the origin of bedded colluvium developed in loess material. Similar sedimentary features were described also by Bertran and Texier (1999) and interpreted as overland flow. As the loess material composes the background of the studied rondel, features of this type are a characteristic result of natural deposition and correspond to the described phenomenon. Surprisingly, these features have not been observed in the Vráble Roman ditch infilling, which is also excavated in loess material. This fact is probably connected with the method of infilling. While the role of humans in case of Neolithic rondel ditch infillings is minimal and the source of loess material might be derived from eroded walls of the ditch as well as from the nearby rampart (if presented), in the Roman ditch infillings the lower part of the ditch was filled by the destroyed rampart deposited intentionally. The possible source of material was therefore minimalized. The bedded colluvium detected in the lowermost parts of the Neolithic rondel ditch infillings might be, according to the field observations (Mücher, 1974), related to the formation during heavy rainstorms when rill erosion occurred on fallow arable land, or on arable land partly covered by crops, which fail to protect the soil from rain splash impact. In deep ditches with steep slopes, the walls composed of easily erodible loess with removed vegetation might be the source of such material (Weicz and Peticzka, 2011; Lisá et al., 2013).

The origin of massive deposits which appear in lower and central parts of the Neolithic rondel might be, according to Bertran et al. (1997), interpreted as overland flow deposits resulting in lenses with lamination or bedding and evidence of sorting. Those deposits originated due to vertical or lateral accretion by rapid or dilute flows (Bertran and Texier, 1999). Karkansas and Golberg (2013) also divided types of slow deposits depending on the amount of energy within cave environments. Lower-energy flows produce less sorted and more crudely bedded microstructures which correspond to the more massive yellow layers of the studied rondel ditch infillings. Sometimes, are layers of rondel ditch infillings composed of rounded aggregates with different degrees of sorting. Mücher et al. (1981) interpreted the appearance of rounded aggregates as a result of disruption caused by running water over subsoil horizons, mostly Bt horizons, which are rather stable during transportation by water. Karkanas and Goldberg (2013) described this type of deposit as a common phenomenon in cave environments. Angular to subangular clay clast layers alternating with finely bedded clays have been accordingly interpreted as the results of episodic high-flow events. Such features were observed within the studied sections only rarely, probably also due to the lack of clayey material typical for rip-up clasts. According to Karkanas and Goldberg (2010), the lower energy process results in microscopically stratified deposits with angular clasts characterised by inclined preferred orientation to the slope are interpreted as flow of liquefied sediments (debris flow). These features were observed commonly in the lowermost part of Těšetice-Kyjovice rondel ditch infilling and within the infillings of some Roman ditches at Mušov.

Massive yellow or dark layers without internal bedding might have also originated from slumping, which is a typical result of mass deposition. According to Karkanas and Goldberg (2013), the slump deposits have a sharp erosional contact with the underlying substrate, and some of the aggregates have a more concave configuration toward the direction of flow. These sediments are in the case of Neolithic rondel ditch infillings as well as in the case of infillings of Roman ditches easily interpretable from a macroscopic point of view, as they form tongue like accumulations. In the Neolithic rondel ditch infillings, these accumulations are usually less thick and more bioturbated than in the Roman ditches. Leopold et al. (2011) call these back-fill sediments.

Another sedimentary process detected only in the infilling of Neolithic rondel ditches are phases of standing water resulting in soil crusts. These graded facies are usually between 0.3 and 4 mm thick, and they are commonly disrupted, which might be caused by bioturbation or drying and swelling processes after sedimentation. This might be a good indicator of repeated redeposition of the ditch infilling (Lisá et al., 2013). These graded facies consisting of repetitive fining upward sequences of sand, silt, and clay usually less than a few millimetres in thickness might be the result of storm events bringing enough water to form temporary small bodies (pools) inside the ditch.

5.2. Deposition caused by humans

The deposition caused by humans can be divided according to two different views. The first one is the explanation of appearance of material which was influenced by humans, i.e. the appearance of charred material as charcoal or daub, by appearance of lithics, or by the appearance of fine grained material obviously mechanically influenced by humans. Identification of these features was well described in many papers (Stoops et al., 2010). Surprisingly, the amount of artefacts or ecofacts is, in the case of Neolithic rondel ditch infillings, distinctively low except in the uppermost parts of infillings. The prevailing anthropogenic material consists of fine grained charcoal. On the other hand, the infillings of Roman ditches revealed influence of humans, identified not only as charcoal, but also abode bricks in case of Mušov. These bricks are in some cases well preserved and visible also macroscopically (Komoróczy, 2008; Tejral, 2008), but in most cases are quite degraded, but still visible in thin sections (Friesem et al., 2011, 2014). A thin section is a thin film of the sediment and therefor might catch only the most common features (Stoops, 2003).

Human influence seems more important in the way the objects were filled in. A typical feature of the lower part of the infillings of Roman ditches is the result of mass movement which is macroscopically visible as coarse grained lenses with tongue like sharp edges. The bodies of this material were not influenced by bioturbation which indicates that they were deposited quickly, covered by another material and the vegetation did not have time to influence them by rooting. This might be explained by the archaeological context. In the Neolithic ditch infillings, mass deposition forced by humans is suggested for the uppermost part of the infilling where the bioturbation is still present. One have to take into account that the material deposited into the ditch was influenced for a long time by vegetation and therefore is rich in organic matter, which was the subject of bioturbation even in deeper parts of the horizon.

5.3. Postdepositional processes

The most typical postdepositional process identified was bioturbation. Macroscopic burrows were rare and occurred mainly in the uppermost part of the infillings. Mesofauna burrows and root bioturbation were more commonly observed. Mesofauna burrows are usually filled with softer material than the surrounding matrix and have loose, heterogeneous and aggregated fabric (Goldberg and Bar-Yosef, 1998). In the case of the studied rondels, the bioturbation is present continually all over the section, but some layers have distinctly higher bioturbation intensity. Such layers are usually also rich in fine-grained organic matter. All microorganisms feed in essence on soil organic matter (Brussaard and Juma, 1996), so their increased activity is quite obvious there. The presence of active soil fauna population is often into relationship with the formation of soil horizons (Davidson et al., 2002). Whole soil horizons can be bioturbated or completely transformed into fine grained particles (Kooistra et al., 1990; Schaefer, 2001). The process of rondel ditch infilling formation as a whole was quite slow, so the bioturbation by plants and mesofauna was more or less continuous. In contrast, the bioturbation of the Roman ditches was usually mainly restricted to the more fine grained material located above the lenses of coarser material relocated by mass deposition.

Another process connected commonly with root bioturbation and with relocation of calcium rich solutions is calcium carbonate accumulations and depletions. The types and identification of different type of calcitic features were described by Durand et al. (2010). Such features are most common in cases where the background substrate is composed of loess, i.e. in Kolín and Těšetice rondels and Vráble Roman ditch, as the presence of carbonate coatings, hypocoatings, infillings, and accumulations is quite common in loess material, because calcium carbonate is easily moved by percolating water in connection with growing vegetation. The root related features are the most common features in case of Neolithic rondel ditches located in loess substrate, while the carbonate infillings are the most common features in Roman ditches located on carbonate claystones. The state of calcium concentrations depends therefore not only on the formation processes, but mainly on the type of geological background and the hydrological conditions connected with the location and the depth of the ditch. Another soluble material which occurs within the studied horizons is clay. Illuvial clay coating, hypocoating, and infillings were reported mainly in the Plotiště rondel and also in the two Roman ditches from Přibice. Pressure facies or neoformation of clay has not been identified, and clays come from the background geology and were deposited by percolating water (Kühn et al., 2010). Their appearance depends mainly on the presence of possible source of clay fractions because the neoformation of clay was not observed, and on hydrological conditions, because the clay matrix is supposed to be deposited by percolating water (Kühn et al., 2010). The third pedofeature connected with water solutions is the presence of redoximorphic features. The recognition of different types of redoximorphic features and their interpretation was described in many papers and recently summarised by Lindbo et al. (2010). These features were detected only in Roman ditches and the reason is probably the proximity to water, i.e. high level of underground water.

One postsedimentary or nearly synsedimentary processes detected in Neolithic rondel ditch infillings is the development of horizontal pores. These features are quite rare, but were presented in brighter as well as in darker horizons and might be probably interpreted as phases of freezing (Van Vliert-Lanoë, 2010), which does not have to be necessarily connected with climate change. The explanation of its possible origin is quite simple. Uncovered soil is more accessible to frost action and such features might originate during one or two seasons.

5.4. Interpretation of archaeological context

The fundamental questions of the formation processes are usually connected with the presence of source of material. On one hand, the relatively high amount of material excavated during the ditch construction might be a possible source of material. The deposition of excavated material from the ditch in the form of some kind of earthwork or rampart is on the other hand an important geomorphological feature for the interpretation of the archaeological context. While the ramparts along the Roman ditches are already corroborated by written sources (Webster, 1985), for the Neolithic rondels the presence of ramparts is only suggested on the base of type of sedimentary infillings or on the base of aerial archaeology (Kovárník and Mangel, 2013; Lenneis, 1977; Modderman, 1983; Němejcová-Pavúková, 1986; Neugebauer, 1986; Oliva, 2004; Válek et al., 2013; Lisá et al., 2013). The presence of a possible rampart close to the Neolithic ditches was also in some cases rejected (Trnka, 1986; Podborský, 1988). The presence of human influenced materials (stones, sands, and mudbricks) implies that the rampart was present in all archaeological structures discussed in this paper. If the earthworks were not present, then the question is where the lithologically varied material transported into the ditch came from. A part of it might have been eroded from the walls of the ditch and from the surrounding area, but the absence of a wide source area for soil material suggests the presence of earthwork which would produce such material. Approximately the lower two-thirds of the infillings of Neolithic rondels origin naturally mainly by slope processes with different intensity, as visible from the textural features and micromorphological descriptions. The upper parts of Neolithic rondel infillings are quite homogenous and considerably bioturbated due to the high amount of humus rich matrix, so the tracking of the original formation processes is quite difficult. We suggest that the material came from the surrounding surface and the deposition took place as a part of landscape levelling for agricultural purposes.

In the Roman ditches the presence of rampart is not discussed, because the building of this structure is well documented in historical sources (Webster, 1985) and also archaeologically confirmed

(Komoróczy, 2008; Tejral, 2008). In spite of this fact, the formation processes detected within the infilling of Roman ditches differ. The bottom of the ditch is composed in most cases by a homogenous mass with no internal clast orientation. Leopold et al. (2011) described similar deposits as backfill deposits, but in this case due to the geomorphological and archaeological context it is obvious that these sedimentary bodies were deposited intentionally by humans. Moreover, in some cases those sedimentary bodies contain material which probably hardened the outer layers of the rampart. Although the upper part of the infilling does not display any preferred clast orientation, we suggest that it was deposited naturally, and the possible layering was destroyed by bioturbation. The question is whether the destruction of the rampart was intentionally done by Roman Army when withdrawing, or by the local German population after the camps were abandoned.

6. Conclusions

The results led to the following interpretations:

1. The infillings of Neolithic rondels consist of two main types. The bedded part of the body composed approximately two-thirds of the lower infilling, whereas generally massive material composed the uppermost part of the infilling. There are macroscopically and micromorphologically visible differences in these two main types of sedimentary bodies. While the massive infill within the uppermost part of the infilling was deposited by human activities, the lower bedded part is mainly the result of natural processes and geomorphological and climatic conditions. The main formation process was colluvial deposition of different intensity, but the low energy formation processes including deposition from standing water took place. It was also possible to detect strong postsedimentary processes including bioturbation, clay illuviation, calcium carbonate concentrations, or freezing processes.
2. The infillings of Roman ditches differ significantly from the Neolithic rondel ditches, although the depth and geological background may be the same. There are thick lenses with sharp edges and tongue-like shapes at the very bottom of the ditch. Their bodies do not contain bioturbation features and also may contain relicts of mudbricks. The material is frequently bioturbated and was deposited naturally. The main formation factor is colluviation. In the Roman ditch infillings phases of standing water or freezing processes have not been detected, indicating, that the infilling process was much quicker than for the Neolithic rondels. Besides bioturbation, the post-sedimentary processes include also clay illuviation, formation of calcium carbonate features, and redoximorphic features. The latter is connected with the geomorphological position, the depth of the ditch, and the presence of underground water.
3. The rampart located near the ditch was the source of material in both types of studied structures. In the Neolithic rondels, the lower parts of the infillings were deposited naturally, and the rampart served as a source of material for a long time. In the Roman ditches, the body of the rampart was destroyd and deposited into the ditches quickly by humans.

Acknowledgements

The contribution was funded by Masaryk University (MUNI/21/VAL/2011), by Grant Agency of Czech Republic (project no. P405/11/1590 – Neolithic rondels from the perspective of micromorphology and formative analysis), by the internal program of Institute of Geology ASCR in Prague RVO 67985831 by the project of the Faculty of Arts of the University Hradec Králové 2013/03/11: The triple rondel of the people with the Stroked Pottery Culture Plotiště nad Labem II. Contribution to the knowledge of construction and function of rondels in the Late Neolithic I and by the Project Platform for landscape formation Reg. No. CZ.1.07/2.4.00/31.0032.). The paper also originated within the frame of the project of the Institute of Archaeology of the Academy of Sciences, Brno and the Austrian Institute of Archaeology, Vienna, no. M300011201. The results of scientific and terrain researches published here are also based on the framework cooperation of the Institute of Archaeology AS CZ Brno, Institute of Archaeology SAS Nitra and Römisch-Germanische Kommission DAI Frankfurt am Main.

References

Bálek, M., Šedo, O., 1998. Příspěvek k poznání krátkodobých táborů římské armády na Moravě. Památky archeologické 89, 159–184.
Bálek, M., Drobertjar, E., Šedo, O., 1994. Die römischen Feldlager in Mähren (1991–1992). Památky archeologické 85, 59–74.
Barham, A.J., Macphail, R.I. (Eds.), 1995. Archaeological Sediments and Soils: Analysis, Interpretation and Management. Institute of Archaeology, London.
Bertran, P., Texier, J.-P., 1999. Facies and microfacies of slope deposits. Catena 35, 99–121.
Bertran, P., Hétu, B., Texier, J.P., van Steijn, H., 1997. Fabric characteristic of subaerial slope deposits. Sedimentology 44, 1–16.
Brussaard, L., Juma, N.G., 1996. Organisms and humus in soils. In: Piccolo, A. (Ed.), Humic Substances in Terrestrial Ecosysrtems. Elseiver, Amsterdam, pp. 329–359.
Bullock, P., Fedoroff, N., Jongerius, A., Stoops, G., Tursina, T., 1985. Handbook for Soil Thin Section Description. Waine Research Publications, Wolverhamton, UK.
Courty, M.A., 2001. Microfacies analysis assisting archaeological stratigraphy. In: Goldberg, P., Holliday, V.T., Ferring, C.R. (Eds.), Earth Sciences and Archaeology. Kluwer, New York, pp. 205–239.
Davidson, D.A., Carter, S.P., Quine, T.A., 1992. An evaluation of micromorphology as an aid to archaeological interpretation. Geoarchaeology 7/1, 55–65.
Davidson, D.A., Bruneau, P.M.C., Grieve, I.C., Young, I.M., 2002. Impacts of fauna on an upland grassland soil as determined by micromorphological analysis. Applied Soil Ecology 20, 133–143.
Durand, N., Monger, H.C., Canti, M.G., 2010. Calcium carbonate features. In: Stoops, G., Marcelino, V., Mees, F. (Eds.), Interpretation of Micromorphological Fatures of Soils and Regoliths. Elseiver, Amsterodam, pp. 149–194.
Fischer, T., 2012. Die Armee der Caesaren (Regensburg).
Friesem, D., Boaretto, E., Eliyahu-Behar, A., Shahack-Gross, R., 2011. Degradation of mud brick houses in an arid environment: a geoarchaeological model. Journal of Archaeological Science 38, 1135–1147.
Friesem, D.E., Karkanas, P., Tsartsidou, G., Shahack-Gross, R., 2014. Sedimentary processes involved in mud brick degradation in temperate environments: a micromorphological approach in an ethnoarchaeological context in northern Greece. Journal of Archaeological Science 41, 556–567.
Goldberg, P., Bar-Yosef, O., 1998. Site formation processes in Kebara and Hyonim caves and their signifikance in Levnatine prehistoric caves. In: Akazawa, E.A. (Ed.), Neanderthals and Modern Humans in Westen Asia. Pienum, New York, NY, pp. 107–125.
Goldberg, P., Macphail, R.I., 2006. Practical and Theroetical Geoarchaeology. Blackwell Publishing, Oxford.
Goldberg, P., Nash, D.T., Petraglia, D., 1993. Formation Processes in Archaeological Context. In: Monographs in World Archaeology No. 17. Prehistory Press, Madison, Wisconsin, p. 188.
Hrnčiarová, T., et al., 2002. Atlas krajiny Slovenskej republiky. Bratislava.
Hüssen, C.M., Ölvecky, R., Rajtár, J., 2014. Výskum dočasných rímskych táborov vo Vrábľoch. AVANS v roku 2011 (in press).
Johnson, A., 1987. Römische Kastelle des 1. und 2. Jahrhunderts n. Chr. In: Britannien und den germanischen Provinzen des Römerreiches. Mainz am Rhein.
Jones, M.J., 1975. Roman Fort-defences to A.D. 117, with Special Reference to Britain. In: British Archaeological Reports British Series 21.
Jones, R.H., 2011. Roman Camps in Scotland. Edinburgh.
Jones, R.H., 2012. Roman Camps in Britain. Amberley.
Karkanas, P., Goldberg, P., 2010. Site formation processes at Pinnacle Point Cave 13B (Mossel Bay, Western Cape Province, South Africa): resolving stratigraphic and depositional complexities with micromorphology. Journal of Human Evolution 59, 256–273.
Karkanas, P., Goldberg, P., 2013. Micromorphology of cave sediments. In: Shroder, J.F., Frumkin, A. (Eds.), Treatise on Geomorphology, Karst Geomorphology, vol. 6. Academic Press, San Diego, pp. 286–297.
Komoróczy, B., 2006. K otázce existence římského vojenského tábora na počátku 1. st. po Kr. u Mušova (kat. Pasohlávky, Jihomoravský kraj). Kritické poznámky z pohledu římsko-provinciální archeologie. In: Droberjar, E., Lutovský, M. (Eds.), Archeologie barbarů 2005, pp. 155–205. Praha.
Komoróczy, B., 2008. Hradisko (Burgstall) u Mušova ve světle výzkumů v letech 1994–2007. In: Droberjar, E., Komoróczy, B., Vachůtová, D. (Eds.), Barbarská

sídliště. Chronologické, ekonomické a historické aspekty jejich vývoje ve světle nových archeologických výzkumů, Spisy Archeologického ústavu AV ČR Brno 37, pp. 391–438. Brno.

Komoróczy, B., 2009a. Marcomannia. Der Militärschlag gegen die Markomannen und Quaden – ein archäologischer Survey. In: Varusschlacht im Osnabrücker Land GmbH – Museum und Park Kalkriese (Ed.), 2000 Jahre Varusschlacht. Konflikt, Stuttgart, pp. 114–125.

Komoróczy, B., 2009b. The character of the internal buildings of the Roman military bases on Burgstall at Mušov (South Moravia, Czech Republic). In: Morillo, A., Hanel, N., Martín, E. (Eds.), Limes XX. 20th International Congress of Roman Frontier Studies, vol. 3. Anejos des Gladius 13, Madrid, pp. 1421–1436.

Komoróczy, B., Vlach, M., 2010. Využití GIS pro výzkum římského vojenského zásahu na barbarské území ve střední Evropě v době markomanských válek – Úvod do problematiky a perspektivy. In: Beljak, J., Březinová, G., Varsik, V. (Eds.), Archeológia barbarov 2009, Archaeologia Slovaca Monographiae. Nitra, pp. 247–290.

Kooistra, M.J., Juo, A.S., Schoonderbeek, D., 1990. Soil degradation in cultivated Alfisols under different management systems in Southern Nigeria. In: Douglas, L.A. (Ed.), Soil Micromorphology: a Basic and Applied Science, Developments in Soil Science, vol. 19. Elsevier Amsterdam, pp. 61–68.

Kovárník, J., 2012. Měly mladoneolitické rondely také valy? Aneb je rondel s valy u Třebovětic, okr. Jičín, klíčem k řešení? Did Late Neolithic Rondels Have Ramparts? Is the Rondel with Ramparts Near Třebovětice, Jičín Dist., a Key to the Solution? (University of Hradec Králové) Živá archeologie. (Re)konstrukce a experiment v archeologii 14/2012, pp. 9–15.

Kovárník, J., 2014. The Discovery of Erosion Layers of Earthworks/Wall/Ramparts in the Inner Ditch of the Triple rondel Plotiště nad Labem II and the Confirmation of the Discovery Earthworks of the rondel near Třebovětice, Jičín Dist. during Archaeological Research (in press).

Kovárník, J., Mangel, T., 2013. Rondel s valy u Třebovětic. Poznámka ke konstrukčním znakům mladoneolitických rondelů. In: Cheben, I., Soják, M. (Eds.), Otázky neolitu a eneolitu našich krajín 2010. Nitra, pp. 133–152.

Kühn, P., Aguilar, J., Miedema, R., 2010. Textural pedofeatures and related horizons. In: Stoops, G., Marcelino, V., Mees, F. (Eds.), Interpretation of Micromorphological Features of Soils and Regoliths. Elseiver, Amsterdam, pp. 217–250.

Lenneis, E., 1977. Siedlungsfunde aus Poigen und Frauenhofen bei Horn. Horn - Wien.

Leopold, M., Hürkamp, K., Völlkel, J., Schmotz, K., 2011. Black soils, sediments and brown calcic luvisols: a pedological description of a newly discovered Neolithic ring ditch system at Stephansposching, Eastern Bavaria, Germany. Quaternary International 243, 293–304.

Lindbo, D.L., Stolt, M.H., Vepraskas, M.J., 2010. Redoximorphic features. In: Stoops, G., Marcelino, V., Mees, F. (Eds.), Interpretation of Micromorphological Fatures of Soils and Regoliths. Elseiver, Amsterodam, pp. 129–148.

Lisá, L., Bajer, A., Válek, D., Květina, P., Šumberová, R., 2013. Micromorphological evidence of neolithic rondel-like ditch infillings; Case Studies from Těšetice-Kyjovice and Kolín, Czech Republic. Interdiciplinaria Archaeologica IV 2, 135–146.

Loishandl-Weisz, H., Peticzka, R., 2011. Mechanismus zaplňování hrotitého příkopu mladoneolitického rondelu na lokalitě Steinabrunn, Dolní Rakousko. Archaeologia Austriaca 91 (2007), 141–162.

Macphail, R.I., Goldberg, P., 2010. Archaeological materials. In: Stoops, G., Marcelino, V., Mees, F. (Eds.), Interpretation of Micromorphological Features of Soils and Regoliths. Elseiver, Amstzterdam, pp. 289–622.

Matthews, W., French, C.A.I., Lawrence, T., Cutler, D.F., Jones, M.K., 1997. Microstratigraphic traces of site formation processes and human activities. World Archaeology 29 (2), 281–308.

Milek, K., 2012. Floor formation processes and the interpretation of activity areas: an ethnoarchaeological study of turf buildings at Thverá, northeast Iceland. Journal of Anthropological Archaeology 31, 119–137.

Modderman, P.J.R., 1983. Einige Gedanken zur Geutung der mittelneolitischen grabenanlagen. Mitteilungen der Österreichischen Arbeitsgemeinschaft für Urund Frühgeschichte 33–34, 347–350.

Mücher, H.J., 1974. Micromorphology of slope deposits: the necessity of a classification. In: Rutherford, G.K. (Ed.), Soil Microscopy. The Limestone Press, Kingston, Ontario, pp. 553–566.

Mücher, H.J., De Ploey, J., Savat, J., 1981. Response of loess materials to simulated translocation by water: micromorphological observations. Earth Surface Processes and Landforms 6, 331–336.

Mücher, H.J., Van Steijn, H., Kwaad, F., 2010. Colluvial and mass wasting deposits. In: Stoops, G., Marcelino, V., Mees, F. (Eds.), Interpretation of Micromorphological Fatures of Soils and Regoliths. Elseiver, Amsterdam, pp. 37–48.

Neugebauer, W., 1986. Neuere Forschungsergebnisse auf dem Gebiet der Hallstattkultur in Nordösterreich. Archäologie Alpen Adria 1, 85–107.

Němejcová-Pavúková, V., 1986. Siedlung un Kreisgrabenanlagen der Lengyen-Kultur in Svodín (Südslovakei). In: Chropovský, B., Friesinger, H. (Eds.), Internationalse Symposium über die Lengyel-Kultur. Nitra-Wien, pp. 177–183.

Oliva, M., 2004. Flint mining, rondels, hillforts… Symbolic works or too much free time? Archeologické rozhledy 56, 499–531.

Pavlů, I., 1982. Die Neolitischen Kreisgrabenanlagen in Böhmen. Arch Rozhledy 34, 176–189.

Podborský, V., 1988. Těšetice-Kyjovice 4. Rondel osady lidu s moravskou malovanou keramikou. Brno.

Podborský, V., 1999. Těšetice-Kyjovice I, okr. Znojmo. In: Podborský, V. (Ed.), Pravěká sociokultovní architektura na Moravě, pp. 115–132. Brno.

Renfrew, C., Bahn, P., 2000. Archaeology. Theories, Method and Practice. Thames and Hudson, London.

Řídký, J., Květina, P., Půlpán, M., Kovačiková, L., Stolz, D., Brejcha, R., Šreinová, B., Šrein, V., 2012. Analýza a interpretace nálezů z příkopu neolitického rondelu ve Vchynicích (okr. Litoměřice). Archeologické rozhledy 64, 628–694.

Schaefer, C.E.G.R., 2001. Brazilian latosols and their B horizon microstructure as long-term biotic constructs. Australian Journal of Soil Research 39, 909–926.

Stoops, G., 2003. Guidelines for Analyses and Descriptions of Soil and Regolith Thin Sections. Science Society of America, Madison WI.

Stoops, G., Marcelino, V., Mees, F. (Eds.), 2010. Interpretation of Micromorphological Features of Soils and Regoliths. Elsevier, Amsterdam.

Šumberová, R., 2012. Neolitické rondely a hroby v trase obchvatu silnice I/38 mimo Kolín. Předběžná informace o průběhu výzkumu v roce 2008. Sborník prací filozofické fakulty brněnské univerzity M 17, 47–64.

Tejral, J., 1999. Zum Stand der archäologischen Forschung über den römischen Militärischen Eingriff in Gebieten nördlich der Donau. Přehled výzkumů 39, 81–164 (1995–1996).

Tejral, J., 2008. Mušov „Hradisko“. Poloha, dějiny výzkumů a bádání. In: Tejral, J., Komoróczy, B. (Eds.), Hradisko u Mušova. Výsledky archeologických výzkumů do roku 2007. Rukopis pro GA ČR. Brno.

Trnka, G., 1986. Ergebnisse zur Untersuchungen der Kreisgrabenanage von Kamegg und Strassertale, Niederösterreich. In: Chropovský, B., Friesinger, H. (Eds.), Internationalse Symposium über die Lengyel-Kultur. Nitra-Wien, pp. 289–295.

Válek, D., Kazdová, E., Kovář, J.J., 2013. Cíle a průběh revizního výzkumu příkopu neolitického rondelu v Těšeticích-Kyjovicích (okr. Znojmo). In: Sborník prací filozofické fakulty brněnské univerzity M, vol. 18. Studia archaeologica Brunensia, pp. 159–169.

Válek, D., Lisá, L., Doláková, N., Uhlířová, H., Bajer, A., 2013. New evidence of origin and artefactual information value of the rondel ditch infilling in Těšetice-Kyjovice (Znojmo district). Acta Musei Moraviae 98, 215–238.

Van Vliert-Lanoë, B., 2010. Frost action. In: Stoops, G., Marcelino, V., Mees, F. (Eds.), Interpretation of Micromorphological Fatures of Soils and Regoliths. Elseiver, Amsterodam, pp. 81–108.

Vokolek, V., 1963. Třebovětice, okr. Jičín. Nálezová dokumentace. Archiv Muzea východních Čech. Nepublikovaná výzkumná zpráva. Hradec Králové.

Webster, G., 1985. The Roman Imperial Army. Totowa.

Welfare, H., Swan, V., 1995. Roman Camps in England. London.

Zeman, A., Havlíček, P., 1988. Geologická expertíza příkopu. In: Podborský, V. (Ed.), Těšetice-Kyjovice 4. Rondel osady lidu s moravskou malovanou keramikou. Brno, pp. 56–64.

Palaeogeography, Palaeoclimatology, Palaeoecology 418 (2015) 344–358

Contents lists available at ScienceDirect

Palaeogeography, Palaeoclimatology, Palaeoecology

journal homepage: www.elsevier.com/locate/palaeo

An integrated rock-magnetic and geochemical approach to loess/paleosol sequences from Bohemia and Moravia (Czech Republic): Implications for the Upper Pleistocene paleoenvironment in central Europe

Jan Hošek [a,g,*], Ulrich Hambach [b], Lenka Lisá [c], Tomáš Matys Grygar [d], Ivan Horáček [e], Sascha Meszner [f], Ilja Knésl [a]

[a] Czech Geological Survey, Klárov 3, Prague 1, Czech Republic
[b] BayCEER & Chair of Geomorphology, University of Bayreuth, D-95440 Bayreuth, Germany
[c] Institute of Geology of Czech Academy of Science, Rozvojová 269, Prague 6, Czech Republic
[d] Institute of Inorganic Chemistry of Czech Academy of Science, Řež 1001, Czech Republic
[e] Department of Zoology, Faculty of Science, Charles University, Viničná 7, Prague 2, Czech Republic
[f] Dresden University of Technology, Institute of Geography, Mommsenstrasse 7, Dresden, Germany
[g] Institute of Geology and Paleontology, Faculty of Science, Charles University in Prague, Albertov 6, Prague 2, Czech Republic

ARTICLE INFO

Article history:
Received 18 June 2014
Received in revised form 27 November 2014
Accepted 30 November 2014
Available online 9 December 2014

Keywords:
Loess/paleosols sequences
Rock-magnetism
Geochemical proxies
Upper Pleistocene
Paleoclimate
Central Europe

ABSTRACT

Two central European loess/paleosol sequences (MIS 6-2), from central Bohemia (Zeměchy) and southern Moravia (Dobšice), situated in the important climatic transition zone between the oceanic (Atlantic) and continental climate regimes, were investigated for rock magnetism, geochemistry, grain size and micromorphology. In both sites the magnetic profile shows good agreement with the standard model of magnetic enhancement in paleosols as established in the Chinese loess. The magnetic signal is dominated by the presence of fine-grained magnetite and maghemite, formed in-situ and controlled by the intensity of soil formation. Magnetic proxies corresponded to proxies of chemical weathering and leaching intensity such as the Chemical Index of Alteration (CIA), the Cation Exchange Capacity (CEC) and the Rb/Sr ratio (correlation coefficient $r = \sim 0.6–0.93$) during the whole Lower Weichselian (MIS 5d–5a) and, in general, also during the Pleniglacial (MIS 4-2). Nevertheless, for the Eemian period (MIS 5e) this relationship was not always valid, either due to weak magnetic enhancement (at Dobšice) or even weak depletion of the magnetic minerals with soil formation (at Zeměchy). The presented data demonstrate that magnetic signals can be overprinted more easily than chemical proxies during later diagenetic events, and are hence not in all cases reliable for deciphering paleoclimate changes during all periods of the studied time interval. Rock-magnetic, geochemical and micromorphological results suggest drier conditions in southern Moravia compared to central Bohemia during the Weichselian Glacial, probably due to the more continental climate in southern Moravia.

1. Introduction

Loess/paleosols sequences (LPSs) of the last climate cycle kaleidoscopically cover wide areas of the European continent and provide a valuable archive of the Upper Pleistocene paleoenvironment there. Yet, as indicated by many large scale geographic comparisons (e.g. Kukla 1977; Pye, 1987; Derbyshire et al, 1988; Bronger and Heinkele, 1989; Pécsi, 1990; Haesaerts and Mestdagh, 2000; Marković et al., 2008; Jary and Ciszek, 2013), European LPSs are marked by regional differences and pronounced facies variability in their pedosedimentary records that complicate finer super-regional correlations (Kemp, 2001). Such complications are especially evident in a transect from sub-oceanic (Atlantic) regions towards more continental areas, apparently due to the influence of the different climate regimes. Detailed studies of geographic and environmental variation in regional responses to general climate trends during the Upper Pleistocene are therefore of high priority for Quaternary science in Europe. A dense network of reliably-dated, high-resolution records from different geographic locations is a basic prerequisite for such spatial analyses (Frechen, 2011; Muhs, 2013).

For a particular LPS, a detailed history of the paleoenvironmental circumstances responsible for the pedogenetic and diagenetic processes (Zhang et al., 2007; Bloemendal et al., 2008) can be reliably reconstructed using instrumental mineral-magnetic and geochemical analyses

* Corresponding author at: Czech Geological Survey, Klárov 3, Prague 1, 118 00; Czech Republic. Tel.: +420 731 905 752.
E-mail addresses: johan.hosek@gmail.com (J. Hošek), ulrich.hambach@uni-bayreuth.de (U. Hambach), lisa@gli.cas.cz (L. Lisá), grygar@iic.cas.cz (T.M. Grygar), ivan.horacek@natur.cuni.cz (I. Horáček), sascha.meszner@tu-dresden.de (S. Meszner).

http://dx.doi.org/10.1016/j.palaeo.2014.11.024
0031-0182/

(Wang et al., 2012). However, in order to reflect the different ways of mineral-magnetic enhancement in sediments and soils (the Chinese vs. Alaskan-Siberian scenario), or the post-depositional loss of ferromagnetic particles (e.g. Begét et al., 1990; Bogucki et al., 1995; Vodyanitskii et al., 2007; Liu et al., 2007; Bábek et al., 2011; Baumgart et al., 2013; Buggle et al., 2013a; Gocke et al., 2014), combining the magnetic and geochemical analyses is quite important. Thus the direct paleoclimatic interpretation of the rock-magnetic record can be corrected and/or improved (Evans and Heller, 2003; Maher et al., 2003).

In European loess research, a large number of studies combining geochemical, rock magnetic and sedimentological approaches have appeared during the last decade. These provide a relatively dense network of continuous LPS records that cover the area of north-western Germany, southern and eastern Poland, western Ukraine and the Danube catchment (e.g., Antoine et al., 2010; Panaiotu et al., 2001; Marković et al., 2006; Kravchinsky et al., 2008; Jordanova et al., 2011; Buggle et al., 2009; Bokhorst et al., 2009; Fitzsimmons et al., 2012; Fischer et al., 2012; Jary and Ciszek, 2013; Baumgart et al., 2013; Vandenberghe, 2013; Rolf et al., 2014; Schatz et al., 2014; Gocke et al., 2014; Újvári et al., 2014). Together, these studies provide a reliable platform for transregional comparisons of climate development during the Upper Pleistocene.

Within the territory of the Czech Republic a range of key loess sites have been investigated (e.g. Dolní Věstonice, Prague-Sedlec, Kutná Hora or Červený Kopec in Brno). These sites have provided detailed paleoclimatic and pedoecological records based on mollusk and vertebrate assemblages (Ložek, 1964; Horáček and Ložek, 1988); pollen data (Urban, 1984); paleopedological analyses (Smolíková, 1982); and archeological findings (e.g. Klíma et al., 1962; Svoboda et al., 1996). Nevertheless, except from the extensive multi-proxy studies of the profile at Dolní Věstonice (Oches and Banerjee, 1996; Bábek et al., 2011; Fuchs et al., 2013; Antoine et al., 2013; Lisá et al., 2014), and the multi-parameter magnetic characterization of the profile at Znojmo (Zhu et al., 2001), representative analytical paleoenvironmental data are still not available for the vast majority of loess series in the Czech Republic.

The present paper reports rock magnetic, geochemical, grain size and micromorphology data for two, until now, poorly-studied Upper Pleistocene series located in the Bohemian and Moravian parts of the Czech Republic more than 200 km apart. The study sites are situated in a relatively dry loess area, in the important transitional zone between Atlantic and continental macro-climatic settings. Regarding their geographical location and the methodological approach, this study helps to fill a gap in European loess research and, furthermore, helps towards a better understanding of the relationship between loess magnetism, chemical weathering and pedogenic intensity.

2. Geological settings

Both study sites are located within a dry loess zone, between north European and Alpine glaciations during glacial periods (Fig. 1). From a paleopedological point of view, both series conform to the standard succession of Upper Pleistocene soil development that is characteristic for this central European zone, as has been established for the area of former Czechoslovakia (Ložek, 1968; Demek and Kukla, 1969) and Upper Austria (Fink and Kukla, 1977; Zöller et al, 1994; Frechen, 2011). The indexing components of the succession, termed pedocomplexes (PK) by Kukla (1961), reveal specific sequences of paleosols, loess and loess derivates that form obvious lithostratigraphic units representing particular stages of climate development. In short, there is a good correlation between particular lithostratigraphic units of loess sequences (PKs) and units of the global climatostratigraphic scale (Marine and Oxygen Isotopic Stages — MIS/OIS). In the region under study, this is also well supported by their numerical dating in many sites throughout central Europe using different means: luminescence techniques (e.g. Musson and Wintle, 1994; Zöller et al., 1994; Frechen et al., 1999; Fuchs et al., 2013); amino-acid racemization chronology (Oches et al., 1996); and radiocarbon dating (e.g. Klíma et al., 1962; Hatté et al., 2001; Lang et al., 2003; Antoine et al., 2013; Kadereit et al., 2013; Újvári et al., 2014). The Upper Pleistocene sequence covers the pedocomplexes: PK III (corresponding to MIS 5e), represented usually by a Bt (zone of clay accumulation in the middle part of a soil) and BC horizons of the Eemian forest brown soil (parabraunerde, luvisol), and an overlying steppe chernozem; PK II (corresponding to MIS 5a and 5c) — two horizons of chernozem separated by colluvial loess sediments (pellet sands sensu Kukla, 1961) (MIS 5b); and PK I (a pedogenetic unit representing MIS 3), which is typically a weak brownish truncated soil of cambisol type .

The descriptions of soils and sediments of the studied sections are based on field observations and micromorphological studies. An overview scheme of the sections and sampled profiles are shown in Figs. 2 and 3.

2.1. Zeměchy

The Zeměchy-section outcrops in a loess gully situated 30 km north of Prague, near the Vltava River. Although the site has become a popular stop of many international field excursions, it has never been studied in detail. Beyond some basic lithological descriptions published as part of excursion guides (Tyráček, 1995; Hošek et al., 2012), or as regional geological reports (Cílek, 1996; Ložek, 1995), only the magnetic susceptibility of the Lower Weichselian part was previously measured (Forster et al., 1996), and five OSL dates were acquired from the Pleniglacial part of the sedimentary record (Zander et al., 2000). The gully is a result of recent erosion; it is 350 m long and 10–15 m wide, incised up to 19 m into a W–E oriented loess "dune" (greda). The pre-Quaternary geological bedrock is composed of weathered carboniferous arkoses. The fluvial gravels and sands accumulated by the Knovíz stream on the bedrock are overlaid by sandy loess corresponding to the Saalian (Riss) glacial (MIS 6, unit number Z 15 in Fig. 3).

A reddish-brown prismatic $Bt_{1(2)}$-horizon and BC horizon of a forest luvisol (parabraunerde) (layer Z14 in Fig. 3) represents the Eemian Interglacial. This horizon, together with brownish pellet sands sensu Kukla (1961) (Z13) and the overlaying chernozem horizon (Z12), represents the 170-cm-thick pedocomplex PK III. A thin layer of coarse sandy loess (Z11) on the surface of PK III may be correlated with the loess marker sensu Kukla (1975). This layer probably represents a phase of strong storm events and has been reported elsewhere in central, western and eastern Europe (Kukla, 1975; Kukla and Cílek, 1996; Antoine et al., 2010; Rousseau et al., 2013). The PK III is overlain by a 90-cm-thick layer of pellet sands (sensu Kukla, 1961) (Z10) and an initial weak brown soil (Z9) developed on colluvial sediment. The 160-cm-thick PK II is composed of a lower dark-gray chernozem (Z8) penetrated by frost wedges and an upper dark to black chernozem (Z6) rich in charcoal. The chernozem soils are separated by brownish pellet sands (Z7) with krotovinas in the uppermost part. The top of PK II is covered by a thin layer of coarse sandy loess (Z5) (marker II) and disturbed by biogenic activity. The described pedocomplexes are overlain by a 6-m-thick accumulation of sandy loess corresponding to the Pleniglacial period (Z4, Z2). The PK I pedocomplex (Z3) from the Middle Pleniglacial (part of MIS 3) is difficult to recognize in the field. It has developed only as a thin, light-brownish layer with a whitish (Ca) horizon below. A gravel layer on the surface of the soil horizon suggests erosional events that may have removed the upper part of the paleosol and, potentially, also some of the overlaying loess. The erosion events probably occurred during warming phases of the MIS 3 interstadial that enhanced the seasonal degradation of the permafrost active layer leading to solifluction-related deformation and alteration of the thin gley horizon (Z2b) preserved above the interstadial soil. The assumption of intensive erosion is also supported by OSL dating (Zander et al., 2000; see Fig. 2). Samples for OSL dating, taken at a distance of 110 cm from the loess above and below the gravel layer (original sample names ZE14 and ZE15, respectively) suggest a considerable hiatus in relatively continuous sedimentation (see OSL ages 51 ky and 22.1 ky). Above the

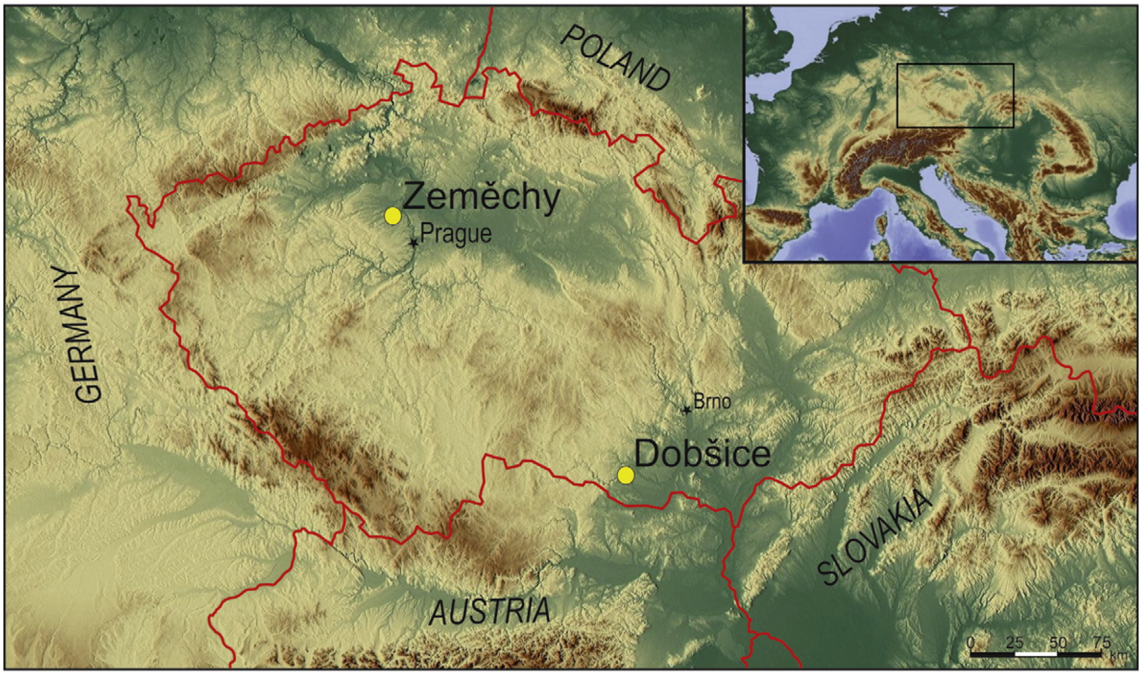

Fig. 1. Location of sites.

position of PK I, Late Pleniglacial loess has accumulated, showing intercalations of several thin gley horizons. The Holocene soil (Z1) is represented by a thin horizon of dark gray, agriculturally-influenced, chernozem soil with a Ca horizon.

2.2. Dobšice

The Dobšice section is situated on the north-western edge of the Pannonian Basin, in the area of surficial contact between the Bohemian Massif and the Carpathian foredeep (Fig. 1). Besides a malacological study of selected horizons (Ložek, 1968), so far only a lithological description, including a micromorphological study, has been published (Havlíček and Smolíková, 1995). The 15-m-thick loess/paleosol sequence has become exposed in the industrial complex of a former brickyard. The sequence overlays a Middle Pleistocene terrace of the Dyje River. The geological bedrock of the area consists of metamorphic rocks of the Bohemian Massif and of Neogene sediments of the Vienna Basin (mainly clay and sands). In general, the pedosedimentary record shows many similarities with the above-described record of Zeměchy. Markers sensu Kukla (1975) are present (unit numbers D12, D7 in Fig. 3) covering both PK III and PK II. The Eemian soil (D14) is developed as a full mature Bt horizon and BC horizon of a luvisol, which is covered by a chernozem horizon (D13). Based on micromorphological analysis (Havlíček and Smolíková, 1995), both soils of the Eemian complex were found to be genetically independent. In comparison with Zeměchy, the chernozems of PK II (D8, D11) are more brownish (in soil taxonomy close to the chernozem/kastanozem transition) and contain higher amounts of silt. In the pellet sands (D9), separating the chernozems of PK II, and also in the Pleniglacial loess (D6), the mollusk *Chondrula tridens* was identified by Ložek (1968). The Dobšice site mostly differs from Zeměchy in its development and preservation of the PK I soil (D5), which corresponds here more to a pararendzina (with cambic features). In the underlying loess (D6), numerous krotovinas are present. In the unit D3, signs of an initial pseudogley process were found. The Holocene soil, similar to that in Zeměchy, is represented by a gray, anthropogenically-influenced soil (D1).

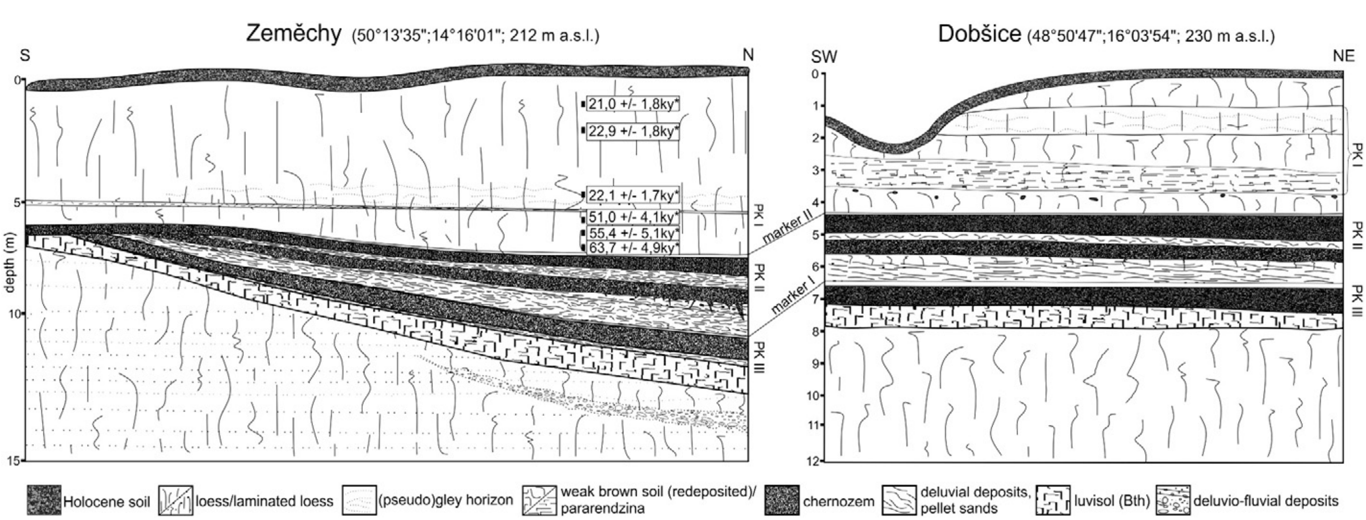

Fig. 2. Lithostratigraphical scheme of the studied sites. *OSL dates (Zander et al., 2000).

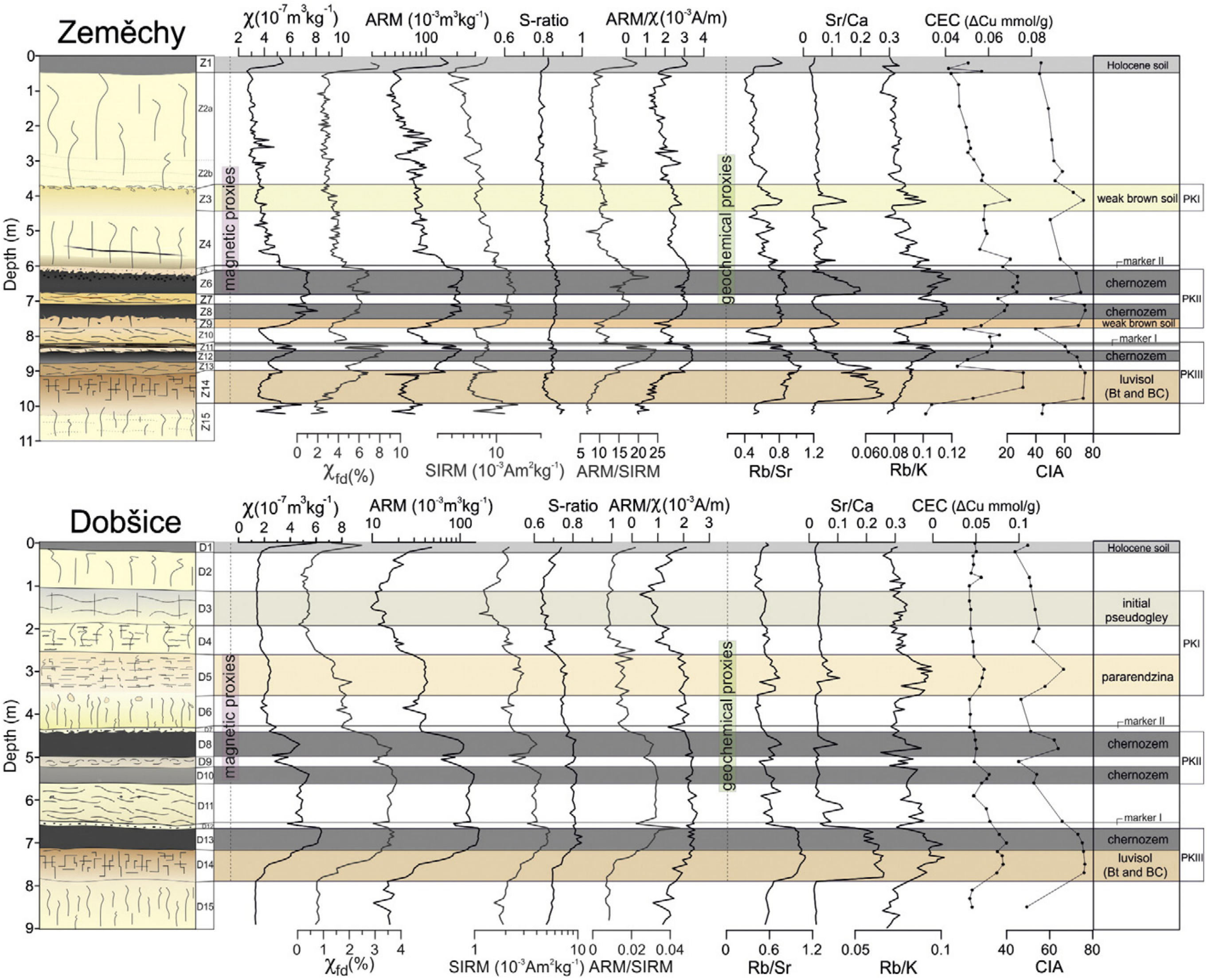

Fig. 3. Magnetic and geochemical proxies of the studied sites together with the lithostratigraphy of the sampled profiles.

3. Methods

3.1. Rock magnetic measurements

Unoriented samples were collected at 3–5 cm intervals from cleaned profiles. The low frequency magnetic susceptibility (χlf, here referred to as χ) was measured at 0.976 kHz, and high frequency magnetic susceptibility (χhf) at 3.904 kHz, using kappabridges MFK1 and KLY-4 (AGICO, Brno). The difference between the two measurements gives the frequency-dependent susceptibility expressed here as a percentage of χfd: $\chi fd\% = (\chi lf - \chi hf) / (\chi lf) \times 100$. The anhysteretic remanent magnetization (ARM) was measured using a LDA-3 demagnetizer with a peak alternating field of 100 mT and a DC biasing field of 0.5 mT.

Values of saturated isothermal remanent magnetization (SIRM) were imparted with a MMPM 10 pulse magnetizer using a field of 2.5 T, and back field remanence measurements were made at 200 mT. The S-ratio was calculated as IRM_0.2 T/IRM 2.5T.

All remanence measurements were made using a JR6-A spinner magnetometer with a noise level of 0.1×10^{-8} A m^2.

The temperature-dependence of the susceptibility (TDS, $\chi - T$) from room temperature up to 700 °C and back to room temperature was measured continuously with a furnace-equipped KLY-3 Kappa-bridge. The powdered whole-material specimens for both loess and paleosol were heated and cooled in an argon atmosphere to prevent possible oxidation.

Frequency dependent susceptibility measurements were carried out at the laboratory of AGICO, s.r.o. in Brno. Magnetic susceptibility of samples from the Dolní Věstonice brickyard (taken in 5 cm intervals) was acquired using a KLY-2 Kappa-bridge (AGICO, Brno) in the Paleomagnetic laboratory of Cologne University within the framework of a project led by one of us in the mid-1990s. Additional rock magnetic measurements were carried out at the Laboratory for Palaeo- and Enviromagnetism of the University of Bayreuth.

3.2. Geochemical and grain size analyses

Element analyses were performed on an X-ray fluorescence (XRF) spectrometer MiniPal4.0 with an Rh tube, maximal primary X-ray energy of 30 keV and a Peltier-cooled ED detector. The XRF signals of some 20 elements were determined, but only the results for Ca, Sr, Rb and K are discussed in this paper.

For selected samples (n = 25 in Zěměchy; n = 22 in Dobšice) conventional silicate analyses after wet decomposition were also carried out. Selected components were used for calculation of the Chemical Index of Alteration (CIA) and as verification of the accuracy of XRF data. The CIA was calculated as $CIA = [Al_2O_3 / (Al_2O_3 + Na_2O + CaO^* + K_2O)]$

× 100. CaO*, referring to silicatic Ca (after Nesbitt and Young, 1982), was obtained by subtracting acid-soluble Ca (in $CaCO_3$) from total Ca content. The cation exchange capacity (CEC) was determined using a procedure proposed by Meier and Kahr (1999) for pure clay mineral specimens and then optimized for sediments and soils (Grygar et al., 2009). $[Cu(trien)]^{2+}$ solution was obtained from $CuSO_4 \cdot 5H_2O$ (Penta, Czech Republic) and trien, triethylenetetramine (1,4,7,10-tetraazadekane, Sigma-Aldrich), and then to the final concentration 0.01 M with potentiometric control of the constant ligand-to-metal ratio.

The solutions were analyzed by Atomic absorption spectroscopy — AAS (Cu and Mg) and Atomic emission spectroscopy — AES (Ca and Na). The sample weight for analysis was adjusted depending on its actual Cation Exchange Capacity (CEC) in order to consume about 50% of $[Cu(trien)]^{2+}$ using the routine described by Grygar et al. (2009).

After removal of carbonate and organic matter by H_2O_2 and HCl respectively, the particle size distribution was measured using a laser granulometer CILAS 1190 LD that provides a measurement range from 0.04 to 2500 μm. For the correlation of magnetic and geochemical parameters the Pearson's correlation coefficient r was used.

3.3. Micromorphology

Oriented soil samples were taken in small Kubiena boxes (dimensions 3 × 5 cm) from each lithological layer. Upon slow drying followed by impregnation with resin, thin sections were produced from samples in the laboratory of the Czech Geological Survey (equivalent to Bullock et al., 1985; Stoops, 2003). The thin sections were studied under polarizing and binocular microscopes in the Institute of Geology ASCR, v. v. i., in Prague at a magnification of 16–800× and interpreted according to Stoops et al. (2010).

4. Results and interpretation

4.1. Magnetic properties

4.1.1. Concentration related magnetic parameters

The rock magnetic records correlate well with the lithology and show many similarities in both sections (Fig. 3). In general, the paleosols are characterized by an enhancement of the magnetic signal compared to loess units and pellet sands.

The values of χ (in 10^{-7} m^3 kg^{-1}) vary from 2.6 to 8.1 in Zeměchy (Z) and from 1.2 to 6.4 in Dobšice (D). In Zeměchy, maximum χ values (8.1) occur in the lower chernozem of PKII (layer Z9), whereas in Dobšice these occur in the chernozem of PKIII (6.4, D13). In both sections, minimum values occur in Saalian and Weichselian-Pleniglacial loess (χ about 1–5 in Z; 1–2 in D), chernozems showing higher values of χ than luvisols, where the magnetic enhancement occurs just in the upper part (Bt-horizon), whereas the underlying BC horizon is characterized by lower values of χ. This is very likely caused by the following process: in a Bt horizon the precipitation of iron oxides occur and consequently a higher amount of pedogenetic magnetite in comparison with the BC horizon can be observed (e.g. Rivas et al., 2006; Torrent et al., 2006; Jordanova et al., 2013). The χ-values of the lower and middle part of luvisols range between 4 and 5 in Zeměchy and 2 and 6 in Dobšice, representing approximately intermediate values between unweathered loess and chernozem paleosols. Pellet sands have higher χ values than loess, probably depending on the amount of top-soil particles in the reworked sediment. The pleniglacial parts of the records exhibit continually-decreasing χ values on the way up to the Holocene soil at both sites. The pararendzina of PK I in Dobšice (D5) show slightly higher values than the over- and underlying loess units (D2, 5) and the pseudogley horizon (D3), whereas the horizon corresponding to the weak brown soil in Zeměchy (Z3) did not show any differences to the loess itself.

The values of SIRM, ARM and χ often represent concentration and grain size-dependent parameters (Evans and Heller, 2003). *SIRM* gives information about the total (ferro-) magnetic mineral concentration with grain size larger than the superparamagnetic (SP)/single domain (SD) threshold (~0.02 μm). Unlike χ, SIRM is not influenced by the presence of para- and dia-magnetic minerals such as phyllosilicates, carbonates or quartz (Thompson and Oldfield, 1986). χfd indicates the proportion of fine viscous magnetic grains just below the SP/SD boundary (~0.02 μm; Thompson and Oldfield, 1986), while *ARM* is sensitive to single domain (SD, ~0.02–0.06 μm) grains of magnetically "soft" minerals like magnetite and maghemite (Maher et al., 1986). Both grain size fractions are preferably formed during pedogenesis (Heller and Evans, 1995).

Generally, ARM and SIRM values, as well as the χfd, follow the χ signal pattern in both sections. Again, values are uniformly low in loess, and enhancement can be observed in chernozems and the upper part of luvisols. Intermediate values are observed in reworked sediments derived from loess and soils. The correlation between χ and remanence parameters (see the highest correlation coefficients between χ and ARM in Table 1) strongly suggests that the magnetic signal of both sections is mainly controlled by the presence of single domain magnetic minerals. In contrast to Zeměchy, the Dobšice section shows less differences of χfd-values between pellet sands and chernozems, suggesting a higher content of SP/SD (pedogenetic) magnetic grains in the sediment.

The plot of χfd and χ is shown in Fig. 4. The increasing χfd and χ values follow the model of magnetic enhancement (i.e. the neoformation of ultrafine magnetite during pedogenesis) proposed, for example, by Heller et al. (1993), whereas decreasing χ with increasing χfd values point to magnetic depletion during low-temperature oxidation of magnetite, likewise leading to a shift of the magnetic domain assemblage towards SP domains. in Zeměchy magnetic enhancement was obvious in all horizons; however, in the upper (Pleniglacial) part of Dobšice signs of depletion of primary MD and SD grains relative to SP particles were found, probably due to the effect of water-logging (initial pseudogley horizons). Similar processes in the Pleniglacial loess have been observed elsewhere, for example in Saxony (eastern Germany) (Baumgart et al., 2013) in the Kraichgau area (western Germany) (Taylor et al., 2014), in Poland, and Western Ukraine (Nawrocki et al., 1996).

In Zeměchy, much higher absolute amounts of ferrimagnetic minerals are present than in Dobšice, resulting in higher ARM and SIRM values (Z: 37.7–227.1 10^{-3} A/m; 4.7–13.9 10^{-3} A/m; D: 9.6–165.2 10^{-3} A/m; 1.2–5.3 10^{-3} A/m). Similarly, χfd is much lower in Dobšice (~0.3–3.5%) than that in Zeměchy (~1.3–8.8%), suggesting that SP grains in chernozems of Bohemian sections are more common than in the equivalent/corresponding Moravian horizons.

4.1.2. Magnetic mineralogy and particle size

The S-ratio is, like the χfd, a concentration-independent proxy indicative of the relative abundance of ferrimagnetic to antiferromagnetic minerals (Maher, 1986; Wang et al., 2012). Elevated values reflect the dominance of magnetite (or maghemite), while lower values represent

Table 1
The correlation of magnetic and geochemical parameters.

		χ	ARM	χ_{fd}	SIRM	Rb/Sr	Rb/K	CEC	CIA
Dobšice	χ		0.99	0.89	0.97	0.5	0.63	0.63	0.53
	ARM	0.99		0.87	0.98	0.58	0.56	0.62	0.52
	χ_{fd}	0.89	0.87		0.84	0.56	0.61	0.56	0.51
	SIRM	0.97	0.98	0.84		0.62	0.67	0.6	0.5
	Rb/Sr	0.5	0.58	0.56	0.62		0.78	0.89	0.76
	Rb/K	0.63	0.56	0.61	0.67	0.78		0.74	0.76
	CEC	0.63	0.62	0.56	0.6	0.89	0.74		0.85
	CIA	0.53	0.52	0.51	0.5	0.93	0.76	0.85	
Zeměchy	χ		0.92	0.7	0.9	0.59	0.77	0.7	0.49
	ARM	0.92		0.78	0.79	0.57	0.79	0.63	0.48
	χ_{fd}	0.7	0.78		0.42	0.78	0.63	0.44	0.48
	SIRM	0.9	0.79	0.42		0.43	0.67	0.79	0.43
	Rb/Sr	0.59	0.57	0.78	0.43		0.65	0.65	0.78
	Rb/K	0.77	0.79	0.63	0.67	0.65		0.74	0.71
	CEC	0.7	0.63	0.44	0.79	0.65	0.74		0.73
	CIA	0.49	0.48	0.48	0.43	0.78	0.71	0.73	

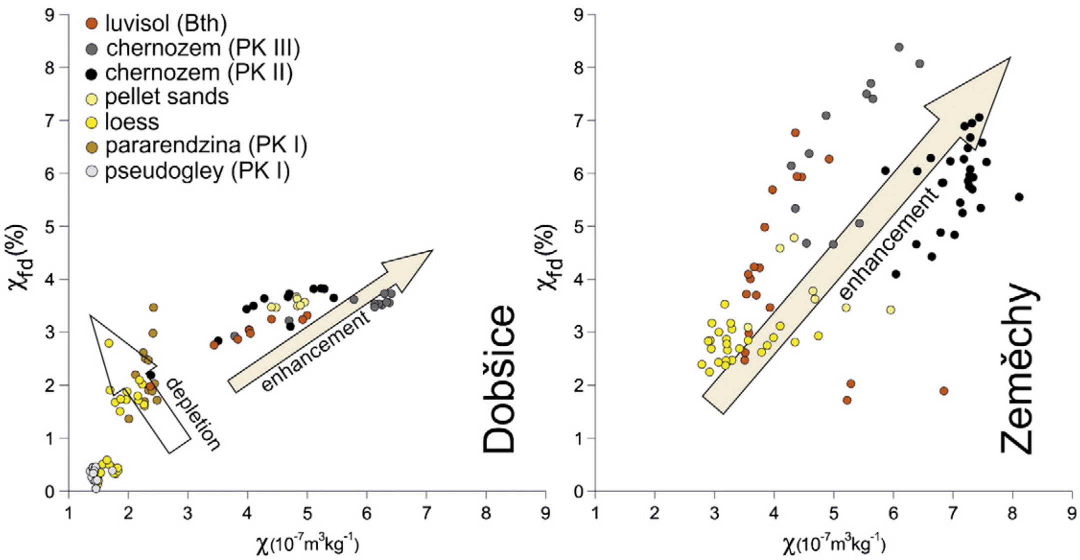

Fig. 4. Scatter plots of χ versus χ_{FD}.

increasing contributions from antiferromagnetic minerals, i.e. hematite or goethite. In both sites the S-ratio ranges between 0.85 and 0.9 in chernozem soils and in the upper part of luvisols, thus reflecting the high concentration of ferrimagnetics in the soil horizons. In both sections, the pleniglacial part of the record typically shows lower values of the S-ratio (0.62–0.8 in Zeměchy, 0.65–0.75 in Dobšice) and a descending trend (more visible in Dobšice) mainly in the loess between PK II and PK I soils. Nevertheless, the relatively uniform values close to 1 through both profiles suggest the dominance of ferrimagnetic minerals and little mineralogical variation. This interpretation is supported by temperature-dependent susceptibility (χ–T; Fig. 6).

Typical χ–T curves for the lower part of chernozems, the middle part of luvisols and Pleniglacial loess are shown in Fig. 6. In chernozems, as well as in loess, there are two major peaks for heating curves around 300 and 510–520 °C, while in luvisols only one peak occurs around 300 °C. The 'rise' in the heating curves at about 300 °C possibly indicates the transition of weakly-magnetic Fe-hydroxides (e.g., lepidocrocite) to maghemite (Oches and Banerjee, 1996). The increase of susceptibility

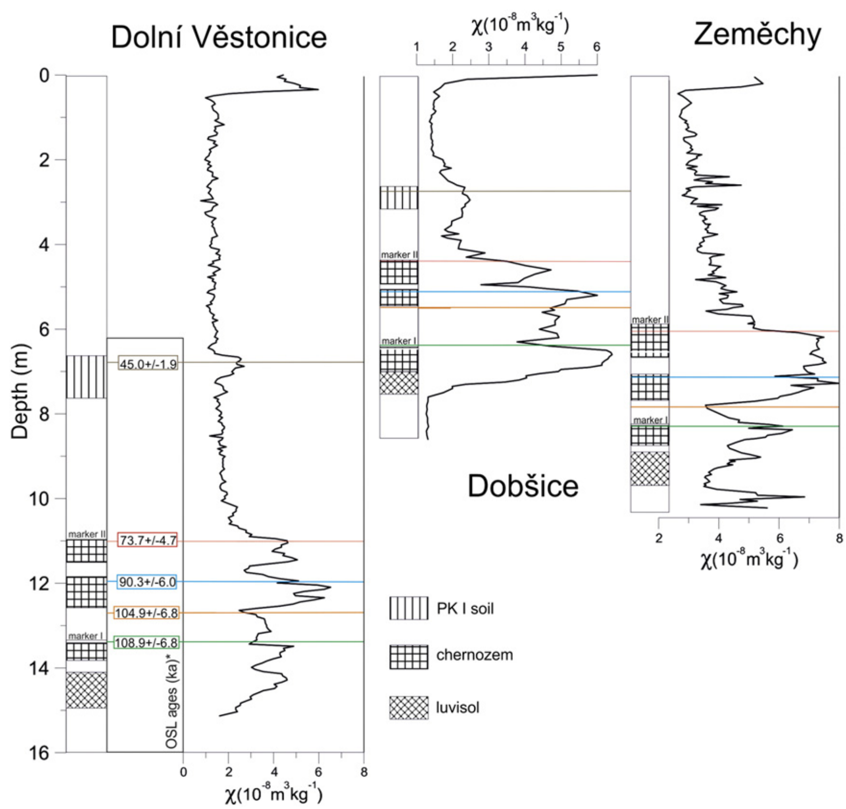

Fig. 5. Correlation of the Dolní Věstonice profile and the studied sections, based on the magnetic susceptibility.
*OSL dates adopted from Fuchs et al. (2013).

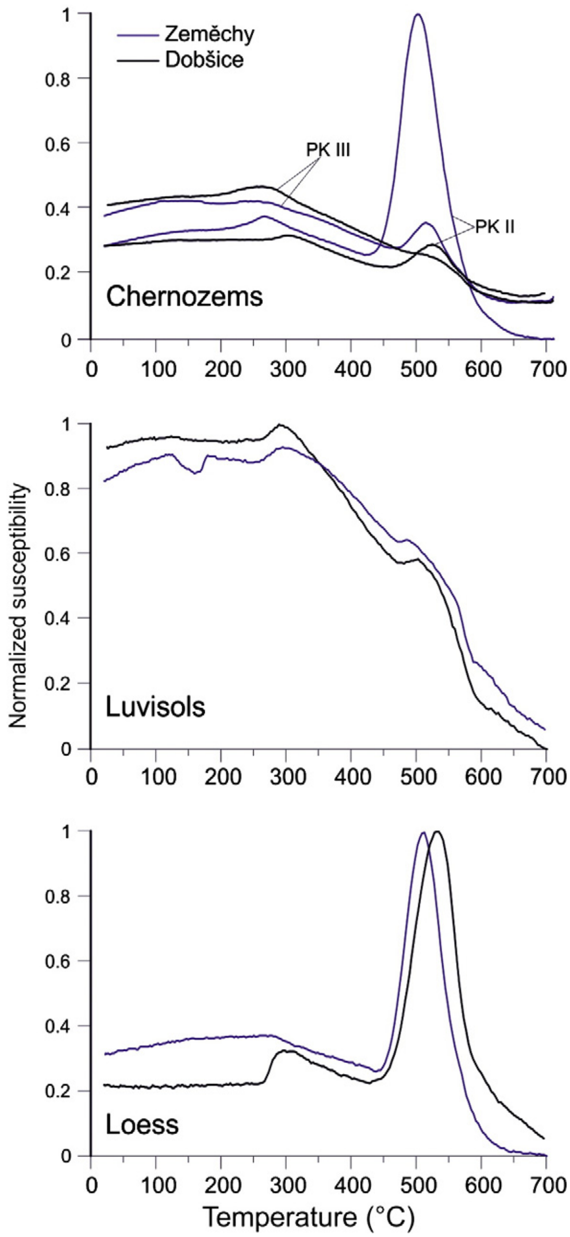

Fig. 6. Temperature dependent magnetic susceptibility of selected horizons. The values were standardized to a variation between zero and one.

between 250 and 300 °C (found in luvisols and loess) was interpreted by Liu et al. (2005) as a result of the gradual unblocking of fine-grained SD particles, which are *multidomain* (MD) at room temperature. The susceptibility drop between ~ 300–450 °C (almost absent for loess samples) has been interpreted as the inversion of *maghemite* to hematite (Sun et al., 1995; Oches and Banerjee, 1996; Liu et al., 2005). Liu et al. (2005) suggest that only the *fine-grained pedogenic particles* can efficiently be converted to hematite between 300 and 400 °C during heating. The rapid increase of susceptibility within the temperature interval of 450–520 °C (absent for luvisols) shows the formation of a new ferromagnetic mineral. This observation can be caused by the reduction of low susceptibility *hematite* to high susceptibility magnetite in an oxygen-free environment (Hunt et al., 1995). The sharp loss of susceptibility of all samples above 520 °C indicates the presence of *magnetite*, with its Curie point of 585 °C, being apparently a major magnetic mineral of the loess/paleosol sequences. A Curie temperature of about 580–585 °C can be observed in all samples. Unlike the warming curves, the cooling curves (not shown here) are dominated by newly-formed magnetite at ~500–400 °C.

In the luvisol of Zeměchy, we found a minor peak of susceptibility at 120 °C and a sharp loss between 120 and 180 °C, which may indicate the presence of *goethite* with a Curie temperature of around 120 °C (Liu et al., 2012).

In general, χ–T experiments suggest magnetite and maghemite enhancement of chernozem horizons as well as partially of pellet sands, while in the middle part of luvisols the enhancement only occurred to a limited extent — and by maghemite rather than magnetite formation. The higher concentrations of hematite in chernozems than in brown soils, and the presence of goethite in brown soils, is in accordance with previous results obtained by diffuse reflectance spectroscopy measured in Dolní Věstonice (Bábek et al., 2011).

Because the SIRM values had no contribution from SP grains, the low values of ARM/SIRM suggest a higher proportion of soft MD or SD magnetic grains, while high values correspond to the presence of stable single domain (SSD) magnetic grains (Evans and Heller, 2003). In Zeměchy, the course of ARM/SIRM with depth suggests the presence of SSD magnetic grains mainly in the upper part of the chernozems, whereas in luvisols, pellet sands and loess horizons larger grains dominated. This is in accordance with the results of the χ–T measurements. In Dobšice, however, the differences between paleosols and loess horizons are not very pronounced; the generally higher amount of SSD grains having been induced by the colluvial sediments. Hence, one almost continuous increase of magnetic parameters can be observed throughout the whole Lower Weichselian. In the Pleniglacial loess (including the weak interstadial soils), a stagnant trend is apparent at both sites. The ARM/χ ratio has been used to investigate the relative contributions of SP and SD grains to the bulk signal (e.g. Zeeden et al., 2010). In general, this record follows the pattern of χfd, proving the contributions of SP/SD grains to the magnetic signal.

The analyses presented above show that the samples contain mainly ferrimagnetic minerals (magnetite and maghemite) and partially antiferromagnetic minerals (goethite, hematite). The chernozem soil horizons are characterized by more fine-grained ferrimagnetic minerals in contrast to loess and luvisols. All these characteristics are, in general, consistent with previous studies of loess/paleosols sequences situated in central Europe (Oches and Banerjee, 1996; Forster et al., 1996; Zhu et al., 2001) and neighboring areas (Süttö, Hungary — Rolf et al., 2014; Lower Austria — Hambach, 2010).

4.2. Chronology of studied sections

The trends of χ with stratigraphy for both investigated sites correspond well to the litho-/pedo-stratigraphical and magnetic susceptibility record obtained from the Dolní Věstonice (DV) brickyard (Fig. 5). We employed the magnetic susceptibility data from DV as a tool to transfer the numerical ages (Fuchs et al., 2013) from DV to the sections under investigation (Fig. 5). For the Pleniglacial part of the record in Zeměchy, OSL dates by Zander et al. (2000) (Fig. 2) were also used to constrain the chronology. As a result, we obtained a composite chronology of all sections, based on OSL and correlation of the χ signals, which was corroborated by direct correlation of the Rb/Sr-weathering index to the global δ^{18}O record on its time scale (Lisiecki and Raymo, 2005).

4.3. Results of geochemical investigations

The results of geochemical analyses are summarized in Fig. 3. During chemical weathering, dissolved ions are transported through the sequences with percolating rainwater, depending mainly on their solubility and ability to be retained by clay (Perel'man, 1977). The weathering process can be divided into the early Ca and Sr removal stage, the intermediate K removal stage and the last Si removal stage (Nesbitt et al., 1980). Therefore, simple ratios of mobile (such as Sr and Ca) to relatively stable (such as Rb, Ti, and K) elements are used. This approach has been widely adopted as an appropriate measure for the degree of chemical weathering and leaching intensity in sediments (Gallet et al., 1996; Nesbitt et al., 1996; Chen et al., 1999; Ding et al., 2001; Muhs et al., 2001; Bokhorst et al., 2009). For the evaluation of the weathering intensity of the silicate component, we used the Chemical Index of Alteration (CIA) (Nesbitt et al., 1980). The interpretation syllogism of the geochemical results is included.

The Rb/Sr ratio of both sections shows maximum values in luvisols and chernozems, being only slightly increased in Middle Pleniglacial weak soils (PK I) and with minimum values in loess. In Dobšice, much less pronounced peaks in the chernozems of PK II occurs compared to Zeměchy. In both sections, a moderate/good correlation was found between Rb/Sr and magnetic parameters (Table 1); however, this did not hold for the luvisol horizons (see Table 1). Rb is usually enriched in K-rich minerals such as muscovite, biotite, K-feldspar and K-rich micas and illite. Furthermore, this element is unaffected by sediment diagenesis and by precipitation and concentrations of Fe and Mn oxihydroxides. It is strongly retained in the weathering zone due to its adsorption or exchange onto clay minerals (Nesbitt et al., 1980). Rubidium fixation in soils is a tracer of the transformation process affecting the 2:1 clay minerals in the acid brown earth-pod's (Herbauts, 1982) weathering sequence: kaolinite, illite, chlorite, vermiculite and smectite. Unlike Rb, Sr is a mobile element bound in Ca-feldspars and primary carbonates; it is easily soluble during leaching and chemical weathering processes. Because Rb is bounded to the clay particles, the resulting ratio is grain-size dependent. Nevertheless the clay in the LPS is mostly a product of the pedogenesis and weathering of the primary (silty) material and hence the Rb/Sr ratio is a sound indicator of loess chemical weathering (Gallet et al., 1996; Chen et al., 1999; Bloemendal et al., 2008; Bábek et al., 2011). It also seems to be a valuable indicator of the Late Glacial paleoenvironmental changes in a lake catchment, as was proved by analysis of non-calcareous lake sediments in Southern Bohemia (Hošek et al., 2014).

Unlike the Rb/Sr ratio, Rb/K shows lower values in the luvisols in both sites, whereas in the upper parts of the profiles the ratio increases again in paleosols and decreases in loess, clearly independent of the dilution by carbonates. This behavior indicates secondary clay enrichment, because Rb substitutes for K in K-feldspars and mica and becomes enriched during weathering, whereas K is more mobile and preferentially leached under moderate/strong chemical weathering (Nesbitt et al., 1980; Zech et al., 2008). The variability of K in the investigated profiles is in agreement with the various correlations between CEC and the elemental signatures that are discussed below. Further, a surprisingly high correlation coefficient between the Rb/K ratio and χfd was found throughout the profiles (see Table 1), suggesting that SD/SP magnetic grain enhancement/depletion in the sediment and soils throughout the profiles, and potassium mobility, may be both driven by related processes.

The highest Sr/Ca ratio is found in the interglacial luvisols in both sections. In Zeměchy, an increase of this ratio also occurs in the lower part of the PK II chernozems, whereas these events are not present in Dobšice. Slightly higher values of the ratio are recorded in the PK I soils of both sites. Ca, as well as Sr, is mainly present in primary carbonates and in relatively soluble carbonate minerals and is hence depleted in the weathering zone (Gallet et al., 1996; Bloemendal et al., 2008). Nevertheless, due to its size, Ca is adsorbed less strongly to clay structures than Sr, and more Ca reprecipitates as secondary carbonates relative to Sr. The vegetation may also play a role in the retention of Ca from wash-out, as the biogenic coefficient of Ca is much higher (0.17) than of Sr (0.06) (Perel'man, 1977). The ratio of Sr/Ca primarily reflects carbonate dissolution and hence mostly increases with increased leaching intensity, during more humid conditions (Bloemendal et al., 2008; Bokhorst et al., 2009). The low correlation between the CIA with Sr/Ca (Pearson correlation coefficient $r = 0.2$ and 0.4, data not shown in Table 1) in both sites suggests that carbonate dissolution was not necessarily accompanied by silicate and feldspar weathering. At Zeměchy, a strong negative correlation ($r = -0.78$) was found between the Sr/Ca ratio and ARM in soil horizons, suggesting that the leaching process also affected fine-grained (0.02–0.06 μm) magnetic particles.

The Chemical Index of Alteration (CIA) gives information about feldspar weathering by relating Al, which is enriched in weathering residues, to Na, Ca and K. Na and K are assumed to be removed from a soil profile in the course of plagioclase and K-feldspar weathering (Nesbitt and Young, 1982). In recent years, this proxy has been relatively frequently used as a suitable tool for the quantitative expression of chemical weathering in loess (e.g. Chen et al., 1999; Buggle et al., 2008; Újvári et al., 2008). The index is referred to as an "Na type" of weathering, whereas the above-described Rb/Sr ratio is considered as a "Sr-type" weathering index (Buggle et al., 2011).

4.4. Cation exchange capacity (CEC)

During the chemical weathering of loess, there occurs an ion exchange and transformation of clay minerals. The $[Cu(trien)]^{2+}$ ion is selectively adsorbed to expandable clay minerals. Increased CEC values obtained by $[Cu(trien)]^{2+}$ can thus be mainly attributed to a higher concentration of the most common expandable clay structure, i.e. smectite (Grygar et al., 2009; Bábek et al., 2011). Expandable clay minerals are characterized by the presence of loosely-bound cations and layers of water-bearing, polarized, organic molecules between the structural sheets. This type of structure is thus typical for more humid environments and their relatively low presence in the sediment suggests that conditions in these sections were most likely arid (and acidic), as they have been largely depleted or at least altered. Illite-type clays are formed under high pH conditions, mostly from weathering of K- and Al-rich minerals such as muscovite and feldspar. The illite/smectite ratio in the loess series thus provides a promising proxy strongly related to soil humidity and its seasonality (Li et al., 2007; Varga et al., 2011; Újvári et al., 2014)

Although CEC has rarely been used for loess/paleosol sequences, several studies have suggested that CEC can be correlated with other indicators of weathering intensity related to precipitation, indicators such as magnetic susceptibility, diffuse reflectance spectroscopy and element ratios of Rb, Ca and Sr (Maher, 1998; Bokhorst et al., 2009; Bábek et al., 2011).

At both sites, the CEC follows the proxies of weathering/pedogenesis intensity; elevated values (interpreted as higher amounts of smectite) coincide with soils, and the highest values correspond with luvisol horizons, for which the most intensive chemical weathering can be expected. In Dobšice, in comparison with Zeměchy, lower values are recorded in chernozems of PK II, especially in the upper one. The middle Pleniglacial soils (PK I) of both sites shows relatively high values, whereas in the overlying loess a gradual decrease occurs. CEC was positively correlated with the Rb/K ratio ($r = 0.74$), which can indicate the conversion of illite to expandable clay minerals (a process accompanied by a partial loss of K^+ ions) and this suggests the presence of K in muscovite and feldspar. The highest correlation between CEC and magnetic parameters was found in the case of χ and SIRM.

4.5. Grain-size analyses

Fig. 7 shows selected grain size distribution parameters of the sediment. Both sites are characterized by a higher content of the clay fraction (<4 μm) in soil horizons (~20%) compared to pellet sands and loess (~10%). The highest enrichment of clay is recorded in the upper parts of the luvisol (Bt horizons) and the overlaying chernozem (PK III) in both sites. A relatively high clay content is also recorded in the middle Pleniglacial part (PK I) of both sites. In general, the amount of clay in the sediment shows a similar pattern to that of the magnetic susceptibility record and proxies of chemical weathering such as Rb/Sr and Rb/K ratios (see Fig. 3), probably due to the pedogenic modification that has changed the grain size composition of the non-quartz component of

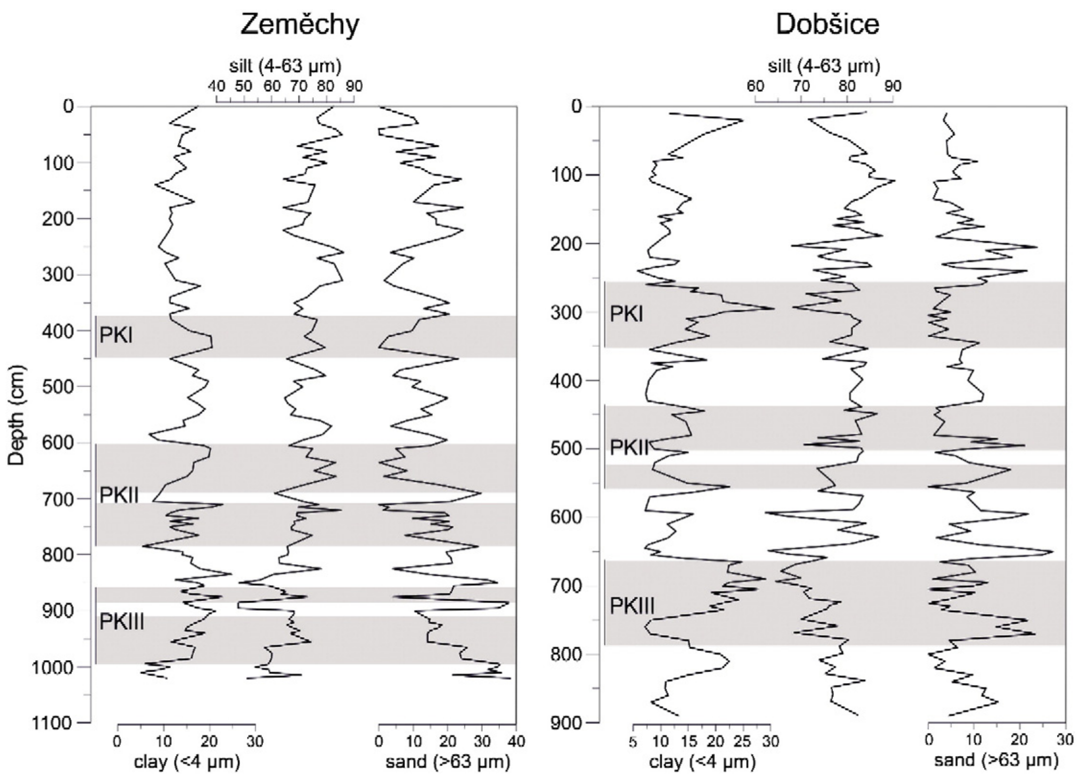

Fig. 7. Results of grain size analyses of the discussed sites.

the original dust. This is in accordance with the correlation between clayey humic soil horizons, magnetic susceptibility or organic carbon content that has been observed in Upper Pleistocene soil complexes from many European sites (e.g. Antoine et al., 1999, 2009, 2013).

The silt fraction (4–63 μm) dominate throughout both profiles (~60–90%). Maxima are typical for upper Pleniglacial loess (above PK I). The sand concentration (>63 μm) ranges from ~1–30%; higher amounts of sand are typical for colluvial sediments (pellet sands) and the upper Pleniglacial loess, as well as for marker horizons (marker I). In general, the amount of sand in Zeměchy is higher than in Dobšice, probably due to a nearby outcrop of carboniferous arkoses, whereas At Dobšice sand originates from Pleistocene fluvial terraces of the Dyje River.

4.6. Micromorphology

Micromorphological features of the main horizons are summarized in Table 2, the characteristics reflecting the local soil and environmental development. While the horizon representing the interglacial luvisol is preserved only by the Bt horizon, with the A horizon missing, the chernozem-like pedo-horizons are characterized by well-developed humified A horizons. During the development of chernozem-type soils, the accumulation of organic matter by humification is the dominant pedogenetic process. For luvisols, besides the strong in-situ weathering, the main pedogenetic process is the translocation of clays down the section. Thus the characteristic feature of such soils is the clay-enriched Bt horizon. The thickness of such horizons usually reflects the intensity and/or temporal duration of the pedogenetic processes. Higher humidity and/or water-logging might be causes for the pedogenetical processes connected with gley formation. Pronounced differences between the sections were found in some horizons, especially in the Lower Weichselian part of profiles (PK II); however, in this respect Dobšice differed from Zeměchy by having a markedly lower level of polygenesis. Secondary redoximorphic features (pseudogley processes) are here present just in the horizon of PK I (D3). Dobšice is also interesting from a pedozoological point of view because, besides the activity of earthworms (Lumbricidae) occurring throughout, the activity of Enchytraeidae (potworms) occurred, or even dominated (D10), in all the paleosols including the pararendzina of PK I.

5. Discussion

5.1. Rock-magnetic and geochemical results and their predictive value as paleoclimate indicators

The rock-magnetic investigation results (Fig. 3) suggest that the magnetic signal at both sites is mostly influenced by fine-grained (SP and SD) magnetite and partially also by maghemite. These components are typically formed during loess weathering and pedogenesis in a relatively warm and humid climate with a pronounced dry season (Fontes and Weed, 1991; Maher, 1998; van Velzen and Dekkers, 1999; Oldfield, 2007; Torrent et al., 2006; Zhang et al., 2007; Buggle et al., 2013a).

The good correlation between magnetic and geochemical proxies through the Weichselian parts of the studied profiles (Fig. 3) suggests that fine-grained magnetite/maghemite formation was accompanied by a more intensive weathering of minerogenic components, and a higher element mobility and clay mineral (trans)formation. For example, the formation of magnetic grains close to the SP/SD boundary (ARM/ χ) clearly correlated with the feldspar weathering and consequently with potassium mobility (Rb/K ratio, CEC). This is probably because, similar to that in pedogenetic bacteria activity, K mobility in soils and sediments (and its availability and diffuse flux for plant uptake) is strongly influenced by soil moisture (Zeng and Brown, 2000). On the other hand, the dissolution and leaching of Sr-rich carbonate minerals (Rb/Sr ratio) did not show such a direct link to magnetic enhancement.

Table 2
Micromorphological characterization of the significant lithological horizons.

Layer	Micromorphological features	Interpretation
Dobšice		
D3	Crack microstructure, sandy loam, crystalitic B fabric, decomposed organic matter — rare, bioturbation, $CaCO_3$ coating — rare, FeOH nodules (pseudogley concretions).	Weakly developed pseudogley (PK I)
D5	Granular to crack microstructure, sandy loam, crystalitic B fabric, $CaCO_3$ coating and infillings, Mn coating and nodules	Weakly developed pararendzina with A and $CaCO_3$ horizon (PK I)
D8	Spongy to granular microstructure, sandy loam, crystalitic B fabric, decomposed organic matter, bioturbation, $CaCO_3$ coating and infillings, excrements, phytoliths.	Upper chernozem (A and $CaCO_3$hor) of PK II
D9	Subangular blocky microstructure, sandy loam, crystalitic B fabric, humous concentratios — aggregates, $CaCO_3$ coating and infilling.	Loess/reworked loess
D10	Spongy to granular microstructure, sandy loam, crystalitic B fabric, decomposed organic matter, partly decomposed wood fragments, bioturbation, $CaCO_3$ and Mn coating and infillings, excrements.	Lower calcareous chernozem (A and $CaCO_3$hor) of PK II
D12	Subangular blocky microstructure, crystalitic B fabric, sandy loam (quartz and feldspar, fragments of granite and quartzite up to 2 mm; obvious positive gradation), $CaCO_3$ and Mn coating and infillings.	Marker loess sensu Kukla (1975)
D14	Spongy to granular microstructure, sandy loam, porostriatic B fabric, partly decomposed wood fragments, charcoal, bioturbation, $CaCO_3$ and Mn coating and infillings, humic concretions — common, excrements.	Luvisol (Parabraunerde) (Bt and $CaCO_3$ horizon) of PK III
Zeměchy		
Z3	Spongy microstructure, enaulic related distribution, 30% micro and mesovoids, vughs and compound packing voids, moderately sorted silt, crystallitic B fabric, light brown matrix, very fine grained black opaque decomposed organic matter (up to 10%), FeOH nodules present (up to 3%).	Weak brown soil (PK I)
Z8	Inter grain vesicular pore microstructure, enaulic related distribution, 30–50% micro and mesovoids, vughs and compound packing voids, moderately sorted silt, crystalitic B fabric, dark brown, fine grained black opaque decomposed organic matter (up to 30–50%),	Lower chernozem of PK II
Z11	Channel microstructure, enaulicrelated distribution, 50% micro and mesovoids, channels, vughs and compound packing voids, moderately sorted silt, crystallitic B fabric, brown, fine grained black opaque decomposed organic matter (up to 10%), charcoal fragments, three phases of calcium carbonate pedofeatures origin: 1.) crystallic pseudomorphoses of root cells due to bioturbation; 2.) hypocoating of channels; 3.) infillings of channels by crystallitic carbonates.	marker loess sensu Kukla (1975)
Z14	Intergrain channel microstructure, enaulic related distribution, 30% micro and mesovoids, channels and vughs, moderately sorted silt to fine sand, porostriatic B fabric, light brown to orange, very fine grained black opaque decomposed organic matter (up to 30%).	Luvisol (Parabraunerde) (Bt and $CaCO_3$ horizon) of PK III

On the contrary, the strong carbonate dissolution may have lead to the loss of fine-grained magnetic particles during the leaching processes.

In contrast to the interstadial chernozem soils, interglacial luvisols showed lower values of magnetic concentration-dependent parameters, as well as weaker magnetite/maghemite enhancement as shown by the χ–T measurements (Fig. 6). This is in contrast to the LPSs from the Pannonian Basin, where a strong magnetic enhancement also occurred within the lower part of the paleosol-complex (S1) corresponding to the Last Interglacial, and where magnetic concentrations were more than twice as high than that for the loess horizons (Marković et al., 2008, 2009; Buggle et al., 2013a). In both sites the Interstadial soils of PK I also exhibited a pronounced maxima of CEC and clay content, and a minima of calcite concentration, that are clear signs of a relatively intensive pedogenesis. However, in the case of Zeměchy, the PK I horizon was not detected by its magnetic measurements (see Fig. 3).

For the last interglacial in central Europe, the malacological, palynological and pedological data generally indicated more humid and warmer conditions (even compared to the Holocene). This favorable climate was replaced during the Lower Weichselian by rather cold and arid conditions with three interstadial oscillations characterized by a warmer, but still relatively dry, climate (Ložek, 1964; Smolíková, 1982; Urban, 1984; Caspers and Freund, 2001). The clear discrepancy between these statements and the above-mentioned surveyed rock magnetic record suggests a non-linear relationship of magnetic parameters with climatic change. This finding should constitute a point of special interest and is further discussed here in more detail.

The influence of climate on a magnetic signal (particularly the magnetic susceptibility) in LPSs and modern soils has already been extensively discussed in many studies (e.g. Heller et al., 1993; Maher et al., 2003; Liu et al, 2007; Buggle et al., 2013a). Nevertheless, the relationships between the state of magnetic variables and the course of the Pleistocene climate are far from being interpreted as linear (Han et al., 1996). This means that some climate changes, clearly documented by well understood proxies – such as pedological or geochemical indicators (Liu et al., 1995; Guo et al., 2001) and malacology (Rousseau and Wu, 1997) – are not necessarily reflected by expected changes in the magnetic susceptibility.

The above-mentioned magnetic enhancement of the studied sequences is mostly the influence of pedogenetic processes (i.e. a China scenario). Thus, it could be expected that the non-linearity of the record with climatic (pedogenetic) development has been probably caused by a post-sedimentary loss of the magnetic signal. We suggest two main reasons for the observed bias between the predicted paleoclimatic development and the recorded magnetic parameters:

(1) Erosion of the humic Ah horizon in the case of PK III
According to the micromorphological studies (see Table 2), the luvisol and overlaying chernozem (PK III) are genetically-independent soils at both sites (proved by the absence of braunlehm plasma in the chernozem horizons). In the case of Zeměchy, they are separated by a thin layer of colluvial sediments (Figs. 2 and 3). These colluvial and/or aeolian sediments are typically present in the PK III of many sites. This documents the higher erosion rate immediately after the climate deterioration at the end of the interglacial. In the case of Zeměchy, the colluvial layer (Z13) contains a small amount (up to 3%) of weak decomposed organic detritus, which might represent the rest of the reworked humic topsoil. Rock-magnetic studies of the Holocene luvisol from the loess area (e.g. Jordanova et al., 2013; Huang et al., 2011) suggest a high concentration of pedogenetic ferrimagnets, as in the humic Ah horizon and in the upper part of the Bt horizon, whereas middle and lower parts of the Bt horizon show significant lower magnetic enhancement. In contrast, geochemical parameters (such as CEC or the ratio of immobile/mobile elements) yield relatively comparable values in both the

Bt and Ah horizons (Duan et al., 2002). Having an Ah horizon missing would therefore be more relevant for an interpretation based on magnetic rather than geochemical proxies.

(2) Leaching and transformation of ferrimagnets in the Bt horizon
As mentioned above, an increase of percolating water could have a major impact on the concentration of ultrafine magnetic particles. Direct leaching can influence magnetic particles, mostly fine-grained, as is suggested by the negative correlation between ARM and the Sr/Ca ratio. Another reason for the χ decrease could be excessive moisture during the Interglacial (as supported by geochemical proxies) that could have caused a transformation of magnetite/maghemite into goethite/limonite (Liu et al., 2007, 2012). This interpretation is supported by the occurrence of goethite in the luvisol as proven by χ–T measurements.

The proxies of chemical weathering (particularly Rb/Sr ratio, CIA and CEC) of the studied profiles (Fig. 3) show the highest values in interglacial soil and they are also enriched in the interstadial paleosol layers relative to the loess (including the PK I soil in Zeměchy which did not even register in the magnetic signal at all, probably due to the erosion of the upper part of the soil horizon, enriched by magnetic minerals — similar to that in the interglacial luvisols). The Rb/Sr ratio and CIA have been used to reflect paleoclimate changes in the loess of north-central China (Chen et al., 1999; Ding et al., 2001), the Danube region (Buggle et al., 2011; Bokhorst et al., 2009; Varga et al., 2011; Újvári et al., 2014) and Germany (Fischer et al., 2012) — in terms of their systematic variations in loess/paleosol sequences. Furthermore, in the Bohemian and Moravian loess/paleosol sequences these proxies reveal in an exemplary way the degree of chemical weathering and reflect the general course of climate development of the Upper Pleistocene — as is apparent through the correlation with deep sea oxygen isotopic records indicating the global climate changes (Lisiecki and Raymo, 2005; Fig. 8).

Despite the correlation between the Rb/Sr ratio and the global benthic $\delta^{18}O$ record being based on a visual comparison, we have several reasons to consider this correlation a reliable one: many lines of evidence indicate that the pedocomplexes PK III and PK II can be assigned to marine oxygen isotope stages MIS 5e–5a and PK I to MIS 3 (e.g. Kukla, 1975; Musson and Wintle, 1994; Zöller et al., 1994; Forster et al., 1996; Frechen et al., 1999; Fuchs et al., 2013). The well-determined pedostratigraphy of the last climatic cycle was mostly established based on detailed studies of the profile Dolní Věstonice (DV) brickyard and thus the successful correlation of the χ and litho-pedostratigraphical records of DV with the studied sections (Fig. 5) have allowed us to compare the obtained proxy records with the global climatic scale. This kind of correlation is supported by OSL dates adopted from DV which in turn can be correlated unambiguously to the sections under study. Yet, it is to be remembered that, in general, an accurate synchronization of land and ocean records and reliable stratigraphic correlation between them is still an unresolved task for several reasons. This also applied to LPSs, where the sedimentary record is often incomplete (as discussed above) and the absolute chronology, based on the OSL dating, is uncertain to often ~5–10 ky. Moreover, as suggested by studies comparing biological and geochemical proxy-records of well-dated varved lake sediments or speleothems with benthic and Greenland $\delta^{18}O$, synchronity often cannot be proven, and these records may not be exactly synchronous (e.g. Sánchez-Goñi et al., 1999; Shackleton et al., 2003; Drysdale et al., 2007; Boch et al., 2011).

In this study we used a simplistic explanation for the correlation between peaks and troughs of the Rb/Sr ratio on one hand and the global benthic $\delta^{18}O$ record on the other hand: benthic foraminiferal marine $\delta^{18}O$ records are directly linked to deep sea water temperature and to global ice volume. Such records may be used as a proxy for the water content of the atmosphere and consequently also for the mainly precipitation controlled climatic humidity on continents. The humidity, in turn, controls weathering and soil formation and therefore the geochemical and magnetic proxies seems to be generally in-phase with the $\delta^{18}O$ records. This assumption has been the basis for a number of studies which have demonstrated a close correspondence of magnetic and geochemical variations within LPSs to signatures of past global climatic change derived from oceanic benthic $\delta^{18}O$ records (e.g. Heller and Liu, 1984; Kukla, 1975; Kukla et al., 1988; Bloemendal et al., 1995; Chen et al., 1997; Heslop et al., 2000; Yang et al., 2004; Buggle et al., 2009; Basarin et al., 2014).

5.2. Paleoenvironmental implications and paleogeographic context

The rock-magnetic and geochemical records (Fig. 3) visually divide both studied sequences into two parts: (1) the lower parts (corresponding to MIS 5), with higher values and fluctuations; and (2) the upper part (interpreted as MIS 4-2), characterized by their lower values and a trend of further decreases towards the top of the sequences. The records reflect the main features of climate development and allow us to correlate these individual profiles.

Sea surface temperature reconstruction for the North Atlantic (Imbrie et al., 1992) or globally benthic $\delta^{18}O$ records (Lisiecki and Raymo, 2005; see also Fig. 8), and also proxy data from Greenland (North Greenland Ice Core Project (NGRIP) Members, 2004), indicates that the beginning of the Weichselian (MIS 5d–a) was on average not dramatically cooler than the Eemian interglacial (MIS 5e). However, this period was characterized by large-amplitude oscillations and with the abrupt appearance of rather drier conditions, which is also widely suggested by the regional biological evidence (Ložek, 1964; Woillard, 1978; Urban, 1984; Behre, 1989; Guiot, 1990; Kühl et al., 2007) and geochemical and sedimentological records (Caspers and Freund, 2001; Sirocko et al., 2005; Rousseau et al., 2006; Drysdale et al., 2007) from the land. In Europe, climate desiccation was most pronounced in continental areas, whereas the region influenced by the Atlantic was considerably wetter (Kühl et al., 2007). This is also reflected in the (paleo) pedological evidence: the east central European soils generally indicate somewhat drier and therefore less favorable conditions for leaching than more westerly areas (Haesaerts and Mestdagh, 2000). Along a transect from northwestern Europe towards the east and south-east, redoximorphic features and pseudogley characteristics in soils (known, for example, from Gleyic Chernozems and Gleyic or Stagnic Phaeozems) decrease and vanish in the Pannonian Basin. Typical steppe chernozem/kastanozem soils become predominant (Eckmeier et al., 2007; Marković et al., 2008; Gozhik et al., 2013).

Our studied LPSs are situated in eastern central Europe in a transitional area of high value for reconstructing past regional atmospheric conditions and their interaction with North Atlantic/continental climate systems (e.g. Kukla, 1977; Rousseau et al., 2013).

In this respect, the situation in the Central Bohemian section Zeměchy shows aspects of the Atlantic part of Europe more clearly than the South Moravian Dobšice section situated on the northwestern edge of the Pannonian Basin. The Pannonian Basin is marked in the Upper Pleistocene by continuous dry continental climate conditions, under the effects of a temperate sub-Mediterranean climatic influence (Sümegi and Krolopp, 2002).

The differences in the proxy records between the two sites can be clearly linked to geographical differences influencing chemical weathering processes. For example, whereas in Zeměchy all interstadial soils show (from the micromorphological point of view) quite pronounced pseudogley features and recalcification processes, in Dobšice these features are only very weakly developed (see Table 2). Regarding the rock-magnetic and geochemical results, the most pronounced differences were found in the lower Weichselian parts of the pedosedimentary records.

A lower Sr/Ca ratio, as well as almost featureless variations of Rb/Sr or CEC in the PK II of Dobšice, indicates weaker pedogenic carbonate dissolution and feldspar weathering, as well as weaker formation/

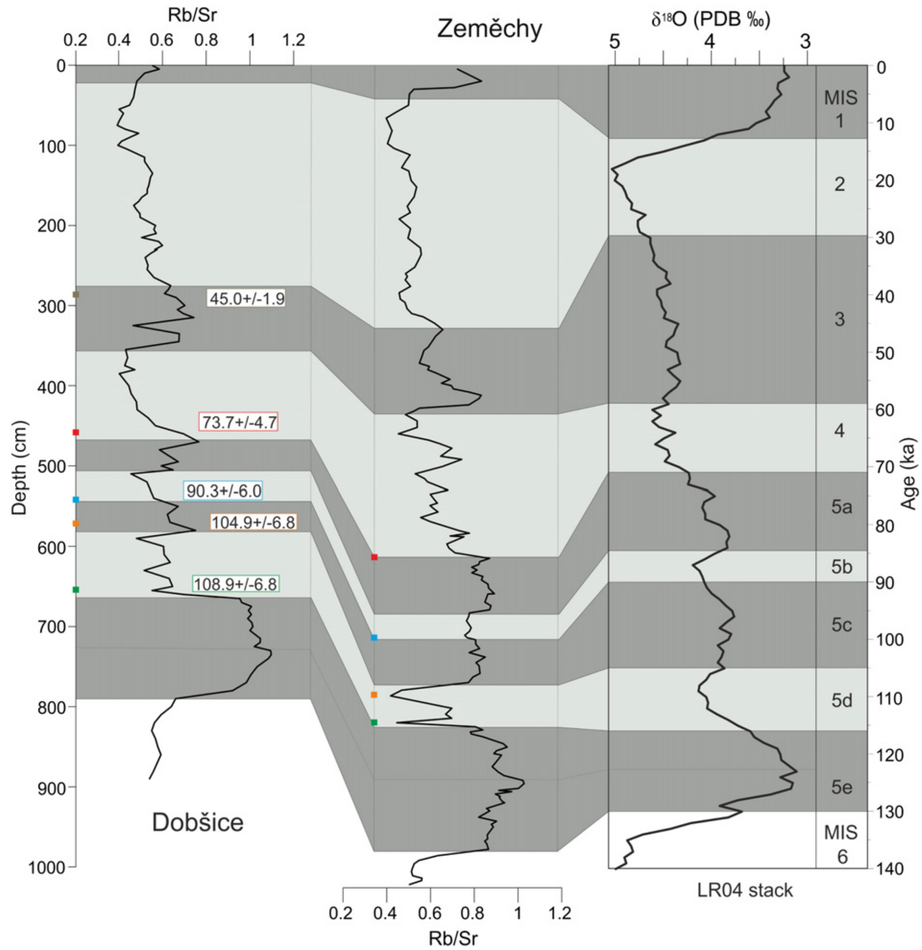

Fig. 8. Correlation of the Rb/Sr ratios from Dobšice and Zeměchy to the $\delta^{18}O$ record from the deep sea (LR04; Lisiecki and Raymo, 2005). OSL dates (color boxes) adopted from Fig. 4.

transformation of clay minerals in the Moravian section compared to the Bohemian (Fig. 3). A stronger leaching process in Zeměchy is also supported by lower concentrations of Ca and Sr, indicating a considerable higher variability of these elements, a leaching of upper soil layers, and the formation of Ca-enriched horizons. In total, the relative concentrations of fine grained ferromagnets (χfd, ARM) are markedly higher in Zeměchy than in Dobšice, suggesting that pedogenic processes were more intense and/or bacterial production of magnetite (and/or maghemite) was higher. An increase in moisture has been found to be the key factor for stronger magnetic enhancement of many LPSs, as long as the soils are not affected by water-logging (e.g. Buggle et al., 2013a).

Regarding the geographical location of the studied sections, we suggest that the pronounced differences in chemical weathering and magnetic enhancement of the pedosedimentary sequences may be caused by differences in the amount of percolating water, which may be representative of the precipitation. Drier conditions during the Pleistocene, or at least a different seasonality with a pronounced dry season in the Pannonian Basin compared to other European regions, are widely supported by geochemical, pedological and biological approaches (Allen et al., 1999; Buggle et al., 2009, 2013b; Bokhorst et al., 2009; Zech et al., 2013; Újvári et al., 2014).

Our findings suggest that the transitional zone between the two climate regions, or the two different modes, of the Upper Pleistocene climate in central Europe could be quite narrow. Yet, to confirm this hypothesis, further data – in a transect from sites towards the Atlantic Ocean and further into the continental area – are required, either confirming or challenging the presented findings.

6. Conclusions

Loess/paleosols sequences from central Bohemia and south Moravia (eastern-central Europe) provide a suitable archive for a detailed study of the Upper Pleistocene paleoenvironmental changes in a transition zone between the oceanic and continental climate regimes. Using a multi-proxy approach combining sedimentological, rock-magnetic, geochemical and micromorphological methods — we demonstrate that:

(i) The stratigraphy of the studied sections conforms well to the general pattern of the Upper Pleistocene loess/paleosol successions in the relatively dry loess of central Europe. This is demonstrated by the correlation of the magnetic susceptibility record with the well-investigated section at Dolní Věstonice.

(ii) The magnetic signal of the studied sediments is dominated by the presence of fine grained (SP/SD) magnetite, and partially maghemite. The origin of these minerals in soils and loess is probably mainly pedogenetic. This is in accordance with the “China scenario” model of magnetic enhancement by pedogenesis.

(iii) Compared to chernozems, the distribution of magnetic minerals throughout the interglacial (MIS 5e) luvisol (para-brown soil) and interstadial (MIS 3) cambisol is nonlinear, probably due to the erosion of the Ah horizons and later leaching of fine-grained magnetic grains. Rock-magnetic properties are thus not always a reliable proxy for deciphering paleoclimatic changes in the study area for the complete last climate cycle.

By contrast, proxies of chemical weathering – such as Rb/Sr ratio, CIA or CEC – reflect the main pattern of climate development through the whole Upper Pleistocene surprisingly well and they promise to provide a suitable correlation tool on the super-regional, or even hemispheric, scale.

(iv) The multi-proxy study reported in this paper revealed well-pronounced interegional differences in the leaching intensity of the loess/paleosols sequences. This suggests more humid conditions in central Bohemia than in south Moravia during the Upper Pleistocene, most probably due to the Moravian site's position close to the Pannonian Basin, where drier conditions during the Pleistocene predominated (in comparison to areas more to the north and west that are more exposed to the North Atlantic Ocean).

Acknowledgments

This research was supported by the Deutscher Akademischer Austausch Dienst (DAAD), Project no. 13-08169S of the Grant Agency of the Czech Republic (GAČR) and internal program of Institute of Geology ASCR in Prague RVO 67985831. We also thank AGICO Brno, s.r.o (especially Martin Chadima) for providing access to measuring equipment. Daniela Valentová is acknowledged for performing the grain-size analysis and Steve Ridgill for improving our English. Christian Zeeden and Gábor Újvári are thanked for their constructive comments, which helped to improve the manuscript enormously.

References

Allen, J.R.M., Brandt, U., Brauer, A., Hubberten, H.W., Huntley, B., Keller, J., Kraml, M., Mackensen, A., Mingram, J., Negendank, J.F.W., Nowaczyk, N.R., Oberhänsli, H., Watts, W.A., Wulf, S., Zolitschka, B., 1999. Rapid environmental changes in southern Europe during the last glacial period. Nature 400, 740–743.

Antoine, P., Rousseau, Moine, O., Rousseau, D.D., Kunesch, S., Hatté, C., Lang, A., Zöller, L., 2009. Evidence of rapid and cyclic eolian deposition during the Last Glacial in European loess series (Loess Events): the high-resolution records from Nussloch (Germany). Quat. Sci. Rev. 28, 2955e2973.

Antoine, A., Rousseau, D.-D., Moine, O., Kunesch, S., Hatté, C., Lang, A., 2010. Rapid and cyclic aeolian deposition during the Last Glacial in European loess: a high-resolution record from Nussloch. Quat. Sci. Rev. 28, 2955–2973.

Antoine, P., Rousseau, D.-D., Degeai, J.P., Moine, O., Lagroix, F., Kreutzer, S., Fuchs, M., Hatté, C., Gauthier, C., Svoboda, J., Lisá, L., 2013. High-resolution record of the environmental response to climatic variations during the Last Interglacial–Glacial cycle in Central Europe: the loess–paleosol sequence of Dolní Věstonice (Czech Republic). Quat. Sci. Rev. 67, 17–38.

Bábek, O., Chlachula, J., Grygar, J., 2011. Non-magnetic indicators of pedogenesis r elated to loess magnetic enhancement and depletion: examples from the Czech Republic and southern Siberia. Quat. Sci. Rev. 30, 967–979.

Basarin, B., Buggle, B., Hambach, U., Marković, S.B., Dhand, K.O.H., Kovačević, A., Lukić, T., 2014. Time-scale and astronomical forcing of Serbian loess–palaeosol sequences. Glob. Planet. Chang. 122, 82–96. http://dx.doi.org/10.1016/j.gloplacha.2014.08.007.

Baumgart, P., Hambach, U., Meszner, S., Faust, D., 2013. An environmental magnetic fingerprint of periglacial loess: records of Late Pleistocene loess paleosol sequences from Eastern Germany. Quat. Int. 296, 82–93.

Begét, J.E., Stone, D.B., Hawkins, D.B., 1990. Paleoclimatic forcing of magnetic susceptibility variations in Alaska loess during the late Quaternary. Geology 18, 40–43.

Behre, K.E., 1989. Biostratigraphy of the last glacial period in Europe. Quat. Sci. Rev. 8, 25–44.

Bloemendal, J., Liu, X.M., Rolph, T.C., 1995. Correlation of the magnetic susceptibility stratigraphy of Chinese loess and the marine oxygen isotope record, chronological and palaeoclimatic implications. Earth Planet. Sci. Lett. 131, 371–380.

Bloemendal, J., Liu, X.M., Sun, Y.B., Li, N.N., 2008. An assessment of magnetic and geochemical indicators of weathering and pedogenesis at two contrasting sites on the Chinese Loess plateau. Palaeogeogr. Palaeoclimatol. Palaeoecol. 257, 152–168.

Boch, R., Cheng, H., Spötl, C., Edwards, R.L., Wang, X., Häuselmann, P., 2011. NALPS: a precisely dated European climate record 120–60 ka. Clim. Past 7 (4), 1247–1259.

Bogucki, A., Maruszczak, H., Nawrocki, J., 1995. Stratigraphic and paleogeographic interpretation of analysis results of magnetic susceptibility of loesses at Bojanice NW Ukraine. Annales Universitatis Mariae Curie Sklodowskao B: Geographia, Geologia, Mineralogia et Petrographia 50, pp. 51–64.

Bokhorst, M.P., Beets, C.J., Marković, S.B., Gerasimenko, N.P., Matviishina, Z.N., 2009. Pedochemical climate proxies in Late Pleistocene Serbiane Ukranian loess sequences. Quat. Int. 198, 113–123.

Bronger, A., Heinkele, T., 1989. Paleosol sequences as witnesses of Pleistocene climatic history. Catena Suppl. 16, 163–186.

Buggle, B., Glaser, B., Zöller, L., Hambach, U., Marković, S., Glaser, I., Gerasimenko, N., 2008. Geochemical characterization and origin of Southeastern and Eastern European loesses (Serbia, Romania, Ukraine). Quat. Sci. Rev. 27, 1058–1075.

Buggle, B., Hambach, U., Glaser, B., Gerasimenko, N., Markovic, S., Glaser, I., Zöller, L., 2009. Stratigraphy, and spatial and temporal paleoclimatic trends in Southeastern/Eastern European loess–paleosol sequences. Quat. Int. 196, 186–206.

Buggle, B., Glaser, B., Hambach, U., Gerasimenko, N., Marković, S., 2011. An evaluation of geochemical weathering indices in loess–paleosol studies. Quat. Int. 240, 12–21.

Buggle, B., Hambach, U., Müller, K., Zöller, L., Markovic, S.B., Glaser, B., 2013a. Iron mineralogical proxies and Quaternary climate change in SE-Central European loess–paleosol sequences. Catena 117, 4–22.

Buggle, B., Hambach, U., Kehl, M., Zöller, L., Marković, S.B., Glaser, B., 2013b. The progressive evolution of a continental climate in SE-Central European lowlands during the Middle Pleistocene recorded in loess paleosol sequences. Geology 41, 771–774.

Bullock, P., Federoff, N., Jongerius, A., Stoops, G., Tursina, T., Babel, U., 1985. Handbook for Soil Thin Section Description. Waine Research Publications, Wolverhampton, UK (396 pp.).

Caspers, G., Freund, H., 2001. Vegetation and climate in the Early- and Pleni-Weichselian in northern central Europe. J. Quat. Sci. 16 (1), 31–48.

Chen, F.H., Bloemendal, J., Wang, J.M., Li, J.J., 1997. High-resolution multi-proxy climate records from Chinese loess: evidence for rapid climatic changes over the last 75 kyr. Palaeogeogr. Palaeoclimatol. Palaeoecol. 130, 323–335.

Chen, J., An, Z., Head, J., 1999. Variation of the Rb/Sr ratios in the loess / paleosol sequences of Central China during the last 130,000 years and their implications for monsoon paleoclimatology. Quat. Res. 51, 215–219.

Cílek, V., 1996. Sprašová rokle v Zeměchách u Kralup nad Vltavou. Zpr. geol. Výzk. v Roce 1995. pp. 31–33 (in Czech).

Demek, J., Kukla, J., 1969. Periglazialzone, Löss und Paläolithikum der Tschechoslowakei. Tschechoslowakische Akademie der Wissenschaften, Geographisches Institut, Brno (158 pp.).

Derbyshire, E., Billard, A., Van Vliet-Lanoë, B., Lautridou, J.-P., Cremaschi, M., 1988. Loess and palaeoenvironment: some results of a European joint programme of research. J. Quat. Sci. 3, 147–169.

Ding, Z.L., Sun, J.M., Yang, S.L., Liu, T.S., 2001. Geochemistry of the Pliocene red clay formation in the Chinese Loess Plateau and implications for its origin, source provenance and paleoclimatic change. Geochim. Cosmochim. Acta 65 (6), 901–913.

Drysdale, R.N., Zanchetta, G., Hellstrom, J.C., Fallick, A.E., McDonald, J., Cartwright, I., 2007. Stalagmite evidence for the precise timing of North Atlantic cold events during the early last glacial. Geology 35, 77–85.

Duan, L., Hao, J., Xie, S., Zhou, Z., Ye, X., 2002. Determining weathering rates of soils in China. Geoderma 110, 205–225.

Eckmeier, E., Gerlach, R., Gehrt, E., Schmidt, M.W.I., 2007. Pedogenesis of chernozems in Central Europe — a review. Geoderma 139, 288–299.

Evans, M.E., Heller, F., 2003. Environmental Magnetism: Principles and Applications of Enviromagnetics. Academic Press, New York (299 pp.).

Fink, J., Kukla, G., 1977. Pleistocene climates in central Europe: at least 17 interglacials after the Oiduvai Event. Quat. Res. 7, 363–371.

Fischer, P., Hilgers, A., Protze, J., Kels, H., Lehmkuhl, F., Gerlach, R., 2012. Formation and geochronology of Last Interglacial to Lower Weichselian loess/palaeosol sequences — case studies from the Lower Rhine Embayment, Germany. E & G Quat. Sci. J. 61, 48–63.

Fitzsimmons, K.E., Marković, S.B., Hambach, U., 2012. Pleistocene environmental dynamics recorded in the loess of the middle and lower Danube Basin. Quat. Sci. Rev. 41, 104–118.

Fontes, M.P.F., Weed, S.B., 1991. Iron Oxides in Selected Brazilian Oxisols: I. Mineralogy. Soil Sci. Soc. Am. J. 55, 1143–1149.

Forster, T., Evans, M.E., Havlíček, P., Heller, F., 1996. Loess in the Czech Republic: magnetic properties and paleoclimate. Stud. Geophys. Geod. 40, 243–261.

Frechen, M., 2011. Loess in Europe. E & G Quat. Sci. J. 60 (1), 3–5.

Frechen, M., Zander, A., Cilek, V., Ložek, V., 1999. Loess chronology of the Last Interglacial/Glacial cycle in Bohemia and Moravia, Czech Republic. Quat. Sci. Rev. 18, 1467–1493.

Fuchs, M., Kreutzer, S., Rousseau, D.-D., Antoine, P., Hatte, C., Lagroix, F., Moine, O., Gauthier, C., Svoboda, J., Lisa, L., 2013. The loess sequence of Dolni Vestonice, Czech Republic: a new OSL based chronology of the Last Climatic Cycle. Boreas 42, 664–677.

Gallet, S., Jahn, B.M., Torii, M., 1996. Geochemical characterization of the Luochuan loess–palaeosol sequence, China, and paaleoclimatic implications. Chem. Geol. 133, 67–88.

Gocke, M., Hambach, U., Eckmeier, E., Schwark, L., Zöller, L., Fuchs, M., Löscher, M., Wiesenberg, G.L.B., 2014. Introducing an improved multi-proxy approach for paleoenvironmental reconstruction of loess–paleosol archives applied on the Late Pleistocene Nussloch sequence (SW Germany). Palaeogeogr. Palaeoclimatol. Palaeoecol. 410, 300–315.

Gozhik, P., Komar, M., Łanczont, M., Fedorowicz, S., Bogucki, A., Mroczek, P., Prylypko, S., Kusiak, J., 2013. Paleoenvironmental history of the Middle Dnieper Area from the Dnieper to Weichselian Glaciation: a case study of the Maksymivka loess profile. Quat. Int. 334–335, 94–111.

Grygar, T., Kadlec, J., Žigová, A., Mihaljevič, M., Nekutová, T., Lojka, R., Světlík, I., 2009. Chemostratigraphic correlation of sediments containing expandable clay minerals based on ion exchange with Cu(II) complex with triethylenetetramine. Clay Clay Miner. 57, 168–182.

Guiot, J., 1990. Methodology of the last climatic cycle reconstruction in France from pollen data. Palaeogeogr. Palaeoclimatol. Palaeoecol. 80, 49–69.

Guo, B., Zhu, R.X., Roberts, A.P., Florindo, F., 2001. Lack of correlation between paleoprecipitation and magnetic susceptibility of Chinese loess/palaeosol sequences. Geophys. Res. Lett. 28, 4259–4262.

Haesaerts, P., Mestdagh, H., 2000. Pedosedimentary evolution of the last interglacial and early glacial sequence in the European loess belt from Belgium to central Russia. Neth. J. Geosci. 79, 313–324.

Hambach, U., 2010. Paleoclimatic and stratigraphic implications of high resolution magnetic susceptibility logging of Würmian Loess at the Upper Paleolithic KremseWachtberg Site. In: Neugebauer-Maresch, C., Owen, L.R. (Eds.), New Aspects of the Central and Eastern European Upper Palaeolithic — Methods, Chronology, Technology and Subsistence. Proceedings of the Prehistoric Commission of the Austrian Academy of Sciences. Vienna, pp. 295–304.

Han, J., Lu, H., Wu, N., Guo, Z., 1996. Magnetic susceptibility of modern soils in China and climate conditions. Stud. Geophys. Geod. 40, 262–275.

Hatté, C., Pessenda, L.C.R., Lang, A., Paterne, M., 2001. Development of an accurate and reliable ^{14}C chronology for loess sequences: application to the loess sequence of Nussloch (Rhine valley, Germany). Radiocarbon 43, 611–618.

Havlíček, P., Smolíková, L., 1995. Vývoj svrchnopleistocenních eolických sedimentů ve Znojmě-Dřevařských závodech. Vest. CGÚ 70/1 pp. 67–74 (in Czech).

Heller, F., Evans, M., 1995. Loess magnetism. Rev. Geophys. 33, 211–240.

Heller, F., Liu, T., 1984. Magnetism of Chinese loess deposits. Geophys. J. R. Astron. Soc. 77, 125–141.

Heller, F., Shen, C.D., Beer, J., Liu, X.M., Liu, T.S., Bronger, A., Suter, M., Bonani, B., 1993. Quantitative estimates of pedogenic ferromagnetic mineral formation in Chinese loess and paleoclimatic implications, Earth Planet. Sci. Lett. 114, 385–390.

Herbauts, J., 1982. Chemical and mineralogical properties of sandy and loamy–sandy ochreous brown earths in relation to incipient podzolization in a brown-podzol evolutive sequence. J. Soil Sci. 33, 743–762.

Heslop, D., Langereis, C.G., Dekkers, M.J., 2000. A new astronomical timescale for the loess deposits of northern China. Earth Planet. Sci. Lett. 184, 125–139.

Horáček, I., Ložek, V., 1988. Paleozoology and Mid-European Quaternary past: scope of the approach and selected results. Rozpr. ČSAV-MPV 94, 1–106.

Hošek, J., Lisá, L., Meszner, S., Knésl, I., 2012. Upper Pleistocene loess/paleosols sequence from Central Bohemia. In: Zöller, L., Peterek, A. (Eds.), From Paleozoic to Quaternary: a field trip from the Franconian Alb to Bohemia. 36. Hauptversammlung der Deutschen Quartärvereinigung DEUQUA, pp. 111–113.

Hošek, J., Pokorný, P., Kubovčík, V., Horáček, I., Žáčková, P., Kadlec, J., Rojik, F., Lisá, L., Bučkuliaková, S., 2014. Late Glacial climatic and environmental changes in Eastern-Central Europe: correlation of multiple biotic and abiotic proxies from the Lake Švarcenberk, Czech Republic. Palaeogeogr. Palaeoclimatol. Palaeoecol. 396, 155–172.

Huang, C., Zhao, W., Liu, F., Tan, W., Koopal, L.K., 2011. Environmental significance of mineral weathering and pedogenesis of loess on the southernmost Loess Plateau, China. Geoderma 163, 219–226.

Hunt, C.P., Banerjee, S.K., Han, J.M., 1995. Rock-magnetic proxies of climate change in the loess–palaeosol sequences of the western Loess Plateau of China. Geophys. J. Int. 123 (1), 232–244.

Imbrie, J., Boyle, E.A., Clemens, S.C., Duffy, A., Howard, W.R., Kukla, G., Kutzbach, J., Martinson, D.G., McIntyre, A., Mix, A.C., Molfino, B., Morley, J.J., Peterson, L.C., Pisias, N.G., Prell, W.L., Raymo, M.E., Shackleton, N.J., Toggweiler, J.R., 1992. On the structure and origin of major glaciation cycles. 1. Linear responses to Milankovitch forcing. Paleoceanography 7, 701–738.

Jary, Z., Ciszek, D., 2013. Late Pleistocene loess–palaeosol sequences in Poland and western Ukraine. Quat. Int. 296, 37–50.

Jordanova, D., Grygar, T., Jordanova, N., Petrov, P., 2011. Palaeoclimatic significance of hematite/goethite ratio in Bulgarian loess–palaeosol sediments deduced by DRS and rock magnetic measurements. In: Petrovsky, E., Ivers, D., Harinarayana, T., Herrero-Bervera, E. (Eds.), The Earth's Magnetic Interior. IAGA Special Sopron Book Series. Springer-Verlag, Berlin.

Jordanova, N., Jordanova, D., Liu, Q., Hu, P., Petrov, P., Petrovský, E., 2013. Soil formation and mineralogy of a Rhodic Luvisol — insights from magnetic and geochemical studies. Global Planet. Chang. 110, 397–413.

Kadereit, A., Kind, C.-J., Wagner, G.A., 2013. The chronological position of the Lohne Soil in the Nussloch loess section e re-evaluation for a European loess-marker horizon. Quat. Sci. Rev. 59, 67–86.

Kemp, R., 2001. Pedogenic modification of loess: significance for palaeoclimatic reconstructions. Earth Sci. Rev. 54, 145–156.

Klíma, B., Kukla, G., Ložek, V., Vries, H., 1962. Stratigraphie des Pleistozäns und Alter des paläolithischen Rastplatzes in der Ziegelei von Dolní Věstonice (Unter-Wisternitz). Anthropozoikum 11, 93–145.

Kravchinsky, V.A., Zykina, V.S., Zykin, V.S., 2008. Magnetic indicator of global paleoclimate cycles in Siberian loess–paleosol sequences. Earth Planet. Sci. Lett. 265, 498–514.

Kühl, N., Litt, T., Schölzel, C., Hense, A., 2007. Eemian and Early Weichselian temperature and precipitation variability in northern Germany. Quat. Sci. Rev. 26, 3311–3317.

Kukla, G.J., 1961. Lithologische Leithorizonte der tschechoslowakischen Lössprofile. Věstník 36, 369–372.

Kukla, G., 1975. Loess stratigraphy of Central Europe. In: Butzer, K.W., Isaac, G.L. (Eds.), After the Australopithecines. Mouton Publishers, The Hague, pp. 99–188.

Kukla, G., 1977. Pleistocene land-sea correlations I. Europe. Earth-Sci. Rev. 13, 307–374.

Kukla, G.J., Heller, F., Liu, X.M., Xu, T.C., Liu, T.S., An, Z.S., 1988. Pleistocene climates in China dated by magnetic susceptibility. Geology 16, 811–814.

Kukla, G., Cílek, V., 1996. Plio-Pleistocene megacycles: record of climate and tectonics. Palaeogeogr. Palaeoclimatol. Palaeoecol. 120, 171–194.

Lang, A., Hatté, C., Rousseau, D.-D., Antoine, P., Fontugne, M., Zöller, L., Hambach, U., 2003. High-resolution chronologies for loess: comparing AMS 14C and optical dating results. Quat. Sci. Rev. 22, 953–959.

Li, G., Chen, J., Chen, Y., Yang, J., Ji, J., Liu, L., 2007. Dolomite as a tracer for the source regions of Asian dust. J. Geophys. Res. 112, D17201. http://dx.doi.org/10.1029/2006JD007924.

Lisá, L., Hošek, J., Grygar, T., Bajer, A., Vandenberghe, D., 2014. Geoarchaeology of Upper Paleolithic loess sites located within transect through Moravian valleys, Czech Republic. Quat. Int. 351, 25–37. http://dx.doi.org/10.1016/j.quaint.2013.08.058.

Lisiecki, L.E., Raymo, M.E., 2005. A Pliocene–Pleistocene stack of 57 globally distributed benthic d ^{18}O records. Paleoceanography 20, 1–17.

Liu, X.M., Rolph, T., Bloemendal, J., Shaw, J., Liu, T.S., 1995. Quantitative estimates of paleoprecipitation at Xifeng, in the Loess Plateau of China. Palaeogeogr. Palaeoclimatol. Palaeoecol. 13, 243–248.

Liu, Q., Deng, C., Yu, Y., Torrent, J., Jackson, M.J., Banerjee, S.K., Zhu, R., 2005. Temperature dependence of magnetic susceptibility in an argon environment: implications for pedogenesis of Chinese loess/paleosols. Geophys. J. Int. 161, 102–112.

Liu, Q., Deng, C., Torrent, J., Zhu, R.X., 2007. Review of recent developments in mineral magnetism of the Chinese loess. Quat. Sci. Rev. 26, 368–385.

Liu, Q., Roberts, A.P., Larrasoaña, J.C., Banerjee, S.K., Guyodo, Y., Tauxe, L., Oldfield, F., 2012. Environmental magnetism: principles and applications. Rev. Geophys. 50, RG4002. http://dx.doi.org/10.1029/2012RG000393.

Ložek, V., 1964. Quartärmollusken der Tschechoslowakei. Rozp. Ú.ú. geol., Praha 31 (374 pp.).

Ložek, V., 1968. Mittel- und jungpleistozäne Löss Serien in der Tschechoslowakei und ihre Bedeutung für die Löss-Stratigraphie Mitteleuropas. INQUA-Report of the VIth International Congress on Quaternary-Warsaw, pp. 525–549.

Ložek, V., 1995. Sprašová rokle u Zeměch. 15/1. Nika Praha, pp. 30–31 (in Czech).

Maher, B.A., 1986. Characterisation of soils by mineral magnetic measurements. Phys. Earth Planet. Inter. 42, 76–92.

Maher, B.A., 1998. Magnetic properties of modern soils and Quaternary loessic paleosols: paleoclimatic implications. Palaeogeogr. Palaeoclimatol. Palaeoecol. 137, 25–54.

Maher, B.A., Alekseev, A., Alekseeva, T., 2003. Magnetic mineralogy of soils across the Russian Steppe: climatic dependence of pedogenic magnetite formation. Paleogeography Paleoclimatololy Paleoecology 201, 321–341.

Marković, S., Oches, E., Sumegi, P., Jovanovic, M., Gaudenyi, T., 2006. An introduction to the Upper and Middle Pleistocene loess–paleosol sequences of Ruma section (Vojvodina, Yugoslavia). Quat. Int. 149, 80–86.

Marković, S.B., Bokhorst, M.P., Vandenberghe, J., Mc Coy, W.D., Oches, E.A., Hambach, U., 2008. Late Pleistocene loess–paleosol sequences in the Vojvodina region, north Serbia. J. Quat. Sci. 23, 73–84.

Marković, S.B., Hambach, U., Catto, N., Jovanović, M., Buggle, B., Machalett, B., Zöller, L., Glaser, B., Frechen, M., 2009. Middle and Late Pleistocene loess sequences at Batajnica, Vojvodina, Serbia. Quat. Int. 198, 255–266.

Meier, L.P., Kahr, G., 1999. Determination of the cation exchange capacity (CEC) of clay minerals using the complexes of copper(II) ion with triethylenetetramine and tetraethylenepentamine. Clay Clay Miner. 47, 386–388.

Muhs, D.R., 2013. The geologic records of dust in the Quaternary. Aeolian Res. 9, 3–48.

Muhs, D.R., Bettis III, E.A., Been, J., McGeehin, J., 2001. Impact of climate and parent material on chemical weathering in loess-derived soils of the Mississippi River Valley. Soil Sci. Soc. Am. J. 65, 1761–1777.

Musson, F.M., Wintle, A.G., 1994. Luminescence dating of the loess profile at Dolní Věstonice, Czech Republic. Quat. Sci. Rev. 13, 411–416.

Nawrocki, J., Wojcik, A., Bogucki, A., 1996. The magnetic susceptibility record in the Polish and western Ukrainian loess-palaeosol sequences conditioned by palaeoclimate. Boreas 25, 161–169.

Nesbitt, H.W., Markovics, G., Price, R.C., 1980. Chemical processes affecting alkalis and alkaline earths during continental weathering. Geochim. Cosmochim. Acta 44, 1659–1666.

Nesbitt, H.W., Young, G.M., 1982. Early Proterozoic climates and plate motions inferred from major element chemistry of lutites. Nature 299, 715–717.

Nesbitt, H.W., Young, G.M., McLennan, S.M., Keays, R.R., 1996. Effects of chemical weathering and sorting on the petrogenesis of siliciclastic sediments, with implications for provenance studies. J. Geol. 104, 525–542.

North Greenland Ice Core Project (NGRIP) Members, 2004. High-resolution record of Northern Hemisphere climate extending into the last interglacial period. Nature 431, 147–151.

Oches, E.A., Banerjee, K., 1996. Rock-magnetic proxies of climate change from loess–paleosol sediments of the Czech Republic. Stud. Geophys. Geod. 40 (3), 287–300.

Oldfield, F., 2007. Sources of fine-grained magnetic minerals in sediments: a problem revisited. The Holocene 17, 1265–1271.

Panaiotu, C.G., Panaiotu, E.C., Grama, A., Necula, C., 2001. Paleoclimatic record from a loess–paleosol profile in southeastern Romania. Phys. Chem. Earth 26, 893–898.

Pécsi, M., 1990. Loess is not just the accumulation of dust. Quat. Int. 7, 1–21.

Perel'man, A., 1977. Geochemistry of Elements in the Supergene Zone. Keterpress Enterprises, Jerusalem (266 pp.).

Pye, K., 1987. Aeolian Dust and Dust Deposit. Academic Press, London (334 pp.).

Rivas, J., Ortega, B., Sedov, S., Solleiro, E., Sychera, S., 2006. Rock Magnetism & pedogenetic processes in Luvisol profiles: Examples from Central Russia & Central Mexico. Quanternary International. 156–157, 212–223.

Rolf, C., Hambach, U., Novothny, A., Horváth, E., Schnepp, E., 2014. Dating of a Last Glacial loess sequence by relative geomagnetic palaeointensity: a case study from the Middle Danube Basin (Sütto, Hungary). Quat. Int. 319, 99–108.

Rousseau, D.-D., Wu, N.Q., 1997. A new molluscan record of the monsoon variability over the past 130,000 yr in the Luochuan loess sequence, China. Geology 25, 275–278.

Rousseau, D.-D., Hatté, C., Guiot, J., Duzer, D., Schevin, P., Kukla, G., 2006. Reconstruction of the Grande Pile Eemian using inverse modeling of biomes and d13C. Quat. Sci. Rev. 25, 2806–2819.
Rousseau, D.-D., Ghil, M., Kukla, G., Sima, A., Antoine, P., Fuchs, M., Hatté, C., Debret, M., Moine, O., 2013. Major dust events in Europe during marine isotope stage 5 (130–74 ka): a climatic interpretation of the "markers". Clim. Past 9, 2213–2230.
Sánchez-Goñi, M.F., Eynaud, F., Turon, J.L., Shackleton, N.J., 1999. High resolution palynological record off the Iberian margin: direct land–sea correlation for the last interglacial complex. Earth Planet. Sci. Lett. 171, 123–137.
Schatz, A.-K., Scholten, T., Kühn, P., 2014. Paleoclimate and weathering of the Tokaj (NE Hungary) loess–paleosol sequence: a comparison of geochemical weathering indices and paleoclimate parameters. Clim. Past Discuss. 10, 469–507. http://dx.doi.org/10.5194/cpd-10-469-2014.
Shackleton, N.J., Sánchez-Goñi, M.F., Pailler, D., Lancelot, Y., 2003. Marine isotope substage 5e and the Eemian interglacial. Glob. Planet. Chang. 36 (3), 151–155.
Sirocko, F., Seelos, K., Schaber, K., Rein, B., Dreher, F., Diehl, M., Lèhne, R., Jäger, K., Krbetschek, M., Degering, D., 2005. A Late Eemian Aridity Pulse in central Europe during the last glacial inception. Nature 436, 833–836.
Smolíková, L., 1982. Fossil soils in loess series. Stud. Geophys. 80, 107–133.
Stoops, G., 2003. Guidelines for Analysis and Description of Soil and Regolith Thin Sections. Soil Science Society of America, Madison, Wisconsin (348 pp.).
Stoops, G., Marcelino, V., Mees, F., 2010. Interpretation of Micromorphological Features of Soils and Regoliths. Elseiver.
Sümegi, P., Krolopp, E., 2002. Quartermalacological analyses for modeling of the Upper Weichselian paleoenvironmental changes in the Carpathian basin. Quat. Int. 91, 53–63.
Sun, W.W., Banerjee, S.K., Hunt, C.P., 1995. The role of maghemite in the enhancement of magnetic signal in the Chinese loess–paleosol sequence: an extensive rock magnetic study combined with citrate-bicarbonatedithionite treatment. Earth Planet. Sci. Lett. 133, 493–505.
Svoboda, J., Škrdla, P., Ložek, V., Svobodová, H., Frechen, M., 1996. Predmosti II, excavations 1989–1992. In: Svoboda, J. (Ed.), Paleolithic in the Middle Danube Region. Spisy Archeologického Ústavu AVČR v Brně, Svazek 5, Brno, pp. 147–171.
Taylor, S.N., Lagroix, F., Rousseau, D.D., Antoine, P., 2014. Mineral magnetic characterization of the Upper Pleniglacial Nussloch loess sequence (Germany): an insight into local environmental processes. Geophys. J. Int. 199 (3), 1463–1480.
Thompson, R., Oldfield, F., 1986. Environmental Magnetism. Allen & Unwin Ltd., London (280 pp.).
Torrent, J., Barrón, V., Liu, Q., 2006. Magnetic enhancement is linked to and precedes hematite formation in aerobic soil. Geophys. Res. Lett. 33, L02401. http://dx.doi.org/10.1029/2005GL024818.
Tyráček, J., 1995. Zeměchy — loess gorge. In: Schirmer, W. (Ed.), Quaternary Field Trips in Central Europe, Eastern Alps Traverse. INQUA, Berlin, pp. 84–86.
Újvári, G., Varga, A., Balogh-Brunstad, Z., 2008. Origin, weathering, and geochemical composition of loess in southwestern Hungary. Quat. Res. 69, 421–437.
Újvári, G., Varga, A., Raucsik, B., Kovács, J., 2014. The Paks loess–paleosol sequence: a record of chemical weathering and provenance for the last 800 ka in the mid-Carpathian Basin. Quat. Int. 319, 22–37.
Urban, B., 1984. Palynology of central European loess–soil sequences. In: Pecsi, M. (Ed.), Lithology and Stratigraphy of Loess and Paleosols. Geographical Research Institute. Hungarian Academy of Sciences, Budapest, pp. 229–247.
van Velzen, A.J., Dekkers, M.J., 1999. Low-temperature oxidation of magnetite in loess–paleosol sequences: a correction of rock magnetic parameters. Stud. Geophys. Geod. 43, 357–375.
Vandenberghe, J., 2013. Grain size of fine-grained windblown sediment: a powerful proxy for process identification. Earth Sci. Rev. 121, 18–30.
Varga, A., Újvári, G., Raucsik, B., 2011. Tectonic versus climatic control on the evolution of a loess–paleosol sequence at Beremend, Hungary: an integrated approach based on paleoecological, clay mineralogical, and geochemical data. Quat. Int. 240, 71–86.
Vodyanitskii, Y.N., Vasil'ev, A.A., Gilev, V.Y., 2007. Iron minerals in soils on red earth deposits in the Cis-Ural region. Eurasian Soil Sci. 40, 432–444.
Wang, F., Sun, D., Guo, F., Wang, X., Li, Z., Zhang, Y., Li, B., Wu, S., 2012. Quantitative reconstruction of paleo-temperature and paleo-precipitation of Lingtai profile in Loess Plateau during the past 7 Ma. J. Earth Environ. 3, 781–791.
Woillard, G., 1978. Grand Pile Peat Bog: a continuous pollen record for the last 140 000 years. Quat. Res. 9, 1–21.
Yang, S.Y., Li, C.X., Yang, D.Y., Li, X.S., 2004. Chemical weathering of the loess deposits in the lower Changjiang Valley China, and paleoclimatic implications. Quat. Int. 117, 27–34.
Zander, A., Duller, G.A.T., Wintle, A.G., 2000. Multiple and single aliquot luminescence dating techniques applied to quartz extracted from Middle and Upper Weichselian loess, Zemechy, Czech Republic. J. Quat. Sci. 15, 51–60.
Zech, M., Zech, R., Zech, W., Glaser, B., Brodowski, S., Amelung, W., 2008. Characterisation and palaeoclimate of a loess-like permafrost palaeosol sequence in NE Siberia. Geoderma 143, 281–295.
Zech, R., Zech, M., Marković, S., Hambach, U., Huang, Y., 2013. Humid glacials, arid interglacials? Critical thoughts on pedogenesis and paleoclimate based on multi-proxy analyses of the loess–paleosol sequence Crvenka, Northern Serbia. Palaeogeogr. Palaeoclimatol. Palaeoecol. 387, 165–175.
Zeeden, C., Hambach, U., Steguweit, A., Anghelinu, M., 2010. Loess stratigraphy using palaeomagnetism: application to the Poiana Cireului archaeological site (Romania). Quat. Int. 240, 100–107.
Zeng, Q.Z., Brown, P.H., 2000. Soil potassium mobility and uptake by corn under differential soil moisture regimes. Plant Soil 221, 121–134.
Zhang, W., Yu, L., Lu, M., Zheng, X., Shi, Y., 2007. Magnetic properties and geochemistry of the Xiashu Loess in the present subtropical area of China, and their implications for pedogenic intensity. Earth Planet. Sci. Lett. 260, 86–97.
Zhu, R.X., Shi, C.D., Suchý, V., Zeman, A., Guo, B., Pan, Y.X., 2001. Magnetic properties and paleoclimatic implications of loess–paleosol sequences of Czech Republic. Sci. China Ser. D Earth Sci. 44, 385–394.
Zöller, L., Oches, E.A., McCoy, W.D., 1994. Towards a revised chronostratigraphy of loess in Austria with respect to key sections in the Czech Republic and in Hungary. Quat. Geochronol. (Quat. Sci. Rev.) 13, 465–472.

5.2.Fluviální procesy

Lisá, L., Lisý, P., Chadima, M., Čejchan, P., Bajer, A., Cílek, V., Suková, L. and Schnabl, P. (2012): Microfacies description linked to the magnetic and non-magnetic proxy as a promising environmental tool: Case study from alluvial deposits of the Nile river. Quaternary International, 266, pp. 25-33.

Grygar, T, Svetlik, I, **Lisa, L**, Koptikova, L, Bajer, A, Wray, DS, Ettler, V, Mihaljevic, M, Novakova, T, Koubova, M, Novak, J, Macka, Z, Smetana, M. (2010): Geochemical tools for the stratigraphic correlation of floodplain deposits of the Morava River in Straznicke Pomoravi, Czech Republic from the last millennium. CATENA , 80, 2, 106-121.

Quaternary International 266 (2012) 25–33

Contents lists available at ScienceDirect

Quaternary International

journal homepage: www.elsevier.com/locate/quaint

Microfacies description linked to the magnetic and non-magnetic proxy as a promising environmental tool: Case study from alluvial deposits of the Nile river

L. Lisa [a,*], P. Lisy [a], M. Chadima [a,b], P. Čejchan [a], A. Bajer [c], V. Cilek [a], L. Sukova [d], P. Schnabl [a]

[a] Institute of Geology, AS CR, v.v.i., Rozvojová 269, 165 00 Praha 6, Czech Republic
[b] Agico, Inc., Ječná 29a, 621 00 Brno, Czech Republic
[c] Faculty of Forestry and Wood Technology, Mendel University, Zemědělská 3, 613 00 Brno, Czech Republic
[d] Czech Institute of Egyptology, Faculty of Arts, Charles University in Prague, Celetná 20, 110 00 Praha 1, Czech Republic

ARTICLE INFO

Article history:
Available online 12 June 2011

ABSTRACT

Alluvial deposits within the Sabaloka Gorge and the Sixth Cataract, the Nile River, Sudan, represent a set of deposits with a high lithological variability. This is due to the geomorphology and short-time and intensive flood events resulting in aggradation and erosion of the alluvial zone. Human maintenance of the alluvial zone also plays a role. Therefore, these sediments seem to be ideal for a methodological case study to show how the lithological facies differ depending on the sedimentary dynamics of the river. Non-magnetic proxies together with TOC values depend on magnetic properties characterized by magnetic susceptibility and its frequency dependence.

1. Introduction

Fluvial sedimentation and erosion in the Nile River Valley is, according to Butzer and Hansen (1968), Williams and Adamson (1982), and Garzanti et al. (2006), driven mainly by flood hydrology and sediment yield of the major headwater catchments which are strongly influenced by Holocene climate changes (Woodward et al., 2001). The sediment source of the Nile River alluvium is usually detected by heavy mineral suites (Butzer and Hansen, 1968; Foucault and Stanley, 1989; Mahmoud and Hamdan, 2002), but recently, new methodologies, such as Sr isotopic measurements (Krom et al., 1999, 2002; Talbot et al., 2000; Weldeab et al., 2002; Stanley et al., 2003), Nd isotopic measurements (Freydier et al., 2001; Weldeab et al., 2002; Scrivner et al., 2004; Padoan et al., 2009), and stable carbon and oxygen isotopic measurements (Williams et al., 2000) have also been applied. Measurements of magnetic susceptibility, a widely used method for the assessment of environmental history and human impact on alluvial plains (Oldfield et al., 1979; Foster et al., 1998; Jordanova et al., 2003; Grygar et al., 2010), has been applied to the Nile alluvial record only rarely (El Fattah and Frihy, 1988).

Most of the work done on the Nile alluvial sediments has concentrated on the Egyptian part of the river. In spite of the fact that one of the first geomorphological and sedimentological works on the Nile River in Sudan was published in 1968 (Berry and Whiteman, 1968), the sedimentological record in the recent Holocene floodplain and the long-term behavior of the Sudanese Saharan Nile are still imperfectly known (Williams et al., 2000, 2010; Woodward et al., 2001).

Authigenic formations of new ferromagnetic minerals in soils, most frequently magnetite, maghemite or greigite, often lead to the enhancement of soil magnetism. As Evans and Heller (2003) pointed out, it should be kept in mind that these strongly magnetic minerals carry only a minor proportion of iron available in soils. With respect to magnetic enhancement, there are several possibilities how the magnetic signal can be influenced. The following five major processes are currently believed to be responsible (Dearing et al., 1996; Evans and Heller, 2003): 1.) The enhancement of magnetic susceptibility signal can be influenced by detrital input provided from the atmospheric fallout of fossil fuel-burning, metallurgical industries and cement factories. After landing, the particles penetrate into the soil profile and accumulate mostly in the uppermost fermentation and humic subhorizons. In this case, magnetic susceptibility will show very little frequency dependence because of the large particle size (Evans and Heller, 2003). 2.) Natural fires or crop burning may cause thermal transformation of magnetic minerals (Kletetschka and Banerjee, 1995). Fires affect the topmost soil layers and the degree of magnetic enhancement is highly variable. 3.) Inorganic *in situ* formation of

* Corresponding author.
E-mail addresses: lisa@gli.cas.cz (L. Lisa), lisy@gli.cas.cz (P. Lisy), chadima@sci.muni.cz (M. Chadima), cej@gli.cas.cz (P. Čejchan), bajer@mendelu.cz (A. Bajer), cilek@gli.cas.cz (V. Cilek), sukova.lenka@gmail.com (L. Sukova).

1040-6182/$ – see front matter © 2011 Elsevier Ltd and INQUA. All rights reserved.
doi:10.1016/j.quaint.2011.05.030

ultrafine-grained magnetite was described mainly for the environment with changing soil moisture and aeration in climate sequences. 4.) The enhancement of magnetic susceptibility in soils is also commonly interpreted as a presence of soil microorganisms which produce very small superparamagnetic minerals (Fassbinder et al., 1990). However, their low population densities in modern topsoils do not seem to provide a substantial contribution to the enhancement of magnetic susceptibility in soils. Frequency-dependent magnetic susceptibility, which is very sensitive to the presence of superparamagnetic grains, may be a useful tool for determining the relative amount of microorganic contribution to the magnetic enhancement of soils. 5.) The weathering of iron-bearing minerals during soil wetting and drying cycles, that is, a change in pedoenvironmental factors such as temperature, soil water activity, pH, organic matter content, and release rate of iron, may produce Fe^{2+} solutions that are oxidized and favored by the presence of organic matter form ferrihydrite when critical concentrations are achieved (Evans and Heller, 2003). The reduction of ferrihydrite in high Eh conditions under the short-lived periods of anaerobicity in well drained soils can be followed by the so-called fermentation when iron-reducing bacteria produce soluble Fe^{2+} ions in soils (Schwertmann, 1988). A partial dehydration and reduction of ferrihydrite to magnetite will finally take place in the presence of excess Fe^{2+} giving rise to the enhancement of soil magnetic properties (Evans and Heller, 2003).

Considering the last mentioned possible reason for magnetic susceptibility enhancement, the total amount of organic carbon (TOC) has to be taken into account. The organic carbon content and grain-size distribution may serve as proxies for, e.g., the intensity of pedogenesis, weathering and palaeowind strength. The possible correlation of magnetic susceptibility with TOC was used by Schatz et al. (in press) and Brachfeld and Banerjee (2000). Organic matter is one of the most important soil components because it influences the physical and chemical properties of soils far out of proportion to the small quantities present. The TOC generally provides information about the amount of organic matter in a sample. Furthermore, organic matter supplies energy and body-building constituents for most of the microorganisms (Brady, 1990).

The aim of this paper is to introduce the highly variable sedimentological record of the Holocene alluvial plain of the Nile River within the Sabaloka Gorge and near the Sixth Cataract in Sudan (Fig. 1), and to show how such high lithological variability can be correlated with the variation in magnetic properties and other factors, such as lithology, micromorphology, grain-size distribution, or the amount of total organic carbon (TOC).

2. Sampling and geological setting

In 2009, the Czech Institute of Egyptology, Charles University in Prague, and the Institute of Geology, Academy of Sciences of the Czech Republic, carried out geoarchaeological research within the area of Sabaloka and the Sixth Nile Cataract in Sudan (Fig. 1). The objective of this research was to attain a better understanding of the history of the Nile, climatic changes in the Holocene, and their impact both on the landscape and the human society. One of the main tasks of the geoarchaeological research was to study the sedimentary record of the Nile alluvial zone.

The area included in this study covers approximately 25 km of the Nile River banks within the Sabaloka Gorge and near the Sixth Cataract (Fig. 1). The present surface of the alluvial plain within the gorge lies generally 5 m above the water level. To date, no sedimentological studies concerning the Holocene alluvial plain within the Sabaloka Gorge have been reported. The background geology is represented by the so-called Sabaloka Igneous Complex.

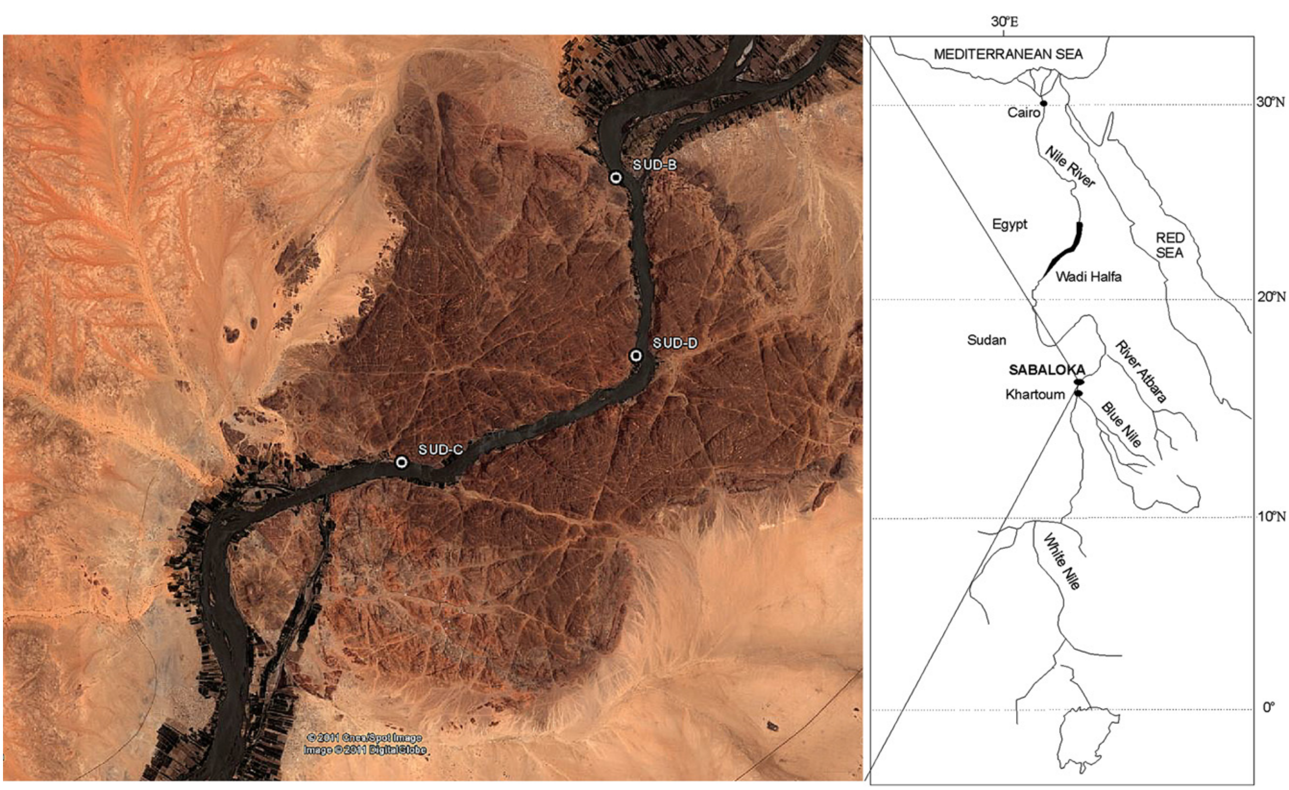

Fig. 1. Location of study area in the context of North Africa together with the location of the studied sections within the Sabaloka Gorge and near the Sixth Cataract. Source: Google Earth 2010.

It represents one of the best exposed granitic complexes in Sudan, and has been dated to the Proterozoic or early Paleozoic. The granite complex is overlain by volcanic rocks and circumscribed by a polygonal zone of ring-fracturing. The fracture system was intruded by a ring dyke of porphyritic microgranite and – at about the same time – mica granite with associated tin–tungsten mineralization was injected into the subsided block (Almond, 1979, 1980).

During the investigation, three, approximately 5-m-high sections (Sections B–D; Fig. 2) were excavated into the exposed banks of the Nile River. These sections were described from the viewpoint of sedimentology and sampled for magnetic, geochemical and grain-size studies at intervals of 10 cm or less when significant lithological or grain-size change occurred. In order to confirm or exclude any possible pedogenic processes, magnetic susceptibility values were correlated with grain-size analyses and the total amount of organic carbon (TOC), and, finally, compared with the results of micromorphological analyses. Additional samples were taken for dating purposes.

3. Methodology

Magnetic susceptibility was measured using an Agico MFK1-FA Kappabridge at two different operating frequencies, $f_1 = 976$ Hz and $f_3 = 15\ 616$ Hz; amplitude of AC field was 200 A/m, peak value. Using this instrument, the variation in the frequency dependence on the order of 1% is well reproducible and the measurements can be interpreted in terms of magnetic granulometry even in weakly magnetic materials (Hrouda and Pokorny, in press). Unconsolidated samples were measured in plastic bags; measured susceptibility was normalized by the mass of each sample and expressed as mass susceptibility [m^3/kg].

Frequency-dependent magnetic susceptibility, κ_{FD}, is characterized by the following commonly accepted parameter (Dearing et al., 1996):

$$\kappa_{FD} = 100 \times \left(\kappa_{f1} - \kappa_{f3}\right) \Big/ \kappa_{f1} [\%]$$

where κ_{f1} and κ_{f3} are susceptibilities at frequency f_1 (976 Hz) and frequency f_3 (15 616 Hz), respectively.

Additional magnetic parameters were measured for each of facies divided on the base of micromorphology. S-parameter is the absolute value of backfield IRM (bIRM) divided by SIRM, which is a dimensionless quantity between 0 and 1. This parameter was calculated for two backfields 100 mT and 300mt. ARM/SIRM ratio is a dimensionless quantity as well. HIRM value was calculated as SIRM value minus absolute value of bIRM(300). Units of this parameter are A/m. Those additional parameters were measured in Paleomagnetic laboratory GLI AS CR, v. v. i. in Pruhonice, Prague.

Grain-size distribution was measured using the Mastersizer laser granulometer, and five grain-size categories were distinguished: 0.1–2 mm (sand); 0.05–0.1 mm (fine sand); 0.01–0.05 (silt); 0.05–0.002 mm (very fine silt); <0.002 (clay). The dependence between magnetic susceptibility, frequency-dependent susceptibility, and grain-size was calculated by means of correspondence analysis.

Total carbon (TC) concentrations (in weight percent) were obtained for subsamples of dry sediment of known weight (~0.5 g) using a PRISMACS analyzer, which combusts the sample in an electric arc at the presence of oxygen and quantifies the carbon dioxide produced to give percentages of total carbon and total sulfur. A further subsample of sediment was fired at 500 °C for 24 h to remove organic carbon, and the carbon content was then determined using a Leco analyzer to obtain total inorganic carbon (TIC) concentrations (in weight percent). The total organic carbon (TOC) content (in weight percent) was determined from the difference between the total carbon and total inorganic carbon concentrations.

Lithologically different strata were sampled into small Kubiena boxes (5 × 3 cm) for the purpose of microstratigraphical studies. Altogether 50 micromorphological samples were taken. The aim was to determine the material composition, its microstructure, the presence of redeposited or *in situ* pedogenic features, and the amount of pores and their relation to the surrounding matrix.

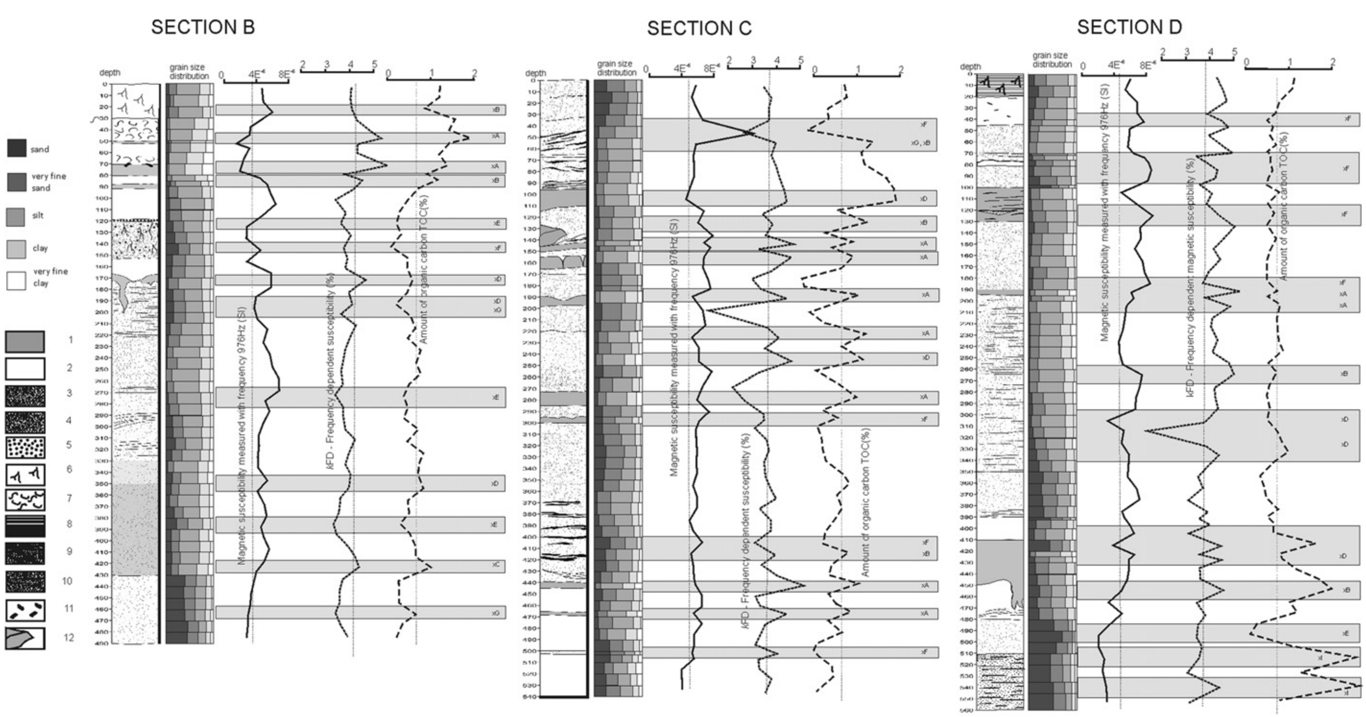

Fig. 2. Correlation among lithology, magnetic susceptibility (κ), frequency-dependent magnetic susceptibility (κ_{FD}), and total amount of organic carbon (TOC) values in Sections B–D.

The samples were dried, impregnated in vacuum, and then thin sectioned. The soil thin sections were studied using a polarizing microscope. The interpretations followed the papers of Stoops (2003), Stoops et al. (2010) and Bullock et al. (1985).

4. Results

4.1. Litho- and pedostratigraphy

The lithological and pedostratigraphic description employs lithological and pedogenic criteria, magnetic susceptibility and frequency-dependent susceptibility variations, grain-size distribution, and TOC values (Table 1). Chosen magnetic proxies were also controlled by additional magnetic properties including ARM, IRM, SIRM, S-ratio (100), S-ratio(300), HIRM and the ratio ARM/SIRM measured of every facies type divided on the base of micromorphological observations (Table 2). The descriptions of the three studied sections are presented in Fig. 2. Generally, the lithology is similar throughout the study area, although the position of soils or organic matter accumulations varies. The lithological and pedostratigraphic descriptions of the studied sections together with the grain-size distributions of different facies (Table 1) show a high variability.

The first of the sections, Section B (Fig. 2), contains macroscopically homogeneous sandy loams below the depth of 180 cm. This part of the section differs mainly by the presence of well expressed sedimentary structures (bedding) at depths of 180–220 cm, 270 cm, 290–300 cm, and 310–330 cm. Gleying is well expressed at the depth of 330–430 cm. The upper parts of Section B show a much higher variability including clearly expressed buried soils at a depth of 120–152 cm and recent soil at a depth of 0–30 cm. The humus-rich intervals may represent Nile mud or redeposited A horizons of newly developed anthropogenic soils. They are macroscopically preserved at depths of 30–50 cm, 50–52 cm, 60–70 cm, 70–80 cm, 91–89 cm, and 170–180 cm. The charcoal concentrations are best expressed at a depth of 70 cm under the surface.

The second of the sections, Section C (Fig. 2), shows much higher lithological variability. The clearly developed buried or recent A horizons of soils are missing. The very base of the section, approximately below the depth of 440 cm, is composed of loam with one sandy interval at a depth of 500 cm and two humus-rich intervals at depths of 440–445 cm and 468–470 cm. This loamy part of the section is overlain, at a depth of 370–440 cm, by sandy loam with visibly preserved lenses rich in partly decomposed organic matter. The same lithological situation is preserved at a depth of 0–95 cm under the surface. The rest of the lithological record is composed of sandy loam with structures typical for ripples and interrupted by intervals of humus-rich material at depths of 95–112 cm, 148–152 cm, 155–165 cm, 190–200 cm, 272–285 cm, and 296–300 cm, which may represent redeposited Nile mud or anthropogenically developed A horizon. Such an interval at a depth of 155–165 cm contains desiccation cracks up to 5 cm wide and up to 10 cm deep.

The third of the studied sections, Section D (Fig. 2), shows a relatively high variability as well. Sandy loams with preserved partly decomposed organic layers constitute the most common sedimentological features and are well expressed mainly at depths of 195–350 cm, 380–390 cm, 470–480 cm, and 510–560 cm. Sandy intervals are well expressed at depths of 350–380 cm and 480–510 cm. The rest of the lithological record is composed of sandy loam with structures typical for ripples and interrupted by intervals of humus-rich material at depths of 100–130 cm, 190–194 cm, and 410–450 cm, which can represent redeposited Nile mud or anthropogenically developed A horizon. Such an interval at a depth of 410–420 cm contains desiccation cracks up to 5 cm wide and up to 10 cm deep. Well expressed A horizon of soil lies on the surface at a depth of 0–20 cm. The loamy interval below, at a depth of 20–45, is rich in charcoal.

4.2. Micromorphology

Based on the distinctive micromorphological characteristics, nine different facies types marked as xA–xI were distinguished. Table 1 provides a summary of the identified facies types together with the typical values of magnetic susceptibility, frequency-

Table 1
Basic facies types of the Nile River alluvial deposits. The indexes used are: $\varkappa_{FD}$ – magnetic susceptibility, $\varkappa$ – frequency-dependent magnetic susceptibility, F1 to F5 – grain-size fractions (F1 – 0.1–2 mm; F2 – 0.01–0.05 mm; F3 – 0.05–0.1; F4 – 0.01–0.002 mm; F5 – <0.002 mm), TOC – total amount of organic carbon.

Faciestype	Distinctive Micromorphological characteristics	Changes in measured values
xA	Nile mud in situ - platy microstructure of laminated loam, prevailing voids are plates and material has close porphyric related distribution. Presence of humus and decomposed organic matter.	$\varkappa$ – average or decrease $\varkappa_{FD}$ – increase TOC – increase
xB	Secondarily redeposited nile mud - granular to inter-grain microaggregate microstructure of redeposited humus-rich loam, single packing voids and compound packing voids, granular structural type, presence of charcoal, decomposed and partly decomposed organic matter.	$\varkappa$ – average or increase $\varkappa_{FD}$ – average or increase TOC – average or increase
xC	Antropogenically influenced horizon of nile mud–intergrain microaggregate and subangular blocky microstructure of sandy loam, compound packing voids and vesicles, porphyric related distribution, partly decomposed organic matter, charcoal, carbonate concentration with microcharcoal, bioturbation.	$\varkappa$ – average $\varkappa_{FD}$ – increase TOC – increase
xD	Ripples composed of heavy minerals and organic matter - layers of opaque mineral concentrations and layers of clay to sandy loam with positive gradation and the diffuse enhancement of humic material. Platy and inter-grain microaggregate microstructure, plates, porphyric related distribution, chambers, rare charcoal and partly decomposed organic matter.	Different behavior according to the prevailing type of material in the measured sample (eg. Section C depth 250 like xA; Section C depth 270 like xG; Section D depth 320 like xF)
xE	Fluvial sands - sands and sandy loam rich in opaque minerals, simple packing voids, and vesicles, mono-related distribution with rare flakes of partly decomposed organic matter and rare presence of opaque mineral lenses.	$\varkappa$–average or decrease $\varkappa_{FD}$ – average or decrease TOC – decrease
xF	Fluvial sands rich in heavy minerals - sands and sandy loam rich of opaque minerals, simple packing voids, and vesicles, mono-related distribution with abundant presence of opaque mineral lenses and rare flanks of partly decomposed organic matter.	$\varkappa$ – average or increase $\varkappa_{FD}$ – average or increase TOC – decrease
xG	Fluvial sands rich in organic matter - platy and microaggregate microstructure of sandy loam, with porphyric related distribution, plates, and horizontally oriented flakes of partly decomposed organic matter.	$\varkappa$ – average $\varkappa_{FD}$ –average or decrease TOC – average or increase
xI	Accumulation of organic matter and charcoal -accumulations of charred and non–charred non–decomposed and partly decomposed organic matter, mono-distribution, single grain microstructure of sandy material.	$\varkappa$ – decrease $\varkappa_{FD}$ – average or increase TOC – increase

Table 2
Values of magnetic proxies measured for facies types divided on the base of micromorphology: S-parameter is absolute value of backfield IRM (bIRM) divided by SIRM, which is dimensionless quantity within interval 0 and 1. This parameter was calculated for two backfields 100 mT and 300mt. ARM/SIRM ratio is dimensionless quantity as well. HIRM value was calculated as SIRM value minus absolute value of bIRM(300). Units of this parameter are A/m.

	χ	χ_{FD}	ARM	IRM	SIRM	S-ratio(100)	S-ratio(300)	HIRM	ARM/SIRM
xA	7.86×10^4	3.19	1.37	31.19	143.28	0.83	0.98	2.23	0.009
xB	6.57×10^4	4.04	1.28	24.77	121.94	0.79	0.94	6.56	0.010
xC	4.99×10^4	4.78	1.20	18.74	82.23	0.78	0.99	0.59	0.014
xD	8.09×10^4	3.23	1.32	33.88	143.88	0.77	0.94	7.46	0.009
xE	5.72×10^4	3.19	1.31	27.16	114.47	0.79	0.98	1.94	0.011
xF	6.68×10^4	3.01	1.00	24.77	116.11	0.79	0.96	4.47	0.008
xG	4.73×10^4	3.07	1.02	19.85	94.47	0.78	0.98	1.49	0.010
xI	4.48×10^4	4.28	0.64	13.11	71.94	0.84	0.99	0.14	0.008

dependent magnetic susceptibility and amount of total organic carbon. The photographic documentation of the different facies types is presented in Fig. 3. Generally, two main types of material were observed. They differ mainly in the grain-size composition and abundance of fine-grained humic material. Within these two types of material, individual facies were distinguished, differing in the presence of charcoal, carbonate concentration, intensity of bioturbation, or the presence of oxidation and reduction features (xA, xB, xC and xI), or in the presence of partly decomposed organic matter accumulations or the accumulations of opaque minerals (xD, xE, xF, xG and xH).

4.3. Magnetic susceptibility and frequency-dependent susceptibility

Most of the magnetic susceptibility values (all three sampled sections taken together) vary between 3.5 and 8.5×10^{-6} m^3/kg. There are no significant differences in magnetic susceptibility values among the three sampled sections, suggesting no or little lateral variability in lithology. Magnetic susceptibility depends on the grain-size of the studied sediments. Using the principal component (PCA-R-MODE) analysis, good correlations were determined among silt, very fine sand and magnetic susceptibility (Fig. 4). Very strong links exist among the frequency-dependent

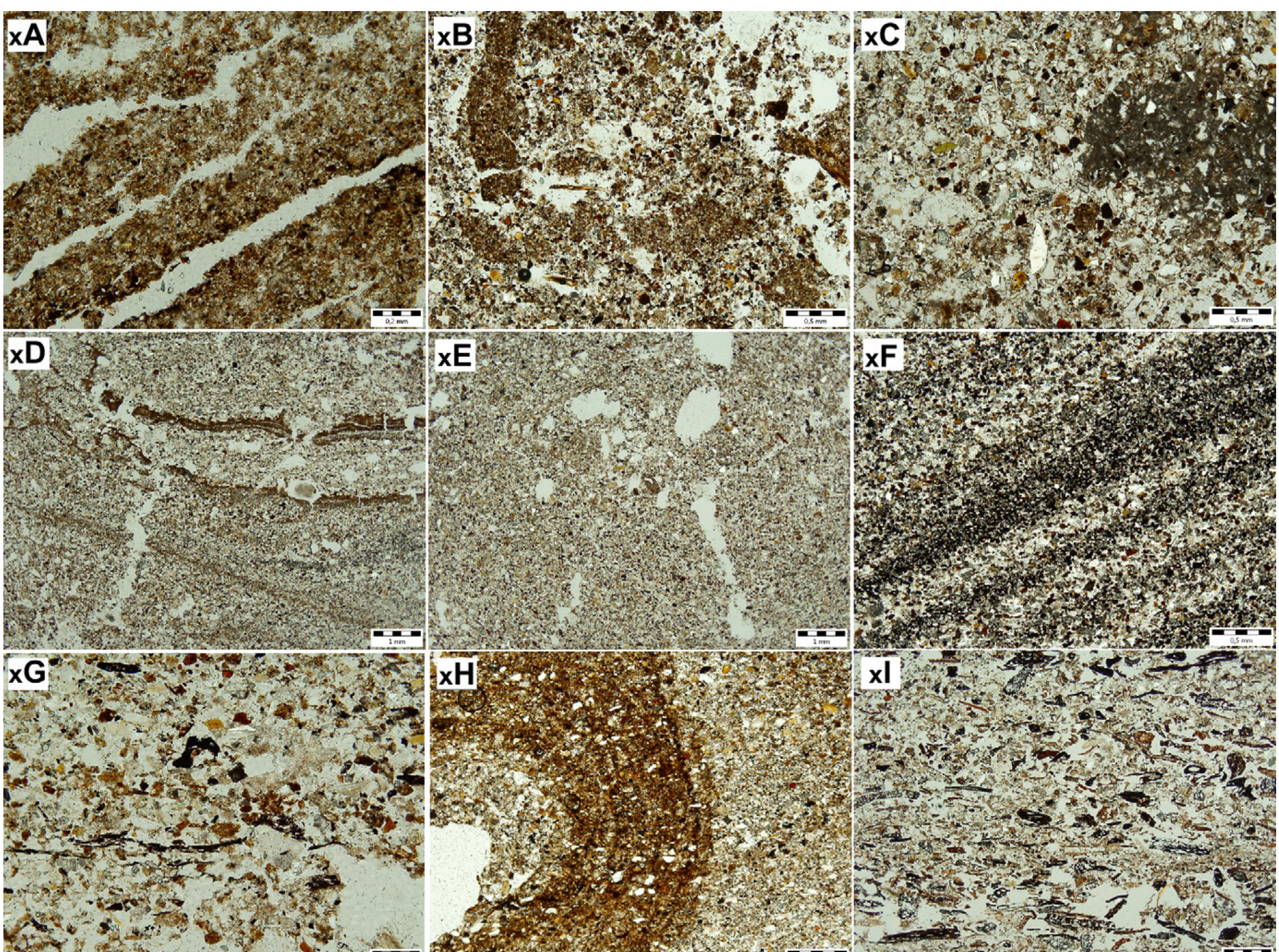

Fig. 3. Microphotographic documentation of the different facies types with the most distinctive micromorphological features.

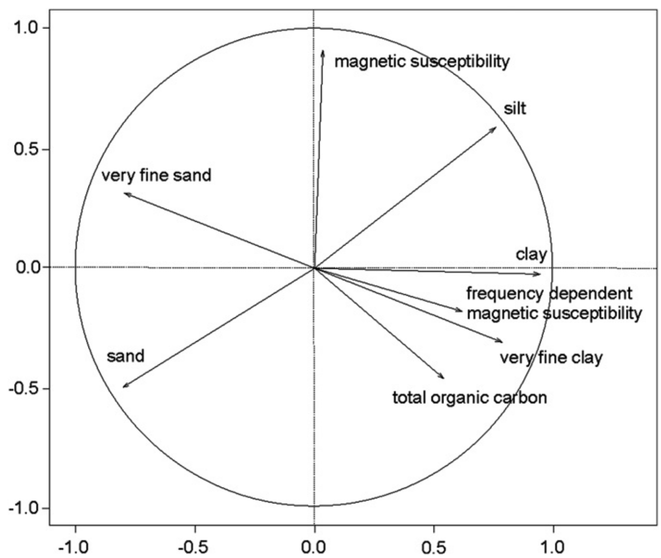

Fig. 4. Results of the principal component (PCA-R-MODE) analysis for Sections B–D. When the arrows meet at a sharp angle, the variables are well correlated; when the arrows meet at more or less right angle, the variables are independent of each other. When the arrows form angles of 180°, the variables are negatively correlated. The length of the arrows is proportional to the degree of variability of the illustrated variables; 50.27 of variability is explained by the axis x and 23.34 of variability is explained by the axis B.

magnetic susceptibility, very fine clay and the values of organic carbon. On the other side, the non-magnetic proxies, i.e. TOC and very fine clay together with sands, do not correlate with the values of magnetic susceptibility; this implies that material of such grain-size possess relatively low magnetic susceptibility (Fig. 4).Coarse-grained sands are mainly composed of diamagnetic minerals such as quartz; their increased presence in a sample decreases the bulk magnetic susceptibility. Fine-grained clays, due to their low depositional energy, do not contain as high proportion of heavy and/or magnetic minerals as slightly coarser silts; as a result, they possess relatively lower susceptibility values.

Most of the values of the frequency-dependent susceptibility range between 2 and 6%. These values are relatively low, suggesting only a little contribution of superparamagnetic grains to magnetic susceptibility. There are no significant differences in the frequency-dependent susceptibility among the three sampled sections. It seems that the frequency-dependent susceptibility depends on the grain-size of the studied sediments with finer-grained fractions (clay and silts) which show elevated values (Fig. 4). Samples with a significant amount of sand fraction show relatively low values of frequency-dependent susceptibility. There is a slight negative correlation between magnetic susceptibility and its frequency dependence; the high-susceptibility samples are less frequency-dependent compared to the low-susceptibility samples (Fig. 2).

4.4. Additional magnetic parameters

The results of the additional magnetic proxy measurements correspond to the interpretations based on sedimenthological and micromorphological interpretations. Facies types xB, xD and xF show not only presence of magnetite, but also presence of hematite and goethite (minerals with high coercivity) while the facies types xA, xC, xE, xF, xG and xI show the appearance of low coercivity minerals, i.e. magnetite and maghemite. The enhancement of very fine-grained minerals is visible in the case of faciesfacies types xA, xB, xC, xD and xE, while the other facies types show the coarser magnetic fractions. The proportion between magnetite and hematite is higher mainly in the case of facies types xA and xI, but as visible from the parameter S ratio (300) the most evident signal is given by the presence of magnetite, which is according to the parameters S ratio (100) and ARM/SIRM probably of single-domain type.

4.5. Grain-size distribution and TOC

The grain-size distribution almost continuously covers all grain-size categories (Fig. 2). This method allows interpretation of the sedimentary dynamics in cases where the material seemed to be macroscopically quite homogeneous. Organic matter was not excluded before the measurement, so the results reflect not only the presence of a coarser fraction, but also the presence of organic matter flakes. It is difficult to mechanically separate fractions with and without organic flakes because a chemical removal of organic matter would also remove very fine humic material which represents an important fraction in some lithological facies. The proportion of organic flakes was therefore determined microscopically.

Generally, humic-rich intervals are more clayey or loamy (Figs. 2 and 4), whereas there is a high variability between the amount of organic matter and sand-sized fraction. There seems to be a trend of the positive grading of the fraction below 0.002 mm at depths of 430–400 cm, 350–270 cm, and 80–0 cm in the case of Section B, and at a depth of 440–300 cm in the case of Section C. This grading reflects sedimentation within a single event, so the section with less variability (Section B) reflects, at the same time, a small number of single events.

The highest amounts of total organic carbon are connected with the macroscopically humus-rich darker intervals and the presence of charcoal or partly decomposed organic matter. Within Section B (Fig. 2), the highest value of TOC is up to 2 percent at a depth of 50 cm. The average proportion of TOC lithologically connected with humic-rich intervals is about 1%. Surprisingly, the macroscopically described horizon A of the buried soil at a depth of 120–150 cm shows the TOC proportion below 0.2%, i.e., the same as the average TOC of sandy loam or sand without macroscopic evidence of decomposed organic matter or humic material. The average TOC proportion in intervals macroscopically rich in partly decomposed organic matter is about 0.8%. In some cases, as in the case of enhanced TOC values in sandy loam at a depth of 420 cm, the presence of high organic content was detected only on a chemical basis. The variability of TOC within Section C (Fig. 2) reflects the lithological variability. Macroscopically humic-rich intervals are reflected by the enhancement of TOC to up to 2% at a depth of 110 cm; generally, the TOC average of 1% within these intervals is the same as in Section B. Also, as in Section B, the average TOC proportion in intervals macroscopically rich in partly decomposed organic matter is about 0.8% and the average TOC proportion in sandy loam without macroscopic evidence of decomposed organic matter or humic material is less than 0.2%. The highest TOC proportion of 2.8% was documented at the base of Section D (Fig. 2). From the viewpoint of lithology, this enhancement is connected with the presence of partly decomposed organic matter or with charcoal. Charcoal, much like organic matter, is relatively light and its accumulation can correspond with erosional processes at the beginning of the flooding event. As in the case of Sections B and C, the highest amount of TOC lithologically connected with humic-rich and charcoal intervals is 2% (at a depth of 450 cm). The average TOC value of intervals lithologically connected with partly decomposed organic matter (except the material below the depth of 510 cm) is about 0.8%. Horizon A of the recent soil has the TOC value of up to 1%. Generally, the value of TOC in Section D is the lowest one of all the compared sections.

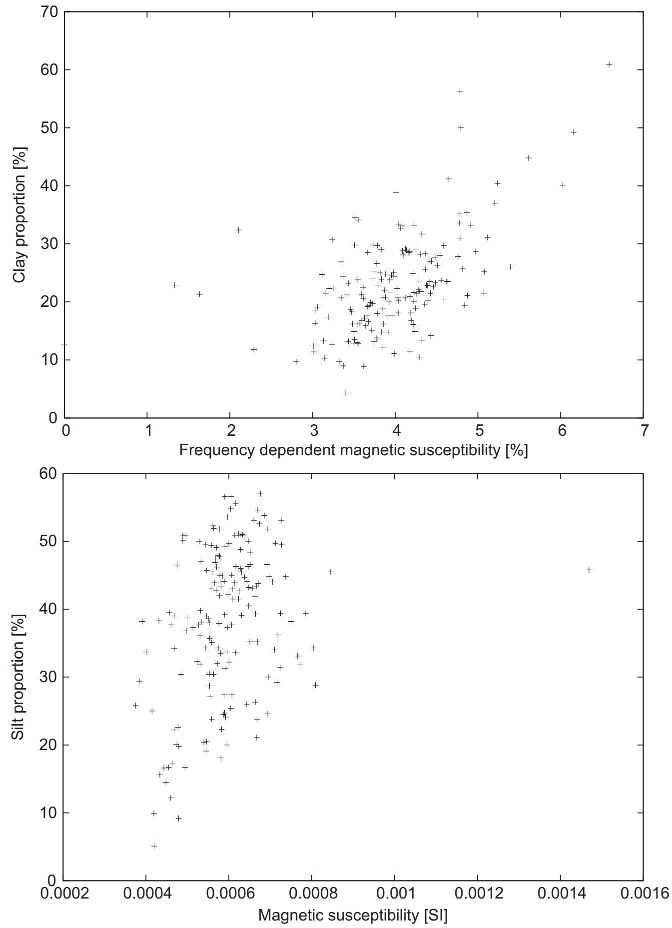

Fig. 5. Cross plot diagram of Magnetic susceptibility and silt fraction and for the frequency-dependent magnetic susceptibility and the clay fraction.

5. Discussion

5.1. Magnetic susceptibility and grain-size distribution as proxies for depositional energy

The grain-size of alluvial deposits reflects the depositional energy (Brown, 1997). While the coarse fraction, composed mainly of the most abundant diamagnetic mineral quartz, needs a relatively strong depositional energy and forms mainly levee structures along river banks, the finer grain-size fraction allows less depositional energy and such deposits form more distal parts of the alluvial plain (Bridge, 2003; Charlton, 2008). The situation within the Sabaloka Gorge is even more complicated, because in some parts the river channel is very narrow, while in others parts it widens to more than 2 km. The lithological variability was characterized from the viewpoint of sedimentology, micromorphology, TOC, magnetic susceptibility (κ) and frequency-dependent magnetic susceptibility (κ_{FD}) by the erection of facies types xA–xI. How and why these types differ in various depositional environments is a question of depositional energy and human influence.

The coarse fraction is usually composed of quartz, but a special type of sedimentation (similar to beach sands) occurs in some cases. These sediments (xD facies type) are rich in heavy opaque and magnetic minerals which can influence the enhancement of (κ). Therefore, the elevated proportions of coarse-grained fraction may correspond to low magnetic susceptibility due to the prevailing quartz (xE facies type) or abundance of flakes of organic matter (xG or xI facies types). In contrast, high magnetic susceptibility of relatively coarse material can occur due to the concentration of magnetic minerals within the heavy fraction (xF facies type). As visible from Figs. 4 and 5, the magnetic susceptibility is dependent mainly on the presence of silt fraction, while the frequency-dependent magnetic susceptibility vary according the presence of clay fractions. The concentrations of heavy minerals can be identified macroscopically as black opaque mineral accumulations. Therefore, the facies types xD, xE, xF and xG can be interpreted as high-energy depositional environments. In spite of the fact facies type xI was included in the above mentioned characteristics of high-energy environment, the organic matter is light enough to be carried and accumulated by low-energy water.

5.2. Correlation between the TOC and depositional energy

A positive correlation was found between the frequency-dependent magnetic susceptibility and the values of total organic carbon (Fig. 4). The total organic carbon is preserved usually as a part of very fine-grained humic matrix within the suspended load, but also as partly decomposed organic matter and charcoal included in relatively coarse fraction, as visible from micromorphological descriptions (Table 1) and field observations. As long as very fine-grained material of suspended load experiences rather upward-directed turbulent motions than the combination of downward-directed turbulent motions and gravitational settling, it will remain in suspension (Bridge, 2003). The timing of the deposition is the final part of the flooding event, and the most suitable parts of the alluvial plain are the morphologically predisposed lateral embayments. Such morphological features act as natural traps for the so-called lag deposits (Charlton, 2008). All three sections described in this paper are located at such positions within the landscape.

In some of the documented situations, the TOC values positively correlated with the coarser fraction (Figs. 2 and 4). These situations are microscopically visible as organic flakes but are sometimes well visible also macroscopically (Fig. 6). Such features are composed of partly decomposed organic matter as well as by charcoal. It seems that the timing of the deposition is the beginning of the flooding event, when the organic matter or charcoal resting on the surface of an antropogenically maintained alluvial plain become redeposited. Charcoal concentrations can be found on the surface of the alluvial plain as a result of the so-called "slash and burnt" management used in a pasture type of management (Abusuwar, 2007; El Tayeb, 2010). The grasses are annually burned to produce fresh new pasture. The accumulations stay undisturbed until the next high flooding event (Fig. 7).

Fig. 6. Origin of structural features within the suspended load macroscopically observed after the flood event.

Fig. 7. Textural features composed of microcharcoal, documenting the initial phases of the flooding event.

5.3. Deposition and redeposition of the Nile mud and agricultural processes

The fine fraction in the Sabaloka alluvial sediments, usually composed of silt and clay, occurs mostly in the form of thin intervals (max. 10 cm) of darker material. This material is the product of suspended load sedimentation which occurs at the end of flooding event, and its provenance from the area of Blue Nile sources can be expected. This suspended load is material derived from the fields, as can be presently observed. Three main facies types (xA–xC) were distinguished in this type of fine-grained material. Facies type xA corresponds to the primary deposited suspended load. Once this material is exposed to oxygen and heat, it starts to dry and shrink (Fig. 5). These post-depositional processes lead to the formation of platy microstructure with prevailing void plates. The high amount of partly decomposed organic matter and humus expressed by a high amount of TOC occurs as a natural part of material deposited from the source areas. Magnetic susceptibility of such material is usually quite low, while the frequency-dependent susceptibility shows a visible enhancement.

When fluvial erosion influences previously deposited suspended load, flakes of the dried mud will be deposited further downstream. The depositional energy must be higher because the material is much coarser. The erosion of once dried and shrunk mud is higher when agriculturally maintained or destructed, for example, by trampling. This facies type was marked as xB. Erosion and depositional processes lead to the origin of granular to intergrain microaggregate microstructure with single packing and compound packing voids. Facies type xB is usually rich in charcoal because redeposition usually takes place some time after the primary deposition, and because of the human presence. Magnetic susceptibility and frequency-dependent magnetic susceptibility of such a material are usually moderate or slightly enhanced due to the mixing with coarser diamagnetic material during redeposition.

Once types xA or xB are anthropogenically influenced, the internal microstructure changes into an inter-grain microaggregate and subangular blocky microstructure with compound packing voids and vesicles and with porphyritic-like distribution. The material is bioturbated and rich in partly decomposed or decomposed organic matter, charcoal or microcharcoal. It is also rich in carbonate due to fertility maintenance and plant growing. Magnetic susceptibility of such material is moderate and the frequency-dependent magnetic susceptibility is enhanced due to the fertility maintenance (burning of organic matter) and bacterial processes during the pedogenesis.

6. Conclusions

Sediments of the alluvial zone within the Sabaloka Gorge, the Sixth Cataract, in Sudan were described and subdivided into nine facies types according to their magnetic properties, grain-size distribution, and the amount of organic carbon. The observed lithological alternations reflect changes in energy of the depositional environment and are also influenced by human activities.

Generally, the high-energy depositional environment is represented by coarse fractions. Magnetic susceptibility enhancement depends mainly on the presence of silt fraction and the heavy mineral accumulations, which are macroscopically visible in lenses of opaque minerals. Frequency-dependent susceptibility is moderate or low in high-energy environment and its enhancement depends mainly on the appearance of clay fractions. The amount of total organic carbon varies and depends on the presence of presence of flakes of partly decomposed organic matter.

The low depositional energy of suspended load environment is represented by intervals of darker silts and clays. Magnetic susceptibility is usually moderate or low, while the frequency-dependent magnetic susceptibility is elevated. The total amount of organic carbon is also high and reflects the presence of organic matter in different stages of decomposition. Three facies types were distinguished within the low-energy depositional environment. The first one, marked as xA and composed of very fine-grained, laminated silt material, represents suspended load as a sedimentological record of the final phases of the flooding event. Once it is exposed to oxygen and heat, it starts to dry and shrink. When agriculturally maintained, the material is enriched in charcoal and becomes liable to erosion. This material is then redeposited by water further downstream (the second facies type marked as xB) or buried as a subfossil agriculturally influenced horizon A (the third facies type marked as xC).

The high depositional energy of the bedload environment is represented by five additional facies types (xE, xF, xG and xI facies types), which differ from one another in their structural features or in the presence or absence of some component, such as heavy mineral accumulations, charcoal or partly decomposed organic matter.

Acknowledgments

The geoarchaeological research in the area of Sabaloka and the Sixth Nile Cataract was financed from the funds granted by the Academy of Sciences of the Czech Republic (international cooperation project No. M100130902 and institutional research plan No. AV0 Z 30130516) and by the Grant Agency of the Charles University in Prague (project No. 15009). We wish to thank the National Corporation for Antiquities and Museums of Sudan for the permission to carry out the works in the area of Sabaloka and to Murtada Bushara, an inspector of the NCAM, for his engagement in the fieldwork.

References

Abusuwar, A. O., 2007. Range management. UNESCO Chair on Desertification, University of Khartoum.

Almond, D.C., 1979. The Sabaloka igneous complex, Sudan. Philosophical Transactions of the Royal Society of London. Series A, Mathematical and Physical Sciences 287 (1348), 595–633.

Almond, D.C., 1980. Precambrian events at Sabaloka, near Khartoum, and their significance in the chronology of the basement complex of North-East Africa. Precambrian Research 13 (1), 43–47.

Berry, L., Whiteman, A.J., 1968. The Nile in the Sudan. The Geographical Journal 134 (1), 1–33.

Brachfeld, S.A., Banerjee, S.K., 2000. Rock-magnetic carriers of century-scale susceptibility cycles in glacial-marine sediments from the Palmer Deep, Antarctic Peninsula. Earth and Planetary Science Letters 176, 443–455.

Brady, N.C., 1990. The Nature and Properties of Soils. Macmillian, New York.
Bridge, J.S., 2003. Rivers and Floodplains, Forms, Processes and Sedimentary Record. Blackwell, Oxford.
Brown, A.G., 1997. Alluvial Geoarchaeology. Cambridge University Press, Cambridge.
Bullock, P., Federoff, N., Jongerius, A., Stoops, G., Tursina, T., Babel, U., 1985. Handbook for Soil Thin Section Description. Waine Research Publications, Wolverhampton.
Butzer, K.W., Hansen, C.L., 1968. Desert and River in Nubia: Geomorphology and Prehistoric Environments at the Aswan Reservoir. University of Wisconsin Press, Madison.
Charlton, R., 2008. Fundamentals of Fluvial Geomorphology. Routledge, London.
Dearing, J.A., Hay, K., Baban, S., Huddleston, A.S., Wellington, E.M.H., Loveland, P.J., 1996. Magnetic susceptibility of topsoils: a test of conflicting theories using a national database. Geophysical Journal International 127, 728–734.
Evans, M.E., Heller, F., 2003. Environmental Magnetism, Principles and Applications of Enviromagnetics. Elsevier Science, Oxford.
El Tayeb, O. Y., 2010. The Shukriya of Central Butana, Pastoralism and Problems of Settlement and Agriculture in New Halfa Scheme. University of Khartoum Printing Press.
El Fattah, T.A., Frihy, O.E., 1988. Magnetic Indications of the position of the Mouth of the Old Canopic Branch on the Northwestern Nile delta of Egypt. Journal of Coastal Research 4 (3), 483–488.
Fassbinder, J.W.E., Stanjek, H., Vali, H., 1990. Occurrence of magnetic bacteria in soil. Nature 343, 161–163.
Foster, I.D.L., Lees, J.A., Owens, P.N., Walling, D.E., 1998. Mineral magnetic characterization of sediment sources from an analysis of lake and floodplain sediments in the catchments of the Old Mill reservoir and Slapton Ley, South Devon, UK. Earth Surface Processes and Landforms 23 (8), 685–703.
Foucault, A., Stanley, D.J., 1989. Late Quaternary palaeoclimatic oscillations in East Africa recorded by heavy minerals in the Nile delta. Nature 339, 44–46.
Freydier, R., Michard, A., De Lange, G., Thomson, J., 2001. Nd isotopic composition of Eastern Mediterranean sediments: tracers of the Nile influence during sapropel S1 formation. Marine Geology 177, 45–62.
Garzanti, E., Andó, S., Vezzoli, G., Abdel Megid, A.A., El Kammar, A., 2006. Petrology of Nile River sands (Ethiopian and Sudan): sediment budgets and erosion patterns. Earth and Planetary Science Letters 252, 327–341.
Grygar, T., Světlík, I., Lisá, L., Koptíková, L., Bajer, A., Wraye, D.S., Ettler, V., Mihaljevič, M., Nováková, T., Koubová, M., Novák, J., Máčka, Z., Smetana, Z., 2010. Geochemical tools for the stratigraphic correlation of floodplain deposits of the Morava River in Straznicke Pomoravi, Czech Republic from the last millennium. Catena 80 (2), 106–121.
Hrouda, F., Pokorny, J. Extremely high demands for measurement accuracy in precise determination of frequency-dependent magnetic susceptibility of rocks and soils. Studia Geophysica et Geodynamica, in press.
Jordanova, D., Veneva, L., Hoffman, V., 2003. Magnetic susceptibility Screening of anthropogenic impact on the Danube River sediments in Northwestern Bulgaria – Preliminary results. Studia geophysica et geodaetica 47 (2), 403–418.
Kletetschka, G., Banerjee, S.K., 1995. Magnetic stratigraphy of Chinese loess as a record of natural fire. Geophysical Research Letters 22, 1341–1343.
Krom, M.D., Cliff, R.A., Eijsink, L.M., Herut, B., Chester, R., 1999. The characterisation of Saharan dusts and Nile particulate matter in surface sediments from the Levantine basin using Sr isotopes. Marine Geology 155, 319–330.
Krom, M.D., Stanley, J.D., Cliff, R.A., Woodward, J.C., 2002. Nile River sediment fluctuations over the past 7000 yr and their key role in sapropel development. Geology 30 (1), 71–74.
Mahmoud, A.M., Hamdan, M.A., 2002. On the stratigraphy and lithofacies of the Pleistocene sediments at Giza Pyramidal area, Cairo. Egypt. Sedimentology of Egypt 10, 145–158.
Oldfield, F., Rummery, T.A., Thompson, R., Walling, D.E., 1979. Identification of suspended sediment sources by means of magnetic measurements: some preliminary results. Water Resources Research 15 (2), 211–218.
Padoan, M., Villa, I.M., Garzanti, E., Galbusera, M., Quistini, S., Peruta, L., El Kammar, A., 2009. Nd isotopes in Nile sediments (Ethiopia, Sudan). Geophysical Research Abstracts 11 EGU Assembly, 2009.
Schatz, A. K., Zech, M., Buggle, B., Gulyás, S., Hambach, U., Marković, S., Sümegi, P., Scholten, T. The late Quaternary loess record of Tokaj, Hungary: Reconstructing palaeoenvironment, vegetation and climate using stable C and N isotopes and biomarkers. Quaternary International, in press.
Schwertmann, U., 1988. Occurrence and formation of iron oxides in various pedoenvironments. In: Stucki, J.W., Goodman, B.A., Schwertmann, U. (Eds.), Iron in Soils and Clay Minerals. Reidel, Dordrecht, pp. 267–308.
Scrivner, A., Vance, D., Rohling, E.J., 2004. New neodymium isotope data quantify Nile involvement in Mediterranean anoxic episodes. Geology 32 (7), 565–568.
Stanley, J.D., Krom, M.D., Cliff, R.A., Woodward, J.C., 2003. Short Contribution: Nile flow failure at the End of the Old Kingdom, Egypt: strontium isotopic and petrologic evidence. Geoarchaeology 18 (3), 395–402.
Stoops, G. (Ed.), 2003. Guidelines for Analysis and Description of Soil and Regolith Thin Sections. Soil Science Society of America, Inc., Madison, Wisconsin.
Stoops, G., Marcelino, V., Mees, F. (Eds.), 2010. Interpretation of Micromorphological Features of Soils and Regoliths. Elsevier, Amsterdam.
Talbot, M.R., Williams, M.A.J., Adamson, D.A., 2000. Strontium isotope evidence for late Pleistocene reestablishment of an integrated Nile drainage network. Geology 28 (4), 343–346.
Weldeab, S., Emeis, K.C., Hemleben, C., Siebel, W., 2002. Provenance of lithogenic surface sediments and pathway of riverine suspended matter in the Eastern Mediterranean Sea: evidence from 143Nd/144Nd and 87Sr/86Sr ratios. Chemical Geology 186, 139–149.
Williams, M.A.J., Adamson, D.A. (Eds.), 1982. A Land between Two Niles: Quaternary Geology and Biology of the Central Sudan. Balkema, Rotterdam.
Williams, M.A.J., Adamson, D., Cock, B., McEvedy, R., 2000. Late quaternary environments in the White Nile region, Sudan. Global and Planetary Change 26, 305–316.
Williams, M.A.J., Williams, F.M., Duller, G.A.T., Munro, R.N., El Tom, O.A.M., Barrows, T.T., Macklin, M., Woodward, J., Talbot, M.R., Haberlah, D., Fluin, J., 2010. Late quaternary floods and droughts in the Nile valley, Sudan: new evidence from optically stimulated luminescence and AMS radiocarbon dating. Quaternary Science Reviews 29, 1116–1137.
Woodward, J.C., Macklin, M.G., Welsby, D., 2001. The Holocene fluvial sedimentary record and alluvial geoarchaeology in the Nile Valley of northern Sudan. In: Maddy, D., Macklin., M.G., Woodward, J.C. (Eds.), River Basin Sediment Systems: Archives of Environmental Change. A. A. Balkema Publishers, Rotterdam.

Catena 80 (2010) 106–121

Contents lists available at ScienceDirect

Catena

journal homepage: www.elsevier.com/locate/catena

Geochemical tools for the stratigraphic correlation of floodplain deposits of the Morava River in Strážnické Pomoraví, Czech Republic from the last millennium

Tomáš Grygar [a,*], Ivo Světlík [b], Lenka Lisá [c], Leona Koptíková [c], Aleš Bajer [d], David S. Wray [e], Vojtěch Ettler [f], Martin Mihaljevič [f], Tereza Nováková [f], Magdaléna Koubová [g], Jan Novák [h], Zdeněk Máčka [i], Mirek Smetana [i]

[a] Institute of Inorganic Chemistry ASCR, v.v.i., 250 68 Řež, Czech Republic
[b] Nuclear Physics Institute ASCR, v.v.i, 250 68 Řež, Czech Republic
[c] Institute of Geology ASCR, v.v.i., Rozvojová 269, 165 00 Prague, Czech Republic
[d] Mendel University of Agriculture and Forestry, Zemědělská 3, 613 00 Brno, Czech Republic
[e] The University of Greenwich at Medway, Chatham Maritime, Kent, ME4 4 TB, UK
[f] Charles University, Faculty of Science, Albertov 6, 128 43 Prague, Czech Republic
[g] Czech Geological Survey, Klárov 3, 118 21 Prague, Czech Republic
[h] University of South Bohemia, Faculty of Science, Department of Botany, Branišovská 31, 370 05 České Budějovice, Czech Republic
[i] Masaryk University, Faculty of Science, Department of Geography, Kotlářská 2, 611 37 Brno, Czech Republic

ARTICLE INFO

Article history:
Received 16 July 2009
Received in revised form 14 September 2009
Accepted 14 September 2009

Keywords:
Fluvial archives
Environmental change
Chemostratigraphy
Proxy analyses

ABSTRACT

The floodplain of the Morava River in Strážnické Pomoraví, south-east Moravia, Czech Republic contains a very valuable record of regional environmental change, which goes back to several thousand years. Its interpretation has been limited by poor stratigraphic correlation and dating of the sediments. We present a geochemical solution to this challenge. We studied 8 outcrops of floodplain deposits from 4 localities along a 6 km long part of the current meander belt of the Morava River in Strážnické Pomoraví using geochemical proxy analyses, magnetic susceptibility measurements, ^{14}C dating of wood remnants, and sediment micromorphology. The proxy methods are based on elemental analysis (EDXRF) and analysis of the cation exchange capacity of clay minerals; granulometric analyses provided the basis for lithological and facies assignment of the sediments. Our geochemical and mineralogical interpretations have further been tested by microstratigraphically studying the optical properties of the fine fraction. Horizons older than about 3 centuries were ^{14}C dated using wood remnants and the age of deposits from the last century was determined on the base of several proxies reflecting their industrial contamination by heavy metals and magnetic particles. The mean depositional rate over the period from about 1000 to about 1900 AD ranged from 0.2 to 0.6 mm y^{-1}, depending on the sedimentary facies. The coeval lithological change in the majority of the studied sections indicated a change of the meander belt structure at between ~1200 AD and ~1600 AD probably as a consequence of changes of channel structure. The alluvial deposition in the 20th century was strongly affected by the river regulation.

1. Introduction

Floodplain deposits are invaluable archives of Holocene fluvial activity (e.g., Macklin et al., 2006; Macklin and Lewin, 2008). The sediments may also contain information about regional environmental changes in countries which have undergone substantial change of land use and industrial development (e.g., Swennen and Van der Sluys, 2002; Lang et al., 2003; Vannière et al., 2003; de Moor et al., 2008). Both the quality and quantity of river-transported solid material can reflect the history of agriculture, anthropogenic adjustments to changing the river dynamics, evidence of chemical pollution, and other aspects of land–human interactions. However, floodplain development is a very dynamic and complex process that requires great care to be taken in the interpretation of overbank deposit sequences (Lewin and Macklin, 2003; Macklin and Lewin, 2008). In many European countries there is lack of continuous environmental sedimentary records such as natural lakes covering the historical and prehistoric periods and documentary archives older than five hundred years are very scattered. The understanding of how to interpret river dynamics has improved in recent years, enabling the production of estimates of river activity extending back several millennia (Macklin et al., 2005, 2006; Starkel et al., 2006; Thorndycraft and Benito, 2006; Hoffmann et al., 2008) allowing workers to identify large, regional, continental, or perhaps global environmental changes in fluvial activity in the multi-millennial time scale. On shorter time- and spatial scales, some local (regional, episodic) changes in the floodplains of rivers with smaller watersheds and alluvial plains have been

* Corresponding author.
E-mail address: grygar@iic.cas.cz (T. Grygar).

0341-8162/$ – see front matter © 2009 Elsevier B.V. All rights reserved.
doi:10.1016/j.catena.2009.09.005

successfully linked to well documented anthropogenic activities (Lang and Nolte, 1999; Swennen and Van der Sluys, 2002; Vannière et al., 2003; de Moor et al., 2008; Notebaert et al., 2009). Larger watersheds has some retention capacity for transport of the materials eroded due to the land use via colluvia and smaller tributaries to the trunk river floodplains that was discussed by Lang et al. (2003), Rommens et al. (2006), Kalicki et al. (2008), and Hoffmann et al. (2009).

The majority of large, naturally meandering rivers in the Czech Republic have been straightened and/or channelized and their floodplains narrowed by flood barriers. Several parts of the Morava River, one of the most important rivers in the Czech Republic from both geographical and historical points of view, have apparently been less affected, one such area is Strážnické Pomoraví (Kadlec et al., 2009). The floodplain in that area has been covered by several metres of fine grained deposits since the end of the Last Glacial Maximum (Havlíček, 1991, pp. 319–341; Havlíček and Smolíková, 1994; Kadlec et al., 2009). The rapid aggradation of the Morava River in the last millennium was assumed by several previous researchers to be connected to changes in land use (e.g., Prudič, 1978). Similarly the dramatic increase in loam deposits on floodplains, where mostly or only peat deposits were formed during the Middle Holocene, has been reported for many European rivers, where catchments were mostly deforested and changed to arable fields (e.g., de Moor et al., 2008; Notebaert et al., 2009; Hoffmann et al., 2009). We have recently started re-examining the floodplain deposits of the lower course of the Morava River and found that its character in a part of Strážnické Pomoraví underwent substantial changes during the last millennium (Kadlec et al., 2009).

The aim of this work is to establish a set of quantitative geochemical laboratory methods which would allow routine analysis of sediments at a sufficient sampling density to facilitate their correlation, and deliver interpretations in conventional lithological and sedimentological terms. These tools should enable floodplain scale correlations, which offer the best approach to the description of the fluvial architecture as demonstrated in numerous successful case studies (Lang and Nolte, 1999; de Moor et al., 2008; Notebaert et al., 2009). We employed cation exchange capacity obtained by $[Cu(trien)]^{2+}$ complex (Meier and Kahr, 1999; Grygar et al., 2005, 2009), X-ray fluorescence element analysis and magnetic susceptibility measurements. To interpret these proxy results, we cross-correlated them with outputs of conventional, more demanding methods such as particle size analysis, micromorphological study of processes within the fine grain matrix of the studied material, and ICP elemental analysis performed on samples from selected sections. The interpretation of the results is also based on ^{14}C dating of wood fragments. The sedimentological analysis, dating, and correlation are used to estimate the mean depositional rate (aggradation plus lateral accretion) over the last millennium.

2. Methods and material studied

2.1. Studied area

Strážnické Pomoraví is one of the last meandering reaches of the Morava River, which is not channelized, however, it is not free of significant modern human impact. The river upstream from Strážnické Pomoraví was straightened, the cross section modified, and the river banks stabilized. These alterations caused a downstream response leading to changes in channel hydraulics and morphology. The Morava River channel has gradually become more deeply incised into the alluvial sediments, the banks have become destabilized and the channel has widened. The changes in the course of the river channel are apparent from Fig. 1. Additionally, in the 1930's flood defences were constructed along the Morava River and its tributaries, limiting the area available for overbank flooding to about 20% of the original floodplain (Fig. 1). Historical maps show an anabranching channel pattern within the area while currently a single channel is active. Parallel channels in the vicinity of Strážnice and Petrov are depicted in several maps from 17th to 19th centuries. The former channel pattern is evident from the map of Moravia compiled in 1665 (Blaeu, 1665) and the maps of the 1st Austrian Military Survey of 1764–1768 and 1780–1783. Side channels called Morawka (Morávka) and Weschka Arm (Věšky) are also recorded on the map from the 2nd Austrian Military Survey (1841). During the 20th century, Morávka and Věšky were both channelized and used as waterway (the Bat'a Channel) and to drain local streams (including the Velička, Věšky, and Radějovka creeks). Other very substantial artificial modifications to the river morphology in the study area were the construction of flood defences and channel straightening and consequent abandonment of meander loops in two places within the study area during the 1930's (Fig. 1).

The map of the 2nd Austrian Military Survey (1841) indicates that the floodplain was dominated by meadows and forests during the first half of the 19th century. Currently the floodplain is mostly forested and a smaller area covered by arable land. The current forests are mostly composed of alder (*Alnus glutinosa*), willows (*Salix* sp.), ash tree (*Fraxinus excelsior*), and oak (*Quercus robur*), but introduced (not domestic) planted species are common in the current river banks, such as poplars (*P. canadensis*, cross-breed *P. canadensis* × *P. nigra*), maple *Acer negundo* = *Negundo aceroides*, ash tree *F. angustifolia*, and walnut *Juglans nigra*.

Our observation after several years of fieldwork is that the lateral movement of the concave banks of meanders in the largest meanders is up to 0.5 to 1 m per year. This is derived from the rate at which previous sampling sites have been removed by lateral erosion.

2.2. Sampling and sample pretreatment

Floodplain sediments were sampled from sections in natural outcrops of the Morava River banks during the seasonal minimum flows. In many places the rate of lateral erosion in the meander loops is about 1 m per year and so after each large seasonal flood relatively fresh deposits are exposed. The outer 0.5 to 1 m of sediment was removed before sampling. Sediments from more distal parts of river channel were retrieved by Auger corers with a diameter of 2 or 3 cm (Ejikelkamp, the Netherlands). Sediments were sampled as cubes with 3 cm edge at 5 or 10 cm intervals, i.e. in a discontinuous manner. Samples were left to dry in an ambient atmosphere. Very gently crushed material was used for the size distribution analysis, clay mineral identification and magnetic susceptibility measurement. Powders obtained by manual grinding in an agate mortar were subjected to geochemical analyses. Micromorphological samples were taken from macroscopically identified lithological layers using small Kubiena boxes.

2.3. Clay mineral identification

Samples for identification of clay mineral composition (clay fraction, $<2\ \mu m$) were obtained by a conventional sedimentation method (Tanner and Jackson, 1948). Oriented specimens for XRD were prepared by pipette method. Approximately 2 ml of suspension was dropped by pipette on the glass slide and air dried. The oriented specimens were analysed air-dried and after overnight saturation with ethylene glycol vapour at 60 °C. Then a part of the suspension was removed and left to evaporate at 40–50 °C and subjected to CEC analysis (discussed below). The clay fraction was analyzed by X-ray diffraction using a Philips X'Pert system (PANalytical, the Netherlands) with $CuK\alpha 1$ radiation. Clay mineral identification was performed using the NEWMOD code (Reynolds, 1985). Relative changes in illite–smectite concentration within the clay fraction were estimated by determining the relative areas of the basal diffraction lines in oriented specimens, estimated by their deconvolution to pseudo-Voigt components using the Peak Fitting Module in Origin7.0 (OriginLab, Northampton, MA, USA).

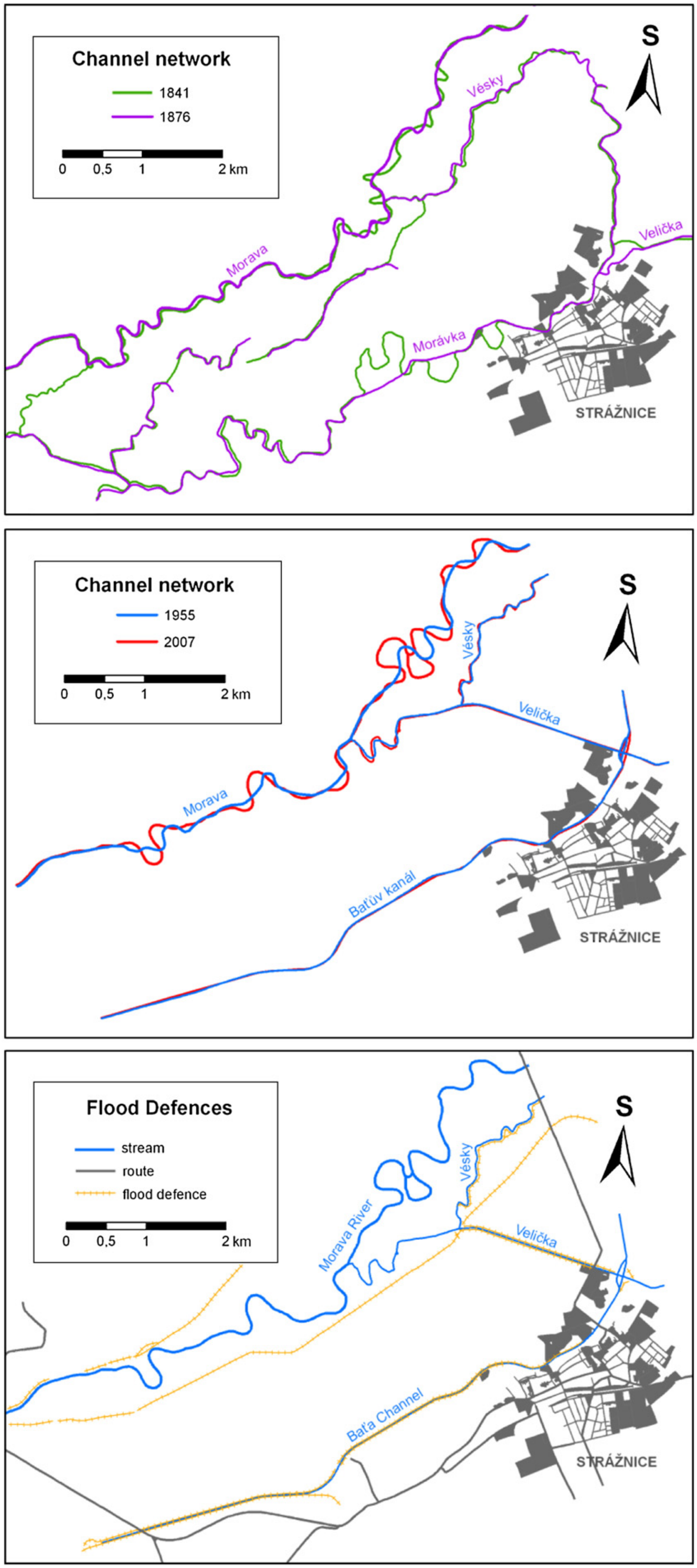
Channel network
1841
1876
0 0,5 1 2 km
S
Vésky
Velička
Morava
Morávka
STRÁŽNICE
Channel network
1955
2007
0 0,5 1 2 km
S
Vésky
Velička
Morava
Baťův kanál
STRÁŽNICE
Flood Defences
stream
route
flood defence
0 0,5 1 2 km
S
Vésky
Velička
Morava River
Baťa Channel
STRÁŽNICE

Table 1
List of studied sections.

Locality	Sections	Former land use (land cover)	Number of ^{14}C dates	Other analyses
Bridge to Bzenec	M215	19th century: forest 1950's: orchard Since 1960's: forest	1	MS, ICP/MS
	M7	19th century: forest 1950's: orchard Since 1960's: forest	3 (taken from Kadlec et al., 2009)	
	M127	19th century: forest 1950's: arable land Since 1980's: forest	no	MS, particle size fractionation, micromorphology
Meadow below Sand Depot	M134	19th century to 1960's: forest 1980's: arable land 1990's: shrubs	no	
	M249	19th century to 1960's: forest 1980's: arable land 1990's: shrubs	no	MS, ICP/MS
Old Piles	M110	19th and 20th century: alterations between meadow and arable land (3 changes of land cover)	4	MS, ICP/MS, particle size distribution function
Jasenová	M107	19th century: forest 1950's: arable land Since 1980's: forest	1	MS
	M108	19th century: forest 1950's: arable land Since 1980's: forest	1	

Only ^{14}C date points from the last millennium relevant to this study are listed. CEC and EDXRF analyses were performed for all sections; other performed analyses are listed in the last column.

2.4. Micromorphology of sediments

Samples were taken into small Kubiena boxes, slowly dried, impregnated by a polymer resin, proceeded into thin sections and then studied according to Bullock and Murphy (1983). A record was made of the microfabric types, structural and porosity features, natural inclusions, anthropogenic inclusions and pedofeatures (Macphail and Cruise, 2001, pp. 241–267).

2.5. Quantitative analysis of expandable clay minerals (CEC)

The cation exchange capacity (CEC) was determined using a procedure proposed by Meier and Kahr (1999) for pure clay mineral specimens and recently tested for sediments and soils (Grygar et al., 2009). $[Cu(trien)]^{2+}$ solution was obtained from $CuSO_4 \cdot 5H_2O$ (Penta, Czech Republic) and trien, triethylenetetramine (1,4,7,10-tetraazadekane, Sigma-Aldrich), to the final concentration 0.01 M with a potentiometric control of the constant ligand-to-metal ratio (Grygar et al., 2009). A fine dry powder (100–500 mg) was placed in a 50 ml beaker, wetted and then suspended by stirring in 5 mL of distilled water; then 5 mL 0.01 M Cu-trien solution was added, and the suspension stirred for a further 5 min using a magnetic stirrer. The suspension was then filtered into a 50 mL flask and the solid washed with several aliquots of distilled water, and the final volume of the filtrate made to 50 mL. The solutions were analyzed by AAS (Cu and Mg) and AES (Ca and Na). The sample weight for analysis was adjusted depending on its actual CEC to consume about 50% of $[Cu(trien)]^{2+}$ using the routine described by Grygar et al. (2009).

2.6. Magnetic susceptibility (MS)

MS of samples from 5 sections was measured using Kappabridge KLY-2 (Agico Brno) operating with magnetic field intensity of 300 A/m and frequency of 920 Hz. Raw data were recalculated to mass-specific MS expressed in m^3/kg, the mass of each sample was 20 to 50 g.

2.7. Particle size fractionation

Particle size fractionation was performed using sedimentation method ISO 11277:1998.

2.8. Particle size distribution function (PSDF)

Particle size distribution was established using a Malvern Mastersizer 2000. Samples of air dried and roughly crushed sediments were gently disaggregated and dispersed in de-ionized water. Organic matter was removed by addition of hydrogen peroxide accompanied by gentle warming at 40 °C until effervescence stopped. The supernatant was removed after centrifugation and the sample rinsed with two changes of deionised water. Samples were then re-homogenised in a minimum of water using a whirlymixer and then sub-sampled for particle size analysis. Two sub-samples were taken from each sample and analysed sequentially, the graphs presented are the mean of the two measurements.

2.9. ICP/MS including Pb isotopic analysis

The sediments were mineralized (dry ashed) in a Linn (Germany) programmable furnace at final temperature 450 °C. The residues were subsequently dampened with deionized water, dissolved in HF and $HClO_4$ and evaporated (twice), then the residue was dissolved in diluted nitric acid and the solutions transferred to volumetric flasks. The metal contents were determined using inductively coupled plasma mass spectrometry (ICP/MS, X Series 2, ThermoScientific). The Pb isotopic composition (ratios $^{206}Pb/^{207}Pb$ and $^{208}Pb/^{206}Pb$) was measured by diluting the solutions to a concentration of <20 µg/L, and a correction for mass bias was performed using SRM 981 (Common Lead, NIST, USA). The detailed instrument parameters are given elsewhere (Ettler et al., 2004). Mean r.s.d. of the $^{206}Pb/^{207}Pb$ and $^{208}Pb/^{206}Pb$ ratio analyses was 0.2%.

2.10. X-ray fluorescence analysis (EDXRF)

The analysis was performed with a PANalytical MiniPal4.0 spectrometer with Peltier-cooled silicon drift energy dispersive detector. The ground samples were analyzed after pouring into measuring cells with a mylar foil bottom. Al and Si were analyzed under He flow, the ratio of their raw signals was used for correlations. The signals of Al, Cu, Pb, Ti, and Zn were calibrated using the results derived from the analysis of a series of sediments by ICP/MS.

2.11. Xylotomy analysis

Identification of the woods remains was carried out using an episcopic microscope. Fragments were broken manually to expose transverse, tangential–longitudinal and radial–longitudinal sections. Taxonomic determinations were made using published works on wood anatomy (Jacquiot et al., 1973; Schweingruber, 1990).

Fig. 1. The development of the channel network of the Morava River in Strážnické Pomoraví according to historical and current maps (2nd Austrian Military Survey, 1841; 3rd Austrian Military Survey, 1876; Topographical Map of the Czechoslovak Army, 1953–1955; Topographical maps of the Czech Republic, 2006–2007) and the actual channel network and flood defence system. The current area of the city of Strážnice is plot in all maps.

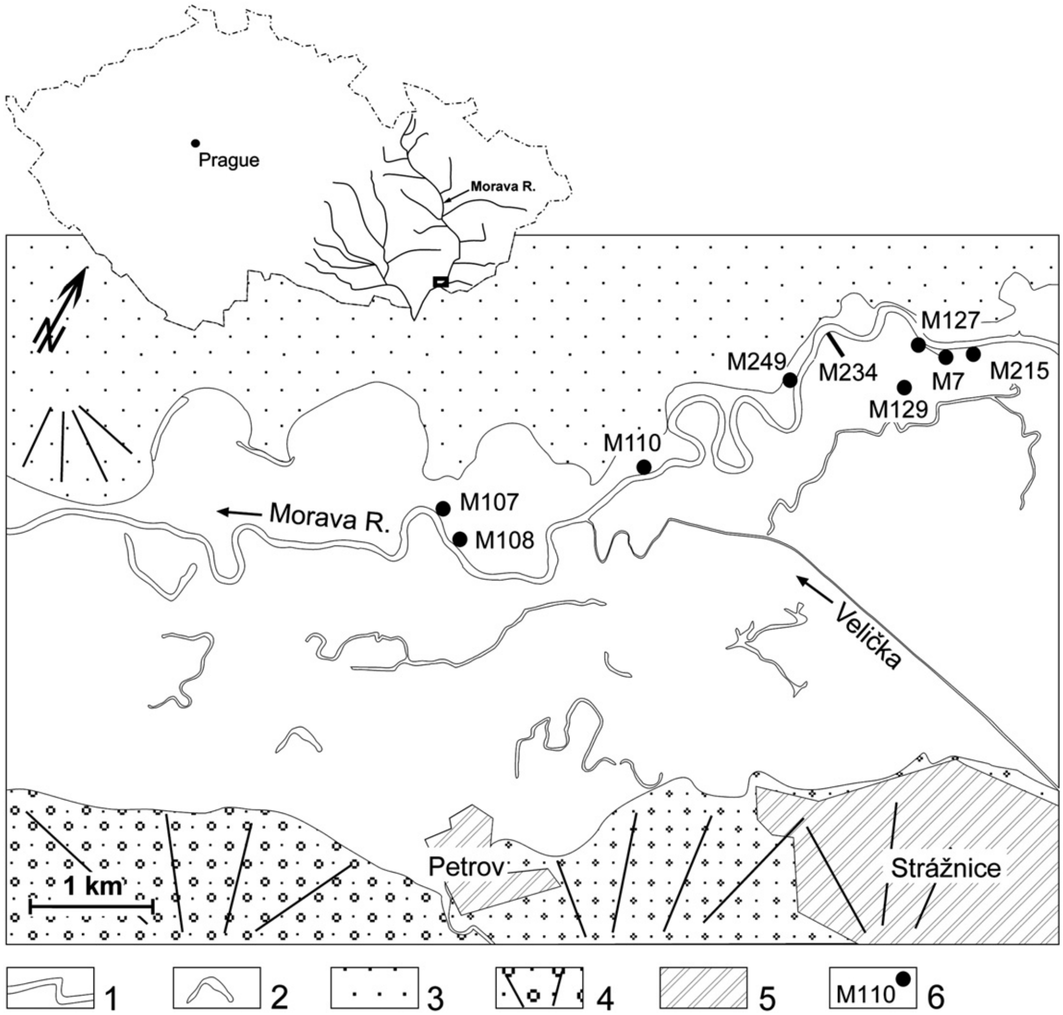

Fig. 2. Map of the Morava River catchment (map at top) with the Strážnické Pomoraví area (black rectangle) with the position of studied sections. Legend: 1 current and 2 abandoned channels within the maximal area of the floodplain (altitude below ~165 m.a.s.l.), 3 eolian sand body, 4 Late and Middle Pleistocene alluvial fans, 5 towns, 6 positions and labels of studied sections.

2.12. ^{14}C dating

Large fragments of wood (trunks, branches) were processed according to the routine procedure entailing Acid/Alkali/Acid pretreatment, combustion and benzene synthesis (Gupta and Polach 1985). The resulting benzene was measured by a low-background liquid scintillation spectrometer (Quantulus 1220). For calibration, the International Standard Certified Reference Material for Contemporary C-14, Oxalic Acid NIST SRM 4990C was used (Schneider 1995). For a background correction, commercially available benzene (Sigma-Aldrich, cat. No. 154628-1 L, benzene, 99 + %, A.C.S., spectrophotometric grade) was used. The resulting conventional radiocarbon age and its uncertainty were converted to an interval of calibrated age utilizing IntCal04 calibration curve for terrestrial samples (Curie, 1995; Reimer et al., 2004).

Dating of small charcoal chips was performed by AMS in Poznań Radiocarbon Laboratory (Poland) and calibrated using the OxCal program.

3. Results

3.1. Lithological, facial and micromorphological description of studied sections

The list of sections included in this study together with methods used to their analyses is shown in Table 1 and their positions are depicted in Fig. 2. Floodplain deposits in the study area are moderately to poorly sorted mixtures of components from fine clay to coarse sand (Figs. 3 and 4). The coarse to fine ratio (C/F) strongly varies according to the chosen coarse limit. Generally, when the lower coarse limit is taken as 100 µm, the C/F ratio varies between 1:5 and 3:1. Sedimentary facies were defined using terminology developed by Cojan and Renard (1999, pp. 322–333), Bridge (2003, pp. 260–295), and Houben (2007) on the basis of field observations, sedimentological, pedological and micromorphological evaluation, and laboratory analyses. The list of facies (Table 2) was obtained by comparison of several sections and an "iterative" evaluation of laboratory analyses using individual approach recommended by Houben (2007) to each studied reach.

From the sequences observed in outcrops (concave banks of meanders) during minimal river flows and material retrieved by the Auger corer farther from the river channel, we focused on fine overbank deposits consisting mostly of clay, silt, and minor fine sand fractions. We avoided horizons containing mostly sandy material through most of their thickness, i.e., we did not systematically study the infill of abandoned channels and deposits on former point bars. The fine-grained overbank sedimentary sequences, up to a thickness of 5 m, lay mostly on early Holocene peat layers (Kadlec et al., 2009) or on channel or point bar deposits older than about several thousand years (e.g., in M127 section, Fig. 3).

The lithological development of the fine overbank deposits in studied area is typical for meandering rivers (Bridge, 2003). The facies

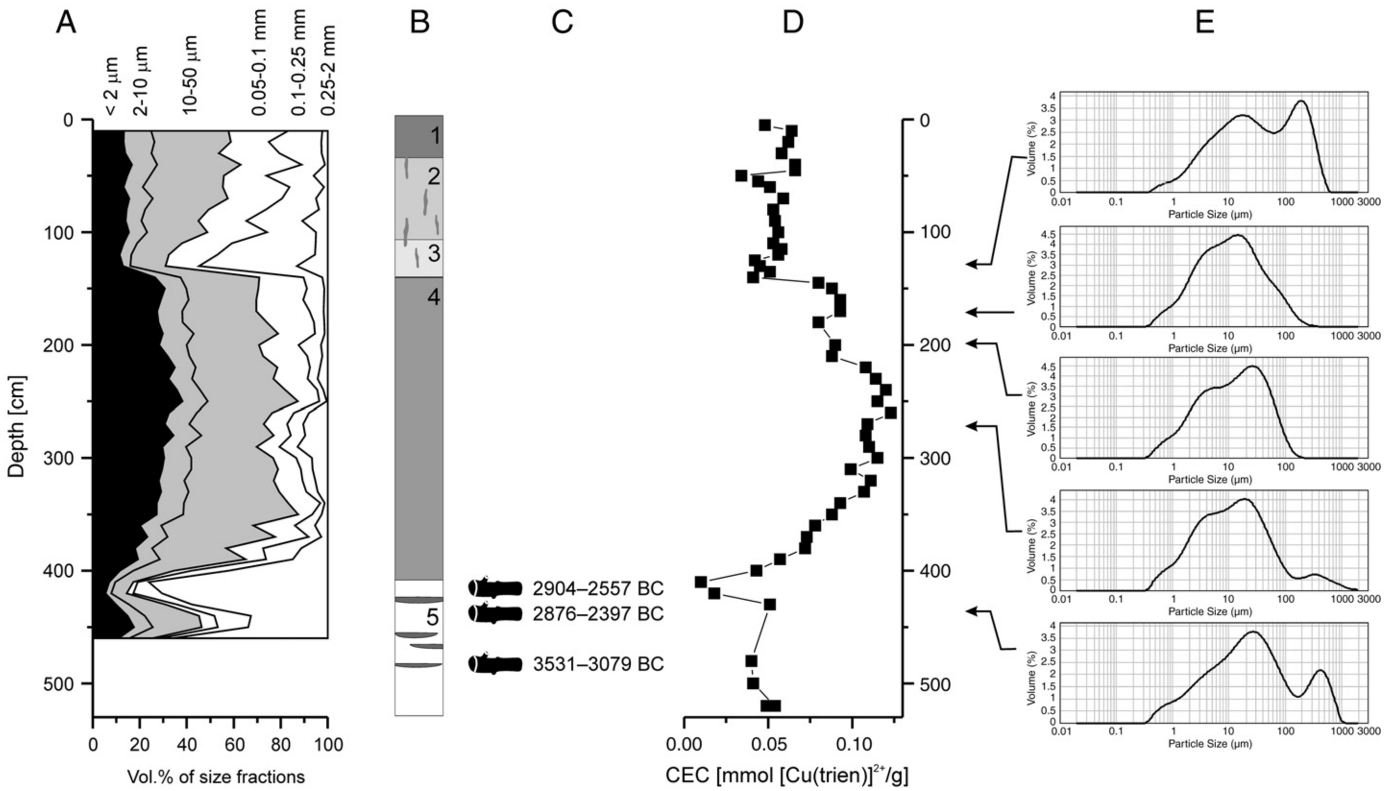

Fig. 3. Characteristics of section M127 with particle size distribution. A: results of particle size fractionation. B: section description, 1 dark brown A horizon (ploughed), 2 light brown soil with coarse polyedric structure, 3 light grey layer with about 1 mm black nodules and about 1 cm rusty stains, 4 grey gleyed layer with up to 0.5 cm rusty stains, 5 grey sand layer with massive grey silty lenses and fossil wood fragments. C: ^{14}C dates of three wood fragments. D: CEC values. E: particle size distribution functions in selected depths.

assignment is supported by the size distribution analyses of sections M127 (Fig. 3) and M110 (Fig. 4). The sedimentary sequence observed in section M127 commences with the fining-upward sandy fill of an abandoned channel or point bar. These coarse sand deposits are overlain by massive sands intercalated with silty layers. The central part of section M127 as well as many other studied sedimentary sequences, is 1–3 m thick and consists mostly of silty–clayey material with <20% fine sand and <10% medium and coarse sand, we consider this to reflect distal or proximal floodplain deposition (the further discrimination is given below). This sedimentary unit always displays signs of gleying with rhizoconcretions and centimetre-sized Fe oxide stains, mostly along desiccation cracks, and it usually has a coarse angular structure. Macromorphologically these stains are Fe,Mn-oxide segregations and hypocoatings. Along these segregations and channels with hypocoatings, depletion features are visible representing the fact that solutions rich in Fe and Mn were transported quite short distances, i.e. on millimetre scale. No dusty or clayey void coatings were observed. Material in this horizon usually has a massive to channel microstructure and a C/F ratio, with the threshold set at 50 μm, varying from 1:1 to 1:2. The upper 1.4 m thick layer of the M127 section has a coarser grain size, dominated by coarse silt and fine sand and with the sum of medium and fine sand totalling about 40%. A C/F ratio of 3:1, with the threshold limit of 200 μm, represents more sandy and unsorted material, but this horizon also contains material with a C/F ratio of 1:1 using a threshold of 50 μm. Samples dominated by coarse-silt to fine-sand fractions can be assigned to the transition from proximal floodplain to levee deposits. Material of this horizon is micromorphologically characterised by the presence of increased bioturbation by roots, redeposited soil fabric fragments, the presence of Fe,Mn-oxides' as well as depletion features. Importantly, there is no visible clay redeposition and segregation as a channel coating. The uppermost parts of sedimentary sequences commonly contain 10–30 cm thick layers covering the buried A horizons perhaps related to agricultural activities. Typical features are bioturbation, the presence of decomposed organic matter, fragments of roots, charcoal, redeposited Fe,Mn-oxide nodules and soil fabric fragments.

The finest grained deposits are assigned to the distal floodplain (backswamp) facies. These are best documented in the central part of section M110. The particle size distribution function of the finest deposits in this section displays the highest proportion of clay-sized material (Fig. 4).

Wood fragments suitable to ^{14}C dating comprised parts of trunks or branches of ash tree or oak. Tree roots were excluded from dating. The wood fragments most commonly occur in the top of clayey layers, in the fining upward abandoned channel deposits, and rather exceptionally in the distal floodplain facies. Charcoal samples are mostly found in deposits with a prevailing fine fraction. The more porous, silty proximal floodplain and sandy levee deposits are usually very poor in fossil wood fragments and charcoal, probably because of oxidative degradation or removal by floods, this substantially hinders their dating and correlation and became a motivation for our chemostratigraphic correlation approach. While ^{14}C dating of the lower parts of the overbank fines can be used to achieve correlation, proxies of industrial anthropogenic pollution were used in their upper parts.

3.2. Geochemical proxy analyses and magnetic susceptibility

Several analytical methods were used to aid interpretation of the large sample series and to increase the number of correlatable sections. To interpret and validate the so obtained proxies, we compared them with the results of well established quantitative methods and performed a regression analysis, which is summarized in Table 3. The most significant correlation is that between CEC and % clay fraction. Correlation of the EDXRF signal of Al/Si and EDXRF signal of Rb with the percentage of the clay fraction are also highly significant.

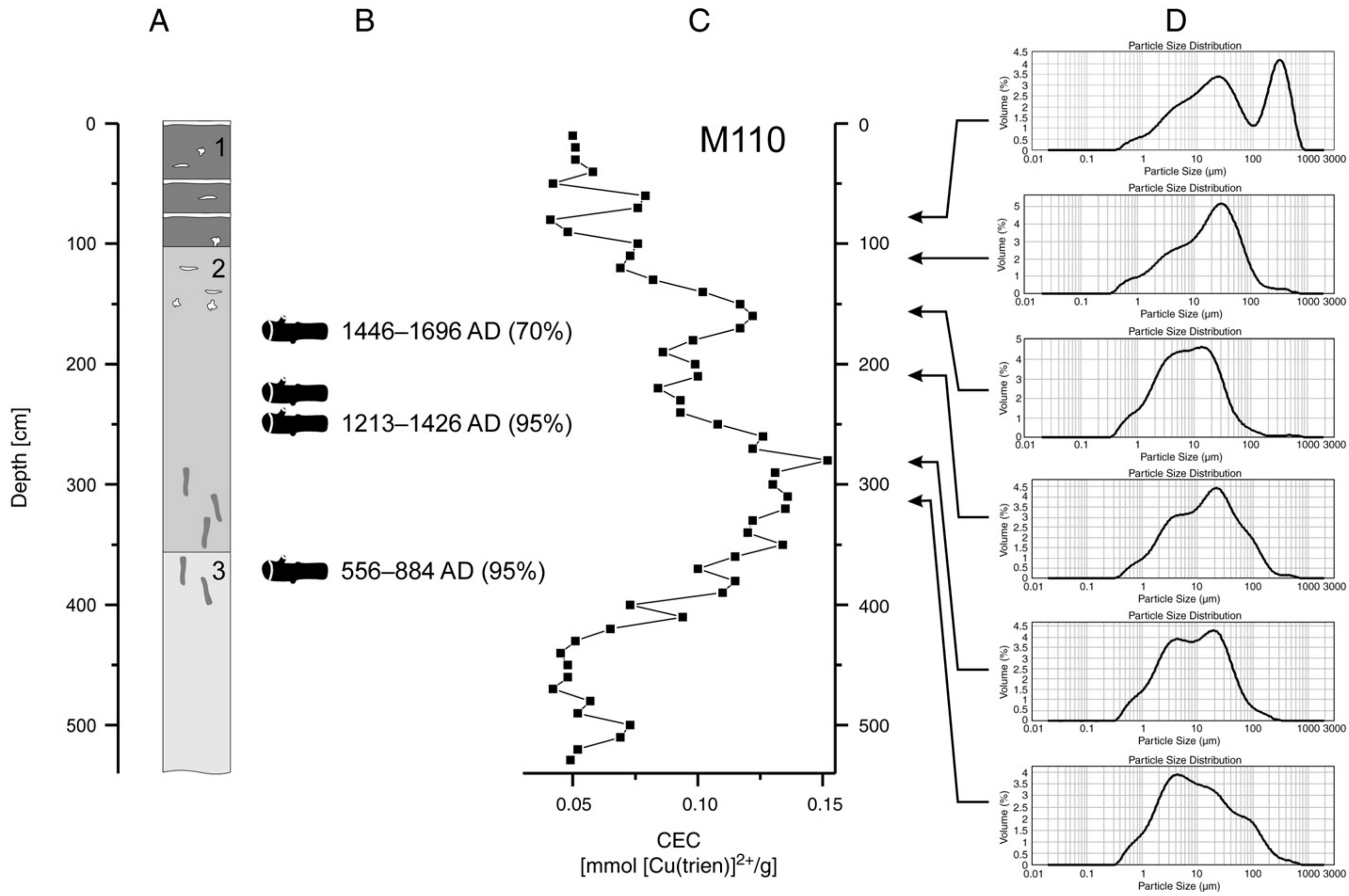

Fig. 4. Characteristics of section M110. A: section description, 1 brown silty sediment with sandy layers and inclusions, 2 brown silty or clayey gleyed material with sand inclusions at top and rhizoconcretions and their pseudomorphs at bottom, 3 mostly anoxic, plastic, unsorted grey sediment with substantial sand component. B: the position of wood fragments with their age obtained by ^{14}C dating. C: CEC log of the section. D: particle.

Preparation and analysis by ICP/MS of a selection of samples enabled the production of calibration lines for lead, titanium and zinc using the EDXRF. We used EDXRF for the majority of measurements because it offers the advantage (over ICP-MS) of a simple, rapid drying and grinding pre-treatment.

The depth of industrially polluted deposits is readily identified from the depth profiles of aluminium-normalised Pb and Zn concentrations, Pb isotopic analysis, and magnetic susceptibility (MS) measurements, as can be seen for 3 sections in Fig. 5. Cu depth profiles (not shown) are very similar to those of Pb and Zn. Heavy metal concentrations were normalized to Al, because it is considered an immobile lithogenic element which is not expected to be anthropogenically affected (Al was also used for the normalization , e.g., by Desenfant et al., 2004; Ettler et al., 2006; and Pasternack and Brown, 2006). The Pb isotopic composition is a very useful tracer of modern industrial pollution (e.g., Novák et al., 2003; Ettler et al., 2004), because common lithogenic Pb in central Europe has a lower abundance of the lighter Pb isotopes, particularly ^{206}Pb than Pb from coal burning and leaded gasoline. Komárek et al. (2008) gave typical $^{206}Pb/^{207}Pb$ values about 1.19–1.22 for Central European natural Pb, 1.18–1.20 for Pb from coal combustion, and 1.12–1.16 for European leaded gasoline. In M215, M219, and M249, $^{206}Pb/^{207}Pb$ ratios of contaminated sediments were 0.189 (σ=0.002), 1.191 (σ=0.001), and 0.188 (σ=0.002), respectively, while the underlying unpolluted sediment in these three sections had mean $^{206}Pb/^{207}Pb$ values 1.200 (σ=0.003). Although the change is not dramatic, it is statistically significant. $^{206}Pb/^{207}Pb$ and $^{208}Pb/^{206}Pb$ ratios are linearly dependent in the studied sediments.

Table 2
Facies description used in this work and "adjusted" for the deposits of the actual studied site.

Facies	Spatial position	Lithology	Structure	CEC
Channel sands	Bottom parts of profiles, occasionally within proximal floodplain deposits	Coarse sand, sometimes with fine gravel	Non-laminated, sometimes with gravel layers	<0.02
Deposits of point bars	Usually on channel sands	Sand layers, silt layers	Usually laminated (cm to dm scale)	<0.05
Distal floodplain sediments	Upward fining of underlying channel sands or point bar deposits	Comparable percentages of clay and silt fractions	Non-laminated, coarse prismatic soil structures	>0.12
Proximal floodplain sediments	Upward coarsening of underlying distal floodplain deposits	Silt fraction larger than clay fraction, minor fine sand	Non-laminated, occasional layers or inclusions of fine sand (mm or cm scale), coarse polyedric soil structure	0.08–0.12
Levee deposits	Topmost layers in outcrops of the current banks	Mainly silt and fine sand fractions	Usually alterations of silt and thin sand layers, fine polyedric soil structure	0.04–0.07

CEC values in mmol [Cu(trien)$^{2+}$] given as mean values for the given facies.

Table 3
Correlations used to interpret and calibrate geochemical proxies.

Proxy (method)	Correlation/calibration analysis	Sections used to correlation	Regression coefficient *r* (number of experimental points)	Proxy interpretation
CEC ($Cu[trien]^{2+}$)	Percentage of fraction below 2 μm	M127	0.9318 (46)	Clay fraction percentage
Al/Si ratio of signals (EDXRF)	Percentage of fraction below 2 μm	M127	0.8575 (46)	Clay fraction percentage
Rb signal (EDXRF)	Percentage of fraction below 2 μm	M127	0.8319 (46)	Clay fraction percentage
Ti signal (EDXRF)	Percentage of fraction 2–50 μm	M127	0.8071 (43)	Silt fraction percentage
Al signal (EDXRF)	Al content (ICP/MS)	M215, M249	0.8647 (87)	Al percentage
Ti signal (EDXRF)	Ti content by ICP/MS	M215, M110, M249	0.8941 (144)	Ti percentage
Zn signal (EDXRF)	Zn content (ICP/MS)	M215, M110, M249	0.9297 (144)	Zn percentage
Cu signal (EDXRF)	Cu content (ICP/MS)	M215, M110, M249	0.7485 (143)	Cu percentage
Pb signal (EDXRF)	Pb content (ICP/MS)	M215, M249	0.8166 (87)	Pb percentage

There is also a minor increase in Pb concentration and a change in the Pb isotopic composition in the Morava River floodplain deposits preceding the major "step" at the top of this minor, and presumably earlier variation is indicated by grey arrows in Fig. 5. It could be caused by a downward movement of Pb ions (Hudson-Edwards et al., 1998; Fernandez et al., 2008) or indicate minor Pb contamination preceding the significant (industrial) increase.

3.3. Proxies based on cation exchange capacity

Cation exchange capacity (CEC) of expandable clay minerals in the sediments was determined by $[Cu(trien)]^{2+}$ method (Meier and Kahr, 1999), which has recently been successfully tested and used in the analysis of the floodplain deposits (Kadlec et al., 2009; Grygar et al., 2009). To interpret the CEC value of the samples in conventional sedimentological terms, we performed detailed mineralogical and granulometric analyses of selected sediment samples. We separated the clay fractions in 11 samples from the M127 section and subjected them to conventional XRD phase identification and CEC determination, producing a specific CEC of the clay fraction (Table 4). XRD of the clay fraction showed that disordered (R0) mixed-layer illite–smectite (with about 50% expandable layers) is the major component, while illite and kaolinite are present at smaller concentrations (Table 4). Depth changes in the % basal diffraction of illite–smectite and CEC of the clay are negligible, showing that the mineralogical composition of the clay fraction is independent of the depth (or age of the sediments). This evaluation is in agreement with the observation that CEC can be used to determine the percentage of clay present using linear regression (Table 3). The regression line of that dependence (with statistically insignificant constant) is:

$$\%\text{clay fraction } (<2\,\mu\text{m}) = 0.6628 \cdot \text{CEC}; r^2 = 0.86$$

where CEC is the consumption of $[Cu(trien)]^{2+}$ in mmol/g.

Another parameter derived from determination of the cation exchange capacity is the Mg/Ca ratio of the exchangeable/soluble fraction. We have already described a very specific Mg/Ca depth profile common in the floodplain deposits in Strážnické Pomoraví (Kadlec et al. 2009, Grygar et al. 2009). Similar depth profiles were obtained in the sections described in this paper (Figs. 6 and 7). We evaluated the correlation of the Mg/Ca ratio with CEC (clay fraction content) and the sample depth, comparing the upper 350 cm of 8 sections. Mg/Ca ratio was statistically weakly dependent on CEC ($r = 0.4702$, 349 points) but it was statistically significantly dependent on the sample depth ($r = 0.7945$, 349 points). The Mg/Ca ratio is hence not primarily derived from sediment lithology, but it is somehow related to the "history" of the sediments.

The general trend found in sedimentary sections is that the Mg/Ca ratio decreases from values around ~0.2 at depths of about 250–350 cm to 0.10–0.15 at the uppermost 50–100 cm, as shown, for example, in Figs. 6 and 7. In agreement with our previous reports (Kadlec et al., 2009; Grygar et al., 2009) we consider the Mg/Ca ratio in the exchangeable/soluble fraction to be very efficient in inter-correlation of the individual sections of floodplain deposits (Fig. 7, panel B).

To exclude some spatial bias in the Mg/Ca ratio of floodplain deposits, we analyzed sediments along a 180 m long transect (M234; Fig. 2) which covers the top layers of a point bar, covered by sparse willows and herbs, through shrubs dominated by *Acer negundo* and *Salix* sp., to the edge of a *Fraxinus* sp. forest at the level of floodplain (total height difference of about 4 m). We found that the Mg/Ca ratio in the top soil layers (Fig. 6) is not dependent on the distance of the site from the channel, because all Mg/Ca values in the top layer of the M234 transect were in the interval 0.09 to 0.15, i.e. within the same range as the top sediments collected from river banks. Additionally, a similar depth trend in the Mg/Ca ratio as in the sections was also found in cores drilled several hundred metres away from the river channel, i.e., outside the range of levee deposits (as demonstrated by core M129 in Fig. 6).

The mean Mg/Ca ratio of water derived from the Morava River (3 samples) is 0.25; this is similar to Mg/Ca ratio of ~0.2, typical for samples in sections of river banks at greater depths. It is also possible that the higher Mg/Ca ratios found in the older (deeper) sediments are due to their slow cation exchange with groundwater derived from the Morava River. If this was the case, the Mg/Ca increase with depth would indicate longer residence of the deeper material in the floodplain.

3.4. Facies description using geochemical proxies

As shown in Table 3, CEC, Rb abundance and the ratio of Al/Si signals from the EDXRF are useful proxies for the abundance of clay fraction material in the sediments. The Si signal of EDXRF is best correlated with the coarse sand fraction (0.25–2 mm), i.e. coarse quartz grains. Variation in the grain size distribution within all studied sections can hence be tracked by the results of geochemical analyses with a high sampling density.

Depth changes in CEC can be used as a sensitive indicator of sand intercalations, which cause sharp minima in CEC/depth profiles (see

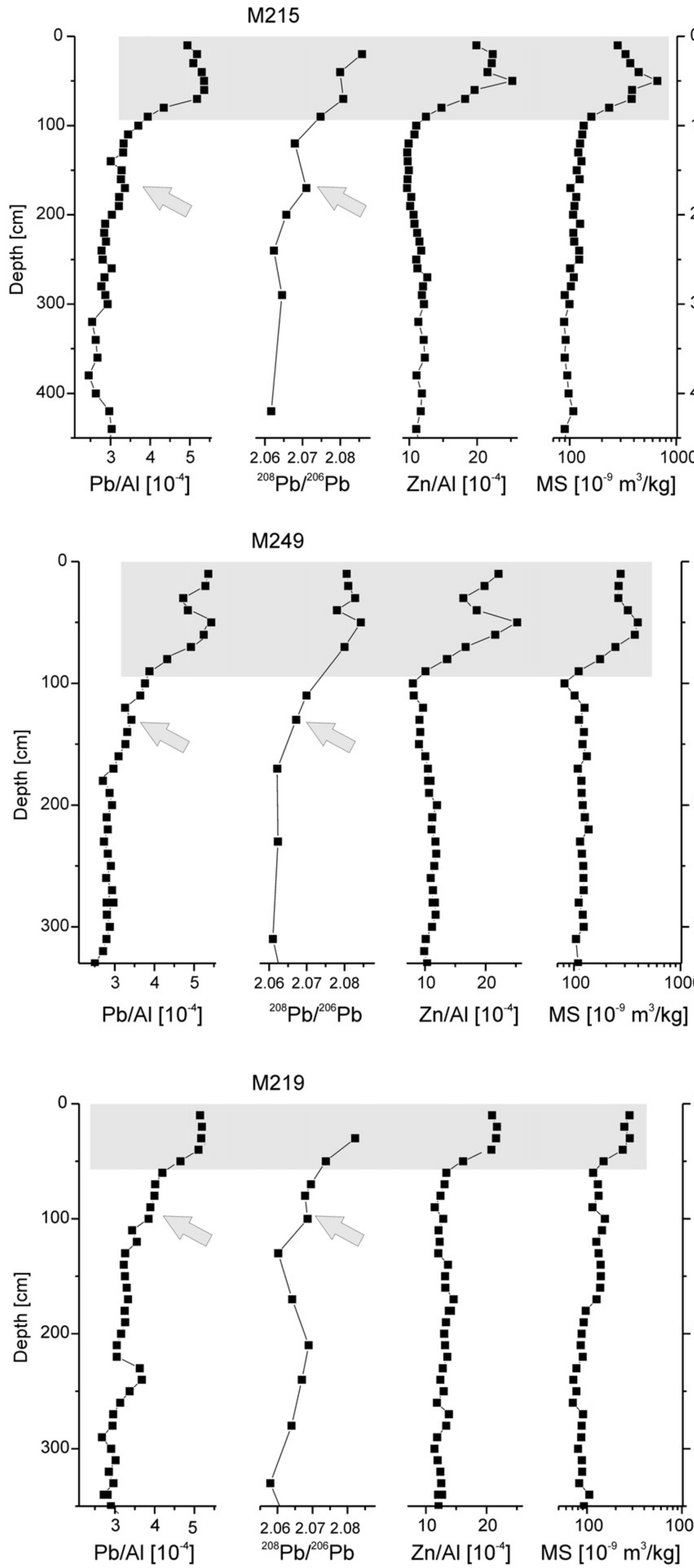
M215
M249
M219
Depth [cm]
0
100
200
300
400
Pb/Al [10^-4]
3 4 5
208Pb/206Pb
2.06 2.07 2.08
Zn/Al [10^-4]
10 20
MS [10^-9 m^3/kg]
100 1000

Table 4
Percentage and characteristics of clay fraction of floodplain deposits from section M127.

Depth [cm]	Sedimentary facies	% clay fraction (<2 μm) [a]	% basal diffraction of illite–smectite [b]	CEC[c] [meq/100 g]
10	Proximal floodplain/levee sediments	13	83	0.205
30	Proximal floodplain/levee sediments	14	81	0.212
70	Proximal floodplain/levee sediments	16	90	0.214
110	Sandy intercalation	13	90	0.219
150	Distal/proximal floodplain sediments	31	93	0.212
190	Distal/proximal floodplain sediments	30	92	0.232
230	Distal/proximal floodplain sediments	32	94	0.251
270	Distal floodplain sediments	31	95	0.263
330	Distal floodplain sediments	29	95	0.250
360	Abandoned channel sediments	20	95	0.251
440	Abandoned channel sediments	15	94	0.202

[a] Obtained by size fractionation according to ISO 11277:1998.
[b] Analysis of clay fraction separated according to Tanner and Jackson (1948), the area of basal diffraction of illite–smectite (diffraction maximum *d* between 13.6 and 14.7 Å) to sum of the areas of basal diffractions of illite–smectites plus micas plus kaolinite.
[c] CEC in mmol $[Cu(trien)]^{2+}$ obtained with the clay fraction (<2 μm) separated according to Tanner and Jackson (1948).

also in Kadlec et al., 2009), but CEC also visualizes stepwise lithological changes development (gradation) within the units of fine overbank floodplain deposits. CEC maxima within units interpreted as distal or proximal floodplain deposits correspond to maxima of clay (<5 μm) and fine silt (<20 μm) fractions, while simple increases in the coarseness of the silt fraction in upward coarsening sequences of distal to proximal floodplain deposits is identified by a decrease in CEC values (Figs. 3 and 4).

A combination of the lithological description and appearance of the sediments with their CEC makes it possible to propose a facies assignment (Table 2). Sediments with a high proportion of clay grade material, considered to be distal floodplain sediments (e.g., in the middle of the section M110), have CEC values higher than about 0.13 mmol $[Cu(trien)]^{2+}$/g, and in some exceptional cases the CEC of the finest sediments is up to 0.16 mmol $[Cu(trien)]^{2+}$/g. The sediments with approximately equal proportions of clay and fine silt fractions, and minor percentage of fine sand, are considered to be proximal floodplain sediments, and have CEC values in the range about 0.08–0.12 mmol $[Cu(trien)]^{2+}$/g. Sediments with CEC values <0.07 always have a significant or even a dominant proportion of coarse silt and/or sand and are considered to be proximal floodplain sediments intercalated with some levee deposits. Levee deposits, the coarsest uppermost sediments, have a CEC of about 0.05 mmol $[Cu(trien)]^{2+}$/g. This sediment sorting, dependent on the distance of the point of deposition from the channel, is typical for floodplains, where the finest particles are deposited over the entire flooded area, while coarser fraction is preferentially settled out closer to the channel (Bridge, 2003). The above described interpretation of the CEC values in the terms of facies is only valid for this particular site in the Morava River floodplain, for which it was "calibrated" by the conventional methods discussed above.

3.5. Lateral stability of the sections

In some localities (such as Bridge to Bzenec) the lateral stability of facies is good at a hundred-metre scale (Fig. 7), while in others (e.g., such as Old Piles) a few metres deep and about 10 m wide palaeochannels are found in the outcrops in close proximity to continuous outcrops of overbank fines. The lateral continuity of outcrops is important to ensure that the chosen sections are representative prior to extending chemostratigraphic correlation and ^{14}C dating to other sections. The sections shown in Fig. 7 are a few hundred metres apart; section M219 is the furthest upstream, M7 is 200 m downstream of M219 and M127 ~400 m downstream of M219 (Fig. 2).

The chemostratigraphic correlation lines for the Bridge to Bzenec location are identified by grey areas in Fig. 7. The topmost layers of the section M127 are thinner, as would be expected from correlation lines 1, 2, and 3, which correspond to industrially polluted layers, the Mg/Ca ratio change, and upward coarsening, respectively. The variable thickness of the industrially polluted layer is probably due to different land use (land cover) in these sections (Table 1). The silt fraction minimum (line 5, clay fraction maximum, distal floodplain sedimentation) within section M127 is at a correspondingly shallower depth. The thickness of proximal to distal floodplain deposits (sediments between lines 3 and 4) is similar in all three sections, implying a similar depositional rate for this unit. The facies development at depths greater than that indicated by line 4 is very different; either the development within the three sections was different due to a different channel position before the Middle Ages, or there is a depositional hiatus in the bottom part of at least two of the three studied sections. The poorer correlation of older deposits is a common consequence of the aggradation dynamics of a meandering river.

3.6. Correlation of sections along the studied meander belt

The lithological development recorded in the eight studied sections can be approximately correlated in their central and upper parts, covering in 3–4 m the last 500–1200 years. This correlation is based on the genetic relationship between the studied sections, which seem to belong to a single meander belt. The location of all studied sections along a single river channel is also apparent from the available maps as discussed above. The timing of the beginning of the coarsening upwards fillings of the abandoned channels (at the base of the sequences of overbank fines) cannot be correlated, because available data are scattered from about 5 to 2 ky BP. The correlation of sedimentation in the sections studied is shown in Fig. 8. Five sections from three localities are displayed, in each of them at least one ^{14}C date of wood fragments or charcoals was determined, which, together with the date point, of approximately 1900 AD derived from the start of the industrially polluted layer — produced five age-depth models.

There are three periods indicated in the sections by grey areas, where some major changes of depositional facies occurred. These changes in individual sections do not always display the same pattern, but they are notably coincident. The start of gradual upward coarsening at ~1200 AD in sections M215, M7, M110, and M107 could indicate the beginning of the gradual approach of the river channel towards these sites. The sediments deposited at ~1600 AD are unusually coarse in the studied sections, and these sediments only briefly fined upward in sections M107 and M110. The final coarsening after 1900 AD is probably due to a combination of the floodplain narrowing due to the construction of flood defences and also an artefact of the substantial accumulation of levee deposits in the studied sections.

Fig. 5. Proxies of industrial pollution in three studied sections. Pb/Al and Zn/Al ratios and Pb isotopic composition obtained by ICP/MS. MS (the right panels) is mass-specific magnetic susceptibility. Grey rectangles indicate industrially polluted top sediments. Grey arrows point to possible increase in Pb concentration and changed isotopic composition before the major change of these parameters.

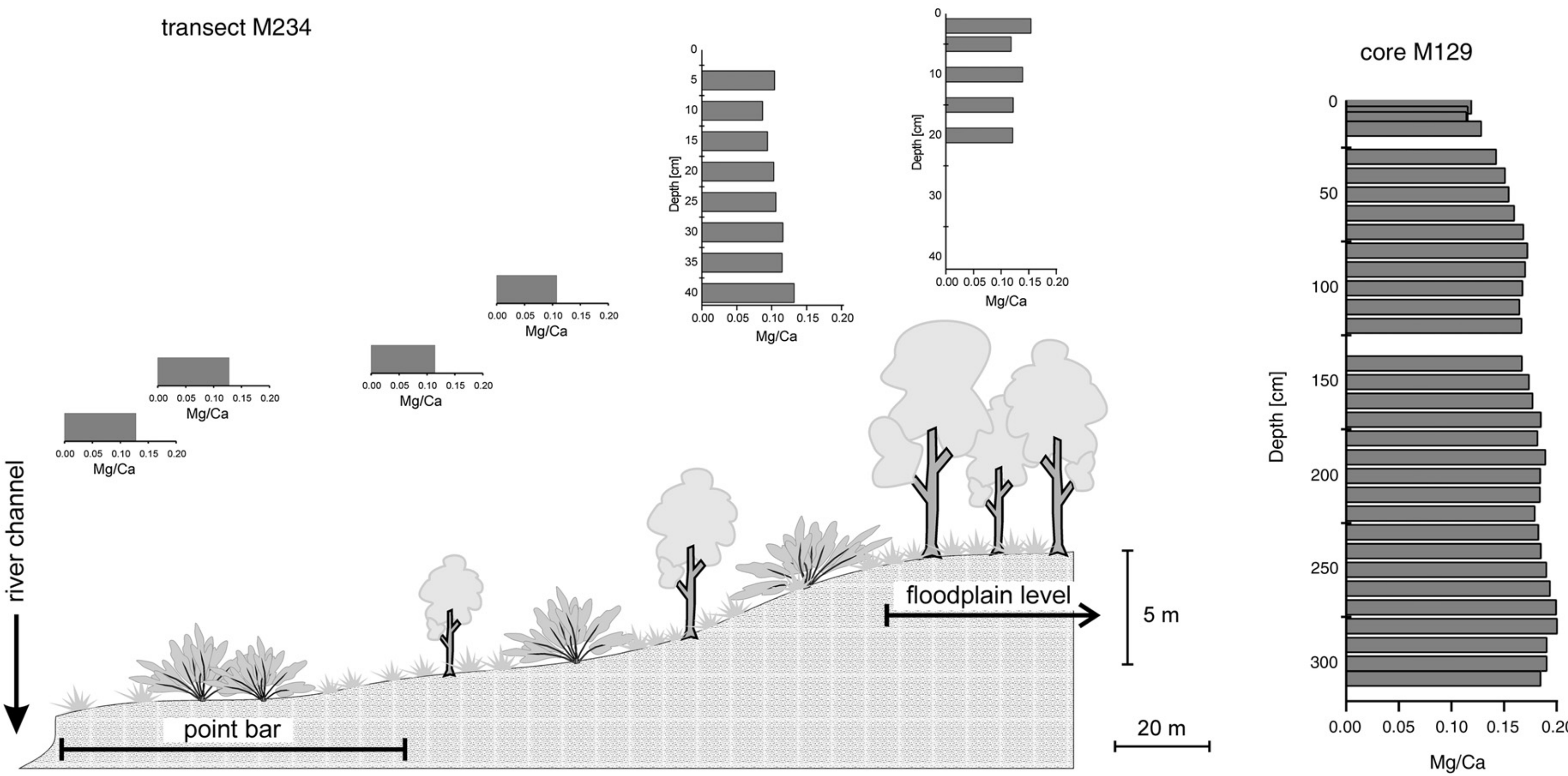

Fig. 6. Mg/Ca in the transect M234 (superficial sampling from the point bar level to the floodplain level) and core M129 (about 200 m far from the river channel). Bar plots show Mg/Ca dependence on the sampling depth.

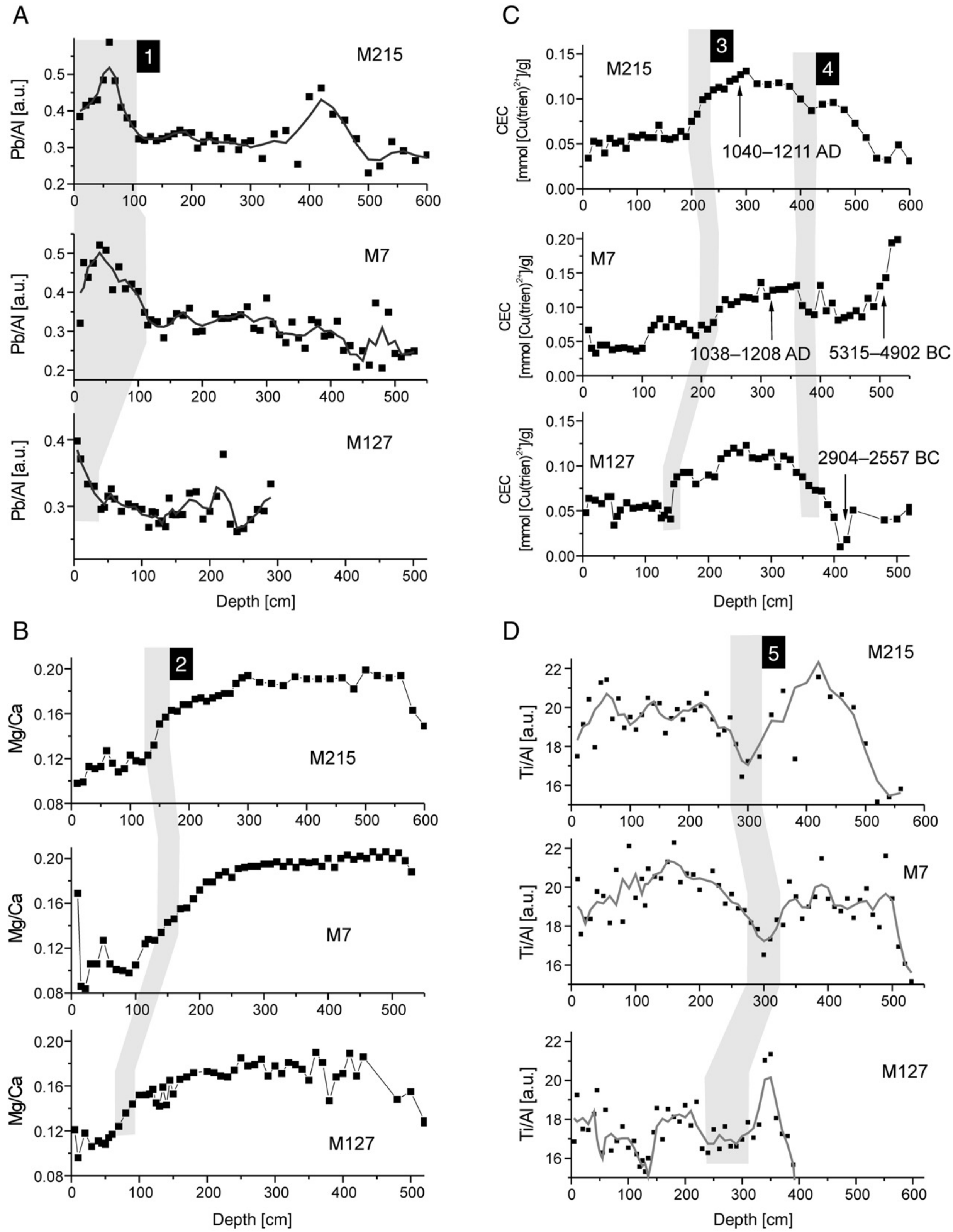

Fig. 7. Lateral stability of three sections in the locality "Bridge to Bzenec" using several chemostratigraphic and lithologic markers. A: the depth of industrially polluted sediments (Pb/Al ratio by EDXRF). B: the inflex point of Mg/Ca ratio in exchangeable/soluble fraction. C: CEC values with selected ^{14}C dates of wood fragments and charcoals. D: Ti/Al minimum, a proxy of silt minimum content (finest sediments of distal floodplain).

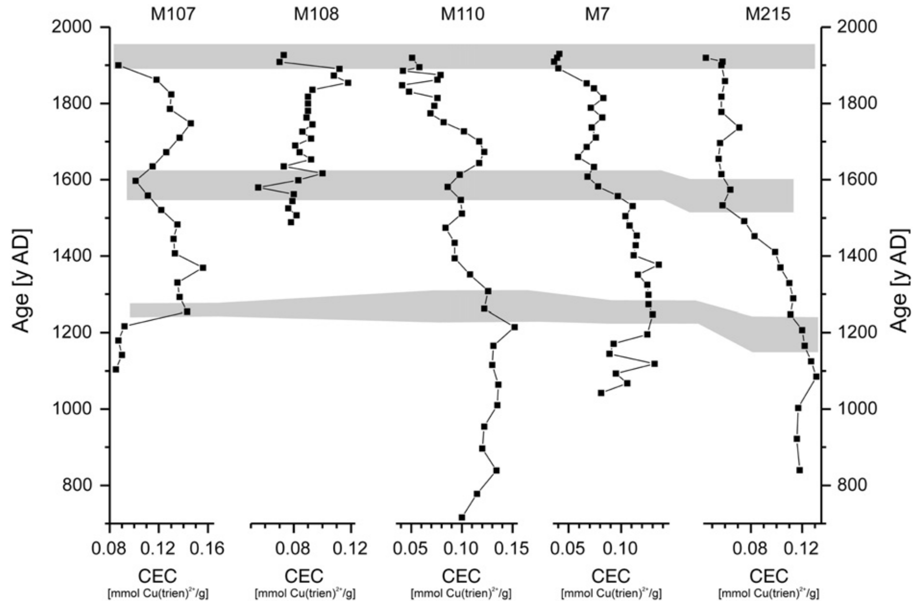

Fig. 8. The depth profiles of CEC in the sections with age models. Three synchronous lithological changes are indicated by grey areas.

4. Discussion

4.1. Use of proxy analyses to facilitate sediment description and correlation

In the studied floodplain deposits we found that CEC values can be used as a proxy for the percentage of clay fraction, which in turn can be used in the assignment of sediment facies. Micromorphological study confirmed that clay horizons or more clayey areas were due to primary sedimentation and that clay redeposition caused by pedogenetic processes is only microscopic (at millimetre scale). If the use of CEC logs is combined with visual sediment examination, it can be used as a substitute for more demanding size fractionation or analysis and allows rapid comparison of data from numerous sections. EDXRF and CEC needs only sample homogenization and grinding, the former method is non-destructive and the latter has sample consumption of up to 0.5 g; each analysis takes several minutes of laboratory work if large sample numbers are routinely processed. The efficiency and low sample consumption are very useful features in checking the lateral stability of the sediments in the studied sites by enabling high density sampling of more sections. Subjective visual evaluation of sediment lithology in the field is seriously hindered by the highly variable degree of gleying, variable development of soil structure, and medium to poor sorting of the overbank fines. The quantitative output of the proxy methods offers a possibility to objectively identify gradation within each sediment subunit (facies).

As shown by the depth profiles in the majority of the studied sections, the Mg/Ca ratio of the exchangeable/soluble fraction has an additional control be it the age of the material deposition, or the time period over which the sediment was subjected to local pedogenesis in the floodplain, or equilibration with groundwater. Our current knowledge is insufficient to discriminate between these hypotheses, but this fact is not essential for correlation purposes. In the sections with a reliable age model, the inflex of the Mg/Ca gradient is centred between 50 cm and 150 cm depth, or in 18th century AD (the letter assignment has a much better consistency). Interpretation of this gradient will be the subject of our further study.

Table 5
Interpolated dates of bottom of Pb polluted layer in selected sections.

Section	Age model (number of 14C dating points)	Locality	Depth of Pb polluted layer [cm]	Interpolated date
S1	3 (taken from Kadlec et al., 2009)	Bridge to Bzenec	30	1910
M110	3	Old Piles	40	1890
M108	1	Jasenová	30	1940

4.2. Chemostratigraphy based on industrial pollution

We had expected individual heavy metals and magnetic particles to display different depth profiles because of their use in different anthropogenic applications (such as corrosion inhibitors, pigments). However, on examination, the individual proxies of the industrial pollution are strongly correlated, i.e. the sharp changes of MS and Zn concentration occurred at practically the same depths in a given section (Fig. 5). The significant increase in Pb concentration and the major change in its isotopic composition also coincide with an increase in MS and Zn levels. This co-variance is in agreement with the results obtained in several previous European studies: in a small watershed of the Arc River in southern France, polluted by fly ash, linked contamination by magnetic particles, Pb and Zn was found by Desenfant et al. (2004). Likewise, a correlation between Cu, Zn, and MS results in riverbed sediments was reported in the Vltava River (Moldau River) in the western part of Czech Republic by Knab et al. (2006).

The estimated age of the industrially polluted deposits in the studied area (grey areas in Fig. 5) can be based on the interpolation of ^{14}C dates, an assumption of a recent deposition of the topmost sediments, and relatively a stable mean depositional rate at the measured section. The last assumption causes the exclusion of sections with thick sandy intercalations in proximal floodplain deposits and/or thick levee deposits on their top. Measured sections meeting the criteria for the interpolation are summarized in Table 5. The mean of the three listed interpolated dates for the lower boundary of the polluted layer is 1910 AD.

Anthropogenic pollution of the topmost floodplain deposits in the study area is probably related to coal combustion and perhaps other industrial processes in the Morava River watershed and, as such, the scheme is generally valid for the Czech Republic (Novák et al., 2003). The recording of elevated concentrations of heavy metals related to the industrial pollution is commonly noted in study of sediment archives (e.g., Swennen and Van der Sluys, 2002; Novák et al., 2003; Ettler et al., 2004; 2006; Pasternack and Brown, 2006). The reliable

Table 6
Mean depositional rates of fine overbank deposits in the studied area.

	^{14}C age BP	Calendar age	Depositional rate [cm·y^{-1}] (time interval)	Sediment character
M107, 90 cm		1900	0.26 (1140–1900)	Mostly clayey, distal floodplain
M 107, 280 cm 8062	901 ± 81	1012 – 1268 (94)		
M107-280, Poz-29491	815 ± 30	1169 – 1269 (95)		
M108, 35 cm		1900	0.55 (1535–1900)	Mostly silty, proximal floodplain
M 108, 210-260 cm, 8063	389 ± 80	1408 – 1661 (95)		
M110, 40 cm		1900	0.42 (1570–1900)	Upward coarsening, silty, proximal floodplain deposits to levee
M110, 178 cm, 8057	273 ± 81	1446 – 1696 (70), 1725 – 1814 (17), 1917 – 1952 (6)		
220 cm, 8066	205 ± 80	1515 – 1598 (11%), 1617 – 1953 (84%) DATUM NOT USED		
250 cm, 8065	672 ± 82	1213 – 1426 (95)	0.20 (720–1320)	Clayey, distal floodplain sediments
370 cm, 8064	1343 ± 83	556 – 884 (95%)		
M215, 90 cm		1900	0.24 (1126–1900)	Upward coarsening from silty to sandy
M215-290, Poz-29494	900 ± 30	1040–1211 (95)		
M7	taken from Kadlec et al., 2009		0.36 (1123–1900)	Upward coarsening silty, proximal floodplain to levee

The depositional rate of the deposits from the last century was not evaluated because of a highly variable proportion of levee deposits in the top of the sections.

identification of the depth profiles of the pollutants may be limited by the weathering of the original contaminant particles and the mobilization of their ions (Hudson-Edwards et al., 1998). This chemical mobilization may be very important in the case of metal sulphide contaminations from historical mining, which considerably decreases pH during their oxidative weathering, and consequently highly mobile free ions are formed (Hudson-Edwards et al., 1998). This is probably not the case in the study area where there are no nearby sources of pollution due to historical or current mining or metal smelting and the pollution probably originates from more remote, global sources. Swennen and Van der Sluys (2002) are rather optimistic with respect to the post-depositional stability of industrial polluted fluvial deposits. The outcrops in Strážnické Pomoraví do not bear signs of systematic translocations of soil particles (illimerization), however, special attention must be paid to the levee deposits and sandy intercalations wherever they are present in the top layers and where metal contamination is observed. The downward particle transport through permeable, coarse sediments in sandy or gravelly river alluvia was observed, e.g., by Cieszewski et al. (2008). Ploughing and bioturbation are also responsible for some downward transport of the atmospherically derived contaminants (Fernandez et al., 2008). The effects blurring the actual lower boundary of the industrial pollution in the measured sections could be responsible for about a decimetre-scale inaccuracy, which is not a significant problem in the studied sections where the depth of industrially polluted layers ranges from 0.3 to 1 m. In spite of all these uncertainties, the lack of reliable dating techniques for the last 100 y makes the industrial pollution an invaluable chemostratigraphic tool for the studied sections.

The pollution of the Morava River watershed by the fallout of fly ash from coal combustion is one possible explanation for the almost step-like growth of heavy metals' and magnetic particles' concentrations observed in sections at the depth of 30 to 100 cm in river banks (Fig. 5). The increase of the magnetic susceptibility signal has previously been attributed to the redeposition of less weathered soil material from intensified agricultural activities since the 1950's (Kadlec et al., 2009). The coincidence of its growth with the growth of heavy metal concentration and Pb isotopic composition can also imply another explanation, such as the contamination of the sediments by fly ash from coal combustion. Such an association of magnetic carriers and heavy metals was experimentally demonstrated in case studies in the Czech Republic by Kapička et al. (1999) and France (Desenfant et al., 2004).

The sharp changes in Pb concentration and isotopic composition observed in the Morava River floodplain sequences closely resemble the observation in sediments of Lake Constance in Switzerland where these signatures started to change around 1900 AD, a pattern that was again attributed to the coal combustion (Kober et al., 1999). Similarly in the Czech Republic, coal combustion was the most important source of atmospheric lead; the first steep growth of coal mining, associated with modern industrialization of Czech lands started at ~1900 and a second growth peak of coal mining followed in the 1950's (Novák et al., 2003). Previously we assigned the change in Pb isotopic signature in the floodplain deposits in Strážnické Pomoraví exclusively to the introduction of leaded gasoline (Kadlec et al., 2009). It is, however, not easy to distinguish the influences of leaded gasoline and coal combustion only from Pb isotopic signatures (Komárek et al., 2008).

4.3. The depositional rates in current floodplain in Strážnické Pomoraví

The depositional rate (aggradation plus lateral accretion) is a very important factor describing the floodplain when an anthropogenic influence is suspected to affect the behaviour of a river or floodplain. In many recent studies, a reported increase of aggradation rates in floodplains has been assigned to an intensification of land use, especially deforestation and ploughing. Such a straightforward relationship seems justified for small watersheds, especially where colluviation and enhanced direct localized erosion can be relevant (e.g., de Moor et al., 2008), but it may be oversimplified in the floodplains of rivers with a large watershed, where the transport of the material from soil erosion to the floodplains of the trunk rivers is delayed in temporal sinks in the higher order valleys (e.g., Lang et al., 2003; Kalicki et al., 2008).

Calculation of the mean depositional rate in Strážnické Pomoraví is hindered by two facts. Firstly, the deposition rate of the topmost sediments in the studied area was probably affected by past changes in land use, flood defence building in Strážnické Pomoraví, and channelization of the river upstream during the 20th century. Evaluation of the depositional rate during the last century would require a much more detailed study than is the scope of this paper. The second limitation is the lack of the recent dating points caused by the equivocality of the radiocarbon calibration curve between 1620 and 1955 AD. The latter problem is partly solved by using the proxies of the industrial pollution, which indicate the sediments deposited after ~1900 AD.

The mean depositional rates in Table 6 were calculated by linear regression using the age of 1900 AD of the bottom of the industrially polluted sediments and ^{14}C date points from the deeper parts of the sections. A facies control on the mean depositional rate is quite clear: the lowest deposition rates (0.2 to 0.3 cm y^{-1}) are typical for distal floodplain sediments (middle, mostly clay (lower part of section M110, mean CEC 0.12 mmol $[Cu(trien)]^{2+}$/g) or upward coarsening clayey sediments grading from distal to proximal floodplain deposits (central parts of sections M7, M107, and M215). The sedimentation rates in section M108 and the upper part of section M110, both with much coarser sediments of proximal floodplain to levee deposits (CEC ~0.09 mmol $[Cu(trien)]^{2+}$/g) was 0.55 and 0.42 cm y^{-1}, respectively. This dependence should be taken into account when mean aggradation rate of floodplains is to be evaluated from large sets of depth-age profiles.

In our previous study (Kadlec et al., 2009) we found a pronounced change in the nature of the sediment, centred on the 16th century, where a shift from more clayey deposits, assigned here to distal floodplain sediments, to more silty deposits, assigned here to proximal floodplain deposits occurred. The current results (Figs. 3, 4, and 8) confirm that substantial lithological (facial) changes occurred in that period in the floodplain part under investigation. The current age model now permits the identification of three simultaneous changes in depositional conditions in four sections from three localities (Fig. 8): one at ~1200 AD, another at ~1600 AD, and the last at ~1900 AD.

The sediment coarsening at ~1600 AD in sections M7 and M110 indicated in Fig. 8 is within the uncertainty of the sediment dating coincident with the sediment coarsening during the 16th century, as reported previously (Kadlec et al., 2009), where one more locality was also included (downstream from sections M107 and M108). For at least the last two centuries all these sections belonged to the same river branch (meander belt). The simultaneous coarsening of the sediments in several sections from that branch allows proposing a hypothesis that the proportion of water flowing through this branch was enhanced in ~1600 AD at the expense of the branch which passed through the vicinity of Strážnice and Petrov (Figs. 1 and 2). This is the most straightforward interpretation reflecting the knowledge on the dynamics of floodplain of meandering and aggrading rivers (Bridge, 2003). To discriminate between such a facies change and an assumed general change in the nature of the sediments, as assumed previously (Kadlec et al., 2009), further analyses will be needed to focus on sections and cores from other areas of the Morava River floodplain, including localities downstream from the current sites and also sections and cores from parts of the river floodplain currently separated from the active river branch by flood defences. This paper presents and verifies tools and approaches suitable for such studies.

5. Conclusions

Geochemical proxies are very useful tools for the study of sedimentary sequences comprised of aggrading meandering rivers due to their ease of generation. The proxy methods were “calibrated” using conventional analytical methods that allowed their interpretation in lithological terms and permit the facies assignment to the sediments. The chemostratigraphic correlation of floodplain horizons with a heavy metal contamination helps to overcome two problems when describing sediment sequences from the last century: firstly by providing a date point of the onset of massive industrial pollution (~1900 AD) into the interval of equivocality of the radiocarbon calibration curve, and secondly by permitting identification of the top layers most affected by river regulations and land use changes in the 20th century. The results of the study produced estimates of mean depositional rates in Strážnické Pomoraví between ~1000 and ~1900 AD in several localities; the actual sedimentation rates depend on the actual depositional facies.

Acknowledgments

The work would never have been performed without the enthusiastic and inspiring work of Jaroslav Kadlec (Geological Institute ASCR, Prague, Czech Republic). We also thank to Libor Petr (Charles University, Prague, Czech Republic) and Anna Píšková (Institute of Inorganic Chemistry ASCR, Řež, Czech Republic) for their help in the field trips. Jana Dörflová, Petr Vorm, and Zuzana Hájková (all three from the Institute of Inorganic Chemistry ASCR, Řež, Czech Republic) substantially contributed by processing and laboratory analyses (CEC and EDXRF) of many hundred samples. The work was funded by project IAAX00130801 (Grant Agency of the Academy of Sciences of Czech Republic) and the EDXRF analyses by the project AV0Z4032918.

References

2nd Austrian Military Survey, 1841. Map sheets no. m137 O 12 IV, m138b O 12 V (Mähren), scale 1:28 800, Austrian State Archive/Military Archive, Vienna; digital processing: © Laboratory of Geoinformatics, University of J.E. Purkyně, Ústí nad Labem, © Agency for nature conservation and landscape protection of the Czech Republic, The Silva Tarouca Research Institute for Landscape and Ornamental Gardening, Branch Brno.
3rd Austrian Military Survey, 1876. Map sheet no. 4458/2, scale 1:25 000, Map collection of the Charles University, Praha; digital processing: © The Silva Tarouca Research Institute for Landscape and Ornamental Gardening, Branch Brno.
Blaeu, J., 1665. The Atlas Maior (Atlas Novus), page 125, available on line at The Regional Archives of Leiden, the Netherlands, http://www.atlasblaeu.com/.
Bridge, J.S., 2003. Rivers and floodplains. Forms, Processes, and Sedimentary Record. Blackwell Publishing.
Bullock, P., Murphy, C.P. (Eds.), 1983. Soil micromorphology. Berkhamsted AB Academic.
Cieszewski, D., Czajka, A., Błażej, S., 2008. Rapid migration of heavy metals and ^{137}Cs in alluvial sediments, Upper Odra River valley, Poland. Environ. Geol. 1577–1586.
Cojan, I., Renard, M., 1999. Sedimentology. A.A. Balkema Publishers Lisse/Abingdon/Exton (PA)/Tokyo.
Curie, L.A., 1995. Nomenclature in evaluation of analytical methods including detection and quantification capabilities. (IUPAC Recommendation 1995). Pure Appl. Chem. 67, 1699–1723.
de Moor, J.J.W., Kasse, C., van Balen, R., Vandenberghe, J., Wallinga, J., 2008. Human and climate impact on catchment development during the Holocene – Geul River, the Netherlands. Geomorphology 98, 316–339.
Desenfant, F., Petrovský, E., Rochette, P., 2004. Magnetic signature of industrial pollution of stream sediments and correlation with heavy metals: Case study from South France. Water Air Soil Pollut. 152, 297–312.
Ettler, V., Mihaljevič, M., Komárek, M., 2004. ICP-MS measurement of lead isotopic ratios in soils heavily contaminated by lead smelting: tracing the sources of pollution. Anal. Bioanal. Chem. 378, 311–317.
Ettler, V., Mihaljevič, M., Šebek, O., Molek, M., Grygar, T., Zeman, J., 2006. Geochemical and Pb isotopic evidence for sources and dispersal of metal contamination in stream sediments from the mining and smelting district of Příbram, Czech Republic. Environ. Pollut. 142, 409–417.
Fernandez, C., Monna, F., Labanowski, J., Loubet, M., van Oort, F., 2008. Anthropogenic lead distribution in soils under arable land and permanent grassland estimated by Pb isotopic compositions. Environ. Pollut. 156, 1083–1091.
Grygar, T., Bezdička, P., Hradil, D., Hrušková, M., Novotná, K., Kadlec, J., Pruner, P., Oberhänsli, H., 2005. Characterization of expandable clay minerals in Lake Baikal sediments by thermal dehydration and cation exchange. Clays Clay Miner. 53, 389–400.
Grygar, T., Kadlec, J., Žigová, A., Mihaljevič, M., Nekutová, T., Lojka, R., Světlík, I., 2009. Chemostratigraphic correlation of sediments containing expandable clay minerals based on ion exchange with Cu(II) triethylenetetramine. Clays Clay Miner. 57, 168–182.
Gupta, S.K., Polach, H.A., 1985. Radiocarbon dating practises at ANU. ANU, Canberra, Australia.
Havlíček, P., 1991. The Morava River Basin during the last 15000 years. In: Starkel, L., Gregory, K.J., Thornes, J.B. (Eds.), Temperate Palaeohydrology: Fluvial Processes in the Temperate Zone During the Last 15, 000 Years. John Wiley & Sons, Chichester, West Sussex, UK.
Havlíček, P., Smolíková, L., 1994. Evolution of south Moravian flood plains. Věst. Čes. Geol. Úst. 69, 23–40 (in Czech).
Hoffmann, T., Lang, A., Dikau, R., 2008. Holocene river activity: analysing ^{14}C-dated fluvial and colluvial sediments from Germany. Quat. Sci. Rev. 27, 2031–2040.
Hoffmann, T., Erkens, G., Gerlach, R., Klostermann, J., Lang, A., 2009. Trends and controls of Holocene floodplain sedimentation in the Rhine catchment. Catena 77, 96–106.
Houben, P., 2007. Geomorphological facies reconstruction of Late Quaternary alluvia by the application of fluvial architecture concepts. Geomorphology 86, 94–114.
Hudson-Edwards, K.A., Macklin, M.G., Curtis, C.D., Vaughan, D.J., 1998. Chemical remobilization of contaminant metals within floodplains sediments in an incising river system: implications for dating and chemostratigraphy. Earth Surf. Process. Landf. 23, 671–684.

ISO 11277:1998. Soil quality — Determination of particle size distribution in mineral soil material — Method by sieving and sedimentation.
Jacquiot, C., Trenard, Y., Dirol, D., 1973. Atlas d'anatomie des bois des Angiospermes. Centre Technique du Bois, Paris.
Kadlec, J., Grygar, T., Světlík, I., Ettler, V., Mihaljevič, M., Diehl, J.F., Beske-Diehl, S., Svitavská-Svobodová, H., 2009. Morava River floodplain development during the last millennium, Strážnické Pomoraví, Czech Republic. Holocene 19, 499–509.
Kalicki, T., Sauchyk, S., Calderoni, G., Simakova, G., 2008. Climatic versus human impact on the Holocene sedimentation in river valleys of different order: examples from the upper Dnieper basin, Belarus. Quat. Int. 189, 91–105.
Kapička, A., Petrovský, E., Ustjak, S., Macháčková, K., 1999. Proxy mapping of fly-ash pollution of soils around a coal-burning power plant: a case study in the Czech Republic. J. Geochem. Explor. 66, 291–297.
Knab, M., Hoffmann, V., Petrovský, E., Kapička, A., Jordanova, N., Appel, E., 2006. Surveying the anthropogenic impact of the Moldau river sediments and nearby soils using magnetic susceptibility. Environ. Geol. 49, 527–535.
Kober, B., Wessels, M., Bollhöfer, A., Mangini, A., 1999. Pb isotopes in sediments of Lake Constance, Central Europe constrain the heavy metal pathways and the pollution history of the catchment, the lake and the regional atmosphere. Geochim. Cosmochim. Acta 63, 1293–1303.
Komárek, M., Ettler, V., Chrastný, V., Mihaljevič, M., 2008. Lead isotopes in environmental sciences: a review. Environ. Int. 34, 562–577.
Lang, A., Nolte, S., 1999. The chronology of Holocene alluvial sediments from the Wetterau, Germany, provided by optical and ^{14}C dating. Holocene 9, 207–214.
Lang, A., Bork, H.R., Mackel, R., Preston, N., Wunderlich, E., Dikau, R., 2003. Changes in sediment flux and storage within a fluvial system: some examples from the Rhine. Hydrol. Process. 17, 3321–3334.
Lewin, J., Macklin, M.G., 2003. Preservation potential for Late Quaternary river alluvium. J. Quat. Sci. 18, 107–120.
Macklin, M.G., Lewin, J., 2008. Alluvial responses to the changing Earth system. Earth Surf. Process. Landf. 33, 1374–1395.
Macklin, M.G., Johnstone, E., Lewin, J., 2005. Pervasive and long-term forcing of Holocene river instability and flooding in Great Britain by centennial-scale climate change. Holocene 15, 937–943.
Macklin, M.G., Benito, G., Gregory, K.J., Johnstone, E., Lewin, J., Michczyńska, D.J., Soja, R., Starke l, L., Thorndycraft, V.R., 2006. Past hydrological events reflected in the Holocene fluvial record of Europe. Catena 66, 145–154.
Macphail, R.I., Cruise, J., 2001. The soil micromorphologist as team player: a multianalytical approach to the study of European microstratigraphy. In: Goldberg, P., Holliday, V.T., Ferring, C.R. (Eds.), Earth Sciences and Archaeology. Kluver Academic.
Meier, L.P., Kahr, P., 1999. Determination of the cation exchange capacity (CEC) of clay minerals using the complexes of copper(II) ion with triethylenetetranine and tetraethylenepentamine. Clays Clay Miner. 47, 386–388.
Notebaert, B., Verstraeten, G., Rommens, T., Vanmontfort, B., Govers, G., Poesen, J., 2009. Establishing a Holocene sediment budget for the river Dijle. Catena 77, 150–163.
Novák, M., Emmanuel, S., Vile, M.A., Erel, Y., Véron, A., Pačes, T., Wieder, R.K., Vaněček, M., Štěpánová, M., Břízová, E., Hovorka, J., 2003. Origin of lead in eight Central European peat bogs determined from isotope ratios, strengths, and operation times of regional pollution sources. Environ. Sci. Technol. 37, 437–445.
Pasternack, G.B., Brown, K.J., 2006. Natural and anthropogenic geochemical signatures of floodplain and deltaic sedimentary strata, Sacramento-San Joaquin Delta, California, USA. Environ. Pollut. 141, 295–309.
Prudič, Z., 1978. The Strážnice floodplain forest in the second half of the 1st millennium A.D. Lesnictví 24, 1019–1036 (in Czech).
Reimer, P.J., Baillie, M.G.L., Bard, E., Bayliss, A., Beck, J.W., Bertrand, C.J.H., Blackwell, P.G., Buck, C.E., Burr, G.S., Cutler, K.B., Damon, P.E., Edwards, R.L., Fairbanks, R.G., Friedrich, M., Guilderson, T.P., Hogg, A.G., Hughen, K.A., Kromer, B., McCormac, G., Manning, S., Ramsey, C.B., Reimer, R.W., Remmele, S., Southon, J.R., Stuiver, M., Talamo, S., Taylor, F.W., van der Plicht, J., Weyhenmeyer, C.E., 2004. IntCal04 terrestrial radiocarbon age calibration, 0–26 cal kyr BP. Radiocarbon 46, 1029–1058.
Reynolds Jr., R. C., 1985. NEWMOD©, a computer program for the calculation of one-dimensional diffraction patterns of mixed-layered clays — R. C. Reynolds, Jr., 8 Brook Dr., Hanover, New Hampshire 03755.
Rommens, T., Verstraeten, G., Bogman, P., Peeters, I., Poesen, J., Govers, G., Van Rompaey, A., Lang, A., 2006. Holocene alluvial sediment storage in a small river catchment in the loess area of central Belgium. Geomorphology 77, 187–201.
Schweingruber, F.H., 1990. Anatomie europäischer Hölzer: Ein Atlas zur Bestimmung europäischer Baum-. Strauch- und Zwergstrauchhölzer, Haupt, Bern, Stuttgart.
Starkel, L., Soja, R., Michczynska, D.J., 2006. Past hydrological events reflected in Holocene history of Polish rivers. Catena 66, 24–33.
Swennen, R., Van der Sluys, J., 2002. Anthropogenic impact on sediment composition and geochemistry in vertical overbank profiles of river alluvium from Belgium and Luxembourg. J. Geochem. Explor. 75, 93–105.
Tanner, C.B., Jackson, M.L., 1948. Nomographs of sedimentation times for soil particles under gravity or centrifugal acceleration. Soil Sci. Soc. Am. Proc. 12, 60–65.
Thorndycraft, V.R., Benito, G., 2006. The Holocene fluvial chronology of Spain: evidence from a newly compiled radiocarbon database. Quat. Sci. Rev. 25, 223–234.
Topographical Maps of the Czech Republic, 2006–2007. Digital version ZABAGED, Map sheets no. 34–22-15, 34-22-19, 34-22-20, scale 1 : 10 000, © Czech Geodetic and Cadastral Institute.
Topographical Maps of the Czechoslovak Army, 1953–1955. Map sheets no. m33119ab, m33119ad, m33119ba, m33119bc, scale 1:25 000, Military Schools, Brno; digital processing: © The Silva Tarouca Research Institute for Landscape and Ornamental Gardening, Branch Brno.
Vannière, B., Bossuet, G., Walter-Simonnet, A.-V., Gauthier, E., Barral, P., Petit, C., Buatier, M., Daubigney, A., 2003. Land use change, soil erosion and alluvial dynamic in the lower Doubs Valley over the 1st millenium AD (Neublans, Jura, France). J. Archaeol. Sci. 30, 1283–1299.

5.3. Eolické procesy

Lisá, L., Buriánek D., Uher P. (2009): New approach to garnet redistribution during aeolian transport.- Geological Quarterly, 53 (3).

Lisa, L., Hosek, J., Bajer, A., Matys Grygar T., Vandenberghe D. (2014): Geoarchaeology of Upper Palaeolithic loess sites located within a transect through Moravian valleys, Czech Republic.- Quaternary International, 351, 25-37.

Geological Quarterly, 2009, **53** (3): 333–340

New approach to garnet redistribution during aeolian transport

Lenka LISÁ, David BURIÁNEK and Pavel UHER

Lisá L., Buriánek D. and Uher P. (2009) — New approach to garnet redistribution during aeolian transport. Geol. Quart., **53** (3): 333–340. Warszawa.

Garnet composition within Late Pleistocene (Weichselian) loess and loess-like deposits was studied in 13 samples of sediment heavy mineral fractions from Moravia and Silesia (Czech Republic). Four areas differing in garnet chemistry were identified, and some regional trends in garnet composition changes were documented. The data obtained support the generally accepted conclusion of prevailing westerly winds during Weichselian loess deposition. Metamorphic rocks of the Bohemian Massif together with contributions from igneous (mainly granitic) and sedimentary rocks were indicated as a source for the Weichselian loess and loess-like deposits studied. Local differences in garnet composition depend on the basement source rocks, on prevailing wind direction, on regional geomorphology and on transport distance.

Lenka Lisá, Institute of Geology, Academy of Sciences of the Czech Republic, Rozvojová 135, 165 02 Praha 6, Czech Republic, e-mail: lisa@gli.cas.cz; David Buriánek, Czech Geological Survey, Leitnerova 2, Brno 602 00, Czech Republic, e-mail: burianek@cgu.cz; Pavel Uher, Department of Mineral Deposits, Comenius University, Mlynská dolina, 842 15 Bratislava, Slovakia, e-mail: puher@fns.uniba.sk *(received: September 24, 2008; accepted: April 04, 2009).*

Key words: Weichselian, Pleistocene, Czech Republic, aeolian sediments, garnet composition, provenance.

INTRODUCTION

The wide compositional range of garnets, leads to their common use as provenance indicators. However, even though their major element chemistry has been known since 1985 (Morton, 1985), they have been very rarely used as provenance indicators for loessic sediments. There are two main reasons why garnet composition is not often used in Quaternary provenance studies. Firstly, the data are inhomogeneous and secondly, sufficient data from provenance source rocks are commonly absent. We demonstrate here that in cases where provenance data are not available, garnet chemistry can be still used as proxies for aeolian sedimentary process. Moravian and Silesian Weichselian loess and loess-like deposits were chosen for this study.

GEOLOGICAL SETTINGS

Loess and loess-like deposits cover more than 20% of the Quaternary surface area in Moravia and Silesia (Fig. 1). Most of these accumulations were deposited during the latest Pleistocene (Late Weichselian, M IS 2) glacial phase (Frechen *et al*., 1999). The average thickness of the youngest Weichselian loess is about 1 to 1.5 m. Garnet-rich loess material was used for provenance studies and also for the study of garnet redistribution across the landscape. The differences between typical South Moravian loess *s.s.* and North Moravian loess-like deposits are in the transparency of the material that reflects carbonate content (Pelíšek, 1949), the different altitudes at which they are found, and different sources (Lisá *et al*., 2005).

Weichselian loess and loess-like deposits in Moravia and Silesia area have been much studied. Detailed sedimentary classifications for local areas were published by Ambrož (1947) and Pelíšek (1949), stratigraphical studies were published by Musil and Valoch (1956), Ložek (1958), Kukla (1961) and Havlíček and Smolíková (1993), provenance studies by Kvítková and Buriánek (2002), Lisá (2004), Lisá *et al*. (2005) and Lisá and Uher (2006). Palaeoclimate studies of the Moravian loess were published by Adamová and Havlíček (1997), Frechen *et al*. (1999), Cílek (2001) and by Adamová *et al*. (2002). However, none of these papers deal with the problem of garnet redistribution.

The most complete source, regarding the garnet chemical composition within the area studied, is by Čopjaková *et al*. (2005). Some other regional publications (Fediuková *et al*.,

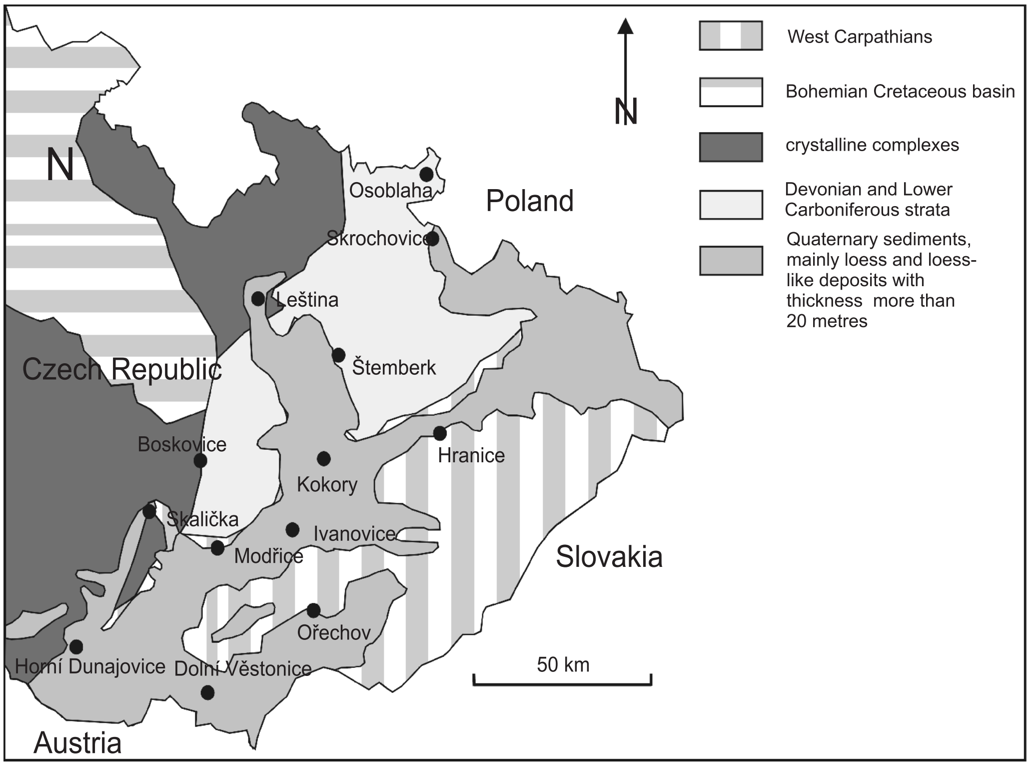

Fig. 1. The distribution of Quaternary, mainly aeolian sediments in Moravia and Silesia and their geological basement, Eastern part of the Czech Republic; location of samples discussed in this paper

1985, Batík and Fediuková, 1992, Nehyba and Buriánek, 2004 and Medaris *et al*., 2005) are used as comparisons in this study.

METHODS

Samples were collected from Weichselian loess sections that have been described by many authors (Macoun *et al*., 1965; Havlíček, 1985; Havlíček and Smolíková, 1993; Adamová and Havlíček, 1995, 1997). In total, 13 sites were selected for detailed garnet analysis (Osoblaha, Skrochovice, Leština, Štemberk, Hranice, Kokory, Boskovice, Skalička, Ivanovice, Modřice, Ořechov, Horní Dunajovice and Dolní Věstonice, Fig. 1).

The most commonly used size fraction in palaeogeographical provenance studies within Moravia, 0.063–0.125 mm, was subjected to the standard procedure of heavy mineral separation in heavy liquid — tetrabromethane of D = 2.96 g/cm^3 (Mange and Mauer, 1992; Mange and Wright 2007). Most of the samples were garnet-rich, so further separation was not necessary. The samples were impregnated with resin and polished. The polished samples were then analysed using a *Cameca SX-100* electron microprobe analyser at the Institute of Geological Sciences (Masaryk University, Brno). The following analytical conditions were used: wavelength-dispersion mode with a beam diameter of 4–5 µm with an accelerating potential of 15 kV and a sample current of 20 nA. A counting time of 20 s was used for all elements. The following standards were used (K_α X-ray lines): wollastonite (Si, Ca), albite (Na), chromite (Cr), Al_2O_3 (Al), MgO (Mg), Fe_2O_3 (Fe), metallic Mn (Mn) and TiO_2 (Ti). Garnet grains separated from the same fraction and mounted on adhesive carbon tape and studied by the same microprobe analyzer were used for micromorphological interpretation. A minimum of three analyses were made, but no zoning was found.

RESULTS

HEAVY MINERAL DISTRIBUTION

The heavy mineral composition is shown in Table 1. Garnets are very abundant in detrital heavy minerals in the fraction studied (0.063–0.250 mm). Their contents range from 5.3% at Ořechov in the south to 44.3% Štemberk in the north. There is no systematic trend in garnet abundance across the area studied, but there is a decrease in garnet from west to east in the south of the area studied and an increase in garnet from west to east in the central and northern parts. A variable proportionality exists between garnet and hornblende quantities (Table 1). The results of the heavy mineral provenance studies have previously been published by Lisá *et al*. (2005).

MAJOR ELEMENT CHEMISTRY OF GARNETS

The garnet chemistry is typified by the predominance of an almandine (Alm) component (Table 2). No pronounced zoning was observed. The garnet with Alm >50% constitutes

Table 1

The concentrations of prevailing non-opaque minerals (%) in the heavy mineral fraction

Locality	Amp	Grt	Zrn	St	Tur	Rt	Ep	Ky	Mnz	Ap	other	
Osoblaha	9.0	34.0	16.7	20.0	3.6	6.7	0.0	5.0	0.2	3.3	1.5	Ttn
Skrochovice	6.6	38.4	7.7	17.4	15.4	10.3	0.0	4.1	0.1	0.0	0.0	
Hranice	8.0	29.3	31.0	0.0	8.0	8.0	9.3	1.3	0.1	0.0	5.0	Cpx
Leština	59.7	24.0	1.9	0.7	0.3	2.5	4.0	0.9	0.3	3.4	2.3	Sil, Ttn
Štemberk	22.4	44.3	4.5	5.0	9.0	1.5	10.1	3.0	0.2	0.0	0.0	
Kokory	57.8	20.3	1.8	1.2	1.2	2.5	3.9	1.2	0.3	3.8	6.0	Sil, Ttn, Cpx
Boskovice	62.5	19.7	3.9	0.5	1.8	0.3	2.5	0.5	0.2	2.1	6.0	Sil, Ttn
Skalička	47.7	24.2	2.9	0.0	5.6	0.0	6.0	0.0	1.2	1.2	0.0	
Modřice	38.6	38.3	1.8	1.8	1.2	2.5	16.6	3.8	2.2	1.9	0.0	
H. Dunajovice	60.2	23.0	1.9	0.9	0.3	2.5	1.7	0.9	0.3	3.4	0.0	
D. Věstonice	61.2	20.9	3.0	0.7	1.8	0.7	2.3	1.4	0.2	2.0	5.8	Sil, Ttn
Ivanovice	31.8	28.8	13.0	3.8	5.0	2.5	6.4	1.3	0.1	5.0	2.3	Cpx
Ořechov	49.5	5.3	15.9	3.9	4.6	11.3	2.0	4.0	0.6	1.4	1.5	Cpx

Amp — amphibole, Grt — garnet, Zrn — zircon, St — staurolite, Tur — tourmaline, Rt — rutile, Ep — epidote, Ky — kyanite, Mnz — monazite, Ap — apatite, Ttn — titanite, Sil — sillimanite, Cpx — Ca clinopyroxene; abbreviations after Kretz (1983)

89%, although groups of garnets can be recognized in which Mg, Mn or Ca components show some differences or anomalies in source provenance rocks. Microchemical analyses of selected detrital garnets from each area are shown in Table 2. Significant differences were found between localities for different parts of Moravia and Silesia. Towards the east, the amount of grossular (Grs) component decreases (Table 2). Another, more significant decrease in this component is a function of latitude in eastern Moravia and Silesia. Towards the south, the Grs component decreases. Another latitude-dependent difference is visible in the western part of Moravia and Silesia (Fig. 2; Table 2). This region is dominated by almandine-rich garnets with variable pyrope (Prp) and spessartine (Sps) components (Table 2). Moravia and Silesia can be divided into four main areas according to such differences: A1, A2, A3 and B1 (see Figs. 2 and 3). Diagrams of relations between Mg/Mn and Ca are demonstrated in Figure 2. These data for garnet distribution in loess of the area studied are shown in four scatter diagrams of Mg/Mn *vs*. Ca (Fig. 2). The first three areas are typified by loess deposits overlying crystalline complexes or surrounded by such complexes. The next two areas have a sedimentary rock basement and a variation of in Grs-rich component garnets can be seen between these two groups. An obvious decrease in the Grs-rich component is visible towards the SE of Moravia. Variations in garnet chemical composition are also visible from north to south. Loess deposits from the southern part of the area studied are typified by a high Mg/Mn ratio (>20; Fig. 3).

MICROMORPHOLOGY OF DETRITAL GARNETS

Garnet grains from the samples studied display typical features of aeolian transport (Fig. 4). This is in contrast with the quartz grains that are more commonly used for micromorphological study (*cf*., Smalley and Cabrera, 1970; Lisá, 2004; Kenig, 2006, 2008; Hladil *et al*., 2008). The garnet grains have a subangular to angular outline, with high to medium relief. There is a noticeable presence of imbricated blocks, large breakage blocks, edge abrasion, and different types of ridges, pits and typical aeolian V-shaped pits or arrows. Most grains are affected by chemical dissolution as documented by solution pits or silica precipitation. Detrital garnets are nearly always found in the form of irregular chips (Fig. 4).

DISCUSSION

The ratio between garnet and hornblende quantities reflects the geological setting of the study area (Lisá *et al*., 2005; Lisá and Uher, 2006). Westerly-lying magmatic and metamorphic Moldanubian rocks, mainly orthogneisses, amphibolites, paragneisses, peridotites, eclogites and granulites (Mísař *et al*., 1983; Fiala *et al*., 1995) produce large amounts of hornblende, garnet and variable amounts of stable heavy minerals such as epidote, apatite or zircon. Towards the east, sedimentary successions of Devonian and Lower Carboniferous age start to appear together with Tertiary deposits of the Carpathian Foredeep. These are connected with large amounts of garnets and other more stable minerals, typical of older strata (Čopjaková *et al*., 2005). Hornblendes are compensated for a more stable mineral — garnet (Table 1). This situation reflects the fact that the studied mineral fraction of loess and loess-like deposits in the conditions of Central Europe (0.063–0.250 mm) were transported at very short distances (Cílek, 2001), mostly about 50 kilometres (Lisá, 2004). Transport was dominantly from the west to the east (Cílek,

Table 2

Typical chemical analyses of garnets from the loess and loess-like localities studied in Moravia and Silesia, Eastern part of the Czech Republic

	Ivanovice/2	Ivanovice/3	Ořechov/4	Ořechov/5	Boskovice/2	Boskovice/8	Leština/3	Leština/5
SiO_2	38.94	38.05	38.98	38.17	37.54	37.36	37.09	37.35
TiO_2	0.22	0.23	0.22	0.37	0.19	0.21	0.33	0.30
Al_2O_3	21.73	21.60	21.70	21.37	20.79	19.89	20.58	20.60
Fe_2O_3	0.00	0.00	0.10	0.00	0.65	0.86	0.89	0.66
FeO	29.42	31.26	25.82	31.04	30.94	21.03	28.04	27.81
MnO	0.67	0.77	0.43	0.38	1.06	16.26	0.56	0.24
MgO	8.43	6.42	9.30	3.74	2.45	2.35	2.60	2.87
NiO	0.00	0.00	0.00	0.00	0.00	0.00	0.00	0.00
ZnO	0.00	0.00	0.00	0.00	0.00	0.00	0.00	0.00
CaO	0.88	1.47	2.76	5.47	6.89	2.01	9.24	9.18
Total	100.29	99.8	99.31	100.54	100.52	99.97	99.33	99.02
Based on 12 oxygens and with Fe^{2+}/Fe^{3+} calculated assuming full site occupancy								
Si	3.009	2.990	3.007	3.003	2.990	3.025	2.972	2.990
Al^{VI}	0.000	0.010	0.000	0.000	0.010	0.000	0.028	0.010
T-site	3.009	3.000	3.007	3.003	3.000	3.025	3.000	3.000
Al^{VI}	1.979	1.993	1.974	1.983	1.945	1.903	1.920	1.973
Ti	0.013	0.014	0.013	0.022	0.011	0.013	0.020	0.018
Fe^{3+}	0.000	0.000	0.006	0.000	0.039	0.052	0.054	0.040
B-site	1.992	2.007	1.993	2.005	1.995	1.968	1.994	2.031
Fe^{2+}	1.901	2.063	1.666	2.053	2.061	1.424	1.879	1.862
Mn	0.044	0.051	0.028	0.025	0.072	1.115	0.038	0.016
Mg	0.971	0.752	1.070	0.439	0.291	0.284	0.311	0.342
Ni	0.000	0.000	0.000	0.000	0.000	0.000	0.000	0.000
Zn	0.000	0.000	0.000	0.000	0.000	0.000	0.000	0.000
Ca	0.073	0.124	0.228	0.461	0.588	0.174	0.793	0.787
A-site	2.989	2.990	2.992	2.978	3.012	2.997	3.021	3.007
Alm	63.4	69.0	55.3	68.9	68.2	46.2	61.8	61.5
Adr	0.0	0.0	0.3	0.0	2.0	2.7	2.7	2.0
Grs	2.5	4.1	7.4	15.5	17.7	3.3	23.8	24.5
Prp	32.7	25.2	36.0	14.8	9.7	9.7	10.4	11.5
Sps	1.5	1.7	0.9	0.9	2.4	38.1	1.3	0.5

Alm — almandine, Adr — andradite , Grs — grossular, Prp — pyrope, Sps — spessartine; T-site means tetrahedral crystallographic sites in garnet structure, dodecahedral A-site is usually occupied by divalent cations, octahedral B-site is usually occupied by trivalent cations

2001; Adamová *et al*., 2002; Lisá *et al*., 2005) and correspond to contemporary wind directions.

The nature of the geological basement determine overall mineral assemblages as well as garnet compositions. By examining the differences between different geological units it is possible to observe patterns of garnet redistribution within the Moravian and Silesian loess and loess-like deposits and divide them into four main areas named A1, A2, A3 and B1 as described above (Fig. 2). It seems that this redistribution depends not only on the rock basement lithology, but also on selection of garnet types during aeolian transport (*cf*., Čopjaková *et al*., 2005). Aerodynamic and diagenetic effects can be minimized by determining the proportion of stable minerals with similar densities. The index values that best reflect the provenance characteristics (Morton and Hallsworth, 1994) are ATi = 100 × apatite count/(apatite + tourmaline), GZi = 100 × garnet count/(garnet + zircone); RuZi = 100 × rutile count/(rutile + zircone) and Mzi = 100 × count monazite/(monazite + zircone).

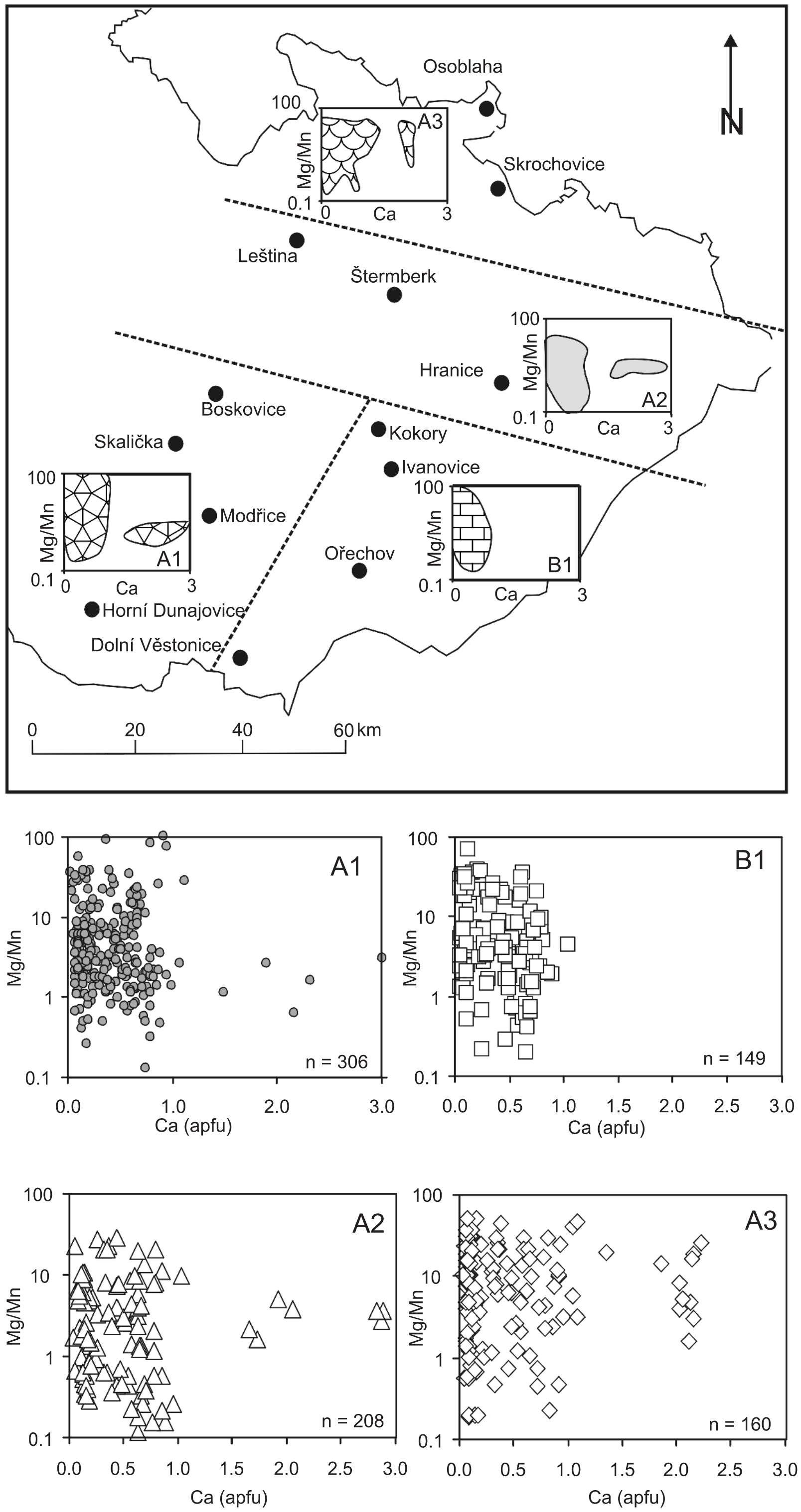

Fig. 2. Diagrams of Mg/Mn *vs*. Ca together with a ternary diagram; this portion is within the loess localities studied from Moravia and Silesia. It is possible to see groups with different garnet chemical compositions

Differences can be found and A1 + B1 groups should be separated from A2 + A3 groups using these indices (Fig. 3). These data support the results published by Lisá *et al*. (2005).

Loess and loess-like deposits with more common almandine-rich garnets are typical mainly of metapelites of the Moravian Nappe (Batík and Fediuková, 1992), paragneisses of the Zábřeh Crystalline Unit (Čopjaková *et al*., 2005) and metamorphic rocks of the Silesicum (Fediuková *et al*., 1985). Low-grossular pyrope-almandine garnets are present in felsic granulites (Čopjaková *et al*., 2005) and pyrope-rich garnets are

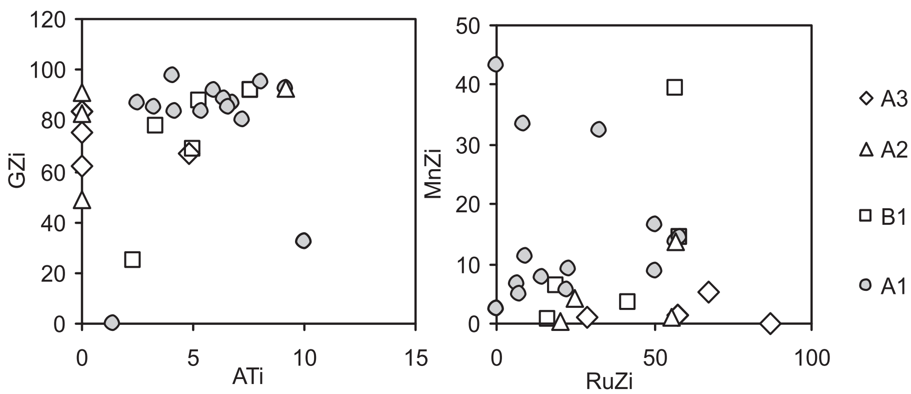

Fig. 3. Diagrams of provenance characteristics according to heavy mineral indices (Morton and Hallsworth, 1994)

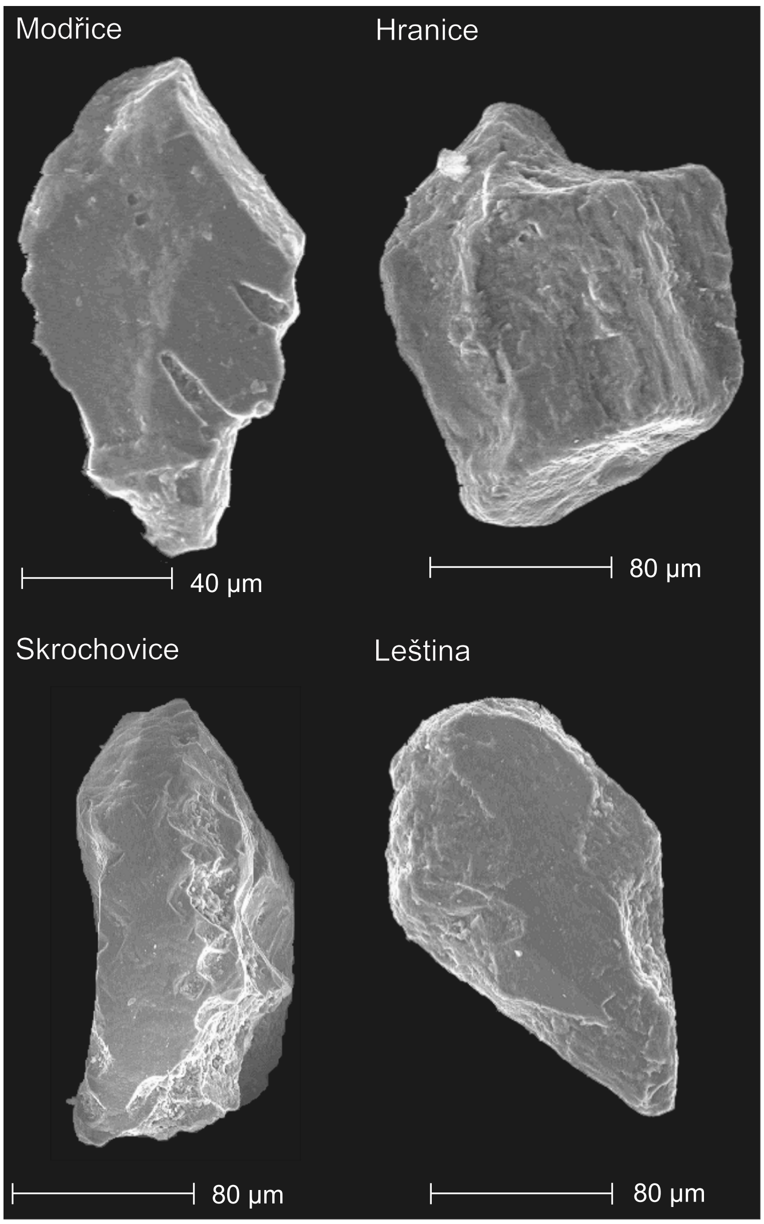

Fig. 4. Garnet grain outlines, morphology and microstructures from selected sites

typical for peridotites from the Moldanubian Zone (Medaris *et al*., 2005). This N–S line primarily covers the main mass of westerly-lying loess and loess-like source rocks. The metamorphic provenance source as a significant part of loess and loess-like deposit material was supported by zircon typology studies (Lisá and Uher, 2006). All sites of loess and loess-like deposits surrounding this line contain variable amounts of garnet with a Grs component (Table 2).

Towards the east, in the provenance area characterized by Tertiary deposits of the Carpathian Foredeep, the amount of Grs-rich garnets rapidly decreases. This is the main trend in loess garnet distribution. This trend could possibly be explained by the fact that the loess material was transported only a limited distance. This explanation fits with the aeolian transport distance results published for this area which are based on radioactivity measurements and abundances of quartz microstructures (Lisá, 2004; Lisá *et al*., 2005). A second explanation for the decreasing amount of Grs-rich garnets towards the east is the changing rock provenance. This is supported by the fact that the garnet geochemical composition of Tertiary deposits from South Moravia is sufficiently variable (Nehyba and Buriánek, 2004); however, garnet grains with a grossular component are very rare in this area. Čopjaková *et al*. (2005) found the same results in the case of Lower Carboniferous Culm strata, where the Grs component is also very rare.

The second trend found in Moravian and Silesian loess and loess-like deposits are the changes in vertical garnet chemical distribution. Garnets with Mg/Mn >20 are present. These types of garnet reflect the presence of different source rocks in the provenance area. Significant differences were found between the A1, A2 and B1 groups. The heavy mineral compositions are very similar for groups A1 and B1 (Fig. 3), as both groups contain garnets with an Mg/Mn ratio of over

30. The only difference between these two groups is the absence of a Grs component in the A1 group. The heavy mineral A2 group differs from the A1 and B1 groups in its composition and also garnet grains from the A2 group differ Mg/Mn ratio, which are not higher than 30. The area A3 contains garnet grains with an Mg/Mn ratio of up to 51.

Areas marked as A1 and A2 have a very similar Ca *versus* Mg/Mn distribution. Garnets in both areas contain a Grs component and have variable amounts of Prp and Grs components. The presumed provenance for these two areas can be seen in rocks lying in southern and central Moravia. The provenance area for southern Moravian loess is probably represented by Moldanubian gneisses, paragneises and migmatites. This mixture of rocks is rich in pyrope and partly also in a spessartine component (Čopjaková *et al*., 2005). The presence of the Grs component is disputable, because some types of rocks are depleted in this component while it is present in others. Source rocks of Central Moravian loess may be represented by the Svratka Zone metapelites, which are mostly rich in Fe with relatively low Mg (unpublished analyses of Novák and Čopjaková in: Čopjaková *et al*., 2005). The area described as A3 probably reflects a source in rocks of the Silesicum. Fediuková *et al*. (1985) distinguished almandine-rich garnets for the Silesicum, but also with variable proportions of Sps and Prp components. Moreover, the same author described Grs-Sps-Alm types of garnets from the Silesicum, originating under conditions of retrograde metamorphism. The widest garnet distribution range (see diagram of Ca *versus* Mg/Mn, Fig. 2) is observed, which reflects a sufficiently wide variability in Silesian garnet chemistry as well as in their source rocks.

Detrital garnets, derived by aeolian process from the source rocks, are mechanically changed into fragments and chips (see Fig. 4). Usually, all grains show some degree of corrosion, but this chemical process is not very marked. There is no evident correlation between the presence of microstructures and the composition of garnets. Čopjaková *et al*. (2005) found the same results in the case of Lower Carboniferous Culm garnets. According to that paper, a low degree of alteration may be suggested by the simultaneous presence of less stable apatite and epidote in heavy mineral assemblages. In the case of loess and loess-like deposits, no significant differences exist in the degree of garnet corrosion between the sites (Fig. 4). This is probably the result of a very recent mechanical erosion and the absence of time for more prominent corrosion processes. It is interesting that the quartz grains from the same samples do not show microstructures that clearly document aeolian transport (Lisá, 2004). The reason for this fact is probably the difference in hardness between quartz and garnet (the hardness of garnet varies from 6.5 to 7.5 while quartz has a hardness of 7). Garnet is shown to be the more informative mineral as regards aeolian transport in this respect.

CONCLUSIONS

The following main conclusions were derived from the data obtained:

1. The use of garnet geochemistry is a new tool for the study of loess deposits and the type of aeolian mineral redistribution.
2. Four different areas in Moravia and Silesia were distinguished based on garnet chemical compositions. These areas reflect different sources of loess material. The aeolian transport distance is recognizable where the almandine component is subdued by other Grs, Prp or Sps components. Such cases are documented by the presence or absence of garnets of anomalous chemical composition.
3. A prevailing westerly wind direction and a short transport distance are best documented in the western part of the study area by the presence of Alm–Prp garnets deflated from Moldanubian metamorphic rocks (especially granulites).
4. The outline (shape, morphology, habitus) of detrital garnets is mostly subangular to angular and reflects aeolian transport more clearly than do quartz grains of the same grain-size category.

Acknowledgements. The authors wish to thank technical staff at the Department of Geological Sciences from Brno for their help and M. Novák (Dept. of Geological Sciences, Fac. of Sci., Masaryk University, Brno) for constructive comments. The research was supported by AVOZ 30130516 Institutional Research Plan.

REFERENCES

ADAMOVÁ M. and HAVLÍČEK P. (1995) — Chemical composition of South-Moravian loesses (in Czech with English summary). Zpr. Geol. Výzk. R., **1994**: 4–19.

ADAMOVÁ M. and HAVLÍČEK P. (1997) — Geochemical characteristics of loess from important Moravian localities (in Czech with English summary). Zpr. Geol. Výzk. R., **1996**: 91–94.

ADAMOVÁ M., HAVLÍČEK P. and ŠIBRAVA V. (2002) — Mineralogy and geochemistry of loesses in southern Moravia. Bull. Czech. Geol. Surv., **77**: 29–41.

AMBROŽ V. (1947) — Rolling upland loesses (in Czech with English summary). Sbor. SGÚ, **14**: 255–280.

BATÍK P. and FEDIUKOVÁ E. (1992) — Garnet chemistry as a indicator of metamorphic development and deformations of the Moravicum in Dyje dome. Bull. Czech Geol. Surv., **67** (1): 1–24.

CÍLEK V. (2001) — The loess deposits of the Bohemian Massif: silt provenance, palaeometeorology and loessification processes. Quatern. Int., **76/77**: 123–128.

ČOPJAKOVÁ R., SULOVSKÝ P. and PATTERSON B. (2005) — Major and trace elements in pyrope-almandine garnets as sediment provenance indicators of the Lower Carboniferous Culm sediments, Drahany Uplans, Bohemian Massif. Lithos, **82**: 51–70.

FIALA J., FUCHS G. and WENDT J. I. (1995) — Stratigraphy of the Moldanubian Zone. In: Pre-Permian Geology of Central and Eastern Europe (eds. R. D. Dallmeyer *et al.*): 418–428. Springer, Berlin.

FEDIUKOVÁ E., FIŠERA M., CHÁB J., KOPEČNÝ V., OPLETAL M. and RYBKA R. (1985) — Garnets of the pre-Devonian rocks in the eastern part of the Hrubý Jeseník Mts. (North Moravia, Czechoslovakia). Acta Univ. Carol., Geol., **3**: 197–234.

FRECHEN M., ZANDER A., CÍLEK V. and LOŽEK V. (1999) — Loess chronology of the last Interglacial/Glacial cycle in Bohemia and Moravia, Czech Republic. Quatern. Sc. Rev., **18**: 1467–1493.

HAVLÍČEK P. (1985) — Quaternary geological research of the South Moravia (in Czech with English summary). Zpr. Geol.Výzk. R., **1985**: 51–52.

HAVLÍČEK P. and SMOLÍKOVÁ L. (1993) — Loess series near Bořetice (southern Moravia) (in Czech with English summary). Věst. ČGÚ, **68**: 11–24.

HLADIL J., STRNAD L., ŠÁLEK M., JANKOVSKÁ V., ŠIMANDL P., SCHWARZ J., SMOLÍK J., LISÁ L., KOPTÍKOVÁ L., ROHOVEC J., BÖHMOVÁ V., LANGROVÁ A., KOCIÁNOVÁ M., MELICHAR R. and ADAMOVÍČ J. (2008) — An anomalous atmospheric dust deposition event over Central Europe, 24 March 2007, and fingerprinting of the SE Ukrainian source. Bull. Geosc., **83** (2): 175–206.

KENIG K. (2006) — Surface microtextures of quartz grains from Vistulian loesses from selected profiles of Poland and some other countries. Quatern. Int., **152**: 118–135.

KENIG K. (2008) — Depositional environments of loesses from the Sandomierz section, SE Poland, based on lithological and SEM studies. Geol. Quart., **52** (2): 169–182.

KRETZ R. (1983) — Symbols for rock-forming minerals. Am. Miner., **68**: 277–279.

KUKLA J. (1961) — Lithologische Leithorizonte der tschechoslowakischen Lössprofile. Věst. ÚÚG, **36**: 369–372.

KVÍTKOVÁ L. and BURIÁNEK D. (2002) — Chemical composition of garnet from the Dyjskosvratecký Úval loesses (in Czech with English summary). Acta Mus., Sc. Geol., **87**: 103–111.

LISÁ L. (2004) — Exoscopy of Moravian eolian sediments. Bull. Geosc., **79**: 177–182.

LISÁ L., BURIÁNEK D. and UHER P. (2005) — Provenance of Würm, Late Pleistocene loess and loess-like sediments from Moravia and Silesia, Czech Republic: Use of heavy mineral assemblage (in Czech with English summary). Acta Mus., Sc. Geol., **90**: 147–154.

LISÁ L. and UHER P. (2006) — Provenance of Würmian loess and loess-like sediments of Moravia and Silesia, Czech Republic: a study of zircon typology and cathodoluminescence. Geol. Carpath., **57** (5): 397–403.

LOŽEK V. (1958) — Research and mapping report of Quaternary cover sequences of the Ostrava and Moravská Brána regions in 1957. Research of Quaternary mollusca of the Moravská Brána region in 1957 (in Czech with English summary). Anthropozoikum, **8**: 277–278.

MACOUN J., ŠIBRAVA V., TYRÁČEK J. and KNEBLOVÁ VODIČKOVÁ V. (1965) — Quaternary of the Ostrava and Moravská Brána regions (in Czech with English summary). ČSAV Press, Prague.

MANGE M. A. and MAURER H. F. W. (1992) — Heavy minerals in colours. Chapman and Hall, London.

MANGE M. A. and WRIGHT D. T. eds. (2007) — Heavy minerals in use. Develop. Sediment., **58**. Elseiver, Amsterdam.

MEDARIS G., WANG H., JELÍNEK E., MIHALJEVIČ M. and JAKEŠ P. (2005) — Characteristics and origins of diverse Variscan peridotites in the Gföhl Nappe, Bohemian Massif, Czech Republic. Lithos, **82** (1–2): 1–23.

MÍSAŘ Z., HAVLENA V. and WEISS J. (1983) — Geology of CSSR I., Bohemian Massif (in Czech with English summary). ČSAV Press. Praha.

MORTON A. C. (1985) — A new approach to provenance studies: electron microprobe analysis of detrital garnets from Middle Jurassic sandstones of the Northern North Sea. Sedimentology, **32**: 553–566.

MORTON A. C. and HALLSWORTH C. R. (1994) — Identifying provenance-specific features of heavy mineral assemblages in sandstones. Sediment. Geol., **19** (24): 12–56.

MUSIL R. and VALOCH K. (1956) — The Vyškov Úval loesses (in Czech with English summary). Pr. Brněn. Zákl. ČSAV, **6**: 28.

NEHYBA S. and BURIÁNEK D. (2004) — Pleistocene fluvial terraces of the Svratka river — facies and provenance study. Geo. Alp., Inst. fur Geologie Uni Innsbruck, Innsbruck.

PELÍŠEK J. (1949) — Contribution to the loess stratigraphy of the Svratka Úval (in Czech with English summary). Pr. Moravskoslez. Akad. Věd Přír., **21** (11): 1–19.

SMALLEY I. J. and CABRERA J. G. (1970) — The shape and surface textures of loess particles. Geol. Soc. Am. Bull., **81**: 1591–1595.

Quaternary International 351 (2014) 25–37

Contents lists available at ScienceDirect

Quaternary International

journal homepage: www.elsevier.com/locate/quaint

Geoarchaeology of Upper Palaeolithic loess sites located within a transect through Moravian valleys, Czech Republic

L. Lisá [a,*], J. Hošek [b,c], A. Bajer [d], T. Matys Grygar [e], D. Vandenberghe [f]

[a] Institute of Geology, Academy of Sciences of the Czech Republic, Rozvojova 269, Prague 165 00, Czech Republic
[b] Czech Geological Survey, Klárov 3, Prague 118 21, Czech Republic
[c] Institute of Geology and Palaeontology, Faculty of Science, Charles University in Prague, Albertov 6, Prague 2, Czech Republic
[d] Faculty of Forestry and Wood Technology, Mendel University, Zemědělská 3, Brno 613 00, Czech Republic
[e] Institute of Inorganic Chemistry, Academy of Sciences of the Czech Republic, 250 68 Řež, Czech Republic
[f] The Research Foundation – Flanders (FWO – Vlaanderen), Laboratory of Mineralogy and Petrology (Luminescence Research Group), Department of Geology and Soil Science, Ghent University, Krijgslaan 281 (S8), B-9000 Gent, Belgium

ARTICLE INFO

Article history:
Available online 3 October 2013

ABSTRACT

The Middle and Upper Palaeolithic sites situated within the system of Moravian and South Silesian valleys are key localities for understanding the patterns of seasonal mobility that enabled humans to exploit the North European Plain, and a possibility to distinguish the importance of the weather and climate for their subsistence practises. Loess accumulations that have covered the best preserved open air Palaeolithic sites in Central Europe display the climatic record covering at least 30,000 years. The sedimentological, microstratigraphical and geochemical record of three studied Upper Palaeolithic loess sites show significant changes, documenting increased precipitation towards the north. A progressive coarsening of the loess deposits during the Upper Pleniglacial, contrasting with the progressive fining toward the North European glaciation was detected. This methodological approach explains more precisely the context of formation processes connected also with human activity within the corridor between the North European Plain and the Danube Basin, through which a wide range of organisms, including humans and their prey species, were channelled.

1. Introduction

Upper Palaeolithic sites located along a transect between the Danube region, Moravian valleys, and the North European Plain offer unique insights into an early episode of modern human adaptations to the landscape (Otte, 1981; Svoboda et al., 2002; Oliva, 2005, 2007; Lisá et al., 2013). The system of Moravian valleys, oriented mainly N–S or NE–SW (Czudek, 1997), provides a valuable archaeological trap for two reasons. First, it constitutes wide river valleys between transcontinental mountain ranges through which a wide range of organisms, including humans and their prey species, were channelled: this has always been the principal access route to the North European Plain from the Danube Basin (Skutil, 1955; Valoch, 1979; Svoboda et al., 2002; Trinkaus and Svoboda, 2006). Second, it is also a trap for wind-blown sediments flowing preferentially from the W or NW, SW to the E or NE, SE (Lisá, 2004; Lisá and Uher, 2006; Lisá et al., 2009) that have accumulated to considerable depths around many a hilly protuberance in that landscape. It is these deep accumulations of loess that have covered the best preserved open air Palaeolithic sites in Europe (Svoboda et al., 2002). The lithological record of those localities was described mainly in the case of the famous Dolní Věstonice old brickyard section (Klíma et al., 1962; Bábek et al., 2011; Antoine et al., 2013), but the geochemical and micromorphological record of other localities situated more northerly in Moravia was less studied. Instrumental sedimentological analyses can bring valuable information about environmental conditions which Palaeolithic hunters had to accept in hunting large mammals. The main question addressed in this paper is, therefore: is it possible to distinguish any significant lithological or geochemical differences between three of the most important Upper Palaeolithic regions within Moravia and use the interpretations of those differences to discuss climatic changes of Middle and Upper Pleniglacial and the reasons which enabled humans to exploit the North European Plain, and subsequently even colder regions?

* Corresponding author.
E-mail address: lisa@gli.cas.cz (L. Lisá).

1040-6182/$ – see front matter © 2013 Elsevier Ltd and INQUA. All rights reserved.
http://dx.doi.org/10.1016/j.quaint.2013.08.058

2. Geographical and sedimentological background

Three key localities for Moravian Upper Palaeolithic history are used in this study. The localities are typical for long term temporary Gravettian occupation (Nývltová Fišáková, 2013) and are situated along a transect between South Moravia (Dolní Věstonice), Central Moravia within Moravian Gate (Předmostí), and North–East Moravia (Hošťálkovice locality near Petřkovice). The imaginary section connecting those three localities provides information about the different sedimentological records preserved, and the differences of environmental conditions which Palaeolithic hunters had to accept in hunting large mammals.

The Last Glacial loess formation within the area of Central Europe was strongly influenced by its geographical position between two glaciers. In that time Moravia and Silesia were situated in the narrowest part of the non-glaciated area and became very important for loess formation as well as for the fauna (Ložek, 1968; Horáček and Ložek, 1988), flora (Frenzel, 1968) and human migrations (Svoboda et al., 2002).

2.1. Dolní Věstonice II (DV II)

This section was excavated in the context of the archaeological research of the Gravettian site during the 2005 season. The studied section is located in anthropogenic terraces on the slope above the famous Dolní Věstonice – old brickyard section. The 4.2 m thick profile DV II covers the Gravettian cultural layer and the Upper Pleniglacial sedimentary record correlated with the upper part of the old brickyard section. The section in the old brickyard represents the most prominent loess section accessible today in Central Europe and, therefore, enormous numbers of different research efforts were made there (Klima et al., 1962; Demek and Kukla, 1969; Haesaerts and Mestdagh, 2000; Fuchs et al., 2012; Antoine et al., 2013). Approximately 18 m of loess, loess like deposits, and paleosols cover a relatively complete Last climatic cycle and display warming, cooling, and wetting trends. The loess was in this case derived mainly from frost shattered and weathered magmatic and metamorphic rocks situated to the west, deposited as eluvial deposits or as river alluvium (Lisá, 2004; Lisá and Uher, 2006; Lisá et al., 2009), and calcareous Miocene deposits (Adamová, Havlíček, 1998). The provenance during the last glacial period did not change (Lisá et al., 2009) and the grain size differences depend mostly on the wind speed or post-depositional weathering.

2.2. Předmostí

Close to the town of Přerov, and to the southern entrance to the Moravian Gate, a series of loess deposits has been extensively excavated. A rescue excavation in the last century produced a considerable body of data relating to various Palaeolithic episodes, mainly of Gravettian Age (Svoboda et al., 1994). Předmostí is located at the southern entrance of the Moravian Gate, one of the most important passing points of prehistoric routes in Central Europe (Svoboda et al., 1994). Originally two limestone formations, at Skalka in the south and Hradisko in the north, emerged from the Neogene and Quaternary deposits. Both of them have nearly disappeared due to limestone exploitation. Several mineral spring sources are known close to the site, which formed travertine deposits (Kovanda, 1971). One, with a constant temperature of 12 °C was located directly at the foot of the former Skalka hill (Svoboda et al., 1994). The cultural content of this locality has been classified as Gravettian or Pavlovian with a hypothetical Aurignacian horizon below. The Gravettian was dated approximately to 26–27 ka (Svoboda et al., 1994).

2.3. Hošťálkovice

Hošťálkovice is situated in Northern Moravia in the Ostrava region. This locality is 1.5 km from Petřkovice, famous for the Venus finding (Svoboda, 2004). Unfortunately, Petřkovice could not be included in this research because of technical problems. Hošťálkovice, nevertheless, offers the similar stratigraphy (Folprecht, 1934; Neruda and Nerudová, 2000) and its location was suitable for our research. The site was excavated in 1992 by P. Neruda (Neruda and Nerudová, 2000). This site lies beyond the Moravian Gate at the opening of the North European Plain. It has also a significant history of archaeological investigation, allowing us to target location of an approximately 1.6 deep test pit to capture the layer with Gravettian artefacts.

3. Methodology

3.1. Micromorphology

Microstratigraphical study, micromorphology in archaeological context, was applied in all three localities. In total, 53 samples for thin sections were taken. A micromorphological approach covers descriptive microstratigraphical analyses (Bullock et al., 1985) including microfabric types, structural and porosity features, natural inclusions, anthropogenic inclusions, and pedofeatures (Macphail and Cruise, 2001). Such application of soil micromorphology to archaeology was introduced mainly by Goldberg (1983) and latelyis well established in the literature (French, 2003; Goldberg and Macphail, 2006). Samples were taken in Kubiena boxes (9×5 cm), slowly dried, impregnated by a polymer resin, processed into thin sections and then studied according to Bullock et al. (1985) and Stoops (2003). A record was made of the microfabric types, structural and porosity features, natural inclusions, anthropogenic inclusions and pedofeatures (Macphail and Cruise, 2001).

3.2. Geochemistry – quantitative analysis of expandable clay minerals (CEC)

The cation exchange capacity (CEC) was determined using a procedure proposed by Meier and Kahr (1999) for pure clay mineral specimens and then optimised for sediments and soils (Grygar et al., 2009). $[Cu(trien)]^{2+}$ solution was obtained from $CuSO_4 \cdot 5H_2O$ (Penta, Czech Republic) and trien, triethylenetetramine (1,4,7,10-tetraazadekane, Sigma–Aldrich), to the final concentration 0.01 M with a potentiometric control of the constant ligand-to-metal ratio (Grygar et al., 2009). A fine dry powder (100–500 mg) was placed in a 50 mL beaker, wetted and then suspended by stirring in 5 mL of distilled water; then 5 mL 0.01 M Cu-trien solution was added, and the suspension stirred for a further 5 min using a magnetic stirrer. The suspension was then filtered into a 50 mL flask and the solid washed with several aliquots of distilled water, and the final volume of the filtrate made to 50 mL. The solutions were analyzed by AAS (Cu and Mg) and AES (Ca and Na). The sample weight for analysis was adjusted depending on its actual CEC to consume about 50% of $[Cu(trien)]^{2+}$ using the routine described by Grygar et al. (2009).

3.3. Bulk magnetic susceptibility (MS)

Unoriented samples were collected at 5 cm intervals from cleaned profiles. Low frequency magnetic susceptibility (χlf) was measured at 0.976 kHz and high frequency magnetic susceptibility (χhf), at 3.904 kHz, using a MFK1 kappabridge (AGICO, Brno). The difference between the two measurements gives the frequency dependent susceptibility, expressed here as a percentage of χfd

($\chi fd\% = (\chi lf - \chi hf)/\chi lf \times 100$). This parameter is widely used to determine the concentration of magnetic particles close to superparamagnetic (SP)/stable single domain (SSD) boundary (Liu et al., 2005). This grain size fraction is proposed to have formed during pedogenesis (Evans and Heller, 2003; Dearing et al., 1996).

3.4. Particle size distribution function (PSDF)

Samples for particle size distribution were collected at 5 cm intervals from cleaned profiles from all three studied section (Figs. 2 and 3). Particle-size analysis (PSA) is a measurement of the size distribution of individual particles in a soil sample (Gee and Bauder, 1986). Particle size distribution was established using a Malvern Mastersizer 2000. Samples of air dried and roughly crushed sediments were gently disaggregated and dispersed in deionized water. Organic matter was removed by addition of hydrogen peroxide accompanied by gentle warming at 40 °C until effervescence stopped. The supernatant was removed after centrifugation and the sample rinsed with two changes of deionised water. The samples were then re-homogenised in a minimum of water using a whirly mixer and then sub-sampled for particle size analysis. Two sub-samples were taken from each sample and analysed sequentially, and the graphs presented are the mean of the two measurements.

3.5. OSL dating

DV II section was sampled in two positions. DV2/1 comes from the depth of 435 cm and corresponds to the base of cultural layer mixed with soil material. DV2/2 comes from the depth of 265 cm and corresponds to the position directly above gley II. layer (Fig. 2). Three locations were sampled at Hošťálkovice. HB 13 came from 160 cm depth at the very base of the section on the contact between redeposited terrace sediments and redeposited loess-like sediments. THV2 came from a depth of 65 cm where some of the artefacts occurred. THV1 came from 35 cm depth, on the contact between E soil horizon and the loess-like sediment below (Fig. 2). Předmostí was not sampled due to the technical problems during the fieldwork organisation.

Samples were dated by OSL in the Laboratory of Mineralogy and Petrology (Luminescence Research Group), Department of Geology and Soil Science, Ghent University in Belgium. by applying the SAR-OSL protocol to sand-sized (63–90 μm) quartz. This fraction was extracted from the inner material of the sampling tubes using conventional sample preparation procedures (HCl, H_2O_2, sieving, heavy liquids, and HF). OSL measurements were performed using an automated Risø TL/OSL-DA-12 reader. The equivalent dose (De) was determined using the single-aliquot regenerative-dose (SAR) protocol as described by Murray and Wintle (2000, 2003). Low-level high-resolution gamma-ray spectrometry was used for the determination of the natural dose rate. The annual dose was calculated from the present-day radionuclide activities using the conversion factors of Adamiec and Aitken (1998). An internal dose rate of 0.013 ± 0.003 Gy ka^{-1} was assumed (Vandenberghe et al., 2008). Both the beta and gamma contributions were corrected for the effect of moisture by generally accepted procedures.

4. Results

4.1. Stratigraphy

4.1.1. Southern Dolní Věstonice section

The lithostratigraphy was examined in a 4.2 m high freshly cleaned vertical section (Fig. 2) containing several horizons with different contexts, coded as DV II. Generally, the profile is mainly composed of fine grained loess and loess-like sediments which

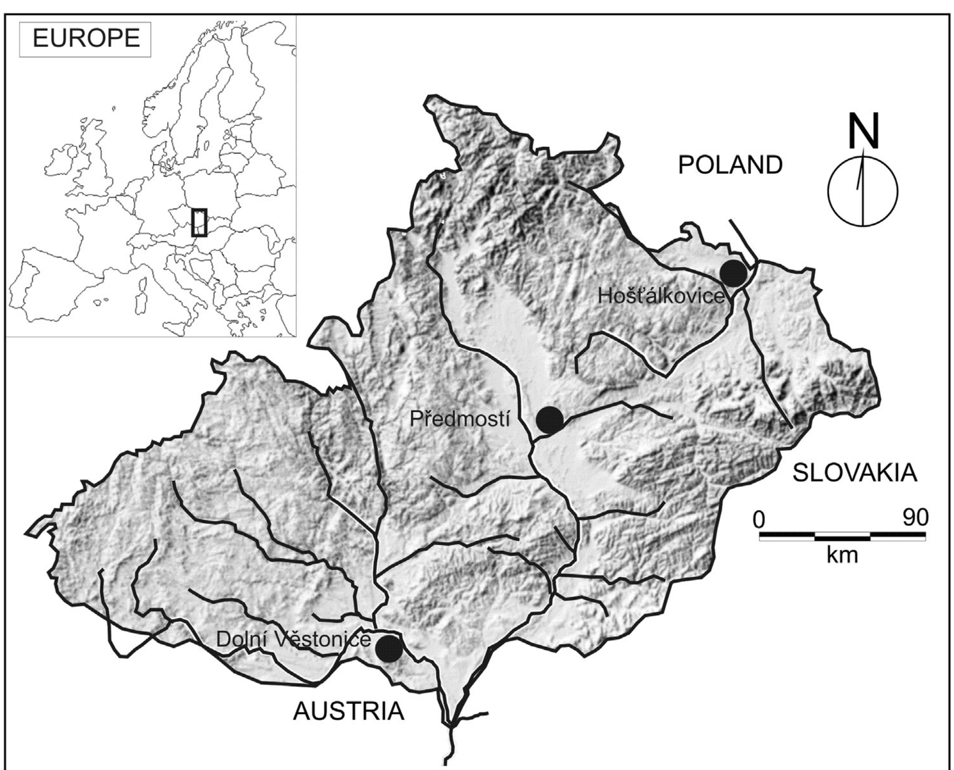

Fig. 1. Location of studied sites.

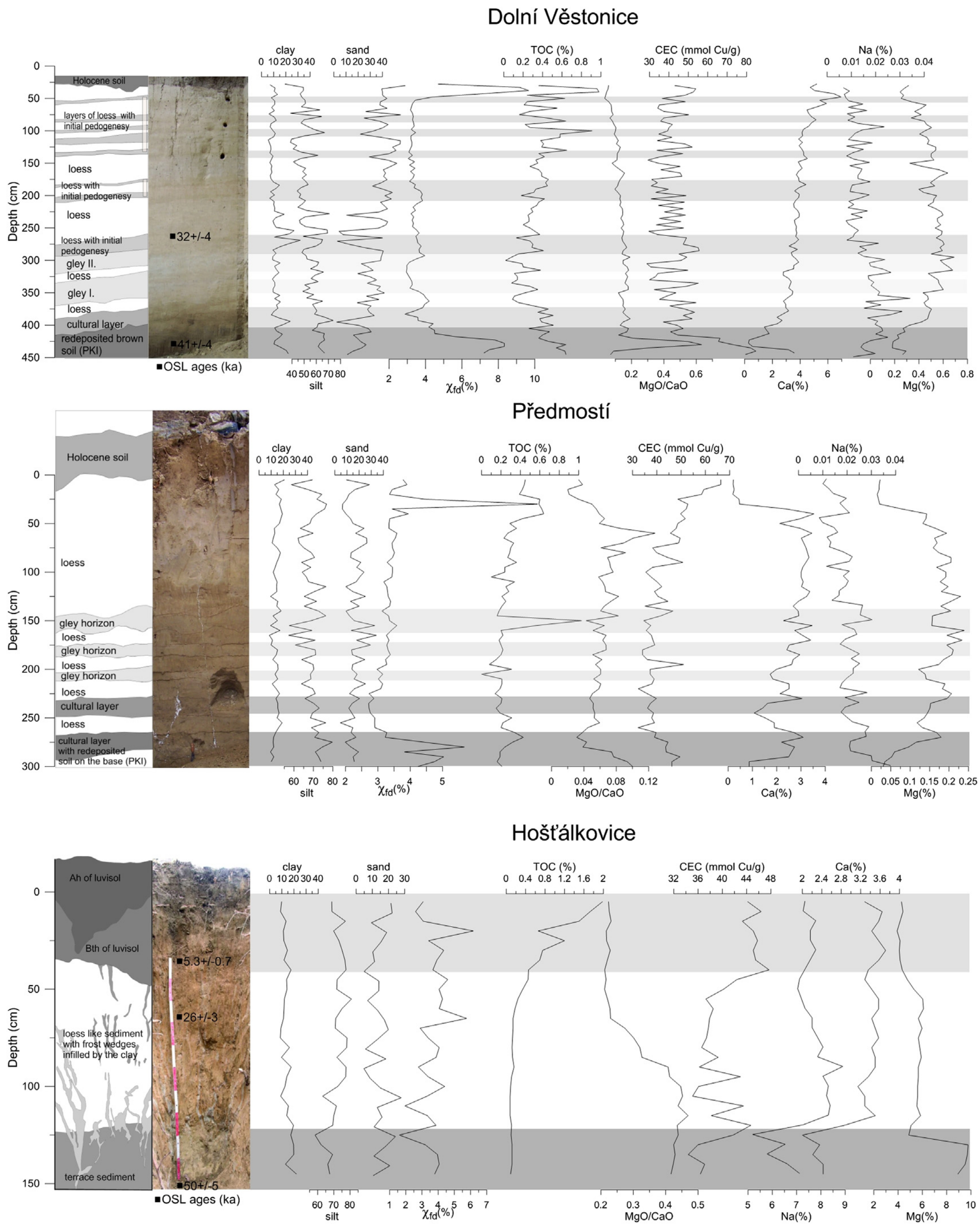

Fig. 2. The sedimentological description of loess sections Dolní Věstonice, Předmostí and Hošťálkovice together with the main geochemical, magnetic and grain size proxies.

were post-depositionally influenced by changing climatic conditions. There is a dark brown horizon of re-deposited laminated soil, probably of Cambisol type (40 cm) found in the very bottom, followed by the complex of thin loess layers (approximately 15 cm each), and one darker layer (10 cm), described as Gravettian occupational layer (10 cm) with the macroscopic presence of charcoal and fine freezing and thawing laminae (less than 1 cm) in the loess layers below and above. The loess deposition grades into two lighter horizons (17 and 10 cm) divided by a loess horizon (10 cm). Those horizons were interpreted as gley horizons. The part of the section above is composed by loessic material with a group of slightly browner horizons (1–5 cm). The section is ended by a dark brown aggraded Chernozem-type Holocene soil horizon.

4.1.2. Intermediate Předmostí u Přerova section

In contrast to the cultural layer excavated in the DV II sections, in which burnt charcoal is a conspicuous hearth component, burnt mammoth bones predominate here, suggestive of a difference in resource availability between the sites (Beresford-Jones et al., 2010). However, another, microcharcoal containing layer was micromorphologically confirmed the cultural layer. The lithological section of Předmostí (Fig. 2) contained a dark brown horizon of re-

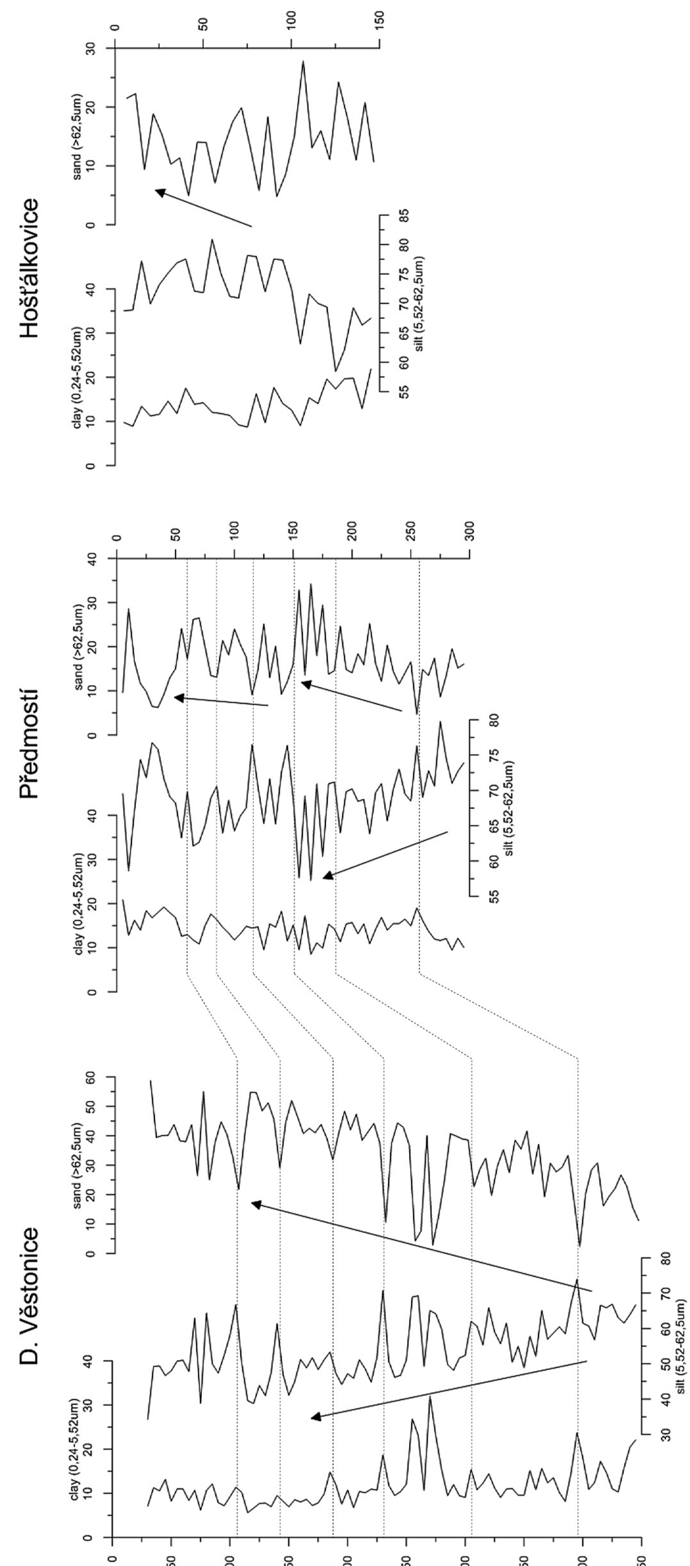

Fig. 3. The grain size distribution within studied sites.

deposited arctic soil in the very bottom followed by a thick cultural layer containing mammoth bones and burned bones together with charcoal and loess-like sediment intercalations (Fig. 2). There is evidently slight re-deposition by gelifluction. This layer is overlain by loess deposits with a number of features typical of frost action, including frost wedges and other micromorphologically detected features. Three thin gley horizons were present. The upper part of the section continues with monotonous loess deposition containing thin darker layers containing decomposed organic matter. The section is capped by a Holocene Cambisol.

4.1.3. Northern Hošťálkovice near Petřkovice loess like sedimentary section

Approximately 1.5 m thick sedimentary cover (Fig. 2) lies on the ridge between Petřkovice and Hošťálkovice. The geological background of Hošťálkovice section is composed of re-deposited terrace deposits. Colluviated loess-like deposits include approximately 30 cm of the section. Gravettian artefacts are distributed mainly on the contact of terrace deposits and loess-like sediments (Fig. 2) (Neruda and Nerudová, 2000), but occasionally were detected within loess-like sediments above. Loess-like deposits contain small frost edges filled by clays as a record of boreal illuviation. The section is capped by a Holocene Luvisol, lately degraded into Pseudogley.

4.2. Microstratigraphy and micromorphology

4.2.1. Dolní Věstonice

The base of the section is composed of re-deposited interstadial soil of the boreal to arctic brown soil type with ferric oxide nodules (Fig. 4C), interpreted as the consequence of relatively humid conditions causing erosion and reduction processes. This soil can be

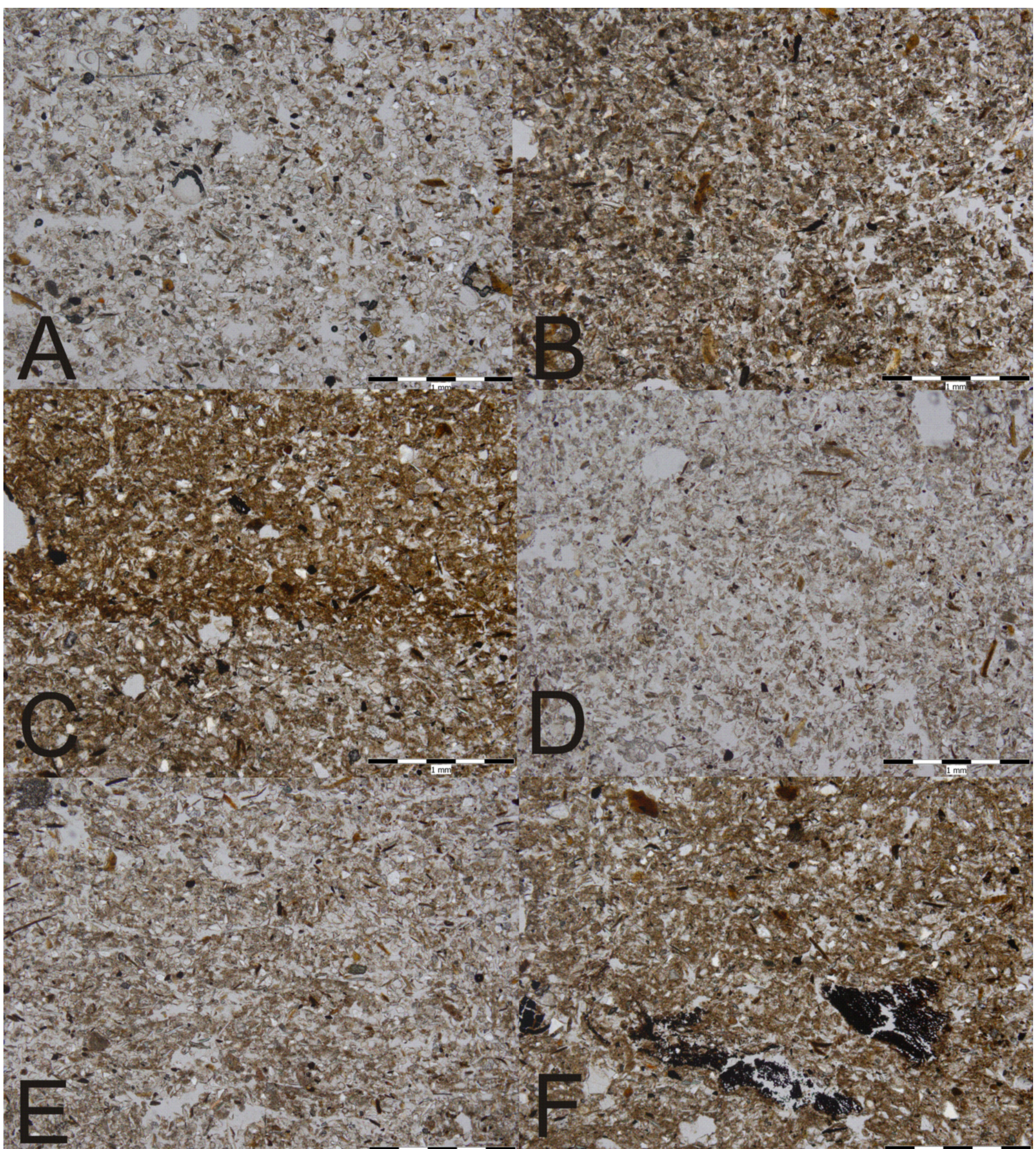

Fig. 4. Typical micromorphogical features from Dolní Věstonice site: A – loess s.s.; B – initial soil horizon with visible brunification, location above Gley II.; C – redeposited arctic brown soil on the base of section with, visible FeOH nodules due to the gleying; D – Gley II with leaching, but without FeOH features typical of gleying; E – horizontal pores documenting phases of freezing and thawing, location above the cultural layer; F – charcoal distributed widely within the cultural layer. This layer also contains redeposited arctic brown soil material.

interpreted as an early stage cambisol. Gelifluction features are connected mainly with the cultural layer (Fig. 4F), which show a continuing relatively cold and humid environment. Freezing – thawing features (Fig. 4E) above the cultural layer indicate frost heaving, related to the development of ice lenses as the consequence of cold and relatively humid conditions. Those features are not very common, in contrast to Předmostí and Hošťálkovice. Two horizons of the frost gley surprisingly do not contain ferric oxide (Fig. 4D) nodules. The absence of freezing – thawing features toward the Holocene layer is probably the result of a cold and dry LGM environment. The slightly darker horizons differ from pure loess (Fig. 4A) by initial brunification (Fig. 4B). The presence of darker horizons (Fig. 4) within this part of the section is therefore the result of transitory periods of increased humidity and initial stages of pedogenic weathering.

4.2.2. *Předmostí*

Re-deposited interstadial soil of the boreal to arctic brown soil type at the base (Fig. 5A) has ferric oxide nodules formed under relatively humid conditions causing erosion and reduction processes. A thick cultural layer with bioturbation (Fig. 5B) indicates stable humid conditions. The cultural layer contains frequently fragments of burned bones (Fig. 5B), but little or no charcoal. A layer which contains microcharcoal was micromorphologically identified above the first cultural layer. The presence of freezing and thawing structures (Fig. 5C) above the cultural layer is the result of persistent cold and relatively humid conditions. The presence of frost wedges (without flat bottoms) and gleying above (Fig. 5D) is the result of cold, humid conditions and probably also an initial stage of permafrost. Continuing freezing and thawing features toward the Holocene horizon with thin horizons containing

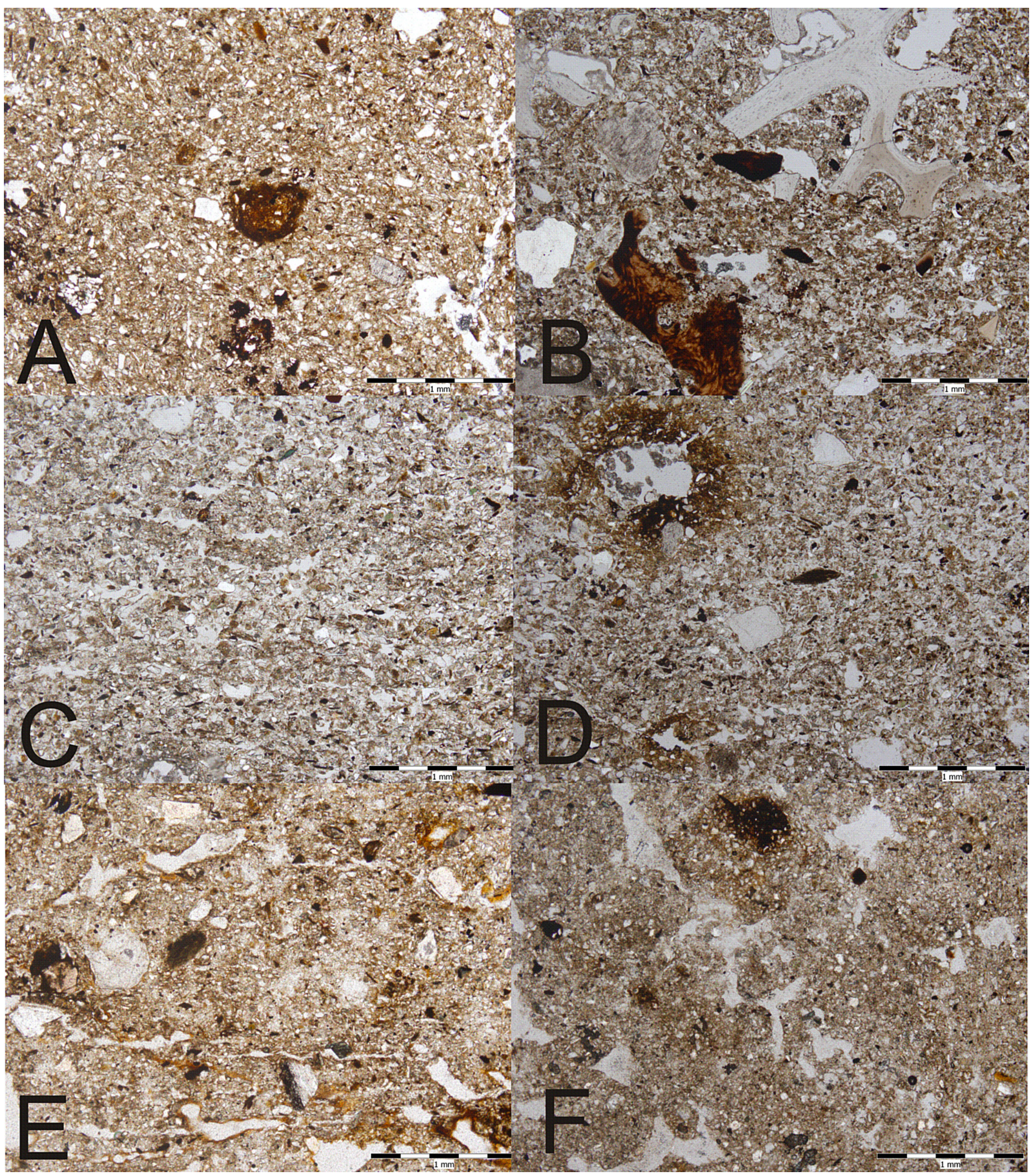

Fig. 5. Typical micromorphological features from Předmostí and Hošťálkovice sections: A – redeposited arctic brown soil at the base of Předmostí section containing nodules of FeOH; B – cultural layer with burned and unburned bones from Předmostí; C – horizontal pores documenting phases of freezing and thawing, location above the cultural layer in Předmostí and appearance of such features within all rest of section; D – Gley horizon with FeOH nodules from Předmostí; E – horizontal pores documenting phases of freezing and thawing (Hošťálkovice). Those pores were secondary during Holocene pedogenesis, iluviated by clays; F – Luvic horizon from locality Hošťálkovice.

decomposed organic matter and initial stages of brunification is the consequence of a cold and relatively wet LGM environment with short stages of increased humidity.

4.2.3. Hošťálkovice

Terrace sediments on the base of the section are partly distributed within the loess-like deposits, overlain by unsorted sediment. This record is the result of gelifluction. The presence of ferric hydroxide nodules and gleying is the consequence of a wet environment responsible for erosion and reduction processes, probably under permafrost conditions. The Gravettian artefacts are more or less incorporated into the re-deposited terrace and loess-like sediments above, probably the result of post-sedimentary cryoturbation. Freezing and thawing features (Fig. 5E) up to the Holocene soil and within the cultural layer can be attributed to persistent cold and relatively humid LGM conditions. Those features are infilled by clay illuviation as a consequence of Holocene pedogenic processes. Desiccation cracks 50 cm below the surface (Fig. 2) are the result of extremely cold and dry conditions. Boreal clay illuviation is the result of the Bölling climate. The sediment was lately influenced by Holocene illimerisation (Fig. 5F).

4.3. Frequency dependent magnetic susceptibility

The values of χfd are basically a concentration-dependent parameter. It depends on the grain-size and amount of magnetic materials present in the sediment, indicating the proportion of fine viscous grains close to the SP/SD boundary (~0.02 μm) in the total (Thompson and Oldfield, 1986). This grain size fraction formed during pedogenesis (Evans and Heller, 2003). χfd vary considerably within the studied localities (Fig. 2), but the trends in Dolní Věstonice and Předmostí are more or less similar. The highest values were detected within the horizon with re-deposited interstadial arctic brown soil (Cambisol) and within Holocene soil cover, whereas the loess typically has lower values (Fig. 2). Předmostí shows a relatively increasing trend of values, in comparison with the consistency at Dolní Věstonice. In the case of Dolní Věstonice, higher values were obtained also within horizons with initial soil horizons. In the case of Hošťálkovice, the highest values were detected within the Holocene Luvisol. The record of the Hošťálkovice section shows high variability with slightly increasing trend toward the Holocene soil (Fig. 2).

4.4. Geochemistry

The geochemical record of the profiles shows numerous similarities and is influenced by lithology (Fig. 2). Cation Exchange Capacity (CEC) of Dolní Věstonice shows a relatively stable trend with microfluctuation, except for enhancement within the lower part of the section, where re-deposited interstadial soil and cultural layer were identified. Increased values were found in the loess with initial pedogenesis, and a slightly increased trend is visible in the upper part of the profile (Fig. 2).

The profile in Předmostí shows a similar trend of CEC to Dolní Věstonice. The elevated values are visible mainly within the lower part of the section where the relicts of interstadial soil were detected. In the middle part of the profile with gley and loess horizons, a stable trend is apparent with slighter higher values in gley horizons. In the upper loess above the gley III increasing trend of values up to the Holocene soil is apparent.

In Hošťálkovice, the highest CEC values were detected within the base of the section where the weathered sandy loam with carbonate pebbles was detected. A sharp decrease of those values follows the appearance of pure loess-like deposits with the artefacts. The percentage content of Na shows a slightly declining trend in the lower part of the profile in Dolní Věstonice, whereas in Předmostí a slightly increasing trend in the whole profile is visible. Mg and Ca contents of the DV profile show the same increasing trend up to the layer of loess with initial pedogenesis. Above this layer, Ca increases whereas Mg begins to decrease to the top of the profile. Ca and Mg content of the Předmostí show slightly increasing trends with relative stagnation in the upper part, above the gley III. In general, contents of Ca and Mg show the highest variations within the gley horizons and initial soil formations above those horizons in both sections. MgO/CaO ratio shows a gradual decrease in both profiles, but in the case of Předmostí this trend is less apparent. For the Hošťálkovice profile, the great difference in elements concentration between the lower and upper part is typical. Ca and Na contents are lowest in the horizon with weathered sandy loam and high in loess-like sediment, whereas the Mg content shows the opposite trend.

Another sharp decrease of measured components is visible within E and A horizons of the Holocene Luvisol. The contents of organic matter within the sections have more or less the same trend: the most obvious is the enhancement of organic matter within the interstadial brown soil of Dolní Věstonice and Předmostí as well as within the Holocene soil formation in all three localities. For Hošťálkovic, a stable trend is typical, with a slight increase below the Holocene soil.

4.5. Grain size

Grain size measurements show the same significant trend in all three studied localities. Toward the Holocene layer significant coarsening of sand fraction is obvious (Figs. 2 and 3), while toward the north there is a fining trend. Dolní Věstonice section has probably the best preserved long-time depositional record, and consequently the deposits have much more fine composition than in other studied localities (Figs. 2 and 3). It is also possible to see a connection between the appearance of darker, more humid layers and the contemporary increase of clay fraction (depth about 1.2, 1.8–2.2 and between 3 and 4 m). In the case of Předmostí and Hošťálkovice this connection was not found. Předmostí and Hošťálkovice sections display much coarser deposits and the trend of coarsening is visible not only toward the Holocene but also toward the north, toward the edge of the North European glaciation. Předmostí section has a visible enhancement of sand fraction within 1.0–1.5 m where the cultural layer was detected. In the case of Hošťálkovice, there is a visible enhancement of clay at the expense of silt in the upper part of the section due to the Holocene pedogenic processes (Figs. 2 and 3).

4.6. Dating

A sufficient amount of pure quartz grains could be extracted from all samples. The quartz extracts showed satisfactory luminescence characteristics in terms of brightness (clearly distinguishable from background), OSL decay (dominated by the fast component), recycling ratio (consistent with unity), recuperation (generally less than 1% of the sensitivity corrected natural OSL signal) and dose recovery (a known dose given to a bleached sample prior to any heating can be accurately measured). These characteristics suggest that the samples are well-suited for optical dating. Sample GLL-091927 behaved differently from the other samples, however, in that a poor dose recovery was achieved using a preheat for 10 s at 240 °C; a lower preheat (200 °C) was required to achieve a good dose recovery. The ages are consistent with the stratigraphic position of the samples. Based on the observed spread in D_e (large aliquots), the date for sample GLL-081901 is not thought to be an accurate sedimentation age. This sample may be affected by postdepositional mixing and/or incomplete resetting.

4.6.1. Luminescence characteristics and D_e-determination

Fig. 1 shows a representative luminescence decay and growth curve for sample GLL-081902. The luminescence signal decays rapidly with stimulation time (Fig. 1, inset); this is characteristic for quartz dominated by the fast component. The dose–response curve can be approximated satisfactorily by the sum of a single saturating exponential and a linear component. Fig. 1 also illustrates the generally good behaviour of the samples in the SAR protocol; the recycling ratios are close to unity (indicating that sensitivity changes occurring throughout the measurement procedure are accurately corrected for) and the growth curves pass close to the origin (demonstrating that recuperation is negligible).

Fig. 2 summarises the dose recovery data. Within analytical uncertainty, the measured dose does not differ from the given dose by more than 5% (Fig. 2A); the average recovered to given dose ratio for the five samples is 1.01 $\pm$ 0.02. Fig. 2B shows the corresponding values for the recycling ratio and recuperation; the average values are 0.98 $\pm$ 0.01 and 0.05 $\pm$ 0.01%, respectively. For each sample, at least 18 replicate measurements of D_e were made. Values were accepted if recuperation did not exceed 5% of the corrected natural OSL signal and if the recycling or depletion ratio did not deviate by more than 10% from unity. The average D_e's ($\pm$1 standard error) are summarised in Table 1.

(Ložek, 1953, 1964; Kukla, 1975; Frechen et al., 1999; Antoine et al., 2013). The Middle Pleniglacial in Europe is marked by the appearance of brown soil complexes as Stillfried-B from Lower Austria (Haesaerts et al., 2003), Vytachiv soil complex of Ukraine (Gerasimenko, 2006), the Gräselberger and Lohne Boden in Germany (Frechen, 1999; Antoine et al., 2009) the Saint-Acheul-Villiers-Adam soil complex in Northern France (Antoine et al., 2003), and Les Vaux soil in Belgium (Haesaerts, 1985). The soil development in this case corresponds to warmer and more humid conditions and it is widely associated with the Hengelo and Denekamp insterstadials. Those periods were interrupted mainly by the phases of erosion, and thus the sedimentary record is usually very fragmented. In Moravia the three interstadials of the Middle Pleniglacial are supposed to be preserved as the PKI pedo-complex described by Klima (1969) and dated at ~30–35 ka, and by the Bohunice soil (Valoch, 1976) dated at ~45–50 ka (Richter et al., 2009). Antoine et al. (2013) mentioned erosion processes resulting from warming phases of one of those interstadials that enhanced the seasonal degradation of the permafrost active layer leading to solifluxion-related deformation and alteration of the gley horizon preserved above the re-deposited interstadial soil.

Two sections included in our research, Dolní Věstonice and Předmostí, contain re-deposited arctic brown soil (Cambisol), which corresponds to one or more of those interstadials. In both cases, the soil sediment was re-deposited and contains ferric oxide nodules indicating the presence of water and buried organic matter

Table 1
Radionuclide concentrations used for dose rate evaluation, estimates of past water content (F^*W), calculated dose rates, equivalent doses (D_e), optical ages, and random (σ_r), systematic (σ_{sys}) and total (σ_{tot}) uncertainties. The uncertainties mentioned with the D_e and dosimetry data are random; all uncertainties represent 1σ.

Sample (field code)	Sample (GLL code)	Depth (cm)	^{234}Th (Bq kg^{-1})	^{226}Ra (Bq kg^{-1})	^{210}Pb (Bq kg^{-1})	^{232}Th (Bq kg^{-1})	^{40}K (Bq kg^{-1})	F^*W (%)	Total dose rate (Gy ka^{-1})	D_e (Gy)	Age (ka)	σ_r (%)	σ_{sys} (%)	σ_{tot} (%)	σ_{tot} (ka)
THV1	081901	35	42 $\pm$ 3	45 $\pm$ 1	39 $\pm$ 1	49.5 $\pm$ 0.3	573 $\pm$ 4	24 $\pm$ 6	2.95 $\pm$ 0.02	$15 \pm 2_{(17)}$	5.3	9.9	9.8	14.0	0.7
THV2	081902	65	36 $\pm$ 2	48 $\pm$ 1	42 $\pm$ 2	52.7 $\pm$ 0.5	600 $\pm$ 5	25 $\pm$ 6	3.03 $\pm$ 0.03	$77 \pm 2_{(18)}$	26	2.3	10.2	10.5	3
HB13	091927	160	36 $\pm$ 3	43 $\pm$ 1	40 $\pm$ 2	47.7 $\pm$ 0.4	521 $\pm$ 5	21 $\pm$ 5	2.81 $\pm$ 0.03	$141 \pm 4_{(24)}$	50	3.3	9.1	9.7	5
DV2/2	091902	265	36 $\pm$ 2	43 $\pm$ 1	39 $\pm$ 1	52 $\pm$ 1	559 $\pm$ 5	23 $\pm$ 6	2.86 $\pm$ 0.02	$92 \pm 6_{(17)}$	32	6.1	9.8	11.5	4
DV2/1	091901	435	45 $\pm$ 3	49 $\pm$ 1	41 $\pm$ 2	57 $\pm$ 1	482 $\pm$ 5	23 $\pm$ 6	2.78 $\pm$ 0.02	$115 \pm 5_{(18)}$	41	4.2	9.9	10.7	4

Radionuclide concentrations used for dose rate evaluation, estimates of past water content (F^*W), calculated dose rates, equivalent doses (D_e), optical ages, and random (σ_r), systematic (σ_{sys}) and total (σ_{tot}) uncertainties. The uncertainties mentioned with the D_e and dosimetry data are random; all uncertainties represent 1σ.

4.6.2. Dose rate determination

The radionuclide activity concentrations and calculated total dose rates are given in Table 1.

4.6.3. Optical ages

Table 1 summarises all analytical results, and shows the calculated optical ages. The present-day dose rate was assumed to have prevailed throughout the entire period of burial. Uncertainties on the luminescence ages were calculated following the error assessment system proposed by Aitken and Alldred (1972) and Aitken (1976). All sources of systematic uncertainty were as quantified by Vandenberghe et al. (2004; see also Vandenberghe, 2004).

For most samples, the systematic uncertainty is dominant in the overall uncertainty on the ages and varies between ~9 and 10% (1 sigma). For sample GLL-081901, both the random and systematic uncertainty are ~10%.

5. Discussion

5.1. Sedimentary and micromorphological record of Middle Pleniglacial (MIS3) and Upper Pleniglacial (MIS 2) in Moravia

The environmental record of the Middle and Upper Pleniglacial in Moravia was studied in detail mainly in context of loess deposits

(Fig. 4). Berendorf-Jones et al. (2011) described this horizon as an Interstadial A Cambisol horizon with the weak B-horizon above and covered by redeposited reworked palaeosol loam. However, micromorphological study did not confirm preservation of the *in situ* A horizon. A similar situation appeared in case of Předmostí locality. The weak interstadial soil horizon was eroded and redeposited. The interstadial soil was not preserved at Hošťálkovice. This finding corresponds to the results of the excavations of Neruda and Nerudová (2000). This type of paleosol is not known from this area, probably because of strong erosion and fragmentation of the sediment record and also because the environment of Northern Moravia and Lower Silesia was probably generally much colder than Central and Southern Moravia. Due to the fragmentation of sedimentary record of the Hošťálkovice section, it is quite difficult to use it for geochemical comparison with the sedimentary record preserved in central and southern Moravia. The first OSL data from Ostrava region concerning this context estimated the base of the section at 50 ka, which indicates that the arctic soil did not develop here or was removed by erosion.

Typical cultural layers containing charcoal or burned bones were described only in Dolní Věstonice and Předmostí, while in Hošťálkovice only the accumulations of artefacts were detected. ^{14}C data recently published by Berensdorf-Jones et al. (2011) from the DV II show a wide range between 25.570 and 28.850 ka uncal. After calibration, this fits the date from the cultural layer by OSL dating, 32 ka. The artefact accumulation from Hošťálkovice was dated as 26 ka, which make the finding a little bit older than the findings from nearby Petřkovice (Svoboda, 2008).

The tundra gley horizons preserved above the soil sediments of the Middle Pleniglacial were described in Dolní Věstonice (Klima et al., 1962; Antoine et al., 2013) and interpreted as cold humid episodes of the Middle and Upper Pleinglacial. In the old Věstonice brickyard, Antoine et al. (2013) have recently described one gley horizon connected with the Middle Pleniglacial which underwent strong solifluction process due to one of the humid interstadial phases of the Middle Pleniglacial (frost creep). The solifluction resulted in thin, discontinuous undulated iron oxide bands throughout the unit, and two gley horizons connected with the Upper Pleniglacial. The section situated above the old brickyard displays only two gley horizons which are *in situ* and have no ferric oxide nodules or accumulations. The third gley horizon was probably redeposited together with the paleosol, which would explain redoximorphic features founded within this redeposited horizon. Such an interpretation would also fit to the findings of Antoine et al. (2013) from the old brickyard. It is quite possible that those ferric oxide accumulations described by Antoine et al. (2013) were formed mainly due to the specific geomorphologic position in the landscape. Berensdorf-Jones et al. (2011) described from this section only lenses of gley above the cultural layer and gleyic features from the cultural layer, but not from redeposited soil below. Our OSL date sampled in the uppermost part of the upper gley horizon was estimated as 32 ka. That position in the old brickyard was in contrast to the date by Fuchs et al. (2012) at 21.7 ka.

One or more gley horizons together with frost features including frost wedges were also mentioned by Žebera et al. (1955) and lately by Svoboda et al. (1994) in Předmostí with no further details of interpretation. Demek and Svoboda (2008) described strong leaching and the presence of frost wedges in Petřkovice. In the same publication, Svoboda (2008) partly rejected Demek and Svoboda's interpretation, and interpreted those wedges as the result of Holocene pedogenesis. According to our OSL data, the infilling of the frost wedges is estimated at 5.3 ka, but the infilling could be much younger than the development of the wedges.

According to Antoine et al. (2013) the transition from Middle Pleniglacial gley horizons to the Upper Pleniglacial loess in Dolní Věstonice is abrupt and marked by a drastic increase in sedimentation rate due to a return of cold and arid conditions. In the studied sections, this phase of the sedimentary record is quite homogenous and the cold and arid conditions are recorded by the increased number of frost features, which are much more evident in Předmostí and Hošťálkovice. In the case of Věstonice and Předmostí, the sedimentary record of wind deposition is interrupted by thin layers of organic-matter rich layers corresponding to short phases of increased humidity. Toward the north there is an evident decrease of the mass of sediment, which could correspond to the increased wind intensity due to the geomorphology and position much closer to the North European glaciation that did not allow aeolian material deposition.

5.2. The interpretation of geochemical, magnetic and grain size proxies of studied sections in context of Middle and Upper Pleniglacial

The profiles from Dolní Věstonice and Předmostí are much more suitable for detailed correlation and paleoenvironmental interpretation from proxy analyses than is Hošťálkovice. The reason is a fragmentation of the sedimentary record and weaker pedogenesis in the case of Hoštálkovice, where the paleoenvironmental record was mainly inferred from micromorphological and sedimentological approaches.

Grain size records of Dolní Věstonice and Předmostí show similar features. Above the interstadial soils, the silt fraction continuously decreases, whereas the sand fraction of the sediment shows an increasing trend. Based on the interval of a higher sand input it is possible to correlate these profiles (Fig. 3). Several cycles can be seen, each being characterised by an abrupt increase of the sand component, followed by a short-term decrease. In these sites strong colluvial or water transport has not been noted. Therefore, these variations can be entirely attributed to the input of aeolian sand associated with climatic deterioration, increase of wind intensity and higher accumulation rate during MIS 2. Grain-size analyses from both sites are generally in accordance with previous measurements from the Upper Weichselian part of the old brickyard profile in Dolní Věstonice (Shi et al., 2003; Antoine et al., 2013). Inputs of coarse aeolian material during the Upper Pleniglacial were also reported and correlated within several sites from sub-Atlantic region to the western Ukraine (Antoine et al., 2009; Bokhorst et al., 2010; Rousseau et al., 2011) as well as in China Loess Plateau (Nugteren et al., 2004). These events were correlated with a dust median in NGRIP record and associated to Heinrich events H3–H1 (Antoine et al., 2009). While a gradual coarsening trend is a significant feature in Dolní Věstonice, in the upper part of Předmostí this trend is not so apparent. That can be a signal of lower wind intensity in the final phase of the Upper Pleniglacial in the Central Moravia in comparison with South Moravia. A distinctly higher percentage of sand in the sediment of Dolní Věstonice as compared with Předmostí indicates lower energy of wind transport during Upper Pleniglacial in Central Moravia. Evident fining of the grain composition toward to the north is also visible (Fig. 3), together with the progressive reduction of the thickness of the deposited material. The fining trend probably reflects the changing provenance (Lisá, 2004; Lisá and Uher, 2006; Lisá et al., 2009) especially the possible appearance of glacial deposits (Lisá, 2004) toward the north. The geomorphology and the lack of westerly situated wide valleys with thick alluvial plain also play a role.

Higher values of frequency dependent magnetic susceptibility suggest the presence of ultra-fine grained (pedogenetic) magnetite or maghemite (Worn, 1998; Liu et al., 2005). In Dolní Věstonice and Předmostí, slightly higher values were found in the horizons with initial pedogenesis (and gley horizons) and significant high values in redeposited brown soil horizons. The magnetic enhancement is probably caused by increased activity of soil bacteria during the Middle Pleniglacial and climatically favourable periods (micro-interstadials) of the Upper Pleniglacial. Good correlation of the frequency-dependent magnetic susceptibility with the organic content was found in both sections. That denotes a connection between vegetation development (humid climate?) and the intensity of pedogenesis. In contrast, weak magnetic signal of pure loess accumulation indicates colder (and drier) condition and minimal pedogenetic processes. With regard to relatively narrow provenance source of the Moravian loess during Upper Pleistocene (Lisá, 2004), changes in the chemical composition in the profiles could relate to postdepositional processes.

Continuously decreasing Mg–Ca ratio (expressed here as MgO/CaO) in the pedo-sedimentary record could be caused by gradual decline of precipitation in the study area during MIS 2. Mg and Ca are present in primary carbonates, abundant in the loess deposits. Free Mg content can be enhanced by weathering of pyroxene, amphibole, and biotite, and Ca mainly from Ca-feldspar. Mg is retained much more strongly on clay than Ca, due to the large difference in atomic diameter (Perel'mman, 1977). A higher amount of percolating rainwater therefore leads to stronger leaching of Ca relative to Mg and increasing of Mg/Ca ratio (MgO/CaO) (Bokhorst et al., 2009). Both elements are also taken up by plants, although Ca is much more important with a biogenic coefficient of 0.17, versus 0.02 for Mg (Perel'man, 1977). The ratio could be, therefore, also influenced by the density of the vegetation cover. In comparison with the decreasing trend in Dolní Věstonice, Předmostí shows a slightly increasing MgO/CaO trend, suggesting wetter conditions in Central Moravia during MIS 2.

During chemical weathering of loess, ion exchange and layers transformation of clay minerals occurs, that leads to modified of their structure and clay neoformation. The $[Cu(trien)]^{2+}$ ion is rather selective to expandable clay minerals, and thus increased CEC values are most likely attributable to a higher concentration of the most common expandable clay minerals, i.e. smectite structures, whereas lower concentrations indicate increased presence of the weak expandable clay mineral, i.e. illite (Bábek et al., 2011). The structure of expanded clay minerals is typical for more humid environments, and its low amount in the sediment suggests that conditions were likely arid (and acidic) and they has been largely depleted or least altered. The smectite/illite ratio in the loess series can be used as a proxy for humidity. Even if CEC has rarely been used for loess/paleosols sequences, several studies suggest CEC can be correlated with other indicators of weathering intensity related to precipitation such as magnetic susceptibility, diffuse reflectance spectroscopy and element ratios of Rb, Ca and Sr (Maher, 1998; Bokhorst et al., 2008; Bábek et al., 2011). In DV and Předmostí, that is suggested by an apparent relationship of CEC with MgO/CaO ratio and magnetic susceptibility that denotes a connection of weathering intensity with pedogenesis and amount of precipitation.

In general, the sedimentological, magnetic and geochemical results from all sections show significant climatic deterioration in Upper Pleniglacial by comparison with Upper Middle Pleniglacial conditions. That is recorded as gradual increasing wind intensity and a relative decline of precipitation. Nevertheless, in comparison with Dolní Věstonice, the proxy record from Předmostí suggests relatively more favorable climatic conditions.

5.3. Gravettian migrations during the Middle and Upper Pleniglacial within Moravian valleys

One of the goals set at the beginning of this paper was to discuss reasons which enabled humans during the Upper Pleniglacial to exploit the North European Plain, and subsequently even colder regions. One of the possible explanations is the presence of the water in the cold, and subsequently very dry glacial landscape (Lisá et al., 2013). Humidity seems to be the most important factor for the presence of vegetation, and subsequently animals and humans. The most important factors limiting the presence of human camps in the landscape is the presence of tectonically predisposed wide open valleys with the river network and with the close proximity of narrowing in the landscape. Oliva (2007) and Svoboda et al. (2003) discuss the importance of the presence of a river network. During the Glacial period, braided rivers (French et al., 2007) resulting from appreciable sediment load, rapid and large variations in discharge, and erosion formed the fluvial landscape of the Paleolithic in Central Europe. The alluvial zone differed from the recent one quite significantly. The presence of water in the landscape raised the temperature below rivers and along the margins, which resulted in further melting of permafrost along the banks and distinct bank morphology. Tectonic activity often brings water to the surface as course and springs. Deep water circulations were probably alsi active during the LGM.

Another important factor is the precipitation, which was probably distributed differently within the Moravian landscape. As visible from the sedimentological micromorphological and the geochemical record, Central and Northern Moravia was during the Middle and Upper Pleniglacial more humid than Southern Moravia. This fact can be connected with the more hilly geomorphology (Czudek, 1997), but also with the shorter distance from the North European glaciation. The proposed movement to the more cold, but subsequently also more humid regions in the transect from the Danube to the North European Plains can be compared with the movement to the Carpathians valleys as described by Svoboda (2001). Those valleys were described as warmer refugia (Musil, 2003), but the key factor was possibly the presence of humidity. Together with the possible presence of permafrost, such areas were much more suitable for the vegetation growth than the drier south. Rich vegetation growing over permafrost, because the permafrost layer catches the humidity, are known from recent arctic areas (Beilman, 2001; Payette et al., 2004). The presence of water connected with growing vegetation is one of the limiting factors of mammoth migrations (Gröning and Saller, 1998), and therefore also the limiting factor for Gravettian hunters' migrations.

6. Conclusions

Studied loess sites from Northern, Southern and Central Moravia provide a suitable archive for detailed study of the palaeoenvironmental changes during Upper Paleolithic period. Using a multi-proxy approach combining micromorphological, sedimentological, rock-magnetic, and geochemical methods, we have demonstrated that:

1. The sedimentary record within the studied transect differs, the amount of deposited or preserved sedimentary record decreases toward the north.
2. The most evident difference in micromorphological record is the increasing presence of freezing and thawing features toward the north. The strong postsedimentary influence at Hošťálkovice precluded detailed study.
3. The particle grain distribution record of three studied Upper Palaeolithic loess sites show a progressive coarsening of the loess deposits during the Upper Pleniglacial. A progressive fining is visible toward the North European glaciation.
4. The geochemical record of the studied sections shows numerous similarities and is influenced by lithology. Cation Exchange Capacity (CEC) of Dolní Věstonice shows a relatively stable trend with microfluctuations except for enhancement within the lower part of the section, where the re-deposited interstadial soil and cultural layer were identified. Increased values were found in the loess with initial pedogenesis, and a slightly increased trend is visible in the upper part of the profile. The profile in Předmostí shows a similar trend. Hošťálkovice section displayed the highest CEC values within the base, due to the weathered sandy loam with carbonate pebbles. A sharp decrease of those values follows the appearance of pure loess-like deposits with the artefacts.
5. New OSL Ages were determined for Dolní Věstonice, and the first OSL dating for Hošťálkovice. In Dolní Věstonice the age of the cultural layer was estimated to 41 ka and the age of the gley layer to 32 ka. Hošťálkovice, the age of the base of the section was estimated to 50 ka, the position of artefact findings 26 ka, and the infilling of frost edges 5.3 ka. OSL dating for Dolní Věstonice and Hošťálkovice brought slightly older dates than expected.
6. The reason that humans could exploit the North European Plain and even colder regions could have been the presence of water in the cold and arid glacial landscape. According to sedimentological and geochemical records, the more northerly regions were more humid than the regions to the south.

Acknowledgements

The authors would like to thank the Archaeological Department of the University of Cambridge and the European Commission Marie Curie Intra-European Fellowship program for support. This research was also financed by the institutional research plan of the Institute of Geology AS CR, v. v. i, No. AV0 Z 30130516 and by the Institutional research plan of FWT Mendel University in Brno, No. MSM 6215648902. We would like to thank Dr. M. Chadima from Agico a.s. company for allowing measurement of magnetic properties of studied sediments, to Prof. Jiří Svoboda and Martin K. Jones to provide us with access to the excavation in Dolni Vestonice, to Mgr. P. Drechsler for providing access to the section in Předmost, and especially to dr. Peter Neruda for the possibility to sample material from the Hošťálkovice locality. Authors would also like to thank Alena Šamonilová for the very helpful comments and editing of the English text.

References

Adamiec, G., Aitken, M., 1998. Dose-rate conversion factors: update. Ancient TL 16, 37–50.
Adamová, M., Havlíček, P., 1998. Fossil soils geochemistry of the most important Moravianlocalities. Zpr. geol. Výzk. v Roce 1997, 54–62.
Aitken, M.J., 1976. Thermoluminescence age evaluation and assessment of error limits: revised system. Archaeometry 18, 233–238.
Aitken, M.J., Alldred, J.C., 1972. The assessment of error limits in thermoluminescence dating. Archaeometry 14, 257–267.
Antoine, P., Catt, J., Lautridou, J.P., Sommé, J., 2003. The loess and coversands of Northern France and Southern England. Journal of Quaternary Sciences 18, 309–318.
Antoine, P., Rousseau, Moine, O., Rousseau, D.D., Kunesch, S., Hatté, C., Lang, A., Zöller, L., 2009. Evidence of rapid and cyclic eolian deposition during the Last Glacial in European loess series (Loess Events): the high-resolution records from Nussloch (Germany). Quaternary Science Reviews 28, 2955–2973.
Antoine, P., Rosseau, D.D., Degeai, J.P., Moine, O., Lagroix, F., Kreutzer, S., Fuchs, M., Hatté, Ch., Gauthier, C., Svoboda, J., Lisa, L., 2013. High-resolution record of the environmental response to climatic variations during the last interglacial-glacial cycle in central Europe: the loess-palaeosol sequence of Dolní Věstonice (Czech Republic). Quaternary Science Reviews 67, 17–38.
Bábek, O., Chlachula, J., Grygar, T.M., 2011. Non-magnetic indicators of pedogenesis related to loess magnetic enhancement and depletion: examples from the Czech Republic and southern Siberia. Quaternary Science Reviews 30, 967–979.
Beilman, D.W., 2001. Plant community and diversity change due to localized permafrost dynamics in bogs of western Canada. Canadian Journal of Botany 79, 983–993.
Beresford-Jones, D., Johnson, K., Pullen, A.G., Pryor, A.J.E., Svoboda, J., Jones, M., 2010. Burning wood or burning bone? A reconsideration of flotation evidence from Upper Palaeolithic (Gravettian) sites in Moravian Corridor. Journal of Archaeological Science 37, 2799–2811.
Beresford-Jones, D., Taylor, S., Paine, C., Pryor, A., Svoboda, J., Jones, M., 2011. Rapid climate change in the Upper Palaeolithic: the record of charcoal conifer rings from the Gravettian site of Dolní Věstonice, Czech Republic. Quaternary Science Reviews 30, 1948–1964.
Bokhorst, S., Bjerke, J.W., Bowles, F.P., Melillo, J.M., Callaghan, T.V., Phoenix, G.K., 2008. Impacts of extreme winter warming in the sub-Arctic: growing season responses of dwarf-shrub heathland. Global Change Biology 14, 2603–2612.
Bokhorst, S., Bjerke, J.W., Davey, M., Taulavuori, K., Taulavuori, E., Laine, K., Callaghan, T.V., Phoenix, G.K., 2010. Impacts of extreme winter warming events on plant physiology in a sub-Arctic heath community. Physiol Plant 140, 128–140.
Bullock, P., Federoff, N., Jongerius, A., Stoops, G., Tursina, T., Babel, U., 1985. Handbook for Soil Thin Section Description. Waine Research Publications, Wolverhampton, UK.
Czudek, T., 1997. Reliéf Moravy a Slezska v kvartéru. SURSUM, Tišnov (in Czech).
Dearing, J.A., Dann, R.J.L., Hay, K., Lees, J.A., Loveland, P.J., Maher, B.A., O'Grady, K., 1996. Frequency-dependent susceptibility measurements of environmental materials. Geophysical Journal International 124, 228–240.
Demek, J., Kukla, J., 1969. Periglazialzone, Löss und Paläolithicum der Tschechoslowakei. Tsechoslowakische Akademie der Wissenschaften, Geographisches Institut, Brno, p. 158 (in German).
Demek, J., Svoboda, J., 2008. Quaternary stratigraphy. In: Svoboda, J. (Ed.), Petřkovice on Shouldered Points and Female Figurines. Institute of Archaeology at Brno, Academy of Sciences of the Czech Republic, Brno, pp. 28–30.
Evans, M.E., Heller, F., 2003. Environmental Magnetism, Principles and Applications of Enviromagnetics. Academic Press, An imprint of Elsevier Science, Oxford.
Folprecht, J., 1934. Výzkumné práce na praehistorickém sídlišti v Petřkovicích. Příroda 27 (3), 77 (in Czech).
Frechen, M., 1999. Upper Pleistocene loess stratigraphy in Southern Germany. Quaternary Geochronology 18, 243–269.
Frechen, M., Zander, A., Cílek, V., Ložek, V., 1999. Loess chronology of the Last Interglacial/Glacial cycle in Bohemia and Moravia, Czech Republic. Quaternary Science Rewiews 18, 1467–1493.
French, Ch.A., 2003. Geoarchaeology in Action: Studies in Soil Micromorphology and Landscape Evolution. Routhledge.
French, C., Lewis, H., Green, M., Allen, M.J., Scaife, R., Gardiner, J., Samarsundera, E., 2007. Studying land use from monuments: archaeology and environment on Bottlebush, Wyke and Gussage Cow Downs'. In: Prehistoric landscape development and human impact in the upper Allen valley, Cranborne Chase, Dorset. McDonald Institute for Archaeological Research, Cambridge.
Frenzel, B., 1968. Grundzűge der pleistozänen Vegetationsgeschichte Nord-Eurasiens. Erdwissenschaftliche Forschungen (I), Wiesbaden (in German).
Fuchs, M., Kreutzer, S., Rousseau, D.D., Antoine, P., Hatté, C., Lagroix, F., Moine, O., Gauthier, C., Svoboda, J., Lisá, L., 2012. The loess sequence of Dolní Věstonice, Czech Republic: a new OSL-based chronology of the Last Climatic Cycle. Boreas. http://dx.doi.org/10.1111/j.1502–3885.2012.00299.x.
Gee, W., Bauder, J.W., 1986. Particle-size analyses. In: Klute, Arnold (Ed.), Methods of Soil Analysis: Part 1—Physical and Mineralogical Methods. SSSA book series 5.1.
Gerasimenko, N., 2006. Upper Pleistocene loess-palaeosol and vegetational successions in the Middle Dnieper Area, Ukraine. Quaternary Int. 149, 55–66.
Goldberg, P., 1983. Applications of micromorphology in archaeology. In: Bullock, P., Murphy, C.P. (Eds.), Soil Micromorphology, Techniques and Applications, vol. 1. AB Academic Publishers, Berkhamsted, United Kingdom, pp. 139–150.
Goldberg, P., Macphail, R.I., 2006. Practical and Theroetical Geoarchaeology. Blackwell Publishing, Oxford, 455pp.
Gröning, K., Saller, M., 1998. Der Elefant in Natur und Kulturgeschichte. Könemann, Köln.
Grygar, T., Světlík, I., Lisá, L., Koptíková, L., Bajer, A., Wray, D.S., Ettler, V., Mihaljevič, M., Nováková, T., Koubková, M., Novák, J., Máčka, Z., Smetana, M., 2009. Geochemical tools for the stratigraphic correlation of floodplain deposits of the Morava River in Strážnické Pomoraví, Czech Republic from last millennium. Catena 80, 106–121.
Haesaerts, P., 1985. Les lœss du Pléistocène supérieur en Belgique ; comparaisons avec les séquences d'Europe centrale. Bulletin de l'Association Française pour l'Etude du Quaternaire 2/3, 105–115.
Haesaerts, P., Mestdagh, H., 2000. Pedosedimentary evolution of the last interglacial and the early glacial sequence in the European loess belt from Belgium to central Russia. Geologie en Mijnbouw/Netherlands Journal of Geosciences 79 (2/3), 313–324.
Haesaerts, P., Borziak, I., Chirica, V., Damblon, F., Koulakovska, L., Van der Plicht, J., 2003. The East-Carpathian loess record: a reference for the Middle and Late Pleniglacial stratigraphy in central Europe. Quaternaire 14 (3), 163–188.
Horáček, I., Ložek, I., 1988. Paleozoology and mid-European quaternary past: scope of the approach and selected results. Rozpravy ČSAV-MPV 94, 1–106.
Klíma, B., 1969. Petřkovice II. Nová Paleolitická stanice v Ostravě. Archeologické Rozhledy 21, 583–595 (in Czech).
Klima, B., Kukla, J., Lozek, V., De Vries, H., 1962. Stratigraphie des Pleistozäns und Alter des Paläolithischen Rastplatzes in der Ziegelei von Dolni Vestonice (Unter-Wisternitz). Antropozoikum 11, 93–145 (in German).
Kovanda, J., 1971. Kvartérní vápence Československa. Anthropozoikum 7, 7–236 (in Czech).
Kukla, G., 1975. Loess stratigraphy of central Europe. In: Butzer, K.W., Isaac, G.L. (Eds.), After the Australopithecines. Mouton Publishers, The Hague, pp. 99–188.
Lisá, L., 2004. Exoscopy of Moravian eolian sediments. Bulletin Geosciences 79 (3), 177–182.
Lisá, L., Uher, P., 2006. Provenance of Wurmian loess and loess-like sediments of Moravia and Silesia (Czech Republic): a study of zircon typology and cathodoluminiscence. Geologica carpatica 57 (5), 397–403.
Lisá, L., Buriánek, D., Uher, P., 2009. New approach to garnet redistribution during aeolian transport. Geological Quarterly 53 (3), 333–340.
Lisá, L., Škrdla, P., Havlín Nováková, D., Bajer, A., Čejchan, P., Nývltová Fišáková, M., Lisý, P., 2013. The role of abiotic factors in ecological strategies of Gravettian hunter-gatherers within Moravia, Czech Republic. Quaternary International 294, 71–81.
Liu, Q.S., Torrent, J., Maher, B.A., Yu, Y.J., Deng, C.L., Zhu, R.X., Zhao, X.X., 2005. Quantifying grain size distribution of pedogenic magnetic particles in Chinese loess and its significance for pedogenesis. Journal of Geophysical Research 110, B11102. http://dx.doi.org/10.1029/2005JB003726.
Ložek, V., 1953. Pleistocénní mekkýši z gravettského sídliště u Dolních Věstonic. Monumenta Archeologica 2, 45–51.
Ložek, V., 1964. Mittel- und jungpleistozäne Löβ-Serien in der Tschechoslowakei und ihre Bedeutung für die Löβ-Stratigraphie Mitteleuropas. Report of the IV International Congress on Quaternary, pp. 525–549. Warschau.
Ložek, V., 1968. Über die malakozoologische Charakteristik der pleistozänen Warmzeiten mit besonderer Berűcksichtung des letzten Interglazials. Berichte der Deutschen Ges. f. Geol. Wiss., R.A 14 (4), 439–469. Berlin.
Macphail, R.I., Cruise, G.M., 2001. The soil micromorphologist as team player: a multianalytical approach to the study of European microstratigraphy. In: Goldberg, P., Holliday, V., Ferring, R. (Eds.), Earth Science and Archaeology. Kluwer Academic/Plenum Publishers, New York, pp. 241–267.

Maher, B.A., 1998. Magnetic properties of modern soils and loessic paleosols: implications for paleoclimate. Palaeogeography, Palaeoclimatology, Palaeoecology 137, 25–54.
Meier, L.P., Kahr, G., 1999. Determination of the cation exchange capacity (CEC) of clay minerals using the complexes of copper (II) ion with triethylenetetramine and tetraethylenepentamine. Clays Clay Miner. 47, 386–388.
Murray, A.S., Wintle, A.G., 2000. Luminescence dating of quartz using an improved single-aliquot regenerative-dose protocol. Radiation Measurements 32, 57–73.
Murray, A.S., Wintle, A.G., 2003. The single aliquot regenerative dose protocol: potential for improvements in reliability. Radiation Measurements 37, 377–381.
Musil, R., 2003. The Middle and Upper Palaeolithic game suite in central and Southeastern Europe. In: van Andel, T.H., Davies, W. (Eds.), Neanderthals and Modern Humans in the European Landscape during the Last Glaciations: Archaeological Results of the Stage 3 Project. McDonald Institute Monographs, Cambridge, pp. 167–190.
Neruda, P., Nerudová, Z., 2000. Archeologická sondáž na lokalitě Hošťálkovice II – Hladová vrch o. Ostrava. Acta Historica et museologica Universitatis Silesianae Opaviensis. 5, 116–122 (in Czech).
Nývltová Fišáková, M., 2013. Seasonality of Gravettian sites in the Middle Danube Region and adjoining areas of Central Europe. Quaternary International 294, 120–134. http://dx.doi.org/10.1016/j.quaint.2011.08.017.
Nugteren, G., Vandenberghe, J., Ko van Huissteden, J., Zhisheng, A., 2004. A Quaternary climate record based on grain size analysis from the Luochuan loess section on the Central Loess Plateau, China. Global and Planetary Change 41 (3-4), 167–183.
Oliva, M., 2005. Palaeolithic and Mesolithic Moravia. MZM, Brno.
Oliva, M., 2007. Gravettien na Moravě. Dissertatiiones archaeologicae Brunheses/Pragensesque Brno, Praha.
Otte, M., 1981. Le gravettien en Europe centrale. Disertationes archeologicae Gandenses 20. Brugge.
Payette, S., Delwaide, A., Caccianiga, M., Beauchemin, M., 2004. Accelerated thawing of subarctic peatland permafrost over the last 50 years. Geophysical Research Letters 31, L18208. http://dx.doi.org/10.1029/2004GL020358.
Perel'man, A.I., 1977. Geochemistry of Elements in the Supergene Zone. Keterpress Enterprises, Jerusalem.
Richter, D., Tostevin, G., Skrdla, P., Davies, W., 2009. New radiometric ages for the Early Upper Palaeolithic type locality of Brno-Bohunice (Czech Republic): comparison of OSL, IRSL, TL and 14C dating results. Journal of Archaeological Science 36, 708–720.
Rousseau, D.D., Antoine, P., Gerasimenko, N., Sima, A., Fuchs, M., Hatté, C., Moine, O., Zöller, L., 2011. North Atlantic abrupt climatic events of the Last Glacial period recorded in Ukrainian loess deposits? Clim. Past 7, 221–234.
Shi, C., Zhu, R., Glass, B.P., Liu, Q., Zeman, A., Suchy, V., 2003. Climate variations since the last interglacial recorded in Czech loess. Geophysical Research Letters 30 (11), 1562.
Skutil, J., 1955. Příspěvek k poznání paleolitika Moravské brány. Anthropozoikum 4, 447–468 (in Czech).
Stoops, G., 2003. Guidelines for Analysis and Description of Soil and Regolith Thin Sections. Soil Science Society of America, Inc., Madison, Wisconsin, USA.
Svoboda, J., 2001. On the Middle to Upper Paleolithic transition in north Eurasia. Archaeol. Ethnol. Anthropol. Eurasia 4 (8), 30–37. Rusko: Institute of Archaeology and Ethnography.
Svoboda, J. (Ed.), 2008. Petřkovice on Shouldered Points and Female Figurines. Institute of Archaeology at Brno, Academy of Sciences of the Czech Republic, Brno.
Svoboda, J., Ložek, V., Svobodová, H., Škrdla, P., 1994. Předmostí after 110 years. Journal of Field Archaeology 21, 457–472.
Svoboda, J., Havlíček, P., Ložek, V., Macoun, J., Musil, R., Přichystal, A., Svobodová, H., Vlček, E., 2002. Paleolithic of Moravia and Silesia. In: The Dolní Věstonice Studies, vol. 8. Brno.
Svoboda, J., Havlíček, P., Ložek, V., Macoun, J., Musil, R., Přichystal, A., Svobodová, H., Vlček, E., 2003. Paleolit Moravy a Slezska, 2., aktualizované vydání – Paleolithic of Moravia and Silesia, 2nd revised edition. Dolní Věstonice Studies vol. 8. Brno 2002.
Svoboda, J., 2004. Continuities, discontinuities, and interactions in Early Upper Paleolithic technologies. In: The Early Upper Paleolithic beyond Western Europe. University of California Press, USA, pp. 30–49.
Thompson, R., Oldfield, F., 1986. Environmental Magnetism. Allen and Unwin, London.
Trinkaus, E., Svoboda, J., 2006. Early Modern Human Evolution in Central Europe: the People of Dolní Věstonice and Pavlov. Oxford University Press, Oxford.
Valoch, K., 1976. Die altsteinzeitliche Fundstelle in Brno-Bohunice, vol. 4. Studi Archeologickeho ustavu Ceskoslovenske Akademie ved v Brne, Brno.
Valoch, K., 1979. Paleolit středního pomoraví. Studie Muzea Kroměříšska 1, 22–35 (in Czech).
Vandenberghe, D., 2004. Investigation of the Optically Stimulated Luminescence Dating Method for Application to Young Geological Samples. Ph.D. thesis. Ghent University.
Vandenberghe, D., Kasse, C., Hossain, S.M., De Corte, F., Van den haute, P., Fuchs, M., Murray, A.S., 2004. Exploring the method of optical dating and comparison of optical and 14C ages of Late Weichselian coversands in the southern Netherlands. Journal of Quaternary Science 19, 73–86.
Vandenberghe, D., De Corte, F., Buylaert, J.-P., Kučera, J., Van den haute, P., 2008. On the internal radioactivity in quartz. Radiation Measurements 43, 771–775.
Worn, H.U., 1998. On the superparamagnetic—stable single domain transition for magnetite, and frequency dependence of susceptibility. Geophys. J. Int 133, 201–206.
Žebera, K., Ložek, V., Kneblová, V., Fejfar, O., Mazánek, M., 1955. Zpráva o druhé etapě geologického výzkumu kvartéru v Předmostí u Přerova na Moravě. Anthropozoikum 4, 291–362.

5.4. Glacigenní procesy

Mentlík P., Minár J., Břízová E., **Lisá L.**, Taborik P. & Stacked V. (2010): Glaciation in the surroundings of Prášilské Lake (Bohemian Forest, Czech Republic).- Geomorphology, 117, 1-2, 181-194.

Krizova, L, Krizek, M, **Lisa, L.** (2011): Applicability of quartz grains surface analysis to the study of the genesis of unlithified sediments. GEOGRAFIE, 116, 1, 59-78

Geomorphology 117 (2010) 181–194

Contents lists available at ScienceDirect

Geomorphology

journal homepage: www.elsevier.com/locate/geomorph

Glaciation in the surroundings of Prášilské Lake (Bohemian Forest, Czech Republic)

Pavel Mentlík [a,*], Jozef Minár [e,f,1], Eva Břízová [b], Lenka Lisá [c,d,2], Petr Tábořík [f], Václav Stacke [f]

[a] Department of Geography, University of West Bohemia in Pilsen, Veleslavínova 42, 306 19, Plzeň, Czech Republic
[b] Czech Geological Survey, Klárov 3/131, 118 21 Praha 1, Czech Republic
[c] Geological Institute Academy of Sciences of the Czech Republic, Rozvojová 269, 165 00 Praha 6, Czech Republic
[d] Department of Archaeology, Cambridge University, United Kingdom
[e] Department of Physical Geography and Geoecology, Comenius University in Bratislava, Mlynská dolina, 842 15 Bratislava 4, Slovakia
[f] Department of Physical Geography and Geoecology, University in Ostrava, Chittussiho 10, 710 00 Ostrava, Czech Republic

ARTICLE INFO

Article history:
Received 2 August 2008
Received in revised form 27 November 2009
Accepted 3 December 2009
Available online 16 December 2009

Keywords:
Pleistocene glaciations
Prášilské Lake
Bohemian Forest
Šumava
Sedimentology
Chronology

ABSTRACT

Comprehensive geomorphological and sedimentological analyses confirmed three phases of Würm glaciation in the surroundings of Prášilské Lake and Stará Jímka, in the Bohemian Forest (Šumava Mountains). Glaciations were affected by a steep east-facing slope, by plateaus on the adjacent ridges and by local geological conditions. A small valley glacier (about 2 km long and 50 m thick) occurred during the first phase. In the second phase, a glacier–rock glacier developed, probably based on remnants of the valley glacier. During the last phase glacial activity was divided into Stará Jímka and the stepped cirque of Prášilské Lake. A further shallow (~3 m deep) lake in Stará Jímka was dammed by slope movements after deglaciation (~14 cal. ka BP) and survived until ~4 cal. ka BP. The Late Pleistocene chronology of the Bohemian Forest seems to be related more closely to the Alps than to northern Europe. In the mid-mountains of central Europe, Pleistocene glaciation decreases significantly eastward, because of increasing continentality. The presence of plateaus (deflation areas), around 1300 m altitude, across the approach of westerly winds was important for the development of glaciers in the Bohemian Forest. The termination of glaciation before the Younger Dryas is specific to the Bohemian Forest in comparison with the Vosges and Krkonoše Mountains.

1. Introduction

Although much attention has been paid to glaciations in Europe (e.g., Ehlers and Gibbard, 2004a,b), some areas remain little known. The Czech part of the Bohemian Forest (in Czech, the Šumava) is an example of such omission, where research was difficult because of proximity to the former 'Iron Curtain' border. The position of the Bohemian Forest between previously glaciated regions — Scandinavia and the Alps in a latitudinal direction, and the Vosges and Western Carpathians in a longitudinal direction — is important for the chronological correlations presented here.

Two basic concepts for the Pleistocene glaciation of the Bohemian Forest have been postulated. Bayberg (1886) and Preihäusser (1934) assumed an extensive glaciation (an ice cap on the Šumavské Plateau with outlets filling the valleys of the bigger rivers, e.g. the Vydra and Otava). On the contrary, Rathsburg (1928) argued that glaciers were located in cirques with tongues only overlapping the sills. The second hypothesis was supported by later research on the Czech side of the Bohemian Forest (Šumava) (Votýpka, 1979; Mentlík, 2002, 2005, 2006; Vočadlová and Křížek, 2005). On the Bavarian side of the Bohemian Forest, however, evidence of a valley glacier up to 3 km long was found in the Arber area (Pfaffl, 1998; Raab and Völkel, 2003; Reuther, 2007) and the presence of glaciers up to 7 km long was postulated by Hauner (1980) for the Rachel–Lusen area.

Papers dealing with the glaciation of the Czech part of the Šumava or Bohemian Forest are outdated (Kunský, 1933; Votýpka 1979) or partial (Mentlík, 2002, 2005, 2006; Vočadlová and Křížek, 2005). Our paper presents the first comprehensive study of a previously glaciated area (the surroundings of Prášilské Lake) in the Šumava using detailed research with dating techniques and a multi-technique and multidisciplinary approach.

This study presents the extent, character and chronology of glaciations. Our results demonstrate a greater diversity of glacial forms than has been mentioned previously (Votýpka, 1979; Raab and Völkel, 2003) and the former presence of an extra post-glacial lake (Stará Jímka).

2. Regional setting

Two glacial cirques creating a step-like system are the predominant erosional glacial forms on the east flank of Poledník Mountain

* Corresponding author. Tel.: +420 777646307; fax: +420 377636582.
E-mail addresses: pment@kge.zcu.cz (P. Mentlík), minar@fns.uniba.sk (J. Minár), eva.brizova@geology.cz (E. Břízová), lisa@gli.cas.cz (L. Lisá), petr.taborik@volny.cz (P. Tábořík), vaclavstacke@seznam.cz (V. Stacke).
[1] Permanent address. Department of Physical Geography and Geoecology, Comenius University in Bratislava, Mlynská dolina, 842 15 Bratislava 4, Slovakia.
[2] Permanent address. Geological Institute Academy of Sciences of the Czech Republic, Rozvojová 269, 16500 Praha 6, Czech Republic.

0169-555X/$ – see front matter © 2009 Elsevier B.V. All rights reserved.
doi:10.1016/j.geomorph.2009.12.001

(1315 m asl), 3.5 km south of Prášily village (Fig. 1). Prášilské Lake (49° 04′ N.,°13° 24′ E.) lies in the well-developed, almost semicircular lower cirque (length 411 m; width 386 m; height of the headwall 141 m) at altitude 1079 m (Fig. 1). The cirque aspect is almost east (azimuth of the median axis: 88°). The second, shallower, more open cirque lies about 25 m higher (length 364 m; width 502 m; height of the headwall 119 m). The plateaus on the adjacent ridges (area 170 000 m^2) (Fig. 1) were important as deflation source areas aiding development of the glaciers (Steffanová and Mentlík, 2007).

Stará Jímka is a 1015-m long and ~70-m wide depression lying ~800 m SSE of the lake, located between the wall and the linear steep slope (~35°) with a predominant eastward aspect (Fig. 1).

The geological conditions are summarized in the 1:50 000 geological maps of Pelc and Šebesta (1994). Although crystalline rocks such as gneiss, migmatite, and quartzite are predominant, relatively small granite areas are morphologically significant (particularly two zones above the lake) (Fig. 2).

3. Materials and methods

Detailed geomorphological mapping by means of elementary forms of relief formed the basis for our multidisciplinary research. Elementary forms are geomorphic primitives delimited by discontinuity of altitude or its derivatives, and characterized by internal uniformity of altitude or some of its derivatives (Minár and Evans, 2008). Mapping of elementary forms was used for two reasons:

(i) elementary forms have strong morphogenetic significance: their properties and discontinuities should be genetically interpretable (Minár and Evans, 2008); and

(ii) their systematic mapping and analysis leads to a holistic understanding of the area of interest (Minár and Evans, 2008) and is a good base for multidisciplinary research.

Investigation of landform genesis and chronology involved multidisciplinary research using sedimentological methods, pollen analysis and relative and absolute dating. Geophysical profiling was used for detection of the internal structure of the landforms and thickness of the sediment.

To distinguish textural groups of sediment, particle size was analyzed in the laboratory of the Department of Physical Geography and Geoecology at the University of Ostrava, Czech Republic. The samples were sieved down from 10 000 to 0.001 µm and the data obtained were entered into a "Gradistat" spreadsheet (Blott and Pye, 2001).

Three methods were used to investigate the origin of the sediments: analysis of particle morphology (shape and roundness), analysis of clast macrofabrics (Benn and Evans, 1998; Hubbard and Glasser, 2005) and analysis of features on the surfaces of quartz grains by SEM (exoscopy).

For analysis of particle morphology the direction and dip as well as the size of the *a*-, *b*- and *c*-axes were measured for each particle. Roundness was classified visually according to Powers' (1953) scale.

Measurements of the axes were plotted on a "tri-plot" spreadsheet (Graham and Midgley, 2000); C_{40} (shape) and RA (roundness) indexes were calculated (Benn and Ballantyne, 1994; Harris et al., 2004). Finally, results were plotted on the RA/C_{40} diagram (Benn and Ballantyne, 1994). This approach was used to discriminate different sedimentological facies and environments (Hambrey and Ehrmann, 2004). Data from the surroundings of near Laka Lake (Mentlík, 2005) were also included, for the sake of completeness (better distinguishing of facies and environments).

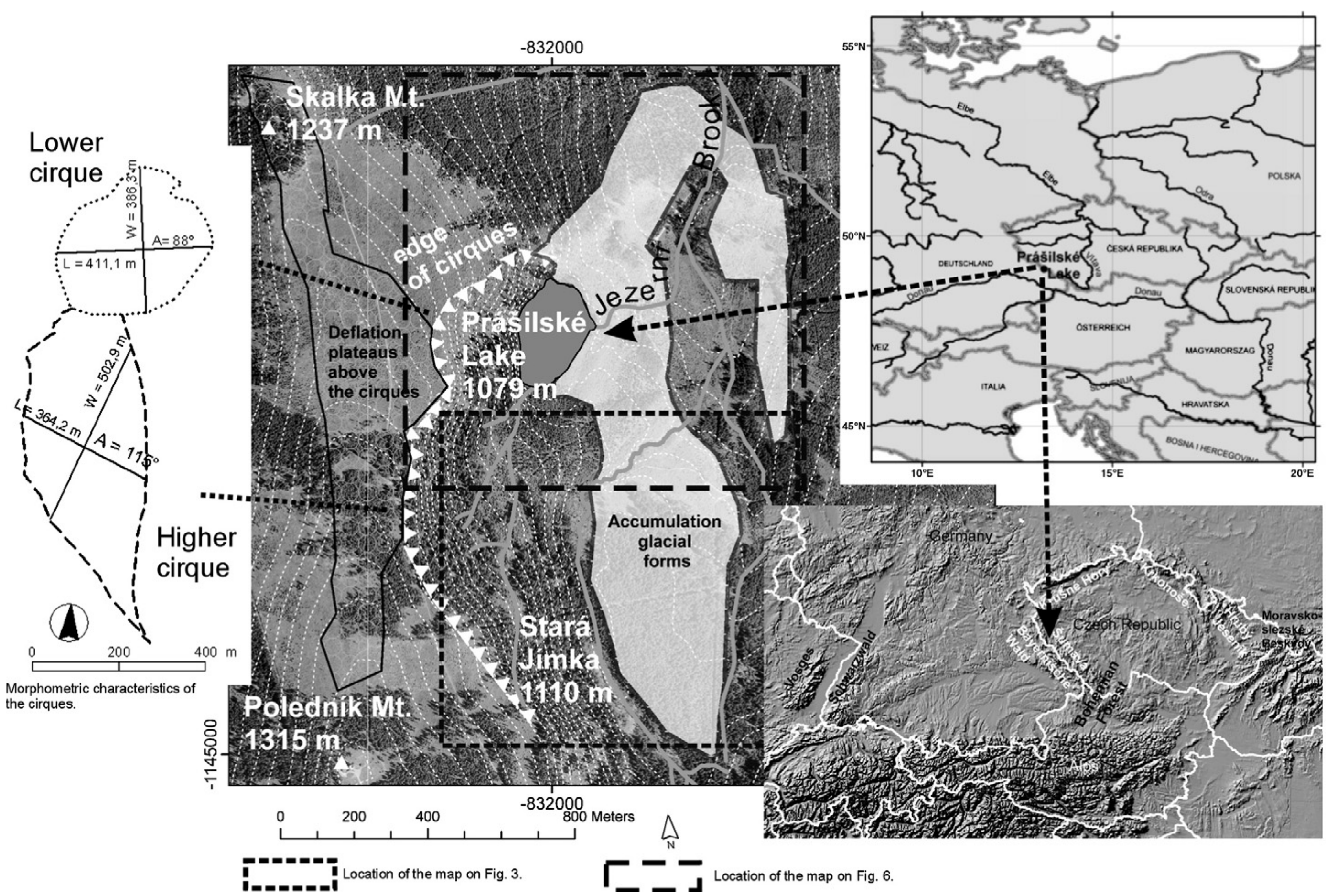

Fig. 1. Location of the area of interest in its European context; morphometric features of the cirque system on the left.

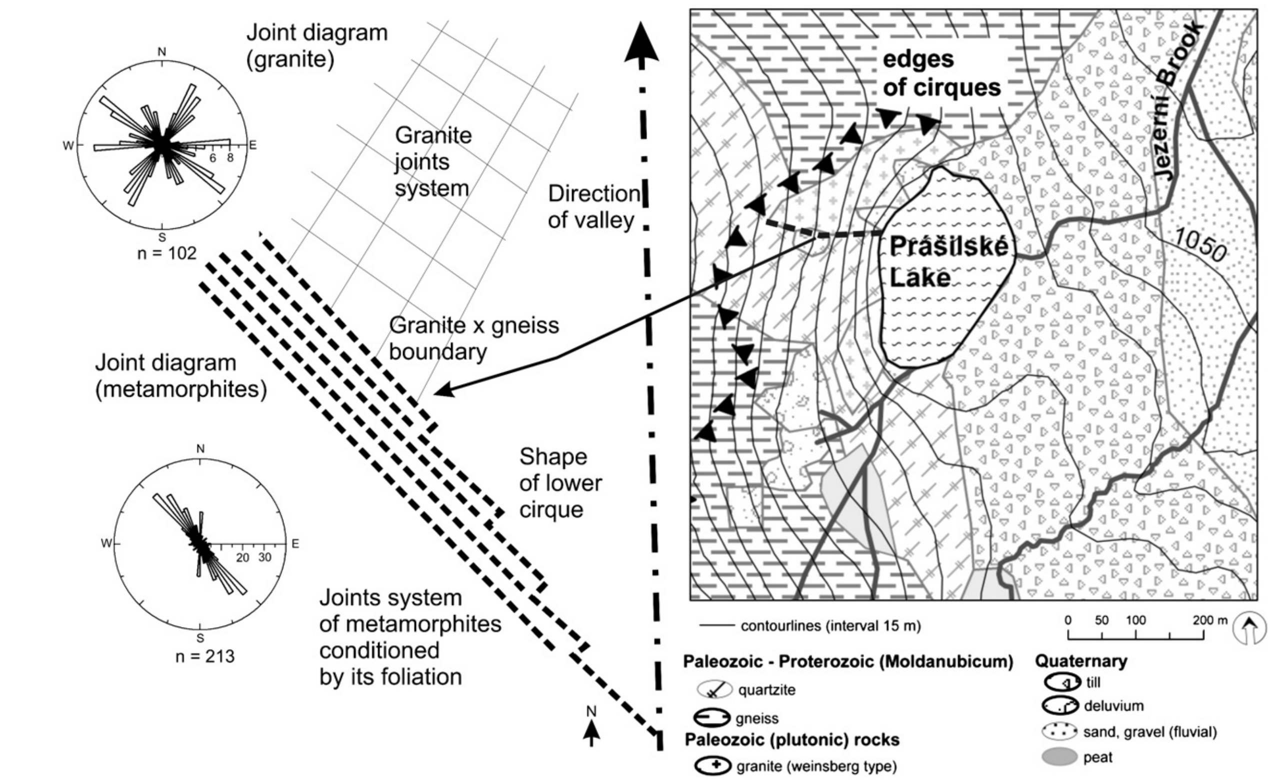

Fig. 2. Geological conditions and their relation with morphology of the lower cirque.

Clast macrofabrics were analyzed with a two-dimensional rose diagram and a three-dimensional contour data diagram. GEOrient 9.2 software (Holcombe, 2005) was used to create the diagrams and for consequent statistical analysis.

Samples for exoscopy observations were wet-sieved (fraction 0.25–0.50 mm) and the calcium carbonates, iron staining, and adhering particles were removed by boiling for 20 min in 10% hydrochloric acid and stannous chloride solution. 30 to 50 grains were then picked randomly, mounted on double-sided graphite adhesive (which is fixed on aluminum specimen stubs), and gold coated for viewing by scanning electronic microscopy (SEM) (Krinsley and Doornkamp, 1973).

Samples were taken within the study area firstly from sites where the genesis of the forms was obvious (debris flows, eluvium, and glacial deposits). They were used as standards for subsequent research and statistically interpreted in histograms (according to Helland et al., 1997; Fuller and Murray, 2002; Mahaney, 2002). Subsequently, the samples with uncertain origin were compared with the standards. This process is necessary for use of SEM in an area where glacial transport distances are short, implying that confusion with grains from different processes (colluvial and fluvial) is likely.

The samples for pollen analysis (sampling interval of 5 cm) were treated by the usual laboratory methods applied for the separation of Quaternary sporomorphs (Erdtman, 1954; Overbeck, 1958; Faegri, 1964). Pollen grains of trees and shrubs, herbs, and spores of ferns and other microfossils were identified and counted in each sample. Identification was based on keys and pollen atlases (Reille, 1992, 1995, 1998) and the Czech Geological Survey's pollen reference collection deposited in Prague. Spores of *Bryophyta* and selected *Fungi* as well as some *Rhizopoda*, *Rotatoria*, *Tardigrada*, etc. were also identified and counted on the pollen slides. Special attention was paid to coccal green algae. The sediments were stratigraphically classified after Firbas (1952). The pollen diagram is presented as a percentage pollen diagram, produced with the PC program POLPAL (Walanus and Nalepka, 1999). Pollen percentage was based on the total sum of AP + NAP = 100% (AP = trees and shrubs, NAP = herbs). The counts of microfossils of other plants and animals were also related to this sum.

Two approaches were used for dating the landforms: relative (position of glacial landforms, Schmidt hammer test, and analysis of roughness of rock surfaces) and absolute (conventional and AMS ^{14}C dating).

It was expected that forms more distant from the source of glaciation would be older (Hubbard and Glasser, 2005). This relative age expectation was tested by measurement of intact rock strength (IRS) with a Schmidt hammer (Mathews and Shakesby, 1984; Goudie, 2006), and by analysis of rock surface roughness (Mentlík, 2006).

Two approaches to use of a Schmidt hammer were employed. First, larger datasets ($n > 60$) were generated using the approach published by Hubbard and Glasser (2005). But the number of measurements was limited by the quantity of appropriate blocks on each form. Thus, a second approach, demanding a smaller number of blocks (Evans et al., 1999), was used simultaneously. The specific R_{max} value was calculated for each landform: methodological details are given in Mentlík (2006). Using both methods allows comparison of two independent views of the relative age of the landforms, and permits dating of landforms with too few suitable boulders for the first method.

Parts of a core taken in Stará Jímka were dated by conventional and AMS radiocarbon dating, in the laboratory of Gliwice Absolute Dating Methods Centre (GADAM), Institute of Physics, Silesian University of Technology, Poland.

Electrical resistivity tomography (ERT), a technique of geophysical sounding, was used for identification of the subsurface structure of glacial landform complexes, as in Otto and Sass (2006). The ERT technique (together with ground-penetrating radar and seismic refraction) seems to be appropriate for determining the depth and internal structure of a form (Schrott and Sass, 2008). The Wenner array, a technique suitable for identification of horizontal structures (Schrott and Sass, 2008), was used preferentially (besides the Wenner–Schlumberger and the Dipol–Dipol arrays).

The parameters of fissure surfaces were measured on 89 outcrops, for determination of structural predisposition of glacial erosional forms.

4. Results

4.1. Connection of geological condition and glacial activity

The following geological features (and their combination) are important factors for development of the step-like cirques (Fig. 2):

(i) fissures of crystalline rock depending on gneissic schistosity with predominant direction NW–SE — determining development of the southern part of the lower cirque and the northern rim of the higher cirque (Fig. 2);
(ii) fissures of granites with predominant directions 120–130° and 20–50°, determining development of the northern part of the lower cirque (Fig. 2); and
(iii) the boundary between crystalline rocks and granites running across the lower cirque, a structural weakness crucial for its development (Fig. 2).

In comparison, the homogenous geological conditions of the gneiss slope above Stará Jímka were unfavourable for development of a glacial cirque, and a linear slope developed there.

4.2. Chronology of glaciation in the Prášilské Lake area

Three main phases of glaciation were distinguished by geomorphological mapping in the Prášilské Lake area (arranged from the oldest and most extensive to the youngest and smallest): the small valley glacier, the combined glacier–rock glacier, and the cirque phase.

4.2.1. The small valley glacier phase

Three types of glacial landforms of this phase were found (I. on Fig. 3): remnants of terminal and lateral frontal moraines, and a block field.

The remnants of the terminal moraine have two spatially connected parts, which are separated by the stream of Jezerní Brook. A 5 m high step created by granite blocks is presented on the left side while a degraded moraine wall exists on the right side (Fig. 3). The step lies partly on the slope and has probably been remodelled by gravitational processes, while the degraded moraine wall occurs on the flat bottom of the valley and is better preserved. However, its level of preservation is significantly poorer than that of the moraines of the younger cirque phase. It is continued southward by a degraded lateral moraine preserving as a step with sporadic erratics. The farthermost position of the terminal moraine shows a maximum glacier length of ~2060 m.

The upper moraine (Fig. 3; photo on the left) is created by granite boulders and blocks (frequently more than 4 m long). These stones are erratics that were transported from the granite parts of the cirque onto the schist bedrock. The form was classified as a remnant of an upper moraine — due to the unrounded shape of the blocks, continuous character of the accumulation and its position behind remnants of the frontal moraine. These geomorphological evidence (remnants of the lateral moraine on the east side of the valley, and the block field of the upper moraine at the rim of the cirque, representing the margin of the glacier) were used to reconstruct the width (~760 m), thickness (~54 m) and surface inclination (~6°) of the former glacier (in the cross profile) (Fig. 4). The inclination of the cross profile can indicate

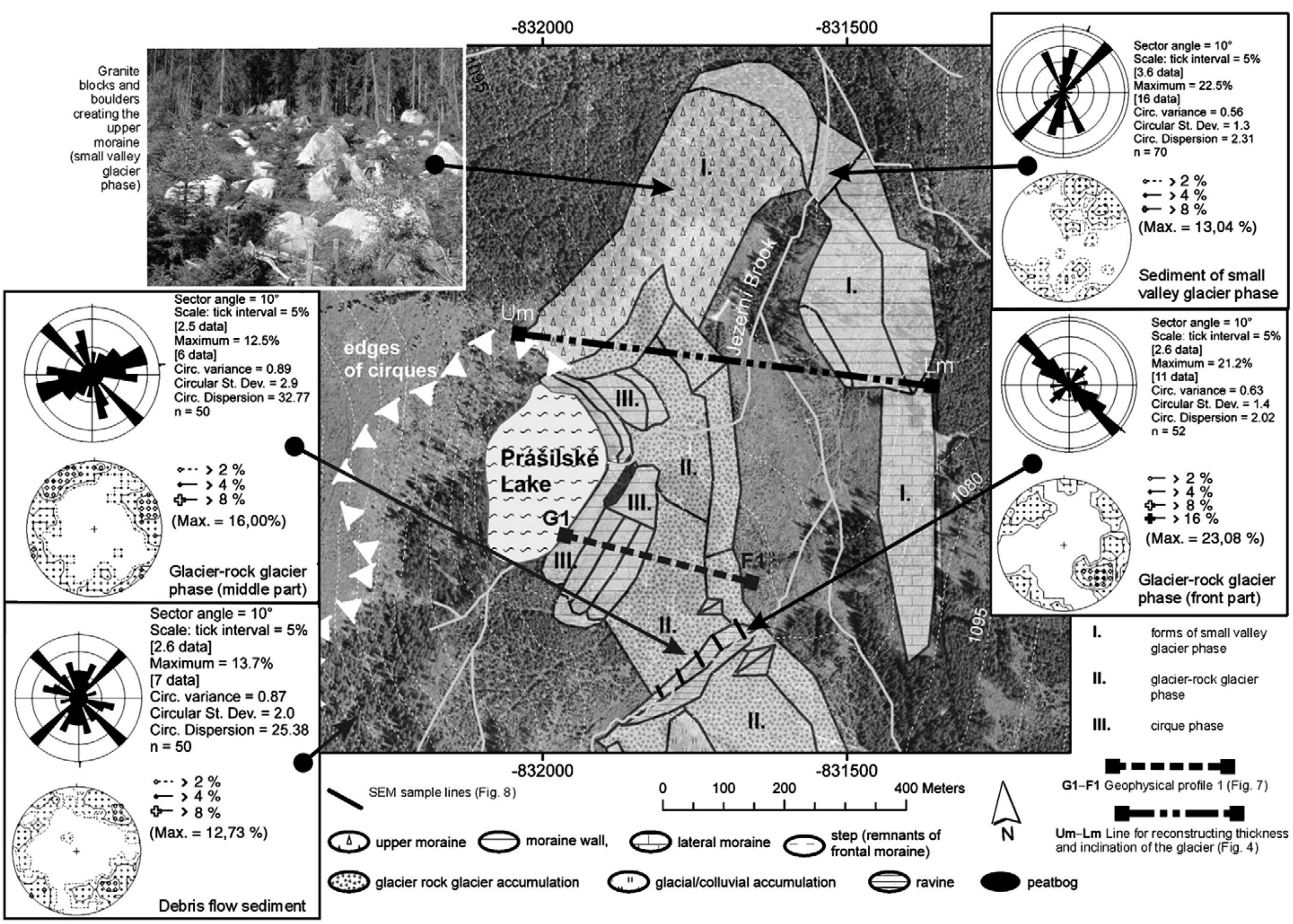

Fig. 3. Landforms and selected documentary materials in the surroundings of Prášilské Lake (location on Fig. 1).

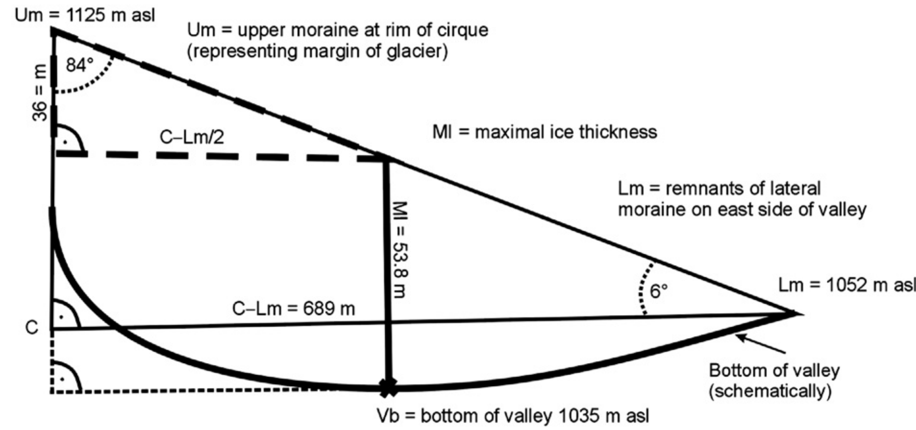

Fig. 4. Reconstruction of thickness and inclination of the former surface of the glacier — small valley glacier phase (location on Fig. 3).

an important source of ice from the cirques area, though the glacier probably filled the whole valley head.

The sediment of this glaciation was classified as a unimodal, extremely poorly sorted, gravelly muddy sand. The hypothesis that the sediments were deposited by a glacier was supported by orientation of macrofabric (22.5% of clasts in one 10°) sector — stronger than in the other sedimentological environments (between 10.7% and 13.7% per sector; apart from 21.2% for the front of the lobe of the glacier–rock glacier; see Fig. 3). Additionally, the main macrofabric directions point to the cirque area (main source of the ice), such that accordance between directions of the main macrofabric and ice flow is evident (Fig. 3).

In comparison with sediments of the other phases, the following facts also support the suggestion of longer glacial transport:

(i) the values of clast shape (C_{40} 36%) and roundness (RA 30%) are lower (Fig. 5); and
(ii) significant striation was found on clasts, but was absent in sediments of the other phases.

SEM could not be used to analyze this phase because of high incrustation on the surfaces of quartz grains. This does, however, support a relatively longer time since deposition.

Due to lack of natural exposures, incorporation of older sediments and landforms into these forms cannot be ruled out, even though the spatial connectivity of the forms suggests development during a single glacial event.

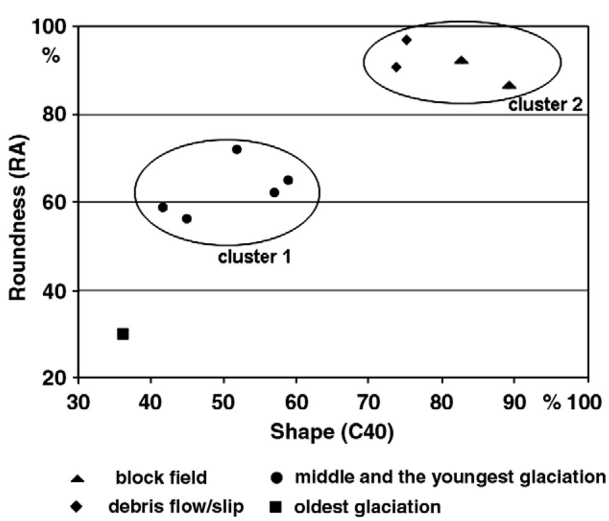

Fig. 5. Results of analysis of clast shapes and roundness from the surroundings of Prášilské and Laka lakes.

4.2.2. The glacier–rock glacier phase

Forms connected with phase II. are morphologically significant and consistent, creating a lobe ~1500 m long: elongate below the steep east-facing slope, 200–300 m wide and ~12 m high (Figs. 3 and 6). The lobe begins in front of the lake, it is superimposed on the southern part of the granite block field and it declines at the end of Stará Jímka, near the valley head (Fig. 6).

According to results of geophysical investigation the morphology and internal structure of the lobe are similar in front of the cirques and in Stará Jímka (Fig. 7). The form is distinctively delimited at the bottom (the sediment thickness is about 20 m, decreasing away from the cirques and the steep slope above Stará Jímka) (Fig. 7). The lobe and the moraine walls (that in front of Stará Jímka and the outer moraine wall of the lower cirque) create unity suggesting compression of previously created sediments of the lobe by later glacial advance (Fig. 7; Geophysical profiles 1 and 3).

The lobe is cut by a stream ravine (~12 m deep and ~280 m long) running from Stará Jímka (Fig. 3, and photo on the right of Fig. 6), creating a useful exposure of sediments on its left bank. Three hypotheses for the origin of this lobe-shaped form, from the results of geomorphological analysis, were tested by sedimentological methods:

(i) repeated spreading of glaciers creating a "continuum" of frontal moraines, suggesting predominantly glacial origin;
(ii) occurrence of a "periglacial rock glacier" (also known as talus-derived or protalus rock glacier: Benn and Evans, 1998), suggesting a predominantly colluvial origin; and
(iii) activity of a glacier–rock glacier combination (Johnson, 1980; Whalley and Martin, 1992; Benn and Evans, 1998), suggesting a mixture of colluvial and glacial sediments.

Two samples were taken for analysis of particle morphology and clast macrofabrics from the very front part and the middle part (30 m from the head of the ravine) of the lobe. Both samples were taken 5 m above the bottom (Fig. 6). The sediment characteristics can be described as trimodal (middle gravel 29.5%, fine sand 9.3% and clay 20.9%) very poorly sorted muddy sandy gravel, and bimodal (31.5% medium gravel and 9.2% clay) extremely poorly sorted gravelly muddy sand.

Greater orientation of macrofabrics in the front part of the lobe (23% in one sector, standard deviation 1.3 and circular dispersion 2.02) indicates glacial origin of the sediment (these characteristics were similar to the sample from the small valley glacier phase) (Fig. 3). Significantly lower roundness (RA 64.7%) and different shapes

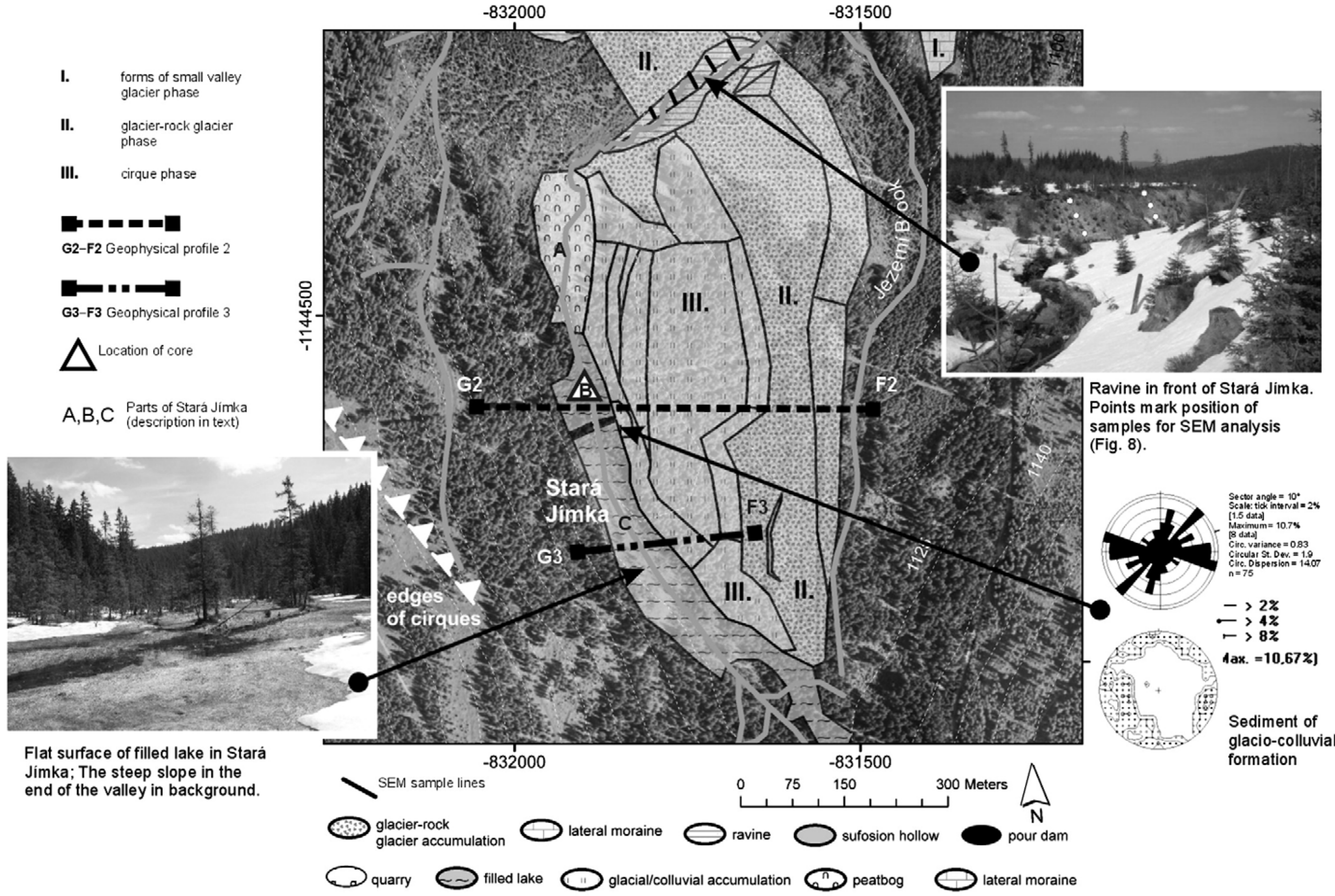

Fig. 6. Landforms and selected documentary materials in the surroundings of Stará Jímka (location on Fig. 1).

(C_{40} 59%) suggest shorter transport than in sediment of the small valley glacier phase (Fig. 5).

The orientation of macrofabrics from the second sample was lower (12.2% in one sector, standard deviation 1.4 and circular dispersion 32.77) while the roundness and shape of clasts were similar (RA 56% and C_{40} 45%) (Fig. 5). This is consistent with different origins for the front part (glacial) and the middle part (colluvial).

To collect further evidence for the origin of the lobe, the left bank of the ravine was sampled in a 3 by 5 grid. Micromorphological structures on the quartz grain surfaces were observed by SEM, and probable origin at a particular place was postulated (Fig. 8). The set of features typical for glacial transport were remarkably well-developed in all samples at the very front part of the lobe — e.g. small (78%) and large (56%) conchoidal fracture, straight (67%) and arcuate (67%) steps, and edge abrasion (61%). Characteristics suggesting longer weathering were not significant (e.g., chemical V-shaped pits 0%, limited silica precipitation 17%, and extensive silica precipitation 5%) (Fig. 8).

Samples from the middle and end parts of the lobe, however, suggest colluvial and/or glacial sediment transported for a short distance (Fig. 8). Mechanical features typical of glacial transport were relatively limited — e.g. small (8%) and large (8%) conchoidal fractures, straight (28%) and arcuate (16%) steps, and edge abrasion (20%) were found on few grains. Nevertheless, features suggesting longer weathering without remodelling by glacial transport (typical for eluvium or sediment from short — 100–200 m — debris flows) were found — e.g. chemical V-shaped pits (13%), limited (28%) and extensive (52%) silica precipitation. Grains with combinations of these features were classified as glacial sediment transported for a short distance.

These results accord with the third postulated hypothesis, suggesting a glacier–rock glacier origin for the lobe and eliminating wholly gravitational or wholly glacial origins.

4.2.3. The cirque phase

Two further accumulation forms developed when the glacier of phase III. occurred in the cirques, and remnants of a glacier survived shaded by the slope in the Stará Jímka area:

(i) two end moraines in front of Prášilské Lake (Fig. 3). The outer moraine, terminal for this phase, is up to 12 m high. It is southeast of the lake and has an asymmetrical position in relation to the lower cirque (Fig. 3). Thus, development by activity of a step-like cirque system is suggested for three reasons: asymmetrical position of the outer moraine wall towards the lower cirque suggests mass coming from the upper cirque; there are no morphologically significant moraines in front of the higher cirque; and on current relief (from DEM analysis) all mass flows from the bottom of the upper cirque into the lower.

The shape of the inner (recessional) moraine (damming the current lake) accords with the sill of the lower cirque. We infer that this moraine developed when the quantity of snow deflated from the plateau decreased, and the activity of the (step-like) cirque glacier system terminated (glacial activity was restricted to the lower cirque).

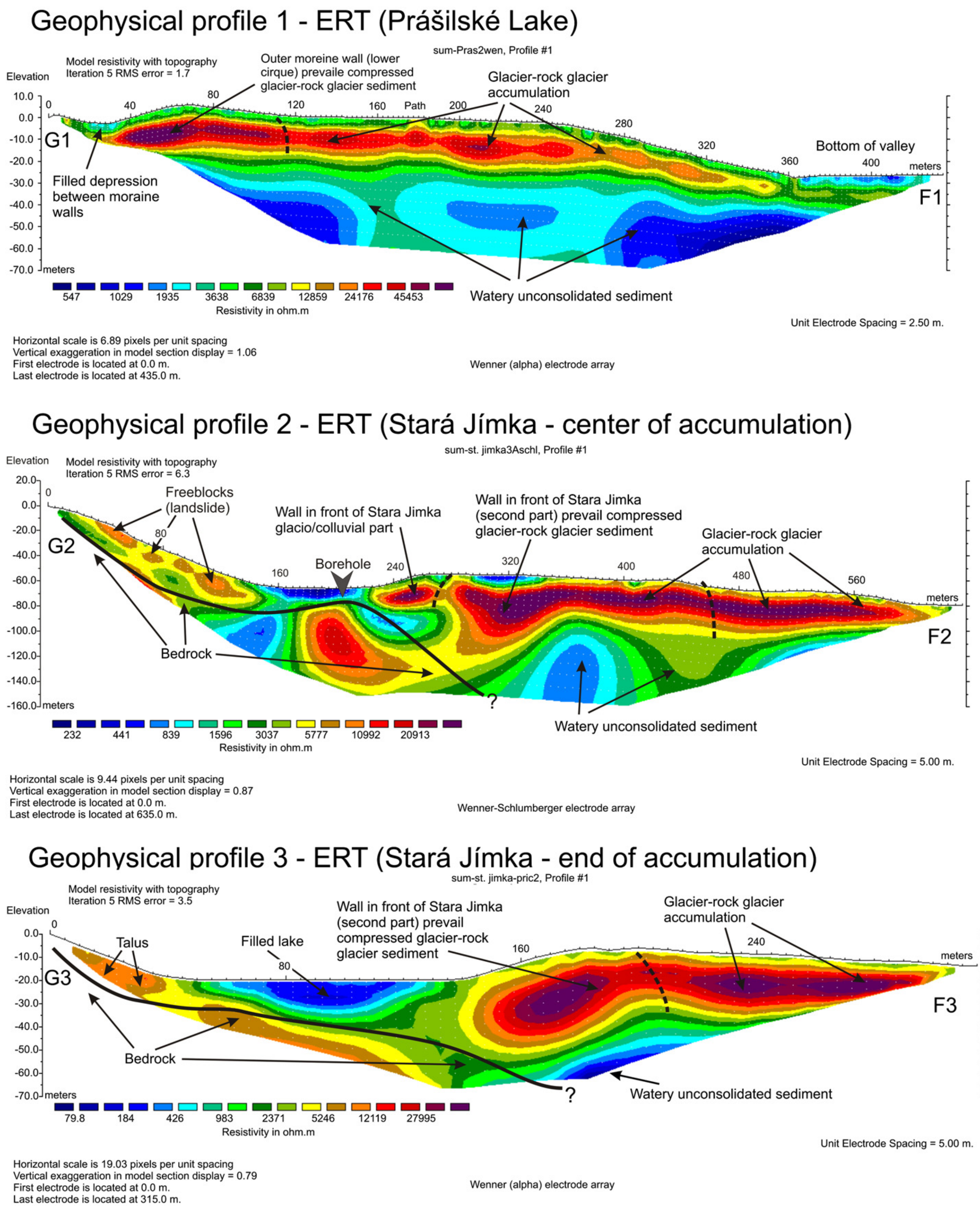

Fig. 7. Geophysical (ERT) profiles in the surroundings of Prášilské Lake (location on Fig. 3) and Stará Jímka (location on Fig. 6).

Mechanical features	Small conchoidal fracture	6
	Large conchoidal fracture	7
	Straight steps	8
	Arcuate steps	9
	Imbricated blocks	10
	Large breakage blocks	11
	Fractured plates	12
	Striations	13
	Edge abrasion	14
	Mechanical Vshaped pits	15
	Straight grooves	16
	Curved grooves	17
	Meandering ridges	18
	Irregular depression	19
	Uptumed plates	20

Morphological features	Angular outline	1
	Rounded outline	2
	Low relief	3
	Medium relief	4
	High relief	5

Chemical features	Solution pits	21
	Chemical Vshaped pits	22
	Adhering particles	23
	Limited silica precipitation	24
	Extensive silica precipitation	25
	Euhedral crystal overgrowths	26

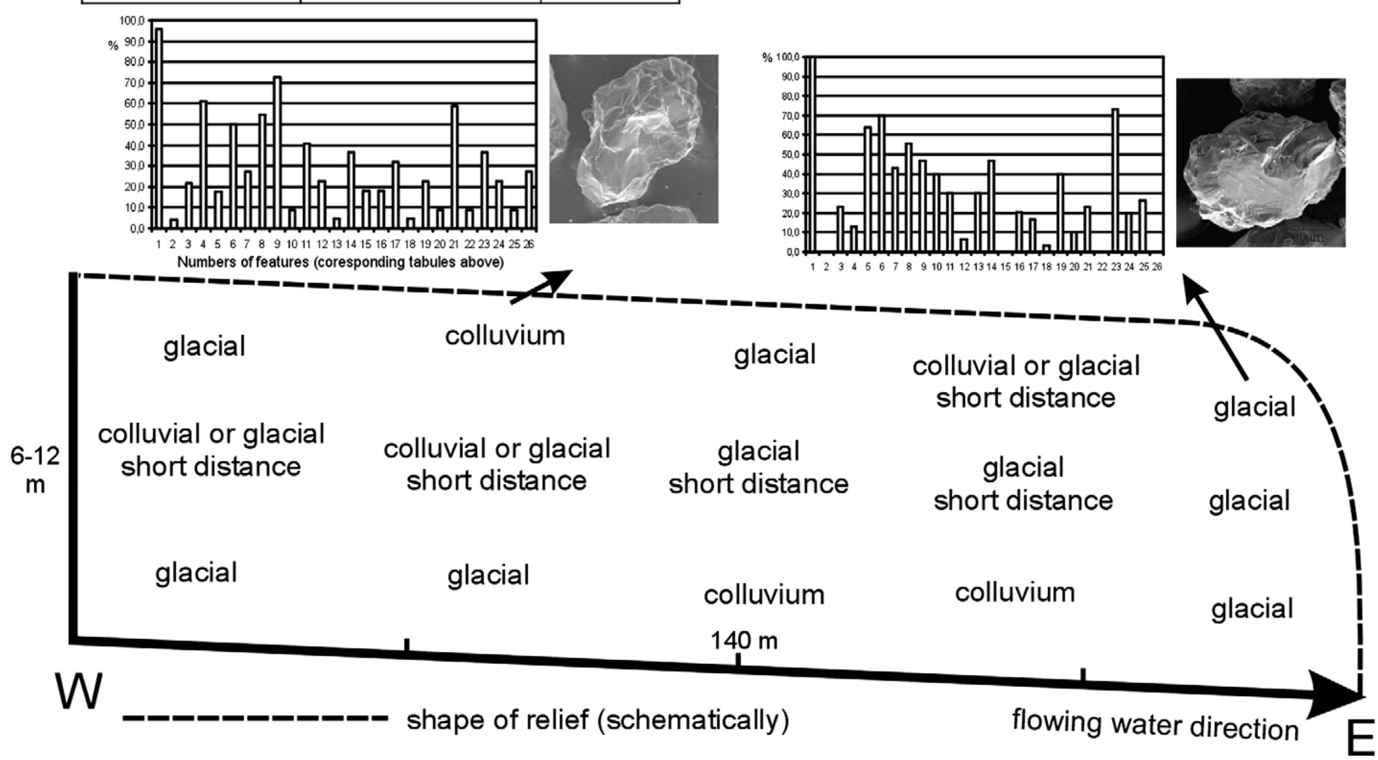

Fig. 8. Results of SEM analysis of the lobe-shaped (glacier–rock glacier) form (location and photo on Fig. 6); the range of microstructures commonly observed on studied material (according to Bull, 1978; Helland et al., 1997; Fuller and Murray, 2002).

(ii) 770 m long wall lying below the linear part of the slope in front of Stará Jímka (Fig. 6).

The wall narrows from north (~220 m) to south (~160 m wide). All of the proximal side has a similar inclination (~20°) but the distal slope is gentle in the north (~11°) and steeper in the south (~19°) (Fig. 7; Geophysical profiles 2 and 3).

From the geophysical results, the original lobe of glacier–rock glacier sediment was compressed by a later glacier forming the walls (Fig. 7; Geophysical profiles 2 and 3). This oscillation probably corresponded with the lower cirque wall development (I. — earlier oscillation). Consequently, remnant ice prevailed in the central part of Stará Jímka and material coming from the slope accumulated in front of this ice created a partly separated wall (this wall is not significant morphologically now because of a peatbog flattening the relief — Fig. 7; Geophysical profile 2).

The sediment of this accumulation was classified as polymodal (medium gravel 14.2%, 9.5% fine sand, 10% very fine sand and 16.7% clay) extremely poorly sorted, muddy sandy gravel. No particular orientation of clasts was found (10.7% in a sector, standard deviation 1.9, and circular dispersion 15.67) (Fig. 6). Roundness (RA 81%) and shape (C_{40} 46.9%) indicate a very short transport. These characteristics are similar to those of glacio-colluvial sediments from the middle part of the glacier rock–glacier phase lobe (Fig. 5). SEM analysis, however, points to glacial modification of the sediment (significant glacial features include small 76% and large 30% conchoidal fractures, straight 58% and arcuate 37% steps, and edge abrasion 57%).

Very low sorting, orientation and shaping of the clasts combined with the glacial features on the surface of the quartz grains imply a combination of glacial and colluvial processes.

Stará Jímka is divided into three main parts (Fig. 6):

(A) shallow (max. 1 m deep) frontal part in the north;
(B) ~5 m deep part where a core was taken (Fig. 9), showing no significant human influence; and
(C) ≤5 m deep artificially dammed part — a reservoir (used for floating logs) — the sediments were possibly removed during clearing of the reservoir.

The boundary between parts A and B is created by a natural dam (~70 m wide and ~50 m long). This is complemented by a

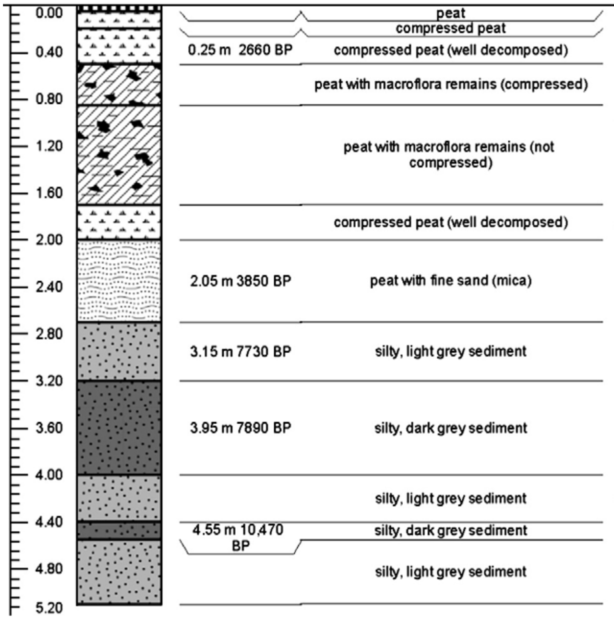

Results of numerical (conventional and AMS ^{14}C) dating of th core.

Laboratory number	Method	Material	Depth (m)	^{14}C age (BP)	Range of Calendar Age (BCE)
Gd-30097	Conven.	Peat, organic fragments	0.2–0.3	2660±250	1050–350; 1400–100
Gd-15745	AMS	Peat	2.00–2.10	3850±170	2600–2000; 2900–1850
GdA-520	AMS	Peat	3.10–3.20	7730±90	8590–8420; 8770–8360
GdA-514	AMS	Peat	3.94–4.00	7890±90	8980–8590; 9050–8450
GdA-516	AMS	Bulk	4.50–4.60	10470±120	12650–12170; 12800–12000

The samples were dated in the laboratory of Gliwice Absolute Dating Methods Centre (GADAM), Institute of Physics, Silesian University of Technology, Poland.

Fig. 9. Core profile and results of radiocarbon dating — the filled lake in Stará Jímka (location on Figs. 6 and 7 — Geophysical profile 2).

semicircular scarp on the adjacent east-facing slope, which probably presents a root area of slope deformation. According to radiocarbon dating and pollen analysis, the depression was dammed directly after deglaciation and before 14 cal. ka BP (Figs. 9 and 10; Table 1).

The former existence of a lake is confirmed by the presence of aquatic organisms (*Isoëtes* and algae) in the core (Fig. 10), and of Late Glacial lake sediment in both the core (Fig. 9) and ERT sounding (Fig. 7).

4.3. Relative dating of landforms

The proposal of three phases of glaciation was supported by the Schmidt hammer results (Fig. 11). This test was applied north of Prášilské Lake, where boulders of granite cover all glacial landforms. Relative dating confirmed the graded sequence of the phases — the older (small valley glacier phase) was the most extensive, while the youngest was connected with the cirques or with the east-facing linear slope (Fig. 11). Within each mapped landform the weathering of boulders was similar: Coefficients of Variation (Fig. 11) were <15%. However, there are two exceptions. Higher coefficients were found firstly in deposits of the oldest glaciation, and secondly on boulders covering the headwall (Fig. 3). Weathering over a long time period possibly caused differences between boulders of the oldest phase (the weathering probably exceeded the range of sensitivity of the Schmidt hammer test). Conversely, variation between relatively older and younger boulders on the headwall suggests continuous activity of rock falling during the Holocene.

5. Interpretation and discussion

Three phases of glaciation (Table 1) were reconstructed in the surroundings of Prášilské Lake and Stará Jímka. The remnants of the most extensive glaciation suggest the former existence of a small valley glacier filling the head of the valley. The distribution of geomorphological forms and the surface inclination of the reconstructed glacier confirm a connection between the glacier, the steep east-facing slope and the deflation plateau (Steffanová and Mentlík, 2007). The approximate altitude of deflation plateaus in the Šumava Mountains was ~1200–1300 m asl (the average altitude of the highest points of the headwalls of six Šumava glacial cirques was 1285 m). Snow was deflated from the plateau, accumulated to leeward, and further transported by snow avalanches. Such connection between the plateau and the cirques implies predominant westerly winds when the glaciers developed, and supports the conclusions of Renssen et al. (2007) that west or northwest winds were dominant in Central Europe during the Weischselian Late Pleniglacial.

We suggest that glacier development followed the build-up of a snow cap on the plateau ~1300 m asl, providing a source for enhanced snow deflation as described by Nesje and Dahl (1992) for western Norway.

If we compare the calculated size of former glaciers from the surroundings of Prášilské Lake and Kleiner Arbersee (Raab and Völkel, 2003) (Table 2), length, and width are similar but the thickness of the Prášilské Lake glacier was only half of that at Kleiner Arbersee. This is probably due to the lower altitude of deflation plateaus on adjacent ridges (less than 100 m) and also the lower relative height of the headwall in the Prášilské Lake area (Table 2).

Conversely, longer former glaciers (up to 7 km) were suggested by Hauner (1980) for the eastern part of the Bavarian Forest (Rachel–Lusen area) with valleys heading south. More favourable conditions for glaciers there might come from the larger and higher (more than 1300 m) deflation plateaus. However, this difference remains as an issue for future research.

The second glacier–rock glacier phase (Table 1) is represented by the elongated lobe-shaped form below the steep slope facing east. The glacial front part and the colluvio-glacial body support the hypothesis of glacier–rock glacier origin. The development of glacier–rock glaciers has been described also from other mountain areas (Whalley and Martin, 1992). For the Prášilské Lake area, the development can be summarized as follows:

(i) after retreat of the small valley glacier, remnants of glacier ice were preserved in the shadow of the steep slope facing east;
(ii) debris from the slope fell on the glacier remnants and the weight of this sediment reactivated glacier flow; while the front part was moving, producing glacial features in the frontal deposit, debris was falling on the rest of the form leading to the colluvio-glacial features which predominate in the middle part; and
(iii) flow velocity reduced and finally stopped due to thinning and ablation of the ice.

This concept suggests a direct connection between first two phases, as remnants of the reduced glacier provided a basis for the glacier rock–glacier phase.

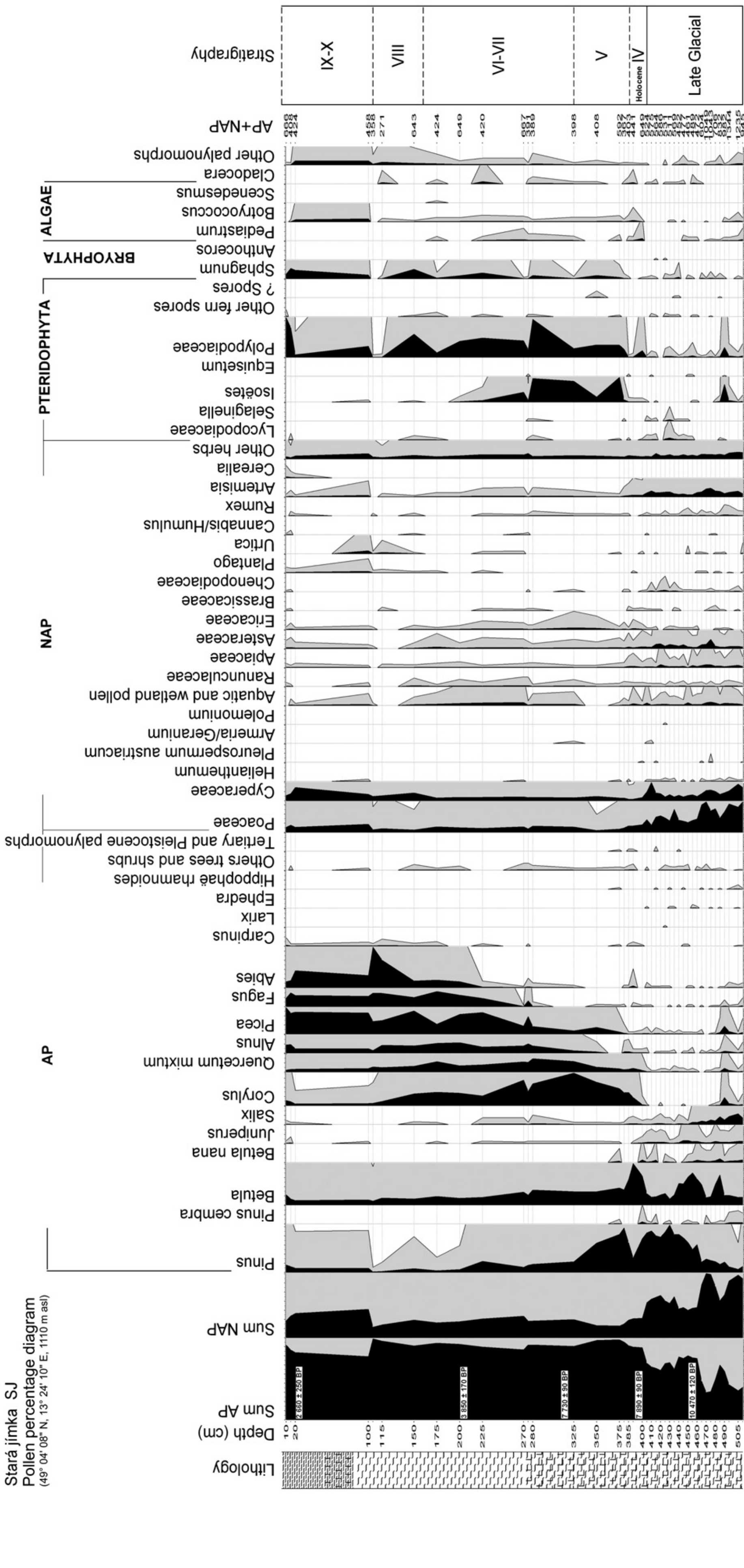

Fig. 10. Results of pollen analysis of the filled lake in Stará Jímka (location on Figs. 6 and 7 — Geophysical profile 2).

Table 1
Summary of landscape development in the surroundings of Prášilské Lake.

Phase of landscape development	Prášilské Lake area (cal. ^{14}C BP)	Type of glacial activity in the Prášilské Lake area	The Alps (Preusser, 2004; Ivy-Osch et al., 2008) (cal. ^{14}C BP)			North Atlantic region (Björk et al., 1998)	
Small valley glacier phase	?	Specific valley glacier (connected with the steep and high east-facing slope and deflation plateaus)		LGM	before 18–19 ka	GS-2c	21 000–18 500
Glacier–rock glacier phase	?	Glacier–rock glacier activity connected with the steep east-facing slope	Oldest Dryas	Phase of early Late Glacial ice decay	18–17 ka	GS-2b	18 500–16 500
Cirque phase	Before 14 ka	Step-like cirque system activity; Glacier in Stará Jímka		Gschnitz	16–17 ka	GS-2a	16 500–15 000
		Cirque glacier (glacier activity only in the lower cirque); remnants of ice in Stará Jímka		Clavadel or Daun	Before 14.7 ka		
Paraglacial phase *sensu stricto*	~14 ka	Unloading of slope: slope movements damming the lake in Stará Jímka	Bølling/Allerød	–	12.9–14.7 ka	GI-1	15 000–13 000
Periglacial processes	~ 14–10 ka	Shrubs —higher activity of rock falling, gelifluctin	Younger Dryas	Egesen	> 12.9 ka	GS1	13 000–11 500
Recent geomorphological processes	~10 ka–present	Occurrence of forest (*Fagus*, *Picea*, and *Abies*) and recent geomorphological conditions (fluvial activity, rockfall etc.)			Holocene		

These Bohemian Forest landforms have generally been interpreted as glacial rather than periglacial (Kunský, 1933; Raab and Völkel, 2003; Vočadlová and Křížek, 2005). Absence of rock glaciers and related forms in the Bohemian Forest and in the whole Czech Massif seems to be very unlikely — rock glacier sediments were observed only in the Krušné Hory Mountains (Růžičková et al., 2001) and the Hrubý Jeseník (Czudek, 1997). This is unexpected, in comparison with other European regions (Harrison et al., 2008).

The final cirque phase (Table 1) was probably connected with a cooler and/or wetter climate and/or strong wind activity favouring snow accumulation in the cirques. Both cirques and Stará Jímka contained ice at the start of this phase, but finally glaciation was limited to the lower cirque.

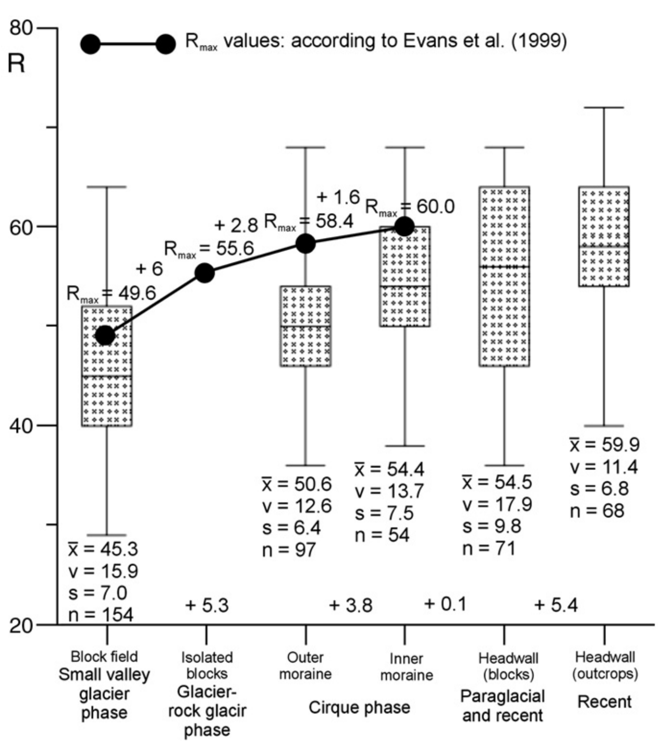

Fig. 11. Results of Schmidt hammer test in the surroundings of Prášilské Lake (v = Coefficient of Variation; s = standard deviation).

According to the radiocarbon dating and pollen analysis (Figs. 9 and 10), the development of geomorphological conditions in the Late Glacial and Holocene may be summarized as follows:

(i) the end of glaciation before ~14 cal. ka BP: the area was ice free before the Younger Dryas. This accords with the conclusions of Raab and Völkel (2003) from the surroundings of Kleiner Arbersee and of Pražáková et al. (2006) from Plešné Lake: the deglaciation of that area is dated at 14.6 cal. ka BP. But the lack of glacial activity in the Younger Dryas distinguishes the Bohemian Forest from some other middle-mountain areas in Central Europe — the Vosges (Mercier and Jeser, 2004) and the Krkonoše Mountains (Mercier et al., 2000; Bourlès et al., 2004);

(ii) instability of slopes connected with higher activity of mass movements occurred in a paraglacial phase after deglaciation. A landslide occurred around 14 cal. ka BP and a lake (~ 3 m deep) was dammed in Stará Jímka;

(iii) cold conditions, documented by aquatic psychrophile algae (*Pediastrum boryanum* var. *longicorne* and *P. integrum*), persist in the profile until ~ 10 cal. ka BP (Fig. 10) — implying periglacial conditions in the shaded areas of the headwall and the cirques. Higher activity of slope mass movements (rockfall and sliding) predominated until development of forest around 10 cal. ka BP stabilized the slopes. This event was connected with lower abundance of *Betula nana*, *Juniperus*, and *Salix* (probably shrubs growing around the lake) (Jankovská, 2006) and *Helianthemum* (growing on the free rock surfaces of the headwalls). Conditions in the Bohemian Forest were significantly milder than in the Krkonoše (Mercier et al., 2000; Bourlès et al., 2004) and even Vosges where permanent ice cover seems to have disappeared around 6 ka (Mercier and Jeser, 2004, p. 117).

(iv) The lake was infilled ~4 cal. ka BP, when aquatic organisms (e.g., *Isoëtes* and various aquatic algae) disappeared (Fig. 10).

Comparison of our results with the conclusions of other work on the glaciation of the Bohemian Forest is problematic because authors have used different methods for evaluating the numbers of glacial readvances (Table 3). Some authors described the quantity of moraines (e.g. the four moraine walls of Raab and Völkel (2003)), while others tried to reconstruct phases of glaciation. Authors using the second approach included moraine walls and other (e.g., step-like) landforms. We prefer this second approach, considering both the

Table 2
Comparison of opinions about former glaciers in areas of selected glacial lakes in the Bohemian Forest.

Area	Maximal length	Maximal. width	Maximal thickness	Lower extension of glacier	Authors	Altitude of adjacent deflation plateau	Highest point in the cirque surroundings
Surroundings of Kleiner Arbersee	2600 m	800 m	115 m	830–880 m asl	Raab and Völkel (2003)	~1300 m	1456 m asl
Surroundings of Prášilské Lake	2060 m	760 m	51 m	1025	This work	~1200 m	1315 m asl

number and the character of glacial landforms in reconstructing the glacial history of the area. According to our results (Table 3), between two and four glacial phases (stadials) occurred in the Bohemian Forest during the last cold period (Würm/Weichselian).

Data on glaciation of the Bohemian Forest can provide connections between European stratigraphical systems in longitudinal directions, with northern Europe and the Alps (Table 1), in terms of:

(i) at least two periods of glacial activity (cold), with the older period being more extensive;
(ii) in a more temperate period between these two the glacier retreated and the glacier–rock glacier developed;
(iii) 32.4 ± 9.4 ka BP (IRSL age) is a maximum age for glaciation in the Bavarian Forest (Raab and Völkel, 2003). This supports the idea that the most extensive Weichselian glaciation probably occurred in MIS 2, as in the Alps (between 21–24 ka BP: Preusser, 2004) and the Vosges (Mercier and Jeser, 2004); and
(iv) glaciation in the Bohemian Forest finished before the Bølling/Allerød and occurred in conditions colder and/or more humid than in the Younger Dryas, when the cirques were ice free (Raab and Völkel, 2003; Pražáková et al., 2006).

We also compared our results and the data from the Alps (Preusser, 2004 and Ivy-Osch et al., 2008) and northern Europe (Björk et al., 1998) (Table 1). The small valley glacier phase can be correlated with the Last Glacial Maximum in the Alps (before 18–19 ka), MIS 2 and stage GS2a in northern Europe. The glacier–rock glacier phase can be correlated with Late Glacial decay in the Alps (17–18 ka BP) and stage GS2b in north Europe (Table 1). Two colder glacial oscillations occurred in the Prášilské Lake area (documented by two moraine walls in the cirque) between the LGM and Bølling/Allerød (stage G1-1 in the north Europe). The first one might correspond with the Gschnitz cold phase in the Alps (16–17 ka BP) (Preusser, 2004) and the second one with Clavadel or Daun phases (dated before 14.7 ka in the Alps). This cold period was not significantly distinct in northern Europe (Björk et al., 1998). Thus we suppose that the glacial chronology of the Šumava Mountains relates to climatic conditions similar to glaciations in the Alps (which are closer than southern Norway).

In a latitudinal direction, it is possible to distinguish a significant eastward decrease in intensity of glaciation in European Hercynian massifs during the last cold period. Valley glaciers (more than 40 km long on the western side and 15 km on the eastern side) occurred in the Vosges (Mercier and Jeser, 2004), a small ice cap in the Schwarzwald, and repeated glaciations despite relatively low altitude (Brocken 1142 m asl) in the Harz (Fiebig et al., 2004). In contrast, cirque glaciers and small valley glaciers (lengths up to 3 km) existed in the Šumava, connected with ridges with altitudes ~1200–1300 m. Finally, small cirque-shaped forms (Malá and Velká Kotlina valleys) existed below ridges with altitudes ~1400 m in the Hrubý Jeseník (Czudek, 1997, 2005) farther east. The difference between sizes of glaciers in the Czech part of the Bohemian Forest (valleys facing north) and in the German part (valleys facing south), where Hauner (1980) described valley glaciers with lengths up to 7 km, remains as a question for future research.

A glacial origin has also been proposed for the cirque-shaped form below Klínovec Mountain. (1244 m asl, in the Krušné Hory Mountains), however Král (1968) argued that it is a remnant of a large rockfall. Similarly, the extensive moraine system described by Pelíšek (1953) below Smrk Mountain (1276 m asl) in the Moravskoslezské Beskydy is more likely a remnant of extensive debris flow activity in the Late Pleistocene and Holocene (Pánek et al., 2009). As glaciers required summit altitudes of ~1200–1300 m asl in the Bohemian Forest, it is probable that lower mountains such as the Krušné Hory did not have sufficient altitude for development of glaciers, whereas drier conditions associated with greater continentality in the eastern Czech mountain ranges (the Moravskoslezské Beskydy) were insufficient for development of glaciers.

Glacial forms in the Bohemian Forest have been investigated by geophysical methods for the first time. As well as the ~20 m thick layer of sediment connected with the glacial landforms, a thick layer (more than 70 m) of unconsolidated sediment was found by the ERT method. The slope above Stará Jímka, and the headwall of the lower cirque, fall very steeply below this material. We hypothesize that the valley is filled by sediment, which may be connected with older glaciations, and we are able to see only the upper parts of the erosional forms at present: further work on these sediments is required.

Table 3
Comparison of ideas on glacial sequences in surroundings of selected glacial lakes in the Bohemian Forest.

Area	Character of glaciation, morphology, and age	Authors
North cirque of Grosse Rachel	4 moraine walls; Würm	Pfaffl (1998)
Grosse Arbersee	4 moraine walls; Würm	Pfaffl (1998)
Kleiner Arbersee	4 moraine walls; Würm	Raab and Völkel (2003)
Plešné Lake	Basal accumulation (probably cryogenic), frontal and passive moraine; 2 phases	Votýpka (1979)
Černé Lake	At least 3 generations of moraine walls	Vočadlová and Křížek (2005)
Prášilské Lake	3 phases of glaciations	This work
Laka Lake	3 moraine walls (2 phases of glaciations)	Mentlík (2005)

6. Conclusions

(i) The development of erosional glacial forms in the Prášilské Lake area is significantly influenced by a combination of geological conditions (fissures of granites, foliation of crystalline schists, and bedrock boundaries);
(ii) geomorphological methods show the presence of small valley glaciers (up to ~2 km long) in the Czech part of the Bohemian Forest at the LGM, followed by cirque glaciers in two stadials possibly correlated with the Gschnitz and Clavadel or Daun cold phases in the Alps. The exact timing, however, must be established by absolute dating. Our results suggest close climatic relations of the Bohemian Forest with the Alps rather than with northern Europe;
(iii) the termination of glaciation before the Younger Dryas in the Bohemian Forest contrasts with that in the Vosges and Krkonoše Mountains;
(iv) in comparison with other previously glaciated areas in central Europe a significant differentiation of glacial landforms was found in the surroundings of Prášilské Lake. Apart from moraine walls, the presence of a glacier–rock glacier combination and of glacio-colluvial formations was determined. Such forms may have been omitted or misinterpreted in similar areas in the Bohemian Forest and Czech Massif;

(v) a shallow (~3 m deep) lake existed in Stará Jímka from 14 to 4 cal. ka BP. The lake was dammed by slope movements in a paraglacial phase after deglaciation;
(vi) comparison with results from the other middle-mountain areas in the Czech Massif suggests dependence of glaciation on altitude (~1200–1300 m) and confirms the eastward decline of humidity and thus of glaciation; and
(vii) although the thickness of glacial sediments belonging to the last glaciation had been identified as ~20 m, preliminary geophysical results suggest an infill more than 70 m thick at the head of the valley, connected with glacial activity. If confirmed, that would indicate much longer and more complicated development of the landscape in the Quaternary than has previously been established from surface evidence.

Acknowledgements

The research was supported by the following grants: grants of the Czech Academy of Science, KJB300460501 and KJB300460803; the integrated project (AV0Z30130516—Earth System) of the Geological Institute Czech Academy of Sciences; grant of Slovak Research and Development Agency No. ESF-EC-0006-07; and grant (research program) MZP000257801 (Ministry of Environment, Czech Republic). Finally, we are very thankful to Dr. Ian S. Evans of Durham University for his critical reading and useful suggestions that helped improve this paper. We also thank to Richard A. Marston and three anonymous reviewers for valuable comments on the manuscript.

References

Bayberg, F., 1886. Geographisch-geologische Studien aus dem Böhmerwalde. Die Spuren alter Gletscher, die Seen und Thäler des Böhmerwaldes. Petermanns Geographische Mitteilungen, Ergänzungsheft 81.
Benn, D.I., Ballantyne, C.K., 1994. Reconstructing the transport history of glacigenic sediments: a new approach based on the covariance of clast form indices. Sedimentary Geology 91, 215–227.
Benn, D.I., Evans, D.J.A., 1998. Glaciers and Glaciation. Arnold, London.
Björk, S., Walker, M.J.C., Cwynar, L.C., Johnsen, S., Knudsen, K.-L., Lowe, J.J., Wohlfarth, B., INTIMATE Members, 1998. An event stratigraphy for the Last Termination in the North Atlantic region based on the Greenland ice-core record: a proposal by the INTIMATE group. Journal of Quaternary Science 13 (4), 283–292.
Blott, J.S., Pye, K., 2001. Gradistat: a grain size distribution and statistics package for the analysis of unconsolidated sediments. Earth Surface Processes and Landforms 25, 1473–1477.
Bourlès, D.L., Braucher, R., Engel, Z., Kalvoda, J., Mercier, J.L., 2004. Deglaciation of the Giant Mountains indicated by ^{10}Be dating. In: Drbohlav, D., Kalvoda, J., Voženílek, V. (Eds.), Czech Geography at the Dawn of the Millennium. Palacky University in Olomouc, Olomouc, pp. 25–33.
Bull, P.A., 1978. Observations on small sedimentary quartz particles analysed by scanning electron microscopy. Scanning Electron Microscopy SL 1, 821–826.
Czudek, T., 1997. Reliéf Moravy a Slezska v kvartéru. Sursum, Tišnov. 213s.
Czudek, T., 2005. Vývoj reliéfu krajiny České republiky v Kvartéru. Moravské zemské muzeum, Brno. . 238 pages.
Ehlers, J., Gibbard, P.L. (Eds.), 2004a. Quaternary glaciations: extent and chronology. Part I: Europe. Elsevier, Amsterdam, The Netherlands.
Ehlers, J., Gibbard, P.L. (Eds.), 2004b. Quaternary glaciations: extent and chronology. Part II: North America. Elsevier, Amsterdam, The Netherlands.
Erdtman, G., 1954. An Introduction to Pollen Analysis. Waltham.
Evans, D.J.A., Archem, S., Wilson, D.J.H., 1999. A comparison of the lichenometric and Schmidt hammer dating techniques based on data from the proglacial areas of some Icelandic glaciers. Quaternary Science Reviews 18, 13–40.
Faegri, K., 1964. Textbook of Pollen Analysis. Copenhagen.
Fiebig, M., Buiter, S.J.H., Ellwanger, D., 2004. Pleistocene glaciations of South Germany. In: Ehlers, J., Gibbard, P.L. (Eds.), Quaternary Glaciations: Extent and Chronology. Elsevier, Amsterdam, The Netherlands.
Firbas, F., 1949, 1952. Spät- und nacheiszeitliche Waldgeschichte Mitteleuropas nördlich der Alpen. – I. Allgemeine Waldgeschichte. II. Waldgeschichte der einzelnen Landschaften. – Jena.
Fuller, S., Murray, T., 2002. Sedimentological investigation in the forefield of an Icelandic surge-type gacier: implication for the surge mechanism. Quaternary Science Reviews 21, 1503–1520.
Goudie, A.S., 2006. The Schmidt hammer in geomorphological research. Progress in Physical Geography 30 (6), 703–718.
Graham, D.J., Midgley, N.G., 2000. Graphical representation of particle shape using triangular diagrams: an excel spreadsheet method. Earth Surface Processes and Landforms 25, 1473–1477.
Hambrey, J.M., Ehrmann, W., 2004. Modification of sediment characteristics during glacial transport in high/alpine catchments: Mount Cook area, New Zealand. Boreas 33, 300–318.
Harris, T., Tweed, F.S., Knudsen, Ó., 2004. A polygenetic landform at Stígá, Öraefajökull, southern Iceland. Geografiska Annaler 86A (2), 143–154.
Harrison, S., Halley, B., Anderson, E., 2008. Relict rock glaciers and protalus lobes in the British Isles: implication for Late Pleistocéne mountain geomorphology and paleoclimate. Journal of Quaternary Science 23 (3), 287–304.
Hauner, U., 1980. Untersuchungen zur klimagesteuerten tertiären und quartären Morphogenese des Inneren Bayerischen Waldes (Rachel–Lusen) unter besonderer Berücksichtigung pleistozän kaltzeitlicher Formen und Ablagerungen. Regensburger Geographische Schriften, Heft 14. Regensbug.
Helland, P.E., Huang, P.H., Diffendal Jr., R.F., 1997. SEM analysis of quartz grain sand surface textures indicates alluvial colluvial origin of the Quaternary "glacial" boulder clays at Huangshan (Yellow Mountains), east-central China. Quaternary Research 48, 177–186.
Holcombe, R.J., 2005. . GEOrient 9.2. www.holcombe.net.au/software/ [online]. Department of Earth Sciences. The University of Queensland, Brisbane, New Zealand.
Hubbard, B., Glasser, N., 2005. Field Techniques in Glaciology and Glacial Geomorphology. John Wiley & Sons Ltd., Chichester, UK.
Ivy-Osch, S., Kerschner, H., Reuther, A., Preusser, F., Heine, K., Maisch, M., Kubik, P.W., Schlüchter, C., 2008. Chronology of the last glacial cycle in the European Alps. Journal of Quaternary Science 23 (6–7), 559–573.
Jankovská, V., 2006. Late Glacial and Holocene history of Plešné Lake and its surrounding landscape based on pollen and palaeoalgological analyses. Biologia 61 (Suppl, 20), 371–385.
Johnson, P.G., 1980. Glacier–rock glacier transition in the southwest Yukon Territory, Canada. Arctic and Alpine Research 12 (2), 195–204.
Král, V., 1968. Geomorfologie vrcholové oblasti Krušných hor a problem paroviny. Rozpravy Československé Akademie Věd 78 (9) 65 pp.
Kunský, J., 1933. Zalednění Šumavy a šumavská jezera. Sborník České Společnosti Zeměpisné 39/1, 33–44.
Mahaney, W., 2002. Atlas of Sand Grain Surface Textures and Applications. Oxford University Press, Oxford, UK.
Mathews, J.A., Shakesby, R.A., 1984. The status of the "Little Ice Age" in southern Norway: relative-age dating of Neoglacial moraines with Schmidt hammer and lichenometry. Boreas 13, 333–346.
Mentlík, P., 2002. Příspěvek ke geomorfologii okolí Prášilského jezera (povodí Jezerního potoka). Silva Gabreta 8, 19–42.
Mentlík, P., 2005. The preliminary results of research of accumulation glacial forms in the surroundings of Laka Lake. Miscellanea Geographica 11, 31–46.
Mentlík, P., 2006. Relative dating of glacial landforms in the surroundings of Prášilské Lake (Šumava Mountains, Czech Republic). Geomorphologia Slovaca 6, 45–54.
Mercier, J.L., Jeser, N., 2004. The glacial history of the Vosges Mountains. In: Ehlers, J., Gibbard, P.L. (Eds.), Quaternary Glaciations — Extent and Chronology. Elsevier B.V.
Mercier, J.L., Kalvoda, J., Bourlès, D.L., Braucher, R., Engel, Z., 2000. Preliminary results of ^{10}Be dating of glacial landscape in the Giant Mountains. Acta Universitatis Carolinae Geographica XXXV, 157–170 Supplementum.
Minár, J., Evans, I.S., 2008. Elementary forms for land surface segmentation: the theoretical basis of terrain analysis and geomorphological mapping. Geomorphology 95, 236–259.
Nesje, A., Dahl, S., 1992. Paleoclimatic implications based on equilibrium-line altitude depressions of reconstructed Younger Dryas and Holocene cirque glaciers in inner Nordfjord, western Norway. Paleogeography, Palaeoclimatology, Palaoecology 94, 87–97.
Otto, J.C., Sass, O., 2006. Comparing geophysical methods for talus slope investigations in the Turtman valley (Swiss Alps). Geomorphology 76, 257–272.
Overbeck, F., 1958. Pollenanalyse quartärer Bildungen. In: Freund, H. (Ed.), Handbuch der Mikroskopie in der Technik. Frankfurt/Main, Germany, pp. 325–410.
Pánek, T., Hradecký, J., Šilhán, K., 2009. Geomorphic evidence of ancient catastrophic flow type landslides in the mid-mountain ridges of the Western Flysch Carpathian Mountains (Czech Republic). International Journal of Sediment Research 24, 88–98.
Pelc, Z., Šebesta, J., 1994. Geologická mapa ČR [Geological Map of the Czech Republic 1:50, 000]. Sheet 22–33 Kašperské Hory, Praha, Czech Republic.
Pelíšek, J., 1953. K otázce zalednění Moravskoslezských Beskyd. Sborník Československé Společnosti Zeměpisné 57, 60–65.
Pfaffl, F., 1998. Glazialmorphologische Untersuchungen am Rachel–Nordkar und am Grossen Arbersee im Bayerischen Wald. Geologische Blätter für NordOst-Bayern 38 (1–2), 7–26.
Powers, M.C., 1953. A new roundness scale for sedimentary particles. Journal of Sedimentary Petrology 23, 117–119.
Pražáková, M., Veselý, J., Fott, J., Majer, V., Kropáček, J., 2006. The long-term succession of Cladoceran fauna and palaeoclimate forcing: a 14,600 year record from Plešné Lake, the Bohemian Forest. Biologia 61 (Suppl. 20), 387–400.
Preihäusser, G., 1934. Über Kare und Karseen des Bayrischen Wales. Der Bayerwald 32, 65–71.
Preusser, F., 2004. Towards a chronology of the Late Pleistocene in the northern Alpine Foreland. Boreas 33, 195–210.
Raab, T., Völkel, J., 2003. Late Pleistocene glaciation of the Kleiner Arbersee area in the Bavarian Forest, south Germany. Quaternary Science Reviews 22, 581–593.
Rathsburg, A., 1928. Die Gletscher des Böhmerwaldes zur Eiszeit. Berichte der Naturwissenschaftlichen Gesellschaft Chemnitz 23, 45–64.
Reille, M., 1992. Pollen et Spores d´Europe et d´Afrique du Nord. Laboratoire de Botanique Historique and Palynologie, Marseillle, France.
Reille, M., 1995. Pollen et Spores d´Europe et d´Afrique du Nord. Supplément 1. Laboratoire de Botanique Historique and Palynologie, Marseillle, France.

Reille, M., 1998. Pollen et Spores d´Europe et d´Afrique du Nord. Supplément 2. Laboratoire de Botanique Historique and Palynologie, Marseillle, France.
Renssen, H., Kasse, C., Vandenberghe, J., Lorenz, S.J., 2007. Weischelian Late Pleniglacial surface winds over northwest and central Europe: a model–data comparison. Journal of Quaternary Science 22 (3), 281–293.
Reuther, A.U., 2007. Surface exposure dating of glacial deposits from the last glacial cycle. Evidence from Eastern Alps, the Bavarian Forest, the Southern Carpathians and the Altai Mountains. Relief Boden Paleoklima, Band, vol. 21. Gebr. Borntraeger, Berlin, Stuttgart, Germany.
Růžičková, E., Růžička, M., Zeman, A., Kadlec, J., 2001. Quaternary Clastic Sediments of the Czech Republic. Czech Geological Survey, Prague, Czech Republic. 92 pp.
Schrott, L., Sass, O., 2008. Application of field geophysics in geomorphology: advances and limitations exemplified by case studies. Geomorphology 93, 55–73.
Steffanová, P., Mentlík, P., 2007. Comparison of morphometric characteristics of cirques in the Bohemian Forest. Silva Gabreta 13 (3), 191–204.
Vočadlová, K., Křížek, M., 2005. Glacial landforms in the Černé Lake area. Miscellanea Geographica 11, 47–63.
Votýpka, J., 1979. Geomorfologie granitové oblasti masívu Plechého. Acta Universitatis Carolinae Geographica XVI/2, 55–83.
Walanus, A., Nalepka, D., 1999. POLPAL. Program for counting pollen grains: diagrams plotting and numerical analysis. Acta Palaeobotanica Suppl. 2, 659–661.
Whalley, W.B., Martin, H.E., 1992. Rock glaciers. II: models and mechanisms. Progress in Physical Geography 16, 127–186.

GEOGRAFIE • ROK 2011 • ČÍSLO 1 • ROČNÍK 116

LENKA KŘÍŽOVÁ, MAREK KŘÍŽEK, LENKA LISÁ

VÝZNAM POVRCHOVÉ ANALÝZY KŘEMENNÝCH ZRN PRO STUDIUM GENEZE NEZPEVNĚNÝCH SEDIMENTŮ

KŘÍŽOVÁ, L., KŘÍŽEK, M., LISÁ, L. (2011): Applicability of quartz grains surface analysis to the study of the genesis of unlithified sediments. Geografie, 116, No. 1, pp. 59–78. – This paper deals with genetic types of unlithified sediments and their characteristics with an emphasis on quartz grain surface microrelief. There are various physical-geographic agents in different sedimentary environments which play an important role in the origin of certain marks on the surface of sedimentary grains. As a result, studying the features of quartz grain surfaces enables us to determine the possible origin of sediments and landforms. Reference samples were chosen from geomorphological landforms of known origin: a moraine in the Labský Důl Valley, a debris flow in the Důl Bílého Labe Valley, a flood accumulation and deluvium from the Důl Bílého Labe Valley in the Krkonoše Mountains and eolian sediment from Klárov in Prague. Significant differences in surface micromorphology were found among these samples.
KEY WORDS: exoscopy – accumulation landforms – weathering – sediments.

Práce vznikla za podpory projektů GAAV KJB301110804 „Recentní aktivita strukturních půd ve vybraných oblastech střední Evropy“ a výzkumného záměru MSM 0021620831 „Geografické systémy a rizikové procesy v kontextu globálních změn a evropské integrace“.

1. Úvod

Nezpevněné sedimenty jsou tvořeny přemístěným a usazeným materiálem, který vznikl rozpadem hornin. Prostor mezi jednotlivými zrny není vyplněn tmelem, na rozdíl od zpevněných sedimentů (Kukal 1986). Nezpevněné sedimenty lze rozlišit podle genetického typu, tedy jejich původu a podmínek vzniku. Základní genetické skupiny kvartérních sedimentů vyskytujících se na území Česka jsou: fluviální, ledovcové, eolické, svahové, jezerní a jeskynní (Růžičková a kol. 2003). Smyslem jejich zkoumání je poznání vývoje a změn fyzickogeografických podmínek v čase. Jedním z hlavních úkolů geomorfologie je určení geneze reliéfu, což lze v některých případech odvodit ze znalosti charakteristik materiálu, který je tvoří. Jednou z metod, která umožňuje odpovědět na otázky geneze sedimentů a tedy i tvarů jimi tvořených, je exoskopie neboli studium povrchových textur na křemených zrnech (Margolis, Krinsley 1971; Fitzpatrick, Summerson 1971; Halley, Krinsley 1974; Le Ribault 1975; Cremer, Legigan 1989; Mahaney 2002). Tato metoda má potenciál, aby byla v budoucnosti více používaná v geomorfologickém výzkumu. Jedním z cílů článku je představit tuto metodu, její možnosti a zejména etablovat českou terminologii, která do dnešní doby buď neexistuje anebo není díky dílčím studiím ujednocena. Dalším cílem je na vzorových příkladech (morény z údolí Labe; mury, povodňových sedimentů a deluvia z údolí Bílého Labe a eolického sedimentu z pražského Klárova) demonstrovat, do jaké míry lze exoskopickou metodou odlišit sedimenty různé geneze.

2. Povrch klastických zrn

Metodu exoskopické analýzy uvedl v roce 1935 André Cailleux pod názvem morfoskopie písku. Princip metody spočívá ve studiu křemenných zrn, která během transportu prodělala signifikantní změny na svém povrchu. Typ fluida, rychlost a délka transportu určuje množství vzniklých texturních prvků a zároveň interpretovatelnost procesů, jimiž křemenná zrna během transportu prošla (Le Ribault 2003a). Povrch křemenných zrn je pozorován pod binokulárním a následně elektronovým mikroskopem při vícenásobném zvětšení. Ideální velikostní frakce zrn pro tuto analýzu je 300 až 500 µm, protože na zrnech této velikosti se nejlépe projevují mechanické i chemické vlivy (Le Ribault 1975; Censier, Tourenq 1986; Cremer, Legigan 1989), jejichž procentuální zastoupení u jemnozrnných sedimentů není zcela jasné (Lisá 2004).

Na povrchu zrn se setkáváme se znaky mechanického nebo chemického původu. Lze rozlišit stupeň lesklosti (lesklý až matný) a skulpturní znaky (rýhování, poškrábání, nárazová deprese, vtisky aj.). Matný povrch křemenných zrn písčité frakce bývá většinou spojován s eolickými pochody, lesklý vzniká nejčastěji dlouhým transportem ve vodním prostředí řek, nebo vývojem v mořském prostředí. V pouštních podmínkách je lesklý povrch vysvětlován tenkým povlakem pouštního laku chemogenního původu (Petránek 1963, Le Ribault 2003b).

3. Mikrotextury podle geneze

Geneze sedimentů určovaná metodou exoskopie odvisí od výskytu charakteristických mikrotextur (viz tab. 1, obr. 1–5) či jejich souborů na povrchu zrn (sensu Le Ribault 1975). Jedná se o takové mirkotextury, které vznikly při zvětrávání, transportu a sedimentaci materiálu a jejichž procentuální zastoupení většinou nepřevyšuje 60 % (Mahaney, Stewart, Kalm 2001). V rámci jednoho prostředí mohou být křemenná zrna ovlivněna několika geneticky odlišnými procesy (Alkaseeva 2005), avšak nejzřetelnější tvary na křemenných zrnech jsou většinou takové, které vznikly během posledního transportu. Kromě procesu který se podílel na posledním typu transportu dokáže exoskopie odhalit na jediném zrnu až 8 epizod vývoje (Le Ribault 1975).

Vztahy mezi eluviálními, fluviálními a eolickými prvky se mění se změnami klimatických podmínek. Vliv procesů na mikroreliéf zrna závisí také na trvání transportu a energii transportního média. Intenzita chemické transformace povrchů křemenných zrn je závislá na době působení chemických procesů, klimatu, textuře sedimentů, velikosti zrn minerálů a na pozici v půdním profilu a v reliéfu (Alkaseeva 2005). Při zkoumání vzorků je třeba mít na zřeteli, že zrna různých genetických typů mohla být během svého transportu smíchána (Mahaney, Kalm 2000).

Tab. 1 – Základní mikrotextury křemenných zrn

	Mikrotextura	Anglický název	Charakteristika	Podmínky vzniku	Literatura	Obr.
Mikrotextury mechanického původu:						
a	Lasturnatý lom	*conchoidal fracture*	Jemné zakřivené lomové plochy s žebrovaným vzhledem.	Vznikají při odlamování od horniny vlivem nárazu. Odpovídají zvláště glaciálním a periglaciálním podmínkám.	1, 5, 6, 7, 8, 10, 12, 14, 17, 19, 20, 21	2, 5
	Lineární subparalelní lomy	*subparallel linear fractures*	Paralelně seskupené stupně s výraznější morfologií než mají lasturnaté lomy.		2, 4, 6, 12, 14, 17, 19	
b	Rovné stupně	*straight steps*	Podobné lasturnatým lomům, ale strmější, s větší hloubkou a rozestupy. Zpravidla tvoří hranice mezi lomovými plochami.		2, 6, 12, 14, 15, 17, 21, 22	4
c	Obloukové stupně	*arc-steps, arcuate steps*			2, 6, 12, 14, 17, 18, 20, 21, 22	4, 5
	Paprsčité lomy	*radial fractures*	Lineární lomy vybíhající ze středu místa, kde došlo k nárazu. S rostoucí silou nárazu se poloměr středu zmenšuje.	Vzniká při nárazu horniny, zvláště v glaciálním a periglaciálním prostředí.	13	
d	Puklinové plochy	*fracture faces*	Velké, hladké a čisté plochy přes 25 % povrchu zrna. Mohou být lehce zakřivené, občas se na nich vyskytují lasturnaté lomy.	Vznikají převážně při mechanickém zvětrávání a v glaciálních podmínkách.	8, 13	2
	Abraze hran	*edge abrasion*	Obroušení hran vlivem transportu. Čím delší transport, tím rozsáhlejší abraze.	Nejvýraznější u eolického a svahového materiálu.		
e	Klikaté hřbítky	*meandring ridges*	Jsou tvořeny křemičitými sraženinami, které kopírují poruchy nebo lomy na povrchu zrna.	Vznikají v periglaciálních a fluviálních podmínkách za nízké kinetické energie.	13	3
f	Paralelní rýhy	*parallel striations*	Paralelně vedoucí brázdy v povrchu zrn.	Typické pro glaciální prostředí.	3, 5, 6, 13, 14, 15, 16	1

Mikrotextura		Anglický název	Charakteristika	Podmínky vzniku	Literatura	Obr.
g	V-jamky	*V-shaped pits*	Drobný impaktní tvar s bočním profilem ve tvaru V.	Glaciální a eolické prostředí o nízké kinetické energii, fluviální prostředí o průměrné kinetické energii.	2, 3, 5, 7, 8, 9, 12, 13, 15, 16	1
	Mísovité jamky	*dish-shaped breakage concavities*	Deprese mísovitého tvaru, které dosahují oproti jiným impaktům větších velikostí.	Glaciální, fluviální a eolické prostředí o vysoké kinetické energii.	2, 4, 5, 8, 9, 11	
h	Srpkovité tvary	*crescent-shaped features*	Srpkovité tvary vznikající nárazem čepelovitých částic na povrch zrn.	Glaciální a eolický transport o průměrné kinetické energii, fluviální transport o vysoké kinetické energii.	4, 5, 9, 12, 13, 14, 19,	2
i	Rovné brázdy	*straight grooves*	Abradované mikroprvky způsobené rytím. Rovné brázdy odpovídají často větší síle a menšímu napětí.	Běžně spojovány s činností ledovců, vznikají však i při gravitačních pochodech.	2, 3, 8, 10, 12, 13, 16	1, 2
j	Obloukové brázdy	*curved grooves*			2, 8, 13, 19, 21	2
	Tvary vzniklé drcením	*grinding features*	Kruhové, hluboké stopy s koncentrickými tvary. Mohou být napojeny na brázdy menších rozměrů.	Glaciální prostředí a gravitační pochody.	5, 8, 11	
	Štěpné plátky	*cleavage plates, upturned plates*	Tenké plátky vystupující z povrchu křemenných zrn. Nejsnáze jsou pozorovatelné na hranách zrn.	Vzniká při odlamování od horniny, výskyt je spojován hlavně s glaciálními podmínkami.	8, 10, 13, 15, 21, 22	
l	Přilnavé částice	*adhering particles*	Malé, ploché křemenné částice přichycené k povrchu zrna elektromagnetickou silou. Po uložení zrna se na nich usazují křemičité sraženiny.	Glaciální prostředí, gravitační pochody. Na zaoblených zrnech se nevyskytují.	1, 2, 4, 8, 9, 13, 15, 16, 18, 20, 21	2, 4

	Mikrotextura	Anglický název	Charakteristika	Podmínky vzniku	Literatura	Obr.
Mikrotextury chemického původu:						
	Tečkování	*pitting*	Shluky velmi malých jamek, které jsou spolehlivěji pozorovatelné při vyšším rozlišení snímků. Iniciální jamky jsou malé a postupně se zvětšují a splývají.	Může být způsobeno omezenou expozicí zrn vůči tající vodě ledovců mírného pásu. Významnou roli hraje pH prostředí, rozpustnost křemene rychle narůstá při pH > 9,0.	1, 4, 6, 8, 11, 13	
	Orientované vyleptané jamky	*oriented etched pits*	Jamky triangulárního tvaru se stejným usměrněním, mohou se velikostně lišit.		1, 2, 3, 4, 5, 6, 7, 8, 10, 15, 16, 22	
	Křemičité globule	*silica globules*	Vysrážené křemičitany pokrývající povrch zrna mají formu skrývky nebo globulí. Když se tyto textury spojí nebo překryjí, utvoří se tenký až silný křemičitý povlak, který může zakrýt tvary vzniklé v předchozích prostředích. Ve vodním prostředí o vysoké kinetické energii může být obroušen a zakryté tvary se mohou opět objevit. Souhrně jsou tyto tvary označovány jako *křemičité sraženiny*.	Vznikají ve vlhkém prostředí s nižší rychlostí transportu a vyskytují se na starších glaciálních uloženinách.	2, 3, 4, 5, 9, 20	
l	Křemičité skrývky	*silica capping*			2, 7	1, 3
m	Křemičitý povlak	*silica pellicle*			2, 4, 5, 8, 9, 13, 20, 21	3
	Nárůsty křemenných krystalů	*quartz crystal overgrowths*	Mají 3 stadia vývoje: 1. vytvoří se malé orientované výčnělky, 2. ty se spojí a vzniknou zřetelné facety, 3. růst končí obrostlým zrnem se vzhledem křemenného krystalu.	Vznikají ve fluviálních podmínkách s nízkou rychlostí proudění.	5, 6, 8, 18, 22	
	Textury vzniklé tlakovým rozpouštěním	*pressure-solution features*	Velmi hluboké, polokruhovité deprese s oblými výčnělky.	Glaciální prostředí.	5, 20, 22	

Citované zdroje: 1 – Alkaseeva 2005; 2 – Cater 1984; 3 – Censier, Tourenq 1986; 4 – Clocchiatti, Le Ribault, Rodrigo 1978; 5 – Cremer, Legigan 1989; 6 – Fitzpatrick, Summerson 1971; 7 – Hellad, Juany, Diffendal 1997; 8 – Krinsley, Doornkamp 1973; 9 – Le Ribault 1975; 10 – Lindé, Mycielska, Dowgiałło 1980; 11 – Lisá 2004; 12 – Mahaney 1995; 13 – Mahaney 2002; 14 – Mahaney, Andres 1991; 15 – Mahaney, Kalm 2000; 16 – Mahaney, Stewart, Kalm 2001; 17 – Mahaney, Vortisch, Julig 1988; 18 – Mellor 1986; 19 – Strand, Passchier, Näsi 2003; 20 – Whalley 1982; 21 – Halley, Krinsley 1974; 22 – Wilson 1978.

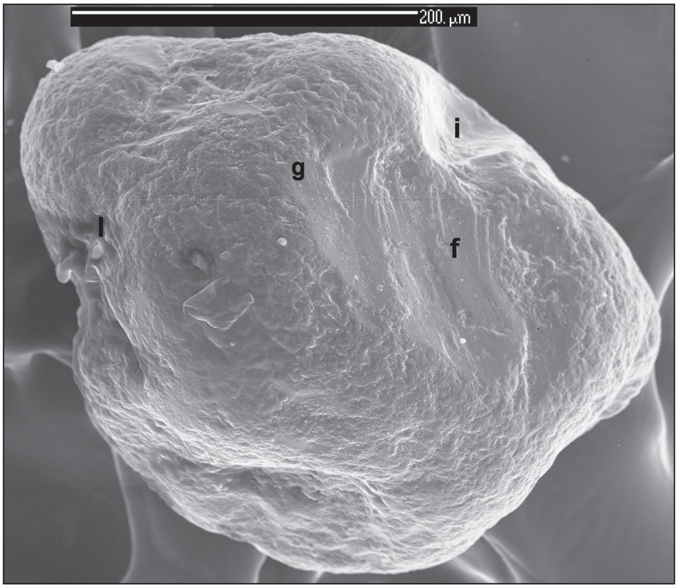

Obr. 1 – Nejčastější tvary vyskytující se na povrchu zrna: f – paralelní rýhy, g – V-jamky, i – rovné brázdy, l – křemičité skrývky. Vzorek eolického sedimentu; Praha-Klárov.

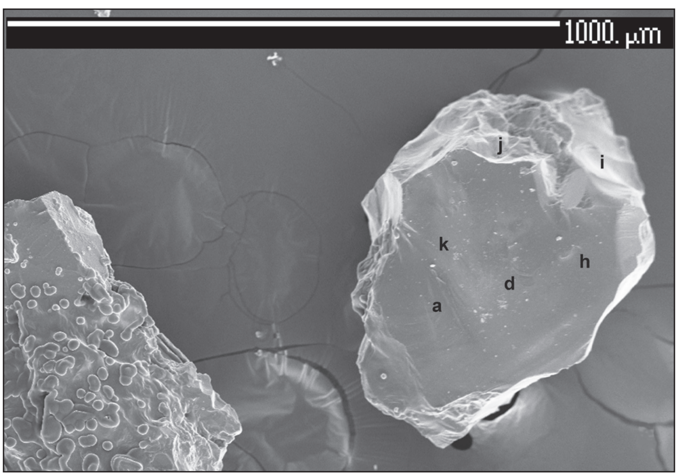

Obr. 2 – Nejčastější tvary vyskytující se na povrchu zrna: a – lasturnatý lom, d – puklinové plochy, h – srpkovité tvary, i – rovné brázdy, j – obloukové brázdy, k – přilnavé částice. Vzorek sedimentu mury; údolí Bílého Labe, Krkonoše.

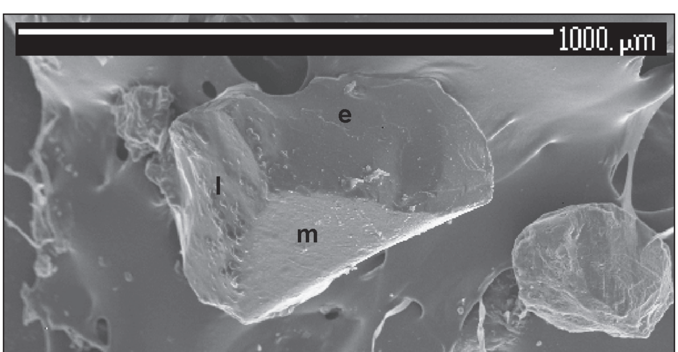

Obr. 3 – Nejčastější tvary vyskytující se na povrchu zrna: e – klikaté hřbítky, l – křemičité skrývky, m – křemičitý povlak. Vzorek fluviálního sedimentu; údolí Bílého Labe, Krkonoše.

Obr. 4 – Nejčastější tvary vyskytující se na povrchu zrna:
b – rovné stupně,
c – obloukové stupně,
k – přilnavé částice.
Vzorek deluvia; údolí Bílého Labe, Krkonoše.

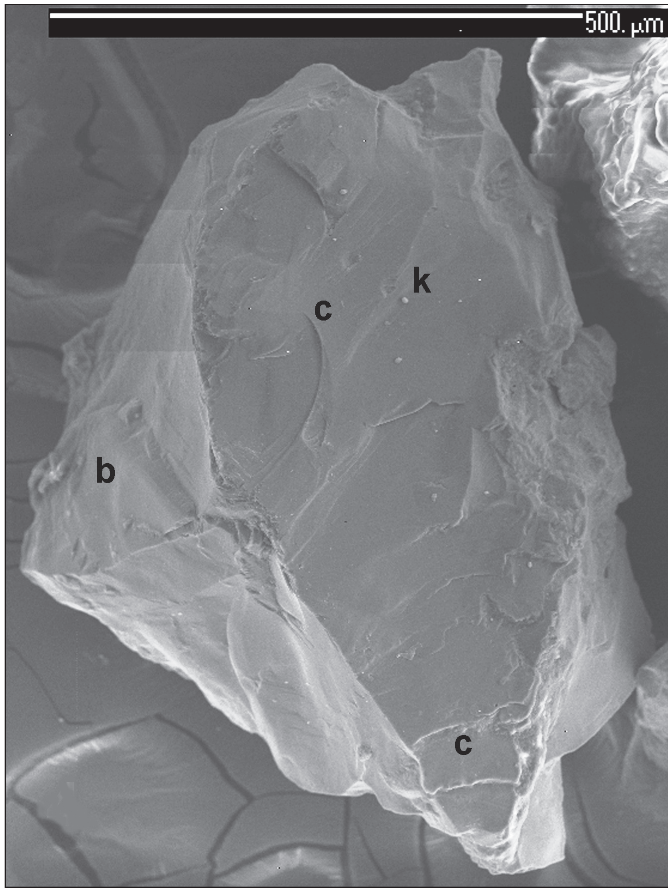

Obr. 5 – Nejčastější tvary vyskytující se na povrchu zrna:
a – lasturnatý lom,
c – obloukové stupně.
Vzorek glaciálního sedimentu; Labské údolí, Krkonoše.

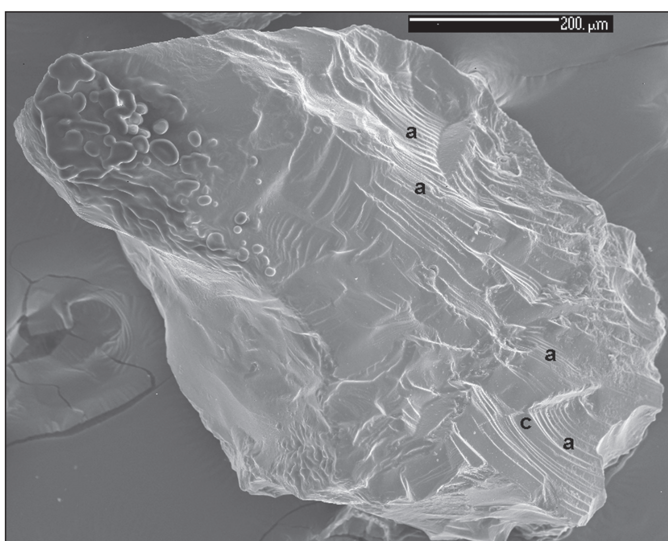

3.1. Eolické sedimenty

Tato genetická třída sedimentů je pro exoskopický popis nejvhodnější. Eolická zrna mají zpravidla nízký, dobře zaoblený reliéf (Mahaney, Stewart, Kalm 2001), jsou matná (Le Ribault 2003b) a lépe zaoblená než fluviální zrna (Lindé, Mycielska-Dowgiałło 1980). Stupeň zaoblení klesá (zrna jsou nepravidelnější) s jejich rostoucí velikostí, což je způsobeno pravděpodobně tím, že klesá i jejich hybnost (Mahaney 2002).

Mikrotextury pozorované na eolických písečných zrnech jsou štěpné plátky, brázdy přibližně 0,5–10 µm velké, prodloužené prohlubně (Mahaney 2002), srpkovité tvary, V-jamky, mísovité jamky, přilnavé částice (Lindé, Mycielska-Dowgiałło 1980), tečkování (Lisá 2004), křemičitý povlak (Le Ribault 2003b). Naopak lineární paralelní lomy a lasturnaté lomy se vyskytují jen minimálně (Mahaney, Stewart, Kalm 2001).

Některé z impaktních tvarů jsou nalézány pouze na větších písečných zrnech. Tyto tvary jsou křehké a obvykle byly odstraněny během eolické abraze a chemického zvětrávání (v horkých pouštních oblastech může pouštní rosa, která je nasycena CO_2, proniknout až do hloubky 2–3 cm; Mahaney 2002). Nejmarkantnějším znakem jsou srpkovité tvary, které jsou tím více uhlazeny, čím jsou starší. Eolickými procesy vznikají na křemenných zrnech také V-jamky a mísovité jamky.

3.2. Glaciální sedimenty

Na subglaciálních zrnech vznikají tvary způsobené drcením ve vlhkém prostředí, ale křemičité sraženiny se vyskytují jen vzácně. Tato zrna bývají nejvíce náchylná k porušení na svých hranách a rozích, zatímco plochy jsou zasaženy méně (Halley, Krinsley 1974). Co se týká písků, předpokládá se, že na těchto zrnech se nalézají pouze zděděné texturní znaky (např. pokud se zrna v ledovci navzájem nedotýkala kvůli jejich menšímu množství), protože zvětráváním se zrna pouze uvolnila a dále byla jen pasivně transportována na povrchu ledovce (Mahaney, Stewart, Kalm 2001). Většina těchto zrn má vysokou sféricitu a ostrohrannost. Typické jsou pro ně štěpné vločky a přilnavé částice, ale pozorovány byly také obloukové stupně a lineární i obloukové brázdy (Halley, Krinsley 1974).

Z exoskopického pohledu jsou glacigenní zrna ostrohranná, nenesou známky uhlazení ani zaoblení, pokud nedošlo k chemickému nebo mechanickému přetvoření, a jejich povrch může být jak matný, tak lesklý (Le Ribault 2003b). Reliéf zrn je proměnlivě hladký (Fitzpatrick, Summerson 1971) až drsný (Le Ribault 2003b) a relativně vysoký, zvláště oproti zrnům pobřežního a eolického prostředí (Krinsley, Doornkamp 1973). Na povrchu glacigenních zrn je možné nalézt nejvyšší počet mikrotextur ve srovnání se zrny, na která působily jiné geomorfologické procesy (Mahaney 2002). Zatímco na zrnech eolického a fluviálního prostředí existují podobné mělké, lasturnaté a lineární paralelní lomy, jejich hranaté tvary, hluboké zasazení do povrchu zrn a časté usměrnění je jedinečným znakem pro zrna glacigenního původu (Mahaney, Kalm 2000). Zrna vlečená na bázi ledovce jsou však pravděpodobně méně ostrohranná a texturovaná než částice pohybující se s ledovcem na jeho povrchu či uvnitř

(Dowdeswell 1982). To samé platí pro zrna glacimarinního původu (Strand, Passchier, Näsi 2003). Všeobecně je mezi englaciálními a supraglaciálními zrny jen málo rozpoznatelný rozdíl (Halley, Krinsley 1974).

Na stupeň poškození zrn má také vliv mocnost ledovce, kterým jsou zrna unášena, a délka jejich transportu. U ledovců o mocnosti mezi 200–800 m (horské ledovce) je výskyt lomů a poruch na povrchu zrna menší (20–30 % zrn ve vzorku), zatímco u kontinentálních ledovců (mocnost větší než 1000 m) je větší. Postupné zvyšování mocnosti ledovce tedy způsobuje větší stupeň poškozování křemenných zrn. Vznikají častěji paralelní hřbítky, lasturnatý lom, obloukové stupně, srpkovité tvary a hluboké brázdy a povrch zrn je značně ostrohranný. Stupeň poškození záleží také na pozici vůči ledovci (od nejmenšího stupně poškození po nejvyšší to jsou zrna supraglaciální, englaciální a bazální) a zda-li má ledovec chladnou (suchou) nebo teplou (vlhkou) bázi, kde u suché báze převažuje křehký smyk a u vlhké báze plastický až plasticko-křehký smyk (Mahaney, Andres 1991; Mahaney 1995).

Za reprezentativní mikrotextury pro glaciální transport jsou považovány lasturnatý lom, lineární subparalelní lomy, rovné a obloukové stupně a hluboké brázdy, tvary vzniklé drcením a tlakovým rozpouštěním, paralelní rýhy a hřbítky, přilnavé částice a štěpné vločky. Vyskytovat se mohou také srpkovité tvary, štěpné plátky, V-jamky a křemičité povlaky. Pro větší zrna je typický lasturnatý lom, zatímco pro malá zrna to jsou štěpné plátky a puklinové plochy podél některých lasturnatých lomů. Pokud byla zrna vystavena drcení, potom je u nich větší variabilita ve velikosti a rozsahu lasturnatých lomů a štěpných plátků, než by bylo normální u nezvětralých zrn (Krinsley, Doornkamp 1973; Mahaney, Vortisch, Julig 1988). Dále se na většině glaciálně transformovaných zrn běžně vyskytují lineární paralelní lomy, přilnavé částice a V-jamky. V-jamky mohou vznikat kolizemi ve vodním prostředí, ale jejich velký rozměr (50 µm) ukazuje spíše na glaciální transport (fluvioglaciální zrna jich mají více) (Mahaney, Kalm 2000).

Z chemických mirkotextur charakteristických pro glaciální sedimenty to jsou tvary vzniklé vysrážením, jako např. vyleptané orientované jamky a tečkování.

3.3. Fluviální sedimenty

V důsledku vodního transportu se povrch zrn zaobluje a reliéf je relativně nízký (Helland, Huang, Diffendal 1997; Mahaney, Stewart, Kalm 2001), přičemž vodní toky s nízkou kinetickou energií znatelně nepřetvářejí povrch transportovaných zrn. Ta se tak podobají více tillům (Mahaney 2002). Málo obroušená zrna se také nacházejí v chráněných místech toku (Censier, Tourenq 1986).

Známkami vodního transportu jsou V-jamky. Čím vyšší energie toku, tím vyšší frekvence výskytu mikrotextur. V systémech horních toků jsou vysoké rychlosti a V-jamky a různé impakty se stávají výrazně velkými a frekventovanými (Mahaney 2002). Mezi další impaktní tvary patří např. mísovité jamky (Clocchiatti, Le Ribault, Rodrigo 1978) a mechanické rýhy (Cater 1984, Lisá 2004). Ve vodním prostředí o vysoké energii je křemičitý povlak na nechráněných částech zrn slabě až silně obroušen (Cremer, Legigan 1989). Při střední energii toku jsou impaktní tvary zahlazovány (Le Ribault 1975; Censier, Tourenq 1986). V oblasti dolního toku řek se mohou vyskytovat zrna jiných genetických typů, např. glacigenního apod., která sem byla dopravena z horních částí povodí. V tomto prostředí o nízké energii se tvoří křemičité sraženiny, orientované vyleptané jamky, nárůsty křemenných krystalů (Cremer, Legigan 1989) a také drobné impaktní tvary vzniklé třením mezi zrny. Ohlazená, lesklá zrna mají silně zhlazené hrany, zatímco místa v dutinách jsou silně zkorodovaná (Censier, Tourenq 1986). Chybí zde brázdy a stupně (Mahaney, Stewart, Kalm 2001).

3.4. Svahové sedimenty

Zkoumání mikroreliéfu křemenných zrn svahových sedimentů metodou exoskopie je nejméně probádanou oblastí. Rychlost pohybů je velmi variabilní (od milimetrů za rok po několik stovek metrů za sekundu) a podle toho se také odvíjí výskyt mikrotextur (Mahaney 2002). Z dostupných dat se zdá, že zvětrávání podloží příliš neovlivňuje povrch zrn (Mahaney 2002).

Na zrnech byly pozorovány mikrotextury, které nebyly v jiných prostředích zatím zaznamenány. Jedná se o hluboké paralelní brázdy s krátkými rozestupy a radiální brázdy. Mimo jiné se hojně objevují puklinové plochy a „mikrofraktury“, které je možné považovat za charakteristické (Mahaney 2002). Důležitým znakem je také výskyt mechanické abraze hran, kterým se svahové sedimenty liší od eluvia.

3.5. Jezerní sedimenty

Rybníky a jezera představují prostředí o nízké kinetické energii fluida, které unáší a zejména ukládá zrna, jež proto nejsou promíchávána a příliš porušována, ale jsou pokryta jílem (Le Ribault 2003b). Zrna si zanechávají na svém povrchu tvary, které se utvořily během předešlého transportu k jezeru. Na povrchu zrn ležících ve vodě se však mohou utvářet křemičité sraženiny a povlaky (Mathur, Mishra, Singh 2009).

4. Metodika

Kopanými sondami byly získány sedimenty z vybraných geneticky různorodých skupin tvarů, tj. z glacigenních, fluviálních, svahových a eolických (tab. 2). Byla snaha provést odběr na relativně malé ploše s obdobnými geologickými a fyzickogeografickými podmínkami i s podobnou historií vývoje reliéfu. Výjimku tvoří jen eolické sedimenty, které se v Krkonoších nenacházejí a pro jejichž odběr byla vybrána poloha eolických sedimentů na pražském Klárově.

Zrna každého ze studovaných vzorků byla rozdělena plavením na velikostní frakci 250–500 μm. Jednotlivé vzorky byly dále vyvařeny v koncentrované HCl, promyty destilovanou vodou a vysušeny. Z takto připraveného vzorku bylo pod binokulárním mikroskopem vybráno 50 křemenných zrn, která byla

Tab. 2 – Charakteristika odebraných vzorků

Genetický typ sedimentu / *Místo odběru*	Stručná charakteristika tvaru a odběrového místa
Moréna / *Labské údolí, Krkonoše*	Lokalita (50°44'53,6" s. š., 15°37'24,9" v. d.) se nachází v nadmořské výšce 828 m na pravém okraji údolního dna Labe. Sedimenty pocházejí z přirozeného odkryvu 8 metrů vysoké proříznuté čelní würmské morény, kterou popsal již Vitásek (1923). Na základě studia sedimentů v Labském dole (Engel a kol. 2005) se podařilo zjistit, že již na konci MIS 3 nebyl ledovec přítomen v karu Labského dolu (Engel a kol. 2010).
Mura / *Údolí Bílého Labe, Krkonoše*	Odběrová lokalita (50°44'13,7" s. š., 15°39'27,8" v. d., 1 110 m n. m.) se nachází v dolní části k severu orientovaného levého svahu údolí Bílého Labe. Zde byl materiál odebrán z bočního valu mury (vzniklé v roce 1994) nad turistickým chodníkem vedoucím na Bílou louku.
Fluviální sediment / *Údolí Bílého Labe, Krkonoše*	Fluviální sediment byl odebrán (50°44'53,6" s. š., 15°37'24,9" v. d., 857 m n. m.) z povodňových akumulací nacházejících se uvnitř koryta a vzniklých v roce 2006.
Deluvium / *Údolí Bílého Labe, Krkonoše*	Deluviální sedimenty byly odebrány z jámy po vývratu v dolní části pravého údolního svahu (sklon 20°) Dolu Bílého Labe (50°46'8,4" s. š., 15°37'9,1" v. d.). Lokalita se nachází 5 metrů nad úrovní současného dna.
Eolický sediment / *Praha-Klárov*	Eolické sedimenty byly odebrány z východně orientovaného svahu vltavského údolí na pražském Klárově (50°5'34,0" s. š., 14°24'33,8" v. d.), kde se dochovaly jejich zbytky v podobě závějí eolik (Kovanda et al. 2001) na letenském souvrství (Chlupáč 1999).

následně připevněna na uhlíkovou pásku a pozlacena a vyfotografována pod elektronovým mikroskopem Cameca SX 100.

Pro zhodnocení výsledků exoskopie jsou používány statistické testy (např. Mahaney 2002). Jedním ze základních prostředků sumarizování dat o mikrotexturách je zakreslování histogramů nebo sloupcových grafů, které znázorňují frekvenci výskytu jednotlivých mikrotextur na každém zrně. Jednou z metod, jak analyzovat sloupcové grafy součtů (rozdělení frekvencí výskytu) pozorovaných mikrotextur na sedimentárních zrnech, je kvantifikace podobných a odlišných znaků mezi porovnávanými vzorky. Pro porovnání podobnosti zrn byl použit koeficient vzdálenosti d (sensu Mahaney 2002):

$$d_{ij} = \sqrt{\sum_{k=1}^{p} (x_{ik} - x_{jk})^2} ,$$

kde d_{ij} je koeficient vzdálenosti mezi dvěma prostředími (i, j), měřenými na dvojicích hodnot frekvence výskytu každého znaku x ze dvou srovnávaných vzorků (prostředí). Pořadí srovnávaných znaků začíná k = 1 (první dvojice) a končí $k = p$ (poslední dvojice). Čím je hodnota d menší, tím jsou si zrna podobnější.

5. Výsledky

Za referenční vzorky byly vybrány sedimenty pocházející z geomorfologických tvarů známé geneze (viz tab. 2): moréna v údolí Labe, mura v údolí Bílého Labe, povodňové sedimenty a deluvium z údolí Bílého Labe a eolický sediment z pražského Klárova.

Fluviální sedimenty se vyznačovaly nižší četností výskytu mikrotextur ve srovnání s jinými typy sedimentů, čímž je lze snadno odlišit od ostatních studovaných vzorků genetických typů sedimentů (obr. 6). Nejcharakterističtějšími znaky fluviálních zrn se ukázaly křemičité sraženiny a povlaky, které vznikají ve vlhkém nebo vodním prostředí, a to v závislosti na energii toku. Opracovanost zrn rostla s délkou transportu. Lasturnatý lom, štěpné plátky a brázdy se vyskytovaly minimálně.

Pro eolickým způsobem transportovaná zrna se ukázal typický výskyt V-jamek a mísovitých jamek, nepravidelných prohlubní a dalších impaktních tvarů (obr. 6). Četnost výskytu V-jamek a mísovitých jamek byla ve studovaných vzorcích 50 %. Tyto mikrotextury měly ovšem nižší procentuální zastoupení, než obloukové stupně, brázdy a abraze hran.

Zrna glaciálních sedimentů byla charakteristická vysokou četností lasturnatého lomu, rovných i zaoblených stupňů a brázd, paralelních rýh a puklinových ploch (obr. 6). S nižším procentuálním výskytem jsou význačné štěpné plátky (> 40 %) a přilnavé částice (> 50 %).

Zrna svahových sedimentů včetně mury pokrývají nejvíce stupňovité textury, lasturnatý lom a brázdy. Ve srovnání s ostatními zrny je výraznější abraze hran a vyskytují se klikaté hřbítky. Reliéf zrn svahové akumulace je vysoký a poloostrohranný, občas s tečkováním, u mury je střední a ostrohranný, navíc obsahuje křemičité sraženiny.

Z hlediska vyhodnocení koeficientů vzdáleností *d* (sensu Mahaney 2002) mezi zrny jednotlivých studovaných genetických skupin sedimentů (tab. 3),

Tab. 3 – Koeficienty vzdálenosti *d* (Mahaney 2002) mezi studovanými vzorky

Vzorky	Fluviální sediment	Moréna Labe	Svahový sediment	Mura	Eolický sediment
Fluviální sediment	0,00				
Labská moréna	1,38	0,00			
Svahový sediment	1,40	0,80	0,00		
Mura	1,24	1,13	1,00	0,00	
Eolický sediment	1,31	0,93	0,89	1,05	0,00

Obr. 6 (na str. 71) – Grafy četností mikrotextur jednotlivých genetických typů sedimentů (Labská moréna, eolické sedimenty, svahové sedimenty – deluvium, murové sedimenty, fluviální sedimenty). 1 – ostrohranné zrno, 2 – poloostrohranné zrno, 3 – polozaoblené zrno, 4 – zaoblené zrno, 5 – nízký reliéf, 6 – střední reliéf, 7 – vysoký reliéf, 8 – malý lasturnatý lom, 9 – velký lasturnatý lom, 10 – rovné stupně, 11 – obloukové stupně, 12 – velké puklinové plochy, 13 – paralelní rýhy, 14 – abraze hran, 15 – V-jamky, 16 – mísovité jamky, 17 – rovné brázdy, 18 – obloukové brázdy, 19 – klikaté hřbítky, 20 – nepravidelné prohlubně, 21 – štěpné plátky, 22 – tečkování, 23 – orientované vyleptané jamky, 24 – přilnavé částice, 25 – omezené křemičité sraženiny, 26 – rozsáhlé křemičité sraženiny, 27 – nárůsty krystalů.

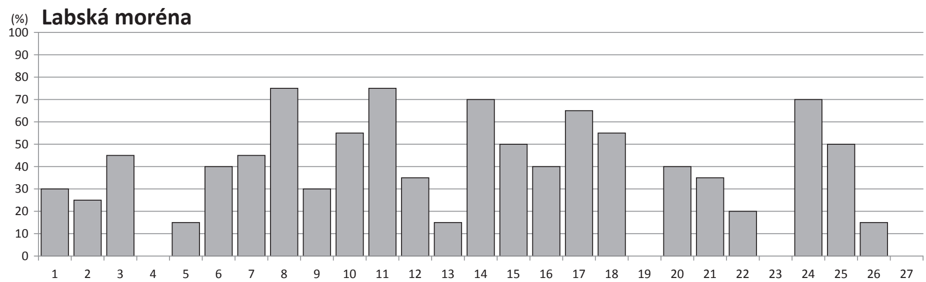
(%)
Labská moréna
0 10 20 30 40 50 60 70 80 90 100
1 2 3 4 5 6 7 8 9 10 11 12 13 14 15 16 17 18 19 20 21 22 23 24 25 26 27

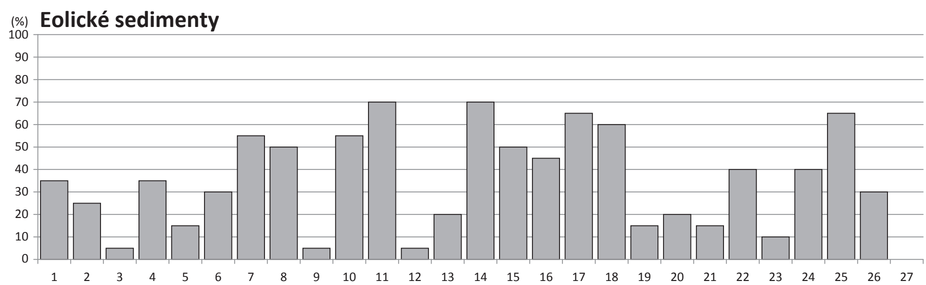
(%)
Eolické sedimenty
0 10 20 30 40 50 60 70 80 90 100
1 2 3 4 5 6 7 8 9 10 11 12 13 14 15 16 17 18 19 20 21 22 23 24 25 26 27

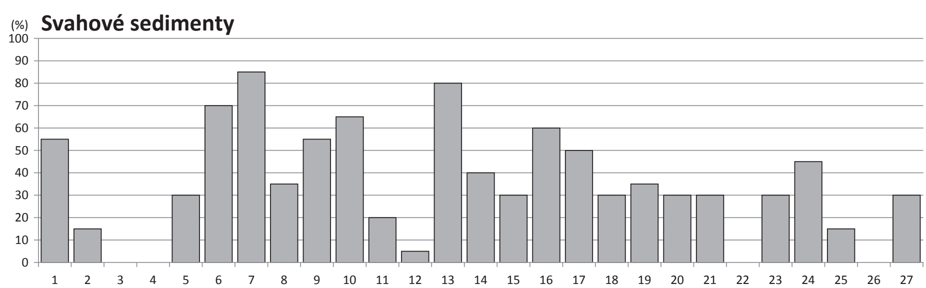
(%)
Svahové sedimenty
0 10 20 30 40 50 60 70 80 90 100
1 2 3 4 5 6 7 8 9 10 11 12 13 14 15 16 17 18 19 20 21 22 23 24 25 26 27

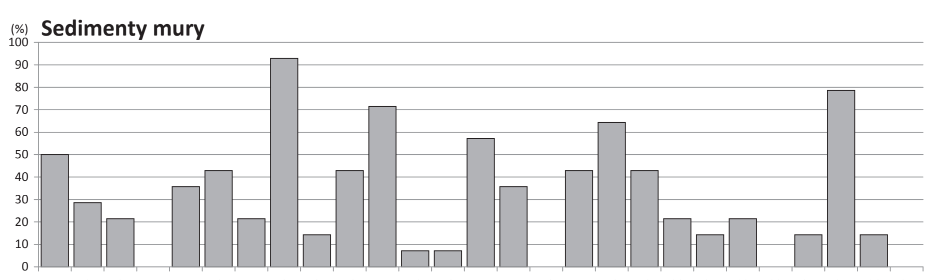
(%)
Sedimenty mury
0 10 20 30 40 50 60 70 80 90 100
1 2 3 4 5 6 7 8 9 10 11 12 13 14 15 16 17 18 19 20 21 22 23 24 25 26 27

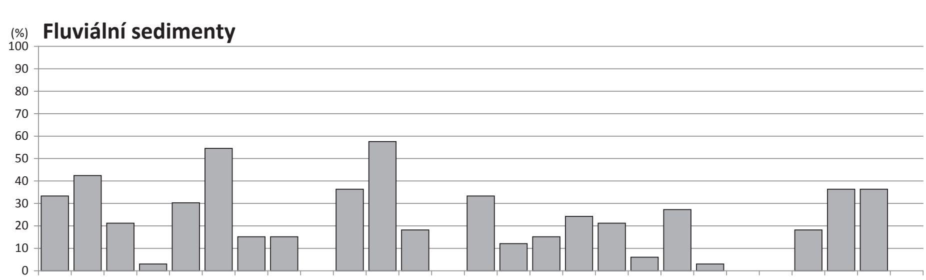
(%)
Fluviální sedimenty
0 10 20 30 40 50 60 70 80 90 100
1 2 3 4 5 6 7 8 9 10 11 12 13 14 15 16 17 18 19 20 21 22 23 24 25 26 27

lze konstatovat, že nejvyšší odlišnost od ostatních vykazují zrna fluviálních sedimentů (průměrná hodnota *d* je 1,333). Následují zrna mury (průměrná hodnota *d* je 1,105), morény (průměrná hodnota *d* je 1,06), eolických sedimentů (průměrná hodnota *d* je 1,045) a svahovin (průměrná hodnota *d* je 1,023), které mají nejvyšší průměrnou podobnost s ostatními studovanými zrny. Vůbec nejvyšší vzájemnou odlišnost vykazují zrna fluviálních sedimentů a svahovin. Naopak nejblíže k sobě mají zrna svahovin a labské morény (tab. 3).

6. Diskuse

S pomocí exoskopie se ze skenovaných vzorků podařilo nejspolehlivěji odlišit fluviální sedimenty, které mají na rozdíl od ostatních studovaných vzorků sedimentů nižší četnosti výskytu všech mikrotextur. Méně zřejmé jsou rozdíly v morfologii zrn svahových a morénových sedimentů, kde je potřeba věnovat vyšší pozornost četnostem a kombinacím charakteristických mikrotextur. Některé genetické typy sedimentů již byly popsány v literatuře (Krinsley, Doornkamp 1973 a Mahaney 2002), dle které se dalo očekávat, že eolická a fluviální zrna se budou charakterem svého povrchu více odlišovat od glaciálních sedimentů. Zatím však v literatuře uvedené charakteristiky nejdou do velkých detailů. Na základě popisů v literatuře tedy nelze interpretovat jemné rozdíly v charakteru zrn patřícím odlišným geomorfologickým tvarům se stejnou genezí. Ukázalo se, že sedimenty, které byly přepracovány gravitačními procesy, nelze snadno odlišit od glaciálních sedimentů, protože mnoho tvarů vyvinutých na křemenných zrnech obou typů sedimentů jsou stejné.

Fluviální zrna se obecně vyznačují křemičitými povlaky (Le Ribault 1975), V-jamkami (Mahaney 2002) a mísovitými jamkami (Clocchiatti, Le Ribault, Rodrigo 1978), popř. nárůsty křemene (Cremer, Legigan 1989). Vzorek fluviálního sedimentu je svými charakteristikami poměrně vzdálen všem ostatním studovaným vzorkům. Na základě koeficientu vzdálenosti je nejpodobnější muře v údolí Bílého Labe, což může mít souvislost s dřívějším vývojem zrn, než začala být unášena vodou. V případě zkoumaných fluviálních zrn byly charakteristické křemičité sraženiny (zejména v podobě křemičitých globulí a skrývek v rozsáhlejší podobě), avšak ve srovnání s ostatními studovanými vzorky sedimentů byl absolutní výskyt tohoto znaku poměrně malý. To mohlo být způsobeno vysokou energií toku v jeho horní části, kde dochází k obrušování křemičitých povlaků, jak popsali Cremer, Legigan (1989). Také četnost výskytu V-jamek a mísovitých jamek nebyla příliš vysoká, zvláště ve srovnání s glaciálními a gravitačními sedimenty. Popisovaná nízká frekvence výskytu V-jamek a mísovitých jamek je v rozporu s tím, co uvádí Le Ribault (1975) pro systémy horních toků s vysokými rychlostmi. Vzhledem k poloze odebraného vzorku nelze očekávat ani dlouhý transport, během kterého by byla zrna více opracována. Stupňovité tvary spíše naznačují, že materiál je ještě poměrně mladý a mohlo jít o odnesené částice ze svahů, popř. morén.

Podobnost zrn svahových sedimentů a morén vyjádřená koeficientem *d* může být způsobena tím, že byl morénový materiál původně (před transportem ledovcem, který však nebyl velký) deluviem či jiným sedimentem, který vznikl gravitačními pochody. Pro zrna studovaných svahových sedimentů je charakteristická abraze hran, výskyt brázd a puklinových ploch. U vzorku deluvia je abraze hran velmi četná (u 80 % zrn), avšak na zrnech není výrazná kvůli minimálnímu transportu. Výskyt dalších mikrotextur také potvrzuje charakteristiku tohoto genetického typu sedimentu, který prozatím nebyl v literatuře příliš zkoumán (zmiňuje se o něm pouze Mahaney 2002), totéž platí i pro mury. Výrazný je vysoký reliéf povrchu zrn deluvií, nízký reliéf se v tomto vzorku nenacházel vůbec. Příčinou je minimální transport deluvia od doby, kdy byl uvolněn od horniny. Tomu nasvědčuje i ostrohrannost zrn ve vzorku.

Zrna morény se obecně vyznačují výskytem štěpných plátků a přilnavých částic na svém povrchu (Krinsley, Doornkamp 1973; Halley, Krinsley 1974 aj.). Stejně je tomu i na zkoumaných zrnech morény Labe. Tyto znaky se pro ně stávají charakteristické zvláště po srovnání s ostatními vzorky z jiných prostředí. Charakteristické pro zrna labské morény jsou také paralelní rýhy a puklinové plochy. Další znaky rovněž odpovídají obecným popisům povrchů zrn morén, tj. výskyt lasturnatých lomů, stupňů a brázd (Whalley, Krinsley 1974 a Mahaney, Vaikmae, Vares 1991 vykládají genezi těchto mirkotextur odlišným způsobem), ačkoli frekvence výskytu lasturnatých lomů je v tomto případě vyšší u deluvia. Důvodem tohoto jevu může být mrazové zvětrávání, které se podílí na formování zdejších skalních výchozů, což lze dokladovat vznikem četných nových úlomků, které se pod výchozy nacházejí po jarní a zimní sezóně.

Mura je z pohledu geneze rovněž tvořena svahovými sedimenty, avšak významnou roli při jejich pohybu hraje voda, která, aby došlo k pohybu, musí nasytit deluvium. To má za následek, že abraze hran křemenných zrn není tak výrazná jako u deluvia. Zrna mury jsou nejméně podobná vzorku fluviálních sedimentů. Ačkoli během vzniku tohoto tvaru působila voda, její vliv byl velmi krátký na to, aby se vytvořily charakteristické znaky pro vodní prostředí. O působení vody vypovídá pouze poměrně velký výskyt omezených křemičitých sraženin na povrchu zrn vzorku, které se pravděpodobně utvářely během osychání jejich povrchu. V literatuře zmínky o exoskopii zrn mur, jakožto samostatného genetického typu, nejsou. Charakteristickými mikrotexturami pro zkoumaný vzorek byly lasturnaté lomy, stupňovité textury, abraze hran, V-jamky a obloukové brázdy. Zároveň bylo pro tato zrna příznačné malé opracování zrn.

Eolický sediment je dle výsledků koeficientu *d* podobný deluviu a moréně Labe. Eolická zrna jsou charakteristická výskytem štěpných plátků, nepravidelných prohlubní a impaktních tvarů, jako jsou V-jamky a mísovité jamky (Lindé, Mycielska-Dowgiałło 1980; Mahaney 2002 aj.). Zrna zkoumaného vzorku eolických sedimentů vykazují četnější výskyt jiných znaků, např. stupňovité textury a brázdy, drobné lasturnaté lomy a abraze hran, které jsou charakteristické spíše pro gravitační pohyby. Po srovnání s ostatními vzorky se však jeví vysoká frekvence výskytu i u V-jamek a mísovitých jamek (cca 50 %), které jsou považovány za charakteristické mikrotextury eolických sedimentů. Dle Mahaneyho (2002) pro eolické sedimenty typické štěpné plátky a nepravidelné prohlubně se však ve zkoumaném vzorku jako charakteristické neprojevily, jelikož ve vysokých četnostech se vyskytují také na křemenných zrnech studovaných glacigenních sedimentů, svahových sedimentů a mur (štěpné plátky) a fluviálních sedimentů (nepravidelné prohlubně).

7. Závěr

Uvedená metoda exoskopie povrchu křemenných zrn umožňuje stanovit způsob transportu, a tedy i genezi sedimentu, respektive daného tvaru, který je jím budován. U vzorků pocházejících z velmi podobného prostředí však nemusejí být výsledky zcela jasné a je zapotřebí použít více vzorků. Také je nutné znát samotné prostředí, kde byl vzorek odebrán, včetně jeho okolí, aby byly procesy formující povrch zrn správně přiřazeny jednotlivým genetickým skupinám.

Pro rozlišení genetických typů sedimentů nelze vždy přesně určit sadu vyskytujících se mikrotextur, spíše lze hovořit o určitých frekvencích výskytu, při kterých by se znak stal charakteristickým. Tyto frekvence výskytu by však nebyly pro všechny znaky stejné. Důležitou roli pro frekvenci výskytu představuje rychlost transportu v prostředí. Lasturnatý lom vzniká např. většinou po prudkých nárazech a odlomení částice od částice větší, což může nastat v kterémkoli prostředí, ale také může vzniknout mrazovým zvětráváním. Tyto nárazy jsou ale ve fluviálním prostředí tlumeny, charakteristická je tedy spíše nepřítomnost lasturnatého lomu pro fluviální sedimenty. Tilly jsou charakteristické naopak velmi vysokou četností lasturnatého lomu, což znamená, že tento znak se u nich vyskytuje alespoň ze cca 70 %. U jiných znaků však stačí menší procentuální podíl výskytu k tomu, aby byly označeny za charakteristické. Zdaleka ne vždy lze ale vysledovat toto přibližné hraniční procento a je potřeba počítat s polohou, s probíhajícími procesy v prostředí, ze kterého vzorky pochází, a nalezenými mikrotexturami. Musíme např. uvažovat nad tím, zda sediment byl donesen z vyšších poloh a jaké procesy probíhaly v těchto vyšších polohách, protože zrno nese na svém povrchu v různé zachovalosti i ty tvary, které byly utvořeny v předešlých prostředích. Podobně i Mahaney (2002) a Le Ribault (1975) upozorňují na to, že zrna si nesou mikrotextury z dřívějších prostředí. Ze znalosti prostředí (např. sklonitosti terénu) jsme schopni odhadnout, v jakých rychlostech zdejší procesy probíhají – v exoskopii např. V-jamky, srpkovité textury a mísovité jamky (Le Ribault 1975) vypovídají o rychlostech média, kterým je sediment unášen – a tím lépe pochopit výsledky exoskopie a určit, kde je přibližná hranice vysokého a nízkého výskytu jednotlivých mikrotextur.

Křemenná zrna glacigenních sedimentů jsou charakteristická výskytem lasturnatých lomů (či štěpných plátků, které jsou typicky vyvinuté na menších zrnech), stupňovitých tvarů, puklinovými plochami a přilnavými částicemi. Eolické sedimenty jsou charakteristické výskytem V-jamek, mísovitých jamek a vyšším zaoblením zrn. Pro deluvium jsou typické lasturnaté lomy, stupňovité tvary, brázdy a zejména abraze hran. Křemenná zrna murových sedimentů byla charakteristická lasturnatými lomy, stupňovitými tvary, brázdami a křemičitými sraženinami. Fluviální sedimenty mají oproti ostatním vzorkům celkově nízkou četnost mikrotextur a typický je pro ně nízký reliéf s vyšší zaobleností zrn a křemičité sraženiny, zvláště křemičité povlaky.

Literatura:

AALKASEEVA, V. A. (2005): Micromorphology of Quartz Grains Surface as Indicator of Glacial Sedimentation Conditions: Evidence from the Protva River Basin. Lithology and Mineral Resources, 40, č. 5, s. 420–428.

CATER, J. M. (1984): An application of scanning electron microscopy of quartz sand surface textures to the environmental diagnosis of Neogene carbonate sediments, Finestrat Basin, south-east Spain. Sedimentology, 31, č. 5, s. 717–731.

CENSIER, C., TOURENQ, J. (1986): Mise en évidence d'une extension occidentale des grés de Carnot (République Centrafricane) par analyses sédimentologiques comparées de gisements alluvionnaires diamantiféres. Géodynamique, 1, č. 1, s. 21–32.

CHLUPÁČ, I. (1999): Vycházky za geologickou minulostí Prahy a okolí. Academia, Praha, 280 s.

CLOCCHIATTI, R., LE RIBAULT, L., RODRIGO, L. A. (1978): Endoscopie et exoscopie de grains de quartz des formations du pliocène et du quaternaire de La Paz (Bolivie). Cahiers O.R.S.T.O.M., série Géologie, 10, č. 1, s. 127–143.

CREMER, M., LEGIGAN, P. (1989): Morphology and Surface Texture of Quartz Grains from ODP site 645, Baffin Bay. Proceedings of the Ocean Drilling Program, Scientific Results, 105, s. 21–28.

DOWDESWELL, J. A. (1982): Scanning electron micrographs of quartz sand grains from cold environments examined using Fourier shape analysis. Journal of Sedimentary Petrology, 52, č. 4, s. 1315–1323.

ENGEL, Z., TREML, V., KŘÍŽEK, M., JANKOVSKÁ, V. (2005): Lateglacial/Holocene sedimentary record from the Labe source area, the Krkonoše Mts. AUC–Geographica, XXXIX, č. 1, s. 73–88.

ENGEL, Z., NÝVLT, D., KŘÍŽEK, M., TREML, V., JANKOVSKÁ, V., LISÁ, L. (2010): Sedimentary evidence of landscape and climate history since the end of MIS 3 in the Krkonoše Mountains, Czech Republic. Quaternary Science Review, 30, s. 1–15. doi:10.1016/j.physletb.2003.10.071

FITZPATRICK, K. T., SUMMERSON, C. H. (1971): Some observations on electrone micrographs of quartz sand grains. The Ohio Journal of Science, 71, č. 2, s. 106–117.

HELLAND, P. E., HUANG, P. H., DIFFENDAL, R. F. (1997): SEM Analysis of Quartz Sand Grain Surface Textures Indicates Alluvial/Colluvial Origin of the Quaternary "Glacial" Boulder Clays at Huangshan (Yellow Mountain), East-Central China. Quaternary Research, 48, s. 177–186.

KOVANDA, J. et al. (2001): Neživá příroda Prahy. Academia, Český geologický ústav, Praha, 215 s.

KRÁLÍK, F., SEKYRA, J. (1969): Geomorfologický přehled Krkonoš. In: Fanta, J. et al. Příroda Krkonošského národního parku. SZN, Praha, s. 59–87.

KRINSLEY, D. H., DOORNKAMP, J. C. (1973): Atlas of quartz sand surface textures. Cambridge, Cambridge University, 91 s.

KUKAL, Z. (1986): Základy sedimentologie. Academia, Praha, 466 s.

LE RIBAULT, L. (1975): Application de l'exoscopie des quartz à quelques échantillons prélevés en Manche orentale. Philosophical Transacations of the Royal Society of London. Series A, s. 279–288.

LE RIBAULT, L. (2003a): LLR et le G5: Exoscopie – Définition scientifique. http://www.leribault.com/exo_definitionscientifique.php, cit. 2007-07-23.

LE RIBAULT, L. (2003b): LLR et le G5: Balade sur un grain de sable. http://www.loic-le-ribault.ch/exo_balademicroscopique_p01.php.

LINDÉ, K., MYCIELSKA-DOWGIAŁŁO, E. (1980): Some experimentally produced microtextures on grain surfaces of quartz sand. Geografiska Annaler A, 62, č. 3–4, s. 171–184.

LISÁ, L. (2004): Exoscopy of Moravian eolian sediments. Bulletin of Geosciences, 79, č. 3, s. 177–182.

MAHANEY, W. C. (1995): Pleistocene and Holocene glacier thickness, transport histories and dynamics inferred from SEM microtextures on quartz particles. Boreas, 24, s. 293–304.

MAHANEY, W. C. (2002): Atlas of sand grain surface textures and application. Oxford University Press, New York, 237 s.

MAHANEY, W. C., ANDRES, W. (1991): Glacially crushed quartz grains in loess as indicators of long-distance transport from major European ice centers during the Pleistocene. Boreas, 20, s. 231–239.
MAHANEY, W. C., CLARIDGE, G., CAMPBELL, I. (1996): Microtextures on quartz grains in tills from Antactica. Palaeogeography, Palaeoclimatology, Palaeoecology, 121, s. 89–103.
MAHANEY, W. C., KALM, V. (2000): Comparative scanning electron microscopy study of oriented till blocks, glacial grains and Devonian sands in Estonia and Latvia. Boreas, 29, s. 35–51.
MAHANEY, W. C., STEWART, A., KALM, V. (2001): Quantification of SEM microtextures useful in sedimentary environmental discrimination. Boreas, 30, s. 165–171.
MAHANEY, W. C., VAIKMAE, R., VARES, K. (1991): Scanning electron microscopy of quartz grains in supraglacial debris, Adishy Glacier, Caucasus Mountains, USSR. Boreas. 20, s. 395–404.
MAHANEY, W. C., VORTISCH, W., JULIG, P. (1988): Relative differences between glacially crushed quartz transported by mountain and continental ice – some examples from North America and East Africa. American Journal of Science, 288, s. 810–826.
MARGOLIS, S. V., KRINSLEY, H. (1971): Submicroscopic frosting on aeolian and subaqueour quartz sand grains. Bull. Geol. Soc. Am. B2, s. 3395–3406.
MATHUR, A. K., MISHRA, V. P., SINGH, J. (2009): Study of quartz grain surface texture by electron microscopy – a tool in evaluating palaeoglacial sediments in Uttarakhand. Current science, 96, č. 10, s. 1377–1382.
MELLOR, A. (1986): Textural and Scanning Electrone Microscope Observations of Some Arctic-Alpine Soils Developed in Weichselian and Neoglacial Till Deposits in Southern Norway. Arctic and Alpine Research, 18, č. 3, s. 327–336.
PETRÁNEK, J. (1963): Usazené horniny: Jejich složení, vznik a ložiska. Nakladatelství ČSAV, Praha, 720 s.
RŮŽIČKOVÁ, E., RŮŽIČKA, M., ZEMAN, A., KADLEC, J. (2003): Kvartérní klastické sedimenty České republiky. Česká geologická služba, Praha, 160 s.
STRAND, K., PASSCHIER, S., NÄSI, J. (2003): Implication of quartz grain microtextures for onset Eocene/Oligocene glaciation in Prydz Bay, ODP Site 1166, Antarctica. Palaeogeography, Palaeoclimatology, Palaeoecology, 198, s. 101–111.
VITÁSEK, F. (1923): O starých ledovcích na Krkonoších. Geografie (Sborník ČSZ), 29, č. 4, s. 196–199.
WHALLEY, W. B. (1982): A preliminary scanning electron microscope study of quartz grains from a dirt band in the Tuto ice tunnel, Northwest Greenland. Arctic and Alpine Research, 14, č. 4, s. 355–360.
WHALLEY, W. B., KRINSLEY, D. H. (1974): A scanning electron microscope study of surface textures of quartz grains from glacial environments. Sedimentology, 21, s. 87–105.
WILSON, P. (1978): A scanning electron microscope examination of quartz grain surface textures from the weathered Millstone Grit (carboniferous) of the Southern Pennines, England: A preliminary report. In: Scanning Electron Microscopy in the Study of Sediments. Univ. East Anglia, Norwich, s. 307–318.

S u m m a r y

APPLICABILITY OF QUARTZ GRAINS SURFACE ANALYSIS TO THE STUDY OF THE GENESIS OF UNLITHIFIED SEDIMENTS

Unconsolidated sediments are formed from redeposited and sedimented material, originating from broken rocks. No cement is involved, in contrast with consolidated sediments (Kukal 1986). We distinguish certain genetic types of loose sediments, which give evidence regarding their origin and the conditions of their formation.

There are several basic genetic groups of quaternary sediments that occur in Czechia: fluvial, glacial, eolian, gravitational and lacustrine. Research of these types of sediments aids in explaining the evolution and change of physical-geographic conditions over time.

One of the aims of geomorphology is to determine the origin of a relief. In some cases this can be deduced from relief material knowledge. Exoscopy is a method used to determine

sediment origin based on an understanding of microscopic surface textures on quartz sand grains (Margolis, Krinsley 1971; Fitzpatrick, Summerson 1971; Whalley, Krinsley 1974; Le Ribault 1975; Cremer, Legigan 1989; Mahaney 2002). We assume that this method will be used more frequently in Czech and Slovak geomorphological work, in the future. Therefore, one of the objectives of this article is to introduce this method and its potential and to establish Czech terminology that either does not exist or is inconsistent. The secondary objective of the article is to illustrate the extent, to which it is possible to distinguish different sediment origins using exoscopy.

Reference samples were chosen from geomorphological landforms of known origin (see Table 2): a moraine in the Labský Důl Valley, a debris flow in the Důl Bílého Labe Valley, flood accumulation and deluvium from a slope in the Důl Bílého Labe Valley in the Krkonoše Mountains and eolian sediment from Klárov in Prague.

The exoscopy method determines sediments' movements and thus their origin as well as the origin of landforms built by these sediments. However, results of samples originating from a very similar environment may not be sufficiently clear. Consequently, it is necessary to use multiple samples of a given landform. To ensure that processes forming the surface of grains are correctly assigned to genetic groups, it is also important to know the environment, from which a sample was taken.

Results suggest that it is not always possible to define an appropriate set of occurring microtextures in order to determine the genetic groups of sediments. Microtextures are characterized by certain occurrence frequencies. These frequencies are different for each microtexture and, so far, no frequencies have been set. Velocity of movement in different environmental conditions plays an important role in the frequencies.

Nonetheless, it is not always possible to observe the approximate characteristic percentages of occurrence in microtextures and it is important to consider connections between sediments and their location, ongoing processes in the local environment and the enumeration of observed microtextures. For example, one must consider the possibility that a sediment might have been moved from higher positions in the terrain and the processes that were occurring in those higher positions. Mahaney (2002) and Le Ribault (1975) also point out that the grains might have microtextures from previous environments.

With a knowledge of slope inclination, we are able to estimate the velocities of local geomorphological processes; for example V-shaped pits, crescent-shaped features and dish-shaped breakage concavities provide evidence concerning the velocity of transport medium (Le Ribault 1975). This can lead to a better understanding of exoscopy results and aid in establishing the approximate boundaries of the high and low occurrence of single microtextures.

Conchoidal fractures (or upturned plates on smaller grains), step forms, fracture faces and adhering particles are typical microstructures in quartz grains from glacigenous sediments. The occurrence of V-shaped pits, dish-shaped breakage concavities and a rather subrounded to rounded grain profile are typical for eolian sediments. Conchoidal fractures, step forms, grooves and especially edge abrasion are typical for deluvium sediments. The sample of debris flow sediment was characterized by the occurrence of conchoidal fractures, step forms, grooves and silica precipitation. Fluvial sediments generally have the lowest occurrence percentage of all microtextures in comparison with other samples and their characteristic forms are silica precipitations, especially silica pellicle and low relief with lower outline.

Fig. 1 – Most frequent forms present on surfaces of quartz grains: f – parallel striations, g – V-shaped pits, i – straight grooves, l – silica capping. A sample of eolian sediment; Prague-Klárov.

Fig. 2 – Most frequent forms present on surfaces of quartz grains: a – conchoidal fracture, d – fracture faces, h – crescent-shaped features, i – straight grooves, j – curved grooves, k – adhering particles. A sample of debris flow sediment; Důl Bílého Labe Valley, Krkonoše Mountains.

Fig. 3 – Most frequent forms present on surfaces of quartz grains: e – meandring ridges, l – silica capping, m – silica pellicle. A sample of fluvial sediment; Důl Bílého Labe Valley, Krkonoše Mountains.

Fig. 4 – Most frequent forms present on surfaces of quartz grains: b – straight steps, c- arcuate steps, k – adhering particles. A sample of deluvium; Důl Bílého Labe Valley, Krkonoše Mountains.

Fig. 5 – Most frequent forms present on surfaces of quartz grains: a – conchoidal fracture, c – arc-steps. A sample of glacigenous sediment; Labský Důl Valley, Krkonoše Mountains.

Fig. 6 – Graphs showing the frequencies of microtextures in the studied genetic types of sediments (moraine, eolian sediments, colluvium, debris flow, flood /fluvial/ sediments). 1 – angular outline, 2 – subangular outline, 3 – subrounded outline, 4 – rounded outline, 5 – low relief, 6 – medium relief, 7 – high relief, 8 – small conchoidal fracture, 9 – large conchoidal fracture, 10 – straight steps, 11 – arcuate steps, 12 – large fracture faces, 13 – parallel striations, 14 – edge abrasion, 15 – V-shaped pits, 16 – dish shaped concavities, 17 – straight grooves, 18 – curved grooves, 19 – meandring ridges, 20 – irregular depressions, 21 – upturned plates, 22 – pitting, 23 – oriented etched pits, 24 – adhering particles, 25 – limited silica precipitation, 26 – extensive silica precipitation, 27 – quartz crystal overgrowths.

Pracoviště autorů: L. Křížová a M. Křížek: Univerzita Karlova v Praze, Přírodovědecká fakulta, katedra fyzické geografie a geoekologie, Albertov 6, 128 43 Praha 2; e-mail: krizova@natur.cuni.cz, krizekma@natur.cuni.cz. L. Lisá: Geologický ústav, AV ČR, v. v. i., Rozvojová 269, 165 00 Praha 6; e-mail: lisa@gli.cas.cz.

Do redakce došlo 3. 2. 2010; do tisku bylo přijato 6. 2. 2011.

Citační vzor:
KŘÍŽOVÁ, L., KŘÍŽEK, M., LISÁ, L. (2011): Význam povrchové analýzy křemenných zrn pro studium geneze nezpevněných sedimentů. Geografie, 116, č. 1, s. 59–78.

5.5. Prostředí jezer a bažin

Libor P., Sádlo J., Žáčková P., **Lisá L.**, Novák J., Pokorný P. (2014): Late-Glacial and Holocene Environmental History of an Oxbow Wetland in the Polabí Lowland (River Elbe, Czech Republic); a Context-Dependent Interpretation of a Multi-Proxy Analysis.- Folia Geobotanica, 49, 2, 137 – 162.

Cílek, V., Bárta, M., **Lisá, L.,** Pokorná, A., Juříčková, L., Brůna, V., Mahmoud, A.M.A., Bajer, A., Novák, J. and Beneš, J. (2012): Diachronic development of the Lake of Abusir during the third millennium BC, Cairo, Egypt. Quaternary International, 266, pp. 14-24

Folia Geobot (2014) 49:137–162
DOI 10.1007/s12224-013-9171-3

Late-Glacial and Holocene Environmental History of an Oxbow Wetland in the Polabí Lowland (River Elbe, Czech Republic); a Context-Dependent Interpretation of a Multi-Proxy Analysis

Libor Petr · Jiří Sádlo · Pavla Žáčková · Lenka Lisá · Jan Novák · Jan Rohovec · Petr Pokorný

Abstract This study presents a palaeoenvironmental reconstruction of an oxbow wetland covering the past 11,500 years. The origin of the oxbow lake and development of the floodplain wetland and changes of the surrounding vegetation are reconstructed using palaeobotanical analyses, radiocarbon dating, detailed sediment stratigraphy and micromorphology of samples taken from a former palaeomeander of

L. Petr (✉) · L. Lisá · J. Rohovec
Academy of Sciences of the Czech Republic, Institute of Geology, Rozvojová 269, CZ-165 00 Prague 6, Czech Republic
e-mail: petr.libor@gmail.com

L. Lisá
e-mail: lisa@gli.cas.cz

J. Rohovec
e-mail: rohovec@gli.cas.cz

P. Žáčková
Department of Botany, Faculty of Sciences, Charles University, Prague, Benátská 2, CZ-128 01 Prague 2, Czech Republic
e-mail: pa.zackova@seznam.cz

J. Sádlo
Academy of Sciences of the Czech Republic, Institute of Botany, CZ-252 43 Průhonice, Czech Republic
e-mail: jiri.sadlo@ibot.cas.cz

J. Novák
Department of Botany, Faculty of Sciences, University of South Bohemia, Branišovská 31, CZ-370 05 České Budějovice, Czech Republic
e-mail: prourou@gmail.cz

P. Pokorný
Center for Theoretical Study, Charles University in Prague and Academy of Sciences of the Czech Republic, Jilská 1, CZ-110 00 Prague 1, Czech Republic
e-mail: pokorny@arup.cas.cz

the river Elbe in the Czech Republic. The sedimentary record of the section *Chrast* was chosen due to its exceptional position within the area of former oxbow lakes. Using a multi-proxy approach, we investigated how this environment reflected climatic changes during the Holocene. Our results show that the *Chrast* section covers the Late-Glacial to the Middle Holocene period, which is climatically very unstable and characterized by extensive vegetation and sedimentological changes. The macrofossil record provides detailed evidence of Allerød vegetation. The sedimentological record reflects changes in fluvial activity (meandering-braided transition in the channel pattern) during Late-Glacial/Holocene and postsedimentological changes (occurrence of a *doplerite* layer) in the middle Holocene. We follow three independent lines of interpretation: (a) a local autogenic environmental-succession process, (b) a regional process driven by climate change, and (c) the role of stochastic and indeterministic processes.

Keywords Floodplain deposits · Macrofossils · Micromorphology · Oxbow wetland · Pollen analysis · Random events · Succession

Introduction

Mire ecosystems can store a wealth of information about past ecological conditions and offer potential clues for understanding the character, strength and periodicity of past climate changes (e.g., Frenzel 1983; Engstrom and Wright 1984). This is because mire vegetation often accumulates organic material year after year. To properly understand and correctly interpret the palaeobotanical record, three conditions must be met: (1) production and accumulation of organic matter must be greater than the rate of its decay; (2) the accumulation of organic matter should happen without interruption; (3) diagnostically essential features of plants must be preserved well.

It is well-documented that these requirements are satisfied in the case of peat or lake sediments, where disintegration or redeposition is minimal, which can lead to the appearance of regularly laminated sediments in lakes (e.g., Saarnisto 1986; Hajdas et al. 1993; Tinner and Lotter 2001; Litt et al. 2001). The palaeoecological record in floodplain fluvial sediments, however, significantly differs from lake or peat sediments because of many disturbances and the influence of stochastic, allochtonous processes.

It is generally accepted that rivers represent geomorphic entities that are highly sensitive to environmental change, but it is ever more recognized that the fluvial response is extremely complex, with considerable spatiotemporal variability (Knox 1983; Törnqvist 2007). The development of any floodplain is based on a dynamic interaction between water, land and biota under the pressure of climatic changes (Mol et al. 2000; Makaske 2001; Vandenberghe 2003; Herget et al. 2007). The floodplain consists of contrasting types of abiotic habitats and vegetation communities that form a complicated pattern, changing spatially over time. The impacts of various climatic, hydrological and biotic conditions, such as dynamics of the water stream, sedimentary processes, successional vegetation stages, disturbance events, animal and human activities, alternate on a scale of years to hundreds of years. Unfortunately, little palaeobotanical work has been done on floodplains, because the alluvial environment is exceptionally heterogeneous, even though they are generally an attractive source for the preservation of the palaeobotanical and sedimentological records. The traditional concept of basin filling suggests the following phases that can be found as layers within the section under study: (a) bedrock material forming the bottom of a flowing river; (b) the early phase of sedimentation possibly with short-lived water and waterfront plants after the emergence of an oxbow lake; (c) the middle phase of sedimentation, which is optimal for littoral species of the lake environment, especially perennial clonal graminoids; (d) the terminal phase of terrestralization with land species including evergreen tree species (Ritchie 1995; Břízová 1998). Törnqvist (2007), for example, reports that climate changes are reflected in rivers through (1) the discharge regime, (2) changes in the channel pattern (fluvial activity); and (3) changes in the longitudinal profile through aggradation or degradation (incision).

In this paper, we focus on interpreting the palaeoenvironmental record of the *Chrast* section (the river Elbe floodplain, Czech Republic). This section records complex sedimentation sequences including abrupt changes in lithology, disturbance events and post-sedimentation processes. During our research, we decided to apply a multi-proxy approach that combines several methods to provide complexity and to compile a detailed reconstruction of the past environment and processes. Our study includes not only a standard pollen analysis but also a macrofossils analysis (Birks and Birks 2000), a charcoal analysis, and geomorphological, sedimentological (Bridge 2003), microstratigraphical (MacCarthy et al. 1998; Stoops 2003; Budek 2010) and geochemical approaches. This enables us to reconstruct an oxbow wetland with local vegetation, trace long-term succession, consider regional landscape patterns and describe sedimentological events from the past 11,500 years. We suggest three independent lines of interpretation, separately focusing on (1) local autogenic environmental-succession processes, (2) a regional process driven by climate change, (3) and the role of stochastic and indeterministic processes.

Study Region

The study area lies along the upper section of the river Elbe, a major watercourse in Central Europe. After the first ten kilometers of its course in the Giant Mountains piedmont, the river falls into a lowland formed by alkaline Mesozoic marine deposits (Czech Cretaceous Basin) mostly covered by acidic Tertiary/Quaternary riverine gravels (Fig. 1). Though the siliceous gravel deposits are nutrient-poor, the floodplain is richer because of the solution percolating from the bedrock. The stratigraphy of the surrounding Pleistocene gravel terraces was studied mainly by Balatka and Sládek (1962) and Žebera (1956). Their interpretation is difficult because of the loess cover and relatively plain relief. Růžičková and Zeman (1994) and Kalicki (2006) described the Holocene alluvial deposits in the study area. Břízová (1998), Dreslerová et al. (2004) and Pokorný (2005) described the Holocene environmental reconstruction based on pollen data from nearby sites Chrást, Kozly and Tišice.

For now, the studied site near the village of Chrást is the only palaeomeander found by the Elbe in the Czech Republic. Its sedimentological record covers the end

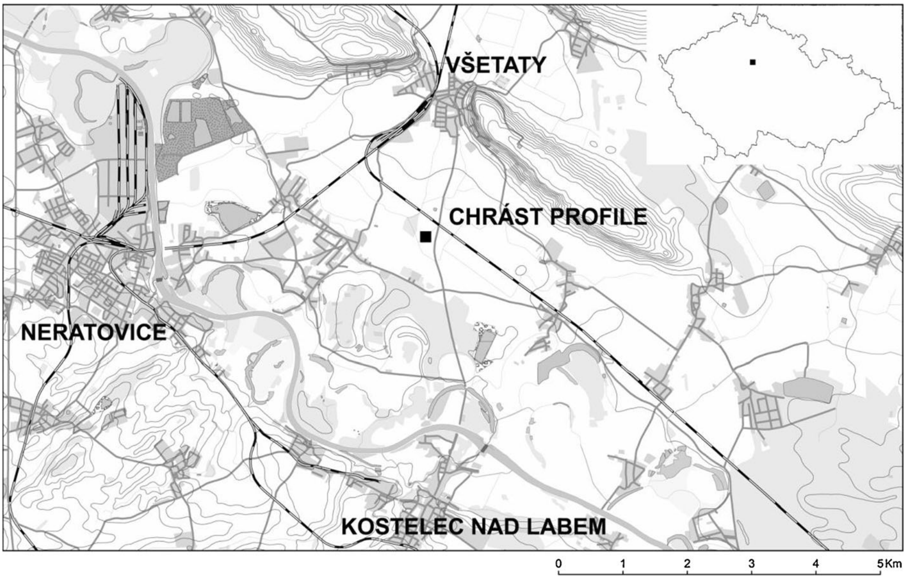

Fig. 1 The location of the section *Chrast*

of the Last Glacial period and the Holocene. The locality is 1.5 km north of the village of Všetaty (50°15′ N; 14°35′ E) in a low river terrace, about 2 km from the current river course and 5 m above its present-day water level (Fig. 1). Cornfields prevail in the surrounding landscape, but semi-natural habitats such as dry pine-oak forest or alluvial wetlands river Elbe are locally present near the present day floodplain of the river Elbe. A narrow strip of the former Late Glacial oxbow is covered by ruderal vegetation on drained soil, now under the influence of fertilization of surrounding intensively exploited arable fields. The present-day annual average temperature in the region is 8.7°C, and the annual precipitation is 527 mm (Culek 1996).

Methods

Trench *Chrast* was excavated to expose a stratigraphic section. The location for this trench was chosen after the completion of a large field survey and detailed screening of the locality using digital maps. The former oxbow lake was identified based on vegetation cues visible in aircraft imagery. The profile was sampled from a 2 × 2 m, 2.85 m deep pit. Samples were taken into steel boxes (10 × 10 × 50 cm). Every 3 cm of the lithological record (or more if sandy layers were present) were sampled for the pollen and geochemical analyses, and samples for macrofossil and charcoal analyses were taken every 10 cm of the section. Lithologically different parts of the section (Fig. 2) were sampled into small Kubiena boxes for micromorphological study. The profile was divided into zones based on lithology (zones marked CH0–CH6 for the entire section). In the pollen analysis, alternative zoning (zones marked 1–3) was

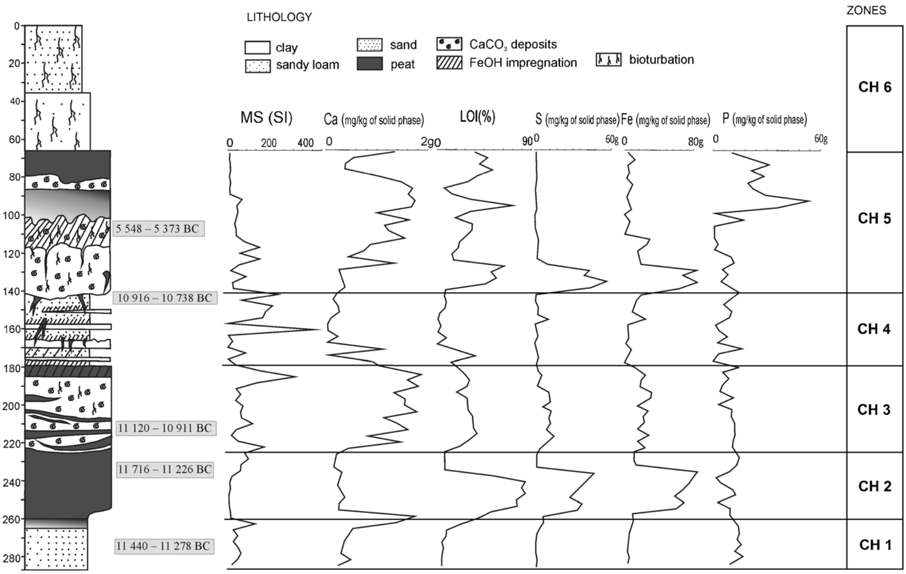

Fig. 2 The section *Chrast* and its geochemical properties and processes. Description of zones: CH1 – Accumulation of organic matter is reflected in increased amount of Fe, S, LOI, P and Mg, while MS and carbonates are low; CH2 – Carbonate precipitation is reflected in increased amount of Ca and Mg; CH3 – FeOH precipitation is reflected mainly by the increased amounts of Fe and slightly increased amounts of MS; CH4 – Magnetic susceptibility reflects predominantly the supply of exogenic very fine grained material, it means clay minerals deposited from suspension; CH5 – Increased amounts of LOI, S and Fe in the facie macroscopically free of FeOH or organic matter reflects the presence of bacterial producing pyrite nodules; CH6 – Most of the traced geochemical and magnetic elements except S and Fe show increased values in the depth of 70 and 90 cm below the surface. This reflects the process of slow oxidation (burning) when P coming from organic matter is fixed into carbonates and CaPO4 originates

made using a cluster analysis (Conslink) implemented within the program POLPAL (Nalepka and Walanus 2003).

Radiocarbon dating was performed following the ^{14}C AMS method in the radiocarbon laboratory in Poznań. The pine trunk was dated using the conventional ^{14}C method in the radiocarbon laboratory of the Nuclear Physics Institute of the Academy of Science of the Czech Republic (hereafter AS CR) in Prague. All of the five radiocarbon dates acquired were calibrated using the program OxCal 4.1. (Bronk Ramsey 2009). The chronostratigraphic division of the Late Glacial and Holocene used in the article follows Walker et al. (1999), and chronological boundaries also consider Björck et al. (1998). A micromorphological approach was taken to answer the question of the Last Glacial and Holocene transition. Small 3 × 4 cm blocks were sampled from the lithological record between 68 and 173 cm below the surface (9 samples). The samples were dried *in situ*, impregnated with resin and thin sectioned in the laboratory of the Institute of Geology AS CR in Prague and followed by the standard description (Bullock et al. 1985; Stoops 2003).

Chemical analyses cover mainly ICP EOS (inductively coupled plasma/emission optical spectroscopy) analyses of main macroelements. The acid leachable fraction of macroelements was measured for each of the lithologically distinct horizons. Each sample (0.5–1 g) was precisely weighed together with 20 ml of a 20 % solution of aqueous hydrochloric acid (ultrapure, Merck) in a beaker covered with watch glass. After the completion of the reaction, the content was left to stand overnight. The remaining solid material was filtered through a piece of filter paper (blue strip) and thoroughly washed with water. Finally, the volume was increased to 100 ml in a volumetric flask. The chemical analyses were performed using the ICP EOS technique on an Intrepid DUO spectrometer (ThermoFisher) at the Institute of Geology AS CR in Prague. The macroelement (Ca, Fe, K, Mg, Mn, Na, P, S) concentrations were measured under standard experimental conditions recommended by the manufacturer using dual plasma view and 2.5 ml/min sample intake. For the calibration, mixed standard solutions were prepared combining commercial 1,000 ppm solutions of single elements in 2 % nitric acid solution. Calcium concentrations are independent of red-ox conditions and do not reflect the amount of oxygen/reducing activity in the mother solution.

Organic matter was measured by a LOI analysis (550°C) according to Heiri et al. (2001) and Holliday (2004). The temperature used for drying was 105°C, and the length of combustion was 3 hours.

Magnetic susceptibility was measured using a kappabridge KLY-4 device at the Laboratory of Paleomagnetism of the Institute of Geology AS CR in Průhonice.

Pollen analyses were performed using the standard acetolysis method using HCl and HF (Moore et al. 1991). Pollen grains were distinguished using pollen keys (Reille 1995, 1998; Beug 2004). The pollen sum in each sample was at least 500 grains. The pollen diagram was plotted in the POLPAL program for Windows (Nalepka and Walanus 2003) including the numerical analyses (Rarefraction, Conslink, PCA) for the visualization and the interpretation of pollen data. Pollen grains were divided into a regional group of terrestrial (Fig. **3**) and a local group (Fig. **4**) of wetland taxa.

Samples for macrofossil analyses (varying between 350–360 ml) were soaked in water and, when necessary, boiled with 5 % KOH. The extraction of plant macrofossils from the sediments followed standard flotation and wet-sieving procedures (Wasylikowa 1986; Pearshall 1989; Jackomet and Kreuz 1999), using a 0.25 mm sieve. Botanical macrofossils were picked out from the recovered fraction and scanned using a stereo-microscope (the magnification 8–56x). Identification was carried out by consulting seed and fruit atlases (Beijerinck 1947; Katz et al. 1965; Schermann 1967; Berggren 1969; Cappers et al. 2006; Velichkevich and Zastawniak 2006) and by comparing samples with recent reference material stored at the Department of Botany, Charles University in Prague.

Antracological and xylotomy analyses of charcoal and wood remains were performed only on fragments from the largest fraction (>2 mm). The identification of charcoal fragments, carried out using an episcopic microscope, was done with an interactive identification key (Heiss 2000) in addition to standard references (Schweingruber 1990). The quantitative and qualitative data obtained from plant macrofossils and charcoal identification are presented in a macrofossils diagram (Fig. **5**) plotted using the POLPAL program for Windows (Nalepka and Walanus 2003).

Lithological zones CH0 and CH6 were not analyzed due to insufficient preservation of the palaeobotanical record.

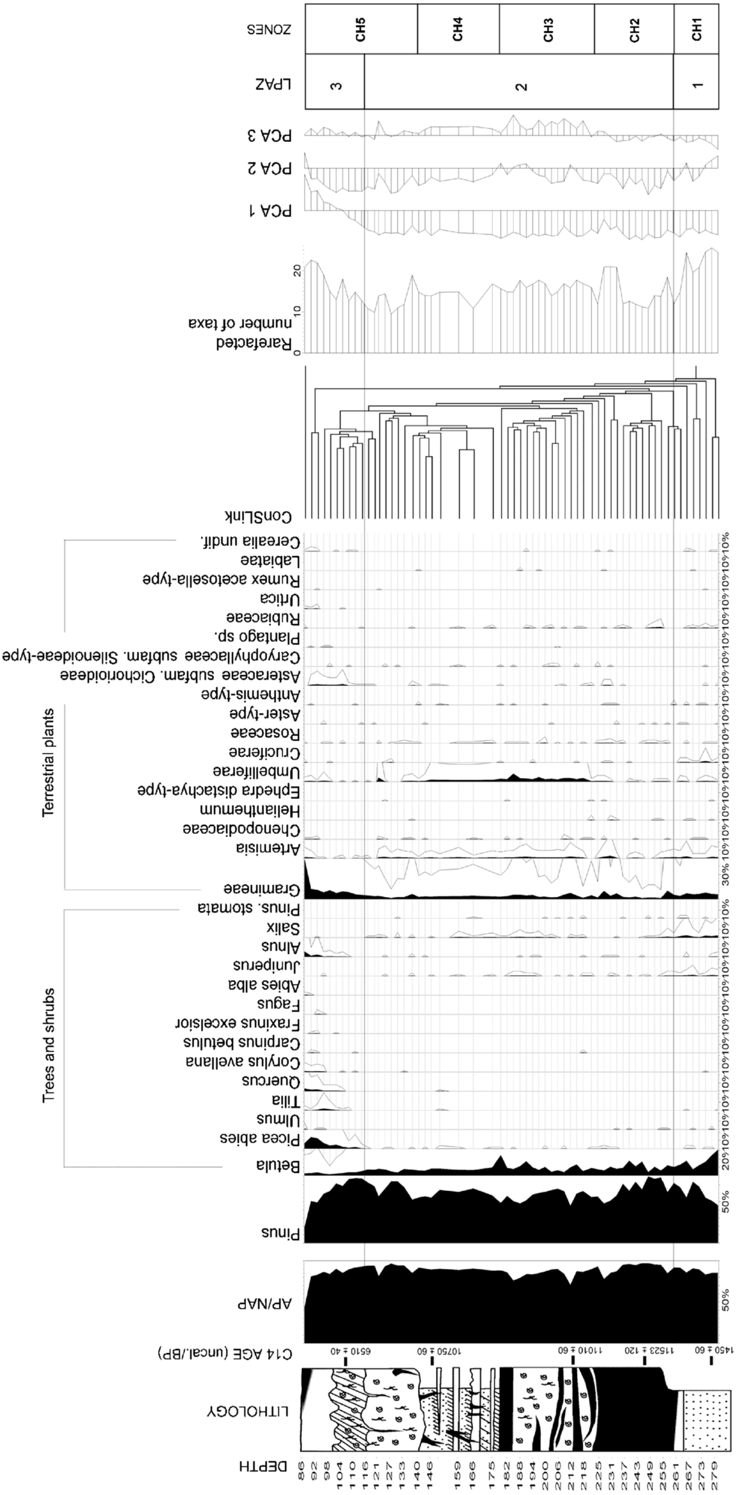

Fig. 3 The pollen diagram of terrestrial species

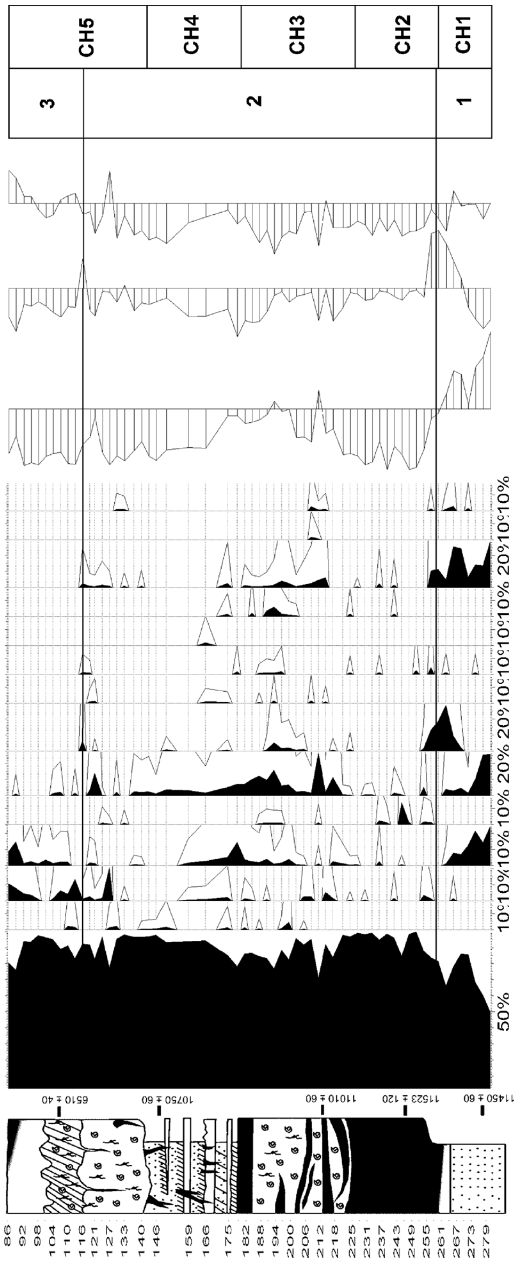

Fig. 4 The pollen diagram of local species

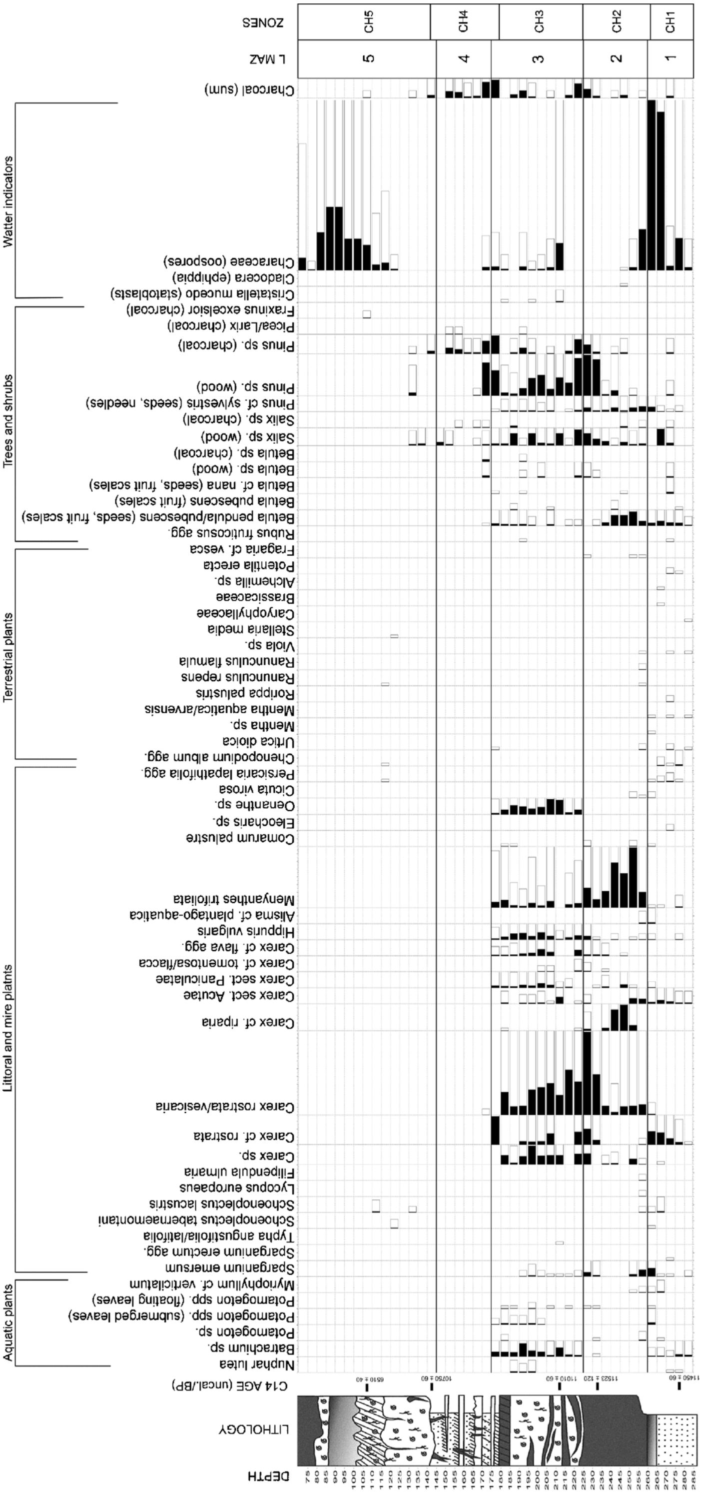

Fig. 5 The macrofossil diagram. *Potamogeton* submerged leaves – CH1 zone: *P. pusilus*, *P. obtusifolius*; CH3 zone: *P. filiformis*

Results

Radiocarbon Dating

The results of radiocarbon dating are presented in Table 1. Dates (Table 1) from the base of the section (11,450±60 BP; 11,523±120 BP) correspond with the Allerød/Bølling interstadial, the date 11,010±60 BP corresponds with the transition from Allerød to the Younger Dryas, while the date 10,750±60 BP corresponds with the beginning of the Younger Dryas. A fragment of charcoal of *Fraxinus excelsior* recovered from the depth of 105–110 cm was dated to the Middle Holocene (6,510 ±40 BP; Middle Atlantic).

Lithology and Micromorphology

Six main lithological zones (CH1–CH6) of the *Chrast* section (Table 2; Fig. 2) were described on the basis of sedimentological and microstratigraphical observations. Micromorphological observations are summarized in Table 3 and Fig. 2.

Chemical Analyses, Loss on Ignition (LOI) and Magnetic Susceptibility (MS)

Calcium concentrations were remarkably high in zones CH1, CH3, CH5 and CH6 (Table 3). In all sections (Fig. 2), calcium concentrations in leachates were well correlated with the clay ratio in the sediment (Table 2) and with the occurrence of mollusc shell fragments (Table 3) and oospores of *Characeae* algae (Tables 3 and 4; Fig. 5). Figure 2 shows the relationship between leachable Fe with sulfur/SO_4^{2-} content at depths of 120–140 cm and 230–250 cm (zone CH2, CH5). Our micromorphological observation confirmed that the layer between 120 and 140 cm is extremely rich in bacterial spherical products (FeS_2 – pyrites). Increased values of phosphorus in zone CH5 at depths of 70–90 cm and 130–140 cm, and in zone CH2 at 240–250 cm correlate with increased values of organic matter measured by LOI and based on the micromorphological observation also

Table 1 Radiocarbon dates (AMS) from the *Chrast* section

Depth (cm)	Lab. nr.	Method	Material	^{14}C age (BP)	Cal. (BC)
105–110	Poz-21028	AMS	Ash charcoal	6,510±40	5,548–5,373
145–150	Poz-20980	AMS	Pine wood	10,750±60	10,916–10,738
210–215	Poz-22832	AMS	Menyanthes seed	11,010±60	11,120–10,911
230–235	Crl-6199B	Con.	Pine trunk	11,523±120	11,716–11,226
275–280	Poz-22833	AMS	Menyanthes seed	11,450±60	11,440–11,278

BC – before Christ, BP – before present (1950)

Table 2 Stratigraphy and lithological description of the *Chrast* section

Depth (cm)	Color	Depositional environment	Lithology
Zone CH0			
Below 285	Not analyzed	Sandy gravel layer strongly saturated by water.	Fluvial
Zone CH1			
285–265	10YR 7/1	Slightly calcareous loamy sand, light gray with a very gradual change toward the overlaying layer. The transition between this and the previous layer is abrupt.	Fluvial/Aeolian/Limnic
265–259	10YR 6/1	Calcareous sandy clay, gray, with an abrupt change and increasing amount of organic matter toward the overlaying layer.	Limnic
Zone CH2			
259–223	7.5YR ¾	Non-calcareous decomposed and compacted peat, dark brown, with an abrupt change toward the overlaying layer.	Terrestrial
Zone CH3			
223–185	10YR 2/2 10YR 8/2	Strongly calcareous laminated layer of clay interrupted by 1–4 cm thin layers of decomposed peat, with an abrupt change toward the overlaying layers. The color varies from very dark brown to very pale brown due to the presence of more calcareous or more peaty material. Root bioturbation is slightly recognizable and the change toward the overlaying layer is abrupt.	Limnic-terrestrial (redeposition, bioturbation)
185–179	10YR 3/1 10YR 5/2	Calcareous, strongly degraded clayey peat impregnated with FeOH-rich solutions coming from decomposed organic matter. Color varies from very dark gray to grayish brown due to the state of the decomposition of peat. The change toward the overlaying layer is abrupt.	Terrestrial-limnic
Zone CH4			
179–142	10YR 6/4	Slightly calcareous sandy layer including thin layers (app.1 cm) of clay and clay loam, with eroded surface at a depth of 159 cm, 169 cm, 166 cm, 175 cm. The color varies between light yellowish brown and light gray due to oxidation	Fluvial-limnic (root bioturbation)

Table 2 (continued)

Depth (cm)	Color	Depositional environment	Lithology
		and reduction processes and due to the grain size changes, with an abrupt change toward the overlaying layer.	
	10YR 7/1 10YR 2/2	Obvious presence of coarse grains of mica. Voids are filled with decomposed organic material of Mn oxides, very dark brown.	
Zone CH5			
142–118	10YR 6/1	Calcareous clay, gray with an abrupt change toward the overlaying layer.	Limnic (bioturbation, ox-reduction)
118–102	5YR 5/8	Calcareous silty clay, yellowish red, with a very gradual change toward the overlaying layer.	Limnic (root bioturbation, oxidation)
102–86	10YR 4/2	Calcareous clay layer, dark grayish brown, with an abrupt change toward the overlaying layer.	Limnic (root bioturbation, oxidation)
86–80	10YR 8/3	Calcareous silty clay, very pale brown, with a gradual change toward the overlaying layer.	Limnic (root bioturbation, oxidation)
80–67	10YR 2/1	Calcareous clay impregnated with organic matter rich solutions, macroscopically described as decomposed black peat with an abrupt change toward the overlaying layer.	Terrestrial-limnic (root bioturbation, oxidation)
Zone CH6			
67–35	10YR 5/2	Degraded calcareous silty peat grayish brown, with an abrupt change toward the overlaying layer.	Terrestrial (root bioturbation)
37–0	10YR 3/2	Very dark grayish brown anthropogenic material.	Anthropogenic (degradation)

Table 3 Micromorphological description of the *Chrast* section (Fig. 2)

Depth (cm); zone	Subzone	Micromorphological characteristic	Interpretation
Sample X1			
173	A (bottom)	Single grain microstructure of sandy material with monic grain distribution	High lithological variability as a result of differing provenience and origin. Phases of unstability and redeposittion are altering with phases of stagnant water with the organic matter accumulation and carbonate precipitation. Postdeposittional presence of redox FeS bacteria.
Zone CH4	B	Intergrain channel microstructure of sandy loam, grey to orange crystallic matrix, carbonate void coating, partly decomposed organic matter.	
	C	Intergrain channel microstructure of sandy loam, horizontal pores and crystallic matrix with grey-orange color, void coating and the presence of partly decomposed organic matter. FeS bacteria products.	
	D (top)	Single grain microstructure of sandy material with monic grain distribution.	
Sample X2			
150	A (bottom)	Intergrain channel microstructure of well-sorted sandy loam. Channels infilled by decomposed and partly decomposed organic matter, FeS bacteria products, crystallic B fabric of light brown matrix.	Phases of unstability presented by washouts with continuous organic matter production. Postdepositional presence of redox FeS bacteria.
Zone CH4	B (top)	Simple packing to intergrain microaggregate microstructure of sandy material, dark brown matrix with decomposed and partly decomposed organic matter, locally very poorly sorted material, lenses of redeposited braunhlem plasma, carbonate concentrations and products of FeS bacteria.	
Sample X3			
135	A (bottom)	Microaggregate to channel microstructure of silty loam, FeOH counting, decomposed and partly decomposed organic matter, products of FeS bacteria, depletion pedofeatures.	Phases of stagnant water and dessication. Postdepositional impregnation by Fe-rich solutions, presence of redox FeS bacteria.
Zone CH5	B	Intergrain microaggregate microstructure of sandy layer, light and dark brown matrix, partly decomposed organic matter, products of FeS bacteria, relicts of horizontal bedding, strong bioturbation.	
	C (top)	Single grain microstructure of silty loam, gefuric related distribution, locally channel microstructure. Crystallic B fabric, hematite microaggregates, FeS products of bacteria rare, decomposed organic matter, bioturbation.	

Table 3 (continued)

Depth (cm); zone	Subzone	Micromorphological characteristic	Interpretation
Sample X4			
120		Intergrain microaggregate and channel microstructure of silty loam, light brown crystalline matrix, carbonate precipitation, mollusc shells, decomposed and partly decomposed organic matter, FeOH impregnation, bioturbation.	Stable alkaline, stagnant environment carbonate precipitation, continuous organic matter production postdepositional impregnation by Fe-rich solutions.
Zone CH5			
Sample X5			
105		Intergrain microaggregate and channel microstructure of silty loam composed of quartz grains and carbonate crystals, channels and chambers, gray brown and crystallic matrix, mollusc shells and *Chara* oogonias very common, FeOH impregnation presented as a *doplerite*, decomposed and partly decomposed organic matter, bioturbation	Long-term stable alkaline conditions, with rich carbonate precipitation, organic matter production postdepositional impregnation by Fe-rich solutions, origin of doplerite appearance
Zone CH5			
Sample X6+X7			
90 + 80		Channel microstructure of silty loam composed of quartz grains and carbonate crystals and aggregates, channels and chambers, grey brown and crystallic matrix, carbonate and mollusc and *Chara* oogonias concentrations postdepositionally corroded and impregnated by ferrum hydroxides. Root bioturbation, presence of decomposed and partly decomposed organic matter.	Long-term stable alkaline conditions, with rich carbonate precipitation, organic matter production postdepositional impregnation by Fe-rich solutions, corrosion of carbonate features, doplerite appearance
Zone CH5			
Sample X8+X9			
75 + 68		Subangular blocky microstructure of organic matter rich matrix, channel and chamber microstructure of carbonate rich matrix. Channels and vughs, cracks, matrix composed mainly of carbonate crystals (fragments of shells occur) or organic-rich solutions. Color of matrix depends on the lithology and varies from light grey to reddish brown.	Long-term alkaline conditions with carbonate precipitation, high organic production, postdepositional impregnation with Fe-rich solutions, corrosion of carbonate, origin of doplerite layers
Zone CH5			

correspond with the appearance of layers rich in organic matter, that is, material precipitated from organic-rich solutions (Table 3). The total magnetic susceptibility varied between 450 and 1.5×10^{-6} SI. The highest values generally reflected the presence of the clay fraction, while the lowest ones reflected the presence of the sandy diamagnetic fraction and organic material (zone CH4).

Table 4 Macrofossils assemblages of the *Chrast* section (Fig. 3)

Depth (cm)	Macrofossil assemblage description
Zone context	
Zone CH1 285–260	Zone CH1 covers early stage of organic sedimentation. This corresponds with the beginning of the vegetation succession. High number of recorded species shows easy way of botanical ecesis and low interspecies competition. High species richness in this zone is remarkable. Different groups of plant communities distinguished here cover species with different requirements for moisture and nutrients; this indicates heterogeneity in habitats under disturbance pressure during dynamic changes in the river channel.
Samples 1-5	Oospores of algae *Chara* are encrusted with calcium. This indicates a shallow carbonate-rich water body with fluctuating water level and clay or loam bottom.
	Diaspores of water macrophytes, sedges and reeds indicate an oligo-mesotrophic lake with littoral vegetation on the shore line.
Zone CH2 260–225	Macrophytes and mire species in zone CH2 indicate the presence of an unstable shallow lake and transitional mire vegetation. High level of organic production caused terrestralization of the water body.
Samples 6-12	Spatial heterogeneity of habitats and pressure of disturbances are lower.
Zone CH3 225–175 Samples 13-20	In zone CH3 has remarkable restoration of a still-water habitat with well-developed littoral vegetation, similar to zone CH1. It shows retrogression of succession and a higher level of disturbances.
Zone CH4 175–140 Samples 21-29	Zone CH4 is extremely poor, and mainly charcoal and wood fragments can be found. Other plant macrofossils are missing. This can be interpreted as a bottom of the river without vegetation, or floodplain under the influence of the big flood episodes or postdeposition loss of macroremains due to the influence of bioturbation and oxidation processes.
Zone CH5 140–86	For Zone CH5 the low content of plant macrofossils is significant. Vegetation cover is poor in species, probably due to the influence of food or bioturbation and high level of mineralization.
Samples 30-43	Presence of oogonias of *Chara* and seeds of *Schoenoplectus tabernaemontani* indicate a mesotrophic water body rich in carbonates.
	Fraxinus charcoal was redeposited. Ruderal species show influence of floods.

Analyses of Plant Macrofossils and Pollen

Results of macrofossil analysis (see Fig. 5), show significant changes. Six local macrofossil assemblage zones (LMAZ) were distinguished using cluster analysis (Conslink) implemented in POLPAL; moreover, in light of sedimentological results, it is clear that macrofossil zones correspond with lithological zones. Species diversity and abundance of plant macrofossils were most marked in zones CH1, CH2 and CH3; in addition, macrofossils (e.g., surface sculpture) were remarkably well preserved in these zones. By contrast, the sandy zone CH4 had a low frequency of subfossil seeds and fruits, but charcoal and wood fragments were common. Zone CH5 contained also a small amount of vascular plant macrofossils, and the surface sculpture of plant macrofossils was considerably degraded; only oospores of green algae *Characeae* in zone CH5 were frequent, as seen in Fig. 5.

Pollen analysis results presented in pollen diagrams (Figs. 3 and 4) show indistinct changes. The observed pollen spectra were rather uniform, therefore only three local pollen assemblage zones (LPAZ), identified using cluster analysis, were distinguished. Apart from zone CH5b, it is difficult to determine any development or changes in the diagram. This was also confirmed in the PCA and Rarefraction analysis (Fig. 3).

Description of Pollen Assemblages

LPAZ 1: 261–279 cm (Zone CH1)

The AP/NAP ratio is about 80 %. The curve of *Pinus* increases from 40 % to 90 % while *Betula* declines from 30 % to 10 %, *Salix* and *Juniperus* form closed curves. *Alnus*, *Picea*, *Ulmus* and *Tilia* pollen was very rare. NAP is dominated by grasses and sedges. *Helianthemum*, *Chenopodiaceae* and *Thalictrum* occur occasionally. Water species were represented, e.g., by *Myriophyllum*, *Batrachium* and algae *Pediastrum*.

LPAZ 2: 120–260 cm (Zone CH2, CH3, CH4, CH5a)

The AP/NAP ratio varies between 50 % and 85 %. *Pinus* (50 %–80 %) and *Betula* (5 %–20 %) dominate whereas *Picea*, *Juniperus*, *Alnus* and *Salix* are rare. In NAP, sedges (30 %) prevail over grasses (5 %). The following pollen taxa had variable occurrence: *Artemisia*, *Ranunculaceae* and *Umbeliferae*. Occurrence of water taxa (*Myriophyllum*, *Potamogeton* and *Pediastrum*) was sporadic.

LPAZ 3: 86–120 cm (Zone CH5b)

The AP/NAP ratio is about 70 %. *Pinus* dominates, but the curve falls from 80 % to 50 %. Only in this zone did broad-leaved woody species of mesophilous habitats expand (*Corylus*, *Fraxinus*, *Quercus*, *Tilia*). The curve of *Betula, Picea, Tilia, Quercus, Corylus* and *Alnus* rapidly increases. *Ulmus*, *Fagus* and *Abies* appear. Grasses and sedges still create an important component of NAP spectra. Other herb taxa (*Artemisia*, *Chenopodiaceae*, *Thalictrum*, *Ranunculaceae* and *Umbeliferae*) are less common. *Cerealia* pollen appears. Wetland taxa are absent, except for *Typha latifolia*. Microcharcoal (including grass types) is extremely common, and its concentration increases from the depth of 100 cm. The quality of preservation in this zone is poor (mechanical and chemical damage of pollen grains).

Pollen grains from the depth of 0–86 cm are largely degraded and not identifiable. The pollen record therefore cannot be used for further interpretation.

Discussion

Interpretation Context 1: Local Environmental Processes

The first approach to the interpretation of the section is based on local changes of the environment and vegetation. Our results document that erosion-accumulation processes and vegetation succession took place during infilling of the inactive river channel.

Sedimentation processes

Our results provide compelling evidence that the development of the palaeoriver channel *Chrast* more or less followed the general scheme described in the Introduction.

Gravels and sands described at the bottom of the section *Chrast* (CH0) represent former channel bed-load of an active river. In the following period (CH1–CH3), the inactive river channel was filled up by overbank deposit (silt and clay), represented by suspended-load sediments that accumulate on floodplains in an environment of slowly flowing to stagnant water. Two types of sediments alternated: (a) loamy or clayey sediments were formed in still water rich in percolated carbonates, whereas (b) nutrient-poor organic sediments were formed on dry land. These changes are illustrated in the geochemical record in zones CH1–CH3 (Fig. **2**); the increase of Ca and Mg positively correlates with carbonate precipitation, while their decrease in zone CH2 (220–260 cm), where S and Fe increase, characterizes the sedimentation phase of organic material and bacterial activity.

A dramatic change is evident at the depth of 179 cm, at the beginning of zone CH4 due to the occurrence of sandy layers. Sandy layers give evidence of the accumulation phase during flood events and represent overbank deposits, as reviewed by Aslan (2007); this is connected with floodplain aggradation, as found by Makaske (2001). A detailed micromorphological investigation revealed the presence of clay layers in zone CH4 (Fig. **2**). The alternating sand and clays resulted from fluvial activity of a braided river in a limnic environment. Several studies have documented braided river system as a typical morphological phenomenon of splitting river channels (e.g., Makaske 2001; Vandenberghe 2003; Törnqvist 2007), and our results provide evidence for such a split channel of the river Elbe.

The record in the CH5 zone is somewhat striking. Despite chemical changes, several remarkable horizons of different colors were found (Fig. **2**). Chemical sedimentation of calcium-rich material was characteristic for this zone. This material is interpreted as lake marl that originated in a shallow limnic environment during a long period of activity of underground water sources rich in carbonates. At the base of zone CH5 (depth range 120–140 cm), intensive bacterial activity was identified chemically and even micromorphologically (Table **3**). At the bottom of zone CH5, carbonate accumulation and organic matter increase (LOI curve up to 70 %); Fe and S values are strikingly high, too. The geochemical structure was largely influenced by post-depositional changes caused by the activity of root systems and the bacterial activity linked to it. Higher parts of zone CH5 (67–120 cm) are remarkable for the significant increase of Ca and Mg and also for the minimal values of MS (probably due to the reaction to diamagnetic carbonate). Also the values of Fe and S are very low. This geochemically homogenous part of zone CH5 is macroscopically light reddish and microscopically black, resembling horizons rich in organics or iron. These layers were identified as *doplerite*. This native hydrocarbon material emerged before total decomposition of topsoil within the largely degraded and anthropogenically influenced fen. The sapric porous horizon (Dinc et al. 1976; Fox 1985) with decomposed organic matter (Manoch 1970; Fox 1985) was transported downward in the section as solutions and, so *doplerite* emerged (Koopman 1988). We found that this substance further precipitated and created a solid, opaque crust. The *doplerite* layer does not contain many plant macrofossils although it resembles a layer rich in organics and also its values of LOI and P indicated the presence of organic acids. We suggest that this appears as a consequence of penetration of these acidic solutions, the subsoil layers rich in carbonates being partially corroded. The sedimentology of this zone is thus based on the competition of several disparate processes: the sedimentation of the clay matrix, carbonate precipitation and the accumulation of organic substance, bioturbation and postsedimentation processes caused the intensification of bacterial activity followed by decomposition of most organic matter including macrofossils, corrosion of carbonate layers, establishment of a *doplerite* solution (Stoops et al. 2010), and its movement through the site.

The youngest zone, CH6, is characterized by sedimentation within a fen that was consequently degraded and largely anthropogenically influenced. The record of local fires can be observed in the form of a black sediment within the studied section and proven thanks to the presence of micromorphologically visible charcoal. Microscopic charcoal particles documenting a human influence were also identified in the pollen slides. The section is covered by an anthropogenic backfill from the second half of the 20th century.

When looking at vegetation succession – history of local vegetation and changes in hydroseries, zone CH1 represents the initial phase of vegetation succession and is characterized by the contemporary occurrence of three groups of species that differ in their habitat requirements. The first group consists of species that can promptly colonize habitats with well utilizable nutrients. These competitively weak species indicate the influence of constant disturbances. This group includes stoneworts (*Chara*) and still water macrophyte plants (*Nuphar lutea*, *Potamogeton filiformis*, *Batrachium* sp.) that occur in shallow water bodies (alluvial pools, oxbows) with stagnant or slowly moving water with mineral sediment. The second group consists of littoral species that can colonize sandbanks and withstand changes in water level (*Alisma, Sparganium*, *Eleocharis*, *Hippuris*, *Schoenoplectus*). The third group is represented by nutrient-demanding herbs growing on alluvial sediment accumulations on the banks (*Persicaria lapathifolia*, *Rorippa palustris*, *Chenopodium*, *Ranunculus repens*, *Mentha, Urtica*). The substrate is usually gravel and sand with a good nutrition supply, as found by Šumberová and Lososová (2011). This "ruderal" group of annual nitrophilous wetland herbs has its optimum in zone CH1 and remarkably recedes due to transitional terrestralization and the competition of perennials and appears in zone CH3 where carbonate and clay sedimentation is renewed.

The group of perennial clonal species, responsible for the extinction of the oxbow lake and the origin of the fen in an undisturbed environment has its optimum in zone CH2 and persists in zone CH3. Clonal perennial plants prevailing here include the following: (a) graminoids (*Carex rostrata/vesicaria*, *C.* sect. *Acutae*, *C.* sect. *Paniculatae*, *C. tomentosa/flacca*, *C. flava*) and (b) dicotyledonous plants (*Menyanthes*, *Comarum*, *Cicuta*). The vegetation is classified as a calcium-rich fen with typical calcium-loving species, for example, *Carex flacca/tomentosa* and *Carex flava*. The sediment contains less calcium as a result of higher organic production (Fig. 2). The presence of woody species in these phases of the succession can be interpreted as an influence of the heterogeneity of the environment (see below).

The succession series in zone CH3 is largely influenced by the increase of hydrological activity, which was connected with the precipitation of carbonates. The plant macrofossils found give evidence of the presence of slow moving or stagnant water with still water macrophytes (*Nuphar*, *Batrachium*, *Potamogeton*) and with macroalgae (*Chara*). Fluctuating water at the shoreline is indicated by species adapted to these conditions (*Hippuris*, *Sparganium*, *Batrachium*, *Oenanthe*). Littoral sedges occurred as well (*Carex rostrata*, *C.* sect. *Paniculatae*, *C. flava* agg.). In zone CH3, the frequent occurrence of *Oenanthe* sp. mericarps is remarkable. *Oenanthe* stands commonly occur in lowland alluvial floodplains, on sites with exposed pond beds or on sites flooded by shallow water, but it can also grow at greater depths of up to 1 m.

In zones CH4–CH6, succession can only be estimated with difficulties on the basis of palaeobotanical data. However, the aforementioned interpretation of the sedimentation processes indicates vegetation that produces a large amount of fast decomposing and mineralizing biomass. The oospores of *Characeae*, with calcium carbonate incrustation, proven in large amounts, indicate shallow water, periodic floods and light. The wood fragments and charcoal (*Betula*, *Salix*, *Pinus*, *Fraxinus*), by contrast, indicate the presence of shrub and forest vegetation in the vicinity of the site under study. The presented evidence suggests an occurrence of eutrophic wetland with the prevalence of tall graminoids (e.g., *Phragmites*). This hypothesis is supported by finds of several achens of *Schoenoplectus tabernaemontani/lacustris*, which indicates reed bed habitats. This eutrophic wetland was, in some episodes, overgrown by a scarce canopy of woody plants. Similar vegetation types and signs of changes of the succession stages are frequent in the area of interest even today. Some human impact to the vegetation is likely, too.

Interpretation Context 2: Large-Scale Environmental Processes

Explaining local patterns of studied deposits using large-scale environmental processes is a common approach in palaeoecology. This approach shows how meander infilling reflects global changes on the landscape level. It was observable that the results from the analyzed section *Chrast* corresponded with general characteristics of environmental development in the Late Glacial and Holocene.

Meander infilling as a result of landscape development and climatic changes

In principle, climatic and environmental changes in the Quaternary period influenced the dynamics of fluvial systems in Central Europe that were not affected directly by the continental ice cover (Maddy et al. 2001; Tyráček 2001; Vandenberghe 2003; Tyráček and Havlíček 2009). We detected different mechanisms of fluvial regime response to environmental-climate factors: (1) changes in hydrological conditions (discharge regime), (2) changes in the channel pattern (fluvial activity) and (3) changes in the longitudinal profile through aggradation or degradation (river incision). On shorter time scales, these changes may result in the formation of river terraces and a river architecture pattern; on the Holocene scale, these changes lead to the genesis of alluvial soils (Törnqvist 2007). These global changes were traced in the sedimentary and palaeoecological record at the *Chrast* site.

Allerød and Bølling

During the interstadial complex Allerød/Bølling, the water regime of the rivers in Central Europe was of a meandering character (Andres et al. 2001; Houben 2003;

Vandenberghe 2003; Pastre et al. 2003). The water flow within the branch in the first part of Allerød is visible in sandy sedimentation in zone CH1 and in macrofossils of short-age plants, which indicate constant disturbances caused by the activity of the river. The second half of Allerød is characterized by fen development without sedimentation of sandy material. This indicates a decrease in fluvial activity. The increased organic production serves as evidence for the improvement of the climate, which allowed for the succession of vegetation in hydroseries.

Younger dryas

The Allerød/Younger Dryas transition is visible as the lithologic interface of zones CH2 and CH3. The presence of water macrophytes and *Characeae* in the macrofossils diagram reflects the transition in the water regime. During the cold stage, Younger Dryas, the river water regime changed frequently from meanders to braided at the site under study, but only indirect evidence is available – the sedimentation of coarse sand with the presence of charcoal and wood fragments of *Pinus* and *Salix* (zone CH4).

Holocene

The beginning of the Holocene is represented by aggradation of fine carbonaceous clays, so called *alm* (or lake chalk; CH5) without a coarse sand fraction. Episodes of sedimentation of *alm* aggradation during the glacial and at the beginning of the Holocene can be explained by the influence of several factors that could act apart or together – the change in hydrological conditions (decrease of flood events), the change in climate (rapid and short periods of instability in climatic conditions followed by years of drought) (Bohncke and Hoek 2007) and the change in the evaporation rate. Ložek and Šibrava (1982) assumed an increased evaporation rate in the river Elbe area for periods of instability during the Late Glacial period. Moreover, the Early Holocene deposition is probably connected with increased spring activity during the Holocene climatic improvement (Ložek 1973; Roberts 1998). The presence of *alm* is well known from the same time period also from other localities within the Elbe lowland (Hrabanovská černava – Petr 2005; Malý Újezd – Ložek 1952).

In zone CH6, sedimentation was influenced by anthropogenic activities in the surrounding landscape. Pollen analysis shows ruderal species and cereal pollen. Macrofossils (charcoal), micromorphology and geochemistry indicated traces of local fires (micro-charcoal of grasses and bent-grass) in the degraded peat.

Development of the vegetation at the regional level

Transported pollen grains and macrofossils from the surrounding landscape can partly explain the vegetation diversity at the regional level. While the origin of shallow water bodies, banks and fens with characteristic vegetation can be seen in local conditions, the presence of other groups of macrofossils can be evaluated as a result of the influence of other vegetation types in the close surroundings of the site. Pine, birch and mesophilous herbs and shrubs (*Fragaria*, *Alchemilla*, *Viola*, *Potentilla erecta*, *Rubus*) could grow in older succession stages on alluvium elevations or in the surroundings of the present alluvium, but also directly on young and frequently disturbed sediment load where long-term plant survival is very difficult whereas the establishment is easy.

At the bottom of the studied section (zone CH1), the number of species as well as the differentiation of their requirement on the environment is the largest. This may suggest a great diversity of plant communities during early development of the inactive river branch in the glacial. Under changeable conditions, water bodies can persist longer or are periodically renewed (Bos 2001).

For the Late Glacial period (zones CH1–CH3), pollen analyses detected that in the surrounding landscape the herbaceous vegetation was species-rich in open habitats where birch (*Betula pendula/pubescens*, *B. nana*), willow (*Salix* sp.) and pine (*Pinus sylvestris*) prevail. The presence of pine wood and needles confirms the local occurrence of pine. Several spruce charcoal particles were recovered from zone CH3. Similarly, spruce is represented in the pollen diagram as well. Its occurrence in the Czech Cretaceous basin on its western boundary is presumed already in the Last Glacial Maximum (Latalowa and van der Knaap 2006). Contrastingly, the sporadic occurrence of pollen of mesophilous woody plants is most likely the result of long-distance transport because there is no macrofossil evidence of their presence at the site. These woody plants have not been detected for the Last Glacial in this part of Central Europe yet (Bittmann 2007).

The Western Carpathians in the Late Glacial period were typically covered with forests (Jankovská 1988; Jankovská and Pokorný 2008). By contrast, open habitats predominated in the western parts of the Czech Republic (Pokorný 2002). The Late Glacial pollen record from the Hrabanovská Černava site is the only one studied in the Central Bohemian lowland (Petr 2005). The former small shallow lake was detected in an area situated 18 km E of the *Chrást* site and 4 km N of the river Elbe. The pollen record from this site is considerably different; open steppe taxa (*Helianthemum*) prevailed and trees were represented only marginally. We can therefore conclude that forest vegetation was restricted to the more favorable habitats along the river. Wet and nutrient-rich soils under mild microclimate conditions were responsible for the development of today's riverine gallery forests in tundras and steppes (Tockner et al. 2009). Similar results are shown in Chytrý et al. (2008) on an example of the recent vegetation of southern Siberia; the continental climate amplifies the dependence of vegetation on local geomorphologic conditions.

Interpretation Context 3: Meander Infilling as a Unique Concomitance Resulting from Random Processes

When interpreting lithological records and researching evidence of local processes, authors commonly present the objects of their study as results of homogenous, global processes. We decided to apply another interpretation to demonstrate randomness and unpredictability in our data by considering coincidences in external influences and circumstances.

The complexity of the value of information

The section studied is a result of various allogenic and autogenic processes (e.g., climate change, vegetation succession) that impact the lithological record. The record is only fragmentary, consisting of several episodes of unknown length. Missing sedimentary records, so-called *hiatuses*, are a very common phenomenon, caused by erosion – processes that interrupt continuous sedimentation. Compared to the development of lakes or peats, there is higher frequency of erosion events in the river systems (e.g., floods, bottom currents), which interrupt local development. The studied record of the *Chrast* section reflects only a part of the local geodiversity (types of sediments) and biodiversity (species, types of vegetation) and their representation in time (stratigraphic sequences, succession lines). The section considered here is therefore unique. There is no such other record for the river Elbe. There are analogous lithological sections at other rivers, but not the same species structure. It is also highly probable that our section is not even representative of all parts of the oxbow lake. The filling of the oxbow lake could be influenced by different processes on spatiotemporal variability. Palaeoecological records can result from large diversity in a small area, at least in this case of largely diversified conditions of a Late Glacial river environment.

Global versus *local processes*

The palaeorecord of the *Chrast* section was formed by random events, which are the result of global processes. In the case of our section, however, they appear as random events. For example, the reintroduction of a gravel-sandy sedimentation that buried the fen's vegetation during the Younger Dryas has been interpreted as a consequence of a general process operating at least throughout Central Europe. Then the deterioration and the instability of the climate were expressed in increased tendency to form a braided pattern of the river instead of genesis of meanders. However, we must admit that this sedimentation regime most probably did not start its activity at once in the whole vast Elbe river alluvium but that it occurred significantly sooner or later, or maybe it did not occur at all under specific conditions. The described change of sedimentation may not be related to the beginning of the formation of the braided pattern of the river. Instead, it could be related merely to a change in the course of the meandering river. Only further excavations and analyses of dated sediments will allow us to decide between these two possibilities.

Conclusion

The sedimentary section of the river Elbe palaeochannel near *Chrast* was discovered after the observation of aerial photographs and maps in the Polabí region, Czech Republic. Our results show that after the abandonment of the channel, the shallow episodical oxbow lake appeared. This event dates to the period of the Late Glacial. The sediment, recovered from the middle part of the palaeochannel, contained the palaeoenvironmental record of changes within the Elbe river alluvium in the period of the Late Glacial and Holocene. Palaeobotanical results suggest that the Elbe river alluvium operated as a favorable micro-climate refuge in the Late Glacial landscape as can be demonstrated by the presence of macrofossils of conifers including spruce charcoal.

The global changes that occurred at the end of the Pleistocene and the beginning of the Holocene periods are evidenced in the form of proxy-data that provide information about changes in the Elbe's fluvial regime. The sedimentary record of the Holocene period provides evidence for complicated formation of the site, which is the best described by the micromorphological analysis. The local development during the Middle and Younger Holocene can only be reconstructed with difficulties on the basis of macrofossils analysis, and the pollen analysis provides information about the surrounding landscape.

The multi-proxy approach to the interpretation of the *Chrast* sedimentary infill enables us to reconstruct the local development of the abandonment of the river channel and observe the vegetation succession and the local sedimentation processes linked on the landscape level in relation to global climate changes. The processes that do not fit the general interpretational frame of global or local changes are emphasized. These processes could occur by chance as a result of the heterogeneity of the alluvial environment.

Acknowledgments This work was supported by grants from the Academy of Sciences of the Czech Republic Nos. IAAX00050801 and IAAX00020701. Additional support came from the Institutional grant AV0Z 30130516 of the Institute of Geology AS CR It was also supported as a long-term research development project No. RVO 67985939. We would like to thank Prof. Kalicki and Prof. Starkel for fruitful discussions. This manuscript was improved by suggestion and thoughtful critiques of anonymous reviewers.

References

Andres W, Bos JAA, Houben P, Kalis AJ, Nolte S, Rittweger H, Wunderlich J (2001) Environmental change and fluvial activity during the Younger Dryas in central Germany. *Quatern Internat* 79:89–100

Aslan A (2007) Fluvial environments. Sediments. In Elias SA (eds) *Encyclopedia of Quaternary Science*. Royal Holloway, University of London, pp 672–685

Balatka B, Sládek J (1962) *Říční terasy v Českých zemích (River terraces in the Czech lands)*. Geofond, NČSAV, Praha

Beijerinck W (1947) *Zadenatlas der Nederlandsche Flora (Seed atlas of the Netherlands Flora)*. H. Veenman and Zonen, Wageningen

Berggren G (1969) *Atlas of seeds and small fruits of Northwest European plant species. Part 2, Cyperaceae*. Swedish Natural Science Research Council, Stockholm

Beug HJ (2004) *Leitfaden der Pollenbestimmung für Mittelereuropa und angrenzende Gebiete*. Verlag Dr. Friedrich Pfeil, München

Birks HH, Birks HJB (2000) Future uses of pollen analysis must include plant macrofossils. *J Biogeogr* 27:31–35

Bittmann F (2007) Reconstruction of the Allerød vegetation of the Neuwied Basin, western Germany, and its surroundings at 12,900 cal BP. *Veget Hist Archaeobot* 16:139–156

Björck, S, Walker MJC, Cwynar LC, Johnsen S,Knudsen K-L, Lowe JJ, Wohlfarth B (1998) An event stratigraphy for the last termination in the North Atlantic region based on the Greenland icecore record: a proposal by the INTIMATE group. *J Quatern Sci* 13:283–292.

Bohncke SJP, Hoek WZ (2007) Multiple oscillations during the Preboreal as recorded in calcareous gyttja, Kingbeekdal, The Nederlands. *Quatern Sci Rev* 26:1965–1974

Bos JAA (2001) Lateglacial and Early Holocene vegetation history of the northern Wetterau and the Amöneburger basin (Hessen), central-west Germany. *Rev Palaeobot Palynol* 115:177–212

Bridge JS (2003) *Rivers and floodplains; forms, processes, and sedimentary record*. Blackwell Publishing, Oxford

Bronk Ramsey C (2009) Bayesian analysis of radiocarbon dates. *Radiocarbon* 51(1):337–360

Břízová E (1998) Změny rostlinných ekosystémů v nivě Labe během pozdního glaciálu a holocénu (pylová analýza) (Changes of plant ecosystems in the Labe river floodplain during Late Glacial and Holocene (pollen analysis)). *Zpr Čes Bot Spol* 34, *Mater* 17:169–178

Budek A (2010) *Genesis and age of the humic horizont in the floodplain at the Carpathian Foreland. Geographical Studies, 222*. Polish Academy of Sciences, Warszaw

Bullock P, Fedoroff N, Jongerius A, Stoops G, Tursina T (1985) *Handbook for soil thin section description*. Waine Research Publications, Wolverhamton

Cappers RTJ, Bekker RM, Jans JEA (2006) *Digital seed atlas of the Netherlands*. Groningen Archaeological Studies 4, Barkhuis Publishing, Eelde. Available at: www.seedatlas.nl

Chytrý M, Danihelka J, Kubešová S, Lustyk P, Ermakov N, Hájek M, Hájková P, Kočí M, Otýpková Z, Roleček J, Řezníčková M, Šmarda P, Valachovič M, Popov D, Pišut I (2008) Diversity of the forest vegetation across a strong gradient of climatic continentality: Western Sayan Mountains, Southern Siberia. *Pl Ecol* 196:61–83

Culek M (1996) *Biogeografické členění České republiky (Biogeographically classification of Czech Republic)*. Enigma, Praha

Dinc U, Miedema R,Bal L, Pons LJ (1976) Morphological and physico-chemical aspects of free soils developer in the Netherlands and their classification. *Netherlands J Agric Sci* 24:247–265

Dreslerová D, Břízová E, Růžičková E, Zeman A (2004) Holocene enviromental processes and alluvial archaeology in the middle Labe (Elbe) valley. In Gojda M (eds) *Ancienit landscape, settlement dynamics and non-destructive archaeology*. Academia, Praha, pp 121–171

Engstrom DR, Wright HE Jr (1984) Chemical stratigraphy of lake sediments as a record of environmental change. In Haworth EY, Lund JWG (eds) *Lake sediments and environmental history*. Leicester University Press, Leicester, pp 11–67

Fox CA (1985) Micromorphological characterisation of Histisols. In Douglas LA, Thompson ML (eds) *Soil micromorphology and soil classification*. Soil Science Society of America Special Publication 15, SSSA, Madison, Wisconsin, pp 85–104

Frenzel B (1983) Mires – repositoriem of climatic information or self – perpetuating ecosystems? In Gore AJP (ed) *Ecosystems of the world 4A. Mires: swamp, bog, fen and moor, general studies*. Elsevier, Amsterdam, pp 35–65

Hajdas I, Ivy SD, Beer J, Bonani G, Imboden D, Lotter AE, Sturm M, Suter M (1993) AMS radiocarbon dating and varve chronology of Lake Soppensee: 6000 to 12000 14C years BP. *Climate Dynamics* 9:107–116

Heiri O, Lotter AF, Lemecke G (2001) Loss on ignition as a method for estimating organic and carbonate content in sediments: reproducibility and comparanility of results. *J Palaeolimnol* 25:101–110

Heiss AG (2000 onwards) *Anatomy of European and North American woods – an interactive identification key*, *Version 2006–08, 22*. Available at: http://www.holzanatomie.at

Herget J, Dikau R, Gregory K, Vandenberghe J (2007) The fluvial systems – Research perspectives of its past and present dynamics and controls. *Geomorphology* 92:101–105

Holliday VT (2004) *Soils in archaeological research*. Oxford University Press, Oxford

Houben P (2003) Spartio-temporally variable response of fluvial systems to Late Pleistocene climate change: a case study from central Germany. *Quatern Sci Rev* 22:2125–2140

Jackomet S, Kreuz A (1999) *Archäobotanik. Aufgaben, Methoden und Ergebnisse vegetations- und agrargeschichtlicher Forschung*. Ulmer Verlag, Stuttgart

Jankovská V (1988) A reconstruction of the Late-Glacial and Early Holocene evolution of forest vegetation in the Poprad-Basin, Czechoslovakia. *Folia Geobot Phytotax* 23:303–319

Jankovská V, Pokorný P (2008) Forest vegetation of the last full-glacial period in the Western Carpathians (Slovakia and Czech Republic). *Preslia* 80:307–324

Kalicki T (2006) *Zapis zmian klimatu oraz działaności człowieka I ich rola w holoceńskej ewolucji dolin środkowoeuropejskich (Reflection of climatic changes and human activity and their role in the Holocene evolution of central European valleys)*. Prace Geograficzne Nr. 24, Polska Akademia Nauk, Warszawa

Katz NJ, Katz SV, Kipiani MG (1965) *Atlas and keys of fruits and seeds occuring in the quaternary deposits of the SSSR*. Nauka, Moscow

Knox JC (1983) Responses of river systems to Holocene climates. In Wright HE, Jr (ed) *Late-quaternary environments of the United States. Volume 2. The Holocene*. University of Minnesota Press, Minneapolis, p 26

Koopman GJ (1988) "Waterhard": A hard brown layer in sand below peat, The Netherlands. *Geoderma* 42:147–157

Latalowa M, van der Knaap WO (2006) Late quaternary expansion of Norway spruce *Picea abies* (L.) Karst. in Europe according to pollen data. *Quatern Sci Rev* 25:2780–2805

Ložek V (1952) Výzkum ložiska sladkovodní křídy u Malého Újezdu na Mělnicku (Research of Calcareous clay deposit near Malý Újezd, Mělník disctrict). *Antropozoikum* 2:29–50

Ložek V (1973) *Příroda ve čtvrtohorách (Nature in Quaternary)*. Academia, Praha

Ložek V, Šibrava V (1982) The Late Glacial of the Labe valley in Bohemia. *Antropozoikum* 14:9–27

Litt T, Brauer A, Goslar T, Merkt J, Balaga K, Miller H, Ralska-Jasiewiczowa M, Stebich M, Negendank JFW (2001) Correlation and synchronisation of Lateglacial continental sequences in northern central Europe based on annually laminated lacustrine sediments. *Quatern Sci Rev* 20:1233–1249

MacCarthy P J, Martini IP, Leckie DA (1998) Use of micromorphology for paleoenvironmental interpretation of complex alluvial paleosols: an example from the Mill Creek Formation (Albian), southwestern Alberta. Canada. *Palaeogeogr Palaeoclimatol Palaeoecol* 143:87–110

Maddy D, Macklin MG, Woodward JC (2001) *River basin sediment systeme: Archive of environmental change*. AA Balkema Publisher, Lisse, Abingdonn, Exton, Tokyo

Makaske B (2001) Anastomizing rivers: a review of their classification, origin and sedimentary products. *Earth Sci Revi* 53:149–196

Manoch B (1970) *Micromorphology of a Saprist.* MSc Dissertation, University of Wisconsin, Madison, Wisconsin

Mol J, Vandenberghe J, Kasse C (2000) River response to variations of periglacial climate in mid-latitude Europe. *Geomorphology* 33:131–148

Moore PD, Webb JA, Collinson ME (1991) *Pollen analysis*. Ed. 2. Blackwell Scientific Publications, Oxford

Nalepka D, Walanus A (2003) Data processing in polen analysis. *Acta Paleobot* 43:125–134

Pastre JF, Limondin-Lozouet N, Leroyer C, Ponel P, Fontugne M (2003) River system evolution and environmental changes during the Lateglacial in the Paris Basin (France*). Quatern Sci Rev* 22:2177–2188

Pearshall DM (1989) *Paleoethnobotany: A handbook of procedures*. Academic Press, San Diego

Petr L (2005) *Vývoj vegetace pozdního glaciálu a raného holocénu v centrální části České kotliny (Late Glacial and Early Holocene vegetation development in the central part of Czech basin)*. MSc Thesis, Charles University, Prague

Pokorný P (2002) A high-resolution record of Late-Glacial and Early-Holocene climatic and environmental change in the Czech Republic. *Quatern Internat* 91:101–122

Pokorný P (2005) Role of man in the development of Holocene vegetation in Central Bohemia. *Preslia* 77:113–128

Reille M (1995) *Pollen et spores d'Europe et d'Afrique du Nord, Supplément 1*. Éditions du Laboratoire de botanique historique et palynologie, Marseille

Reille M (1998) *Pollen et spores d'Europe et d'Afrique du Nord, Supplément 2*. Éditions du Laboratoire de botanique historique et palynologie, Marseille

Ritchie JC (1995) Current trends in studies of long-term plant community dynamics. *New Phytol* 130:469–494

Růžičková E, Zeman A (1994) Holocene fluvial sediments of Labe River. In Růžičková E, Zeman A (eds) *Holocene flood plain of the Labe river*. Geological Institute of Academy of Sciences of the Czech Republic, Praha, pp 3–25

Roberts N (1998) *The Holocene: an environmental history*. Ed. 2. Blackwell, Oxford

Saarnisto M (1986) Annually laminated lake sediments. In Berglund BE (ed) *Handbook of holocene palaeoecology and palaeohydrology*. Wiley, Chichester, pp. 343–370

Schermann S (1967) *Magismeret II (Transpation)*. Akadémiai Kiadó, Budapest

Schweingruber FH (1990) *Mikroskopische Holzanatomie*. Swiss Federal Institute of Forestry Research, Birmensdorf

Stoops G (2003*) Guidelines for analysis and description of soil and regolith thin section*. Soil Science Society of America, Madison, Wisconsin

Stoops G, Marcelino V, Mees F (eds) (2010) *Interpretation of micromorphological features of soils and regoliths*. Elsevier, Oxford

Šumberová K, Lososová Z (2011) Vegetace jednoletých nitrofilních vlhkomilných bylin (Vegetation of annual nitrophilous wetland herbs). In Chytrý M (ed) *Vegetace České republiky. 3, Vodní a mokřadní vegetace (Vegetation of the Czech Republic. 3, Aquatic and wetland vegetation)*, Academia, Praha, pp 347–384

Tinner W, Lotter AF (2001) Central European vegetation response to abrupt climate change at 8.2 ka. *Geology* 29:551–554

Tockner K, Uhelinger U, Robinson CT (2009*) Rivers of Europe*. Elsevier, Oxford

Törnqvist TE (2007) Fluvial environments: responses to rapid environmental change. In Elias SA (eds) *Encyclopedia of quaternary science*. Royal Holloway, University of London, pp 686–694

Tyráček J (2001) Upper Cenozoic fluvial history in the Bohemian Massif. *Quatern Int* 79:37–53

Tyráček J, Havlíček P (2009) The fluvial record in the Czech Republic: A review in the context of IGCP 518. *Global Planet Change* 68:311–325

Vandenberghe J (2003) Climate forcing of fluvial system development: an evolution of ideas. *Quatern Sci Rev* 22:2053–2060

Velichkevich FYu, Zastawniak E (2006) *Atlas of the Pleistocene vascular plant macrofossil of Central and Eastern Europe, Part 1*. W. Szafer Institute of Botany, Polish Academy of Science, Kraków

Walker MJC, Bjorck S, Lowe JJ, Cwynar LC, Johnsen S, Kundsen KL, Wohlfahrt B (1999) Isotopic events in the GRIP ice core: a stratotyp for the Late Pleistocene. *Quatern Sci Rev* 18:1143–1150
Wasylikowa K (1986) Analysis of fossil fruits and seeds. In Berglund BE (ed) *Handbook of Palaeoecology*. John Wiley, Chichester, pp 571–590
Žebera K (1956) Stáří přesypů a navátých písků ve středočeském Polabí (Age of sand dunes in the central Bohemian Polabí lowland). *Antropozoikum* 5:77–93

Received: 16 November 2011 / Revised: 14 September 2012 / Accepted: 20 September 2012 / Published online: 28 September 2013

Quaternary International 266 (2012) 14–24

Contents lists available at SciVerse ScienceDirect

Quaternary International

journal homepage: www.elsevier.com/locate/quaint

Diachronic development of the Lake of Abusir during the third millennium BC, Cairo, Egypt

Václav Cílek[a], Miroslav Bárta[b], Lenka Lisá[a,*], Adéla Pokorná[a,c], Lucie Juříčková[d], Vladimír Brůna[e], Abdel Moneim A. Mahmoud[f], Aleš Bajer[g], Jan Novák[c], Jaromír Beneš[c]

[a] Institute of Geology AS CR, Rozvojová 269, Praha 6, 165 00, Czech Republic
[b] Charles University in Prague, Czech Institute of Egyptology, Celetná 20, 110 00, Praha 1, Czech Republic
[c] Laboratory of Archaeobotany and Palaeoecology, Faculty of Science, University of South Bohemia, České Budějovice, CZ 37005, Czech Republic
[d] Department of Zoology, Faculty of Science, Charles University in Prague, Viničná 7, Praha 2, CZ 12000, Czech Republic
[e] Laboratory of Geoinformatics, Faculty of Environment, J.E Purkyne University in Usti nad Labem, Czech Republic
[f] Education of Earth Sciences & Space Unit, Faculty of Education, Ain Shams University, Roxy, Misr el Gadida, Cairo, Egypt
[g] Faculty of Forestry and Wood Technology, Mendel University, Zemědělská 3, Brno 613 00, Czech Republic

ARTICLE INFO

Article history:
Available online 31 December 2011

ABSTRACT

The paper introduces results of the survey of the Lake of Abusir, performed by the Czech Institute of Egyptology over the last few years. A detailed sedimentological description of four trenches located within the area of the so-called Lake of Abusir is given, together with the micromorphological results of selected strata, molluscs and archaeobotanical findings. All the presented results document the paleoenvironmental and geoarchaeological history of the study area. Five main developmental phases of the Lake of Abusir are interpreted. The area was used as a principal entryway to the cemeteries of Saqqara and Abusir during the third millennium BC. These cemeteries were built to serve the capital of ancient Egypt, the White Walls, which was established around 3000 BC. The old Nile terrace deposits constituted the background for the tiled pavement built during the Old Kingdom period. Later, this pavement was partly destroyed by heavy outwash, and the anthropogenic features were overlain by a layer of pure sand. Subsequent sedimentological development is characterized by increased desiccation interrupted by several phases of elevated moisture due to the activity of the local hydrological system. Due to the function of Wadi Fetekti, thick colluvial deposits were preserved.

1. Introduction

Fluvial environments can be used as good indicators of paleogeographical and paleoclimatic changes (Brown, 1997; Vandenberghe, 2003). The Lake of Abusir, the depression attached to extensive ancient Egyptian cemeteries of Saqqara and Abusir, Cairo, Egypt (5000–400 BC), represents a major topographic feature connected with the organization of the pyramid landscape (Figs.1 and 2) (Jeffreys and Tavares, 1994; Bárta, 2005). The lake was used as a principal access route to the cemeteries of North and Central Saqqara and Abusir during most of the Old Kingdom (Bárta, 1999). The water reservoirs often played a significant role in the design of the Old Kingdom royal mortuary complexes (Verner, 1994; Bárta, 2005). The Lake of Abusir was also associated with the goddess Heqet, ancient Egyptian goddess of birth and rejuvenation (Bárta, 1999).

Looking for the evidence and development of the lake during the Old Kingdom (2592–2218 BC, Hornung et al., 2006, 490–91) involved examining its sediments to find additional information about the function of the lake during the Old Kingdom period and about the possible transitional climate conditions during the Holocene. Surprisingly, several mastabas and remnants of different architectonic features dated to the Third and Fourth Dynasties (2592–2436 BC; Hornung et al., 2006, 490–91) were discovered approximately 1.5 m below the present floodplain (Bárta, 2009) at about 18 m a.s.l. This paper presents the lithology and palaeoecology of the Lake of Abusir deposits and discusses the origin and the function of this depression in relation to the background geology, climate and the role of the River Nile.

* Corresponding author.
E-mail addresses: cilek@gli.cas.cz (V. Cílek), miroslav.barta@ff.cuni.cz (M. Bárta), lisa@gli.cas.cz (L. Lisá), adepo@seznam.cz (A. Pokorná), lucie.jurickova@seznam.cz (L. Juříčková), bruna@geolab.cz (V. Brůna), bajer@mendelu.cz (A. Bajer), prourou@gmail.com (J. Novák), benes.jaromir@gmail.com (J. Beneš).

1040-6182/$ – see front matter © 2011 Elsevier Ltd and INQUA. All rights reserved.
doi:10.1016/j.quaint.2011.12.025

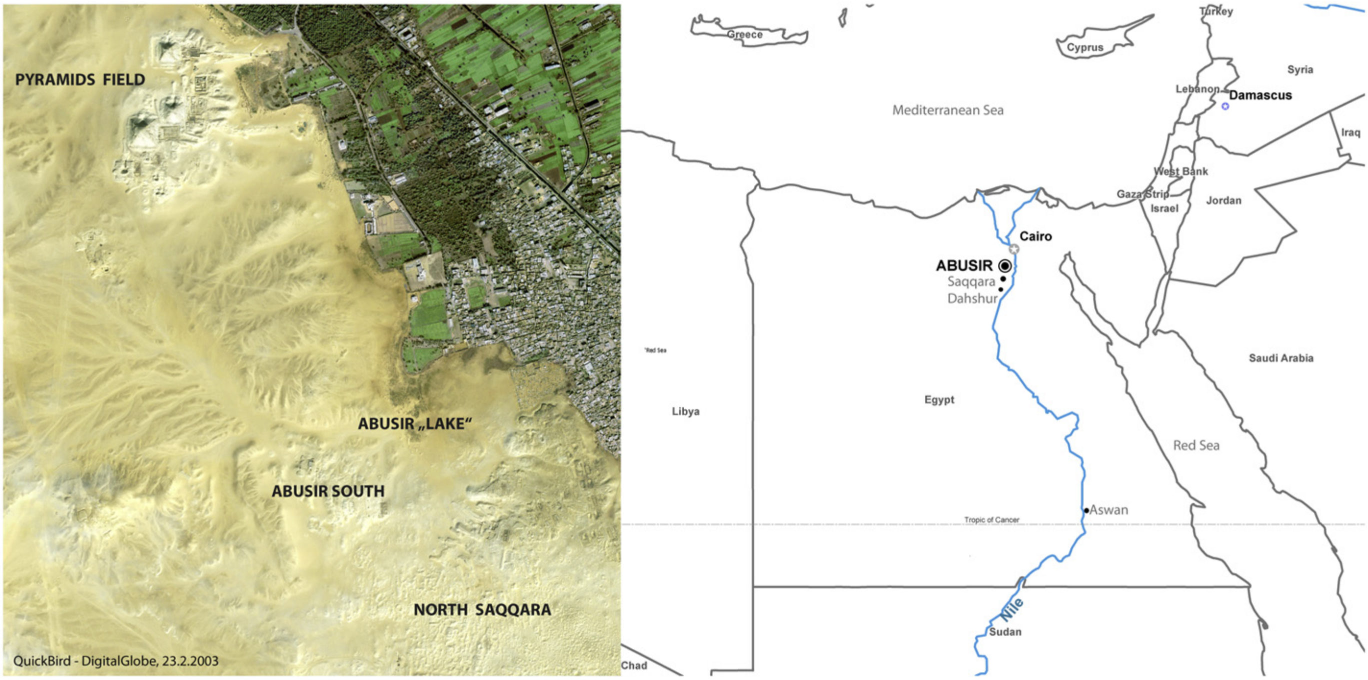

Fig. 1. Map showing the location of the Abusir Lake area within the North Africa and the landscape view of Abusir Lake area. Marked positions Dahshur, Saqqara, Abusit Lake and Pyramid fields of Abusir: Dahshur – 29.799712° N, 31.213655° E; Saqqara – 29.871053° N, 31.216682° E; Abusir Lake – 29.885166° N, 31.212735° E; Pyramid Fields of Abusir – 29.896171° N, 31.203543°.

2. History of the study area

The Lake of Abusir appears on the early maps of Karl Richard Lepsius, Jacques de Morgan, Ludwig Borchardt and other Egyptologists and cartographers of the 19th and early 20th centuries (Bárta and Brůna, 2006). It is rendered as a rather prominent and isolated body of water. The lake was reported to exist occasionally until the mid-1960s. According to reliable reports from the local inhabitants, it was a seasonal feature, 1–2 m deep, and fed by water leaking from the ground. The lake was used for swimming, fishing and cattle washing. The lake existed only seasonally, during August–October/November, and chronologically was connected with the annual Nile flooding which caused a general rise of the water table in the whole valley (Butzer, 1976; Schenkel, 1978). It started to disappear with the completion of the Aswan Dam in the 1960s. Today, the Lake of Abusir is a slightly moist depression covered with a sparse ruderal vegetation at the transition between the cultivated area and the desert (Dittmer et al., 2003) and is dominated by the clonal plant *Desmostachya bipinnata* (halfa grass). Other species encountered at the site are those typical of ruderal stands: *Spergularia media, Setaria pumila, Echinochloa crus-galli, Chenopodium sp., Sonchus oleraceus, Hordeum murinum, Xanthium spinosum,* and *Cassia cretica,* or those typical of desert margins (*Alhagi graecorum*) or bottoms of wadis (*Panicum thurgidum*) or those which are connected with oases or more or less humid environments, such as *Phoenix dactylifera, Arundo donax, Tamarix nilotica, Imperata cylindrical,* and *Cyperus laevigatus* (Pokorný et al., 2009).

The lake depression is situated on the edge of the present Nile floodplain (Figs. 1 and 2), with the modern surface at 20 m a.s.l. The Lake of Abusir is thought to be a remnant of an extensive water reservoir fed by groundwater and superficial water of the Nile River (Mahmoud, 1986; Pokorný et al., 2009). According to recent observations, the exact role of the lake is rather enigmatic because no typical clayey lacustrine deposits have been found (Reader, 2009). Mathieson (2000) reported concentrations of freshwater bivalve molluscs that formed a stable shoreline of the lake during the Old Kingdom. Dittmer et al. (2003) claimed that before coverage by recent windblown sand deposits, this area was subject to deposition of fine dark-coloured organic-rich soils. This suggests that the area probably functioned as an inundation basin, fed exclusively by seasonal flooding associated with the Nile.

The Lake of Abusir was studied in detail by Mathieson (2000), mostly by various geophysical methods, and by Jeffreys (2001, 2006a, 2006b) who focused on Holocene stratigraphy and settlement remains by using coring. Mathieson thoroughly mapped the area and found a mixture of sand-dominated sediments up to 5 m thick. Similar results were provided also by Jeffreys, who observed that the large open areas in front of the valley temples of the Abusir funerary complexes were filled exclusively with sand deposits. The area of the lake was later investigated by the Czech Institute of Egyptology (2002, 2009).

The main geomorphological features in the close vicinity of the Lake of Abusir are the Fetekti and Abusir wadis (Fig. 2). The Fetekti wadi is a short dry tributary of east–west orientation, descending from the Western Desert plateau towards the lake. Originally, it was an insignificant shallow valley, but it was later deepened by torrential rains. The Abusir wadi is a major dry valley of the area that stretches from South Abusir to the northeast and opens into the Lake of Abusir.

3. Geological background

The prevailing geological formations of the Abusir area are the Late Eocene Maadi limestone, clayey limestone and marls (tafla). The upper member of the Maadi Formation, Giran el Ful, is developed mostly as porous brown sandy limestone tempestite facies (Strougo, 1985). The only known outcrops appear more to the west (Lion Hill) but scattered fragments of these low-quality building limestone rocks can be found almost everywhere. The studied area

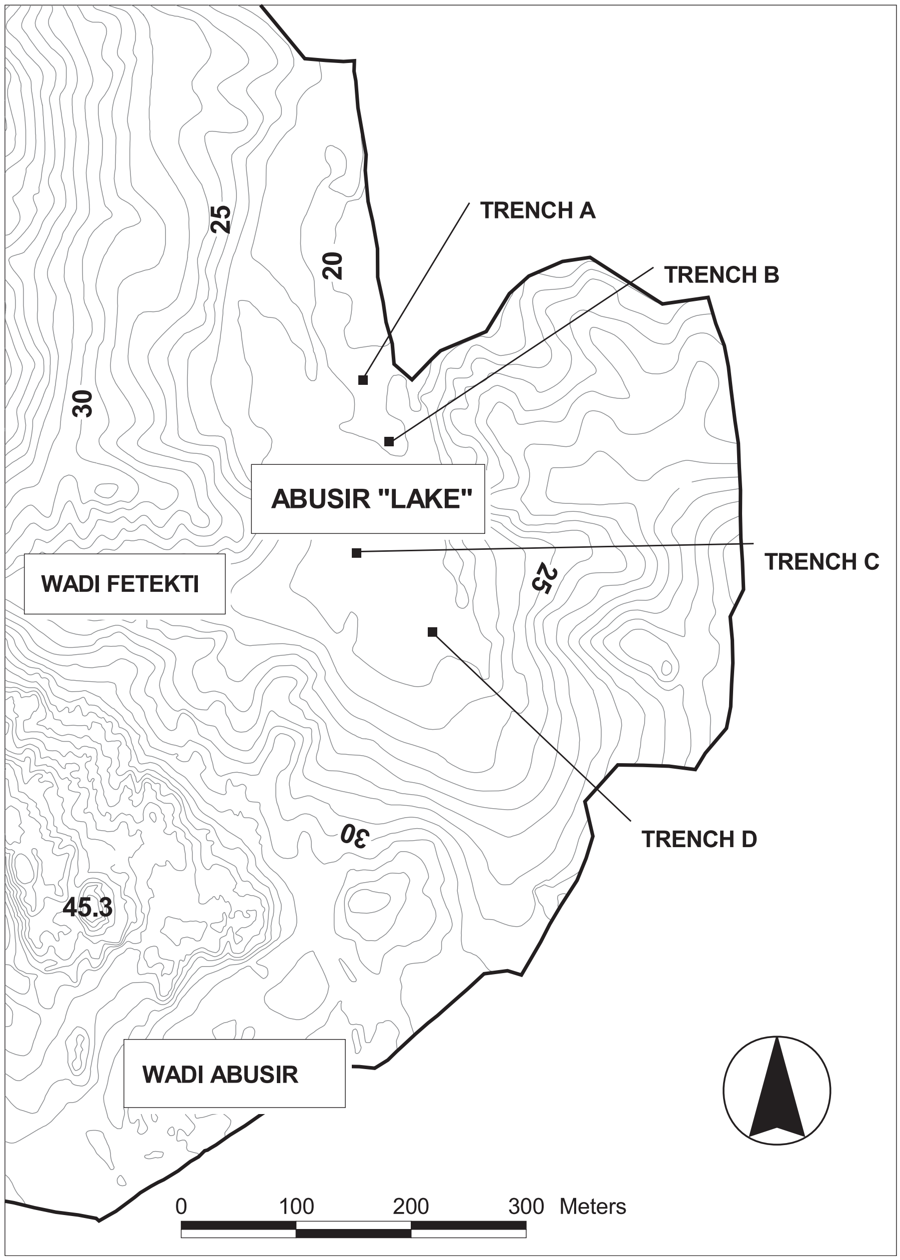

Fig. 2. Contour map showing the location of trenches and basic geomorphology of the Abusir Lake area.

is completely formed by the Saqqara Member which consists of alternating strata of structureless, 40–120 cm thick beds of yellowish limestone and 20–60 cm thick beds of light grey marls (Said, 1993; Issawi and al-Jiyūlūjīyah al-Misrīyah, 1999; Reader, 2009).

The Quaternary sediments are developed as slope deposits derived from older Nile terraces of Pleistocene age (Mahmoud and Hamdan, 2002) as well as aeolian sands. Other materials such as remobilized river gravels and sands cemented by calcium carbonate are rare. The Nile sediments are easily distinguishable by the presence of concretional and laminar brown cherts (hornstones, flints) derived from Middle Nile Eocene limestone rocks, weathered pink granodiorites from the Aswan area, epidotized green metamorphic rocks from the basement complex of the Eastern Desert, rare carnelians and other rocks (Mahmoud and Hamdan, 2002). However, rounded quartz pebbles are the most common material in all Pleistocene terraces. The reddish Pleistocene Edfu sands of the upper Nile terrace above Abusir were sieved and used for making very commonly used pink gypsum mortars and plasters during the Old Kingdom and much younger (Roman) periods. Dittmer et al. (2003) reported only sands and no soil layers from their investigations of the Lake of Abusir. Their stratigraphic sections consisted of recent windblown sand up to 2 m thick, overlying soils which were predominantly granular but contained varying proportions of dark humic material. Within the dark-coloured soils, mud-brick structures were encountered, together with fragments of red/black pot and occasional shell fragments.

4. Methodology

During the 2007 field season (April 7–24), four trenches 2–3 m wide and 1.8–3.2 m deep were excavated. The trenches were located approximately in the north–south axis of the remnant lake, as judged by its extent given in historical maps (especially by K. R. Lepsius and later sources, Bárta and Brůna, 2006) (Fig. 1). Methods applied to the study of environmental record include mainly basic facial analyses, microstratigraphy studied by the method of micromorphology, study of the surface of quartz grains, macro-remain and anthracological studies and the study of malacofauna.

The excavated sections were sedimentologically logged. Bulk samples used for the study of the surface quartz grain micromorphology were taken according to the lithological change. Three micromorphological samples were taken into Kubiena boxes, dried, impregnated by resin, hand thin sectioned and studied under a polarizing microscope. The quartz grain surface analysis was performed on the spot together with the determination of ceramic fragments and pebble provenance analysis. Each 10 cm of material from sections a and b were wet sieved on the spot for the purpose of grain-size distribution. All studied sections included in this paper are dated by the presence of archaeological remains.

Five main lithologically different layers were sampled and flotated (20 L each) for the purposes of botanical, anthracological, and mollusc analyses. Extraction of macrofossils, charcoal and molluscs from the soil material followed the standard flotation and wet sieving procedure (Jacomet and Kreuz, 1999), using staggered sieves with a mesh size of 0.25 mm. Molluscan and plant macro-remain analyses were performed from eight lithological intervals from Section A. The volume of all the processed samples was 20 l with the exception of the sample from the bottom of the section (175–185 cm). The volume of this one did not exceed 3 l. All the samples were treated by water flotation with the sieve size of 0.5 and 0.25 mm immediately after sampling. The dried samples were then sorted under a light microscope at ×l0 to ×15 magnifications. Seed atlases by Cappers et al. (2006, 2009) were used for the plant macro-remain determination. Characteristics of the wild plants follow the Flora of Egypt by Boulos (1999, 2000, 2002, 2005).

5. Results

5.1. Sedimentology and microstratigraphy

Aquatic sedimentation of the deepest lacustrine facies (Trench A and B) was expected (Figs. 3 and 4), with lake deposits being overlain by wadi sedimentation (Trench C and D) (Fig. 5). The facial analysis of studied sections confirmed those expectations. This is why Trench C was located at the intersection of the axis of the Lake of Abusir and the Fetekti wadi (Fig. 2), to reveal the role of flash floods and torrential rains. Trench A was located approximately in the centre of the Lake of Abusir depression and close to the fields of the floodplain, lying some 1.2–1.4 m below the present surface of the Lake of Abusir. Trench B was located close to the axis of the depression and near the Abusir wadi (Fig. 2). It was confirmed that sections in trenches A and B represented the deepest part of the depression, whereas the section in Trench C is strongly influenced by the Fetekti wadi, and that in Trench D by the Abusir wadi. Trench D was located near the southern extension of the lake close to the wide Abusir wadi. The trench excavation had to be stopped at the level of groundwater some 1.8–2.0 m below the present flood

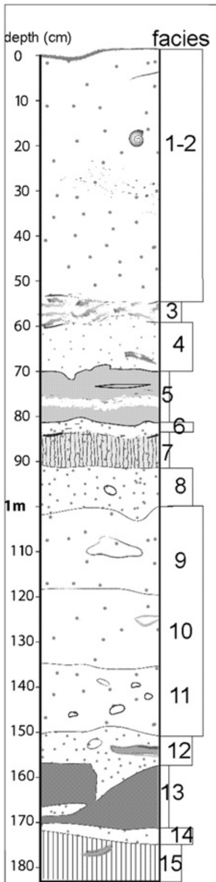

Depth	Facies	Lithology	Depositional environment
Trench A			
0-70	1-4	Sand, yellow aeolian sand, occasional stains of the dark humic soil from decomposed mudbricks, frequent water snails, tubular root krotovinas.	The pure sand fluviatile sedimentation ends some 15 cm above Old Kingdom platform of the Third to early Fourth Dynasty. The upper part of the profile is formed by distinctly different aeolian sands interrupted by dark sandy loams of an intermittent “lake”. The soil material is most probably coming from the eroded mudbricks or irrigation channels feeding field systems that are very common in the whole area. The mudbrick platform (other platforms of this type were possibly identified nearby by georadar) could be a part of the landing installations for boats arriving to the cemetery as witnessed by frequent iconographic evidence (Bárta 1999). It means that the water table had to be slightly below 18 m. a. s. l even during the high flood season during the Third to early Fourth Dynasty.
70-90	5-7	27-35 cm thick strata of grey sandy loam derived from mudbricks or recent field system with two layers of aeolian sand, and no bioturbation.	
90-150	8-11	Grey and yellow fine grained aeolian sands	
150-160	12	Grey and yellow fine grained sands, pure, coarse grained, fluviatile sands with quartz and flint pebbles	
160-170	13	Mudbrick platform (tilled pavement), partly well preserved, partly decomposed by humidity, frequent pieces of Fifth Dynasty ceramic. The tilled pavement is eroded by stream water containing sandy material (wash outs) (Cooke et al, 1993).	
Below 170	14-15	Fluvial, quartz dominated pebbles, flints and sands	

Fig. 3. Lithostratigraphy and depositional history of Abusir “Lake” trench A.

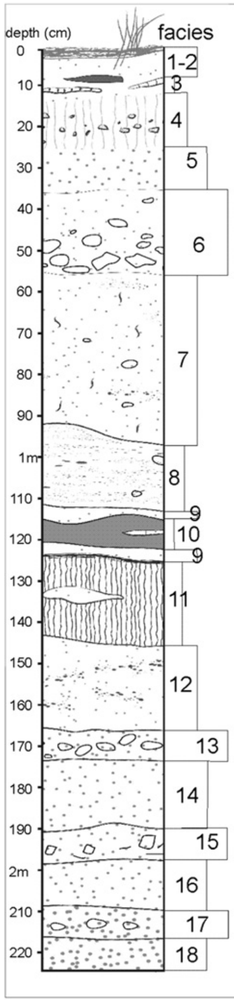

Depth	Facies	Lithology	Depositional environment
Trench B			
0-58	1-5	Yellow and grey sand, small lenses of clay, some gravel deposits form the overlying layer.	Profile B has the same pattern as the previous profile. It can be divided in the lower more humid fluviatile phase and the upper arid aeolian sedimentation phase. The boundary between these two series is located aprox. 20 cm above the Third to early Fourth Dynasty mudbrick marker. The intermittent "lake" is recorded here as well in the layer 7 – it may belong to the Pre-Coptic period, but a cross proof such as OSL dating is still missing due to the administrative barriers.
58-9	7	Correlates to the lacustrine sedimentation of layers 5-7 of A profile, grey sandy loam deposited in stagnant water, but the bioturbation is present probably due to the cattle treading (water buffalo ?).	
92-115	8	Pure, coarse grained sand and gravel of colluvial origin.	
115-140	9-11	Rewashed mudbricks accompanied by ceramic fragments of the Third-early Fourth Dynasty and divided like in profile A by fluviatille sand deposition.	
140-230	12-18	Alternating strata of pure fluviatile sands and gravels.	

Fig. 4. Lithostratigraphy and depositional history of Abusir "Lake" trench B.

plain (ca. 20 m a.s.l.). The detailed description of sedimentary facial analyses together with the basic interpretations is documented in Figs. 3–5.

Micromorphological analyses were used to find out the composition and origin of the sand-dominated material below the tiled pavement, the properties of the darker loamy intervals within the sandy loam of Trench A (at a depth of 75 cm) and the thin cracked clay interval in Trench B (depth of 25 cm). An example of photodocumentation with the distinctive micromorphological characteristics and the descriptions and interpretations is presented in Fig. 5. Each sample presented in this figure reflects a different environment within the Lake of Abusir depression.

5.2. *Palaeobiological analyses*

Plant macro-remains and charcoal found in studied strata were very limited. The plant macro-remains originally present in these strata may have been present only in very small amounts. However, some grassland species (Poaceae) *Echium* sp. and a clover (*Trifolium* sp.) were present together with a wetland species of spike-rush (*Eleocharis* sp.) and hood canarygrass (*Phalaris paradoxa*). One fragment of a charred cereal caryopsis was also found (Figs. 5 and 6). Samples contained also very small pieces of fresh and charred wood. Among species prevailed fragments of acacia (Acacia nilotica) and tamarix (*Tamarix* sp.), reflecting the presence of common local trees and shrubs. Fragments of fresh wood and charcoal were small, not exceeding 2–3 mm. Their amounts and sizes indicate secondary deposition in the strata. Among archaeobotanical samples, there are exceptional samples from mud-brick structures connected with the Old Kingdom period. Macro-remains from mud-brick structures, namely from Trench A, were more frequent in amount, but they could be not directly connected with natural and semi-natural alluvial deposits and will be evaluated separately.

Mollusca shells or their fragments founded in studied sediments contain 7 main species. Those species are typical mainly of fresh water environments, with flowing or slowly flowing water, but terrestrial snail shells also were identified. The results of the analyses are summarized in Fig. 6. Ecological interpretations of the individual taxa are listed in Fig. 8.

6. Discussion

6.1. *Water source for feeding the Lake of Abusir depression*

The sedimentological record can be considered rather discontinuous due to the episodic sedimentation, erosional events and scraping of the upper aeolian sand by farmers protecting their fields against desertification. Three human-made sand rims can be observed along the western edge of the lake. They contain aeolian

Trench C

Located at the edge of Abusir Lake in the axis of Fetekti wadi. The sedimentology is typical for desert wadis. Aeolian and rewashed aeolian sands alternate with gravels washed down by flash floods. An limestone altar of unique historical value and a mudbrick structure was revealed approx. 70 cm below the recent surface. The unplanned rescue archaeological research revealed top of an Old Kingdom tomb. This finding is important for determination of water table level during the Old Kingdom Period. The upper part of the false door was located 1.00 m below the present surface. The stela was 50 cm high and the floor of this offering chapel was at a depth of 1.50 m below the present surface, i.e. about 18.80 m a.s.l.. (for details see Bárta 2009). It correlates with the mudbrick platform of Profile A (-180 cm + two cubits = approx. 3 m below the present surface, i.e. 17.20 m a.s.l..) and situation in Profile D. Also mastaba AS 33 in South Abusir seems to provide some interesting evidence in this respect. During the excavation of its substructure, one room (Room X, a well-shaft?) was found flooded to a height of 17.30 m a.s.l.. (Bárta 2010, 70).

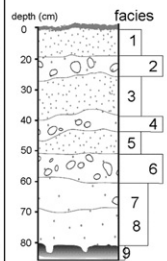

Trench D

It was located still within the limits of the lake but close to Abusir wadi. When we refer to the lake limits we take as the basis the flat lake-like surface covered by vegetation and the extent of a "lake" as recorded by Lepsius´s and other maps. The excavation was arduous because of the constant finds of pottery fragments and animal bones – both rewashed and in situ positions. All the layers up to the depth of 290 cm (again a similar boundary of aprox. 3 m) are somehow influenced by human activities. We observed the layers with mudbrick admixture, blocks of limestone up to 50 cm long from some nearby building and other human traces. The surface of Abusir wadi seems to be a continuous burial place sometimes affected by flash flood erosion. However in the lowermost part of the profile D (290-340 cm) we found the same pure, fluviatile sand and gravel strata as in the A and B profiles.

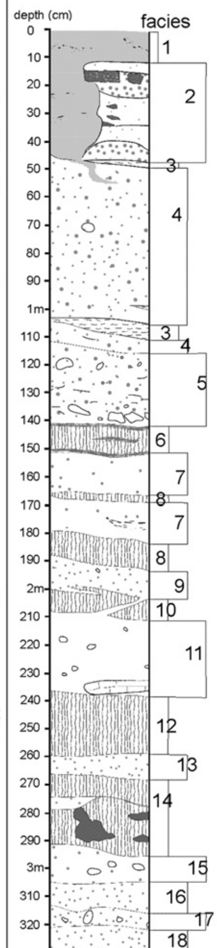

Fig. 5. Lithostratigraphy and depositional history of Abusir "Lake" trench C and D.

sand constantly blown by desert winds to the Nile floodplain. There is a visible lack of any fluvial sediments or typical organic-rich material within the sedimentological record of the studied sections (Figs. 3–5). However, the source of water was not contaminated by black Nile loam rich in organic matter. The only possible explanation seems to be that the lake was fed by ground water collected below Eocene rocks. The elevated activity of groundwater seepage probably reflects the flooding periods of the Nile River. It seems this system works on the principle of connected vessels. The water of Nile flooded not only the surrounding alluvial plain but also penetrated into geological background represented by the local Eocene sand basement. This infiltration initiated the activity of groundwater which is now at the level of 18 m a.s.l., and this water started to discharge on the surface in the form of springs, i.e., to the lowermost area of the Abusir depression, the Lake of Abusir. When the flood receded, the water body in the depression slowly infiltrated or even dried completely. Some water could be collected from occasional flash floods and sands of the Abusir wadi catchment as well (Abusir wadi was a principal discharge valley in the local topography). The closest existing analogue of the Lake of Abusir is probably the intermittent Dahshur Lake some 10 km to the south.

6.2. Landscape of the Lake of Abusir during the Old Kingdom

All the studied sections show a quite similar sedimentological trend (Figs. 3–5), strongly influenced by the local geomorphology (Figs. 1 and 2). Surprisingly, the groundwater level was found at the altitude of 18 m which is approximately 2 m below the present surface of the flood plain (Jeffreys, 2006a, p.17; Bárta, 2010, p.70). The bottom of all sections were represented by fluvial sands and pebbles, overlain by a tiled pavement dated to the interval between the Third and Fifth Dynasties of the Old Kingdom according to the ceramic shreds, approximately before 2460 BC. This date correlates well with the first stage of desiccation in the Middle East which occurred around 2500 BC, while the main droughts occurred around 2200 BC (Weiss and Bradley, 2001; Bárta and Bezděk, 2008). Clearly, fluvial activity with no prevailing aeolian deposition dominated the landscape during the use of the pavement. The likely function of the mud-brick pavement which was about 2 m wide and oriented NE–SW was probably to serve as one (of many) access routes from the lake to the cemeteries. It can be supposed that some true or symbolic (see below) landing facilities may have been located at some distance to the east or northeast, close to the third millennium main branch of the Nile. During this period, the Nile branch was most likely situated to the

Context	Distinctive micromorphological characteristics	Interpretation
Sample A, located in the depth of 170 cm of the trench A, below the toled pavement (PPL) (plane polarized light) 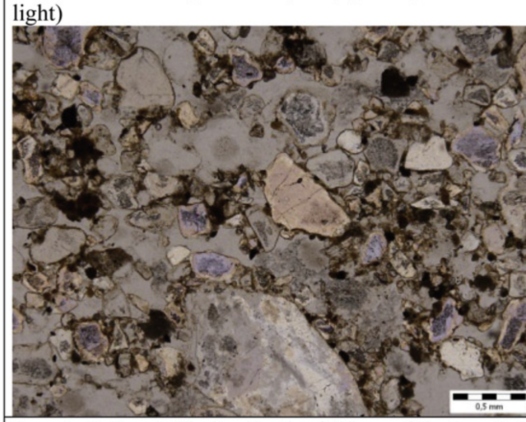	The bridge grain microstructure with gefuric related distribution decomposed organic matter composing the bridges between coarse material. Coarse material is moderately sorted and composed of quartz, plagioclase mainly. c/f (0.3mm) = 80:20. The percentage of organic matter is 20 %.	Surface organic horizon of weakly developed arid soil.
Sample B, located in the depth of 75 cm of the trench A (PPL) 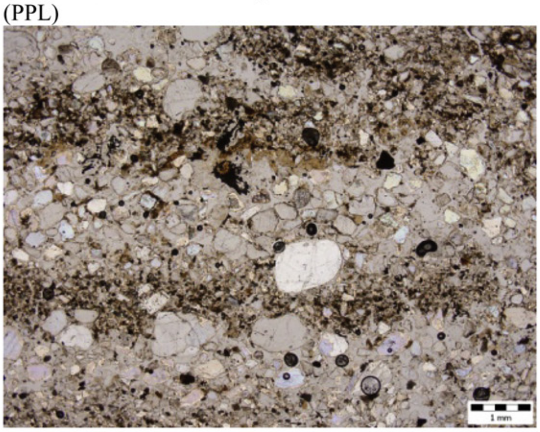	Four buried organic matter rich horizons marked as facie x and three pure sandy horizons marked as *facies* y. X - homogenous, apedal, salt free clayey groundmass, rare vesicles. The c/f related distribution pattern is monic, with the ratio c/f(0.2 mm) = 50:50. The micromass is yellowish-brown calcitic crystalitic b-fabric Y – moderately to well sorted sand composed mainly of quartz. The ratio c/f(0.5 mm) = 95:5.	X - buried takyric *horizon* reflecting the phases of increased moisture and organic matter production. Y - buried aeolian sand reflecting the phases of *desiccation.*
Sample C, located in the depth of 25 cm of the trench B, macroscopically visible as a cracked thin clay layer (XPL) (cross polarized light). 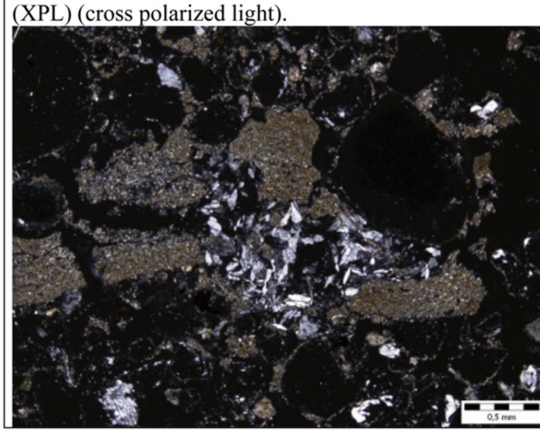	0.5 thin fragments visible on the picture on the left are composed of very fine grained dusty material. c/f related distribution is porfyric with the ratio c/f(0.02mm)= 50:50. Brown calcitic matrix has crystalitic b-fabric. The crystals of gypsum salts occur in the middle of the picture and reflect quick desiccation.	Desiccation cracks of matrix originated within the slope or small shallow pool after the heavy rain. Evaporite crystals grow and disrupt the soil matrix because of the presence of ion rich soil solution and relatively high formation/dissolution frequencies in relation to horizontal processes (Schaetzl and Anderson, 2005).

Fig. 6. Micromorphological observations and interpretations of facies.

west of ancient Memphis. Based on the latest results, it can be supposed that the modern Bahr Libeini (now about 2 km east of the Abusir pyramid field) was the main channel of the River Nile in antiquity (Giddy, 1994; Lutley and Bunbury, 2008; Spencer, 2010, 29). Later, during the late Old Kingdom (ca. 2300 BC), the area around the lake became occupied by tombs of lesser officials of the state starting at the altitude of about 19 m (Bárta, 2010).

The altitude of 18 m, where the tiled pavement was found, lies 3.5–4.0 m above the reconstructed inundation levels of the Old Kingdom period (14–14.5 m a.s.l.) (Lehner, 2009a, 2009b). This means that the encountered pavement was built on a dry fluvial terrace and not flooded at all. This suggests a similar symbolical phenomenon as in the case of the valley temple of Unas and other Old Kingdom royal complexes. The base line of the harbour walls in the valley temple of Unas lies at the altitude of about 18 m. (Jeffreys, 2006a, 17). In his opinion, it was impossible to reach the harbour by water.

The most recent studies that the Old Kingdom floodplain must have been situated considerably at lower altitudes than the 18 m a.s.l. structures discovered in the Lake of Abusir. The seminal study by Jeffreys and Tavares (1994, p. 158) made it clear that the majority of settlement in the area of Old Kingdom Memphis is situated above the floodplain level which was typically about 13–14 m a.s.l. Supposing that a standard Nile flood reached a height of 1.5 m (Willcocks, 1889, 44), it is logical to suppose that most settlement of the period was located at around 15.5 m a.s.l. and higher. This estimate matches the results of coring materials from Dahshur. The borings carried out by the German expedition (Alexanian and Seidlmayer, 2002, p. 23–5) have shown that the Fourth-Sixth Dynasty settlement level was situated somewhere between 16 and 17.5 m a.s.l. Contrary to this, Casey has concluded during his survey of Saqqara that the valley floor of the Old Kingdom (based on the elevation of the harbour in the funerary complex of Pepy II) was lying around 16–16.5 m a.s.l. In this connection it is interesting to mention that the floors of the valley temples of Sahure and Nyuserre in Abusir lie at the altitude of 17.5 and 19.0 m a.s.l., respectively (Seidlmayer, 2001, 48).

Possible changes in moisture can be reconstructed from the micromorphological observations. The bridge grain microstructure of sandy matrix with gefuric-related distribution (Fig. 4) is usually interpreted as a friable Bh horizon or A or E horizon of podzols (Wilson and Righy, 2010). However, podzolization should not be considered in this type of environment. The presence of this material suggests organic matter accumulation and decomposition. The dark brown organic pigment is typical for the surface horizons according to Gerasimova and Lebedeva-Verba (2010) and Adderley et al. (2010). It is possible that relicts of surface horizons of desert soils were preserved below the tiled pavement. These soils are extremely thin, only a few centimetres in thickness. The moisture needed for the production of this kind of organic matter accumulation was probably provided by an already existing hydrological system, as described above. This means that the area of the Abusir depression was inundated by pushing groundwater in relation with the Nile River inundation phases.

Mollusc shells found below the pavement are very rare and cannot be used as statistical proof. They were interpreted as xerophilous African land snails which usually occur in northwestern Africa, or as common freshwater snails inhabiting a wide range of aquatic environments. These findings correspond with the conclusion that the lake was in existence only seasonally, during the flooding period.

On the other hand, the botanical interpretation of this period is not very clear. In general, the palaeobotanical study of botanical macro-remains (no pollen could be determined) preserved in mudbricks of individual archaeological objects shows that there was a major tendency towards desiccation of the area throughout the third–first millennia BC (Pokorný et al., 2009). Macrobotanical remains toward the younger deposits are very rare. Together with the decreasing amount of macroremains, deposition of windblown material containing aeolian quartz grains is interrupted by thin clay layers produced by occasional heavy rains followed by rapid dessication (Fig. 8).

	0-65	65-90	90-100	100-135	135-150	150-160	170-175	175-185
Aquatic molluscs								
Bithynia tentaculata	2	2	1					
Bulinus truncatus	7	8	1					
cf. *Belamya unicolor*		16						
cf. *Valvata nilotica*	1							
Gabbiella cf. *senaariensis*							1	
Melanoides tuberculata						1		2
Terrestric molluscs								
Trochonanina/Martensia spp.								1 fragm.
Aquatic and wetland plants								
Characeae	38	169		3				
Damasonium alisma Mill.	78	24	4	10	18			
Alisma plantago aquatica L.	30	7		6	9			
Heliotropium aegyptiacum Lehm.	15	2	2	3	5			
*Scirpoides holoschoenus*Sojak	2							
*Ranunculus sceleratus*L.	1							
Cyperaceae	2							
Eleocharis cf. caduca (Delile) Schult.		1					1	
Elatinaceae					1			
Weeds of cultivation								
Buglossoides/Echium	1			1		1		
Fallopia convolvulus(L.)		1						
cf. *Fumaria* spec.		1						
Chenopodium murale				1				
Grassland plants								
Poaceae		3					1	1
cf. *Trifolium* spec.						1		

Fig. 7. The appearance of the taxa of molluscs and plant macro-remains found in the Abusir "Lake" deposits (profile A). The individual samples are identified by their depth (in cm) under the recent surface.

6.3. Erosion event by the end of Fourth Dynasty

The tiled pavement buried below a surprisingly thin layer of sand and sandy loam (150–180 cm) has a deeply eroded surface horizon (Figs. 3 and 4). An approximately 15 cm thick layer of sand overlying and partly destroying the Old Kingdom pavement was described as a result of purely sand-sized alluvial (colluvial) sedimentation. The glossy surfaces of quartz grains derived from this sand-sized material are rounded, bearing typical fluvial bowl-like features. This could suggest a possible fluvial origin, but a much higher-energy depositional environment is suggested by the clearly visible pavement destruction. The possible explanation is alluvial (colluvial) redeposition of sand coming from older fluvial terraces above. Such a high-energy event is compatible with a heavy rain period(-s).

A similar and a more precisely dated erosional event, comparable with the erosion of tiled pavement of the Lake of Abusir, was found by Polish expeditions within the area of Necropolis of West Saqqara (Trzcinski et al., 2006). Based on the geoarchaeological results of the Polish expedition of 2006, geodynamic processes in this area were reconstructed. They suggest a natural environment shaped indirectly by human activity. Archaeological interpretation of the finds indicates that these processes could have taken place during the first phase of use of the Lower Necropolis, between 2700 and 2600 BC. At the beginning of this phase, the relatively dry and warm climate appears to have changed for a cooler and more humid one. The type of weathering observed on the surface of the limestone points to a warm climate characterized by cyclical alternation of humid and dry periods, with the latter predominating (Trzcinski et al., 2006). Another remark on heavy rains and the need to build some kind of protection was made by Welc (2007). He excavated the remains of a casing wall at the Netjerikhet funerary complex and interpreted its later use also at the end of the Old Kingdom. Similar evidence, e.g. heavy muddy downwashes, was observed in several burial chambers of late Third Dynasty mastabas at Abusir (Bárta, 2010).

Although no mollusc remains were found in the strata representing humid environments, the plant remains (*Damasonium alisma, Alisma plantago-aquatica, Heliotropium aegyptiacum,* Elatinaceae) (Figs. 7 and 8) indicate humid conditions persisting during

Mollusca	**Ecology**
Aquatic molluscs	
Bithynia tentaculata (Linnaeus, 1758)	Common European species of various aquatic habitats. The occurrence of this species in Abusir is surprising, because of its recent known range extends to Morocco and Algeria only.
Bulinus truncatus (Audoin, 1827)	Common African species of all types of freshwater habitats.
cf. Bellamya unicolor (Olivier, 1804)	This species occur in lakes and slowly flowing rivers of tropical Africa, common also in fossil records
cf. Valvata nilotica (Jickeli, 1874)	The species of slowly flowing waters with dense aquatic vegetation. Occurs in Lower Egypt and the Ethiopian Highlands.
Gabbiella senaariensis (Küdter, 1852)	The species of large rivers and lakes, recently known from the Nile and Southern and Western Africa. Fossil records from Fayum (Egypt), the second Nile Cataract (Sudan) and also from Chad and Nigeria.
Melanoides tuberculata (Müller, 1774)	Common freshwater snail of wide range of aquatic environments.
Terrestric molluscs	
Trochonanina/Martensia spp.	Xerophilous African terrestrial snails occurring in North-western Africa.
Plants	**Ecology**
Aquatic and wetland plants	
Characeae	Green algae found in shallow fresh water, particularly in limestone areas, sometimes in in brackish even maritime waters.
Damasonium alisma Mill.	Inundated land, muddy canal banks. The species was fairly common in the basin lands which were regularly inundated in summer time for several months by the annual Nile flood. But after the construction of the Aswan High Dam in 1964, which allowed the control of the annual flood, the basin lands were subjected to a network of irrigation canals and the plant became rare. Perennial.
Alisma plantago-aquatica L.	Nile banks, ditches and marshy ground. Perennial.
Heliotropium aegyptiacum Lehm.	Nile banks, moist stony ground. Short- lived perennial.
Scirpoides holoschoenus (L.) Sojak	Moist ground, swamps, canal banks. Annual.
Ranunculus sceleratus L.	Littoral marshes, Nile and canal banks, wet meadows. Perennial.
Cyperaceae	Moist ground or shallow water, canals, ditches.
Eleocharis caduca (Delile) Schult.	Wet meadows, springs, canal banks and lakes. Perennial.
Elatinaceae	Irrigation canals, moist ground. Annual.
Weeds of cultivation	
Buglossoides/Echium	Cultivated ground, waste land, sandy and stony soils.
Fallopia convolvulus (L.)	Weed of cultivation. Annual.
cf. Fumaria spec.	Weed of cultivation. Annual.
Chenopodium murale L.	Weed of cultivation and waste ground. Annual.
Grassland plants	
Poaceae	Grasses. Broad range of biotopes.
cf.Trifolium spec.	Moist to sandy ground, orchards, edges of cultivation.

Fig. 8. Overview of the present taxa and their ecological interpretation. Characteristics of molluscs are according to Van Damme (1984), Kerney et al. (1983) and Boettger (1910). Characteristics of the wild plants are according to Flora of Egypt by Boulos (1999, 2000, 2002, 2005).

sediment deposition between 0 and 150 cm depth. However, no definite evidence for a persistant aquatic environment was found. The plant species found here typically grow on moist and marshy ground, on banks and wet ditches and on temporally inundated land. Goosefoot (*Chenopodium murale*) and *Echium* sp. can be interpreted as weeds of cultivation or indicators of waste ground.

6.4. Buried takyric horizons as a reflection of the past

The most continuous aeolian sedimentation of the Lake of Abusir area not destroyed by the Fetekti wadi function is preserved in trenches A and B (Figs. 3 and 4). Sediments in these two sections are represented by distinctly different aeolian sands interrupted by dark sandy intercalations. These loams were formed due to the inundation of the Lake of Abusir depression as described above. The only difference is that the period of the accumulation of the intercalations lasted during and after the maximum desiccation period around 2200 BC (Weiss and Bradley, 2001). The sand-dominated material may be regarded as "mirrors" (Dokuchaev's expression) of the present-day environment (Gerasimova and Lebedeva-Verba, 2010), whereas "the subsoil, i.e., the darker humic loam layers, reflects the events that happened under more humid condition" (Lobova, 1967; see; Souirji, 1991), in this case, moistening due to regional geomorphic conditions. A similar life cycle is typical for most of the wadi systems and had a profound impact on the settlement strategies pursued by the ancient Egyptians with regard to wadi mouths (Dufton and Branton, 2009).

Micromophological observations confirmed the presence of the so-called takyric horizon or its very first stages. Repetition and common appearance of these horizons is due to the repeated moistening/inundation and desiccation. Microlamination is formed under such circumstances (Fig. 6). According to Gerasimova and Lebedeva-Verba (2010), "these horizons are characterized by a homogeneous, apedal, salt-free clayey groundmass, with few to abundant vesicles and few planes". The c/f related distribution pattern is mostly a fine monic, with few coarse mineral grains. Micromass is yellowish-brown to light brown with mainly calcitic crystallitic and locally stipple speckled b-fabric (Fig. 6). According to Fedoroff and Courty (1987), aeolian transport of fine sand separating the tacric horizons is very common. Mollusc species found within the horizons are usually common African species, living mainly in different substrates in stagnant or slowly flowing waters, in lakes and gently flowing rivers of tropical Africa or another freshwater habitats (Kerney et al., 1983; Van Damme, 1984). The most common taxon, cf. *Bellamya unicolor* (Olivier, 1804), was found in damaged fragments and is common also in fossil record, which indicates that it could have been probably redeposited by wind erosion together with the aeolian material. The appearance of *Bithynia tentaculata* (Linnaeus, 1758), a common European species of various aquatic habitats, was quite surprising because the present distribution of this taxon is only limited to Morocco and Algeria (Van Damme, 1984).

Plant macro-remains found in strata beneath the present surface (0–90 cm) strongly indicate aquatic environment. A total of 166 specimens of wetland and aquatic plant species were present in the uppermost interval, representing 7 taxa. The appearance of Characeae, green algae typical of shallow, clear water, together with *Daphnia magna ephipia* (aquatic crustacean) supports the interpretation of the presence of an aquatic environment. On the other hand, many wetland species (some identical with those mentioned in the previous section) indicate humid conditions with no superficial water over several months in a year. Several remains of weeds were also found here, indicating the presence of a humid environment which is usually connected with cultivated land in the surroundings. Unlike the upper strata, the interval directly below the organic-rich matter (90–100 cm) was very poor in plant macro-remains. It is unclear whether this is a result of poor taphonomic conditions or evidence for rapid accumulation. However, wetland species were present here.

7. Conclusions

1. The background geomorphology of the Lake of Abusir and other natural depressions under the steep slopes of the Abusir and Saqqara area were very probably formed by an older, now abandoned Early–Mid Holocene river course. Such irregular linear depressions are a common feature of all riverine systems. The river erodes or undercuts the slope and then, after a flood or megaflood, shifts its course closer to the central part of the wide valley. Aggradations take place there. The former river course under the slopes remains in spite of some aeolian sedimentation, and water seeps in, resulting in a formation of a marsh or even a "lake".
2. The sections observed in the excavated trenches can be roughly divided into five parts:
   1) the lower part is formed by "pure" sands and gravels of fluvial origin with probable relicts of humic horizon
   2) mud-brick pavement overlain by wash-out sandy alluvial deposits
   3) the upper parts of the sections are dominated by desert aeolian sedimentation interrupted by stages of elevated moisture and the origin of takyric horizons
   4) aeolian sands are occasionally intercalated by flash-flood wadi deposition (medium-sized gravels, trenches B and C)
   5) desiccation cracks as the result of heavy rains sedimentations followed by quick desiccation occur in the uppermost parts of the sections.
3. The lower fluvial sedimentation reflects the changes in hydrological regimes witnessed by a sand-gravel rhythm. Wadis must have functioned at least as perennial rivers during and after the Old Kingdom period.
4. The Abusir wadi seems to be older than the Fetekti wadi because fragments of the local limestone rocks are abundant in Trench D but almost lacking in the other trenches. The Fetekti wadi probably acted as a water piracy agent. Its sediments probably formed a transversal aggradation rim that cut off the southern smaller part of the lake from the lake main body.
5. Possibly the main result is that the change of the sedimentation from fluvial to aeolian occurred some 10 cm above the horizon dated to the interval between the Third through the Fifth Dynasty of the Old Kingdom, approximately after 2460 BC. This date correlates well with the first stage of the Middle East desiccation at around 2500 BC, while the main droughts appeared much later, at around 2200 BC (Weiss and Bradley, 2001).

Acknowledgement

The research was supported by the MSM Research Plan No. 0021620826 (Czech Institute of Egyptology), Academic International Project "Environmental history of Egyptian Western Desert" No. M100130902, by the Institutional Research Plan of the Institute of Geology AS CR, v. v. i, No. AV0Z 30130516 and by the MSM Research Plan No. 6007665801 (University of South Bohemia, Faculty of Science). This study has been supported by the Grant Agency of the Czech Republic, Grant nos. P405/11/1873 and P206/09/1564.

References

Adderley, W.P., Wilson, C.A., Simpson, I.A., Davidson, D.A., 2010. Anthropogenic features. In: Stoops, G., Marcelino, V., Mees, F. (Eds.), Interpretation of

Micromorphological Features of Soils and Regoliths. Elseiver, Amsterdam, pp. 569–588.
Alexanian, N., Seidlmayer, J.S., 2002. Die Residenznekropole von Dahschur. Erster Grabungsbericht, Mitteilungen des Deutschen archäologischen Instituts. Abteilung Kairo 58, pp. 1–28 (in German).
Bárta, M., 1999. The Title "Priest of Heket" in the Egyptian old Kingdom. Journal of Near Eastern Studies 58 (2), 107–116.
Bárta, M., 2005. Location of the old Kingdom pyramids in Egypt. Cambridge Archaeological Journal 15 (2), 177–191.
Bárta, M., 2009. An Old Kingdom book for the afterlife. In: Magee, D., Bourriau, J., Quirke, S. (Eds.), In Sitting beside Lepsius. Studies in Honour of Jaromir Malek at the Griffith Institute. Orientalia Lovaniensia Annalecta, vol. 185. Peeters, Leuven–Paris, pp. 23–38.
Bárta, M., 2010. Mastaba AS 33. Architecture. In: Bárta, M., Coppens, F., Vymazalová, H. (Eds.), Abusir IX. Tomb of Hetepi (AS 20), Tombs AS 33–35, and AS 50–53. Serifa, Prague, pp. 6–17.
Bárta, M., Bezděk, A., 2008. Beetles and the decline of the old Kingdom: climate change in ancient Egypt. In: Proceedings of the Conference, Chronology and Archaeology in Ancient Egypt (The Third Millennium BC). Czech Institute of Egyptology, Prague, pp. 214–222.
Bárta, M., Brůna, V., 2006. Satellite Atlas of the Pyramids: Abu Ghurab, Abusir, Saqqara, Dahshur, Dryada, Mníšek pod Brdy.
Boettger, O., 1910. Die Molluskenausbeute der Erlangerschen Reise nach Nordost-Afrika. Abhandlungen der Senckenbergischen Naturforschenden Gesellschaft 32, 1–52.
Boulos, L., 1999. Flora of Egypt (Azollaceae-Oxalidaceae), vol. 1. Al Hadara Publishing, Cairo, Egypt.
Boulos, L., 2000. Flora of Egypt (Geraniaceae-Boraginaceae), vol. 2. Al Hadara Publishing, Cairo, Egypt.
Boulos, L., 2002. Flora of Egypt (Verbenaceae-Compositae), vol. 3. Al Hadara Publishing, Cairo, Egypt.
Boulos, L., 2005. Flora of Egypt (Alismataceae-Orchidaceae), vol. 4. Al Hadara Publishing, Cairo, Egypt.
Brown, A.G., 1997. Alluvial Geoarchaeology. Cambridge University Press, Cambridge.
Butzer, K.W., 1976. Early Hydraulic Civilization in Egypt: A Study in Cultural Ecology of Prehistoric Archeology and Ecology. University of Chicago Press, Chicago.
Cappers, R.T.J., Bekker, R.M., Jans, J.E.A., 2006. Digital Seed Atlas of the Netherlands. Barkhuis, Eelde.
Cappers, R.T.J., Neef, R., Bekker, R.M., 2009. Digital Atlas of Economic Plants. Barkhuis, Eelde.
Dittmer, J., Gallorini, C., Ikram, S., Leahy, A., Lines, D., Mathieson, I., Reader, C., 2003. Saqqara Geophysical Survey Project 2003. Glasgow Museums, Scotland.
Dufton, D., Branton, T., 2009. Climate change in early Egypt. Egyptian Archaeology 36, 36–37.
Fedoroff, N., Courty, M.A., 1987. Morphology and distribution of textural features in arid and semiarid regions. In: Fedoroff, N., Bresson, M., Courty, M.A. (Eds.), Micromorphologie des Sols, Soil micromorphology. AFES, Paris, pp. 213–219.
Gerasimova, M., Lebedeva-Verba, A., 2010. Topsoils – Mollic, takyric and yermic horizons. In: Stoops, G., Marcelino, V., Mees, F. (Eds.), Interpretation of Micromorphological Features of Soils and Regoliths. Elseiver, Amsterdam, pp. 351–368.
Giddy, L., 1994. Memphis and Saqqara during the late Old Kingdom: some topographical considerations. In: Berger, C., Clerc, G., Grimal, N. (Eds.), Hommages à Jean Leclant. Études pharaoniques. Bibliothéque d'Etudes 106/1, vol. 1. French Archaeological Institute, Cairo, pp. 189–200.
Hornung, E., Krauss, R., Warburton, D., 2006. Ancient Egyptian Chronology. Brill, Leiden.
Issawi, B., al-Jiyūlūjīyah al-Misrīyah, M., 1999. The Phanerozoic Geology of Egypt. A Geodynamic Approach The Egyptian Geological Survey. Special Publication 76, Cairo.
Jacomet, S., Kreuz, A., 1999. Archäobotanik: Aufgaben, Methoden und Ergebnisse Vegetations und Agrargeschichtlicher Forschung. Ulmer, Stuttgart.
Jeffreys, D., 2001. High and dry? Survey of the Memphite escarpment. Egyptian Archaeology 19, 15–16.
Jeffreys, D., 2006a. Field work 2005–06. Memphis: escarpment survey. Journal of Egyptian Archeology 92, 16–19.
Jeffreys, D., 2006b. The survey of Memphis: recent results. Egyptian Archaeology 32, 14–15.
Jeffreys, D., Tavares, A., 1994. The Historic Landscape of Early Dynastic Memphis, vol. 50. Mittelungen des Deutschen archäologischen Instituts, Abteilung Kairo. 143–173.
Kerney, M.P., Cameron, R.A.D., Jungbluth, J.H., 1983. Die Landschnecken Nord– und Mitteleuropas. Verlag Paul Parey, Hamburg und Berlin.
Lehner, M., 2009a. Capital zone walk-about 2006: spot heights on the third millennium landscape. In: Lehner, M., Kamel, M., Tavares, A. (Eds.), 2009a. Giza Plateau Mapping Project Seasons 2006–07 Preliminary Report, Giza Occasional Papers, vol. 3. Ancient Egypt Research Associates, Boston, pp. 97–151.
Lehner, M., 2009b. Valley complex for a queen who would be king. AERAGRAM 10, 7–9.
Lobova, E.V., 1967. Soils of the Desert Zone of the USSR. Israel Programme for Scientific Translations, Jerusalem.
Lutley, C., Bunbury, J., 2008. The Nile on the move. Egyptian Archaeology 32, 3–5.
Mahmoud, A.M.A., 1986. Geological studies of the Quaternary sediments, East Nile. M.Sc. Thesis, Fac.Sc.Ain Shams University, Cairo.
Mahmoud, A.M.A., Hamdan, M.A., 2002. On the stratigraphy and lithofacies of the Pleistocene sediments at Giza Pyramidal area, Cairo, Egypt. Sedimentology of Egypt 10, 145–158.
Mathieson, I., 2000. The National Museums of Scotland Saqqara survey report 1990–2000. In: Bárta, M., Krejčí, J. (Eds.), Abusir and Saqqara in the Year 2000. Oriental Institute AS CR, Prague, pp. 33–42.
Pokorný, P., Kočár, P., Sůvová, Z., Bezděk, A., 2009. Paleoecology of Abusir South according to plant and animal remains. In: Bárta, M. (Ed.), Abusir XIII. Tomb Complex of the Vizier Qar, His Sons Qar Junior and Senedjemib, and Iykai. Abusir South 2. Czech Institute of Egyptology, Prague, pp. 29–41.
Reader, C., 2009. The geology of Abusir. In: Bárta, M., Bezděk, A. (Eds.), Abusir XIII: Abusir South 2: Tomb Complex of the Vizier Qar, His Sons Qar Junior and Senedjemib and Iykai. Czech Institute of Egyptology, Prague, pp. 11–16.
Said, R., 1993. The River Nile. Geology, Hydrology and Utilization. Pergamon Press, New York.
Schenkel, W., 1978. Die Bewässerungsrevolution im alten Ägypten Zabern, Mainz.
Seidlmayer, S.J., 2001. Historische und moderne Nilstände: Untersuchungen zu den Pegelablesungen des Nils from der Frühzseit bis in die Gegenwart. Achet (Series) A 1. Achet Verlag, Berlin.
Spencer, P., 2010. Egypt exploration expeditions. Egyptian Archaeology 36, 29.
Souirji, A., 1991. Classification of aridic soils, past and present: proposal of diagnostic desert epipedon. In: Kimble, J.M. (Ed.), Characterization, Classification and Utilization of Cold Aridisols and Vertisols. Proceedings of the International Soil Correlation Meeting (ISCOM). USDA, Soil Conservation service, National Soil Survey Center, Nebraska, pp. 175–185.
Strougo, A., 1985. Eocene stratigraphy of the Giza Pyramid Plateau. M.E.R.C. Aim Shams Univ., Earth Science Research Series 5, pp. 79–99.
Trzcinski, J., Kuraszkiewicz, K.O., Welc, F., 2006. Preliminary report on geoarchaeological research in West Saqqara. Polish Archaeology in the Mediterranean IXI Reports 2007, Warsaw.
Vandenberghe, J., 2003. Climate forcing of fluvial system development: an evolution of ideas. Quaternary Science Reviews 22, 2053–2060.
Van Damme, D., 1984. The Freshwater Mollusca of Nothern Africa. Distribution: Biogeography and Paleoecology. Developments in Hydrobiology. Junk Publishers, Dordrecht, Boston, Lancaster.
Verner, M., 1994. Forgotten Pharaohs, Lost Pyramids. Abusir. Academia/Škodaexport, Prague.
Weiss, H., Bradley, R.S., 2001. What drives societal collapse? Science 291, 609–610.
Welc, F., 2007. Some remarks on the Early Old Kingdom structures adjoining the enclosure wall of the Netjerykhet funerary complex. Polish Archaeology in the Mediterranean XVIII, Reports 2006, pp. 175–179.
Willcocks, W., 1889. Egyptian Irrigation. Spon Ltd., London.
Wilson, M.A., Righy, D., 2010. Spodic materials. In: Stoops, G., Marcelino, V., Mees, F. (Eds.), Interpretation of Micromorphological Features of Soils and Regoliths. Elseiver, Amsterdam, pp. 49–68.

5.6. Procesy v jeskyním prostředí

Lisá L., Neruda P., Nerudová Z., Bajer A. (2013): Geoarcheologický záznam středního a mladého paleolitu v jeskyni Kůlně, Moravský kras.- Acta Musei Moraviae. Scientiae sociales = Časopis Moravského muzea. Vědy společenské. 98, 2: 197-214.

Kadlec J., Chadima M., **Lisá L.**, Hercman H., Osintsev A., and Oberhänsli H.(2009): Clastic cave deposits in Botovskaya Cave (Eastern Siberia,Russian Federation). - Journal of Cave and Karst Studies, NSS. 70, (3), p. 142-155.

ISSN 0323-0570 *Acta Mus. Moraviae, Sci. soc.*
XCVIII: 2, 197–214, 2013

GEOARCHEOLOGICKÝ ZÁZNAM STŘEDNÍHO A MLADÉHO PALEOLITU V JESKYNI KŮLNĚ, MORAVSKÝ KRAS

GEOARCHAEOLOGICAL RECORD OF MIDDLE AND UPPER PALEOLITHIC IN KŮLNA CAVE, MORAVIAN KARST

LENKA LISÁ[1] – PETR NERUDA[2] – ZDEŇKA NERUDOVÁ[2] – ALEŠ BAJER[3]
[1] Geologický ústav Akademie věd ČR, v. v. i.,
[2] Ústav Anthropos, Moravské zemské muzeum, v. o.,
[3] Ústav geologie a pedologie, Mendelova univerzita

ABSTRACT:
The Kůlna Cave provides relatively unique sedimentary record containing not only artefacts of Upper and Middle Palaeolithic, but also information on changing climatic conditions within isotope stages MIS6 – MIS2. There are studied two major sections in context of sedimentology, micromorphology and other auxiliary proxy as are magnetic properties or particle-size distribution. One of the sections is located in the central part of the cave, the second one in its entrance part. By combining of these two sections a complete record of sedimentary development of layers 5 to 11 was obtained. Based on the set of geoarchaeological analyses it was possible to make detailed interpretation of provenance of cave sediments and their formation history which provides new information on long discussed chronostratigraphic questions of this locality.

KEY WORDS: Middle and Upper Palaeolithic, Kůlna cave, cave deposits, formation processes, micromorphology.

1. ÚVOD

Jeskyně Kůlna (Moravský kras; obr. 1) je jednou z nejdůležitějších středo- a mladopaleolitických lokalit střední Evropy. Nachází se cca 45 km severně od Brna, na severním okraji Moravského krasu. Je to v podstatě 87 m dlouhý tunel s maximální výškou 25 m a šířkou 8 m (Valoch *et al.* 2011, 10). Jeskyně má dva vchody, menší orientovaný směrem na sever a větší orientovaný směrem na JJZ do Sloupského údolí (obr. 1). Geomorfologie celé oblasti je zvýrazněna Sloupským údolím, na sever široce rozevřeným, které směrem k jihu přechází do úzkého Pustého žlebu.

Geologické podloží (obr. 1) je tvořeno devonskými vápenci, na západě částečně překrytými devonskými arkózami a slepenci. Na východě se devonské vápence stýkají s drobami kulmu Drahanské vrchoviny. Tyto horniny se nacházejí již cca 400 metrů od severního vchodu do jeskyně. Dno údolí je vyplněno fluviálními štěrky a písky, z části překrytými sprašemi a sprašovými hlínami či koluvii odvozenými od okolní geologie.

Komplexní interdisciplinární výzkum probíhal v jeskyni v letech 1961–1976 pod vedením K. Valocha (1988b), který řídil i předstihový výzkum ve vstupní části jižního vchodu v roce 1995–1997 (Valoch 2002). V souvislosti se zpracováním nalezených archeologických památek byla provedena celá řada přírodovědných analýz, z nichž mezi nejdůležitější patří detailní datovací studie metodami ^{14}C (Mook 1988), AMS ^{14}C (Neruda – Nerudová v tisku-a), ESR (Rink *et al.* 1996), OSL (Nejman *et al.* 2011), U/Th (Michel *et al.* 2006, Patou-Mathis *et al.* 2005) nebo magnetostratigrafické studie (Sroubek *et al.* 2001, Sroubek *et al.* 1996). Dodnes však nebyl pro tuto jeskyni proveden detailnější sedimentologický výzkum, na jehož podkladě by bylo možné popsat formační procesy vzniku sedimentů

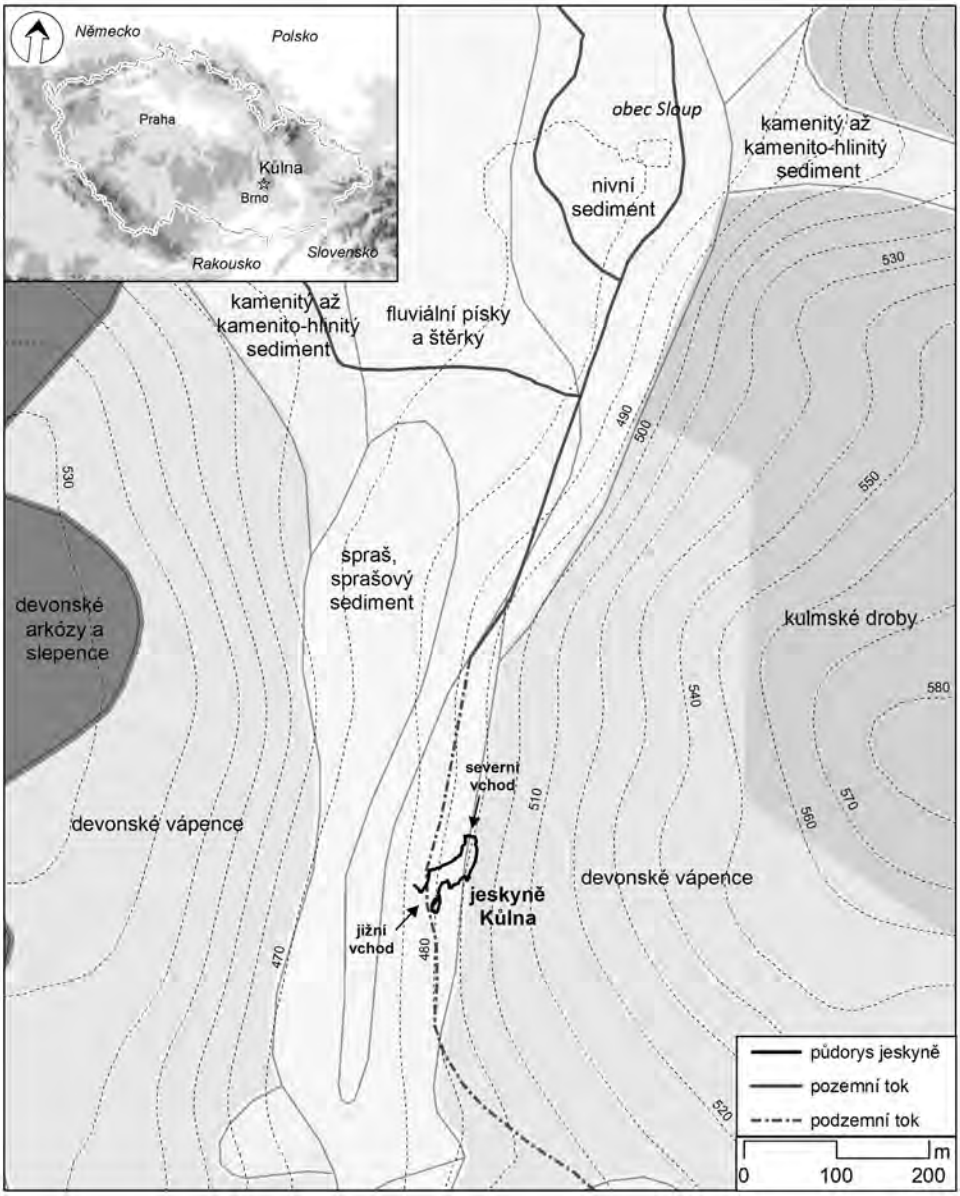

Obr. 1. Poloha jeskyně Kůlny v Moravském krasu a její vztah ke geologii údolí Sloupského potoka a Pustého žlebu. Podklad pro geologickou mapu (GEOČR50 2013).

a jejich vztahu k relativnímu či absolutnímu datování, archeologickému kontextu, či možnému environmentálnímu záznamu. Cílem této studie je základní vyhodnocení formačních procesů, které hrály roli v utváření jednotlivých vrstev vyčleněných při archeologickém výzkumu, a zároveň propojení sedimentárního záznamu v oblasti vchodu s centrální částí jeskyně. Nedílnou součástí práce je i diskuse o měnícím se prostředí, které je v sedimentech zachyceno, a jeho vztahu k řešení chronostratigrafických otázek této lokality.

2. ZÁKLADNÍ CHRONOSTRATIGRAFICKÝ KONCEPT

Plochu jeskyně rozčlenil K. Valoch do několika sektorů (obr. 2). Nejúplnější stratigrafii popsal ve vstupní části jeskyně, kde postupně rozlišil celkem 14 hlavních geologických vrstev, složených především z klastických sedimentů, které se liší homogenitou a zrnitostí od prachu po brekcie tvořené devonskými vápenci či písky a štěrky (schematický profil obr. 3).

Sedimentární i archeologický záznam jeskyně rozdělil K. Valoch do několika chronologicko-kulturních jednotek (Valoch 1988b). Nejstarší osídlení jeskyně (obr. 3,

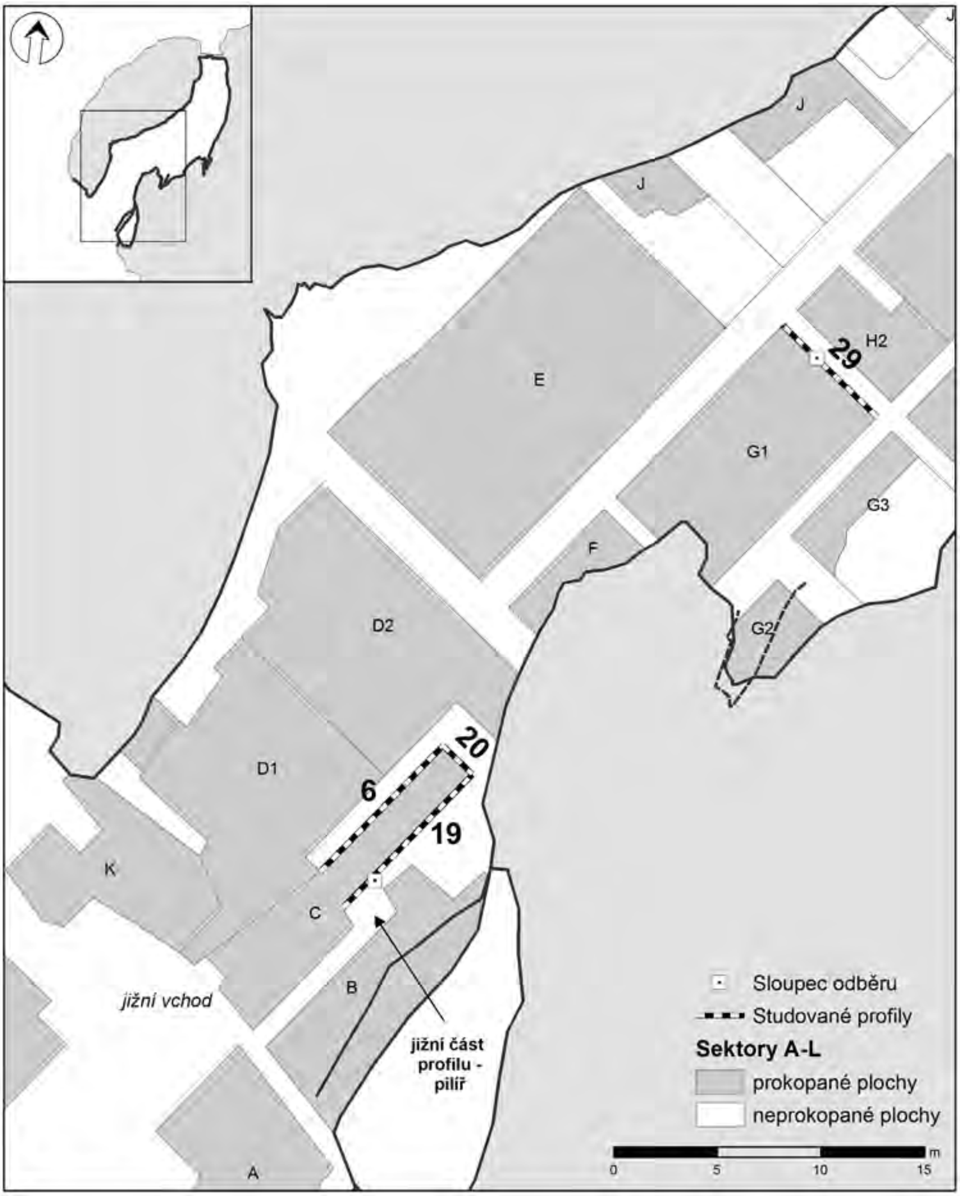

Obr. 2. Členění jeskyně Kůlny na sektory a poloha analyzovaných profilů 6, 19, 20 a 29.

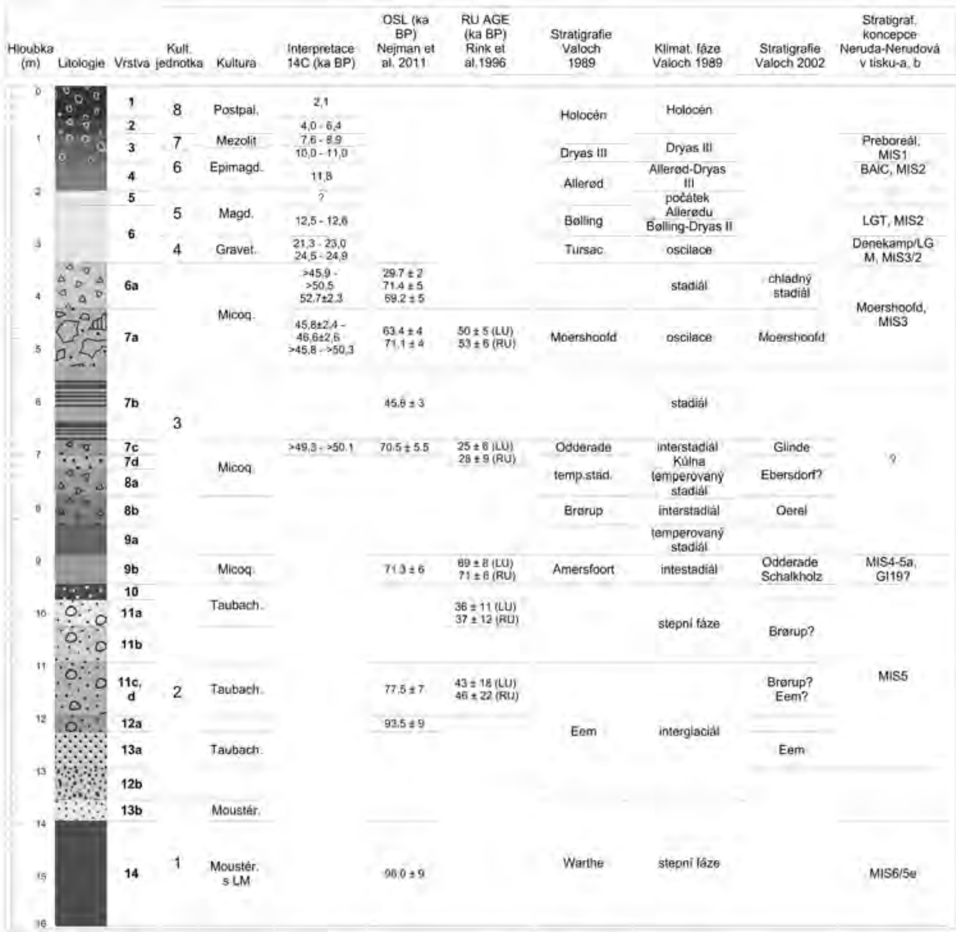

Obr. 3. Chronostratigrafická koncepce sedimentární výplně jeskyně Kůlny. MIS – *Marine Isotope Stage*, GI – *Greenland Interstadials*, LGM – pozdně glaciální maximum, LGT – pozdní glaciál, BAlC – Bølling-Allerød komplex.

jednotka 1) je reprezentováno moustérienskými nálezy z vrstvy 13b a 14, ve které se v nepočetné kolekci podařilo identifikovat i doklady levalloiské metody sbíjení jader (Neruda 2011; Valoch 1970). Na základě interdisciplinárního studia (mikrofauna, Musil 1988) je tato vrstva spojována s koncem glaciálu Saale (MIS6).

Druhá kulturní jednotka (vrstvy 13a–10) poskytla artefakty středopaleolitického taubachienu (Valoch 1988b; 1988a), který je na podkladě malakologické analýzy (Kovanda in Valoch *et al.* 1969) a vyššího obsahu humusu v sedimentu 11 (Pelíšek in Valoch *et al.* 1969) relativně datován do posledního interglaciálu (Valoch 1989; 2002; Valoch *et al.* 2011).

Pozice třetí vyčleněné chronologicko-kulturní jednotky (vrstvy 9–6a) je poměrně komplikovaná, přičemž většina vrstev (9b, 8a, 7d, 7c, 7a a 6a) obsahovala nálezy středopaleolitického micoquienu (Valoch 1988b). Z hlediska datování se můžeme opřít o ucelený soubor dat pro vrstvu 9b, která na podkladě metody ESR (Rink *et al.* 1996) spadá do období okolo 71 000 let BP (RU AGE), a lze ji považovat za jeden z důležitých markerů kůlenské stratigrafie. Druhým podobným markerem by mohla být vrstva 7b, která měla reprezentovat chladný stadiál (Valoch 1989, 2002), nejspíše pak první glaciální maximum posledního klimatického cyklu Visla (MIS4). Šroubek *et al.* (2001) ji ale na základě magnetických studií interpretovali jako soubor krátkodobých teplotních výkyvů, při kterých se utvářela půda (období se zvýšeným srážkovým úhrnem). Za hlavní stratigrafický marker třetí chronologicko-kulturní jednotky je považována vrstva 7a, protože v jejím případě korelují výsledky získané metodou ESR (Rink *et al.* 1996), ^{14}C (Mook 1988) i AMS ^{14}C (Neruda – Nerudová 2013, v tisku-a) a kladou její stáří do období cca 50 000 let BP kalibrované chronologie. Můžeme ji tudíž spojovat s interstadiály Moershoofd či Glinde (Behre – Plicht 1992).

Mladší fáze MIS3 není v jeskyni Kůlně samostatně sedimentárně ani archeologicky doložena. V jeskyni zcela chybí artefakty starší fáze mladého paleolitu (EUP). Čtvrtou chronologicko-kulturní jednotku, spadající do období MIS 3/2, tedy tvoří nálezy z mladší fáze gravettienu, které byly dochovány zejména ve vnitřní části jeskyně. V jižní vstupní části rozlišeny nebyly, ale nová radiokarbonová data ukazují, že i zde se nacházely zvířecí kosti, které zřejmě souvisejí s touto fází osídlení (Neruda – Nerudová v tisku-b).

Pátá kulturní jednotka je reprezentována artefakty magdalénienu z vrstev 6 a 5, které jsou v dnešní době zachovány jen v severním profilu v sektoru G1. Nově je vrstva 6 datována do období okolo 14 800 BP kalibrované chronologie (Neruda – Nerudová v tisku-b). Svrchní část stratigrafické sekvence (vrstvy 4–1) již není v jeskyni Kůlně dochována, a není proto v tomto článku zpracována.

3. METODIKA

Geoarcheologické analýzy popsané v této práci zahrnují základní sedimentární popis jednotlivých vrstev, jejich mikromorfologickou charakteristiku, charakteristiku magnetických a zrnitostních proxy.

Celkem 15 mikromorfologických vzorků o rozměrech 6 × 9 cm bylo odebráno ze čtyř profilů různých částech jeskyně. 11 z nich pochází ze vchodu jeskyně a zahrnují především vrstvy 9b–6a, další 4 potom pocházejí z vnitřní části jeskyně a pokrývají vrstvy 6a–5 (obr. 4). Vzhledem k tomu, že sedimenty byly nezpevněné a často obsahovaly větší klasty, bylo nutné v některých případech použít místo tetrapakových kubiena-boxů i vypěnění přímo ve stěně, ze které byly vzorky odebírány. Vzorky byly dále zpracovány Julie Boreham (Reach, UK) do formy výbrusů. Následně byly studovány při různém zvětšení (40–800×) pod binokulárním či polarizačním mikroskopem s připojenou fluorescencí. Popisy vzorků byly provedeny dle Stoopse (2003), Bullocka a Murphyho (1983) a interpretovány především na základě Goldberga – Macphaila (2006) či Stoopse *et al.* (Stoops – Marcelino – Mees 2010).

Spolu s mikromorfologickými vzorky byly měřeny magnetické vlastnosti a zrnitostní charakteristiky sedimentů. Vzorky byly odebírány v intervalu 5 cm, a to v sektoru C z profilu 19 (jižní část – pilíř, čtv. N/5–6) a z profilu 29 uvnitř jeskyně (obr. 2, sektor G1). Po odebrání byly sedimenty za sucha prosety, aby byla odstraněna frakce větší než 2 mm, která je ve většině případů tvořena výhradně devonskými vápenci. Magnetická susceptibilita a frekvenčně závislá magnetická susceptibilita byla měřena na kapamůstku firmy Agico (MFK1-FA), a to při dvou frekvencích, f1 = 976 Hz a f3 = 15 616 Hz, amplituda AC pole byla 200 A/m. Vzorky byly změřeny v plastových sáčcích a následně zváženy, aby mohla být vypočítána hmotnostní susceptibilita [m^3/kg]. Frekvenčně závislá magnetická susceptibilita byla potom přepočítána dle obecně akceptovaného vzorce (Dearing *et al.* 1996) jako kFD = 100 × (kf1 – kf3) / kf1 [%], kde kf1 a kf3 jsou měření susceptibility při frekvencích 976 Hz a15 616 Hz.

Zrnitostní analýza byla provedena laserovým granulometrem značky CILAS 1190. Vzorky byly dispergovány v destilované vodě s přídavkem KOH a následně pipetovány do přístroje. U každého vzorku byla provedena minimálně dvě měření a výsledek zprůměrován.

4. VÝSLEDKY

4.1. Sedimentární popis a stratigrafie popisovaných vrstev

Materiál vrstev 5, 6 a 6a zachovaných uvnitř jeskyně v profilu 29 sektoru G1 (obr. 4) byl popsán jako žlutohnědá prachovitá hlína s minimálním obsahem vápencových klastů. Přechod mezi těmito vrstvami je špatně znatelný a rozdíl byl stanoven především na základě odlišného zabarvení (vrstvy 6 a 6a měly pouze mírně tmavší odstín) a zvýšeného podílu hrubších klastů ve vrstvě 6a. V těchto vrstvách byly identifikovány 1–2 mm velké klasty rozvětralých úlomků hornin, mikromorfologicky následně identifikovaných jako droby. Makroskopicky identifikovatelné texturní znaky zde nebyly rozpoznány. Podobnou litologii vykazuje i vrstva 6a ve vchodu, zachycená v profilu 19 (jižní část-pilíř) sektoru C.

Ve vchodové části jeskyně byly vrstvy dokumentovány na celkem třech na sebe navazujících profilech (obr. 2; sektor C, profil 20 kolmý na profil 6, profil 19 střední část a profil 19 jižní část-pilíř). Z těchto profilů byly odebírány mikromorfologické vzorky (obr. 4). Profil 19 jižní část-pilíř (čtv. N/5–6) byl stratigraficky nejkomplexnější, a proto byl vybrán i pro odběr sypkých vzorků na další analýzy. Fotodokumentace celého profilu byla krajně obtížná, proto je v tomto příspěvku představen schematickým nákresem (obr. 6). Ve vchodové části jeskyně v sektoru C byly zachyceny vrstvy 6a (báze)[1], 7a, b, c, d, souvrství 8 (8a + 8b), 9b a 11. Vrstva 6a měla podobné parametry jako vrstva 6a uvnitř jeskyně. Vrstva 7a, identifikovaná jako prachovitá hlína, měla hnědou barvu a byla typická obsahem drobnější sutě o velikosti do 1 cm (cca 30 %), ale i hrubších vápencových klastů do velikosti až desítek cm (5 %). Vrstva 7b tvoří nejmocnější a texturně nejvýraznější část studovaných profilů. Její mocnost dosahuje cca 1 m a je typická výskytem milimetrových až centimetrových tenkých lamin složených z písčitoprachovitého materiálu červenohnědé barvy. Dalším texturním prvkem této vrstvy je horizontální odlučnost prachovitého materiálu. Vrstvy 7c a 7b jsou si zrnitostně i texturně velmi podobné a jsou tvořeny prachovitojílovitou hlínou hnědé barvy s obsahem jemnozrnného vápencového detritu. Rozdíl mezi těmito vrstvami je makroskopicky ve vyšším obsahu větších vápencových klastů v rámci vrstvy 7c. Souvrství 8, zachycené pouze v profilu 19 (jižní část-pilíř), je tvořené šedě hnědou jílovito-prachovitou hlínou s občasným výskytem větších vápencových klastů do 5 cm (max. 10 %). Vrstva 9b byla odkryta taktéž pouze v profilu 19 (jižní část-pilíř); má podobnou charakteristiku jako nadložní vrstva s tím rozdílem, že podíl vápencových klastů plošně kolísá.

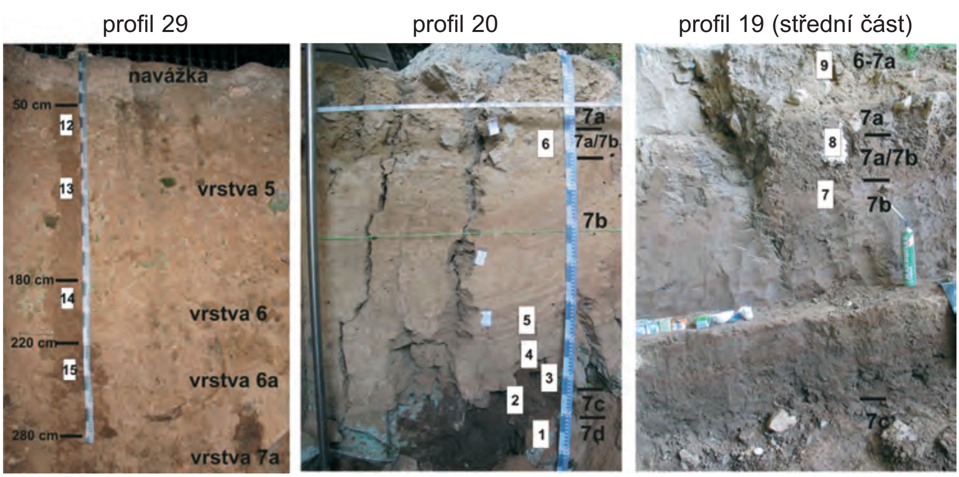

Obr. 4. Fotodokumentace stratigrafie a odběru mikromorfologických vzorků z profilu uvnitř jeskyně, sektor G1 profil 29, a ve vchodu jeskyně, profily 19 (střední část) a profil 20 (foto L. Lisá).

Vrstva 11 byla částečně odkryta na bázi téhož profilu a byla tvořena především jemnozrnným vápencovým detritem a oblázky (Valoch 2011). Matrix této vrstvy má šedou barvu a jílovitý charakter.

4.2. Mikromorfologická charakteristika

Obecně lze zkoumané sedimenty popsat jako nevytříděnou prachovou hlínu s C/F poměrem (poměr hrubé a jemné frakce) s limitem 50 µm okolo 20 : 80, což je typická hodnota pro spraš. Vrstvy 5 a 6 vykazují lentikulární mikrostrukturu, typickou pro intenzivní

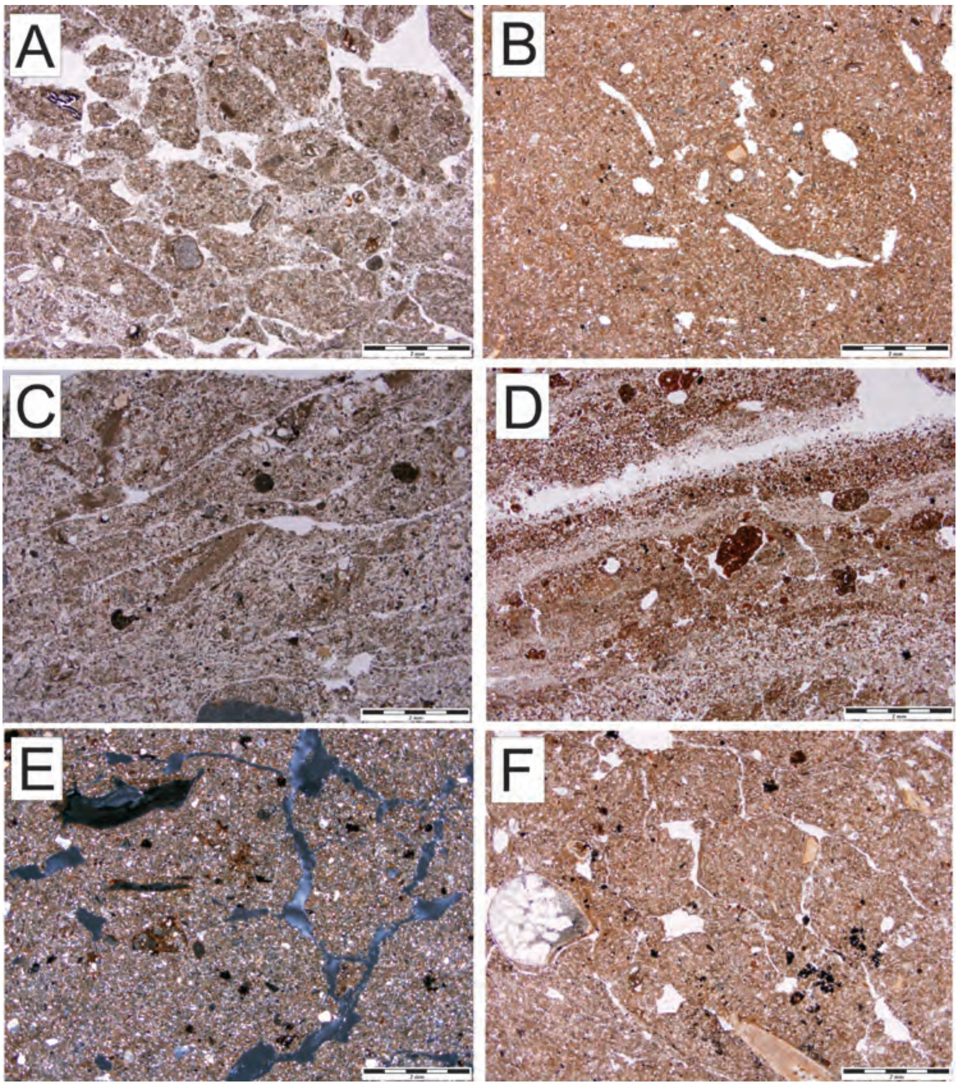

Obr. 5. Fotodokumentace hlavních typů mikrostruktur zachycených ve studovaných vzorcích. A – lentikulární mikrostruktura, vzorek 12, vrstva 5, profil 29; B – kanálkovitá mikrostruktura, vzorek 1, vrstva 7d, profil 20; C – planární mikrostruktura, vzorek 9b, vrstva 6a/7a, profil 19 (střední část); D – planární mikrostruktura s laminami a rip-up klasty, vzorek 5, vrstva 7b, profil 20; E – subangulárně bloková mikrostruktura, vzorek 10, vrstva 8(a + b), profil 19 (pilíř); F – subangulárně až subováln
ě bloková mikrostruktura, vzorek 11, vrstva 9b, profil 19 (pilíř).

Tab. 1. Mikromorfologická chrakteristika jednotlivých vzorků.

Číslo vzorku a kontext	Mikro-struktura	Orientace matrix	Póry	Zrnitost	Matrix	Dvojlom	Organická hmota	Uhlíky	Kosti	Pedogenní znaky
Vzorek 1 vrstva 7d profil 20	masivní až kanálkovitá	bez orientace	dutiny a kanálky (5–10 %)	C/F(50 µm)=20:80; prachovitá hlína	hnědá	krystalický	dekomponovaná tmavá (20 %), hnědá (5 %); částečně dekompo-novaná (3 %)	3–5 %	5 %, 1–2 mm, angulární až subangulární	guano (3 %) občasné potahování zrn
Vzorek 2, vrstva 7c s reliktem vrstvy 7d profil 20	subangulární bloková	bez orientace erozní povrch	meziagregátové póry (20 %) dutiny (10 %)	C/F(200 µm)= 5:95; C/F(50 µm)= 20:80; prachovitá hlína s malými klasty zvětralého vápence	světle hnědá	striatický, granostriatický	dekomponovaná černá a hnědá (10 %)	vzácně	5 %, 1–2 mm, angulární až subangulární	vzácně nodule FeOH, časté povlékání zrn
Vzorek 3, vrstva 7b profil 20	dutinová, misty planární	usměrnění pod úhlem ve směru redepozice	dutiny (10 %)	5:95; C/F(50 µm)= 20:80; vrstvy s rip-up klasty C/F(200 µm)= 90:10; nevytříděná prachovitá hlína až písčitá hlína	světle hnědá, hnědá, oranžová	krystalický vzácně striatický	dekomponovaná černá a hnědá (10 %)	5% ve svrchní části vzorku	5%, 1-2 mm, angulární a subangulární ve svrchní části vzorku	vzácně nodule FeOH, častá přítomnost půdních krust
Vzorek 4 vrstva 7b profil 20	dutinová, misty planární	usměrnění pod úhlem ve směru redepozice	dutiny (10 %)	5:95; C/F(50 µm)= 20:80 vrstvy s rip-up klasty C/F(200 µm)= 40:60 nevytříděná prachovitá hlína až písčitá hlína	světle hnědá, hnědá, oranžová	krystalický vzácně striatický	dekomponovaná černá a hnědá (10 %)	vzácně	5 %, 1–2 mm, angulární a subangulární	FeOH nodule v jemnozrnných částech vzorku, častější přítomnost jemnějších lamin
Vzorek 5 vrstva 7b profil 20	dutinová, misty planární	usměrnění pod úhlem ve směru redepozice	dutiny (10 %)	5:95; C/F(50 µm)= 20:80 vrstvy s rip-up klasty C/F(50 µm)= 40:60 nevytříděná prachovitá až písčitá hlína	světle hnědá, hnědá, oranžová	krystalická, vzácně striatická	dekomponovaná černá a hnědá (10%)	vzácně	5 %, 1–2 mm, angulární a subangulární	bioturbace kořeny
Vzorek 6 pozice mezi vrstvami7a a 7b profil 20	subangulárně bloková, misty plátovitá	misty horizontální, zvlněné?	meziagregátové póry (10 %) dutiny (20 %)	C/F(200 µm)= 10:90; C/F(50 µm)= 30:70; C/F(20 µm)= 50:50 prachovitá až písčitá hlína, dle vrstev	světle hnědá	místy striatická a granostriatická	dekomponovaná černá a hnědá (10 %)	vzácně	5 %, 1–2 mm, angulární a subangulární	FeOH nodule (5 %);
Vzorek 7 vrstva 7b profil 19	subangulárně bloková misty lentikulární	misty horizontální	dutiny (10 %) praskliny (10 %)	C/F(200 µm)= 5:95; C/F(50 µm)= 20:80; prachovitá hlína	světle hnědá	striatická a granostriatická	dekomponovaná černá a hnědá (10 %)	vzácně	5 %, 1–2 mm, angulární a subangulární	akumulace karbonátů (30 %), FeOH nodule (10 %), povlékání zrn (3 %)
Vzorek 8 pozice mezi vrstvami 7a/7b profil 19	subangulárně bloková misty lentikulární	horizontální	meziagregátové póry (20 %) dutiny (3 %)	C/F(200 µm)= 5:95; C/F(50 µm)= 20:80; prachovitá hlína	světle hnědá	striatická a granostriatická	dekomponovaná černá a hnědá (10 %)	vzácně	5 %, 1–2 mm, angulární a subangulární	CaCO3 (3 %); FeOH nodule 3 %); povlékání zrn (10 %)

Tab. 1. Pokračování.

Vzorek 9 pozice mezi vrstvami 6a/7a profil 19	planární až lentikulární	horizontální	dutiny (20 %)	C/F(200 µm)= 5:95; C/F(50 µm)= 50:50; partly C/F(20 µm)= 50:50 nevytříděná prachovitá až písčitá hlína	světle hnědá	striatická a granostriatická	dekomponovaná černá a hnědá (10 %)	vzácně	3 %, 0,5 mm, subangulární a zakulacené	CaCO3 (3 %); FeOH nodule (3 %); povlékání zrn (10 %); deformované půdní krusty (20 %)
Vzorek 10 vrstva 8 v profil 19 pilíř	Subangulárně bloková	Misty horizontální	pukliny (3 %), dutiny nepravidelného tvaru (max. 10 %)	C/F(200 µ) = 5:95; C/F(50 µ) = 25:75; zrnitost prachovitá hlína	hnědá	krystalická, striatická	tmavá opákní do 10 %, hnědá do 3 %,	vzácně	do 3 %, velikost 1–2 mm, subangulární a angulární	vrstevnaté FeOH nodule
Vzorek 11 vrstva 9 profil 19 pilíř	puklinová až dutinová, místy náznaky subangulárně blokové	bez, náznaky bioturbace	dutiny (15 %), pukliny (5 %); tvar dutin nepravidelný	C/F(200 µ) = 3:97; C/F(50 µ) = 30:70; zrnitost prachovitá hlína	světle hnědá	krystalický, misty striatický	tmavá opákní do 10 %, hnědá do 3 %	vzácně	do 3 %, velikost 0,5–2 mm, subangulární a angulární	Mn nodule and FeOH nodule
Vzorek 12 vrstva 5, profil 29	planární až lentikulární	horizontální	meziagregátové pukliny až 40 %; tvar dutin odpovídá lentikulární mikrostruktuře	C/F(200 µ) = 5:95; C/F(50 µ) = 60:40; zrnitost prachovitá hlína	světle hnědá až hnědošedá	krystalická	tmavá opákní do 3 %, hnědá do 3 %	ne	ne	povlékání zrn
Vzorek 13 vrstva 5 profil 29	subangulárně bloková a přechody do lentikulární	mrazové třídění, usměrnění díky geliflukci	meziagregátové pukliny až 40 %; tvar dutin odpovídá lentikulární mikrostruktuře	C/F(200 µ) = 5:95; C/F(50 µ) = 60:40; zrnitost prachovitá hlína	světle hnědá až hnědošedá	krystalická	tmavá opákní do 3 %, hnědá do 3 %	ne	ne	povlékání zrn
Vzorek 14 vrstva 6 profil 29	subangulárně bloková a přechody do lentikulární až granulární	mrazové třídění, usměrnění díky geliflukci, místy bioturbace,	meziagregátové pukliny až 40 %; tvar dutin odpovídá lentikulární mikrostruktuře	C/F(200 µ) = 5:95; C/F(50 µ) = 60:40; zrnitost prachovitá hlína	světle hnědá až hnědošedá	krystalická	tmavá opákní do 3 %, hnědá do 3 %	ne	ne	povlékání zrn, redeponované a deformované půdní krusty
Vzorek 15 vrstva 6a profil 29	subangulárně bloková až granulární	mrazové třídění, usměrnění díky geliflukci	meziagregátové pukliny až 40 %; tvar dutin odpovídá granulární mikrostruktuře, tj. nepravidelné jak do velikosti, tak do tvaru	C/F(200 µ) = 5:95; C/F(50 µ) = 60:40; zrnitost prachovitá hlína	světle hnědá až hnědošedá	krystalická	tmavá opákní do 3 %, hnědá do 3 %	ne	ne	povlékání zrn, redeponované a deformované půdní krusty

zmrzání a rozmrzání (obr. 5). Zároveň je u nich zřetelné usměrnění matrix, což je důsledkem geliflukce. Texturně nejzajímavější vrstva 7b obsahovala laminy litologicky odlišného materiálu. Ten byl popsán jako tzv. *rip-up* klasty vzniklé intenzivní erozí starších půdních sedimentů. Výsledky mikromorfologické analýzy jsou shrnuty heslovitě v tab. 1; hlavní typy mikrostruktur popsaných ve studovaných vzorcích jsou dokumentovány v obr. 5.

4.3. Magnetické vlastnosti studovaných sedimentů

Magnetická susceptibilita a frekvenčně závislá magnetická susceptibilita měřená na profilu 19 jižní část – pilíř ve vchodové části profilu koreluje s dříve provedenými měřeními (Sroubek *et al.* 2001). Sedimenty uvnitř jeskyně mají magnetickou susceptibilitu o řád nižší, což je pravděpodobně dáno jejich složením i typem ukládání. Hodnoty frekvenčně závislé magnetické susceptibility sedimentů uvnitř jeskyně svědčí o absenci pedogenně ovlivněné matrix. Mírně zvýšené hodnoty kFD se objevují na bázi profilu, ve vrstvě 6a. V případě sedimentů zachycených v profilu v jižním vchodu jeskyně lze říci, že přinejmenším ve vrstvách 7a, 7b, 7d, 9b a 11 byly identifikovány sedimenty obsahující pedogenně ovlivněnou složku (obr. 6).

4.4. Zrnitostní charakteristika studovaných sedimentů

Zrnitostní distribuce pro studované profily, ve které nejsou zohledněny případné rozdíly mezi minerální a organickou složkou, jsou znázorněny na obr. 6. Sedimenty jsou

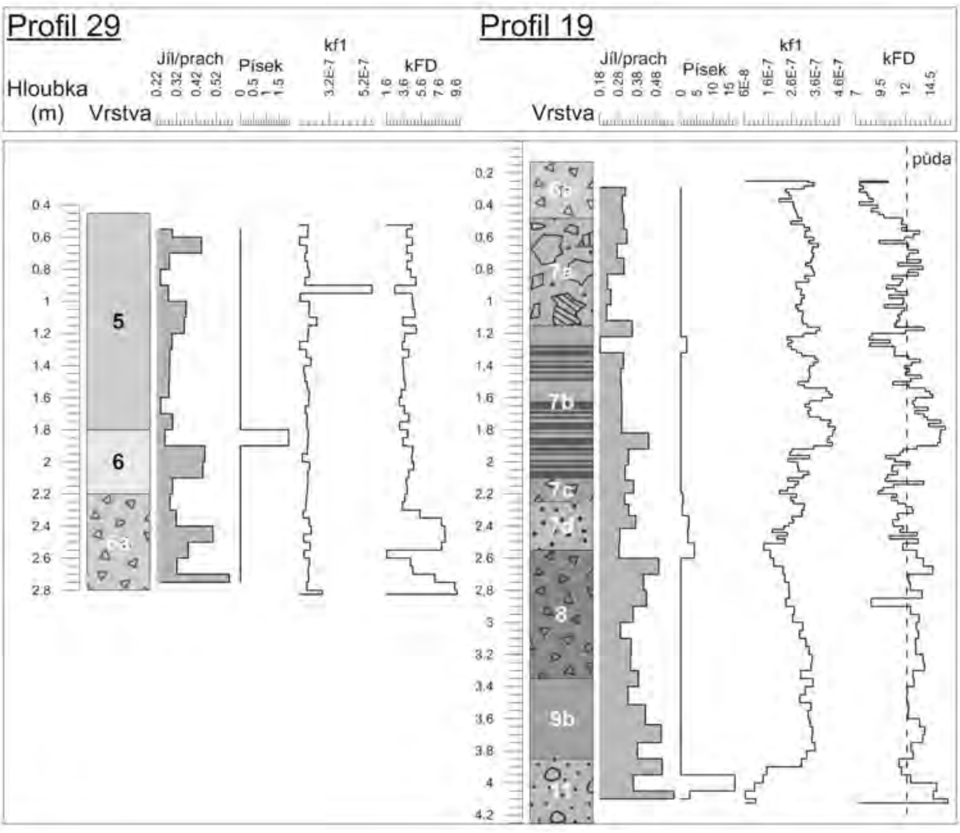

Obr. 6. Hodnoty magnetické susceptibility kf1, frekvenčně závislé magnetické susceptibility kFD, indexu zvětrávání (podíl jíl/prach) a zrnitostní distribuce analyzovaných profilů jeskyně. Hodnota 12 u kFD je obecně považována za známky pedogeneze.

vždy bimodální. Obsah jílové frakce se pohybuje okolo 20–30 %, písčitá frakce je zastoupena minimálně, a to především v profilu pocházejícího ze vchodu jeskyně. Poměrem jílovité a prachovité složky, který určuje míru zvětrání (Sroubek *et al.* 2001) dobře koreluje s hodnotami frekvenčně závislé magnetické susceptibility (obr. 6).

5. DISKUSE

5.1. Provenience jeskynních sedimentů

Karel Valoch (1988b) a později například P. Šroubek (Sroubek *et al.* 2001) považují za hlavní zdroj sedimentů jeskyně Kůlny spraše. Signál magnetické susceptibility a frekvenčně závislé magnetické susceptibility tomu odpovídá především v případě vrstev 6a, 6 a 5 uvnitř jeskyně a v rámci některých facií ve vchodu jeskyně (vrstva 6a, světlejší vrstvy v rámci vrstvy 7b, část vrstvy 7c). Ostatní vrstvy identifikované ve vchodu jeskyně potom vykazují hodnoty frekvenčně závislé magnetické susceptibility podobné spíše půdám (obr. 6). Zrnitostní analýza identifikovala ve všech sedimentech převládající prachovitou frakci (obr. 6).

Typická spraš je obyčejně velmi dobře vytříděna s více jak 70 % zrn velikosti mezi 10–50 µm (Kukal 1971; Pécsi 1990). Během pedogeneze však dochází ke zvětrávání alumosilikátů a následně bimodálnímu složení výsledného sedimentu. Průměrná zrnitost tak klesá spolu s formováním jílových minerálů (Martini – Chesworth 1992). Poměr jíl/prach tudíž může odrážet intenzitu pedogenního procesu (Sroubek *et al.* 2001) a v případě studovaných sedimentů velmi dobře koreluje s magnetickým signálem, tj. stoupá v intervalech, v nichž zároveň narůstají hodnoty frekvenčně závislé magnetické susceptibility. Sedimenty uvnitř jeskyně mají magnetickou susceptibilitu o řád nižší, což je pravděpodobně dáno jejich složením a v návaznosti na to i typem depozice.

Navýšení signálu magnetické susceptibility může mít několik důvodů, například atmosférický spad (Evans – Heller 2003), termální alteraci díky ohni (Kletetschka – Banerjee, 1995) nebo anorganickou tvorbu ultrajemného magnetitu v důsledku zvětrávání minerálů s obsahem Fe, a to v prostředí s měnící se půdní vlhkosti (Evans – Heller 2003). Takové podmínky předpokládáme ve vrstvách 6a–5 uvnitř jeskyně (Lisá *et al.* 2013), kde sice magnetický signál žádné výrazné navýšení neukazuje, ale mikromorfologické popisy podobné podmínky indikují. Podobně je tomu i v případě vrstvy 9b zachycené ve vchodu do jeskyně, která podobné navýšení magnetického signálu rovněž indikuje.

Sedimenty vchodové části jeskyně jsou mnohem variabilnější jak po stránce formačních procesů, tak jejich litologie a s tím související provenience. V jejich případě je nutné diskutovat i možnost navýšení magnetického signálu v důsledku přítomnosti superparamagnetických minerálů vzniklých bakteriálně během pedogeneze (Fassbinder 2010). Musí se však zákonitě jednat o pedogenezi proběhlou mimo jeskyni s následnou redepozicí pedogenně ovlivněného materiálu do vnitřních částí jeskyně. Takový záznam byl identifikován především ve vrstvách 9b a 11, dále potom ve vrstvách 7d, svrchní části souvrství 8 a i ve vrstvě 7a. Palynologická spektra (Doláková 2002) ukazují na mírně teplejší podmínky ve vrstvách 8a (svrchní část vrstvy 8) a 7c. V rámci vrstvy 7b byly potom identifikovány červenohnědé sedimenty v rámci jemných lamin. Na základě mikromorfologie byla matrix těchto klastů popsána jako výrazně jílovitá s velkým obsahem FeOH. Může se jednat napříkad o relikt starší půdy typu rothlem či *terrae calcis*.

5.2. Formační procesy v jeskyni

Na podkladě zrnitostní analýzy a měření magnetických vlastností byla provenience studovaných vrstev přisouzena původně eolickým sedimentům (např. Sroubek *et al.* 2001). To však není důvod k závěrům, že tyto sedimenty byly do jeskyně deponovány výhradně větrnou energií. Podle dosavadních studií týkajících se jeskynních sedimentů a jejich klasifikace (souhrnně Karkanas – Goldberg 2013) je nečastějším depozičním faktorem gravitační proud či splachy. Prostřednictvím tohoto procesu dochází k přínosu sedimentů jak z osypového kužele vchodové facie, tak z výplní komínů. Z hlediska morfologie jeskyně, nepřítomnosti typických komínů s kontaktem na povrch a umístění v terénu je však jeskyně Kůlna poměrně atypická. Relativně široký, k jihu otevřený portál je mírně vytočený na západ, a proto zde evidentně nevznikal typický jeskynní kužel. Pokud se přece jen, alespoň v omezené míře, v některých epochách vytvářel, pak musel být erodován tokem, který vstup do jeskyně porušoval (souvrství 12, VALOCH 2011, 55, 57–58). Zdroj materiálu byl tak pravděpodobně suplován především osypovým kuželem při východním okraji jižního portálu (NERUDA 2013, obr. 1). Původní morfologie vchodu je značně poškozena masivním zásahem za druhé světové války (k problému NERUDA 2013). Není vyloučené, že část prachovitého materiálu byla do otevřeného jižního vchodu deponována eolickými procesy (SROUBEK *et al.* 2001). Texturní prvky, které by tuto doměnku dokládaly, však nebyly nikde uspokojivě doloženy. P. Šroubek a kol. (SROUBEK *et al.* 2001) dokládají prostřednictvím mikromorfologie povrchu křemenných zrn velmi dobré opracování související s intenzivním eolickým transportem; toto jsou však textury související s transportační historií samotných křemenných zrn a nutně nemusí dokládat primární formační procesy, kterými byl sediment uložen.

Zajímavým fenoménem jsou červenohnědé vrstvičky v rámci vrstvy 7b, interpretované P. Šroubkem a kol. (SROUBEK *et al.* 2001) jako odrazy krátkodobých oteplení. J. KadleC (2012) vysvětluje textury vrstvy 7b jako důsledek splachových událostí a předpokládá na bázi vrstvy 7b malé jezírko, v němž by docházelo k usazování ze suspenze. Tomu však jen stěží odpovídá sklon těchto sedimentů, dodnes viditelný např. na profilu 20. N. DOLÁKOVÁ (2002) identifikovala v rámci této vrstvy 7b přítomnost spor vodních řas; tyto se však vyskytují v podložních i nadložních vrstvách a indikují spíše přítomnost vodní plochy v blízkosti jeskyně. Ta by mohla souviset s činností Sloupského potoka. Pomocí mikromorfologické analýzy se podařilo odhalit, že v případě červenohnědých vrstviček jde o tzv. *„rip-up“* klasty (KARKANAS – GOLDBERG 2013). Podle současných přestav jsou facie s těmito klasty, střídajícími se např. s jemně laminovanými vrstvami jílu, důsledkem epizodických vysokoenergetických událostí. Například bouřkové eventy, během nichž jsou deponovány větší klasty (v tomto případě jílem stmelené části půdy), jsou většinou následovány pomalejší sedimentací, při které ze suspenze pomaleji vypadává jemnozrnný materiál (KNAPP *et al.* 2004).

P. Šroubek a kol. (SROUBEK *et al.* 2001) předpokládá, že prachový materiál, více či méně ovlivněný pegodenezí v závislosti na klimatických podmínkách, byl transportován do jeskyně ze směru jižního vchodu. J. KadleC (2012) později upřesňuje, že sedimenty byly do jeskyně pravděpodobně přemísťovány srážkovými vodami, a to ze severního vchodu směrem do jeskyně díky přítomnosti závrtovité deprese, jejíž relikty jsou v terénu údajně dodnes patrné. Je tedy zřejmé, že na vzniku sedimentů uvnitř a ve vchodu jeskyně se podílí různé faktory. Jeskyně samotná je tvořena dvěma vchody, přičemž severně orientovaný vchod, jehož rozsah lze dnes odhadovat jen na podkladě dobových zpráv, je dle písemných záznamů dostatečně velký pro redepozici velkého množství sedimentů (KADLEC 2012; souhrnně NERUDA 2013). Zároveň má velký geomorfologický potenciál pro to, aby z tohoto směru byly přinášeny sedimenty. Svahy v okolí severního vchodu jsou vhodným zdrojem materiálu, a to ať již sprašového sedimentu, tak písčité složky tvořené rozvětralým eluviem spodnokarbonských drob Drahanské vysočiny (cf. obr. 1). Droby, které zde mimochodem zmiňuje již Martin KŘÍŽ (1889), byly identifikovány makroskopicky i mikromorfologicky. V neposlední řadě jsou v sedimentech zastoupeny i vápencové klasty. Vnitřní mikrostruktura sedimentů studovaných na profilu uvnitř jeskyně ukazuje, že při depozici a těsně po ní docházelo k výraznému mrazovému ovlivnění (VLIET-LANOË 2010). Mrazové struktury zde dokládají jak fáze zmrzání a rozmrzání, tak i geliflukci. Sediment byl do své současné pozice tedy s největší pravděpodobností deponován pomalým creepem, a to v důsledku gravitace a mrazových procesů, což podporuje i imbrikace vápencových klastů naznačující směr transportu odseveru k jihu, kterou zmiňuje J. KADLEC (2012).

Poměrně odlišná situace však panuje v prostoru jižního vchodu do jeskyně, kde je sedimentární situace mnohem variabilnější. Objevují se zde sedimenty usazené gravitačně či eolicky. Zdroj gravitačních sedimentů můžeme hledat ve svrchní hraně portálu jeskyně nebo v prostoru osypového kužele umístěného při východní hraně jižního vchodu. J. Kadlec (2012) pro tuto část jeskyně předpokládá jak splachy ve srážkově bohatších obdobích, tak nevylučuje ani transport v důsledku svahových geliflukčních procesů ani eolické procesy. Zároveň však přítomnost velkých vápencových klastů interpretuje jako opad ze stropu jeskyně při ústupu čela jižního portálu.

5.3. Chronostratigrafická problematika sedimentárního záznamu

Současná chronostratigrafická interpretace sedimentárního a archeologického záznamu jeskyně Kůlny (Neruda – Nerudová v tisku-a; v tisku-b; Valoch 1988b; 1989; 2002) evokuje několik zásadních otázek. Jedním z nich je identifikace rozdílů mezi vrstvami 5 a 6 uvnitř jeskyně. Na jediném, v současné době dostupném profilu, kde jsou příslušné sedimenty dochovány, tyto vrstvy K. Valoch nerozlišil (cf. Valoch 1974, Beilage I). Obě vrstvy nebylo možné rozlišit ani na základě mikromorfologie složení identifikované z výbrusu, tj. mineralogická a organická složka jsou víceméně stejné. Odlišnosti jsou však identifikovatelné v zrnitostním rozložení, resp. v poměru jíl/prach, jinak charakterizovaném jako míra zvětrávání (Sroubek *et al.* 2001). Rozdíly těchto proxy jsou viditelné i v případě hodnot frekvenčně závislé magnetické susceptibility, nicméně zvýšené hodnoty v rozmezí 8–9 odpovídají pouze vrstvě 6a. Tyto hodnoty jsou srovnatelné s výsledky měření frekvenčně závislé magnetické susceptibility pro intestadiální půdu PK I v Dolních Věstonicích (Lisá *et al.* v tisku).

Další pro archeologii důležitou otázkou je, zda lze na základě provedených analýz vydělit sedimentaci, která probíhala v období 30–40 tisíc let BP nekalibrované chronologie. V archeologickém inventáři (EUP komplex) toto období zachyceno není. Jeho existenci dokládá pouze jedno radiokarbonové datum v nové sérii dat pro nejmladší středopaleolitickou vrstvu 6a, ovšem vzorek kosti nenesl na svém povrchu stopy po manipulaci člověkem a vzhledem k absenci nálezů, které by mohly odpovídat kulturám EUP komplexu, se zdá pravděpodobnější, že se jedná o doklad činnosti šelem (Neruda – Nerudová v tisku-a). Chronostratigraficky by se měl příslušný sediment nacházet mezi vrstvou 6a a 6. V jižní vstupní části jeskyně není ale tato úroveň dochována, a nelze ji proto analyzovat, ve vnitřní části ji nelze vyčlenit. Vysvětlení lze hledat v hiátu, způsobeném kryogenními pochody, které odstranily část původních sedimentů, na jejichž místo byly deponovány sedimenty vrstev 6 a 5.

Jednou z dlouhodobě diskutovaných otázek je stratigrafické zařazení sterilní vrsvy 7b jako případného markeru MIS4. Tuto interpretaci předpokládal K. Valoch, který tuto vrstvu spojoval se stadiálem (1989) nebo chladným stadiálem (2002). Později však P. Šroubek a kol. (Sroubek *et al.* 2001) interpretovali tutéž vrstvu jako sled krátkodobých oteplení v rámci MIS3. V současné chronostratigrafické koncepci spadá MIS4 do období mezi 74–60 tisíc let BP kalibrované chronologie a představuje první výrazné ochlazení posledního klimatického cyklu. Toto období má dvě fáze, přechodnou v počáteční fázi s velkými teplotními výkyvy a chladnou v terminální fázi (Van Andel – Davies 2003). Během chladné fáze se boreální les a tajga postupně mění v rozlehlou a otevřenou tundru (Van Andel – Tzedakis 1996). Obecně lze tedy říci, že během tohoto období muselo dojít k výrazné změně vegetace, a s tím pak souvela i zvýšená eroze. A vrstva 7b je právě důsledkem opakujících se erozních událostí, což dokládají jak sedimentologické, tak mikromorfologické analýzy. Magnetická proxy ukazují střídání extrémně zvýšených a snížených hodnot, které byly interpretovány jako důsledek krátkodobých oteplení během MIS3 (Sroubek *et al.* 2001). Na základě mikromorfologických pozorování a zrnitostní analýzy je však zřejmé, že tyto rozdíly jsou ovlivněny jak typem redeponovaného materiálu, tak i jeho zrnitostním složením. Například písčitější složka, kterou již na bázi popsal J. Kukla (1975) jako *„pellet sands"* a která se objevuje opakovaně v rámci celé vrstvy 7b, je tvořena křemenem, jež je výrazně diamagnetický (Evans – Heller 2003). Naopak jílem bohaté polohy, které odpovídají tzv. *rip-up* klastům (Karkanas – Goldberg 2013), obsahují magnetickou složku vzniklou v důsledku chemického zvětrávání a pravděpodobně i pedogenního procesu (Evans – Heller 2003; Fassbinder – Stanjekt – Vali 1990). Otázkou však zůstává, jak vysvětlit zvýšenou erozi v podobě splachů v tak aridním prostředí, jaké panovalo v terminální fázi MIS4. Teplou oscilaci v rámci počáteční fáze MIS4, která je teplotně i srážkově poněkud příznivější, dokládá zřejmě vrstva 9b (71 tisíc let BP RU AGE), která je od nadložní vrstvy 7b navíc oddělena ještě dalšími horizonty 8(a+b)–7c. Pokud by zvýšená eroze v jejímž důsledku vznikla vrstva 7b měla být odrazem zvýšených srážkových úhrnů, potom je nutné počítat spíše s vlivem výrazně humidnějšího období, které se objevilo na počátku MIS3 (Guiot *et al.* 1989).

Dalším důležitým problémem je chronologická pozice druhé kulturní skupiny nálezů a příslušných archeologických vrstev (vrstvy 13a–10). Na podkladě vrstevního sledu, malakofauny a obsahu humusu předpokládáme, že by sedimentace těchto vrstev měla souviset s posledním interglaciálem (obr. 3). V námi zkoumaných profilech byla zachycena pouze vrstva 11 (profil 19, jižní část-pilíř), přičemž ale nebyla analyzována metodou mikromorfologie, protože vzorek nebylo možné z technických důvodů odebrat. Na základě měření frekvenčně závislé magnetické susceptibility a zrnitostního složení lze důvodně předpokládat, že vrstva 11 obsahuje pedogenně ovlivněný materiál. Hodnoty frekvenčně závislé magnetické susceptibility jsou v rozmezí 12–16, což zřetelně indikuje pedogenezi. Podobné i když mírně nižší hodnoty byly indikovány pouze na přechodu vrstev 8, 7d a 7a a dále v kontextu výše diskutovaných červenohnědých vrstviček v rámci vrstvy 7b. Poměry zvětrávání (jíl/prach) velmi dobře korelují s hodnotami frekvenčně závislé magnetické susceptibility. Tyto hodnoty indikují pedogenezi, nicméně neurčují stáří sedimentu. Korelace by byla možná s podobnými paleopůdami. Pro srovnání lze uvést např. hodnoty kFD pro interstadiální půdu PKI v Dolních Věstonicích, kde měření kolísají kolem hodnoty 9 (Lisá *et al.* v tisku), což je na hraně indentifikace sedimentu jako pedogenně ovlivněného. V tomto porovnání však není zohledněn půdní typ, i když zdrojový materiál (spraš) byl pravděpodobně totožný.

Pro správnou interpretaci formování archeologických struktur v jeskyni je důležitá identifikace vrstev, které jsou ovlivněny kryogenními pochody. Pozitivně se podařilo tyto postdepoziční procesy rozpoznat v několika horizontech. Ve vrstvách 5, 6, 6a, povrch 7a byla identifikována typická lentikulární mikrostruktura, která vzniká v důsledku kryogenních pochodů ovlivňujících především povrchové části sedimentu (Vliet-Lanoë 2010). Méně vyvinutá je tzv. planární mikrostruktura, která byla zachycena ve vrstvách 6a/7a, 7a/7b, 7a a 7c ve vchodu jeskyně. Některé z těchto vrstev vykazovaly přechody do třetího mrazově ovlivněného typu mikrostruktury, a tou je mikrostruktura subangulárně bloková. Ta může vznikat i v hlubších částech sedimentárního tělesa v důsledku procesů probíhajících na povrchu. Van Vliet-Lanoë (2010) uvádí doklady působení až 80 cm pod povrchem. Směrem do hloubky je pak tato mikrostruktura hůře vyvinuta. Je tedy zřejmé, že přítomnost podobné mikrostruktury nemusí výslovně odrážet enviromentální podmínky panující při primární tvorbě vrstvy. Takto je například ovlivněno souvrství 8, zatímco ve vrstvě 9b je vliv již méně zřetelný. Naopak vrstva 7d známky subangulárně blokové mikrostruktury nevykazuje. Z hlediska mikromorfologie lze tedy říci, že souvrství 8 bylo ovlivněno chladným klimatem, výsledky ostatních analýz však ukazují, že geneze této vrstvy je mnohem složitější. Subangulárně bloková mikrostruktura byla zachycena také ve vrstvě 7c a částečně i ve vrstvě 7a. Protože jde o strukturu sekundárně vzniklou v důsledku procesů v nadloží, lze předpokládat, že u vrstvy 7a je výsledkem působení klimatu v době vrcholu posledního zalednění (LGM), zatímco v souvrství 8 v důsledku jiných chladnějších fází spojených pravděpodobně s MIS4.

Důležitým zjištěním mikromorfologické analýzy je doložení výrazného postdepozičního ovlivnění vrstvy 7a kryogenními pochody, především pak zmrzáním a rozmrzáním, v důsledku kterých vznikají různé mikrostruktury, v tomto případě subangulárně bloková mikrostruktura (Vliet-Lanoë 2010). Sekundárním jevem těchto procesů je postdepoziční vertikální posun artefaktů v sedimentu, což je jev, který lze doložit i v současných klimatických podmínkách (Mihevc 2009). Tímto způsobem lze vysvětlit rozpor mezi výsledky prostorové distribuce nálezů ve vrstvě 7a, které naznačují, že ukládání artefaktů nemohlo probíhat po dlouhou dobu (spíše opakované návštěvy stejné skupiny lidí), a velkým vertikálním rozptylem artefaktů, který by naznačoval dlouhodobé opakované využívání jeskyně (Neruda – Lázničková-Galetová – Dreslerová 2011).

6. ZÁVĚRY

Geoarcheologické studium sedimentů jeskyně Kůlny v Moravském krasu přineslo následující poznatky:

1. Mikromorfologickou analýzou byly vyčleněny jednotlivé fáze odpovídající různým formačním procesům. Nejvýraznějšími strukturami, identifikovanými především ve vrstvách 5–7a byly tzv. *„freezing structures“*, tj. mikrostruktury související s intenzivním promrzáním. Archeologicky sterilní vrstva 7b obsahuje tzv. *rip-up* klasty reliktní jílovité půdy a na podkladě mikromorfologické analýzy kombinované se zrnitostním či magnetickým studiem byla popsána jako výsledek rychlých erozních událostí, souvisejících s vyššími srážkami. Mikrostruktury jednotlivých vzorků v kombinaci s dalšími proxy-daty zároveň ukazují, že výrazně chladnější období panovalo během ukládání vrstev 5–6a, 7c a 8. Naopak vrstvy 11 a 9b vykazují známky relativně teplejšího a humidnějšího klimatu, což rámcově koresponduje s dosud uznávanou stratigrafickou koncepcí (cf. obr. 3). Podobné podmínky, i když pouze mírně teplejšího charakteru, pravděpodobně převládaly i v době ukládání vrstvy 7a. Následně však tato vrstva byla postdepozičně mrazově postižena, což zřejmě způsobilo vertikální redepozici archeologických nálezů.
2. Magnetická susceptibilita a frekvenčně závislá magnetická susceptibilita měřená na profilu 19 (jižní část-pilíř) ve vchodové části jeskyně koreluje s měřeními P. Šroubka a kol. et al. (Sroubek *et al.* 2001). Sedimenty uvnitř jeskyně mají magnetickou susceptibilitu o řád nižší, což je pravděpodobně dáno jejich složením a i typem depozice. Hodnoty frekvenčně závislé magnetické susceptibility sedimentů uvnitř jeskyně svědčí o jejich nulové pedogenní příměsi (až na bazální části vrstvy 6a), zatímco v případě sedimentů z profilu ve vchodu jeskyně lze říci, že tyto obsahují minimálně ve vrstvách 7a, 7b, 7d, 9b a 11 pedogenně ovlivněnou složku.
3. Studované sedimenty jsou vždy bimodální a jejich zrnitostní složení odpovídá spraším, tj. jílová složka je obsažena cca 20 %, jinak převládá prach. Poměr jíl/prach posloužil jako vhodná proxy pro určení míry zvětrávání a dobře koreluje s hodnotami frekvenčně závislé magnetické susceptibility.
4. Na základě provedených analýz bylo možné definovat možné odpovědi související s dlouho diskutovanou chronostratigrafickou situací jeskyně Kůlny. Rozdíl mezi vrstvami 5 a 6 lze identifikovat na základě zrnitostního složení, resp. míry zvětrávání; na základě měření hodnot frekvenčně závislé magnetické susceptibility lze odlišit vrstvu 6a od vrstev 6 a 5. Sedimentace, která probíhala v rámci starší fáze mladého paleolitu (EUP) byla buď značně omezená, nebo byla poškozena pravděpodobně v důsledku kryogenních pochodů. V každém případě se v sedimentární výplni objevuje nejméně jeden hiát, který by se měl nacházet mezi mezi vrstvami 6a a 6. Vrstva 7b mohla vznikat během chladnější fáze MIS4, kdy docházelo k výrazné změně vegetace a s tím související možné erozi. Pokud byl však důvodem eroze humidnější event, lze tuto vrstvu interpretovat spíše jako důsledek zvýšeného srážkového úhrnu na počátku MIS3. MIS4 by potom mohlo být na základě mikromorfologických pozorování kladeno spíše do vrstvy 8. Teplejší a humidnější klima, které je dle chronostratrigrafického kontextu předpo-

kládáno pro vrstvu 11–13, lze doložit pouze na základě výrazně zvýšených hodnot frekvenčně závislé magnetické susceptibility a indexu zvětrávání charakterizovaného poměrem jíl/prach. Velký vertikální rozptyl artefaktů ve vrstvě 7a lze interpretovat jako výsledek promrzání sedimentu, při kterém dochází k vertikálnímu pohybu.

PODĚKOVÁNÍ

Práce vznikla za podpory Grantové agentury České republiky (projekt P405/11/0406, Chronostratigrafická revize unikátní paleolitické lokality jeskyně Kůlny).

LITERATURA

BEHRE, K.-E. – PLICHT, J., 1992: Towards an absolute chronology for the last glacial period in Europe: radiocarbon dates from Oerel, northern Germany. Vegetation History and *Archaeobotany* 1, 2, 111–117.

BULLOCK, P. – MURPHY, C. P. (eds.), 1983: Soil micromorphology. A. B. Academic Publishers, Berkhamsted.

DEARING, J. A. – HAY, K. L. – BABAN, S. M. J. – HUDDLESTON, A. S. – WELLINGTON, E. M. H. – LOVELAND, P. J., 1996: Magnetic susceptibility of soil: an evaluation of conflicting theories using a national data set. *Geophysical Journal International* 127/3, 728–734.

DOLÁKOVÁ, N., 2002: Palynologické studium sedimentů šošůvské části Sloupsko-Šošůvských jeskyní a spodní části opěrného profilu v jeskyni Kůlna. *Acta Musei Moraviae, Sci. geol.* 87, 275–288.

EVANS, M. E. – HELLER, F., 2003: Environmental magnetism, Principles and Applications of Enviromagnetics. Academic Press, An imprint of Elsevier Science, Oxford.

FASSBINDER, J., 2010: Magnetometry for archaeologists. A. Aspinall, C. Gaffney and A. Schmidt. Editors L. B. Conyer and K. L. Kvamme Altamira Press, 2008. No. of pages: 208. ISBN: 0-7591-1106-5. *Archaeological Prospection* 17/4, 271–272.

FASSBINDER, J. W. E. – STANJEKT, H. – VALI, H., 1990: Occurrence of magnetic bacteria in soil. *Nature* 343/6254, 161–163.

GEOČR50, 2013: Geologická mapa České republiky 1 : 50 000, wms.geology.cz, Česká geologická služba, 3. 11., 2013.

GOLDBERG, P. – MACPHAIL, R., 2006: Practical and theoretical geoarchaeology. Blackwell Publishing, Malden, MA; Oxford.

GUIOT, J. – PONS, A. – DE BEAULIEU, J. L. – REILLE, M., 1989: A 140,000-year continental climate reconstruction from two European pollen records. *Nature* 338/6213, 309–313.

KADLEC, J., 2012: Sedimenty ve Sloupsko-šošůvských jeskyních a v Kůlně – klíč k porozumění podzemním procesům. *Speleofórum* 31, 26–33.

KARKANAS, P. – GOLDBERG, P., 2013: Micromorphology of Cave Sediments. In: J. F. SHRODER – FRUMKIN, A. (eds.): Treatise on Geomorphology, Vol. 6, Karst Geomorphology, 286–297. Academic Press, San Diego.

KLETETSCHKA, G. – BANERJEE, S. K., 1995: Magnetic stratigraphy of Chinese loess as a record of natural fires. *Geophysical Research Letters* 22, 11: 1341–1343.

KNAPP, E. P. – TERRY, D. O. – HARBOR, D. J. – THREN, R. C., 2004: Reading Virginia's paleoclimate from geochemistry and sedimenthology of clastic cave sediments. In: I. D. SASOWSKY – MYLROIE, J. (eds.): Studies of cave sediments: Physical and Chemical Records of Paleoclimate, 95–106. Kluwer/Plenum, New York.

KŘÍŽ, M., 1889: Kůlna a Kostelík. Dvě jeskyně v útvaru devonského vápence na Moravě. Bádání a rozjímání o pravěkém člověku. Musejní spolek brněnský, Brno.

KUKAL, Z., 1971: Geology of Recent Sediments. Academia–Academic Press, Praha.

KUKLA, G. J., 1975: Loess Stratigraphy of Central Europe. In: K. W. BUTZER – ISAAC, G. L. (eds.): After the Australopithecines, 99–188. Mouton Publishers, The Hague.

LISÁ, L. – HOŠEK, J. – BAJER, A. – GRYGAR, T. M. – VANDENBERGHE, D., in press: Geoarchaeology of Upper Palaeolithic loess sites located within a transect through Moravian valleys, Czech Republic. Quaternary International.

LISÁ, L. – LISÝ, P. – BAJER, A. – KUBÁLEK, P., 2013: Geoarcheologický posudek sedimentů jeskyně Kůlna, Moravský kras. Nepublikovaná výzkumná zpráva pro MZM Brno. Geologický ústav AV ČR, v. v. i. Praha, 1–41.

MARTINI, I. P. – CHESWORTH, W. (eds.), 1992: Weathering, Soils & Paleosols Elsevier, Amsterdam.

MIHEVC, A., 2009: Cryoturbation of the sediments at the cave entrances – case studies from Skednena jama, Potočka zijalka and Bestažovca cave. In: 51st Annual Meeting in Ljubljana 14th–18th of April, 2009, 26–27. Hugo Obermaier-Gesellschaft, Erlangen.

MICHEL, V. – BOCHERENS, H. – VALOCH, K. – YOKOYAMA, Y., 2006: La grotte de Kůlna : analyses physico-chimique et radiométrique des os et dentines de grands mammifères des niveaux de Paléolithique moyen. *ArcheoSciences, Revue d'archéométrie* 30, 137–142.

MOOK, W. G., 1988: Radiocarbon-Daten aus der Kůlna-Höhle. In: K. VALOCH (ed.): Die Erforschung der Kůlna-Höhle 1961–1976, 285–286. Moravské zemské muzeum, Brno.

MUSIL, R., 1988: Ökostratigraphie der Sedimente in der Kůlna-Höhle. In: K. VALOCH (ed.): Die Erforschung der Kůlna-Höhle 1961–1976, 215–255. Moravské muzeum – Anthropos Institut, Brno.

NEJMAN, L. – RHODES, E. – ŠKRDLA, P. – TOSTEVIN, G. – NERUDA, P. – NERUDOVÁ, Z. – VALOCH, K. – OLIVA, M. – KAMINSKÁ, Ľ. – SVOBODA, J. A. – GRÜN, R., 2011: New Chronological Evidence for the Middle to Upper Palaeolithic Transition in the Czech Republic and Slovakia: New Optically Stimulated Luminiscence Dating Results. *Archaeometry* 53/5, 1044–1066.

NERUDA, P., 2011: Střední paleolit v Moravských jeskyních. Middle Palaeolithic in Moravian Caves. Masarykova Univerzita, Brno.

NERUDA, P., 2013: Morfologie jeskyně Kůlny před II. světovou válkou. *Acta Musei Moraviae, Sci. soc.* 98: 2, 183–195.

NERUDA, P. – LÁZNIČKOVÁ-GALETOVÁ, M. – DRESLEROVÁ, G., 2011: Retušéry a kosti s rýhami z jeskyně Kůlny v Moravském krasu. Interdisciplinární analýza tvrdých živočišných materiálů ze středopaleolitických horizontů. *Anthropos-Studies* 33 (N. S. 25). Moravské zemské muzeum, Brno.

NERUDA, P. – NERUDOVÁ, Z., 2013: The Middle-Upper Palaeolithic transition in Moravia in the context of the Middle Danube region. *Quaternary International* 294/0, 3–19.

NERUDA, P. – NERUDOVÁ, Z., v tisku-a: New radiocarbon data from Micoquian layers of the Kůlna Cave (Czech Republic). *Quaternary International*, http://dx.doi.org/10.1016/j.quaint.2013.10.015.

NERUDA, P. – NERUDOVÁ, Z., v tisku-b: Chronology of the Upper Palaeolithic Sequence in the Kůlna Cave. Archäologisches Korrespondenzblatt.

PATOU-MATHIS, M. – AUGUSTE, P. – BOCHERENS, H. – CONDEMI, S. – MICHEL, V. – MONCEL, M.-H. – NERUDA, P. – VALOCH, K., 2005: Les occupations du Paléolithique moyen de la grotte de Külna (Moravie, République Tchèque): nouvelles approches, nouveaux résultats. In: A. TUFFREAU (ed.): Peuplements humains et variations environnementales au Quaternaire. Colloque de Poitiers, 18–20 septembre 2000, 69–94. Ed John and Erica Hedges Ltd, Oxford.

PÉCSI, M., 1990: Loess is not just the accumulation of dust. *Quaternary International* 7–8/0, 1–21.

RINK, W. J. – SCHWARCZ, H. P. – VALOCH, K. – SEITL, L. – STRINGER, C. B., 1996: ESR Dating of Micoquian Industry and Neanderthal Remains at Kůlna Cave, Czech Republic. *Journal of Archaeological Science* 23/6, 889–901.

SROUBEK, P. – DIEHL, J. F. – KADLEC, J. – VALOCH, K., 2001: A Late Pleistocene palaeoclimate record based on mineral magnetic properties of the entrance facies sediments of Kulna Cave, Czech Republic. *Geophysical Journal International* 147/2, 247–262.

STOOPS, G. (ed.), 2003: Guidelines for Analysis ond Description of Soil and Regolith Thin Sections. Soil Science Society of America, Inc., Madison.

STOOPS, G. – MARCELINO, V. – MEES, F. (eds.), 2010: Interpretation of micromorphological features of soils and regoliths. Elsevier, Amsterdam.

ŠROUBEK, P. – DIEHL, J. F. – KADLEC, J. – VALOCH, K., 1996: Preliminary study on the mineral magnetic properties of sediments from Kůlna Cave (Moravian Karst), Czech Republic. *Studia Geophysica et Geodaetica* 40/3, 301–312.

ŠROUBEK, P. – DIEHL, J. F. – KADLEC, J. – VALOCH, K., 2001: A Late Pleistocene palaeoclimate record based on mineral magnetic properties of the entrance facies sediments of Kulna Cave, Czech Republic. *Geophysical Journal International* 147/2, 247–262.

VALOCH, K., 1970: Early Middle Palaeolitic (Stratum 14) in the Kůlna Cave near Sloup in the Moravien Karst (Czechoslovakia). *World archaeology* 2/1, 28–38.

VALOCH, K., 1974: Eine datierte Feuerstelle des Magdaléniens in der Kůlna-Höhle bei Sloup im Mährischen Karst. *Anthropozoikum* 10, 111–130.

VALOCH, K., 1988a: Le Taubachien et le Micoquien de la grotte Kůlna en Moravie (Tchécoslovaquie). In: L'homme de Néanderthal, vol. 4, La technique. 205–207, Liège.

VALOCH, K., 1988b: Die Erforschung der Kůlna-Höhle 1961–1976. Anthropos Studien 24 (N. S. 16). Moravské muzeum, Brno.

VALOCH, K., 1989: Osídlení a klimatické změny v poslední době ledové na Moravě. *Acta Musei Moraviae, Scientiae sociales* 74, 7–34.

VALOCH, K., 2002: Eine Notgrabung in der Kůlna-Höhle im mährischen Karst. *Acta Musei Moraviae, Scientiae sociales* 87, 3–34.

VALOCH, K., 2011: Stratigrafie sedimentů. In: K. Valoch a kol.: Kůlna. Historie a význam jeskyně, 47–58. Správa jeskyní České republiky, Průhonice.

VALOCH, K. a kol. 2011: Kůlna. Historie a význam jeskyně. Správa jeskyní České republiky, Průhonice.

VALOCH, K. – PELÍŠEK, J. – MUSIL, R. – KOVANDA, J. – OPRAVIL, E., 1969: Die Erforschung der Kůlna-Höhle bei Sloup im Mährischen Karst (Tschechoslowakei). *Quartär* 20, 1–45.

VAN ANDEL, T. H. – DAVIES, W. (eds.), 2003: Neanderthals and modern humans in the European landscape during the last glaciation : archaeological results of the Stage 3 Project. McDonald Institute for Archaeological Research, Cambridge.

VAN ANDEL, T. H. – TZEDAKIS, P. C., 1996: Palaeolithic landscapes of Europe and environs, 150,000–25,000 years ago: An overview. *Quaternary Science Reviews* 15/5–6, 481–500.

VLIET-LANOË, B. V., 2010: 6 – Frost Action. In: G. STOOPS – MARCELINO, V. – MEES, F. (eds.): Interpretation of Micromorphological Features of Soils and Regoliths, 81–108. Elsevier, Amsterdam.

POZNÁMKA

1 Dochována pouze v tomto místě v podobě mírně narušeného fragmentu mezi stěnami starších sond. V původním kresleném profilu 19 nebyla dokumentována.

SUMMARY

The main aim of the study is a geoarchaeological evaluation of sediments of the Kůlna cave in Moravian Karst. During the rescue excavation in 2011, a section at the cave entrance (profile 19 southern part-pillar) have been uncovered again. This was the basis for geochemical sampling of layes 11–6a that according to chronostratigraphic classification document the period Eemian – Weichselian. Stratigraphically related sediments (layers 6a–5) were then sampled in section 29 in sector G1 in the middle of the cave. Besides samples for magnetic parameters and particle-size measurements, micromorphological samples documenting particular chronostratigraphically determined layers were taken from three related sections at the entrance and from section 29 inside the cave.

By micromorphological analysis particular structural elements corresponding to different formation processes were defined. The most significant structures identified mostly in 5–7a layers were so called “freezing structures”, i.e. microstructures corresponding to very intensive freezing. Archaeologically sterile layer 7b contains so called rip-up clasters of relict clayey soil, and due to micromorphological analysis combined with particle-size and magnetic study this layer was described as a set of fast erosion events caused by increased precipitation. Due to microstructure of particular samples in combination with other proxies it is possible to say that significantly colder period prevailed during deposition of layer 5–6a, 7c, and 8. On the contrary layers 11 and 9b show signs of warmer and more humid climate. This kind of climate possible prevailed also during deposition of layer 7a (also layers 7b and 7d). However, this layer was then secondarily affected by frost, which also caused discrepancies in classification of archaeological findings.

The analyses provided possible answers related to long-discussed chronostratigraphic situation in the Kůlna cave. The difference between layers 5 and 6, that were not distinguished inside the cave in G1 sector by K. Valoch, can be identified based on particle-size distribution or weathering index. Distinguishing of layer 6a from layers 6 and 5 is possible on the basis of measurement of values of frequency dependent magnetic susceptibility. Sedimentation occuring within EUP complex was damaged presumably due to cryogenic processes, and can be relic preserved within transition betwen layers 6a and 6. Layer 7b could be formed during colder phase MIS4 when there was significant change of vegetation and related eventual erosion. However, if erosion was caused by increased precipitation (more humid event), then this layer could be rather associated with the beginning of MIS3. A warmer and more humid climate that is, in context of chronostratigraphy, assumed for layers 11–13, can be demonstrated only on the basis of extremely increased values of frequency dependent magnetic susceptibility and weathering index characterized by clay/dust ratio. The large vertical dispersion of artefacts in layer 7a can be interpreted as a result of sediment freezing where there is vertical movement, which corresponds to the results of spatial distribution of findings.

J. Kadlec, M. Chadima, L. Lisá, H. Hercman, A. Osintsev, and H. Oberhänsli – Clastic cave deposits in Botovskaya Cave (Eastern Siberia, Russian Federation). *Journal of Cave and Karst Studies,* v. 70, no. 3, p. 142–155.

CLASTIC CAVE DEPOSITS IN BOTOVSKAYA CAVE (EASTERN SIBERIA, RUSSIAN FEDERATION)

Jaroslav Kadlec[1], Martin Chadima[1], Lenka Lisá[1], Helena Hercman[2], Alexandr Osintsev[3], and Hedi Oberhänsli[4]

Abstract: Botovskaya Cave is a typical example of a two-dimensional maze with a total length of explored passages exceeding 60 km, which represents the longest limestone cave system in the Russian Federation. The clastic cave sediments filling the cave passages differ in both mineral and mineral magnetic properties and were deposited under different hydrological conditions. The older portion of the clastic cave fills was derived from overlying sandstones, whereas the properties of younger cave sediments show closer affinity to the soils and weathering products originating on the plateau above the cave. The cave sediments underwent repeated periods of deposition and erosion during the Tertiary (?) and Pleistocene. The last catastrophic erosion event occurred in the cave more than 350 ka based on flowstone dating. Water seeping through the overlying sandstone body causes collapses of sandstone slabs from the cave passage ceilings, forming the youngest portion of the clastic cave fills.

Introduction

It has been demonstrated that the study of the clastic cave deposits can contribute to better understanding of the cave system development as well as to the local hydrological processes. Sedimentological and mineralogical studies together with radiometric or paleomagnetic datings of both clastic and chemogenic deposits have commonly been applied in cave sediment research (e.g., Häuselmann et al., 2007; Kadlec et al., 2001). The mineral magnetic approach has been used only occasionally to understand climatic, hydrological and anthropogenic processes controlling sediment deposition in caves (Ellwood et al., 1996, 2004; Sroubek et al., 2001, 2007). The assemblage of magnetic minerals found in sediments is controlled by the character of the source rocks, weathering, mode and energy of transporting medium, and by depositional as well as post-depositional processes.

The aim of this paper is an examination of Botovskaya Cave deposits using methods operating with magnetic and heavy minerals and with quartz grain exoscopy. Obtained mineral characteristics were used for correlations from the point of view of sediment source and mode of transportation into the cave passages. Radiometric and paleomagnetic datings of the cave carbonate bed allowed us to estimate the age of both depositional and post-depositional processes.

Geographical and Geological Settings

Botovskaya Cave (55° 18′ N, 105° 20′ E) is located on the Angarsko-Lensky Plateau of the southern Siberian Craton about 500 km north of Irkutsk City (Fig. 1). The area reaches altitudes of 1100 m a.s.l., and belongs to the Zhigalovo District of the Irkutsk Area. The plateau is dissected by river valleys up to 400 m deep. Cave entrances lie at a relative elevation of 310 m above the Lena River level, in a valley of the Garevogo Creek, the left tributary of the Boty River, which joins the Lena River. The cave system, dipping gently to the north, has developed in an Early Ordovician limestone formation with a thickness of 6 to 12 m. The limestone bed is underlain by Middle and Late Cambrian sandstone, siltstone, marl and gypsum and overlain by Middle Ordovician sandstone, limestone and argillite (Filippov, 2000).

The cave system developed under confined (artesian karst) settings (Klimchouk, 2000, 2003; Filippov, 2000). The speleogenesis of the Botovskaya Cave system was interpreted by Filippov (2000) and is due to two different processes, (i) corrosion involving meteoric artesian water and (ii) ascending deep circulating artesian water spanning the time period between Late Mesozoic and Early Neogene. The clastic cave deposits fill the bottom portion of the cave passages and are not usually exposed sufficiently for study. The deposits from the cave were preliminarily described by Filippov (2000). Breitenbach (2004) described in detail a recently excavated section of cave sediments (the same section is labeled Section 1 in this paper).

The cave is divided into two parts: the Old World and the New World. All studied sections of cave sediments are situated in the Old World, 200–400 m east of the Central and Medeo entrances (Fig. 2). The key Section 1 and Section 2 are exposed in two test-pits excavated in the sedimentary fill close to survey stations PK0122 and PK042. The smaller Section 3 and Section 4 are located

[1] Institute of Geology AS CR, v.v.i., Rozvojova 269, CZ-165 00 Praha 6, Czech Republic, kadlec@gli.cas.cz
[2] Institute of Geological Sciences, PAN, Warszawa, Poland
[3] Speleoclub Arabica, Irkutsk, Russia
[4] GeoForschungsZentrum Potsdam, Germany

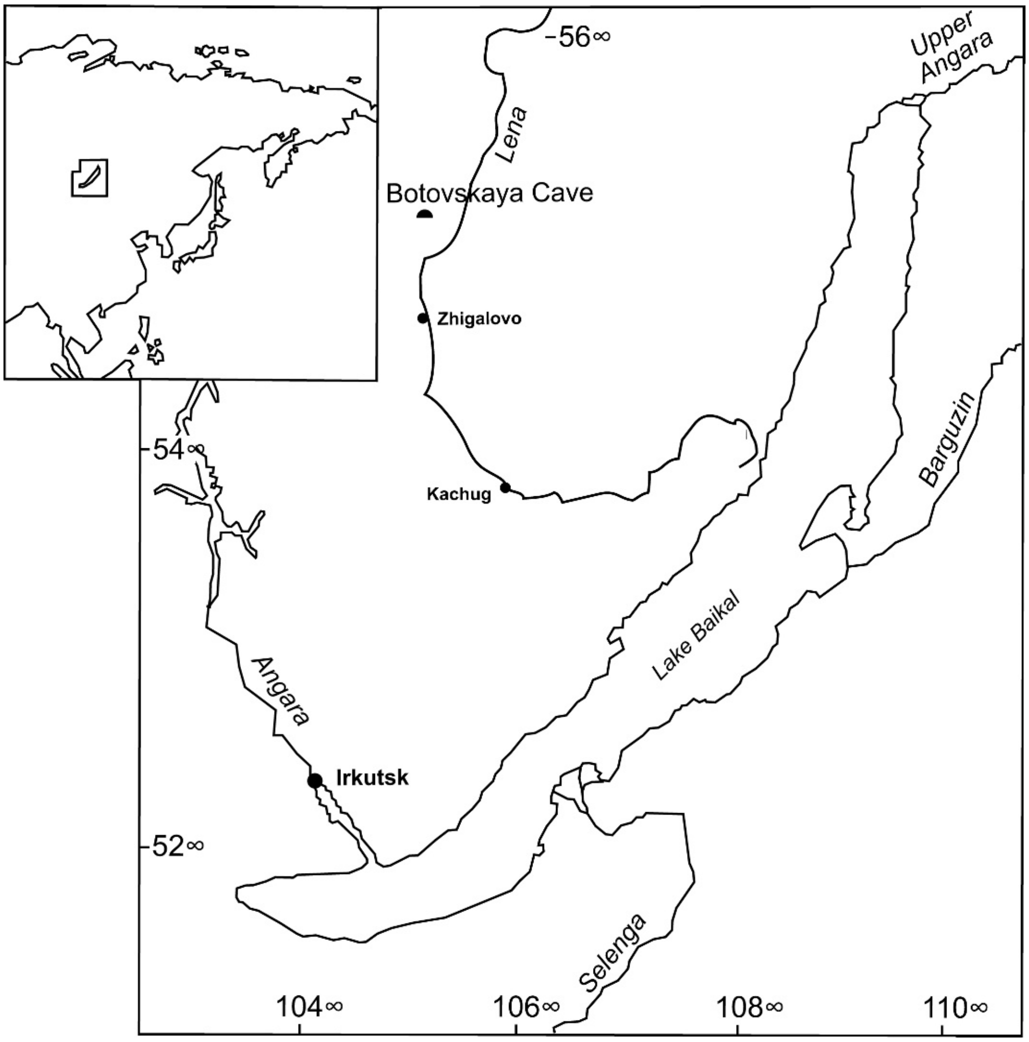

Figure 1. Location of Botovskaya Cave in Eastern Siberia.

close to survey stations PK0186 and PK0342, respectively. A small relic of flowstone bed used for Th/U dating is preserved on the limestone wall W of Section 1 ca 1.7 m above the present passage floor.

Materials and Methods

The studied sections of the cave deposits were documented with special reference to lithology, sedimentary structures and aggradation and erosion event records. Mineral magnetic characteristics such as low field bulk magnetic susceptibility (MS) and anhysteretic remanent magnetization (ARM) together with anisotropy of magnetic susceptibility (AMS) help to find the source of the cave fills and estimate a mode of sediment transport to the cave passages. While MS values are influenced by the concentration of magnetic particles, mineralogy and grain size of the minerals (ferro-, para-, and diamagnetic) in the sediments, ARM is sensitive only to the concentration, mineralogy and grain size of ferromagnetic minerals present in sediments. AMS reflects the preferred orientation of magnetic minerals and can be used for texture interpretation in sedimentary rocks. Magnetic anisotropy can be visualized by an ellipsoid with three perpendicular principal axes ($k_1 \geq k_2 \geq k_3$). The maximum axis (k_1) is denoted as magnetic lineation and the plane perpendicular to minimum axis (k_3) defines a magnetic foliation. The AMS ellipsoid magnitude can be presented as a ratio k_1/k_3, known as the degree of anisotropy, *P* (Nagata, 1961). The AMS ellipsoid shape can be described by the shape parameter, *T* (Jelínek, 1981); oblate shapes correspond to $0 < T \leq 1$, prolate shapes correspond to $-1 \leq T < 0$. The degree and shape of the AMS depend on the lithology and compaction imposed on the deposit.

Oriented samples of clastic cave sediments were collected in plastic boxes (volume 6.7 cm^3). For each sample MS and AMS were measured using Agico KLY-4 Kappagridge (alternating field amplitude of 425 A/m and operating frequency of 875 Hz) in the Paleomagnetic Laboratory of the Institute of Geology AS CR, v.v.i. in

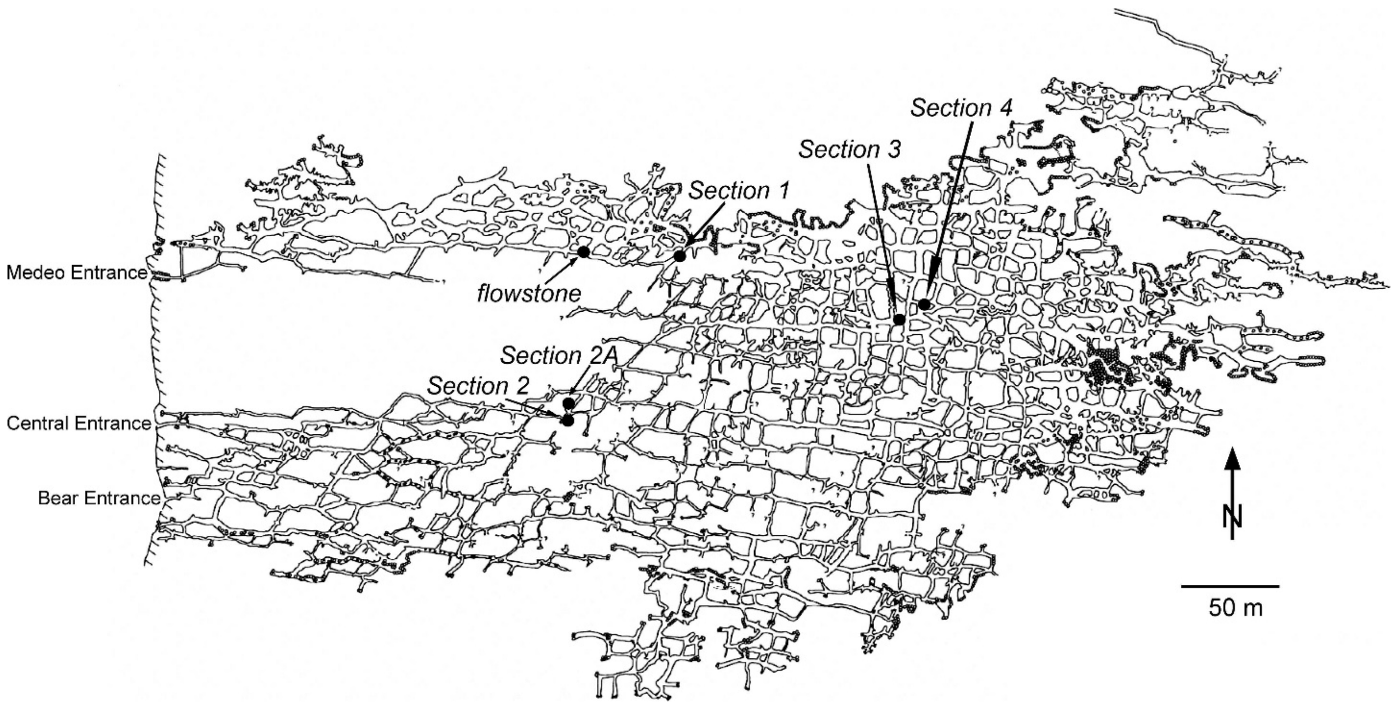

Figure 2. Botovskaya Cave (The Old World) map (adopted from Göbel and Breitenbach, 2003) with indication of studied sections and dated flowstone.

Prague. The ARM was imparted on demagnetized samples (using an Agico AF demagnetizer/magnetizer LDA-3/ AMU-1A and measured on an Agico JR-6A spinner magnetometer). Frequency dependent magnetic susceptibility as a proof for the presence of superparamagnetic particles was tested in low- and high-frequency measurements conducted on a Bartington MS2 magnetic susceptibility meter. For the purpose of paleomagnetic polarity measurements three 8 cm^3 samples were cut from the flowstone bed. Samples were thermally demagnetized and measured using a 2G Enterprises superconducting rock magnetometer in the Laboratory for Natural Magnetism ETH Zurich.

The character of quartz grain surfaces indicates transportation and post-depositional history of clastic sediments. Exoscopic observations were performed on quartz grains larger than 0.25 mm separated from either clastic cave deposits or from the Ordovician sandstone bedrock after wet sieving and boiling in HCl. The cleaned grains were stuck on a carbon tape and observed using the BS 340 electron microscope. Heavy minerals were separated after wet sieving from the grain-size fraction of 0.25–0.063 mm using tetrabromethane (density 2.964 g cm^{-3}) and observed in Canadian balsam. At least 300 grains of transparent heavy minerals were determined in each sample.

The flowstone bed used for the paleomagnetic polarity measurements was also dated by the $^{230}Th/^{234}U$ radiometric method. Uranium and thorium were separated from three samples using a standard chemical procedure (Ivanovich and Harmon, 1992). The samples were dissolved in 6 M nitric acid, and uranium and thorium were separated by a chromatographic method using the DOWEX 1 × 8 ion exchanger. The efficacy of chemical separation was controlled by addition of a $^{228}Th/^{232}U$ spike. Activity measurements (alpha spectrometry) were taken with the OCTETE PC device of the EG&G ORTEC company. Spectral analysis and age calculation were performed using URANOTHOR 2.5. software (Gorka and Hercman, 2002).

Description of the Cave Deposits

Section 1

The section is exposed in the excavated test-pit 2.8 m deep (Breitenbach, 2004). A SW face of the test-pit shows dark gray to black, medium-grained sand deposited on the bedrock bottom of the passage (Bed 15 in Fig. 3). The sand layer contains rare laminae of light medium-grained brown sand and sporadic aggregates of SiO_2-cemented sand up to 1 cm large. The overlying gray to yellow brown sand bed contains frequent, up to 2 cm large aggregates of sand cemented with SiO_2 (Bed 14). Deposition continued with brown clayey medium-grained sand with laminae and lenses of light brown sand (Bed 13), light brown, medium-grained sand (Bed 12) and with overlying dark gray clayey medium-grained sand with small lenses to laminae of light fine-grained sand (Bed 11). This bed was partly eroded before the deposition of brown laminated clayey medium-grained sand (Bed 10) with fragments of brown clay on the

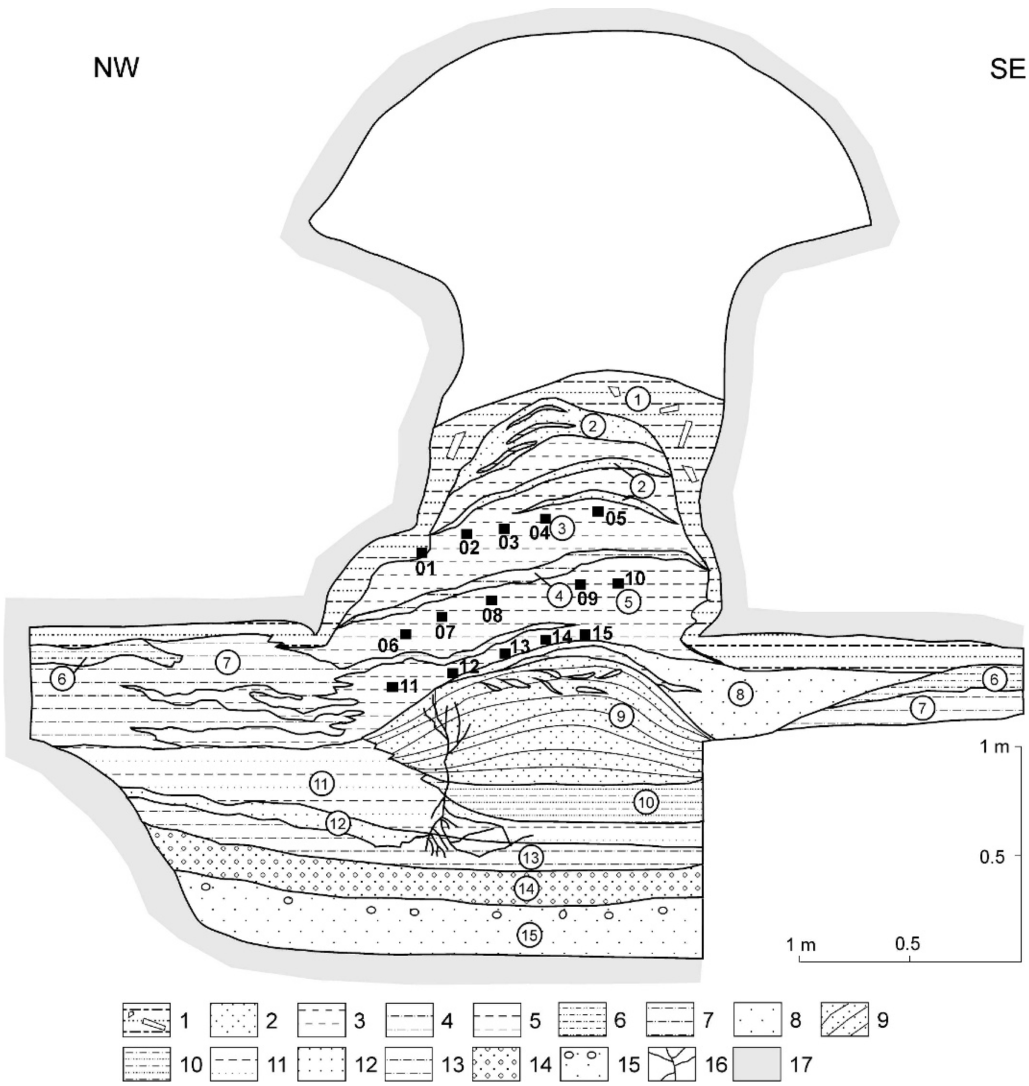

Figure 3. Section 1 — SW face

1 – clay, sporadic angular clasts of sandstone; 2 – sand; 3 – clay; 4 – sandy clay to clayey sand; 5 – clay; 6 – sandy clay; 7 – slightly sandy clay; 8 – sand; 9 – sand, fine-grained; 10 – clayey sand, laminated; 11 – clayey sand; 12 – sand; 13 – clayey sand; 14 – sand with sandy aggregates; 15 – sand; 16 – carbonate cementation along fissures; 17 – bedrock wall; black squares with numbers – collected samples. For more detailed description see text.

erosional top of the bed. The above lying loaf-like bed (Bed 9) is formed by light and dark brown laminae of fine-grained sand 1–15 mm thick with brown clay fragments of up to 2 cm in size at the erosional surfaces and relics of cemented laminae (up to 7 mm thick) in the upper portion of the bed. Beds 9 to 13 were disturbed by fissures filled with carbonate-cemented fine sand. Bed 8 is formed by light brown fine-grained sand with chaotic small lenses or laminae of darker medium-grained sand and rare fragments of light gray fine-grained sand. This is followed by light brown, slightly sandy clay with black smudges at the base (Bed 7) and red sandy clay preserved only in relics (Bed 6). The above lying brown to brown-red clay (Bed 5), massive in the lower portion and containing 1–3 mm thick laminae in the upper portion, is overlain by gray to yellowish sandy clay to clayey medium-grained sand (Bed 4) and brown clay (Bed 3) containing lenses of light brown, medium-grained sand (Bed 2). The section is covered with brown-red clay with sporadic angular clasts of sandstone up to 7 cm in size filling the space formed by water running along the limestone walls.

The NE face of the test-pit shows a similar succession as the opposite SW face of the section (Fig. 4). Minor unconformities and clay fragments are noticeable in the laminated fine-grained sands forming Bed 9 (Fig. 3). Laminated sediments in the left part of the bed were disturbed by a fissure. Small fragments (< 1 mm) of disintegrated darker laminae concentrate along this fissure.

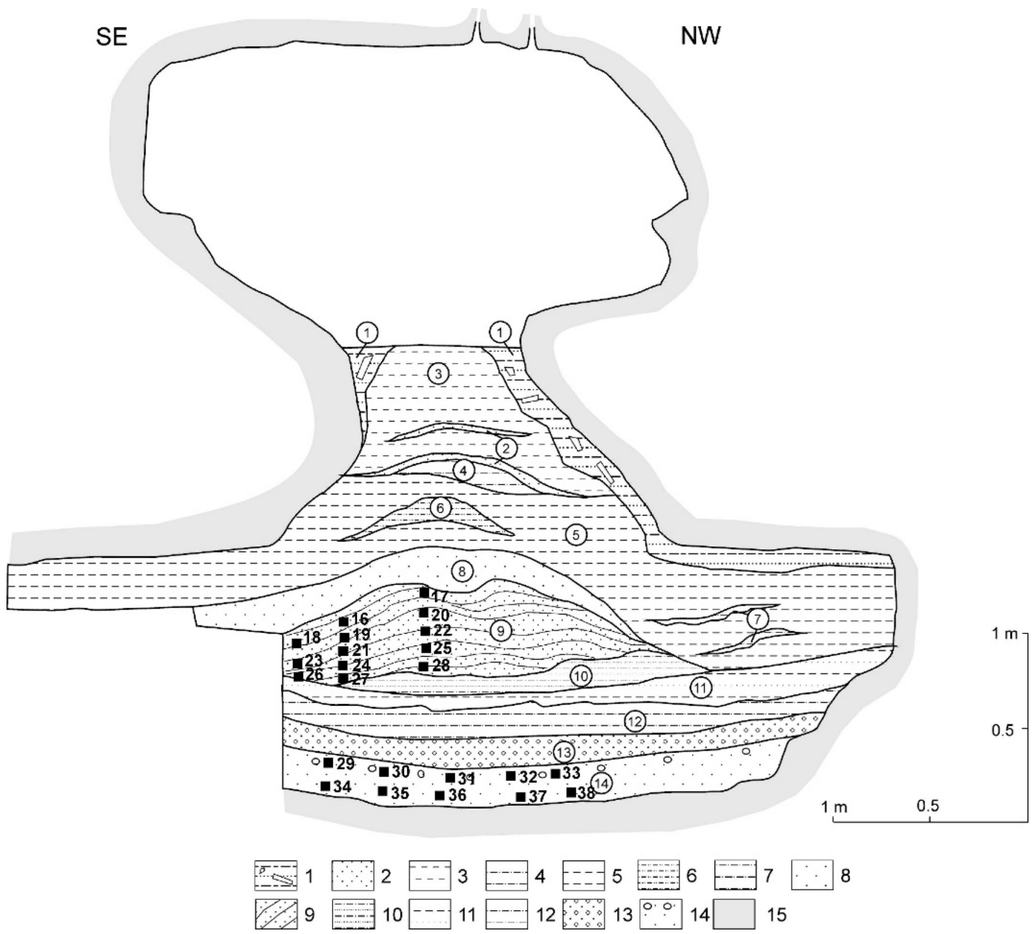

Figure 4. Section 1 — NE face

1 – clay, sporadic angular clasts of sandstone up to 7 cm large; 2 – sand; 3 – clay; 4 – clay; 5 – clay; 6 – sand; 7 – slightly sandy clay; 8 – sand; 9 – sand, fine-grained; 10 – clayey sand, laminated; 11 – clayey sand; 12 – clayey sand; 13 – sand with sandy aggregates; 14 – sand; 15 – bedrock wall; black squares with numbers – collected samples. For more detailed description see text.

SECTION 2

The section is exposed in an older excavated test-pit. Dark brown to gray, medium-grained sand with sporadic clasts of SiO_2-cemented sand up to 1.5 cm in size and rare fragments of brown clay up to 4 cm in size were deposited at the bedrock bottom (Bed 7 in Fig. 5). The above lying gray to yellow brown medium sand with sandy aggregates (Bed 6) contains aggregates of SiO_2-cemented sand up to 1.5 cm in size. Dark gray medium-grained clayey sand layers with lighter stains containing irregular lenses of yellow-brown sand and fragments of brown massive clay up to 1.5 cm in size deposited on the surface of the bed designated as Bed 5. The younger Bed 4 is formed by dark gray, fine-grained silty sand, partly laminated with 1 mm thick laminae of yellow-brown fine sand in the lower portion and lenticular fragments of brown clay indicating erosional surfaces of laminae. The above lying light brown, slightly clayey, medium-grained sand contains relics of cemented sand on its surface (Bed 3). Brown to slightly red laminated clay colored by Mn-oxides in the upper portion represents Bed 2. The top of the succession is formed by light brown to yellow-brown, medium-grained clayey sand containing angular sandstone clasts 5–15 cm in size and fragments of brown and black clay coloured by Mn-oxides (Bed 1). A limestone block up to 0.5 m large is present in the youngest bed.

SECTION 2A

This sedimentary section is exposed in a phreatic conduit about 0.5 m above the top of Section 2. It consists of brown-red, medium-grained sand (Bed 2) and is overlain by light brown clay (Bed 1 in Fig. 5).

SECTION 3

The lowermost Bed 3 of the section is formed by dark gray medium-grained sand beds (1–1.5 cm thick) with brown clayey medium-grained sand and brown clay (0.5–2 cm thick) (Fig. 6). The above lying Bed 2 comprises

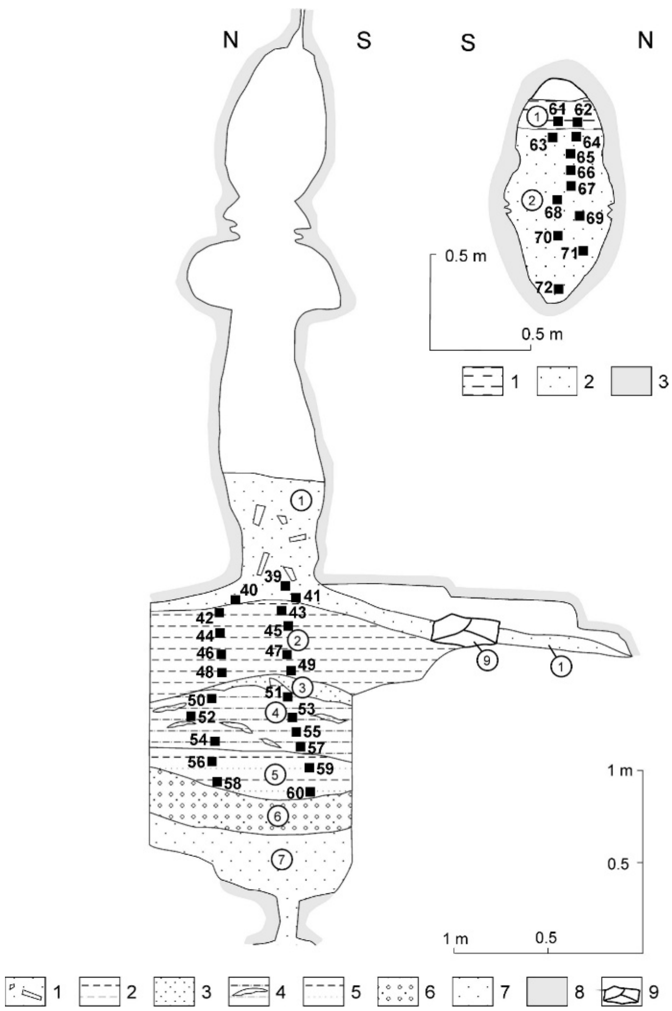

Figure 5. Section 2

1 – clayey sand, rare angular sandstone clasts 5–15 cm large and fragments of clay; 2 – clay, laminated in the upper portion; 3 – slightly clayey sand; 4 – silty sand; 5 – clayey sand; 6 – sand with sandy aggregates; 7 – sand, sporadic sandy concretions up to 1.5 cm large and rare fragments of brown clay up to 4 cm large; 8 – bedrock wall; 9 – block of bedrock; black squares with numbers – collected samples. For more detailed description see text.

Section 2A (top right)

1 – clay; 2 – sand; 3 – bedrock wall.

alternating dark gray laminae of medium-grained clayey sand. The deposition was terminated by a gray to gray-black, medium-grained sand bed with irregular lenses of light brown sand (Bed 1).

Section 4

Yellow-gray, medium-grained sand is exposed in the lowermost Bed 4 (Fig. 7). Light brown, medium-grained sand with gray-brown lenticular stains was deposited in the above lying Bed 3. Bed 2 is formed by dark gray, fine- to medium-grained sand laminae alternating with light brown

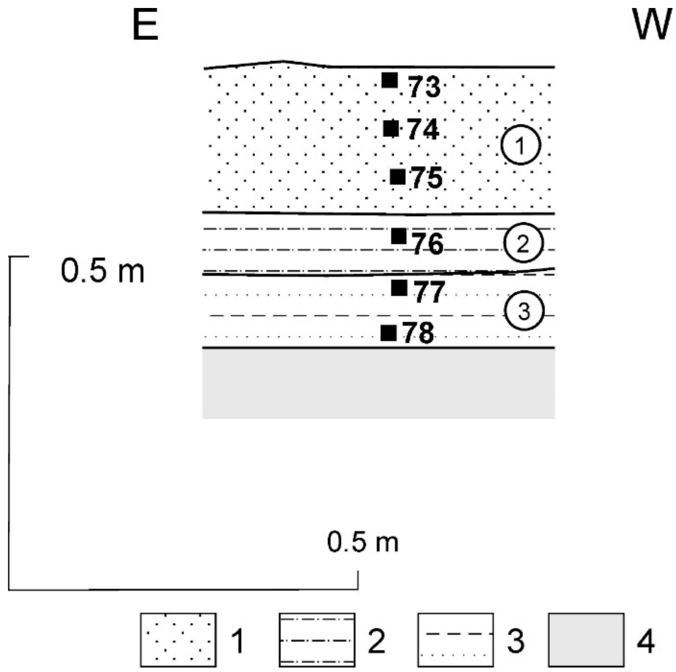

Figure 6. Section 3

1 – sand; 2 – clayey sand; 3 – alternating of layers of sand with clayey sand and clay; 4 – bedrock bottom; black squares with numbers – collected samples.

sand laminae. The section is topped by brown clay alternating with irregular beds of gray, medium-grained clayey sand (Bed 1). A black lamina coloured by Mn-oxides occurs at the base of this bed.

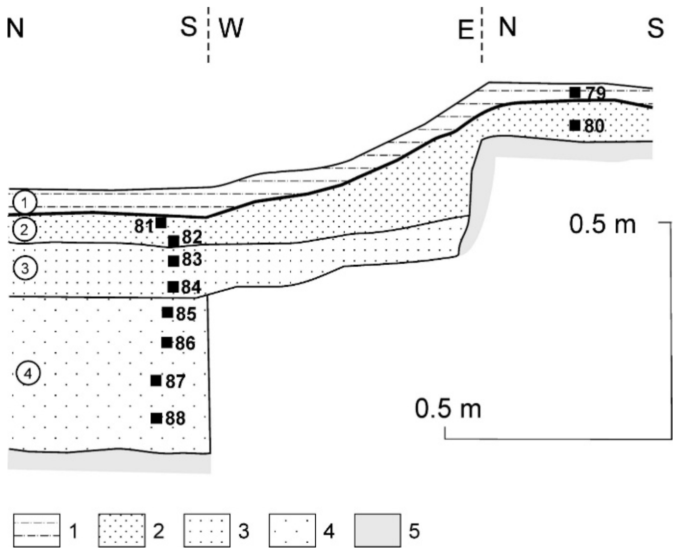

Figure 7. Section 4

1 – clay; 2 – sand; 3 – sand; 4 – sand; 5 – bedrock bottom; black squares with numbers – collected samples.

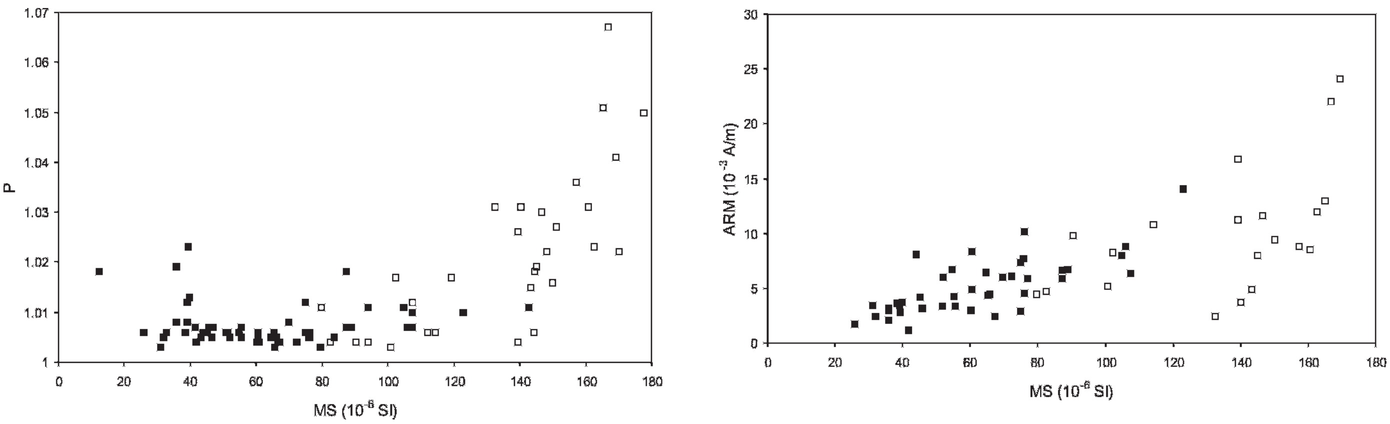

Figure 8. Correlation between magnetic susceptibility (MS) and degree of magnetic anisotropy (*P*) – left; correlation between magnetic susceptibility (MS) and anhysteretic remanent magnetization (ARM) – right. Black squares – bottom sedimentary beds (samples 16–41, 50–60, 63–72, 79–88); empty squares — top sedimentary beds (samples 01–15, 42–49, 61–62, 73–78).

Results

Mineral Magnetic Characteristics and Magnetic Fabric

The MS values slightly increase from sandy bottom sediment beds to the above lying clay dominating sediments (Fig. 8). In Section 1, the values range from 23–63 × 10^{-6} SI (Bed 14) to 30–119 × 10^{-6} SI (Bed 9) and 90–149 × 10^{-6} SI (Beds 3 and 5). Similar variations were measured in Section 2 with 37–73 × 10^{-6} SI (Beds 4 and 5), 67–127 × 10^{-6} SI (Bed 2) and 56–90 × 10^{-6} SI (Bed 1). Basal sands in Section 2A yielded MS values of 22–55 × 10^{-6} SI (Bed 2), whereas the above lying clay bed has MS values of 121–123 × 10^{-6} SI (Bed 1). MS values of sediments exposed in Section 3 range between 76 and 124 × 10^{-6} SI, whereas the values in Section 4 slightly increase from 10–35 × 10^{-6} SI (in beds 3 and 4) to 26–94 × 10^{-6} SI (Bed 2). The highest MS values (up to 410 × 10^{-6} SI) were measured in the modern topsoil collected above the Medeo Entrance, whereas the bedrock sandstone showed MS values between 7 and 25 × 10^{-6} SI and MS values of limestone are about 10 × 10^{-6} SI. The ARM values ranging between 1 and 22 × 10^{-3} A/m plot versus the MS show steep increase in the top beds (Fig. 8). The AMS degree also increases in these beds (Fig. 9). The magnetic fabric of the sediments is mostly oblate. Basal sands in sections 1, 2 and 4 show more prolate fabric as expressed by negative *T* values (Fig. 9).

The magnetic lineation directions in the top sedimentary beds show concentration in NW to SW directions (Fig. 10, top left) with the mean direction tending to the WSW. The poles to magnetic foliation are usually concentrated around the center of the projection. N-S elongation of the pole directions was found in sediments from Section 3 (Fig. 10, top right). The magnetic lineation directions measured in the bottom sedimentary beds show almost random distribution accompanied by large dispersion of poles to magnetic foliation (Fig. 10, bottom).

Exoscopy of Quartz Grains

Three types of microstructures were observed on quartz grain surfaces: (i) precipitation of SiO_2 on the surface of grains in lace-like patterns, (ii) corrosive etched microstructures, and (iii) overgrowth with quartz crystals. The bedrock Ordovician sandstone forming the ceiling of the cave passage above Section 2 contains rounded quartz grains about 1 mm in diameter (Fig. 11, top left). The grain surfaces show weak dissolution and precipitation of SiO_2 (Fig. 12, bottom left). The cross-bedded sandstone forming intercalations in the limestone contains smaller quartz grains cemented with SiO_2 into aggregates with an average length of 1 mm (Fig. 11, top right). The basal sand in Section 1 consists of separate rounded grains with average size of about 0.5 mm (Fig. 11, bottom left). Surfaces of many grains are modified by conchoidal fractures and corrosion features. Grain aggregates with weakly corroded

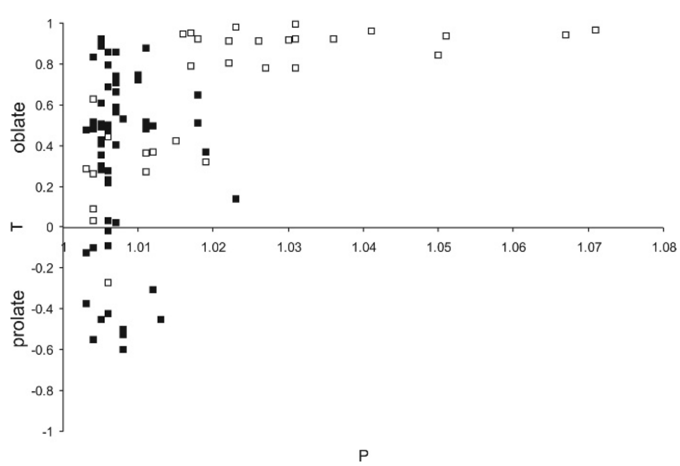

Figure 9. Correlation between degree of anisotropy (*P*) and shape of anisotropy ellipsoids (*T*). Sample symbols are the same as in Fig. 8.

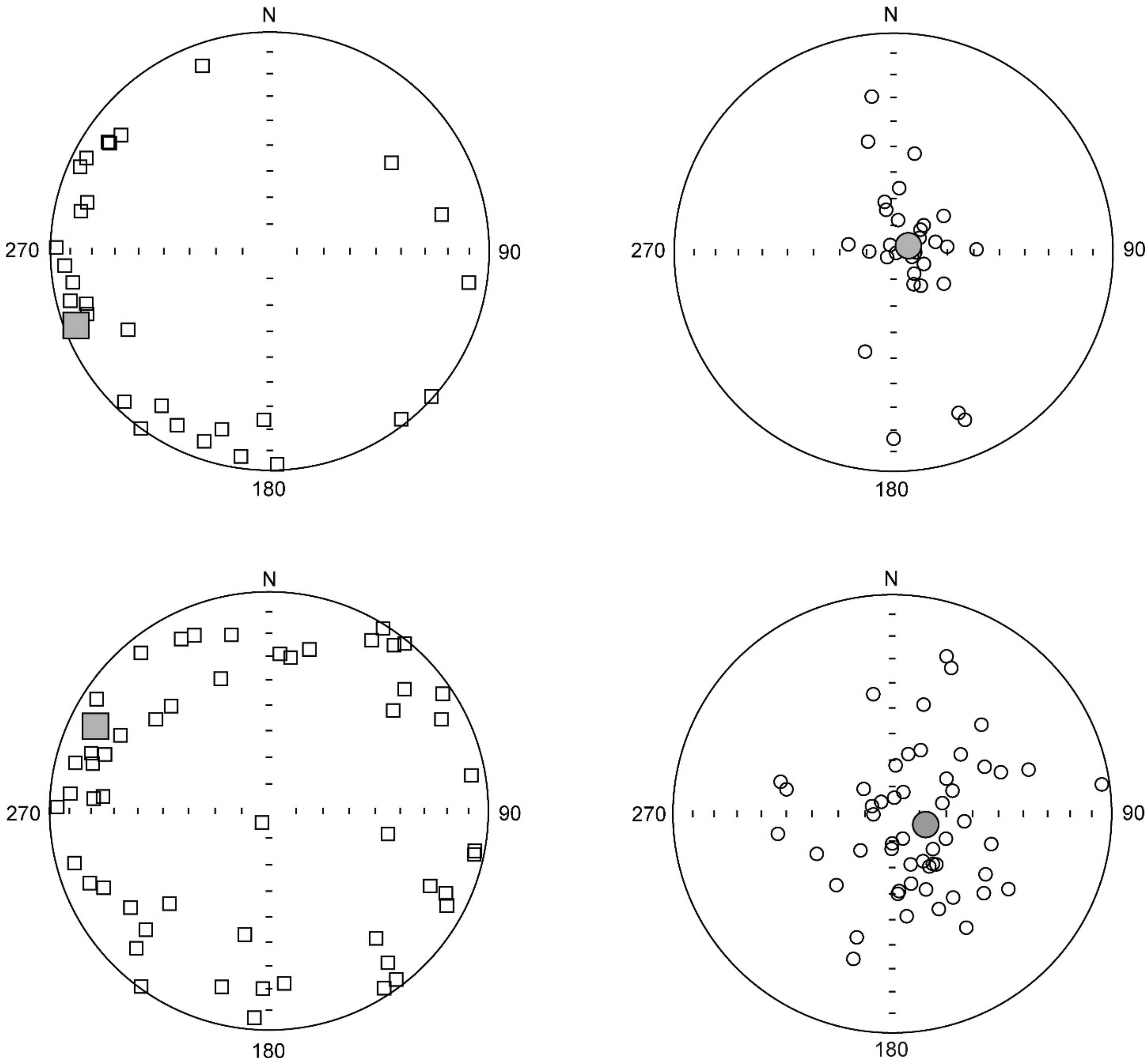

Figure 10. Principal directions of magnetic fabric of sediments indicated by anisotropy of magnetic susceptibility; equal-area projection on the lower hemishere. Top left – magnetic lineation in bottom sedimentary beds; top right – pole to magnetic foliation in bottom sedimentary beds; bottom left – magnetic lineation in top sedimentary beds; bottom right – poles to magnetic foliation in bottom sedimentary beds; larger gray squares and circles represents mean directions.

surfaces dominate in the above lying Bed 9 (Fig. 11, bottom right). Angular flat mineral particles (micas?) dominate in Bed 3, separate quartz grains and aggregates are present in smaller amounts (Fig. 12, top left). Quartz grains in sand deposited in the bottom beds in Section 2 (Beds 6 and 7 in Fig. 5) form cemented aggregates up to 1 mm large as in the bottom beds of Section 1. Grain surfaces often bear lace-like silica coatings. The above lying Bed 4 in Section 2 is composed of a mixture of free grains (30 %) and cemented aggregates (70 %) with lace-like silica coatings. Angular mineral particles are rarely present in the bed. Sub-angular to rounded grains up to 1 mm in size prevail in Bed 1 against cemented grain aggregates showing weak roundness. Sand from Bed 2 in Section 2A shows predominantly free rounded quartz grains coated with lace-like silica (Fig. 12, bottom right). Exoscopic analyses were completed with images from modern soil collected at the Medeo Cave entrance. Free rounded quartz grains up to 1.5 mm in size dominate in the soil (Fig. 12, top right).

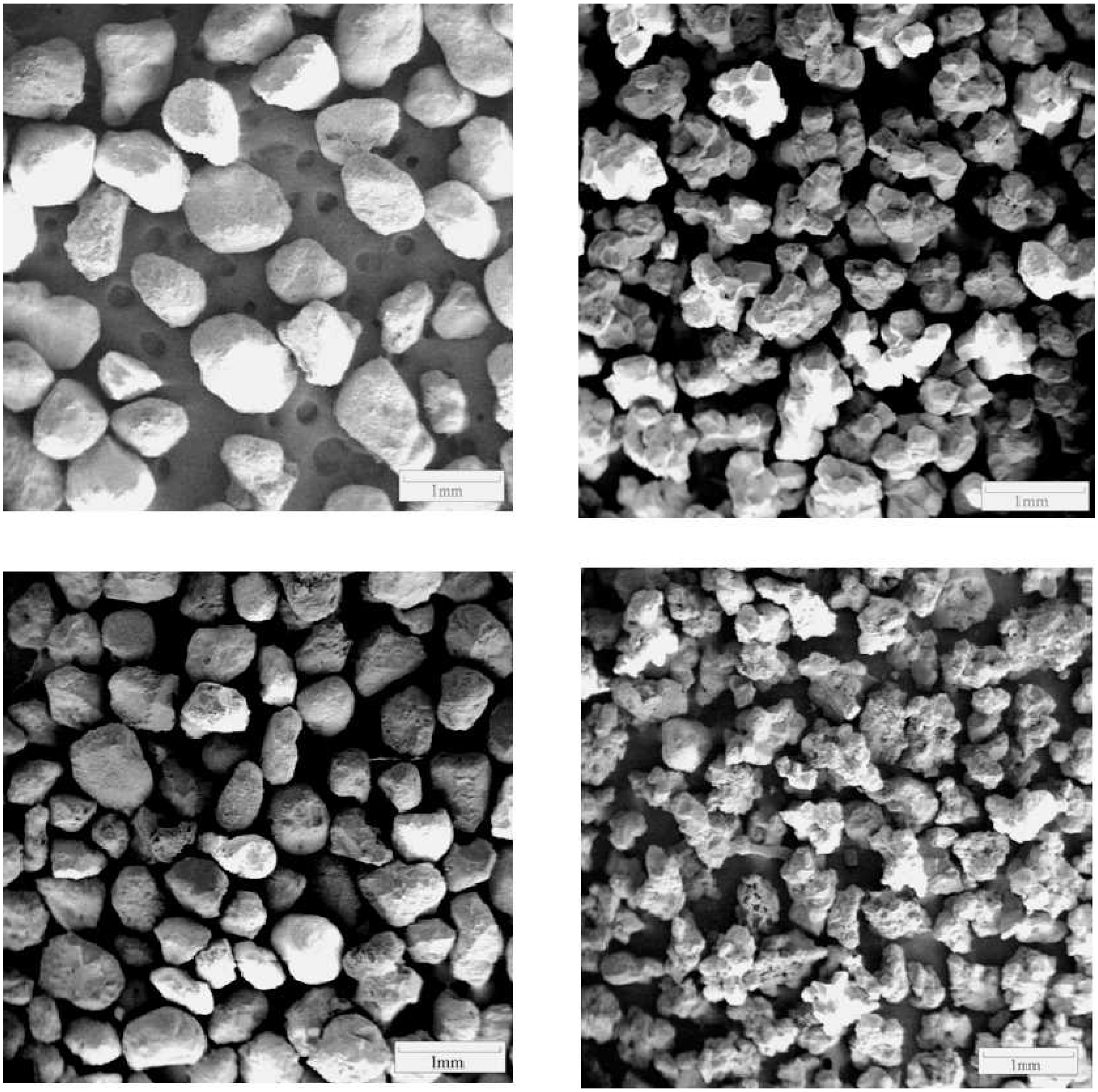

Figure 11. Surface of quartz grains. Top left – quartz from bedrock sandstone; top right – quartz aggregates from cross-bedded sandstone intercalated within the limestone; bottom left – quartz from Bed 15 in Section 1; bottom right – quartz aggregates from Bed 9 in Section 1.

The quartz grain aggregates isolated from Bed 14 in Section 1 were put through an experiment using a kitchen blender simulating transport of sediments in a turbulent flow. The aggregates were almost completely disintegrated after 5 minutes of mixing. The silica coatings on grain surfaces were destroyed after 15 and 30 minutes of mixing.

Heavy Mineral Content

The studied samples of the bedrock and cave deposits show monotonous association of stable heavy minerals. Grains of transparent heavy minerals are rounded, while the opaque mineral grains are mostly angular. Beds in the upper portions of Sections 1 and 2 contain greater amounts of garnet, similar to modern soil (Table 1).

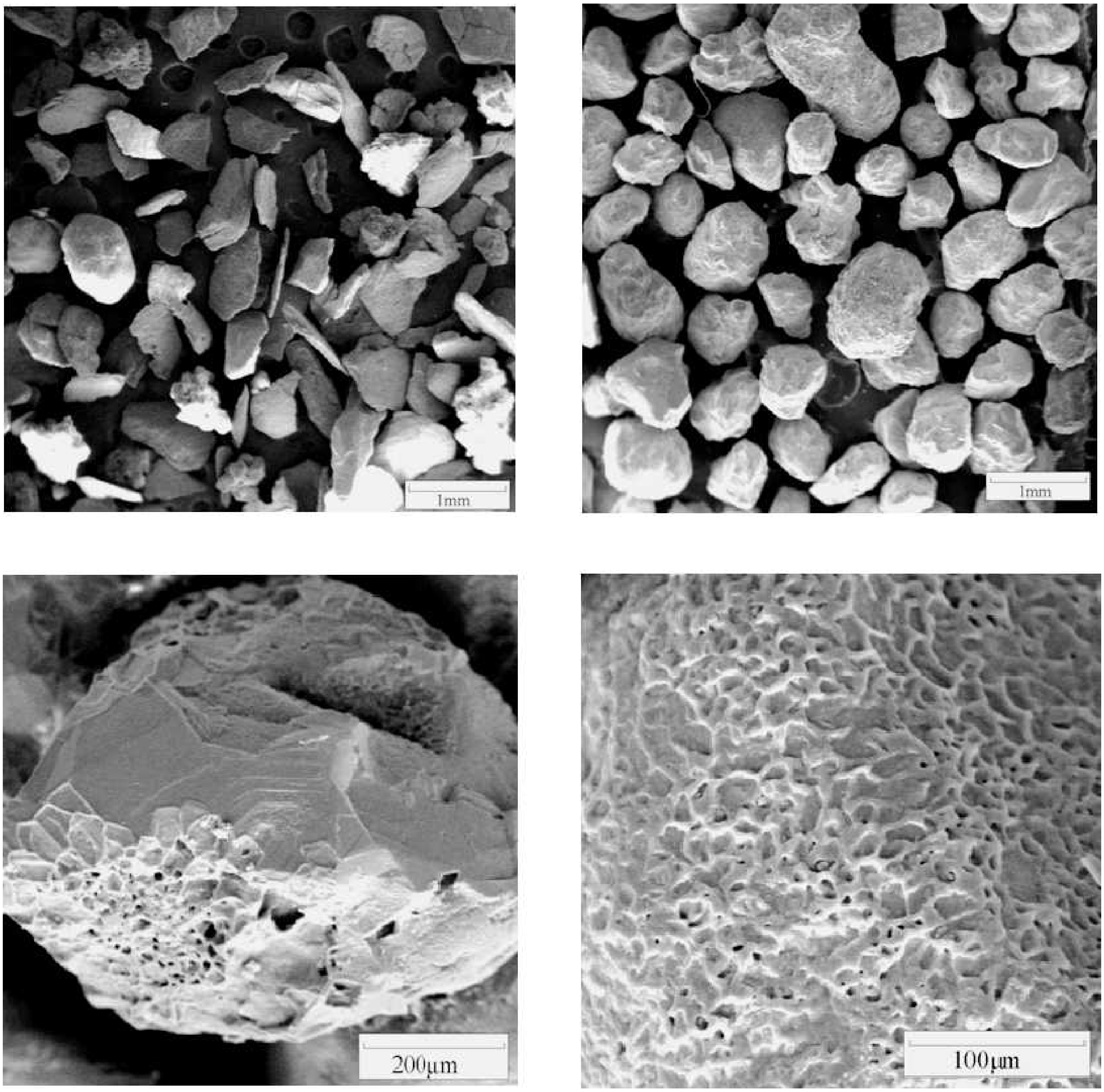

Figure 12. Surface of quartz grains. Top left – mixture of quartz and angular grains from Bed 3 in Section 1; top right – quartz from modern soil; bottom left – a detail of quartz corrosion from Bed 15 in Section 1; bottom right – a detail of newly-formed quartz precipitates from Bed 2 in Section 2A.

These deposits reveal an opaque/non-opaque mineral ratio 1:3 while other sediments studied contain a higher proportion of opaque minerals. Higher concentrations of garnet were also determined in the basal sand from Bed 14 in Section 1. Staurolite dominates in sediments with lower garnet content, including the bedrock sandstone (Table 1).

Flowstone Dating

Radiometric dating of the flowstone bed by ^{230}Th/^{234}U method reveals that the age of three dated samples exceeds 350 ka (limit of the dating method). However, the flowstone age higher than 1.2 Ma cannot be eliminated based on ^{234}U/^{238}U ratio (Table 2). During thermal demagnetization experiments magnetic moment decreased

Table 1. Heavy mineral content in modern soil, cave deposits and bedrock (values are in percent).

Cave Deposit	Garnet	Staurolite	Zircon	Rutile	Opaque/Non-Opaque Mineral Ratio
Modern Soil	72	24	2	3	1:3
Section 1 – Bed 3	80	5	15	1	1:3
Section 1 – Bed 9	4	89	5	2	1:1
Section 1 – Bed 14	3	85	7	5	1:1
Section 1 – Bed 15	45	49	3	3	8:1
Section 2 – Bed 1	35	56	2	8	1:1
Section 2 – Bed 4	7	82	9	2	1:1
Section 2 – Bed 6	9	80	7	4	1:1
Section 2A – Bed 2	50	36	10	4	1:3
Ordovician Sandstone	4	86	5	5	1:1

with increasing temperatures (Fig. 13, bottom). Directional variations of magnetic vector during the demagnetization process are expressed in the Zijderveld diagram and in the stereographic plot (Fig. 13, top). The mean paleomagnetic direction is: Declination = 18°, Inclination = 61°. Based on these paleomagnetic data, it is evident that the flowstone records normal polarity of the Earth magnetic field from the time of the carbonate deposition.

Discussion of Results

Based on obtained results the sedimentary beds exposed in the studied sections were subdivided in two parts with the bottom (older) beds (beds 9–14 in Section 1, beds 4–7 in Section 2, Bed 2 in Section 2A and beds 2–4 in Section 4) and top (younger) beds (beds 1–8 in Section 1, Bed 1–3 in Section 2, Bed 1 in Section 2A, beds 1–3 in Section 3 and Bed 1 in Section 4).

The bottom beds reveal similar lithological, magnetic and heavy metal properties (except of sand in Bed 14). Basal sand deposited on the bedrock bottom shows a lower MS, similar to the bedrock sandstone. The exoscopic quartz grain characteristics are similar, too. It can therefore be proposed that the deposits filling the bottom part of cave corridors were derived from the local bedrock formed by Early Ordovician sandstones. The good roundness of quartz grains is a result of grain reworking in a high-energy Ordovician marine environment. Later, long distance redeposition of these quartz grains by Cenozoic streams can be excluded by the results of liquidizer experiment testing of the resistance of quartz grain aggregates during turbulent fluvial transport. No source of larger SiO_2-cemented aggregates (max. 2 cm long) common in beds 13 and 14 in Section 1 was found. These aggregates were cemented *in situ* during different climatic conditions allowing SiO_2 dissolution and precipitation. Sands in beds 11–13 in Section 1 and in Beds 6 and 7 in Section 2 lack prominent lamination or cross bedding (unlike the overlying sediments). It can be therefore assumed that these beds also belong to the bottom fill of cave passages.

The younger cross-bedded and laminated, mostly clayey sands in beds 8–10 (Section 1) and beds 3 and 4 (Section 2) were deposited after partial erosion of the basal deposits. The deposits reveal slightly higher MS values. The exoscopic observation shows cemented quartz grain aggregates indicating the source in the local cross-bedded sandstone (comp. Fig. 11, top right and Fig. 11, bottom right). The inner structures of these laminated sediments (small unconformities, redeposited fragments of clay, laminae partly cemented by carbonate and erosional surface of Bed 10) show a frequent alternation between local aggradation and erosion events. The sediments were deposited during heavy precipitation events, when water penetrated into the cave corridors from the surface through the swallow holes and along open cracks. The water escape structures (e.g., the fissure in beds 9–11, Section 1) were formed during the compaction of sediments. Sand grains accumulating along the fissures were later partly cemented by carbonate. Pore fluids moved during repeated liquefaction of the sediments and disturbed the primary magnetic fabric of these deposits, resulting in the tilting of the magnetic foliation to the NW (Fig. 10, bottom right). However, it is not possible to determine the flow direction

Table 2. Th/U age of the flowstone relic.

Sample Name	Sample Lab. No.	U (ppm)	$^{234}U/^{238}U$	$^{230}Th/^{234}U$	$^{230}Th/^{232}Th$	Age (ka)
BT 2	W 1302	28.2 ± 0.7	1.005 ± 0.005	1.064 ± 0.005	> 1000	> 350
BT 3	W 1301	19.8 ± 0.7	1.002 ± 0.007	1.002 ± 0.007	450 ± 40	> 350
BT 6	W 1303	11.9 ± 0.4	1.009 ± 0.008	1.083 ± 0.008	520 ± 60	> 350

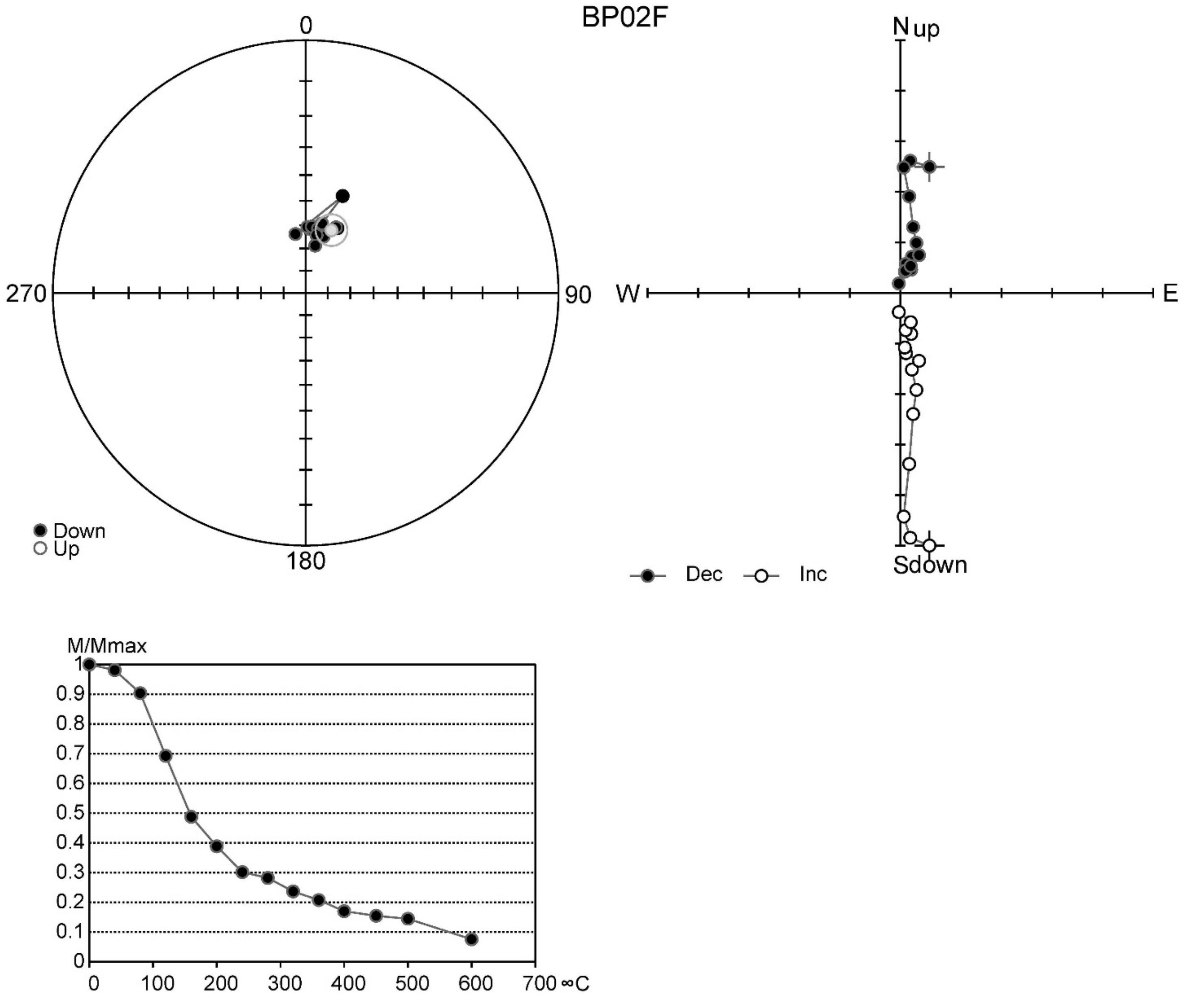

Figure 13. Thermal demagnetization of the flowstone sample BP02F. Top left – directions of magnetization vector during demagnetization process, black circles – projection of vector directions to the lower hemisphere, gray point in the circle – interpreted direction of the primary component of the magnetization vector; top right – Zijderveld diagram, black circles – projection of vector directions into horizontal plane, white circles – projection of vector directions into vertical plane; bottom left – normalized magnetization intensity values during the thermal demagnetization.

due to random dispersion of magnetic lineation directions measured in the bottom bed sediments.

Clayey sands forming the top portions of Section 1 (Beds 2–7) and Section 2 (Bed 2) reveal still higher MS values and higher garnet content, similar to the modern soil from the surface above the cave. The magnetic lineation and foliation indicate a calmer sedimentary environment with slow sediment transport directions from NW, W and SW (Fig. 10, top). Elongation of k_3 orientations in N-S direction measured in Section 3 could be a result of post-depositional deformation of the cave sediments caused by frost when the sedimentary layers filling narrow cave passage could be deflected due to volume changes. In the cave sediments with higher clay content, the MS increases together with the degree of anisotropy (Fig. 8, left). Different heavy mineral content of the sediments, compared to the bottom portions of the sections, indicates a different source of these deposits. The sediments could have been originally transported by wind to the area of Botovskaya Cave, from where they were vertically transported by precipitation waters through swallow holes and along open cracks to the cave. This assumption could be supported indirectly because angular flat mineral particles are missing in bottom cave sediments. Higher MS values of the clayey sediments correspond with the high MS of the topsoil at the cave surface. Most part of the iron present in the modern soil is the paramagnetic Fe^{3+} form (almost 80 %, identified by Mössbauer spectroscopy), which may be the result of weathering of paramagnetic minerals during pedogenic processes (e.g., Evans and Heller, 2004). The presence of superparamagnetic (SP) minerals originating during pedogenesis or taiga forest fires cannot be excluded (Thompson and Oldfield, 1986). However, results of frequency dependent magnetic susceptibility measurements, usually supporting SP mineral presence (e.g., Dearing, 1999), are not very reliable due to low MS values of the cave sediments.

MS of sand filling the karst conduit with Section 2A (Bed 2) is similarly low as in the basal sands in Section 2. Nevertheless, it differs from the latter in the high proportion of garnet (much like in Bed 14 in Section 1). The overlying clay in this section has similar properties to the youngest deposits in Sections 1 and 2 and the modern soil. However, precipitation waters flowing vertically from the surface through open fissures also transported the clay. Heavy precipitation events resulted in the erosion of the top part of the sediment in both Sections 1 and 2 and resulted in the deposition of clay-dominated sediments with chaotically arranged angular clasts of sandstones and with limestone blocks (Bed 1 in both sections).

Taiga forest fires could control the mechanism of sediment transportation from the surface above the cave to the underground passages. The topsoil retention ability is usually dramatically decreased after forest fires due to damaged vegetation. Precipitation would then percolate very fast into the cave. Evidence of a past catastrophic erosion event is preserved about 50 m west of Section 1 (Fig 2). A relic of flowstone bed is preserved on the limestone wall 1.7 m above present passage floor. The flowstone bed was originally deposited on the top of the clastic deposits, which filled the passage. The radiometric and paleomagnetic polarity dating suggests a likely age for the carbonate bed between 350 and 780 ka (i.e., older than $^{230}Th/^{234}U$ method age limit and but still within the present normal-polarity Brunhes Chron). However, we cannot entirely exclude the flowstone deposition during any older normal-polarity periods. In such case the flowstone should be older than 2.58 Ma (i.e., Matuyama-Gauss paleomagnetic boundary). We do not suppose a speleothem deposition during relatively short normal-polarity Jaramillo or Olduvai subchrons. Anyway, in the time of the flowstone deposition the artesian aquifer regime was already disrupted due to surrounding valley incision and vadose conditions dominated in the cave system. The later intensive erosion removed clastic sediments from under the flowstone bed and destroyed the entire flowstone. This erosional event had to be triggered by unusually heavy precipitation, which entered the bedrock through vertical ruptures opened both in sandstone and limestone due to differential subsidence of the massif (see below). The surrounding valleys supporting this vertical movement should be developed. Therefore, we suppose that the erosion occurred most probably during the Middle or Late Pleistocene. At that time the local surface streams were incised at a much lower position than the Botovskaya Cave. Results of this catastrophic cave flood could be the chaotic sediments deposited in Bed 1 in the Sections 1 and 2.

The morphology of the cave passages documents transverse flow under confined hydrological conditions in the artesian aquifer connected with upward solution of limestone (Klimchouk, 2000, 2003; Filippov, 2000). In the subsequent period lower parts of the passages were widened to the shape of a relatively broad channel with a flat ceiling. It should indicate a long-term dissolution, when the passages were permanently flooded with stagnant water. It is not easy to reconstruct this period in the cave system development, because this channel is completely filled with clastic cave deposits and is noticeable only in the excavated test-pits. We assume a period of relative stability and propose that the cave system was lying near the level of the ground-water table prior to the incision of the present deep valleys (Lena River) in the vicinity of the cave system. This stage should be dated to the Miocene, because the cave is located above the Pliocene river terrace level (Filippov, 2000).

Structures preserved in the clastic sediments filling the cave passages indicate deposition mostly in vadose conditions with frequent alternations of deposition and erosion. The water escape structures detected in sediments similar to silty laminae cemented by carbonate (Bed 9 in Fig. 3) support our assumption that the clastic deposition occurred in cave passages, which were not completely filled with water.

The following incision of surrounding valleys was probably triggered by a substantial Late Pliocene uplift recorded in the Lake Baikal Cenozoic sediments (Mats et al., 2000). Stability of the sedimentary massif comprising the Botovskaya Cave deteriorated as a result of this Pliocene-Pleistocene incision.

This was accompanied by gravity-induced opening of N–S joints parallel to the slope of the Garevogo Creek, where cave entrances are located, and by NE–SW opened joints parallel to the Lake Baikal rift structure indicating ongoing uplift connected with extension of the area (cf., Zorin et al., 2003). These ruptures detected at many places in the Old World of the Botovskaya Cave are now used by water seeping from the surface above the cave. These vertical pathways are also used for the underground transport of clastic sand- and clay-dominated sediments from the surface above the cave. Such a place is located east of Section 1. Sandstone blocks fallen from the ceiling are covered by light brown sands and clays (much like in Section 2A). Relicts of clayey sand are also preserved in hanging positions on rock ledges above the test-pit with Section 1. These clastic sediments do not, however, cover blocks pertaining to a younger phase of ceiling destruction. It is probable that the last falling of ceiling slabs also took place recently. Erosion caused by flowing water results, in turn, in further stability deterioration of the sandstones under- and overlying the limestone bed. Such weak points in the cave system then experience large collapse of the sandstone slabs from the ceiling and formation of chokes. Intensive water flow is also responsible for the growth of flowstone decorations at such places.

Conclusions

Three specific conclusions can be drawn from this study. First, the sections in detrital cave sediments in Botovskaya Cave (in The Old World part) evidence periodical sediment deposition. It cannot be excluded that the individual beds are separated by long hiatuses. Sediments of the cave fill are of two different types: the older, bottom sands are derived from weathered bedrock sandstones and were probably horizontally transported over a short distance. The overlying sediments dominated by clay and clay/sand were transported vertically with precipitation waters from the surface above the cave. The contrasting mineralogical and magnetic parameters of these top sediments indicate a different (more distant?) source.

Second, if the bottom sand was transported horizontally through the cave by flowing water, it must have taken place before the incision of the present deep valleys, probably in the Late Tertiary. Finer sediments should be transported by wind and deposited on the surface above the cave. From there, they were removed by precipitation waters together with weathered surface products and deposited in cave passages. These processes, most probably of Quaternary age, were lacking any direct link to the local hydrologic network.

Third, morphologies of passages in Botovskaya Cave document two stages of the cave system development: the older, characterized by confined hydrological conditions in the artesian aquifer. Passages formed during this older stage were later partly remodeled by stagnating water corrosion. This younger stage affected the cave system probably in the Tertiary, before the deep river valleys were formed.

Acknowledgements

The project was supported by the INTAS Program No. 03-51-4152: Speleothems and other cave sediments from Siberia: an archive from the boreal climate zone with the potential for climate reconstruction on an annual to decadal basis (SPELEOARCH) and it is a part the research project of the Institute of Geology AS CR, v.v.i. No. AV0Z30130516.

References

Breitenbach, S., 2004, High-resolution isotope measurements ($\delta^{18}O$ and $\delta^{13}C$) from Siberian stalagmites as potential palaeoclimatic proxies [MSc. thesis], Humboldt Universität, 72 p.

Dearing, J., 1999, Magnetic susceptibility, *in* Walden, J., Oldfield, F., and Smith, J., eds., Environmental magnetism: A practical guide, Quaternary Research Association, Technical Guide No.6, p. 35–62.

Ellwood, B.B., Petruso, K.M., Harrold, F.B., and Korkuti, M., 1996, Paleoclimate Characterization and Intra-Site Correlation Using Magnetic Susceptibility Measurements: An Example from Konispol Cave, Albania: Journal of Field Archaeology, v. 23, p. 263–271.

Ellwood, B.B., Harrold, F.B., and Benoist, S.L., 2004, Magnetic susceptibility applied as an age-depth-climate relative dating technique using sediments from Scladina Cave, a Late Pleistocene cave site in Belgium: Journal of Archaelogical Science, v. 31, no. 3, p. 283–293.

Evans, M.E., and Heller, F., 2004, Environmental Magnetism: Principles and Applications of Enviromagnetics, San Diego, Academic Press, 299 p.

Filippov, A.G., 2000, Speleogenesis of Botovskaya Cave, Eastern Siberia, Russia, *in* Klimchouk, A.B., Ford, D.C., Palmer, A.N., and Dreybrodt, W., eds., Speleogenesis, Evolution of Karst Aquifers, Huntsville, Ala., National Speleological Society, p. 282–286.

Göbel, E., and Breitenbach, S., 2003, Die Peschera Botovskaja, die längste Höhle Russlands: Mitteilungen des Verbandes der Deutchen Höhlen - und Karstforscher, v. 49, no. 2, p. 42–45.

Gorka, P., and Hercman, H., 2002, URANOTHOR v. 2.5., Delphi Code of calculation program and user guide: MS, Archive of Quaternary Geology Department, Institute of Geological Sciences, PAS, Warsaw, 65 p.

Häuselmann, P., Granger, D.E., Lauritzen, S.E., and Jeannin, P.Y., 2007, Abrupt glacial valley incision at 0.8 Ma dated from cave deposits in Switzerland: Geology, v. 35, no. 2, p. 143–146.

Ivanovich, M., and Harmon, R.S., 1992, Uranium Series Disequilibrium: Applications to Environmental Problems, Oxford, Clarendon Press, 2nd edition, 910 p.

Jelínek, V., 1981, Characterization of the magnetic fabric of rocks Tectonophysics, v. 79, T63–T67

Kadlec, J., Hercman, H., Beneš, V., Šroubek, P., Diehl, J.F., and Granger, D., 2001, Cenozoic history of the Moravian Karst (northern segment): Cave sediments and karst morphology: Acta Musei Moraviae, Scientiae Geologiae, v. 85, p. 111–161.

Klimchouk, A., 2000, Speleogenesis under deep-seated and confined settings, *in* Klimchouk, A.B., Ford, D.C., Palmer, A.N., and Dreybrodt, W., eds., Speleogenesis, Evolution of Karst Aquifers, Huntsville, Ala., National Speleological Society, p. 244–260.

Klimchouk, A., 2003, Conceptualisation of speleogenesis in multi-storey artesian systems: a model of transverse speleogenesis, http://www.speleogenesis.info/archive/publication.php?PubID=24&Type=publication&keyword=Klimchouk

Mats, V.D., Khlystov, O.M., De Batist, M., Ceramicola, S., Lomonosova, T.K., and Klimansky, K., 2000, Evolution of the Academician Ridge Accommodation Zone in the central part of the Baikal Rift, from high-resolution reflection seismic profiling and geological field investigations: International Journal of Earth Science, v. 89, p. 229–250.

Nagata, T., 1961, Rock Magnetitism, Tokyo, Maruzen, 2nd edition, 350 p.

Sroubek, P., Diehl, J.F., Kadlec, J., and Valoch, K., 2001, A Late Pleistocene paleoclimatic reconstruction based on mineral magnetic properties of the entrance facies sediments of Kulna Cave, Czech Republic: Geophysical Journal International, v. 147, no. 2, p. 247–262.

Sroubek, P., Diehl, J.F., and Kadlec, J., 2007, Historical climatic record from flood sediments deposited in the interior of Spirálka Cave, Czech Republic: Palaeogeography, Palaeoclimatology, Palaeoecology, v. 251, p. 547–562.

Thompson, R., and Oldfield, F., eds., 1986, Environmental Magnetism, Allen and Unwin, London, 227 p.

Zorin, Y.A., Turutanova, E.Kh., Mordvinovaa, V.V., Kozhevnikova, V.M., Yanovskayab, T.B., and Treussovc, A.V., 2003, The Baikal rift zone: the effect of mantle plumes on older structure: Tectonophysics, v. 371, p. 153–173.

5.7. Procesy v antropogenním kontextu

Dejmal, M., **Lisá, L.,** Nývltová Fišáková M., Bajer A., Petr, L., Kočár, P., Kočárová R., Nejman L., Rybníček M., Suvová Z., Culp, R., Vavrčík H. (2014): Medieval horse stable; The Results of Multi Proxy Interdisciplinary Research.- Plos One, 9, 3, e89273.

Novak J., **Lisá L.**, Pokorný P., Kuna M. (2012): Charcoal analyses as an environmental tool for the study of Early Medieval sunken houses infills in Roztoky near Prague, Czech Republic.- Journal of Archaeological Science, 39, 808 – 817.

Medieval Horse Stable; The Results of Multi Proxy Interdisciplinary Research

Miroslav Dejmal[1], Lenka Lisá[2]*, Miriam Fišáková Nývltová[3], Aleš Bajer[4], Libor Petr[2,5], Petr Kočár[5], Romana Kočárová[5], Ladislav Nejman[6], Michal Rybníček[4], Zdenka Sůvová[5], Randy Culp[7], Hanuš Vavrčík[4]

1 Archaia Brno, o. p. s., Brno, Czech Republic, **2** Institute of Geology AS CR, v. v. i., Prague, Czech Republic, **3** Institute of Archaeology of AS CR in Brno, v. v. i., Brno, Czech Republic, **4** Faculty of Forestry and Wood Technology, Mendel University in Brno, Brno, Czech Republic, **5** Department of Archaeology, University of Western Bohemia, Pilsen, Czech Republic, **6** Centre for Applied Isotope Studies, University of Georgia, Athens, Georgia, United States of America, **7** School of Social Science, University of Queensland, St Lucia, Australia

Abstract

A multi proxy approach was applied in the reconstruction of the architecture of Medieval horse stable architecture, the maintenance practices associated with that structure as well as horse alimentation at the beginning of 13th century in Central Europe. Finally, an interpretation of the local vegetation structure along Morava River, Czech Republic is presented. The investigated stable experienced two construction phases. The infill was well preserved and its composition reflects maintenance practices. The uppermost part of the infill was composed of fresh stabling, which accumulated within a few months at the end of summer. Horses from different backgrounds were kept in the stable and this is reflected in the results of isotope analyses. Horses were fed meadow grasses as well as woody vegetation, millet, oat, and less commonly hemp, wheat and rye. Three possible explanations of stable usage are suggested. The stable was probably used on a temporary basis for horses of workers employed at the castle, courier horses and horses used in battle.

Citation: Dejmal M, Lisá L, Fišáková Nývltová M, Bajer A, Petr L, et al. (2014) Medieval Horse Stable; The Results of Multi Proxy Interdisciplinary Research. PLoS ONE 9(3): e89273. doi:10.1371/journal.pone.0089273

Editor: Terry Brown, Manchester Institute of Biotechnology, United Kingdom

Received June 26, 2013; **Accepted** January 17, 2014; **Published** March 26, 2014

Funding: The research was supported by the Czech Grant Agency project no. P405/11/1729 (Veselí nad Moravou – Medieval Castle in alluvial plain). The grant agency of CR supported financially the analyses, manuscript preparation and publication.

Competing Interests: The authors have declared that no competing interests exist.

* E-mail: lisa@gli.cas.cz

Introduction

Despite the fact that horses were a common part of the Medieval culture, there is a dearth of information about horse husbandry in the Central European Middle Ages. Occasional references can be found in written documents [1–3] as well as in archaeological research [4–5], but the identification of architectonical structures is usually very difficult and stabling deposits are not commonly preserved.

Important information about stable deposits can be inferred from microstratigraphic studies [6–9] Floor deposits in particular can be a source of high-value information. Variations in floor residues are being profitably examined in order to understand uses of space and the nature of activities in a settlement [7] [10–17], but archaeological stratigraphies that may contain floors are usually difficult to identify when not composed of lithologically varied materials. One of the well recognizable types of floor deposits are those composed of stabling deposits. Micromorphological research of stable floor deposits has been reported from different environments but such studies are rare. An experimental stable was studied in Butser ancient farm [18].

A unique opportunity to perform interdisciplinary research including a classic archaeological approach, combined with geology and micromorphology, bioarchaeology and isotope studies of a well preserved Medieval stable presented itself in 2009, when during rescue excavations in Veselí nad Moravou, occupation deposits were found within a bailey dated to an early phase of castle construction. This paper discusses what Medieval stable architecture looked like and how the stable was maintained. Both, the specific diet of horses which occupied the stable during the last phase of its use, and the vegetation growing in the castle surroundings are discussed in this paper.

The study site: Medieval bailey in Veselí nad Moravou, Czech Republic

Veselí nad Moravou is situated in the southeastern part of the Czech Republic in South Moravia. The study site is located on the right bank of the Morava River (Fig. 1). The archaeological rescue research was performed during renovation of the castle in 2008–2010 [19]. Within the castle grounds, located features include a nobleman residence and a wooden bailey which was separated from the castle itself by a moat. Also, well preserved occupational deposits covering an area of 500 m^2 were identified. These deposits were 1.6 meters thick and consisted mainly of wooden chips and organo-mineral material. Only the uppermost part of the occupational deposit was destroyed by decomposition typical for dry open air environments. In total, 16 wooden objects were detected, but the function of these structures was proposed in only three cases. One of them was interpreted as a bakery, the second one as a hayloft and the third one, discussed in this paper, as a horse stable (Fig. 2) [19]. The reason why the structure was interpreted as a horse stable is mainly due to the presence of well preserved stabling material containing horse hairs as well as

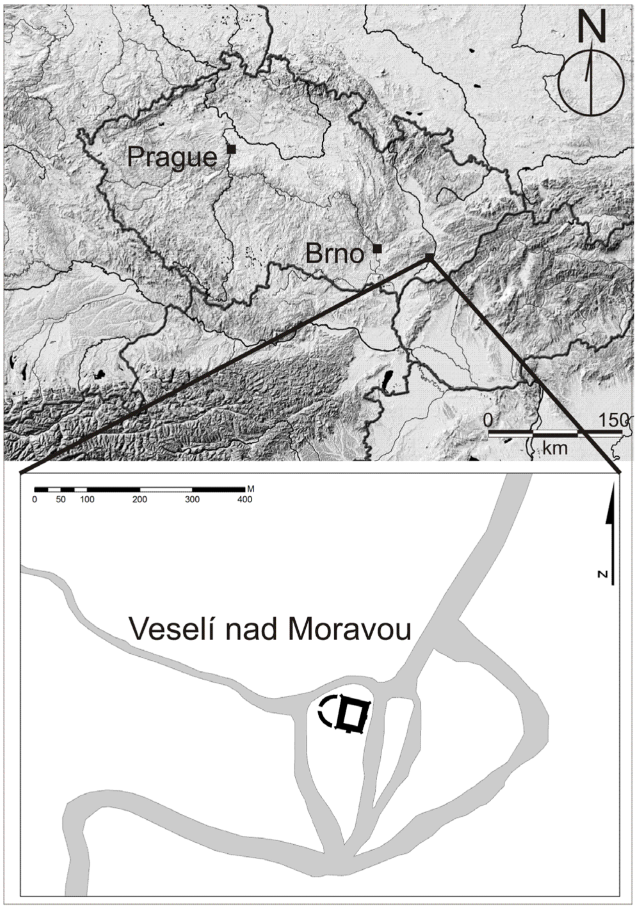

Figure 1. The location of Veselí nad Moravou within the context of Central Europe and within the local geomorphology.
doi:10.1371/journal.pone.0089273.g001

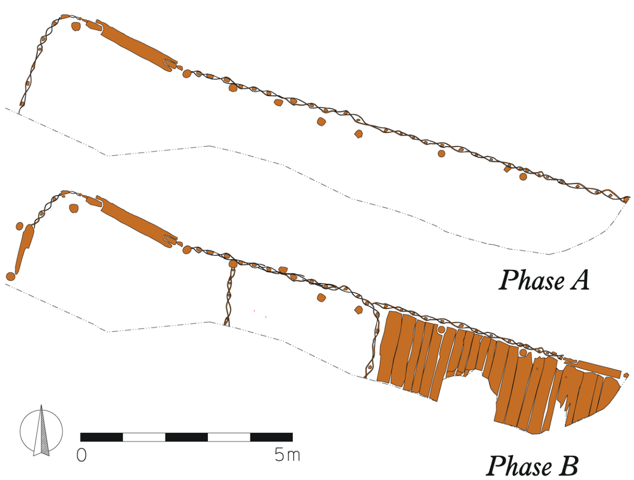

Figure 2. Archaeological evidence of horse stable.
doi:10.1371/journal.pone.0089273.g002

artefacts which are typically used in the context of horse husbandry.

Research methods

1. Ethics statement

We declare that no living animals were used in this research. The samples used for zooarchaeological research and isotope studies were collected from an archaeological context dated to the 13th century. The archaeological company conducted the excavations under a government permit and following the heritage law of Czech Republic (No. 20/1987), all excavated material including the osteological material is interpreted as archaeological material so no further permits are required for the presented study.

2. Archaeology

The excavation area was divided into 5×5 squares. Those squares were then excavated in 2×2 subsquares and a control section 0.5 m wide was left unexcavated along each square. In some cases, sectors were selected irregularly, based on specific contexts. This method of excavation was selected for better orientation in a stratigraphically difficult situation. The excavation was systematically documented with drawings and photographs. Coordinates of archeological features and artefacts were recorded. The Harris matrix showing the connections between different contexts was applied. Dominant structures were differentiated from other contexts (layers, constructions and ditches). Finally, recovered artefacts and their spatial connections were analysed.

3. Sedimentological description, micromorphology

The stratigraphic section which included the stable infill and underlying sediment (Fig. 3) was approximately 80 cm thick. It was sedimentologically logged and lithological changes were described. Seven micromorphological samples were then collected from the studied section based on visible lithological changes, placed into plastic Kubiena boxes (5×9 cm) and prepared according to standard procedure by Julie Boreham in Reach (www.earthslides.com). Thin sections were studied under a binocular and polarising microscope at different magnifications and described according to Bullock et al. [20] [21] and Stoops [22] [23].

4. Pollen and phytolith analysis

Four samples for pollen and phytolith analyses were collected from the top 20 cm of the stable infill, i.e. from the horse stabling material. Preparation followed the standard acetolysis method [24]. For phytolith samples, the wet oxidation method was used [25]. Pollen grains and phytoliths were distinguished using published guides [26–30]. Each sample contained a minimum of 500 grains or fragments. The pollen diagram includes phytoliths and was plotted in POLPAL program for Windows [31] including numerical analyses (Rarefraction, Conslink, PCA) for the visualization and the interpretation of pollen data.

5. Macroremains and anthracology

Macroremains and anthracological analyses were performed on samples from different parts of the stable infill. In total, 7 samples were processed, three from the horse stabling and four from the waste material underlying the horse stabling. Extraction of macrofossils from the soil material followed the standard flotation and wet sieving procedure [32], using staggered sieves with 0.25 mm mesh. The dried samples were then sorted under light microscope at ×10 to ×15 magnifications. Seed atlases by Cappers et al. [33] [34] were used for plant macro-remains determination.

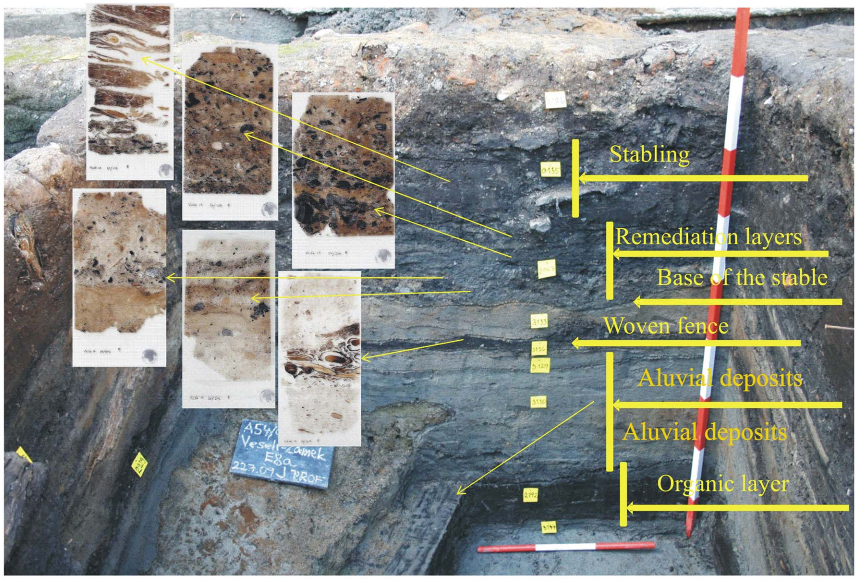

Figure 3. Micromorphological sampling position with the sedimentary facies interpretation.
doi:10.1371/journal.pone.0089273.g003

Fresh refractive surfaces of wooden fragments and charcoal were analysed under a light microscope at 50×, 100× and 200× magnifications. The number of fragments was counted. Identification followed mainly Schweingruber [35] and a web key [36].

6. Isotopes

Six samples of horsehair were divided into three centimeter (cm) sections (Tab. 3), and analyzed for their respective δ13C and δ15N values. The analyses were performed at the University of Georgia's Center for Applied Isotope Studies, Athens, Georgia, USA, using standard procedure. Approximately 200–600 micrograms of horsehair from each sample was analysed. Two interpretation diagrams based on [37–40] were constructed (Fig. 8 and 9) and used in the general interpretations.

7. Dendrochronology and dendrology

Samples for dendrochronological analysis from separate structures identified within the bailey were collected using a drill. The analysis was performed in correspondence with standard dendrochronological methodology [41]. The average age was counted from 6 samples taken within bailey structures. Samples labelled as 110 and 111 come from the stable material. Dendrological analyses of the stable structure were performed using standard identification keys.

8. Zooarchaeology

Bone fragments were collected and bagged during the archaeological excavation. The identification was performed using standard zooarchaeological keys. The osteological material is stored in the depository of Archaia o.p.s. company, Bezručova 15, 602 00, Brno.

Results

1. Archaeological evidence of horse stable

The horse stable was 14×2.5 meters in size, but may have originally been larger (its original size has not been determined). It was excavated in the southeastern part of what is currently the castle courtyard. Parts of the building were obliterated by later Medieval activities and construction works in the 1990s. Two construction phases designated as A and B were identified on the basis of different construction features such as walls, pillars and floors (Fig. 2).

Rough-hewn girders 0.06×0.04 m in size were used during construction phase A. The space between these girders was filled with a hurdle fence and covered by a thick layer of daub from both sides. The roof of the building was supported by 0.16 m thick pillars located regularly every two meters along the walls. The 1.6 m wide relict of an entrance was located in the northern part of the building. The entrance structure consisted of a pair of vertical window frames with an added doorstep. Divisions inside the stable were not identified for this construction phase.

During construction phase B the building was completely rebuilt. The former building was destroyed and only the foundations, which were re-used, remained in their original position. The construction technique was very similar to the previous one. New walls mirrored the shape of the former walls and the entrance located in the northwestern part of the building was replaced by a new entrance located in the same position and within the same construction proportions. In contrast to the original building, the interior of the new building was divided by two partition walls. The first wall divided the eastern room (approx. 6 m^2 in size). The partition wall was constructed in the same way as the outside wall and a hurdle fence was also present. The eastern room had a wooden floor consisting of rough-hewn, criss-crossing planks up to 0.4 meters wide. The 1 meter wide entrance was located in the northern section and consisted of double window frames and a doorstep. The second partition wall, 3.5 metres long, divided the central room. The partition wall was constructed as a hurdle fence and was not joined to the outside wall. It appears that a 1 meter wide entrance facing west was also added. All the doorsteps were raised 0.25 m above the floor. The organic layers deposited on the floor of the stable originating in the second construction phase of contain evidence of horse presence with horseman equipment such as horse shoes, bridle-bits, currycomb, buckles and spurs. Two complete sickles were also recovered.

2. Sedimentology and micromorphology of the deposits

2.1. Fluvial deposits and trampling periods. The underlying material of the horse stable consists of 10 cm thick, partly decomposed organic material (wood) followed by a 30 cm thick fluvial deposit of grey colour consisting of sands and silts (Tab. 1). The fluvial deposition of sands ends with a layer of organic material, macroscopically identified as part of a collapsed hurdle fence followed by a thin layer of fluvial sands. The organic matter of this structure is not decomposed as seen in Fig. 4B. The sandy material above the fence differs somewhat from the sandy material below. Repeatedly appearing thin, dark brown layers composed of decomposed organic material were identified (Fig. 4A). Those organic intercalations document the phases when the area was not inundated by water and was probably being trampled by humans. The thick fluvial section ends with a partly decomposed organic material macroscopically identified as a relict of a hurdle fence, followed by yellowish sandy material 5 cm thick (Fig. 3).

2.2. Infill of the horse stabling structure composed of domestic waste. The basal layer consists of 15 cm thick occupation deposits composed of construction material, charcoal, decomposed organic matter and ashy material (Tab. 1, Fig. 4C). Layering is macroscopically visible within this layer (Fig. 2). The material in each layer differs somewhat in grain size, the amount of daub and ceramic sherds. Within this stratum, visible minute layering corresponds to phases of accumulation. These individual sublayers are composed of different types of material and the grain size varies considerably, but differences in lithological composition are small.

2.3. Horse stabling. The section and the infilling of the horse stable is capped by well preserved horse stabling, i.e. organic material deposited during the last usage of this structure (Tab. 1, Fig. 4D). Horsehair is common in this layer but it is difficult to identify and is observed mainly as round-shaped cross sections (Fig. 10).

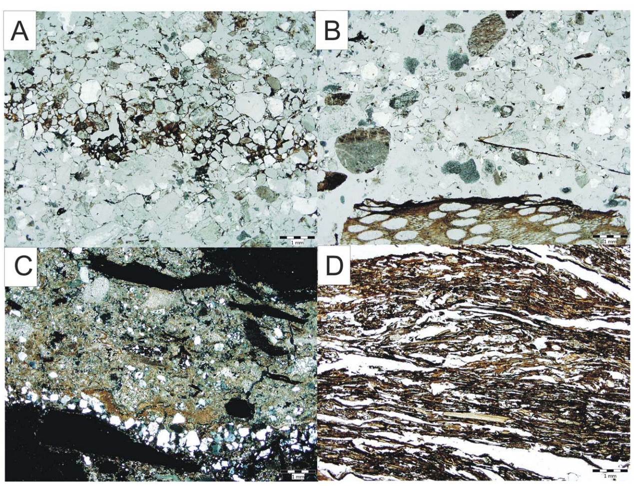

Figure 4. Characteristic micromorphological features in studied section. A - Fluvial deposits with trampling periods and thin layers of decomposed organic matter; B - Fence relict composed of undecomposed organic matter followed by the last phase of inundation; C - Infilling of the stable composed of domestic waste; D - Horse stabling composed of partly decomposed organic matter and mineral components.
doi:10.1371/journal.pone.0089273.g004

3. Pollen and phytolith analyses

Pollen spectra found in the 20 cm thick layer of horse stabling include mainly herbs. Tree palynomorphs are very rare. Most of the herb palynomorphs are wild grasses. Intestinal parasites were not recorded, except for an Ascaris spore in a sample located 10–15 cm below the surface (Fig. 5).

Phytolith spectra are relatively uniform with low type diversity. Dendritic-type phytoliths occur most frequently and elongate-type phytoliths have the second highest frequency. Based on the abundance of Dendritic-type and Polylobate-type types, most of the phytoliths come from wild grasses of subfamilie Poideae. Panicoideae grasses (Bilobate-type) are rare; this type is likewise rare in present day vegetation of Southern Moravia. Phytoliths from trees and cereals were not recorded. The phytolith spectra reflect meadow vegetation where wild grasses and sedges dominate.

4. Macroremains and anthracological analyses

Macroremains and anthracological spectra identified within the Medieval stable infill in Veselí nad Moravou are quite heterogeneous (Fig. 6 and Fig. 7, tab. 2). Samples from the stable have the highest concentration of macroremains (compared to other units) and lower concentrations of wood fragments and charcoal (Fig. 6). The proportion of individual ecological groups which could be significant for stabling (the concentration of wetland species) or feeding (the concentration of crop plants) varies greatly (Tab. 2). Also, the proportion of macroscopically identifiable components (hay, straw, wood annual shoots) varies significantly in the samples (Fig. 6). After examining 2150 pieces of plant macroremains (mainly seeds and fruits), 104 taxons of higher plants were identified and divided into 5 ecological groups according to their ecological requirements known from recent times (Tab. 2). Those groups are: 1) meadows, pasture, wetland; 2) cereal weeds; 3) economic crops; 4) ruderal plants; 5) wood, glade.

The remediation layers in the stable commonly contained charcoal fragments providing clues to wood vegetation in the surrounding area. The most common taxa are typical for oak forests and oak-hornbeam forests including hardwood forests of lowland rivers (*Quercus robur*, *Fraxinus angustifolia subsp. danubialis*, *Fraxinus excelsior*, *Acer campestre*, *Ulmus laevis*). The species typical for willow-poplar forests (*Populus nigra*, *Populus alba*, *Salix alba*, *Salix* fragilis) and alder forests (*Alnus glutinosa*) were present in lower quantities. Charcoal fragments of beech were very rare.

5. Isotope analysis of horse hair

Three centimeter long sections of horse hair were analyzed. Since one millimeter of horse hair grows each day, this section represents one month of hair growth [42]. Surprisingly, the results of isotope analyses differ for each sample (Tab. 3), corresponding to different water stress and feeding provenance through time and for each individual. In the case of sample K228, a significant shift into negative values (2‰) for the $\delta 13C$ measurement implies that the horse spent the first three months mainly in parks and meadows while the next three months correspond to wood vegetation (tree leaves, shrubs) (Fig. 8 and Fig. 9). Six centimeters of horse hair in sample 1268 were divided into 4 parts and they do not show any significant changes in feeding or environment. This individual lived or was fed (at least for the four month period tested) on meadow grass and/or in a sparsely wooded environment. Nine centimeter sections of horse hair in sample 3318, representing 3 months, changed significantly in the second and the third months. This change was tracked to a change in environment as well as in the type of feeding. The first change shows movement from meadow grasses to a wooded environment

Table 1. Micromorphological description of different lithological contexts.

Context	Description
4.2.1. Fluvial deposits with trampling periods	Moderately sorted subangular to subrounded clasts mainly composed of quartz between 0.2 to 1 mm in size. The prevailing types of pores are simple packing voids and the microstructure of these deposits is porphyric with monic related distribution. Chitonic distribution is associated with decomposed organic matter (Fig. 4 A). Bioturbation was not observed. Charcoal or partly decomposed organic matter occasionally occurs. The main postdepositional process is leaching.
4.2.2. Infill of the horse stabling structure composed of domestic waste	Poorly sorted material composed of charcoal, quartz grains, burned bones, ceramic fragments, partly decomposed organic matter and matrix rich in micritic calcium phosphate compose the infilling of horse stable structure and was interpreted as domestic waste coming mainly from ovens (Fig. 4 C). Its microstructure is porphyric, with porphyric related distribution of angular to subrounded clasts of varied origin and with rare occurrence of compound packing voids. Leaching and accumulations of phosphate rich solutions are visible within the matrix. No bioturbation was observed.
4.2.3. Horse stabling	The horse stabling is composed mainly of partly decomposed organic material, and a large number of horse hairs. The organic material is visibly degraded in the uppermost part of the section. Stable crust is microscopically composed of laminated plant fragments embedded in a calcium phosphate-rich, autofluorescent (blue light) cement of hydroxyapatite (Fig. 4D).

doi:10.1371/journal.pone.0089273.t001

and then a significant movement back to the cultural landscape and meadows (Fig. 8 and Fig. 9). The horse hair of another individual (sample 3318B) measured 21 cm and was divided into 7 parts. Interestingly, no change in δ13C was detected between these seven sections. This individual was fed in a wooded environment. The last part of the sample shows significant improvement of environment and food and movement into a more humid environment (Fig. 8 and Fig. 9). Another individual (sample K1268B) provided a 9 cm long hair which was divided into three sections. The first two sections have isotopic values corresponding to a dry environment (Fig. 8 and Fig. 9). This individual was probably fed on hay. The third section of this sample shows a change to a woody, humid environment (Fig. 8 and Fig. 9). Sample K228B recorded two months of the individual's life and suggested that the environment and food did not change during this period. This individual lived in a humid environment and was fed on grass and tree leaves (Fig. 8 and Fig. 9).

6. Dendrochronology and dendrology

The average tree-ring series was dated using the Czech oak tree-ring chronology CZGES 2010 [43] to the year 1228. The period of tree felling could be established for sample no. 111 dated to 1230–1248 because it contained sapwood tree rings (ks); within the territory of the Czech Republic oak sapwood usually contains 5–25 tree rings depending on the age of the tree and location [44]. Sample No. 110 dated to the year 1202 did not contain sapwood tree rings (oak); therefore, we could only ascertain the year after which the tree was felled (Tab. 4).

The individual construction components differ in the type of wood used. Poles supporting the roof and frames of the single entrances were made of oak. Doorstep from the wide northerly

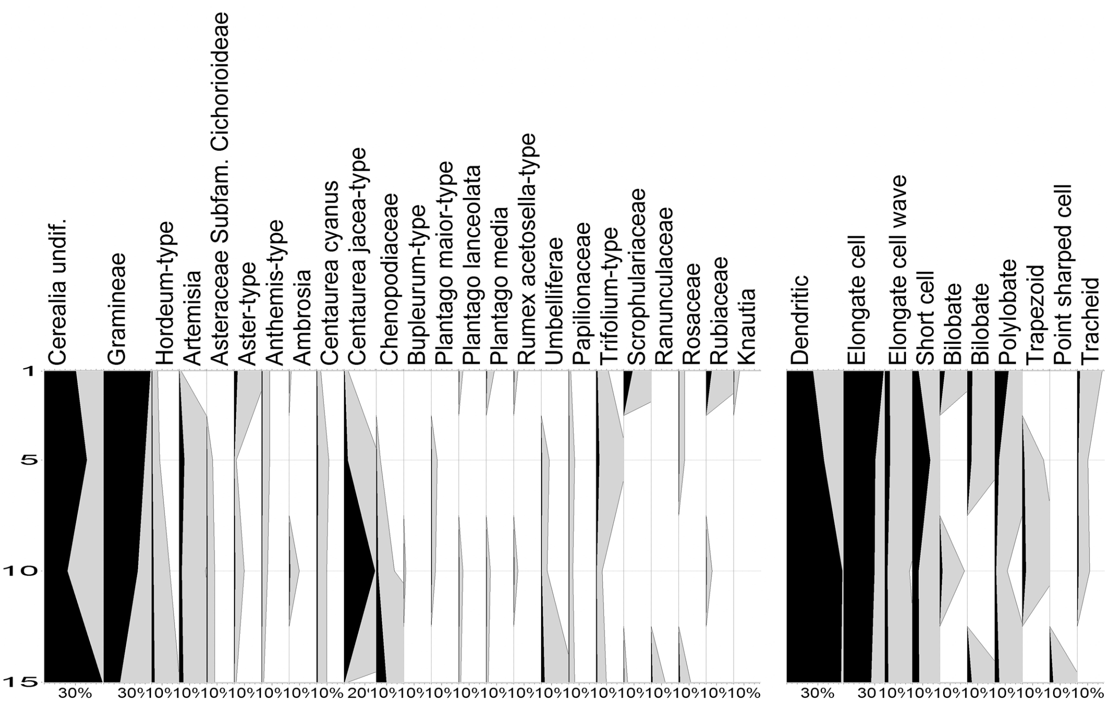

Figure 5. Pollen and phytolith diagram from Veselí nad Moravou Medieval stabling.
doi:10.1371/journal.pone.0089273.g005

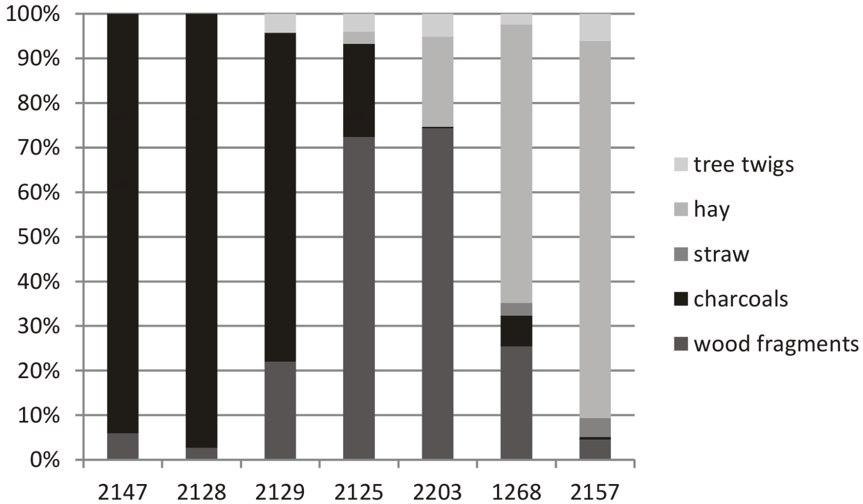

Figure 6. The proportion of macroscopically identifiable components (hay, straw, wood annual shoots). Samples of archaeological contexts 2147, 2129 and 2128 are from the waste aggradation while the samples of the contexts 2157, 2203, 2125 and 1268 are from the stabling.
doi:10.1371/journal.pone.0089273.g006

oriented entrance was made of oak and alder. The walls of the building were made from entwined sticks of unidentifiable broad-leaved wood, but the presence of a hazelnut suggests that this tree was used. Twenty vertical joists were also analysed. Nineteen were identified as oak wood and one as elm wood. Elm was also used for floor boards found in the eastern room. Wood found under the wooden floor was identified as elm and oak.

7. Zooarchaeology

Six species of animals were identified from 207 fragments (weighing a total of 2844.7 grams) recovered from the remediation (waste) layer and organic layers in the stable. The average weight of one fragment was 13.7 grams. Unburned fragments of mammal and bird bones were identified within remediation layers as well as within the organic part of the stabling. The following taxa were identified: Aves, *Anser domesticus*, Galliformes, *Gallus domesticus*, Mammalia, *Sus scrofa*, *Sus domesticus*, *Ovis/Capra*, *Bos Taurus*. Also taphonomic changes induced by humans and animals were identified. Butchering was evident on 29% of the fragments and tooth prints on 5% of the fragments. Weathering of bone surfaces was not significant.

Discussion

1. Medieval horse stabling structures

Medieval stables are quite rare in the Central European archaeological record [45], probably because horses were often left outside on the pastures during summer and stables were usually used as a winter refuge only. The discovery of a Medieval stable in Veselí nad Moravou presents a unique opportunity to study not only architecture, but also stable maintenance and the type of horse alimentation.

The stable investigated in this project has two identified construction phases (Fig. 2). During the first phase (A) the stable served as a simple room with an entrance oriented to the NE. The structure was made from intertwined sticks, which was commonly

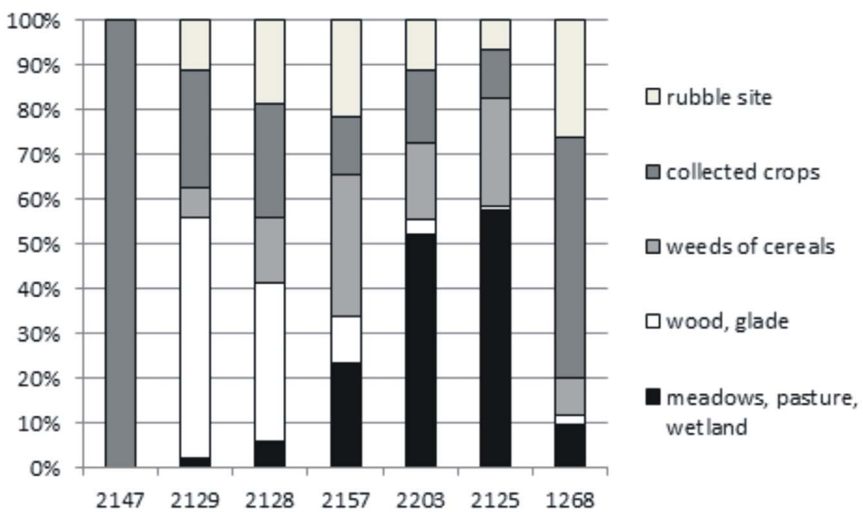

Figure 7. Ecological groups identified within the studied samples (samples of archaeological contexts 2147, 2129 and 2128 are from waste aggradation while samples 2157, 2203, 2125 and 1268 are from stabling.
doi:10.1371/journal.pone.0089273.g007

Table 2. The types and numbers of macroremains of different contexts (samples of archaeological contexts 2147, 2129 and 2128 come from the remediation layer while samples 2157, 2203, 2125 and 1268 come from stabling).

	context	waste aggradation					horse stabling		
	context number	**2147**	**2129**	**2128**	**2203**	**2157**	**1268**	**2125**	**total**
Type of plants	meadows, pasture, wetland		6	4	80	125	274	65	554
	wood, glade		158	25	35	8	4	13	243
	weeds of cereals		19	10	107	41	116	56	349
	collected crops	2	77	18	44	39	51	358	589
	rubble site		33	13	73	27	31	176	353
	total amount	2	293	70	339	240	476	668	2088

doi:10.1371/journal.pone.0089273.t002

used in Medieval times. Unlike the common types known from iconography [46], the stable from Veselí nad Moravou has plastered walls and the structure was quite robust. Such structures are also known from iconography, but rarely [47]. The structure itself was supported by posts and according to their positions, the building appears to have been 4–5 meters wide. Such joists can be easily made from common trees [48] [49]. If the spatial arrangement was equivalent to known data from 19th century, i. e. 1.3×3.5 m [50], the stable excavated in Veselí nad Moravou could have accommodated 7 horses.

The roof of the stable was not found. Stable roofs are not known from iconography, but ethnographic sources confirm their existence [51]. The 1.6 meter wide entrance was quite robust. In ethnography there are known doorways built from sticks, sealed up in winter by straw [51] [52]. The second phase of stable construction follows more or less the first phase. The differences are in the internal division of space where the second phase structure changes from one to three separate rooms. Also, two of the new rooms have a wooden floor. One of those rooms probably served for superior horses or pregnant mares, the second one probably as a preparation room. Preparation rooms are known from iconography [47]. The walls contained hazelnuts, which mean that this structure was built sometime in the late summer [53].

Other interpretations were also considered. For example, the structure may have been used as a storage room for feed, or for stabling of animals other than horses. Unfortunately there is not enough information about the differences between stabling structures used for different types of animals so we have only been able to compare our data with iconographic and etnographic works [46] [47] [51]. In interpreting the stabling deposits, the key features were the presence of organic matter and the internal

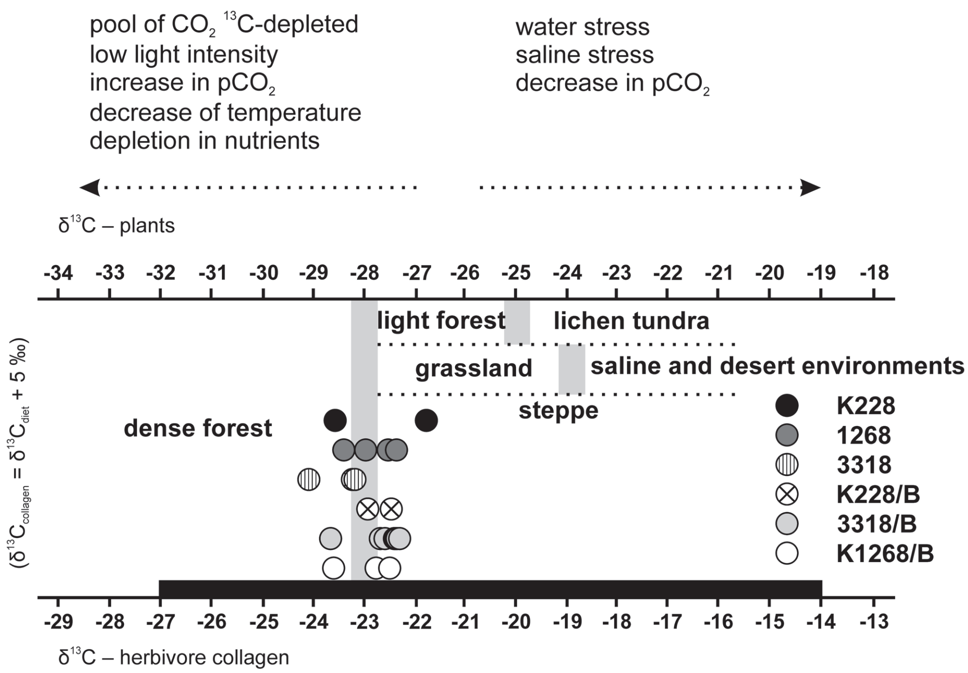

Figure 8. δ^{13}C values obtained from horse hair excavated at the Medieval site Veselí na Moravě. The obtained values show that the individuals lived and moved in different types of environments. Environmental data was taken from Bocherens (2003), Nelson *et al.* (1986), Bocherens *et al.* (1994, 1996, 2000), Rodière et al. (1996).
doi:10.1371/journal.pone.0089273.g008

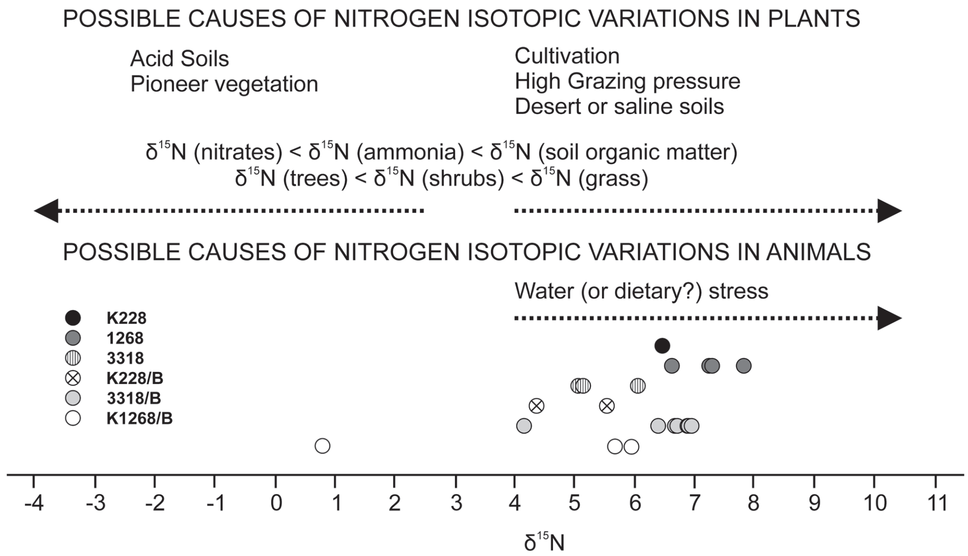

Figure 9. δ^{15}N values obtained from horse hair excavated at the Medieval site Veselí na Moravě. The obtained values show that the individuals moved during the year in different environments. The environmental data was taken from the Bocherens (2003), Nelson *et al.* (1986), Bocherens *et al.* (1994, 1996, 2000), Rodière et al. (1996).
doi:10.1371/journal.pone.0089273.g009

structure of this part of the infill (compare with chapter 4.2.3) which is composed of organic matter as well as a mineralogical fraction interbedded within the organic matter. Such structure cannot form just from the deposition of organic matter; trampling during the deposition of organic matter must also have taken place [6]. The presence of horse hairs and artefacts typically used in horse husbandry contexts have also contributed to the final interpretation. If the structure was used as a storeroom, trampled horizons within the floor layers would be expected, instead of the organic matter that was actually found [54].

Table 3. δ^{13}C and δ^{15}N values obtained from horse hair samples.

Sample	Lot	δ^{13}C	±1 σ	δ^{15}N	SD
Horse hair	K228/1	−21.79	0.21	6.46	0.20
Horse hair	K228/2	−23.57	-	4.48	-
Horse hair	1268/1	−23.40	0.35	7.84	1.21
Horse hair	1268/2	−22.39	0.18	7.25	0.34
Horse hair	1268/3	−22.54	0.20	6.62	0.16
Horse hair	1268/4	−22.97	0.16	7.30	0.30
Horse hair	3318/1	−23.18	0.21	6.05	0.74
Horse hair	3318/2	−24.09	0.17	5.07	0.29
Horse hair	3318/3	−23.23	0.78	5.15	0.64
Horse hair	3318/1B	−23.66	0.48	6.71	0.46
Horse hair	3318/2B	−22.69	0.11	6.67	0.17
Horse hair	3318/3B	−22.60	0.04	6.95	0.11
Horse hair	3318/4B	−22.38	0.08	6.90	0.01
Horse hair	3318/5B	−22.42	0.09	6.88	0.11
Horse hair	3318/6B	−22.32	0.03	6.39	0.36
Horse hair	3318/7B	−22.37	0.19	4.16	0.43
Horse hair	K1268/1B	−22.51	0.44	5.94	0.21
Horse hair	K1268/2B	−22.77	0.06	5.66	0.01
Horse hair	K1268/3B	−23.60	0.17	9.17	0.79
Horse hair	K228/1B	−22.93	0.90	5.54	1.27
Horse hair	K228/2B	−22.48	0.14	4.37	0.10

doi:10.1371/journal.pone.0089273.t003

2. Maintenance practices in a Medieval stable

Maintenance practices of horse stables are not known from historical or archaeological sources. In the case of Veselí nad Moravou, we have opted to apply a sedimentological and micromorphological approach to determine the sediment composition and to track possible maintenance practices that were used. Analogous micromorphological studies concerning stabling or floor deposits from sites such as Veselí nad Moravou are difficcult to find because a micromorphological approach is still not widely used for such contexts. However, stabling has been identified and micromorphogically studied in tell sites by Matthews et al. [12]. These authors report stables, but in contrast to Veselí nad Moravou, usually without prepared surfaces. This could be due to different geological and geomorphological backgrounds. As in Veselí nad Moravou, the background is composed of easily erodible sediments with potential for a high water level. Accumulated deposits of tell stables are interbedded lenses of

Table 4. Dating of wood samples excavated within a Medieval bailey in Veselí nad Moravou.

Number of sample	Species	Length	End	Dating
110	elm	51+6ak	1191	after 1202
111	oak	107+2ks	1228	1230–1248
150	oak	46+19ak	1193	after 1217
159	oak	61+31ks	1196	1227–1241
162	oak	62+1ks	1222	1224–1244
205	oak	189+20ak	1188	after 1213

doi:10.1371/journal.pone.0089273.t004

fragmented dung pellets with postdepositional changes typical mainly for organic staining, salts and bioturbation. In Veselí nad Moravou, the organic staining in calcium carbonate rich lenses of organic waste were preserved below the horse stabling, which is again also probably connected with the permeable geological units and the position within the alluvial zone of the Morava River.

Most of references concerning the study of object infillings are concerned with whether the infill originated naturally or anthropogenically [55] [56]. In the case of the Veselí nad Moravou stable, from the sedimentological and micromorphological view it is evident that the infilling originated antropogenically during remediation. Such examples are known for example from Hallstatt sunken houses [57] and from Viking houses [58]. Maintenance of Viking sunken houses in Iceland can be used as a comparison. The remediation layers have a sanitation effect and they increase the amount of easily erodible material on the surface. Floor surface erosion in Iceland is due to the volcanic background [58] [59]. In Veselí nad Moravou it is due to the sandy erodible background and the fact that during the removal of stabling the background is repeatedly removed as it adheres to the stabling. Due to such maintenance practices, at least 10 aggradation layers were preserved composed of waste from ovens and also common domestic waste as visible from the appearance of animal bones which were not burnt. On the other hand, such waste has a sanitation effect and and protects against hoof inflamation.

Preserved stabling was quite fresh due to the lack of ruderal species, i.e. waiting to be removed. Its pollen composition shows that the organic part of the stabling itself comes from the end of summer. But from an etnographic source [45] it is known that horses were stabled after the 16th of October (Feast Day of St. Havel). Until that time horses were pastured and lived outside 24 hours a day.

3. Horse alimentation in Medieval times and the origin of Veselí nad Moravou horses

Surprisingly, information about horse alimentation in Medieval Europe is limited [45] [60] [61]. It is a fact that during feudalism there was a shortage of adequate alimentation for animals, especially during the winter period [2] [3]. On the other hand the recent research in Siberia show, that livestok is able to fed outside the farm independently also during the winter periods, becuase the nutrition value of trees and shrubs is suficcient [62], but there must be evidently also limited number of animals per adequate area. We know from writen sources, that during summer, horses were kept in pasture or in the woods where they required minimal attention [63]. It is known that in the Late Middle Ages, it was common practice to collect branches with leaves suitable for feeding in the woods [2] [45]. Free pasture was possible during the 13th century and was enshrined in law - the so-called "the right of mare field", which means that mares were allowed to move freely in the landscape during the time period before harvest [2] [45].

The oldest known record of purposeful horse feeding is from Ibrahím Ibn Jakúb from the mid-10th century. More information is available from Medieval England [64], mainly from accounting records [65]. In spite of the fact that 14^{th} century England differs culturally to Central Europe, the differences in alimentation appear to be small. Horses in Medieval England were fed on oats in winter and were pastured during summer. Also, hay and straw was commonly used as feed, with chaff, bran, horse bread, legumes (peas, beans, vetches) a minor component [65]. Horses in Bohemian countries were fed mainly on barley and later on oats [45]. Graus [2] claims that in the pre-Hussite period horses in Bohemian countries were fed oats, vetches and mélange. Draff was also used. Ethnographic sources reveal that draught horses in Southern Moravia were fed vetches and hay during summer because pasture was not sufficient [66]. During winter, horses were fed straw from vetches, lentils, peas or millet and hay. Also, rye and wheat straw as well as other fodder was used as feed [66].

The most frequently found types of macroremains in the stable sediments in Veselí nad Moravou are plants that typically grew in meadows, pastures, and harvested fields. Less frequently occurring macroremains belonged to rubble sites, weed of cereals and wood glade. It is difficult to differentiate between feeding and stabling material. Sources suggest wood glade was also used as feed [2] [45]. Veselí nad Moravou is situated on an alluvial plain, so the element rich alluvial grass was also probably used as stabling material and as a substitute for straw. On the other hand, we know from ethnographic sources that at the beginning of the 20th centrury, stabling with straw was less common than today. As fodder was in short supply, other materials may have been used [66]. Animal bone fragments were also detected; it appears likely that any material at hand was used as stabling material, but the overall amount of stabling material was small and most of the material described from Veselí nad Moravou probably comes from feed left by horses on the floor.

We do know for a fact that pasture was an important component of horse feed. The examined samples indicate Cynosurus pasture species (for example *Prunella vulgaris*). The presence of willow sprouts (*Salix sp.*), small blackberries (*Rubus sp.*), hornbeam nuts (*Carpinus betulus*) and fragments of acorns constitute evidence of horses being fed in wooded pastures. Cereals such as millet, oat and hemp seeds were also detected. Straw is commonly used as stabling material today. We know from ethnographic sources that it was often used as horse feed in Southern Moravia [66]. Such a spectrum of horse fodder is much greater than what we know from references for Central Europe or for England.

It is also possible to obtain valuable information about horse feeding from analyses of C and N isotopes. The changes in these isotopes show environmental or seasonal changes [42] [67] [68]. Data about horse alimentation as interpreted from isotopic analyses of horse hairs (confirmed macroscopically and microscopically (Fig. 10) in large numbers), does not significantly differ from the horse alimentation generally presumed for Medieval horses in Central Europe [69]. Horse hair from Veselí nad Moravou shows significant changes in alimentation, or alternatively changes in the environment (Fig. 8 and Fig. 9) i.e. the transition between meadows to more humid woods and humid meadows (see Fig. 8 and 9). This transition can be interpreted as a seasonal change in alimentation (i.e. pasture during the vegetation season and feeding on hay during winter), or as structural differences in horse alimentation. For example, one of the horses often moved in the landscape where enough feed and water were available and moved between ecosystems. Another horse was kept in close surroundings of the castle and its opportunities for a varied diet were restricted.

The results published in this paper show that the fresh stable in Veselí nad Moravou was deposited in late summer. The horse population stabled in Veselí nad Moravou was quite varied. This inference can be explained in different ways. For example, the stable may have been used as temporary shelter for horses of peasants who came to work for the owner of the castle. Alternatively, the observed variability can correspond to different functions of the stable. If the stable was also servicing an inn, a number of courier houses could have been stabled there [70]. The third possible explanation for the presence of a large number of horses with different backgrounds in the one place is the possible presence of horses used in battle. In Medieval times, battle horses were commonly sourced from local inhabitants. One of the last

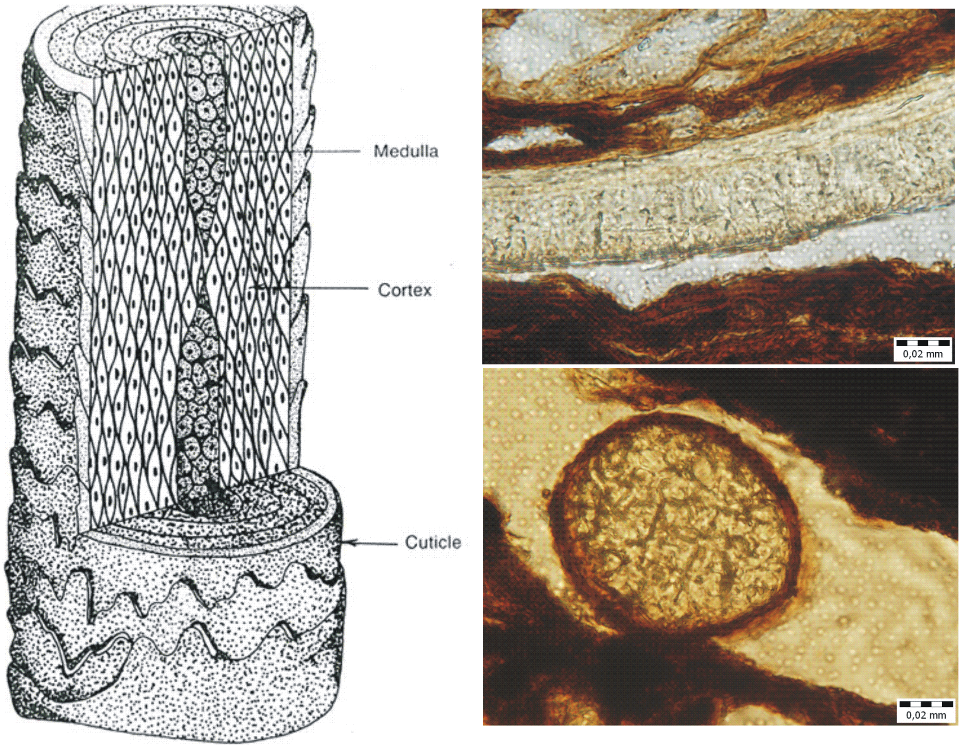

Figure 10. Micromorphology and the internal structure of horse hair.
doi:10.1371/journal.pone.0089273.g010

references to Veselí nad Moravou dates to the year 1315 when Jan Lucemburský battled Matúš Čák Trenčianský and conquered the castle in Veselí nad Moravou during the late summer [71]. The excavated stabling could represent the last usage of this stable up to this event, but unfortunately it is difficult to confirm this hypothesis.

4. Medieval vegetation along the Morava River

The archaeobotanical record from stable deposits in Veselí nad Moravou also reflects the composition of surrounding vegetation, to varying degrees. As we are dealing with anthropogenic deposits, in interpreting them it is neccessary to take into account the fact that the species present in the stable were selectively introduced by humans (so they are not an accurate reflection of the actual vegetation structure) [72]. The deposits include two separate sources (airborne and humans & animals), so the information obtained from pollen, phytolith, macroremains and anthracological analyses must be interpreted separately.

The remediation layers contain burnt firewood which offers probably the best evidence of the structure of the surrounding vegetation [56]. Charcoal of oak forest and oak-hornbeam forest species, including hardwood forests of lowland rivers (*Quercus robur*, *Fraxinus angustifolia subsp. danubialis*, *Fraxinus excelsior*, *Acer campestre*, *Ulmus laevis*) dominate. Due to the presence of species such as *Rubus ssp.* or *Clinopodium vulgare*, i.e. indicators of woodland which can be interpreted as a form of forest management. Such type of forest produces firewood at the expense of structural wood that was probably imported from more distant and less populated areas. Beech charcoal was identified in the samples, but beech does not grow in a riverine environment. Species of willow-poplar forest (*Populus nigra*, *Populus alba*, *Salix alba*, *Salix fragilis*) and alder forest (*Alnus glutinosa*), i.e. wood coming from near the Morava River floodplain were also reported. This picture of riverine vegetation is quite different from an Early Medieval site in Roztoky near the Vltava River. This site is typical for fir, Scots pine, and beech, along with coppiced and light-demanding species [56].

The second type of deposit being interpreted in the stable infilling is the horse stabling which contains plant macroremains and wood fragments. These remains indicate the presence of alluvial forests, alluvial meadows and tilled fields. It seems to represent horse feed and stabling material rather than the surrounding vegetation which can be seen in natural organogenic deposits, such as oxbow or peat [24].

Within the Medieval surroundings of Veselí nad Moravou we can postulate the existence of wet meadow/pasture communities (Morava River floodplain), in particular mesic meadows and to a smaller extent, dry and very dry grasslands. Meadow vegetation of the region (Lesser Carpathians) is already documented at least 2 500 years ago and is mainly the result of human activities [73]. The fields where the horse feed was harvested were fertile and rich in carbonates (for example the weed *Bupleurum rotundifolium*). The substrate of such fields is often loess as well as colluvial and alluvial deposits, so the horse feed was probably sourced locally. Even pest species are typical for warmer parts of Moravia (*Glaucium corniculatum*, *Chenopodium murale*) and correspond with the modern-day local situation [74].

Conclusions

The following conclusions can be made:

1. Average age of the wood found in Veselí nad Moravou Medieval bailey was determined to date to the year 1228. The investigated stable had two construction phases. Whilst the older phase involved a simpler structure, in the subsequent phase, part of the structure had a wooden floor.

2. The infilling of the stable reflects maintenance practices. Ashy material was deposited to provide remediation effects and its aggradation also served to reduce difference between the interior and the exterior of the stables.

3. Well preserved horse stabling in the uppermost part of the horse stable structure infilling accumulated within a few months at the end of summer. The stabling material was composed mainly of wetland grasses and wooden annual shoots. Differences in horse alimentation identified within stabling were probably due to differences between individuals. Horses were fed on meadow grasses as well as woody vegetation, millet, oat and less often on hemp, wheat and rye.

4. The results of isotope analyses suggest that the horses accommodated in the stable came from varied backgrounds. Three possible explanations of stable usage can be inferred. It may have been used as a temporary stable for horses of peasants from outside the castle, courier horses or battle horses.

5. Within the Medieval surroundings of Veselí nad Moravou we can postulate the existence of communities of wet meadow/pastures (floodplain of the Morava River), common types of mesic meadows but also (to a smaller extent) dry and very dry grasslands. Woody vegetation includes oak and oak-hornbeam forests including hardwood forests of lowland rivers (*Quercus robur*, *Fraxinus angustifolia* subsp. *danubialis*, *Fraxinus excelsior*, *Acer campestre*, *Ulmus laevis*). Low forests (*Quercus robur*, *Carpinus betulus*) were probably cultivated.

Acknowledgments

We would like to thank Daniel Nývlt for helpful comments on this paper.

Author Contributions

Analyzed the data: MD LL RC LP PK RK HV MFN ZS AB. Contributed reagents/materials/analysis tools: MD AB. Wrote the paper: LL MD PK MR MFN ZS AB LN.

References

1. Kühtreiber T (2010) Alimentation and Meat at Medieval Castles – Social Practice and Economic Structures from the Archaeologists's Perspective. The Zooarchaeological Contribution from Religious, Rural and Fortified Sites. In: Pluskowski A, Kunst GK, Kucera M, Bietak M, Hein I, editors. Bestial Mirrors: Using Animals to Construct Human Identities in Medieval Europe. Animals as Material Culture in the Middle Ages. Viena: Institute of Archaeological Science. pp. 66–76.
2. Graus F (1953) Dějiny venkovského lidu v Čechách v době předhusitské I., Dějiny venkovského lidu od 10. stol. do první poloviny 13. stol. Praha: ČSAV. 375 p.
3. Graus F (1957) Dějiny venkovského lidu v Čechách v době předhusitské II., Dějiny venkovského lidu od poloviny 13. století do roku 1419. Praha: ČSAV. 632 p.
4. Ewald J, Tauber J (1975) Die Burgruine Scheidegg bei Gelterkinden. Berichte über die Grabungen 1970–1974. Olten-Freiburg/Breisgau: Schweizer Beiträge zur Archäologie und Kulturgeschichte des Mittelalters, 2. 531 p.
5. Friedrich W (2006) Die sozialen Strukturen in der Burg Romrod anhald des archäologischen Fundmaterials In: Ettel P, Flambard HA, McNeill TE, editors. Château et Peuplement. Caen: Château Gaillard 22. pp. 163–174.
6. Goldberg P, Macphail R (2006) Practical and theoretical geoarchaeology. London: Blackwell Publishing. 454 p.
7. Courty MA, Goldberg P, Macphail RI (1989) Soils and Micromorphology in Archaeology, Cambridge Manuals in Archaeology. Cambridge: Cambridge University Press. 344 p.
8. Courty MA (2001) Microfacies analysis assisting archaeological stratigraphy In: Goldberg P, Holliday VT, Ferring CR, editors. Earth Sciences and Archaeology. New York: Kluwer Academic/Plenum Publishers. pp. 205–239.
9. Brochier JE, Villa P, Giacomarra M (1992) Shepherds and Sediments: geo-ethnoarchaeology of pastoral sites. Journal of Anthropological Archaeology 11: 47–102.
10. Matthews W, Postgate JN, Paney S, Charles MP, Dobney K (1994) The imprint of living in an early Mesopotamian city: questions and answers In: Luff R, Rowley-Conway P, editors. Whither environmental archaeology? Oxford: Oxbow Monograph 38. pp. 171–212.
11. Macphail RI, Goldberg P (1995) Recent advances in micromorphological interpretations of soils and sediments from archaeological sites In: Barham AJ, Macphail RI, editors. Archaeological sediments and soils: analysis, interpretation and management. London: Institute of Archaeology, University College. pp. 1–24.
12. Matthews W (1995) Micromorphological characterization and interpretation of occupation deposits and microstratigraphic sequences at Abu Salabikh, Southern Iraq In: Barham AJ, Macphail RI, editors. Archaeological sediments and soils: analysis, interpretation and management. London: London: Institute of Archaeology, University College. pp. 41–74.
13. Matthews W, French CAI, Lawrence T, Cutler DF (1996) Multiple surfaces: the micromorphology In: Hodder I, editor. On the surface: Çatalhöyük 1993–95: Cambridge: MacDonald Institute for Research; London: British Institute at Archaeology of Ankara. pp. 301–42.
14. Matthews W, French CAI, Lawrence T, Cutler DF, Jones MK (1997) Microstratigraphic traces of site formation processes and human activities. World Archaeology 29: 281–308.
15. Hodder I, Cessford C (2004) Daily practice and social memory at Çatalhöyük. American Antiquity 69: 17–40.
16. Matthews W (2005) Life-cycle and life-course of buildings In: Hodder I, editor. Çatalhöyük perspectives. Reports from the 1995–1999 seasons by members of the Çatalhöyük team. Cambridge: McDonald Institute Monographs; London: British School at Ankara. 125–49.
17. Karkanas P, Efstratiou N (2009) Floor sequences in Neolithic Makri, Greece: micromorphology reveals cycles of renovation. Atiquity 83: 955–967.
18. Macphail RI, Cruise GM, Allen MJ, Linderholm J, Reynolds P (2004) Archaeological soil and pollen analysis of experimental floor deposits; with special reference to Butser Ancient Farm, Hampsihre, UK. Journal of Archaeological Science 31: 175–191.
19. Dejmal M, Merta M (2011) Výzkum hradu ve Veselí nad Moravou. Archaeologia historica. 36, 1: 125–137.
20. Bullock P, Murphy CP (1983) Soil micromorphology, Berkhamsted: AB Academic. 705 p.
21. Bullock P, Fedoroff N, Jongerius A, Stoops G, Tursina T (1985) Handbook for soil thin section description. Wolverhamton, UK: Waine Research Publications. 152 p.
22. Stoops G, Marcelino V, Mees F (2010) Interpretation of micromorphological features of soils and regoliths, Amsterdam: Elseiver. 720 p.
23. Stoops G (2003) Guidelines for Analysis and Description of Soil and Regolith Thin Sections, Madison, Wisconsin, USA: Soil Science Society of America. 184 p.
24. Moore PD, Webb JA, Collinson ME (1991) Pollen analysis, second edition, Oxford: Blackwell Scientific Publications. 237 p.
25. Piperno DR (2006) Phytoliths. A Comperhative Guide for Archaeologists and Paleoecologists, Lantam: Altamira Press. 238 p.
26. Beug HJ (2004) Leitfaden der Pollenbestimmung für Mitteleuropa und angrenzende Gebiete, München: Verlag Dr. Friedrich Pfeil. 542 p.
27. Reille M (1995) Pollen et spores d'Europe et d'Afrique du Nord, Supplément 1. Marseille: Éditions du Laboratoire de botanique historique et palynology. 327 p.
28. Reille M (1998) Pollen et spores d'Europe et d'Afrique du Nord, Supplément 2. Marseille: Éditions du Laboratoire de botanique historique et palynologie. 521 p.
29. Madella M, Alexandre A, Ball T (2005) International Code for Phytolith Nomenclature 1.0. Annals of Botany 96: 253–260.
30. Madella M, Powers-Jones AH, Jones MK (1998) A simple method of extraction of opal phytoliths from sediments using a non-toxic heavy liquid. J Arch Sci 25: 801–803.
31. Nalepka D, Walanus A (2003) Data processing in polen analysis. Acta Paleobot 43: 125–134.
32. Jacomet S, Kreuz A (1999) Archäobotanik: Aufgaben, Methoden und Ergebnisse Vegetations und Agrargeschichtlicher Forschung, Stuttgart: Ulmer. 363 p.
33. Cappers RTJ, Bekker RM, Jans JEA (2006) Digital Seed Atlas of the Netherlands. Eelde: Barkhuis. 502 p.
34. Cappers RTJ, Neef R, Bekker RM (2009) Digital Atlas of Economic Plants. Barkhuis, Eelde. 445 p.
35. Schweingruber FH (1978) Mikroskopische Holzanatomie. Eidgenössische Anstalt für das forstliche Versuchswesen, Birmensdorf (Ed.). Kommissionsverlag Zürcher AG, Zug. 226 p.
36. Schweingruber FH (2001) Dendroökologische Holzanatomie. Anatomische Grundlagen der Dendrochronologie, Haupt, Bern, Stuttgart, Wien: Haupt Werlag. 274 p.
37. Bocherens H (2003) Isotopic biogeochemistry and the paleoecology of the mammoth steppe fauna. Deinsea 9: 57–76.
38. Bocherens H, Fizet M, Mariotti A, Gangloff RA, Burns JA (1994) Contribution of isotopic biochemistry (13C, 15N, 18O) to the paleoecology of mammoths (Mammuthus primigenius). Historical Biology 7: 187–202.
39. Nelson BK, Deniro MJ, Schoeninger MJ, De Paolo DJ, Hare PE (1986) Effects of diagenesis on strontium, carbon, nitrogen and oxygen concentration on isotopic composition of bone. Geochimica et Cosmochimica Acta 50: 1941–1949.

40. Rodière É, Bocherens H, Angibault JM, Mariotti A (1996) Particularités isotopiques chez le chevreuil (Capreolus capreolus L.): implications pour les Reconstitutions paléoenvironnementales – Comptes Rendus de l'Académie des Sciences, Paris 323: 179–185.
41. Cook ER, Kairiukstis LA (1990) Methods of Dendrochronology – Applications in the Environmental Sciences. Dordrecht, Boston, London: Kluwer Academic Publisher and International Institute for Applied Systems Analysis. 394 p.
42. Ayliffe LK, Cerling TE, Robinson T, West AG, Sponheimer M, et al. (2004) Turnover of carbon isotopes in tail hair and breath CO2 of horses fed an isotopically varied diet. Oecologia 139: 11–12.
43. Kolář T, Rybníček M, Kyncl T (2012) The New Oak Standard Chronology for the Czech Republic and its Teleconnection on a European Scale, Dendrochronologia. DOI 10.1016/j.dendro.2012.02.002 (in print)
44. Rybníček M, Vavrčík H, Hubený R (2006) Determination of the number of sapwood annual rings in oak in the region of southern Moravia, Journal of forest science 52, 3: 141–146.
45. Beranová M, Kubačák A (2010) Dějiny zemědělství v Čechách a na Moravě, Praha: Libri. 432 p.
46. Krása J (1990) České iluminované rukopisy 13./16. století, Praha: Odeon. 455 p.
47. Vařeka J, Frolec V (2007). Lidová architektura, Encyklopedie, Praha: Grada. 87 p.
48. Úradníček L, Maděra P, Tichá S, Koblížek J (2009). Dřeviny České republiky (Woody species of Czech republic). 2nd edition, Kostelec nad Černými Lesy: Lesnická práce. 792 p.
49. Wagenführ R (2000) Holzatlas (Atlas of wood). 5th edition. München: Fachbuchverlag Leipzig im Carl Hanser Verlag. 707 p.
50. Zbranek H (2013) Zámecká jízdárna v Lednici - multifukční centrum. Brno: Rkp. nálezové zprávy 22/2013 uložené v archivu Archaia Brno o.p.s. 55 p.
51. Štěpánek L (1978) Ustájení zvířat v rolnických usedlostech Čech. Vědecké práce zemědělského muzea 18/1978: 195–215.
52. Niederle L (1918) Moravské Slovensko sv. 1, Národopis lidu Československého díl I., Praha: Národopisné museum Československé. 399 p.
53. Hejný S (1990) Květena České republiky 2, Praha: Academia. 540 p.
54. Lisá L, Kolařík V, Bajer A (2008) The geoarchaeological and micromorphological reconstruction of medieval food store room floor layers; the case study from Tišnov, Czech Republic. Frankfurter Geowissenschaftliche Arbeiten. Serie D, Band 30: 67–75.
55. Parma D, Lisá L, Jarošová M, Petr L (2011). Geoarchaeology of La Tène Sunken Houses at Syrovice, Czech Republic: Importance for Understanding Living Strategies. Interdisciplinaria Archaeologica 2(1): 15–25.
56. Novák J, Lisá L, Pokorný P, Kuna M (2012) Charcoal analyses as an environmental tool for the study of Early Medieval sunken houses infills in Roztoky near Prague, Czech Republic. Journal of Archaeological Science 39: 808–817.
57. Jarošová M, Lisá L, Přichystal A, Parma D, Petr L, et al. (2010) Geoarcheologický výzkum halštatské zemnice v Modřicích u Brna.- Geol Výzk Mor Slez Brno 2010: 39–45.
58. Milek K (2012) The Roles of Pit Houses and Gendered Spaces on Viking-Age Farmsteads in Iceland. Medieval Archaeology 56: 85–130.
59. Milek K (2012) Floor formation processes and the interpretation of site activity areas: An ethnoarchaeological study of turf buildings at Thverá, northeast Iceland. Journal of Anthropological Archaeology 31: 119–137.
60. Černý V (1932) Crescentius v Čechách, k dějinám čsl. Období humanism. Sborník prací věnovaných J. B. Novákovi k 60. tým narozeninám: 105–118.
61. Eis G (1939) Meister Albrants Rossarzneibuch im deutschen Osten, Liberec: Olms Presse. 329 p.
62. Hejcman M., Hejcmanová P, Stejskalová M, Pavlů V (2014) Nutritive value of winter collected annual twigs of main European woody species, mistletoe and ivy and its possible consequences for winter foddering of livestock in prehistory. The Holocene: in press.
63. Curwen EC, Hatt G (1953) Plough and Pasture, the early history of farming. New York: Henry Schuman. 329 p.
64. Clark J (2004) The Medieval horse and its equipment, London: Boydell Press in association with Museum of London. 185 p.
65. Langdon J (1982) The economics of Horses and Oxen in medieval England. Agricultural History Review 30: 31–40
66. Kuns L (2006) Osedlý rolník. Rolnictví na východní Moravě od baroka do II. světové války, Rožnov pod Radhoštěm: Valašské museum v přírodě. 340 p.
67. West AG, Ayliffe LK, Cerling TE, Robinson TF, Karren B, et al. (2004) Short-term diet changes revealed using stable carbon isotopes in horse tail-hair. Functional Ecology 18: 616–624.
68. Zazzo A, Harrison SM, Bahar B, Moloney AP, Mohanan FJ, et al. (2007) Experimental determinativ of dietary carbon turnover in bovin hair and hoof. Can J Zool 85: 1239–1248.
69. Müldner G, Richards MP (2005) Fast or feast: reconstructing diet in later medieval England by stable isotope analysis. Journal of archaeological Science 32: 39–48.
70. Dušek J (1995) Kůň ve službách člověka – středověk, Praha: Apros.
71. Dejmal M (2012) Struktura vrcholně středověkého osídlení ve Veselí nad Moravou. Archaeologia Historica 37: 209–232.
72. Pearsall DM (2000) Paleoethnobotany: A Handbook of Procedures, Second Edition, San Diego: Academic Press. 700 p.
73. Hájková P, Roleček J, Hájek M, Horsák M, Fajmon K, et al. (2011) Prehistoric origin of the extremely species-rich semi-dry grasslands in the Bílé Karpaty Mts (Czech Republic and Slovakia). Preslia 83(2): 185–204.
74. Chytrý M (2009) Vegetace České republiky 2. Ruderální, plevelová, skalní a suťová vegetace/Vegetation of the Czech Republic 2. Ruderal, Weed, Rock and Scree vegetation. Praha: Academia. 520 p.

Journal of Archaeological Science 39 (2012) 808–817

Contents lists available at ScienceDirect

Journal of Archaeological Science

journal homepage: http://www.elsevier.com/locate/jas

Charcoal analyses as an environmental tool for the study of Early Medieval sunken houses infills in Roztoky near Prague, Czech Republic

Jan Novák[a], Lenka Lisá[b,*], Petr Pokorný[c,d], Martin Kuna[c]

[a] Department of Botany, Faculty of Science, University of South Bohemia, Branišovská 31, 370 05 České Budějovice, Czech Republic
[b] Institute of Geology of the Academy of Sciences of the Czech Republic, v.v.i., Rozvojova 269, 165 00 Praha 6, Czech Republic
[c] Institute of Archaeology of the Academy of Sciences of the Czech Republic, v.v.i., Letenská 4, 118 01 Praha 1, Czech Republic
[d] Center for Theoretical Studies, Charles University in Prague and the Academy of Sciences of the Czech Republic, Jilská 1, 110 00 Praha 1, Czech Republic

ARTICLE INFO

Article history:
Received 13 January 2011
Received in revised form
16 June 2011
Accepted 21 June 2011

Keywords:
Anthracology
Geoarchaeology
Pollen analysis
Early Medieval
Sunken houses
Vegetation
Firewood
Post-depositional processes

ABSTRACT

The research was focused on the testing of possible information value of charcoal analysis from infills of archaeological objects, when methodologically different approaches are used in the combination with the micromorphological and pollen-analytical approach. The case study site chosen for this type of study is the unique Early Medieval settlement at Roztoky, Czech Republic. The comparative study includes the infills of 20 pithouses from the extensive settlement comprising about 750 (323 excavated) such archaeological structures situated along the left bank of Vltava River close to what today is the city of Prague. A combination of three anthracological outcomes (the number of charcoal fragments, the anthracomass, and the qualitative frequency of charcoal species) proves to be a powerful tool in determining the vegetation pattern in the surrounding landscape. The study revealed a major effect of post-depositional processes and quantification methods on the final anthracological interpretation. A modification of the anthracological record in different layers was traced in order to assess the applicability of sedimentology and micromorphology in the interpreting of the primary use and ending of the objects found. The reliability of anthracological interpretations are then compared with the results of micromorphological analyses and with regional vegetation patterns interpreted from pollen analyses of an off-site pollen profile.

1. Introduction

One of the key questions, often discussed in final archaeological interpretations, is the information value of the infills of archaeological features. The composition of these infills has been long discussed in studies focused on the construction technology and the purpose of archaeological features, their usage, and the reasons of their abandonment (Dolukhanov, 1996, Simpson et al., 1999; Einarsson, 2008). Usually, the subdivision into horizons within the studied features was based on a combination of visual attributes, archaeological or archaeobotanical remains.

Organic matter has a high information value in archaeological record. One of the usually best preserved organic remains, connected with humans since the Palaeolithic, is charcoal. Wood charcoal analysis provides site-related information on the species occurrence and the woodland composition and, as such, becomes an integral part of archaeological research, especially when a combination with pollen analysis is possible (Asouti and Austin, 2005; Nelle et al., 2010). Charcoal fragments found in archaeological deposits usually represent either firewood remains or burned vestiges of structural timber resulting from catastrophic conflagrations (Chabal, 1992; Dufraisse, 2008). Firewood collection provenance is generally interpreted to be completed in the area close to the settlement with all species gathered proportionally according to their occurrence in the surroundings (Asouti and Austin, 2005). In addition to societal factors and combustion processes, post-depositional agents are very important filters between the vegetation and the charcoal assemblage (Théry-Parisot et al., 2010).

Another important methodological tool used in the study of composition of archaeological features is micromorphology in archaeological context (Courty et al., 1989; Goldberg et al., 2001; Goldberg and Macphail, 2006). Micromorphological investigation is primarily based on the coarse fraction, matrix, voids, organic material and features typical of sedimentary and post-sedimentary

* Corresponding author. Tel.: +420 607706585; fax: +420 220922670.
E-mail addresses: prourou@gmail.com (J. Novák), lisa@gli.cas.cz (L. Lisá), pokorny@arup.cas.cz (P. Pokorný), kuna@arup.cas.cz (M. Kuna).

0305-4403/$ – see front matter © 2011 Elsevier Ltd. All rights reserved.
doi:10.1016/j.jas.2011.06.026

processes (Courty et al., 1989) and, in combination with charcoal analysis and other geochemical data, provides a complex information about the studied layers (Goldberg et al., 2001; Goldberg and Macphail, 2006).

The subject of our research is the Early Medieval settlement agglomeration dated to the 6th and 7th century AD, discovered at Roztoky near Prague. The unusually high number of the Early Medieval sunken houses, the estimated time span of the settlement existence of 150 years, and its location on the floor of a deep, canyon-like valley is unique in the whole area of the Prague-Korčak (also the Prague-type) culture (Sedov, 1982; Gojda, 1991; Dolukhanov, 1996, Kuna and Profantová, 2005). This settlement represents a puzzle considering the enormous number of house remains and its specific interpretation. A combination of three complementary methods – charcoal analysis in context of micromorphology and pollen analysis, which are not a standard approach in archaeo-environmental research yet, may contribute to a better understanding of the character of the surrounding landscape. We attempt to answer the following questions: How is the anthracological record modified by post-depositional processes in different layers? What does the anthracological record in context of sedimentology or micromorphology say about the use, abandonment and decay of the studied objects? We will also discuss the reliability of the combined methods used.

2. Study area

2.1. Early Medieval settlement at Roztoky near Prague

The Early Medieval settlement discovered during the last twenty years in the close vicinity of Roztoky near Prague (settlement with the estimated number of more than 750 sunken houses accumulated over the period of 120–150 years) (Fig. 1) is unique to the whole area of the Slavic spread (Kuna and Profantová, 2005). The site is located on the floor of the deep Vltava River canyon, where sunken features interpreted as sunken houses were discovered. These findings belong to the so-called Prague-type culture which is usually believed to represent the earliest Slavic populations that moved into the Central Europe from the East. Although some relatively large sites have been reported from the surrounding countries – for instance, Germany (Krüger, 1967), Poland (Parczewski, 1989), Ukraine (Baran, 1988), Moldova (Zeman, 1976; Teodor, 1994) and Romania (Dolinescu-Ferche, 1992) – the Roztoky settlement site is larger than any other site of this culture known so far. However, it is characterized by a very short period of use (120–150 years; Curta, 2008), which complicates a comparison with similar localities, but provides excellent conditions for studying this unique site.

2.2. The geographical and archaeological context

The studied settlement is situated in the Vltava River canyon on a fluvial terrace separating rocky slopes of the valley from the stream (Fig. 1). The terrace is only 120 m wide and the level of the Early Medieval settlement is at present situated 5 m above mean water level. Local Quaternary deposits are characterized by sandy loams and morphologically comprise an older river terrace level gently sloped toward the river channel. It is obvious from the study of sunken house infills that the location was situated well above the water level, being therefore rarely flooded during periodical flood events. The stratigraphy of sunken house infills shows no evidence of catastrophic events assignable to a repeated cycle of the destruction and building of the houses. The number of artefacts left on the floors of the sunken houses is not very high, suggesting that the houses were abandoned slowly and peacefully. Both the movable finds and architecture are basically similar to what we know from other sites of this period, the main explanation problem being the extremely high number of houses discovered (Kuna and Profantová, 2005).

3. Materials and methods

3.1. Charcoal analysis

In total, 101 anthracological samples from 20 sunken houses were analyzed and nearly 11,000 charcoal fragments were included into the final interpretations. Soil samples of 20–35 kg, rarely 50 kg were collected. The extractions of charcoal from the samples were subjected to the standard flotation procedure using staggered sieves with a mesh size of 0.25 mm. The charcoal analysis was performed only on fragments from the largest fraction (>2 mm). The charcoals were identified using an episcopic interference microscope (Nikon Eclipse 80i) with 200–500× magnification and the reference collection. The additional standard identification keys were also used (Schweingruber, 1990; Heiss, 2000).

The relative species abundance was expressed in the number of charcoal fragments (e.g., proposed by Delhon, 2006), charcoal anthracomass (e.g., Carcaillet and Thinon, 1996), and the qualitative

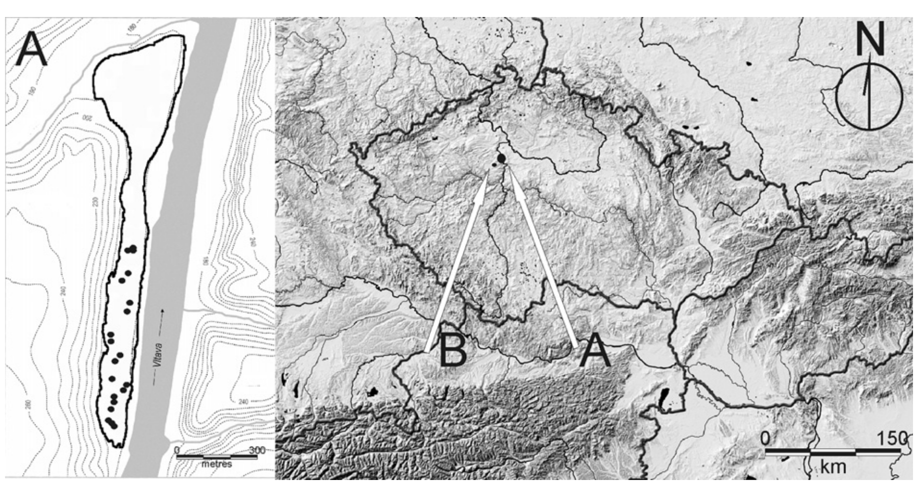

Fig. 1. Location of the Prague – Korčak site at Roztoky (20.6 ha) situated on the bottom of a canyon-like valley of the Vltava River, Czech Republic. Left part of the figure refers to the location of sampled sunken houses. Arrow A refers to the location of the studied site, arrow B refers to the pollen site "Břve".

frequency of identified species (the qualitative approach where taxa are recorded as a presence/absence data; e.g., Willcox, 1974; Neumann, 1989; Figueiral, 1992). The individual taxa were weighted with an accuracy of 0.001 g. The sediment anthracomass (mg charcoal per kg of sediment; Talon et al., 1998) was derived from the charcoals larger than 2 mm.

3.2. Micromorphology

The micromorphogical samples were taken from 20 houses in the different parts of the settlement (Fig. 1). Sampling was done usually for each divided layer, but in some cases intentionally chosen horizons were sampled. The sampling and the preparation followed the standard procedures. Samples from the different lithological units of the sunken infills were taken into the "Kubiena boxes", dried, impregnated by resin in vacuum and thin sectioned. Thin sections were studied by binocular microscope Olympus SZX 16 and by polarizing microscopes Olympus DP 70 at different magnifications ranging from 10–800x and described according to Stoops (2003) and Bullock et al. (1985).

3.3. Pollen and micro-charcoal analysis

The nearest site suitable for performing off-site pollen analyses has been discovered 13 km SW from the studied settlement at Roztoky. Present soils and vegetation conditions around the studied pollen site quite resembles that around Roztoky settlement, if we do not take into the account the interior of the Vltava River valley.

The study pollen site is small calcareous spring mire that lies in the western edge of the city of Prague (50°04′00″N, 14°14′20″E; 362 m a.s.l.; see Fig. 1). Today the site is drained off and strongly affected by management, especially over-fertilization from the surrounding cultural landscape (fields and settlements). The local vegetation is drying-out open *Carex*-dominated fen with spreading reed (*Phragmites australis*) population. The organic sediment at the sampling spot is 200 cm deep and was sampled from an open pit dug with spades. The entire section consists of calcareous fen peat without visible stratigraphic transitions.

AMS radiocarbon measurements were carried out on plant macrofossils (small twigs with buds) at the *Physikalisches Institut der Universität Erlangen-Nürnberg*, Germany (Erl-4308; Erl-4309; Erl-4310; See Table 2). Calibration was made using INTCAL 09 calibration set (Reimer et al., 2009). Absolute chronology was then obtained using linear interpolation between the midpoints of the calibrated ranges (95% confidence interval) of its three ^{14}C dates. No reservoir effect was assumed. Sediment surface (0 cm) was included in the depth-age model and was assumed to have an age of 2000 BC/AD.

Sediment samples for pollen analysis were treated by acetolysis after pre-treatment by cold, concentrated HF for 10 h. Usually more than 700 pollen grains were counted per sample. Pollen diagram is based on total terrestrial pollen sum (AP + NAP = 100%). The percentages of aquatic taxa and all non-pollen objects (like microscopis charcoal particles) are related to this sum. Pollen nomenclature follows Czech Quaternary Palynological Database – PALYCZ (Kuneš et al., 2009). The key of Beug (2004) was the main source for pollen determination besides reference collection. Zonation of the pollen diagram was performed using subjective evaluation criteria. Curves of trees and anthropogenic indicators were given stronger relative weight during this procedure.

Microscopic charcoal particles were counted directly from pollen slides using a simple method described by Kangur (2002): Particles larger than 100 μm^2 were registered at the same area where pollen was counted. The area of every charcoal particle was

Table 1
The quotation of quantitative frequency, anthracomass and the number of charcoal fragments of different charcoal taxa from the Early Medieval settlement, Roztoky, Czech Republic. The σ means the expression for the standard deviation.

Charcoal taxa	Qualitative frequency (%)				Antracomass (mg/kg)								Number of charcoal fragments (n/kg*100)							
	Layer G	Layer C	Layer B	Layer E	Layer G	σ G	Layer C	σ C	Layer B	σ B	Layer E	σ E	Layer G	σ G	Layer C	σ C	Layer B	σ B	Layer E	σ E
Abies alba	14.3	33.3	22.7	47.2	0.067	0.22	0.101	0.20	0.270	1.00	3.075	9.36	3.10	0.1	2.26	0.04	2.99	0.08	55.30	1.41
Acer sp.	25.0	6.6	40.9	22.2	0.366	1.64	0.031	0.14	0.622	1.75	0.103	2.98	4.45	0.18	0.53	0.02	5.30	0.11	1.42	0.03
Alnus sp.	10.7	13.3	22.7	22.2	0.128	0.52	0.077	0.29	1.212	5.17	0.805	4.22	1.84	0.07	0.51	0.02	2.90	0.05	5.73	0.25
Betula sp.	50.0	40.0	72.7	80.6	0.357	0.6	0.243	0.46	0.596	0.90	1.589	3.1	6.54	0.10	4.80	0.08	9.57	0.13	27.25	0.42
Carpinus betulus	46.4	60.0	77.2	66.7	1.367	3.19	1.062	2.27	3.697	9.41	2.551	7.3	21.65	0.54	10.95	0.22	29.39	0.41	21.74	0.37
Cornus sp.	3.6	0.0	4.5	0.0	0.007	0.04	0.000	0.10	0.019	0.27	0.000	3.8	0.15	0.01	0.00	0.01	0.79	0.02	0.00	0.00
Corylus avellana	27.6	7.1	31.8	30.6	0.224	0.56	0.011	0.10	0.082	0.26	0.182	2.94	1.78	0.04	0.27	0.00	1.62	0.04	1.77	0.04
Fagus sylvatica	10.7	28.6	31.8	50.0	0.445	2.22	0.056	0.11	0.33	0.93	14.716	67.2	0.31	0.01	1.29	0.02	2.49	0.04	163.07	6.67
Fraxinus excelsior	17.6	20.0	13.6	11.1	0.028	0.09	0.132	0.46	0.083	0.29	0.043	3.3	0.89	0.02	2.77	0.07	1.47	0.04	0.68	0.02
Juniperus communis	7.1	0.0	2.7	0.0	0.018	0.09	0.000	0.10	0.002	0.28	0.000	3.7	0.46	0.02	0.00	0.00	0.06	0.05	0.00	0.00
Pinus sylvestris	46.4	46.7	59.1	55.6	0.704	1.53	0.227	0.43	0.881	2.17	1.68	5.22	13.75	0.26	4.96	0.07	12.92	0.27	20.58	0.48
Picea abies	0.0	0.0	4.5	16.7	0.000	0.00	0.000	0.10	0.013	0.27	0.043	3.3	0.00	0.00	0.00	0.00	0.45	0.02	1.34	0.04
Pomoideae	17.2	0.0	4.5	11.1	0.051	0.19	0.000	0.10	0.011	0.27	0.151	3	1.35	0.03	0.00	0.00	0.17	0.01	1.23	0.03
Prunus sp.	0.0	0.0	4.5	2.7	0.000	0.00	0.000	0.10	0.004	0.27	0.001	3.7	0.00	0.00	0.00	0.00	0.09	0.01	0.03	0.00
Quercus sp.	100.0	100.0	100.0	100.0	26.535	31.79	17.446	24.55	33.323	52.71	47.822	92.58	274.47	2.3	211.01	1.2	277.59	1.85	417.18	5.22
Salix/Populus	7.1	6.6	9.1	11.1	0.056	0.27	0.012	0.10	0.010	0.27	0.141	2.99	0.79	0.04	0.28	0.01	0.33	0.01	1.24	0.04
Tilia sp.	14.3	6.6	13.6	11.1	0.133	0.59	0.406	1.51	0.159	0.59	0.058	3.2	1.78	0.07	9.60	0.38	4.6	0.18	0.74	0.02
Ulmus sp.	7.1	6.6	22.7	11.1	0.232	0.90	0.021	0.11	0.197	0.55	0.116	2.98	2.13	0.09	1.11	0.04	2.99	0.08	1.42	0.04
Σ					30.72		19.83		41.51		73.08		335.35		250.34		354.91		720.72	

Table 2
Results of AMS radiocarbon analyses used to date the studied pollen sequence from Bř̌ve locality.

Depth	Material	Measured value	Lab. no.	Calibration result (95%)
40 cm	Carex seeds	813 ± 58 BP	Erl-4308	1055 AD–1275 AD
130 cm	Small twigs with buds	2080 ± 52 BP	Erl-4309	330 BC–30 AD
180 cm	Small twigs with buds	2344 ± 54	Erl-4310	720 BC–240 BC

estimated by multiplying the lengths of the longest and shortest axes. The charcoal particles curve displayed in the pollen diagram shows the ratio between number of charcoal particle units (each unit = 100 μm^2) and total pollen sum.

4. Results

4.1. Sedimentological and micromorphological analysis of the studied objects

Sedimentological background of the Roztoky site is represented by alluvial deposits of the Vltava River. Because there were observed similar sedimenthological and micromorphological features within the studied objects, the description used in this paper is generalized and refers to the description based on the micromophological study of 20 houses and the sedimenthological study of minimally 50 houses. Former sunken houses excavated at Roztoky near Prague were originally about 1 m deep, but the preserved sedimentary infill 40–70 cm thick is composed of three to four layers marked as P, G, C and B (Fig. 2). Each of the studied sunken houses has an oven in the corner and layer E, which was divided on the base of archaeological context and sedimenthological observations, refers to the infill of the oven.

Description: *layer P* – A typical floor layer is usually missing or trampled by a background more rich in clay minerals. In some cases, a low number of voids are preserved. Organic matter is present in the form of punctuations, and forms a natural occurrence of organic matter within the alluvial zone. This layer does not contain any charcoal found in other archaeological remains. In some parts of the houses, this trampled layer has nearly disappeared or has not been preserved. This fact was interpreted as the result of cleaning activities inside the house, or the presence of wooden floor during the occupation phase (Fig. 3).

Layer G – The layer above is sometimes preserved as a dark, moderately sorted, silty, non-calcareous layer 1–5 cm thick. It is rich in organic matter decomposed to a variable degree, bone remains, and a large amount of charcoal characteristic of strong bioturbation. The microstructure is typical by the presence of vughs (Fig. 3). This lithological unit is preserved in ca. 30% of the studied objects. The layer is interpreted either as a residue of the last human activities in the house before the destruction, or as a part of a destructed roof.

Layer C – this layer is situated above layer G; it is largely free of archaeological remains, charcoal fragments or other remains of human activities. It is composed of light brown, non-calcareous silty loam, very similar to the material of the sedimentological background at the studied locality. The thickness of this layer is usually 10–50 cm and is continuous throughout the extent of the sunken house. The shaping [top surface] of this layer is usually reminiscent of a bowl with edges rising toward the peripheries of the house. The layer was macroscopically described as smeared on, which, in terms of micromorphology, means small concentrations of clay minerals originated due to the post-sedimentary processes caused by activities within the objects.

Layer B – The final destruction layer usually contains a huge amount of archaeological remains, charcoals, partly decomposed organic remains, burned bones, and stones from destroyed ovens. This layer is dark brown, non-calcareous silty loam approximately 10–50 cm thick, filling the uppermost part of the studied objects. This dish-shaped lithological layer was found in all objects at the studied locality. The dark brown colour of the layer is caused by a high concentration of micro-charcoal.

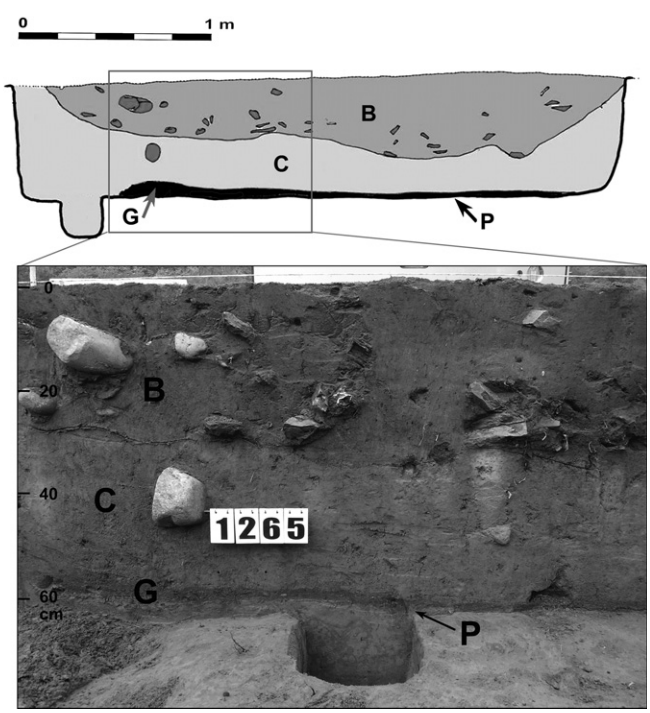

Fig. 2. Section of a typical house infill (house 1265). B, C, G, P: Distinctive layers of the house infill.

4.2. Anthracological analysis

The concentration of charcoal fragments was found to be rather low (Table 1). The average degree of the charcoal fragmentation was counted as 5 mm. The radial cracks within the charcoal fragments were observed in 8% of charcoal fragments. The results of the anthracological study are quite similar to those from the sedimentological record. All the layers show a very similar vegetation composition, except for Layer E which is identified as an oven infill (Fig. 4). A combination of three anthracological outcomes (the number of charcoal fragments, the anthracomass, and the qualitative frequency of charcoal species) was used for determining the sunken house layers and the reconstruction of vegetation patterns in the surrounding landscape.

4.2.1. The number of charcoal fragments

In total 10,731 charcoal fragments of eighteen tree taxa were identified. Oak (*Quercus* sp.) clearly dominated, while hornbeam (*Carpinus betulus*), birch (*Betula* sp.), Scots pine (*Pinus sylvestris*) and maple (*Acer* sp.) were also commonly preserved (Fig. 4). A mosaic of oak-hornbeam forest, sparse coppice and brushwood used for pasture probably surrounded the settlement. Remarkably, two woody species indicating pastures were discovered: rarely preserved juniper (*Juniperus communis*) and cornel (*Cornus* sp.). Despite the locality being situated on the bank of the Vltava River, the presence of the riverine species (alder, willow/poplar) was low.

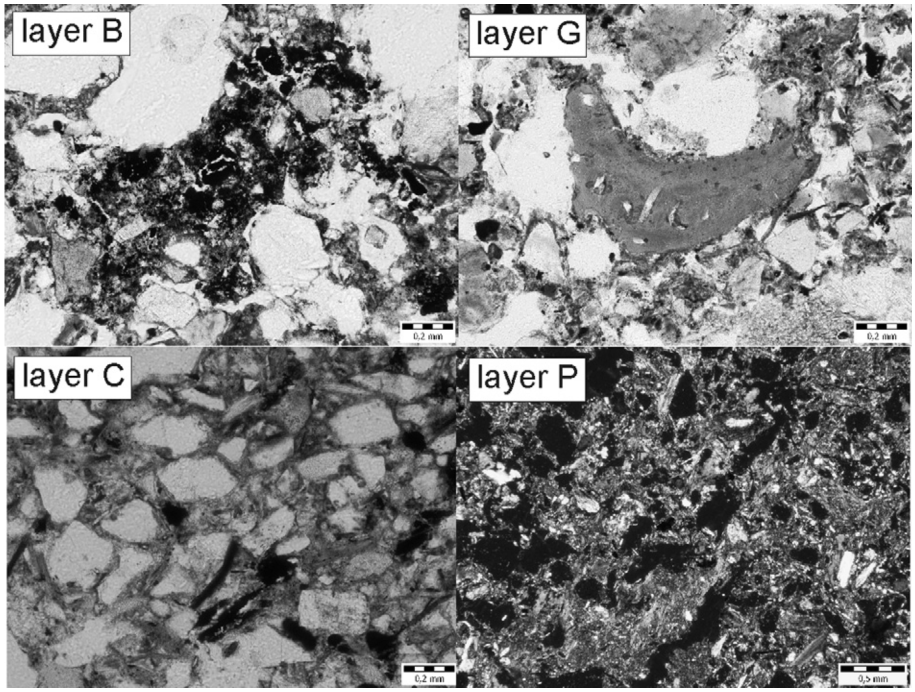

Fig. 3. Typical micromorphological features observed in the sedimentary infill of the Early Medieval sunken houses. B – micromorphological features of layer B; unsorted material of minerals, charcoal and decomposed matter dumped into the uppermost infill of a house (plan- polarized light). C – accumulations of clay minerals as the typical micromorphological features of layer C. (cross-polarized light) G – bioturbated material composed mainly of decomposed and non-decomposed organic matter, charcoal, unsorted material and fragments of bones. (Plan-polarized light) P – compacted structure of the uppermost part of layer P. (plan-polarized light).

Ovens (layer E) were relatively specific structures of the former sunken houses and contained the highest amount of charcoal fragments. The spectrum of species represents the composition of wood used as fuel from a short time before the abandonment of the house (Fig. 4). Layer E differs from other layers in its high proportion of beech (*Fagus sylvatica*), fir (*Abies alba*), Scots pine and birch charcoals.

A relatively high number of charcoal fragments were found in layer B. The cover of layer B, which also contains a high proportion of bones and macrofossil remains, is interpreted as a dump layer. The number of charcoal fragments in layer G is only slightly lower than in layer B, however, a slightly higher number of beech charcoal fragments were found in layer B. The lowest number of fragments (and charcoal species) was found in layer C.

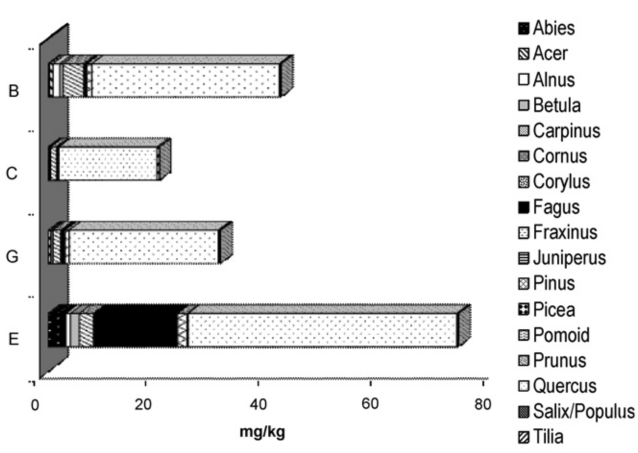

Fig. 4. Histogram of charcoal species in distinguished layers from twenty Early Medieval houses a) number of charcoal fragments b) anthracomass c).

4.2.2. *The anthracomass*

The highest average anthracomass was found in the ovens. Layer E is the richest (73.08 mg/kg), followed by layer B (41.50 mg/kg). Layer G has an average anthracomass of 30.72 mg/kg, and layer C contained the lowest average anthracomass (19.83 mg/kg). Oak represented the highest anthracomass among all layers. Hornbeam, pine, birch, alder and maple reached lower values accordingly. The anthracomass of the rest of the found species was relatively low (Fig. 4). Remarkable are the high anthracomass values of fir, Scots pine and beech in the ovens (layer E).

4.2.3. *Qualitative frequency of charcoal taxa*

The contexts of layers E and B are outstanding for the higher taxa frequencies (see Table 1). Oak, the light-demanding and coppiced wood, is quite frequent for most of the oven infills but fir, beech or Scots pine also form a significant part (Fig. 5). Layer B is dominated by oak, birch, hornbeam, Scots pine but also maple, beech, hazel (*Corylus avellana*) and elm (*Ulmus* sp.). Many species with a low anthracomass were quite frequent in layers G and C.

Oak was present everywhere. Other high frequented species were birch, hornbeam, Scots pine, and also ash (*Fraxinus excelsior*). Layer C is characterized by relatively higher frequencies of fir and beech. The frequencies of maple and hazel reached higher values in layer B.

4.3. *Regional vegetation*

Fig. 6 shows the results of pollen-analytical corroboration of the studied off-site sedimentary profile. Based on these results, we will now briefly describe regional vegetation development using the advantage of the pollen diagram zonation.

In zone BRV-1 the local mire had nutrient-rich alder carr (*Alnus*, monolete fern spores), the close surroundings had *Corylus* shrublands, and natural forest remnants contained *Tilia*, *Ulmus*, and *Fagus*. During zone BRV-2 the local fen was less nutrient-rich with

	Abies	*Acer*	*Alnus*	*Betula*	*Carpinus*	*Cornus*	*Corylus*	*Fagus*	*Fraxinus*
E	47.2	22.2	22.2	80.6	66.7		30.6	50.0	11.1
G	14.3	25.0	10.7	50.0	46.4	3.6	27.6	10.7	17.6
C	33.3	6.6	13.3	40.0	60.0		7.1	28.6	20.0
B	22.7	40.9	22.7	72.7	77.2	4.5	31.8	31.8	13.6

	Juniperus	*Pinus*	*Picea*	*Pomoid*	*Prunus*	*Quercus*	*Salix/Populus*	*Tilia*	*Ulmus*
E	2.7	55.6	16.7	11.1	2.7	100.0	11.1	11.1	11.1
G	7.1	46.4		17.2	3.6	100.0	7.1	14.3	7.1
C		46.7				100.0	6.6	6.6	6.6
B		59.1	4.5	4.5	4.5	100.0	9.1	13.6	22.7

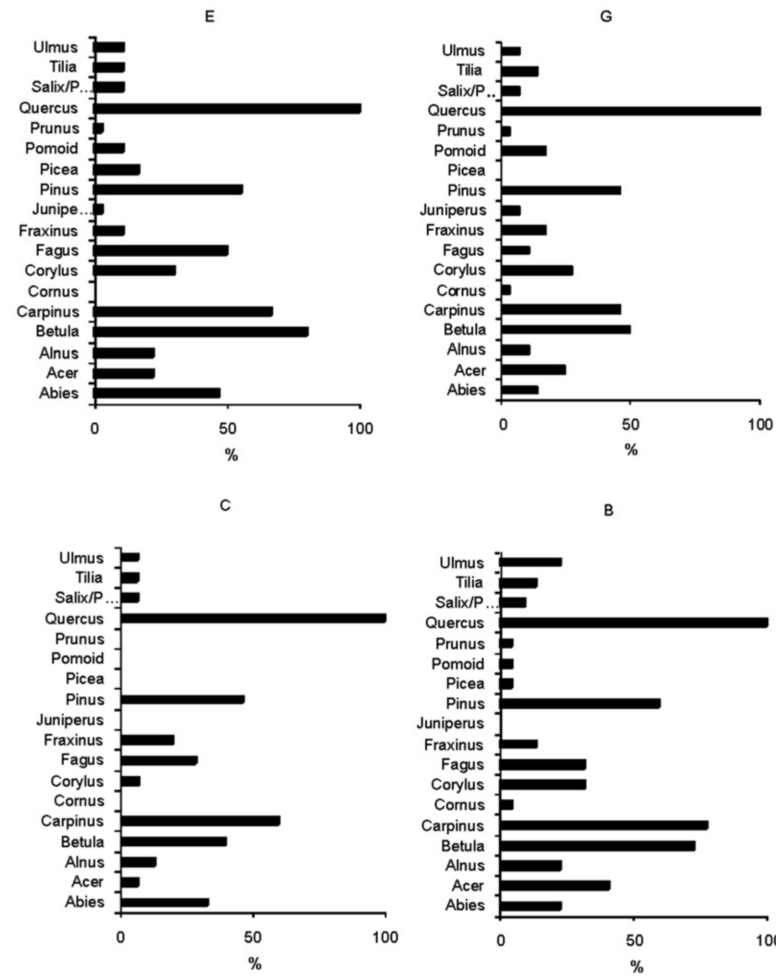

Fig. 5. Qualitative frequencies of charcoal species in distinguished layers (B, C, G, E).

Betula, Cyperaceae, *Potentilla*-type, and Gramineae, while *Tilia* and *Ulmus* disappeared from the surroundings. The compositional changes in the woodlands can be attributed to increased human influence as indicated by rising curves of most of anthropogenic indicators. During zone BRV-3, the dominance of *Pinus* (surely *P. sylvestris*) and the scarcity of herbal taxa suggest open, nutrient-poor forest.

During zone BRV-4, maxima of *Quercus* and *Abies* and increase of *Fagus*, *Corylus*, and *Alnus* indicate partial forest recovery in the surrounding region. Local fires (shown by microscopic charcoal particles curve) might have decimated the *Pinus* trees near the site. The transition between zones BRV-4 and BRV-5 is dated back to the Early Medieval period. This is the time when the studied settlement at Roztoky was in full prosperity. Pine (*Pinus*), oak (*Quercus*) and silver fir (*Abies alba*) had special importance in the regional vegetation at this particular period of time.

Grazing indicators increase stepwise in zones BRV-5, 6, and 7. Crop cultivation (*Secale cereale* etc.) became dominant in zone BRV-7 that dates to High Medieval and Modern periods.

5. Discussion

5.1. Composition of surrounding vegetation

The rich collection of anthracological material (a total of 10,731 charcoals representing 18 species) allows us to make a rather precise inference of the tree species composition in the settlement's surroundings. The concentration of charcoal fragments was generally rather low. Due to this, the low concentrations of charcoal allowed us to determine all fragments in the samples. Low numbers of charcoals in the samples were caused by the short period of the existence of the settlement. Therefore, the charcoal in all studied

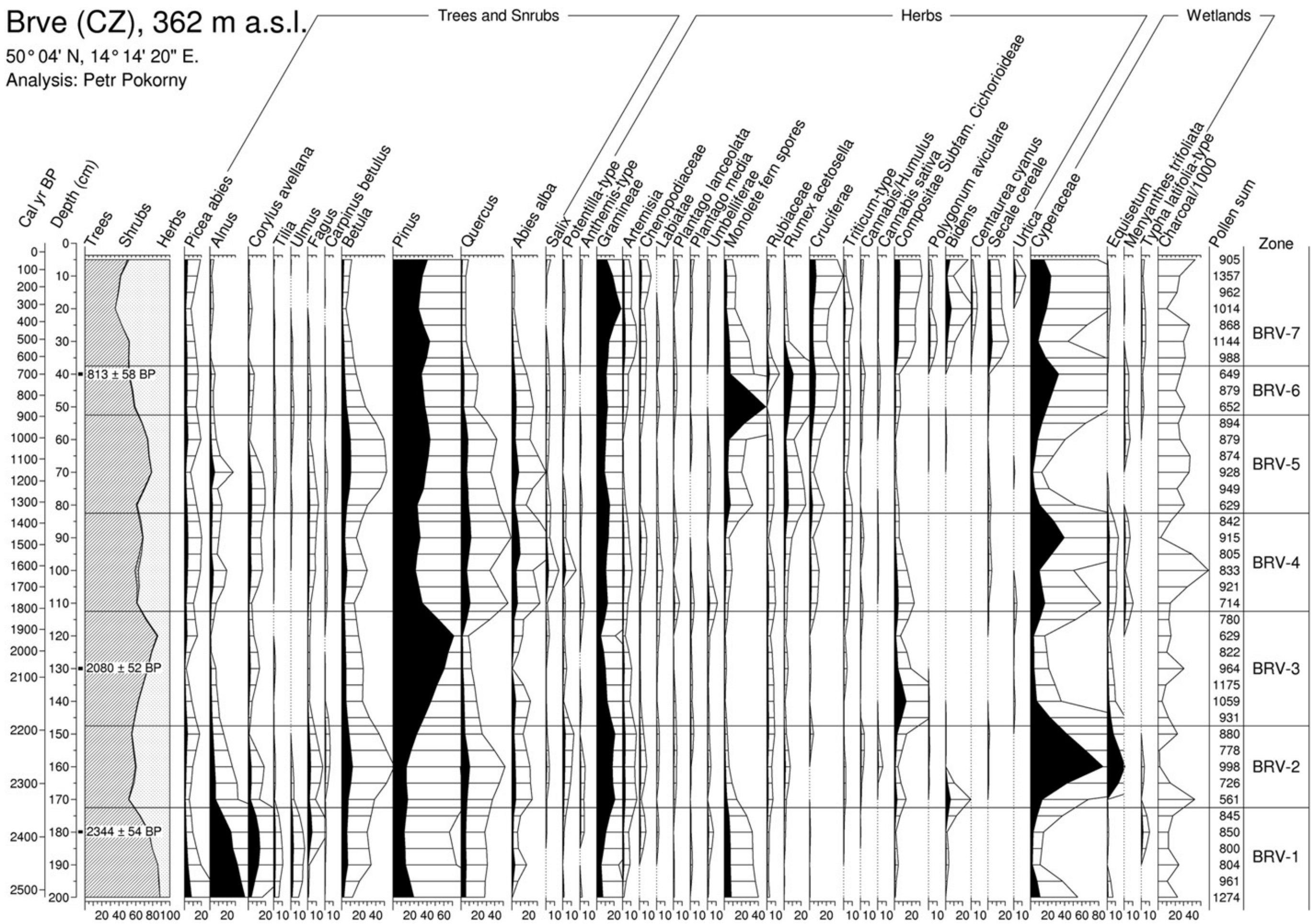

Fig. 6. Percentage pollen diagram from the studied sections of organic sediments (peat) analyzed by P. Pokorný. The period of interest overlaps roughly with the depth 80–90 cm (6th to 7th centuries A.D. according to the interpolations of radiocarbon measurements).

layers is probably, in various ways, a modified picture of the same vegetation.

Charcoal of layer B represents common firewood. The cover of layer B, which also contains a high proportion of bones and macrofossil remains, is interpreted as a dump layer. This charcoal content of the layer is less transformed than charcoal content of layers marked as C and G, and probably better represents the composition of common firewood. This interpretation is supported by higher anthracomass, a higher amount of charcoals per kilogram, and also a higher qualitative frequency of the species than in layers G and C. Layers B, G, E are of the same species diversity (17 species), whereas layer C is relatively poorer in charcoal species (13 species). The ascertained differences reflect the origin of the layers and also the way houses were used and the way they decayed and filled in.

Layer E is the infill of an oven. It contains charcoal left in the oven before the house was abandoned. The anthracomass in it was found to be the highest of all studied layers. Similarly to other data sets from the ovens, the species composition is a result of a specific activity. A high abundance of fir, Scots pine, and beech charcoal fragments, along with coppiced and light-demanding species is very common. Coniferous wood could have been collected selectively as structural timber. This suggests a burning of the construction by the inhabitants before they left, or burned waste wood from newly built dwellings. Burning beech wood produces heat for a very long time, which points to the use of the beech firewood for a specific activity.

An interpretation toward the common presence of above mentioned trees in regional vegetation is supported by the results of pollen analyses from relatively nearby sedimentary sequence "Brve" and also by previous regional vegetation-historical study (Pokorný, 2005). At the period of interest, regeneration of woods took place in the wider region. Both coniferous and broadleaf taxa were involved in this woodland regeneration. Nevertheless, pine was dominant as the results of continuous human presence and influence.

A comparison with anthracological data sets from other Prague-Korčak culture sites is rather difficult due to the following reasons: i) published results are based on small data sets (Beneš, 2005); ii) published charcoal data sets are related to younger phases of the Early Middle Ages (Petrlíková and Beneš, 2008); iii) published Early Medieval data sets are linked with different vegetation types (Opravil, 2000). On the other hand, comparisons with neighboring anthracological data sets dated to the Bronze Age, Hallstatt, La Tene and Roman periods (e.g., Novák, 2007; Šmejda and Kočár, 2007) give us a very similar picture to that of the vegetation composition of the localities. The presented anthracological data from Roztoky, as well as regional pollen data from the same period, are remarkable for the high frequency of trees resistant to pollarding and coppicing. Most of the found species are typical of the early succession stages and high pasture pressure.

All the above mentioned founds are very probably the result of an intensive, long-term human impact on vegetation in the region. The short-term character of the Early Medieval settlement at

Roztoky and the tree species composition imply the probable long-term human impact on the vegetation before the appearance of the Prague-type Culture. This result is well confirmed by studied pollen record. Species richness documented by the charcoal data is much higher compared to previous studies where, generally, oak-hornbeam forests or the riverine willow/alder/poplar-dominated forests were documented. In the charcoal remnants, the relative abundance of species typical of alluvial forests is relatively low, indicating that the riverbeds were mostly devoid of trees.

A high abundance of charcoal with radial cracks is worth noting. Radial cracks in charcoal, caused by rapid dehydration and conflagration, may indicate burning of green wood (e.g., Théry-Parisot, 2001). Dry firewood was may be unavailable due to a dense settlement with an intensive wood consumption, or, more interestingly, it was used for specific purposes such as fish smoking (we expect a high abundance of salmon in the Vltava River at that time) or repelling of insects.

5.2. The charcoal information value in the sedimentological context

The representativeness of charcoal from archaeological contexts and their potential for paleoecological reconstructions is a long discussed topic (e.g., Clark et al., 1998; Delhon, 2006). The anthracomass is usually interpreted as one of the best indicators of the abundance of species in the analyzed file (Carcaillet and Thinon, 1996). This is caused by the fragmentation, post-depositional processes, separation and/or drying procedures. The correlation of anthracomass with the wood hardness of species (species with soft wood are less abundant due to easier burning) is still questionable.

The amount of charcoal pieces is positively correlated with the anthracomass in the presented study with exceptions: the fragment/anthracomass ratio was apparently higher for fir and low for beech. The qualitative frequency of species was used to highlight the species diversity. However, the results of our study show that the final anthracological interpretation is controlled not only by human practices and combustion processes: additional factors are post-depositional agents, sampling and quantification methods.

5.3. The interpretation of the origin of layers

Our interpretation of sedimentary units recognized in the infills of Prague - Korčak sunken houses at Roztoky is primarily based on field observations made during the archaeological excavations and later verified by the method of micromorphology (microstratigraphy of sedimentary units). Based on this type of data, we can assume that layer P developed due to the porosity reduction of the background overbank deposits of the Vltava River due to compaction by trampling (Simpson et al., 1999; Rentzel and Narten, 2000). The absence of the cultural layer may be the result of cleaning activities but the presence of a wooden floor is also taken into account. Gebhardt and Langohr (1996) observed a complete disappearance of wooden floor within the oxidation zone in the medieval motte at Werken (Belgium), in contrast to its perfect preservation in the reduction zone. Small fragments of organic matter are preserved in the studied sections. Therefore, if a wooden floor existed there, it was probably removed before the house was abandoned. The cleaning, resulting in a depletion process, usually involves the removal of refuse from the activity area (La Motta and Schiffer, 1999). The absence of the accumulation of the clay fraction was probably due to the repeated maintenance of the floor. During the use of the houses, coarser material was swept away periodically but finer particles remained and became incorporated into the floor (Davidson et al., 1992). The very fine mineral material might also be carried into the houses on the soles of feet or as an airborne dust (Macphail et al., 1990; Milek, 1997). The presence of the small pit features within studied features is, on one side, an indirect indicator showing that the floors were maintained, disturbed in some way and not really covered by a wooden floor (compare with Miller et al., 1998) or skin (Jones et al., 2010). On the other hand, however, holes in the wooden floor would provide additional support to sticks or bars purposely and repeatedly driven into the sediment below.

The interpretation of layer G is based mainly on the high abundance of decomposed and non-decomposed organic matter, mesofauna excrements, bone fragments, charcoal and bioturbation; all this with no sign of compaction. This can happen when the central part of the roof collapses (due to the human or natural influence) (Simpson et al., 1999). The present waste causing increased bioturbation (Jones et al., 2010) is probably of a post-abandonment origin, very probably a stochastic waste deposition in the ruined house/house pits. No gradual accumulation and compaction of domestic debris was observed (Simpson et al., 1999). Structural collapse can also introduce objects onto the room floors, primarily through the deposition of objects used as construction material (Schiffer, 1985, 1996), or the waste deposited on the roof during long-term usage of the houses (Goldberg and Macphail, 2006). Another possibility for the origin of layer G is the deposition of an upper soil horizon from the new house built nearby. Soil surface enclosing the Early Medieval houses probably contained decomposed organic matter, mesofauna excrements, bone fragments and charcoal. This hypothesis supports a secondary use of construction timber from the abandoned houses.

Layer C represent an infill of a house pits either “naturally”, after a collapse after abandonment, or with an intension to deposit the redundant material from the new house built nearby; this can be a very quick process and these layers usually lack organic contamination.

Surface layer B aggraded probably as a dump (compare with Simpson et al., 1999); it contains a large amount of ash, which was commonly washed to layer C. It probably served as a secondary refuse deposition (La Motta and Schiffer, 1999) for that also produced by cleaning activities (compare with interpretations of the uppermost part of layer P).

6. Conclusions

A combination of sedimentological observations and micromorphological analyses provided a good context for the interpretation of the environmental history of the study area.

The presented anthracological data are remarkable for their high frequency of woods resistant to pollarding and coppicing. Most of the ascertained species are typical of the degraded pasture or early succession stages and high pasture pressure. The settlement was probably surrounded by a mosaic of oak-hornbeam forest, sparse coppice and brushwood used for pasture. The abundance of species typical of alluvial forests is relatively low, indicating that the riverbeds were mostly devoid of trees. This interpretation has been confirmed by pollen analysis of relatively nearby, continuous and radiocarbon-dated peat profile.

The rather low concentration of charcoal fragments in the infills of the studied sunken houses was most likely caused by the short period of the Early Medieval settlement. Charcoals in all studied layers probably represent, in various ways, a modified picture of the same vegetation. Together with coppiced and light-demanding species, the high abundance of silver fir, Scots pine and beech charcoals was very common. A high number of coniferous charcoals may indicate residues of structural timber. Nevertheless, coniferous trees were rather common element in regional vegetation, as revealed by pollen analyses.

Frequently found charcoals coming most probably from the originally fresh wood suggest its usage either as an alternative fuel or for specific purposes (fish smoking, repelling of insects).

The combination of several independent interpretation methods (charcoal qualitative frequency, anthracomass, and the number of charcoal fragments/kg, pollen analyses) provides the best picture of a vegetation cover in the vicinity of the studied locality. However, the results of our study show that not only human practices and combustion processes, but above all post-depositional effects, sampling and quantification methods can significantly contribute to the final interpretations.

Acknowledgments

The authors thank Jiří Sádlo, Tomáš Bešta and Albert Krovinar for inspiring critical comments on the manuscript, Václav Cílek for positive spirit, and Petr Kuneš for his help with the picture. The research was funded by a project of the Czech Science Foundation: GAČR P405/10/2289, the Ministry of Education of the Czech Republic grant project MSM 600 766 5801, and Research Program AV0Z 30130516 of the Institute of Geology AS CR, v. v. i. The Grant Agency of the Academy of Sciences of the Czech Republic (project No. IAAX00020701) supported pollen-analytical part of the investigation.

References

Asouti, E., Austin, P., 2005. Reconstructing woodland vegetation and its relation to human societies, based on the analysis and interpretation of archaeological wood charcoal macro-remains. Environ Archaeol 10, 1–18.

Baran, V.D., 1988. Pražskaja kultura Podnestrovja. (Prague culture Podnestrovja). Naukova Dumka, Kijev.

Beneš, J., 2005. Antrakologická analýza uhlíků ze slovanských zásobních jam ve Statenicích. (Anthracological analysis of charcoal from the Early Medieval storage pits from Statenice). Archeologie Ve Středních Čechách 9, 557–559.

Beug, H.J., 2004. Leitfaden der Pollenbestimmung für Mitteleuropa und angrenzende Gebiete. Verlag Dr. Friedrich Pfeil, München.

Bullock, P., Fedoroff, N., Jongerius, A., Stoops, G., Tursina, T., 1985. Handbook for Soil Thin Section Description. Waine Research Publications, Wolverhamton, UK.

Carcaillet, C., Thinon, M., 1996. Pedoanthracological contribution to the study of the evolution of the upper treeline in the Maurienne Valley (North French Alps): methodology and preliminary data. Rev Palaeobotany Palynology 91, 399–416.

Chabal, L., 1992. La représentativité paléoécologique des charbons de bois archéologiques issus du bois de feu. Bulletin de la société botanique de France. Actualités Botaniques 139, 213–236.

Clark, J.S., Lynch, J., Stocks, B.J., Goldammer, J.G., 1998. Relationships between charcoal particles in air and sediments in westcentral Siberia. The Holocene 8, 19–29.

Courty, M.A., Goldberg, P., Macphail, R., 1989. Soils and Micromorphology in Archaeology. Cambridge University Press, Cambridge.

Curta, F., 2008. Utváření Slovanů (se zvláštním zřetelem k Čechám a Moravě). (The making of the Slavs (with a special emphasis on Bohemia and Moravia)). Archeologicke Rozhledy 60, 643–694.

Davidson, D.A., Carter, S.P., Quine, T.A., 1992. An evaluation of micromorphology as an aid to archaeological interpretations. Geoarchaeology 7, 55–65.

Delhon, C., 2006. Palaeo-ecological reliability of pedo-anthracological assemblages. In: Dufraisse, A. (Ed.), Charcoal Analysis: New Analytical Tools and Method for Archaeology, 1483. BAR international series, pp. 9–24.

Dolinescu-Ferche, S., 1992. Habitats des VIe et VIIe siècles de notre ère à Dulceanca IV. Dacia NS 36, 125–177.

Dolukhanov, P.M., 1996. The Early Slavs, Eastern Europe from the Initial Settlement to the Kievan Rus. Longman, London and New York.

Dufraisse, A., 2008. Firewood management and woodland exploitation during the late Neolithic at Lac de Chalain (Jura, France). Vegetation Hist. Archaeobotany 17, 199–210.

Einarsson, B.F., 2008. Blót houses in Viking age farmstead cult practices new findings from south-eastern Iceland. Acta Archaeologica 79, 145–184.

Figueiral, I., 1992. Méthodes en anthracologie - Étude des sites du Bronze Final et de l'Âge du Fer du Nord-Ouest du Portugal. Bulletin de la Société Botanique de France 139, 191–204.

Gebhardt, A., Langohr, R., 1996. Archaeo-Pedological study of post-occupational processes from a medieval motte in Werken (West Flanders, Belgium). Geoarchaeology 14, 595–620.

Gojda, M., 1991. The Ancient Slavs. Settlement and Socicety. Edimborough University Press, Edimborough.

Goldberg, P., Macphail, R., 2006. Practical and Theoretical Geoarchaeology. Blackwell Publishing, Malden, Oxford, Victoria.

Goldberg, P., Holliday, V.T., Ferring, C.R., 2001. Earth Sciences and Archaeology. Kluwer Academic/Plenum Publishers, New York.

Heiss, A.G., 2000. Anatomy of European and North American woods – an interactive identification key. http://www.holzanatomie.at/ (accessed 22.08.06).

Jones, R., Challands, A., French, Ch., Card, N., Downes, J., Richards, C., 2010. Exploring the location and Function of a late Neolithic house at Crossiecrown, Orkney by Geophysical, geochemical and soil micromorphological methods. Archaeol Prospect 17, 29–47.

Kangur, M., 2002. Methodological and practical aspects of the presentation and interpretation of microscopic charcoal data from lake sediments. Vegetation Hist Archaeobotany 11, 289–294.

Krüger, B., 1967. Dessau-Mossigkau. Ein frühslawischer Siedlungsplatz im mittleren Elbgebiet. Akademie-Verlag, Berlin.

Kuna, M., Profantová, N., 2005. Počátky raného středověku v Čechách. Archaeologický výzkum sídlištní aglomerace kultury pražského typu v Roztokách. (The onset of the Early Middle Ages in Bohemia. Archaeological research at a large settlement site of the Prague-type culture at Roztoky). ARÚ AVČR, Praha.

Kuneš, P., Abraham, V., Kovařík, O., Kopecký, M., Břízová, E., Janovská, V., Knipping, M., Kozáková, R., Nováková, K., Petr, L., Pokorný, P., Rozková, A., Rybníčková, E., Svobodvá-Svitavská, H., Wacnik, A., 2009. Czech Quaternary Palynological Database – PALYCZ: review and basis catatistics of the data. Preslia 81, 209–238.

Macphail, R.I., Courty, M.A., Goldberg, P., 1990. Soil micromorphology in archaeology. Endeavour 14, 163–171.

Milek, K.B., 1997. Micromorphology and the medieval urban environment: examples from Ely and Peterborough, Cambridgeshire, England. In: Boe, G., Verhaeghe, F. (Eds.), Environment and Subsistence in Medieval Europe: Papers of the Medieval Europe. Zellik. Instituut voor het Archeologisch Patrimonium, pp. 155–168.

Miller, J., Dikson, J.H., Dixon, T.N., 1998. Unnusual floor plants from Oakband Cranog, Loch Tay, Scottish Highlands: cloudberry, opiumpoppy and spelt wheat. Antiquity 72, 805–811.

La Motta, V., Schiffer, M.B., 1999. Formation processes of house assemblages. In: Allison, P.M. (Ed.), The Archaeology of Household Activities. Routledge, London.

Nelle, O., Dreibrodt, S., Dannath, Y., 2010. Combining pollen and charcoal: evaluating Holocene vegetation composition and dynamics. J. Archaeological Sci 37, 2126–2135.

Neumann, K., 1989. Vegetationsgeschichte der Ostsahara im Holozän. Holzkohlen aus prähistorischen Fundstellen. In: Kuper, R. (Ed.), Forschungen zur Umweltgeschichte der Ostsahara. Heinrich-Barth-Institut, Köln, pp. 13–181.

Novák, J., 2007. Antrakologická analýza vybraných objektů časně laténského sídliště v Chržíně. (Analysis of selected features from the early La tene settlement of Chrzin). Archeologické Rozhledy 59, 517–522.

Opravil, E., 2000. Holz aus frühmittelalterlichen Gräberfeldern in Mähren. In: Polaček, L., Marek, O., Skopal, R. (Eds.), Zum Burgwall von Mikulčice. Bd. 4.Brno, Archäologisches. Institut der Akademie der Wissenschaften der Tschechischen, Republik Brno, pp. 171–176.

Parczewski, M., 1989. Żukowice pod Głogowem w zaraniu średniowiecza. (Żukowice pod Głogowem at the dawn of the Middle Ages). Anfangdes Mittelalters, Głogów.

Petrlíková, V., Beneš, J., 2008. Antrakologická analýza uhlíků ze sídelního areálu doby laténské, římské a hradištní v Lovosicích a z výrobního centra doby římské v Kyjicích. (Anthracological analysis of charcoal fragments from the La Tène, Roman and the Early Medieval settlement area in Lovosice and from the Roman period production centre in Kyjice). Archeologické Rozhledy 60, 93–113.

Pokorný, P., 2005. Role of man in the development of Holocene vegetation in Central Bohemia. Preslia 77, 113–128.

Reimer, P.J., Baillie, M.G.L., Bard, E., Bayliss, A., Beck, J.W., Blackwell, P.G., Bronk Ramsey, C., Buck, C.E., Burr, G.S., Edwards, R.L., Friedrich, M., Grootes, P.M., Guilderson, T.P., Hajdas, I., Heaton, T.J., Hogg, A.G., Hughen, K.A., Kaiser, K.F., Kromer, B., McCormac, F.G., Manning, S.W., Reimer, R.W., Richards, D.A., Southon, J.R., Talamo, S., Turney, C.S.M., van der Plicht, J., Weyhenmeyer, C.E., 2009. INTCAL 09 and MARINE09 radiocarbon age calibration curves, 0–50,000 years Cal BP. Radiocarbon 51, 1111–1150.

Rentzel, P., Narten, G. B., 2000. deZur Entstehung von Gehniveans in sandiglehmigen Ablagerungen-Experimente und archäologische Befunde. Jahresberichte der Archäologischen Bodenforschung, Basel-Stadt.

Schiffer, M.B., 1985. Is there a Pompeii Premise in archaeology? J. Anthropological Res 41, 18–41.

Schiffer, M.B., 1996. Formation Processes of the Archaeological Record. University of Utah Press, Salt Lake City.

Schweingruber, F.H., 1990. Microscopic wood anatomy, third ed. Eidgenössische Forschungsanstalt für Wald, Schnee und Landschaft.

Sedov, V.V., 1982. The Eastern Slavs in the 6th-13th centuries AD. In: Vostochnye slavjane, vol. VI-XIII. Archeologia SSSR, Moscow.

Simpson, I.A., Milek, K.B., Guðmundsson, G., 1999. A reinterpretation of the great pit at Hofstaðir, Iceland using sediment thin section micromorphology. Geoarchaeology 14, 511–530.

Šmejda, L., Kočár, P., 2007. Botanické makrozbytky z knovízského sídliště v Praze-Hostivaři: vektorová syntéza dat. (Botanical Macro-Remains from the Late Bronze Age (Knovíz-Culture) settlement at Prague-Hostivař: a Vector Synthesis). In: Šmejda, L., Vařeka, P. (Eds.), Opomíjená archeologie 2005–2006. KAR ZČU, Plzeň, pp. 192–208.

Stoops, G., 2003. Guidelines for analysis and description of Soil and Regolith Thin Sections. Soil Science Society of America, Medison, Wisconsin.

Talon, B., Carcaillet, Ch, Thinon, M., 1998. Études pédoanthracologiques des variations de la limite supérieure des arbres au cours de l'Holocene dans les Alpes Francaises. Géographie physique et Quarternaire 52, 1–14.
Teodor, D. Gh., 1994. Slavii la nordul Daunarii de Jos in secolele VI–VII d. h. (The Slavs at the North of the Lower Danube in the VI–VII Centuries). Archeologica Moldovei 18, 223–225.
Théry-Parisot, I., 2001. Economie des combustibles au Paléolithique. Expérimentation, anthracologie, Taphonomie. D.D.A. 20. CNRS-Editions, Paris.
Théry-Parisot, I., Chabal, L., Chrzavzez, J., 2010. Anthracology and taphonomy, from wood gathering to charcoal analysis. A review of the taphonomic processes modifying charcoal assemblages, in archaeological contexts. Palaeogeography Palaeoclimatology Palaeoecology 291, 142–153.
Willcox, G., 1974. A History of Deforestation as Indicated by Charcoal Analysis of Four Sites in Eastern Anatolia. Anatol Stud 24, 117–133.
Zeman, J., 1976. Nejstarší slovanské osídlení Čech - Die älteste slawische Besiedlung Böhmens. Památky Archeologické 67, 115–236.

3. Shrnutí

Studium jeskynních sedimentů a pokus o aplikaci provenienčních metod v mé diplomové práci (**Lisá a Přichystal, 2001**) v podstatě předurčily další směřování mé vědecké kariéry. Studie zaměřené na provenienci eolických sedimentů (hlavním téma mé dizertační práce) prohloubily mé znalosti o provenienčních metodách zaměřených na studium asociací těžkých minerálů (**Lisá et al, 2005**) studium geochemie granátů (**Lisá et al., 2009**) nebo typologie zirkonů (**Lisá a Uher, 2006**). Výstupem těchto prací byly jedny z prvních a prozatím nejkomplexnějších prací zaměřených na provenienci sprašových sedimentů na území naší republiky. Současně se mi podařilo začlenit do metodiky provenienčních studií i mikromorfologii povrchu křemenných zrn (**Lisá, 2004**), kterou jsem později několikrát s úspěchem použila v jinak směřovaných studiích (**Nývlt et al., 2011**; **Mentlík et al., 2010**; **Engel et al., 2010**; **Křížová et al., 2011**). Přínosem této metodiky bylo například rozpoznání sedimentů transportovaných ledovcem v případě Šumavských jezer nebo sedimentů transportovaných eolickými procesy v případě Labského dolu. Přestože i v současnosti publikuji studie specializované na změny klimatu (**Hošek et al., 2014, 2015**; **Bešta et al., 2015**; **Antonie et al., 2013**; **Fuchs et al., 2012**; **Wisniewski et al., 2015**; **Petr et al., 2013**; **Cílek et al., 2013**; **Lisá et al., 2013a,b**), mé další profesní směřování ovlivnilo začlenění do projektu Cambridge University a počátek spolupráce s archeology. Postupně vzniklo několik studií v rámci tohoto projektu orientovaných na vztah měnícího se klimatu, formačních procesů v krajině a lidského impaktu (**Lisá et al., 2012, 2013c, 2014**), a to především během MIS3 (marinní izotopové stádium 3).

Studie zaměřené na interpretace formačních procesů v přirozeném a archeologickém kontextu by však nebylo možné provádět bez hlubších znalostí geoarcheologických metod a aplikace metod, jako je mikromorfologie, environmentální magnetismus nebo geochemická charakteristika studovaných sedimentů. Postupně bylo možné sestavit určitou metodiku geoarcheologie (**Bajer ed., 2014**; **Lisá a Bajer, 2014**), která je dnes běžně používána v České republice a přednášena na několika universitách. Nejdůležitější projekty posledních let sponzorované především agenturou GAČR zahrnovaly například výzkum dřevěného předhradí (**Plaček et al., 2015),** v rámci kterého byla například publikována komplexní celosvětově ojedinělá multioborová studie směřovaná na údržbu středověké stáje (**Dejmal et al., 2013**), výzkum neolitických rondelů, při kterém jsme provedli první studii zaměřenou na porovnání výplní hrotovitých příkopů z doby neolitu a doby římské (**Lisá et al., 2015**) a výzkum ranně středověké lokality Roztoky u Prahy, kde bylo možné identifikovat a interpretovat vznik, vývoj a zánik objektů a především jejich podlahových horizontů (**Novák et al., 2012**; **Kuna et al., 2013**). Další podobné menší projekty byly směřovány na studium podlahových horizontů v rámci pravěkých a středověkých kontextů (**Parma et al., 2012**; **Beran et al., 2014**) nebo konceptu Dark Earth (**Parma et al., 2015**).

Studium formačních procesů je dnes již nezbytnou součástí environmentálních studií a je zde viditelná snaha začleňovat tento metodický pohled i do projektů zaměřených na archeologii. Metodické přístupy používané v tomto směru se neustále rozvíjejí a do budoucna má tento obor před sebou velký potenciál.

4. Použitá literatura

Aalkaseeva, V.A. (2005): Micromorphology of Quartz Grains Surface as Indicator of Glacial Sedimentation Conditions: Evidence from the Protva River Basin.- Lithology and Mineral Resources, 40, č. 5, s. 420–428.

Adamová, M., Havlíček, P. (1996): Geochemická charakteristika spraší významných moravských lokalit.- Zprávy o geologických výzkumech v roce 1996, s. 91 – 94.

Antoine, P., Rousseau, D.D., Degeai, J.P., Moine, O., Lagroix, F., Kreutzer, S., Fuchs, M., Hatté, Ch., Gauthier, C., Svoboda, J., **Lisá, L.** (2013): High-resolution record of the environmental response to climatic variations during the Last Interglacial-Glacial cycle in Central Europe: The loess-palaeosol sequence of Dolní Věstonice (Czech Republic).- Quaternary Science Reviews. 67, s. 17-38.

Bárta, M. (2005): Location of the old Kingdom pyramids in Egypt. Cambridge Archaeological Journal 15 (2), 177e191.

Bajer, A. (2003): Forest site relationships with parrent material: site conditions on various parent rocks in particular forest territories in the Czech Republic.- Ekológia, 22, č. 3, s. 5-18.

Bajer, A., Ložek V., Lisá L., Cílek V. (2015): Krajina a geodiverzita; neživá příroda jako základ krajinných a kulturních hodnot.- Mendelova univerzita v Brně, 159s.

Bastin, B. (1979): L'analyse pollenique des stalagmites: une nouvelle possibilité d'approche des fluctuations climatiques du Quaternaire.- Ann. Soc. Géol. Belg, 101, s. 13–19.

Besta, T., Novak, J., Dreslerova, D., Jankovská V., Bernardová, S., **Lisá L.**, Valentová D. (2015): Mid-Holocene history of a central European lake: Lake Komorany, Czech Republic.- BOREAS, 44, 3, s.563-574.

Beran V., Hajnalová M., Kos P., **Lisá L.,** Parma D. (2013): Geoarcheologický výzkum raně středověké kovárny z Modřic u Brna.- Rekonstrukce a experiment v archeologii.- živá archeologie, 15, s. 25-31.

Bosák, P. (2008): Karst processes and time.- Geologos vol. 14 (1), 2008, s. 15-36.

Bosch, R.F., White W. (2004): Lithofacies and transport of clastic sediments in karstic aquifers. In: Sasowsky, I.D., Mylroie, J. (ed.).Studies of Cave Sediments; Physical and Chemical Records of Paleoclimate.- Kluwer Academic/Plenum Publishers, New York, s. 1 – 22.

Burkhardt, R., Šerebl, Z. (1965): Možnosti metody težkých minerálu ve výzkumu krasových oblastí. - Kras v Ceskoslovensku 1, Brno.

Canti, M. G. (2003): Aspects of the chemical and microscopic characteristics of plant ashes found in archaeological soils.- Catena 54, s. 339-361.

Censier, C., Tourenq, J. (1986): Mise en évidence d'une extension occidentale des grés de Carnot (République Centrafricane) par analyses sédimentologiques comparées de gisements alluvionnaires diamantiféres. Géodynamique.- 1, č. 1, s. 21–32.

Cílek, V., Bárta, M., **Lisá, L.,** Pokorná, A., Juříčková, L., Brůna, V., Mahmoud, A.M.A., Bajer, A., Novák, J. and Beneš, J. (2012): Diachronic development of the Lake of Abusir during the third millennium BC, Cairo, Egypt.- Quaternary International, 266, s. 14-24.

Cílek, V., **Lisá, L.,** Bárta, M. (2010): The Holocene of the Abusir area. Abusir and Saqqara in the year 2010. Vol. 1. Prague: Czech Institute of Egyptology, Faculty of Arts, Charles University in Prague, 2011 - (Bárta, M.; Coppens, F.; Krejčí, J. eds.), s. 312-326

Cohen, K.M., Finney, S.C., Gibbard, P.L., Fan, J.-X. "International Chronostratigraphic Chart 2013" (PDF). http://www.stratigraphy.org/icschart/chronostratchart2013-01.pdf. ICS. Retrieved 15 June 2014

Cremer, M., Legigan, P. (1989): Morphology and Surface Texture of Quartz Grains from ODP site 645, Baffin Bay.- Proceedings of the Ocean Drilling Program, Scientific Results, 105, s. 21–28.

de Moor, J.J.W., Kasse, C., van Balen, R., Vandenberghe, J., Wallinga, J. (2008):Human and climate impact on catchment development during the Holocene – Geul River, the Netherlands.- Geomorphology 98, s. 316–339.

Dearing, J.A., Dann, R.J.L., Hay, K., Lees, J.A., Loveland, P.J., Maher, B.A., O'Grady, K. (1996): Frequency-dependent susceptibility measurements of environmental materials.- Geophysical Journal International 124, 228e240.

Dejmal, M., **Lisá, L.,** Nývltová Fišáková M., Bajer A., Petr, L., Kočár, P., Kočárová R., Nejman L., Rybníček M., Suvová Z., Culp, R., Vavrčík H. (2014): Medieval horse stable; The Results of Multi Proxy Interdisciplinary Research.- Plos One, 9, 3, e89273.

Engel Z., Nyvlt D., Krizek M., Treml V., Jankovska V., **Lisa L.** (2010): Sedimentary evidence of landscape and climate history since the end of MIS 3 in the Krkonose Mountains, Czech Republic.- Quaternary science reviews, 29, 7-8, s. 913-927.

Evans, M.E., Heller, F. (2003): Environmental Magnetism, Principles and Applications of Enviromagnetics.- Academic Press, An imprint of Elsevier Science, Oxford.

Fairchild, I., Baker, A (2012): Speleothem science: from process to past environments.- John Wiley & Sons, New York.

Ford, D and Williams, P W. (2013): Karst hydrogeology and geomorphology. John Wiley and Sons, New York.

French, Ch. (2002): Geoarchaeology in Action: Studies in Soil Micromorphology and Landscape Evolution.- Routledge.

Frolec, I. (2003): Kovářství.- Grada Publishing, Praha.

Fuchs, M., Kreutzer, S., Rousseau, D.D., Antoine, P., Hatté, Ch., Lagroix, F., Moine, O., Gauthier, C., Svoboda, J., **Lisá, L.** (2013): The loess sequence of Dolní Věstonice, Czech Republic: A new OSL-based chronology of the Last Climatic Cycle.- Boreas. Roč. 42, 3, s. 664-677.

Goldberg, P., MacPhail, R. (2006): Practical and Theoretical Geoarchaeology.- Wiley, London.

Grygar, T., Svetlik, I., **Lisa, L.**, Koptikova, L., Bajer, A., Wray, D.S., Ettler, V., Mihaljevic, M., Novakova, T., Koubova, M., Novak, J., Macka, Z., Smetana, M. (2010): Geochemical tools for the stratigraphic correlation of floodplain deposits of the Morava River in Straznicke Pomoravi, Czech Republic from the last millennium.- CATENA , 80, 2, s. 106-121.

Haesaerts, P. (1985): Les loess du Pléistoce`ne supérieur en Belgique. Comparaison avec les sequences d'Europe Centrale.- Bulletin A.F.E.Q. 22, s. 105–115.

Haesaerts, P., Teyssandier, N. (2003): The early Upper Paleolithic occupations of Willendorf II (Lower Austria): a contribution to the chronostratigraphic and cultural context of the beginning of the Upper Paleolithic in Central Europe. In: J. Zilhčo – F. d'Errico eds., The Chronology of the Aurignacian and of the Transitional Technocomplexes. Trabalhos de Arqueologia 33, Lisboa, 133–151.

Hays, J. D., Imbrie, J., Shackleton, N. J. (1976): Variations in the Earth's Orbit: Pacemaker of the Ice Ages". Science 194 (4270): 1121–1132. doi:10.1126/science.194.4270.1121. PMID 17790893

Hladil, J., Strnad, L., Šálek, M., Jankovská, V., Šimandl, P., Schwarz, J., Smolík, J., **Lisá, L.**, Koptíková, L., Rohovec, J., Böhmová, V., Langrová, A., Kociánová, M., Melichar, R., Adamovič, J. (2008): An anomalous atmospheric dust deposition event over Central Europe, 24 March 2007, and fingerprinting of the SE Ukrainian source.- Bulletin of Geosciences, 83, 2, s. 175-206.

Hoffmann, T., Erkens, G., Gerlach, R., Klostermann, J., Lang, A. (2009): Trends and controls of Holocene floodplain sedimentation in the Rhine catchment.- Catena 77, s. 96–106.

Hosek, J., Hambach, U., **Lisá, L.,** Matys Grygar, T., Horáček, I., Meszner, S., Knésl, I. (2015): An integrated rock-magnetic and geochemical approach to loess/paleosol sequences from Bohemia and Moravia (Czech Republic): Implications for the Upper Pleistocene paleoenvironment in central Europe.- Palaeography Palaeoclimatology Palaeoecology. 418, s. 344-358.

Hošek, J., Pokorný, P., Kubovčík, V., Horáček, I., Žáčková, P., Kadlec, J., Rojík, F., **Lisá, L.,** Buckuliaková, S. (2014): Late Glacial climatic and environmental changes in eastern-central Europe: Correlation of multiple biotic and abiotic proxies from the lake Svancemberk, Czech Republic (2014): Paleogeography, Paleoclimatology, Palaeocology, 396, s. 155 – 172.

Hradecký, J., Pánek, J. (2008): Deep-seated gravitational slope deformations and their influence on consequent mass movements (case studies from the highest part of the Czech Carpathians).- Natural Hazards 45, 2, s. 235-253.

Hurník, S. (1969): Příspěvek ke geologické problematice tzv. Komořanského jezera. Mostecko-Litvínovsko. Regionální studie.- Příroda, 6, s. 5–14.

Jarošová, M., **Lisá, L.,** Přichystal, A., Parma, D., Petr, L., Kos, P. (2010): Geoarcheologický výzkum halštatské zemnice v Modřicích u Brna.- Výzkumy na Moravě a ve Slezsku, 1-2, s. 39 - 45.

Kadlec, J., Grygar, T., Světlík, I., Ettler, V., Mihaljevič, M., Diehl, J.F., Beske-Diehl, S., Svitavská-Svobodová, H. (2009): Morava River floodplain development during the last millennium, Strážnické Pomoraví, Czech Republic.- Holocene 19, s. 499–509.

Kadlec, J., Chadima, M., **Lisá, L.**, Hercman, H., Osintsev, A., and Oberhänsli, H. (2009): Clastic cave deposits in Botovskaya Cave (Eastern Siberia,Russian Federation). - Journal of Cave and Karst Studies, NSS. 70, (3), s. 142-155.

Komoróczy, B., Vlach, M., Hüssen, C.M., **Lisá, L.**, Lenďáková, Z., Groh, S. (2014): Projekt interdisciplinárního výzkumu římských krátkodobých táborů ve středním Podunají.
[Interdisciplinary research project of the Roman temporary camps in the Middle Danube region.]
Sociální diferenciace barbarských komunit ve světle nových hrobových, sídlištních a sběrových nálezů (Archeologie barbarů 2011). Brno : Archeologický ústav AV ČR, Brno, v. v. i., 2014 - (Komoróczy, B.), s. 341-367 ISBN 978-80-86023-25-0. - (Spisy archeologického ústavu AV ČR Brno. 44)

Krizova, L., Krizek, M., **Lisa, L.** (2011): Applicability of quartz grains surface analysis to the study of the genesis of unlithified sediments.- GEOGRAFIE, 116, 1, s. 59-78

Krystek, I. (1981): Použití výzkumu společenstev těžkých minerálů v sedimentárních komplexech. – Folia Fac. Sci. Natur. Univ. Purk. Brun, Geologia 22, 3, s. 101-107.

Kukla, J., Ložek, V. (1958): K problematice výzkumu jeskynních výplní. - Československý Kras, 11, s. 19-83.

Kubiena, W. (1938): Micropedology. Collegiate Press Ames, Iowa 1938.

Kukal, Z. (1986): Základy sedimentologie. – Academia Praha.

Kukla, J. (1969): Die Lösskurve und ihre absolute Datierung. In: Demek – Kukla Hrsg. 1969, s. 94–95.

Kuna, M., Hajnalová, M., Kovačíková, L., **Lisá, L.,** Novák, J., Bureš, M., Cílek, V., Hošek, J., Kočár, P., Majer, A., Makowiecki, D., Cumming, L.S., Suvova, Z., Svetlik, I., Vandenbenberhe, D., Van Nieuland, J., Yost, C.L., Zabilka-Kunek, M. (2013): The Early Medieval site at Roztoky; The evidence of ecofacts.- Památky Archeologické, 104, s. 59 – 147.

Kvítková, L. (2002): Distribuce přirozeně radioaktivních prvků v moravských spraších.- Geol. Výzk. Mor. Slez. v Roce 2001, s. 11-12.

Kvítková, L., Buriánek, D. (2002): Chemical composition of the Dyjskosvratecký úval valley loess.- Acta Mus. Moraviae, Sci. geol., 87, s. 103-111.

Le Ribault, L. (1975): Application de l'exoscopie des quartz à quelques échantillons prélevés en Manche orentale. Philosophical Transacations of the Royal Society of London. Series A, s. 279–288.

Le Ribault, L. (2003a): LLR et le G5: Exoscopie – Définition scientifique. http://www.leribault.com/exo_definitionscientifique.php, cit. 2007-07-23.

Le Ribault, L. (2003b): LLR et le G5: Balade sur un grain de sable. http://www.loic-leribault.ch/exo_balademicroscopique_p01.php.

Lisá, L. (2004): Exoscopy of Moravian eolian sediments. Bulletin of Geosciences, 79, 3, s. 177-182.

Lisá L. (2011): 28. O kolapsech skrytých pod povrchem krajiny. In: Bárta M. (ed).: Kolapsy moderních společností.

Lisa, L., Komoroczy, B., Vlach, M., Válek, D., Bajer, A., Kovárník, J., Rajtár, J., Hüssen, C.M., Šumberová, R. (2015): How were the ditches filled? Sedimentological and micromorphological classification of formation processes within graben-like archaeological objects.- Quaternary International, 370, s. 66-76.

Lisá L., Bajer, A. (2014): Manuál Geoarcheologa.-Mendelova Universita v Brně.

Lisa, L., Hosek, J., Bajer, A., Matys Grygar T., Vandenberghe D. (2014): Geoarchaeology of Upper Palaeolithic loess sites located within a transect through Moravian valleys, Czech Republic.- Quaternary International, 351, s. 25-37.

Lisá, L., Škrdla, P., Havlín Nováková, D., Bajer, A., Čejchan, P., Nývltová Fišáková, M., Lisý, P. (2013a): The role of abiotic factors in ecological strategies of Gravettian hunter–gatherers within Moravia, Czech Republic.- Quaternary International, 294, s. 71 – 81.

Lisá, L., Neruda, P., Nerudová, Z., Bajer, A. (2013b): Geoarcheologický záznam středního a mladého paleolitu v jeskyni Kůlně, Moravský kras.- Acta Musei Moraviae. Scientiae sociales = Časopis Moravského muzea. Vědy společenské. 98, 2: s. 197-214.

Lisá L., Bajer, A., Válek D., Květina P., Šumberová R. (2013c): Micromorphological Evidence of Neolithic Rondel-like Ditch Infillings; Case Studies from Těšetice-Kyjovice and Kolín, Czech Republic.- Interdisciplinaria Archaeologica 4(2): s. 135–146.

Lisá, L., Lisý, P., Chadima, M., Čejchan, P., Bajer, A., Cílek, V., Suková, L. and Schnabl, P. (2012): Microfacies description linked to the magnetic and non-magnetic proxy as a promising environmental tool: Case study from alluvial deposits of the Nile river. Quaternary International, 266, pp. 25-33.

Lisá, L., Buriánek D., Uher P. (2009): New approach to garnet redistribution during aeolian transport.- Geological Quarterly, 53, 3, s. 333 - 340.

Lisá, L., Kolařík, V., & Bajer, A. (2008): The geoarchaeological and micromorphological reconstruction of medieval food store room floor layers; the case study from Tišnov, Czech Republic.- Frankfurter Geowissenschaftliche Arbeiten. Serie D, Band 30, 67-75, Archaeological Soil Micromorphology - Contributions to the Archaeological Soil Micromorphology Working Group Meeting 3rd to 5th April 2008.

Lisa, L., Uher, P. (2006): Provenance of Wurmian loess and loess-like sediments of Moravia and Silesia (Czech Republic): a study of zircon typology and cathodoluminiscence. Geologica Carpatica, 57, 5, s. 397-403.

Lisá, L., Buriánek, D., Uher, P. (2005): Provenance of Wurmian loess and loess like sediments inMoravia and Silesia, Czech Republic: using of heavy minerals associations.- Acta Musei Moraviai, Sci. geol, 90, s. 147-154.

Mahaney, W.C., Kalm, V. (2000): Comparative scanning electron microscopy study of oriented till blocks, glacial grains and Devonian sands in Estonia and Latvia. Boreas, 29, s. 35–51.

Mahaney, W.C., Stewart, A., Kalm, V. (2001): Quantification of SEM microtextures useful in sedimentary environmental discrimination. Boreas, 30, s. 165–171.

Matys Grygar, T., Novakova, T., Mihaljevic, M., Strnad, L., Svetlik, I., Koptikova, L., **Lisa, L.**, Brazdil, R., Macka, Z., Stachon, Z., Svitavska-Svobodova, H., Wray, D.S. (2011): Surprisingly small increase of the sedimentation rate in the floodplain of Morava River in the Straznice area, Czech Republic, in the last 1300 years.- CATENA, 86, 3, s. 192-207

Mentlík, P., Minár, J., Břízová, E., **Lisá, L.**, Taborik, P. & Stacke, V. (2010): Glaciation in the surroundings of Prášilské Lake (Bohemian Forest, Czech Republic).- Geomorphology, 117, 1-2, s. 181-194.

Milek, K. (2012): Floor formation processes and the interpretation of activity areas: an ethnoarchaeological study of turf buildings at Thverá, northeast Iceland. Journal of Anthropological Archaeology 31, s. 119-137.

Nerudová, Z., Neruda, P., **Lisá, L.** (2012): Rescue excavation of the Upper Palaeolithic sites in Brno-Styrice in the context of Brno Region.- Archeologické Rozhledy, 64, 4, s. 591 – 627.

Novak, J., **Lisá, L.**, Pokorný, P., Kuna, M. (2012): Charcoal analyses as an environmental tool for the study of Early Medieval sunken houses infills in Roztoky near Prague, Czech Republic.- Journal of Archaeological Science, 39, s. 808 – 817.

Notebaert, B., Verstraeten, G., Rommens, T., Vanmontfort, B., Govers, G., Poesen, J. (2009): Establishing a Holocene sediment budget for the river Dijle.- Catena 77, s. 150–163.

Nyvlt, D., Kosler, J., Mlcoch, B., Mixa, P., **Lisa, L.**, Bubik, M., Hendriks, B.W.H. (2011): The Mendel Formation: Evidence for Late Miocene climatic cyclicity at the northern tip of the Antarctic Peninsula Palaeogeography Palaeoclimatology, Palaeoecology, 299, 1-2, s. 363-384.

Pánek, T., Tábořík, P., Klimeš, J., Komárková, V., Hradecký, J., Šťastný M. (2011): Deep-seated gravitational slope deformations in the highest parts of the Czech Flysch Carpathians: Evolutionary model based on kinematic analysis, electrical imaging and trenching.- Geomorphology 129 (1), s. 92-112.

Parma, D., **Lisá, L.**, Jarošová, M., Petr, L. (2011): Geoarchaeology of La Tène Sunken Houses at Syrovice, Czech Republic: Importance for Understanding Living Strategies. Interdisciplinaria Archaeologica 2(1), s. 15-25.

Parma, D., Vejrostová, L., **Lisá, L.**, Bajer, A., Pacina, J., Gottvald, Z. (2015): Neolithic Occupation of Svratka Alluvial Plain; Case Study from Brno-Přízřenice, Czech Republic.- IANSA (v tisku)

Petr L., Sádlo J., Žáčková P., **Lisá L.**, Novák J., Pokorný P. (2014): Late-Glacial and Holocene Environmental History of an Oxbow Wetland in the Polabí Lowland (River Elbe, Czech Republic); a Context-Dependent Interpretation of a Multi-Proxy Analysis.- Folia Geobotanica, 49, 2, s. 137 – 162.

Petránek, J. (1963): Usazené horniny: Jejich složení, vznik a ložiska. Nakladatelství ČSAV, Praha, 720 s.

Plaček, M., Dejmal, M. (eds.) (2015): Veselí nad Moravou; středověký hrad v říční nivě.- Archaia Brno o.p.s., Brno.

Neustupný, E. (1985): K holocénu Komořanského jezera. Památky archeologické, 76, s. 9–70.

Neustupný, E., Dobeš, M., Turek, J. & Zápotocký, M. (2008): Archeologie pravěkých Čech 4: Eneolit. Archeologický ústav AVCR, v. v. i., Praha. 185 s.

Pokorný, P., Šída, P., Chvojka, O., Žáčková, P., Kuneš, P., Světlík, I., Veselý, J. (2010): Palaeoenvironmental research of the Schwarzenberg Lake, southern Bohemia, and exploratory excavations of this key Mesolithic archaeological area.- Pamatky Archeol., 101, s. 5–38.

Prudič, Z. (1978): The Strážnice floodplain forest in the second half of the 1st millennium A.D. Lesnictví 24, s. 1019–1036.

Musil, R. (1993): Moravský kras : labyrinty poznání.- Jaromír Bližňák, GEO program, Adamov.

Neruda, P. In press: GIS analysis of the spatial distribution of Middle Palaeolithic artefacts in Kůlna Cave (Czech Republic). Quaternary International. DOI: 10.1016/j.quaint.2015.10.028

Nývlt, D., Engel, Z., Tyráček, J. (2011): Pleistocene Glaciations of Czechia. In: Ehlers, J., Gibbard, P.L., Hughes, P.D. (eds): Quaternary Glaciations – Extent and Chronology, A closer look. Developments in Quaternary Science, 15, s. 37–46.

Roberts, N. (2014): The Holocene; an environmental history, third edition, Wiley Blackwell, New Yordk.

Růžičková, E., Růžička, M., Zeman, A., Kadlec, J. (2003): Kvartérní klastické sediment České republiky; struktury a textury hlavních genetických typů.- Česká geologická služba, Praha.

Řeháková, Z. (1986): The Postglacial history of diatom-bearing sediments of the former Lake Komořany (North-West Bohemia). Anthropozoic 17, s. 87–134.

Smalley, I., O'Hara-Dhand, K., Wint, J., Machalett, B., Jary, Z., Jefferson, I. (2009): Rivers and loess: The significance of long river transportation in the complex event-sequence approach to loess deposit formation.- Quaternary International, 198, 1-2, s. 7-18.

Smolíková, L. (1969): Mikromorphologie der fossilen Böden in den Löss-Serien. In: Demek – Kukla Hrsg. 1969, s. 34–38.

Smolíková, L. (1973): Paleogeografický a paleoklimatický význam půd v kvartéru.- Acta Universitatis Carolinae 1973. Geographica 2, Praha, s. 37–46.

Stoops, G., Marcelino, V., Mees, F. (2010): Interpretation of Micromorphological Features of Soils and Regoliths. Elseiver.

Šída, P., Pokorný, P., Kuneš, P. (2007): Dřevěné artefakty raně holocenního stáří z litorálu zaniklého jezera Švarcenberk.- Přehled Výzkumů 48, s. 55–64.

Šilhán, K., Pánek, T. (2010): Fossil and recent debris flows in medium–high mountains (Moravskoslezské Beskydy Mts, Czech Republic).- Geomorphology 124, 3, s. 238-249.

Škrdla, P., Tostevin, G., Nývlt, D., **Lisá, L.,** Mlejnek, O., Prichystal, A., Richter, D. (2009): Tvarozna-Za skolou. The results of 2008 excavation season.- Přehled výzkumů 50, s. 11-24.

Thér, R., Droberjar, E., Gregor, M., **Lisá, L.,** Kočár, P., Kočárová, R. (2010): Roman Age lime kilns in Tuněchody near Chrudim, eastern Bohemia.- Archeologické Rozhledy, 62, 2, s. 326 – 347.

Thompson, R., Oldfield, F. (1986): Environmental Magnetism. Allen and Unwin, London.

Valoch, K. (2012): K historii členění würmského/viselského glaciálu v českých zemích.- Archeologické rozhledy, 64, s. 129-135.

Valoch, K. (2011): Stratigrafie sedimentů. In: K. Valoch a kol.: Kůlna. Historie a význam jeskyně, s. 47–58. Správa jeskyní České republiky, Průhonice.

Valoch, K. (2002): Eine Notgrabung in der Kůlna-Höhle im mährischen Karst. Acta Musei Moraviae, Scientiae sociales 87, s. 3–34.

Valoch, K. (1988): Die Erforschung der Kůlna-Höhle 1961–1976. Anthropos Studien 24 (N. S. 16). Moravské muzeum, Brno.

Valoch, K. (1971): Der zeitliche und kulturelle Ablauf des Altwürm in Mitteleuropa. Archeologické rozhledy 23, s. 716–724.

Valoch, K., Pelíšek, J., Musil, R., Kovanda, J., Opravil, E. (1969): Die Erforschung der Kůlna-Höhle bei Sloup im Mährischen Karst (Tschechoslowakei). Quartär 20, s. 1-45.

Šroubek, P., Diehl, J.F., Kadlec, J., Valoch, K. (2001): A Late Pleistocene palaeoclimate record based on mineral magnetic properties of the entrance facies sediments of Kulna Cave, Czech Republic.- Geophysical Journal International, 147/2, s. 247–262.

Tichý, R., Dohnálková, H., **Lisá, L.** (2010): Odpadní jámy nebo blátivé louže? : zaplňování archeologických objektů/vznik výplní jako klíčový faktor pro širší interpretace.- Živá archeologie, 11, s. 138 – 142.

Wisniewski, A., Plonka, T., Zdzislaw, J., **Lisa L.,** Traczyk, A., Kufel-Diakowska, B., Raczyk, J., Bajer, A. (2015): The early Gravettian in a marginal area: New evidence from SW Poland. Quaternary International. 359, s. 131-152.

Zalasiewicz, J., Williams, M., Haywood, A., Ellis, M. (2011): The Anthropocene: a new epoch of geological time?". Philosophical Transactions of the Royal Society A 369 (1938): s. 835–841. doi:10.1098/rsta.2010.0339. PMID 21282149.

Zupan Hajna, N., Mihevc A., Pruner, P., Bosák, P. (2008): Palaeomagnetism and Magnetostratigraphy of Karst Sediments in Slovenia.- Karst Research Institute, Carsologica 8, Ljubljana.